THE UNIVERSITY
of EDINBURGH

Detection, Assessment and Modulation of Myocardial Inflammation

Syed Shirjel Rizwan Alam

MBChB, MRCP, MRCS, MRCA

Degree of Doctor of Philosophy

University of Edinburgh

2017

Abstract

Coronary atherosclerosis and plaque rupture leads to acute coronary thrombosis and myocardial infarction. Current treatment involves re-establishing vessel patency, but no treatments have been developed to target post-infarction inflammatory pathways. Such treatments may reduce cardiomyocyte injury, attenuate adverse remodelling and improve clinical outcome.

Inflammation within the infarcted myocardium is associated with chemotaxis of neutrophils and monocytes to the site of injury. Early reperfusion therapy amplifies this inflammatory cell influx. Neutrophil release a variety of pro-inflammatory factors, including human neutrophil elastase (HNE). HNE has a wide range of substrates. Preclinical studies have demonstrated that neutrophil depletion or inhibition of neutrophil elastase attenuates post-ischemic inflammatory reperfusion injury within the myocardium. Recruitment of monocytes into the infarcted myocardium is followed by maturation and differentiation into macrophages. Macrophages play a key role in orchestrating inflammation and repair. Therapeutic manipulation of this healing process will only come from understanding mechanisms and targeting reparative pathways.

"Ultrasmall superparamagnetic iron oxide particles" (USPIOs) extravasate through capillaries and are phagocytosed by tissue inflammatory cells. These cells are predominately macrophages, but neutrophils have also been shown to take up USPIOs. USPIO-enhanced MRI can identify areas of inflammation in models inflammation in various tissues. Therefore we hypothesised that USPIO enhanced

MRI could identify and assess cellular inflammation of the myocardium.

During coronary artery bypass graft surgery (CABG), the myocardium receives an immediate ischaemic insult that is exacerbated by post-ischaemic reperfusion inflammatory responses leading to increased myocardial injury. CABG surgery can therefore be used as a clinical model of myocardial infarction and inflammation. We investigated this with blood markers of inflammation, MRI scanning and USPIO.

Elafin inhibits the destructive and inflammatory HNE enzyme. Beyond this elafin inhibits inflammatory cytokines and modulates the innate and adaptive immune systems. In preclinical studies elafin treatment is associated with reduced myocardial injury. As such, elafin has a marked potential for the treatment of cardiovascular disease involving inflammation. Therefore, we hypothesised that elafin will reduce perioperative ischaemic myocardial injury and inflammation in patients undergoing elective coronary artery bypass graft surgery.

We demonstrated for the first time that USPIOs are taken up by the infarct tissue in patients with recent myocardial infarction and by the peri-infarct myocardium to a lesser degree. This represents a novel non-invasive method to further study cardiac inflammation and therapeutic interventions.

All patients undergoing CABG surgery demonstrated >10-fold elevation above the 99^{th} centile of cardiac troponin by high sensitivity assay (hs-cTnI) indicating the current universal definition of type 5 myocardial infarction lacks specificity. A peak hs-cTnI at 6 hours following CABG surgery appears to be related to the surgical process and non-specific myocardial injury whilst a continuing increase at 24 hours

suggests myocardial infarction. We would suggest hs-cTnI sampling at 6 and 24 hours post CABG surgery together with ECG assessment for the routine detection and diagnosis of type 5 MI. Differing levels of humoral makers inflammation post CABG surgery occurred, and did not correlate directly with the length of cardiopulmonary bypass time or hs-cTnI release. For the first time we identified differing levels of inflammatory cell infiltrate into the myocardium post CABG. This varied from none to levels similar to infarcted myocardial tissues.

Elafin did not attenuate myocardial ischemia-reperfusion injury and inflammation. Post-hoc analysis identified reduced cTnI concentrations at 6 hours in Elafin treated patients and it is possible that a bigger dose would have conferred protection out to 48 hours. Elafin did not attenuate the cellular infiltration into the myocardium post CABG surgery, but did appear to reduce inflammation in renal tissue. USPIO enhanced CMR holds major promise in the non-invasive assessment of myocardial inflammation post surgery.

Contents

Table of Figures

Table of Tables

Abbreviations

cTnT	**-**	**Cardiac Troponin T**
cTnI	**-**	**Cardiac Troponin I**
cTnC	**-**	**Cardiac Troponin C**
IL	**-**	**Interleukin**
MCP	**-**	**Monocyte chemoattractant protein**
HNE	**_**	**Human neutrophil elastase**
M-CSF	**-**	**Macrophage colony stimulating factor**
TNF	**-**	**Tumour necrosis factor**
CABG	**-**	**Coronary artery bypass surgery**
CPB	**-**	**Cardio-pulmonary bypass**
CMR	**-**	**Cardiac magnetic resonance**
WHO	**-**	**Who health organisation**
MMP	**_**	**Matrix metallo-proteinases**
TIMP	**-**	**Tissue inhibitor of metallo-proteinases**
TFPI	**-**	**Tissue factor pathway inhibitor**
LPS	**-**	**Lipopolysaccharide**
PAR	**-**	**Protease activated receptor**
SLPI	**-**	**Secretory leukocyte protease inhibitor**

α1-PI	**-**	**Alpha-1 antitrypsin**
NF-κB	**-**	**Nuclear factor kappa-light-chain-enhancer of B cells**
KDa	**-**	**Kilo-Daltons**
Pg	**-**	**Picogram**
MRI	**-**	**Magnetic resonance imaging**
USPIO	**-**	**Ultrasmall superparamagnetic iron oxide particles**
MI	**-**	**Myocardial Infarction**
ROI	**-**	**Region of Interest**
LV	**-**	**Left Ventricle**
hs-TnI	**-**	**Troponin I by high sensitivity assay**
hs-CRP	**-**	**C-reactive protein by highly sensitive assay**
AUC	**-**	**Area under the curve**
ECG	**-**	**Electrocardiogram**
TWI	**-**	**T-wave Inversion**
BBB	**-**	**Bundle branch block**
SEM	**-**	**Standard error of mean**
MPO	**-**	**Myeloperoxidase**
95% CI	**-**	**95% Confidence Interval**
IQR	**-**	**Inter-quartile range**
mL	**-**	**Millilitre**

ng	**-**	**Nanogram**
mg	**-**	**Milligram**
CAD	**-**	**Chronic allograft damage**
NGAL	**-**	**Neutrophil gelatinase-associated lipocalin**
AKI	**-**	**Acute kidney injury**
ICAM	**-**	**Intercellular adhesion molecule**
VCAM	**-**	**Vascular cell adhesion protein**

Declaration

This thesis represents research that I have undertaken in the British Heart Foundation University of Edinburgh Centre for Cardiovascular Science and the Edinburgh Heart Centre, Royal Infirmary of Edinburgh between August 2011 and August 2014.
I was personally involved in composition and every aspect of the work presented in this thesis. In keeping with the collaborative nature of this work, assistance was received and is acknowledged. Dr Ninian Lang & Miss Jennifer Richards undertook the preliminary design of the study presented in Chapter 3. Dr Peter Henriksen conceived and undertook the preliminary design of the study presented in Chapter 4.
This thesis has not been submitted elsewhere in application for a university degree, and all sources of information have been acknowledged. All studies were undertaken in accordance with the regulations of the Scotland Research Ethics Committee, the Lothian Local Research Ethics Committee, the Medicines and Healthcare products Regulatory Agency and the Declaration of Helsinki of the World Medical Association. The written informed consent of each participant was obtained before entry into the studies.
The British Heart Foundation funded myself through a Clinical Research Training Fellowship (FS/12/83/29781). This work was funded by the Medical Research Council (G1001339) and Chest Heart and Stroke Scotland (R11/A135).

The Wellcome Trust Clinical Research Facility and Clinical Research Imaging Centre are supported by NHS Research Scotland (NRS) through NHS Lothian. The work was greatly aided by Lynsey Milne, Samantha Thomas and Ronald Harkess.

Preface

بِسْمِ اللَّهِ الرَّحْمَٰنِ الرَّحِيمِ

رَبِّ أَوْزِعْنِيٓ
أَنْ أَشْكُرَ نِعْمَتَكَ ٱلَّتِيٓ أَنْعَمْتَ عَلَيَّ وَعَلَىٰ وَٰلِدَيَّ وَأَنْ أَعْمَلَ صَٰلِحًا تَرْضَىٰهُ
وَأَصْلِحْ لِي فِي ذُرِّيَّتِيٓ ۖ إِنِّي تُبْتُ إِلَيْكَ وَإِنِّي مِنَ ٱلْمُسْلِمِينَ

IN THE NAME OF ALLAH, THE ENTIRELY MERCIFUL, THE ESPECIALLY MERCIFUL

MY LORD, ENABLE ME TO BE GRATEFUL FOR YOUR FAVOUR WHICH YOU HAVE BESTOWED UPON ME AND UPON MY PARENTS AND TO WORK RIGHTEOUSNESS OF WHICH YOU WILL APPROVE AND MAKE RIGHTEOUS FOR ME MY OFFSPRING. INDEED, I HAVE REPENTED TO YOU, AND INDEED, I AM OF THE MUSLIMS.

Acknowledgements

I would like to thank all the people who have both tolerated and supported me during this time of research.

Most of all my parents Sabiha and Khursheed Alam who worked so hard and sacrificed so much to allow me to become a doctor.

My fellow researchers - Nikhil Joshi, Anoop Shah, Gareth Barnes and Amanda Hunter. To this day, friendships formed during the time have endured.

Professor Dave Newby gave me the opportunity to undertake this period of research, and this intervention rescued me from a career in anaesthetics, and allowed me to pursue cardiology. For this I am grateful and am indebted.

Dr Andrew Flapan has mentored me throughout my clinical career, and has continually encouraged me to finally write up this thesis. I greatly value his friendship and support.

The Medical Research Council is thanked for their grant. The British Heart Foundation and Chest, Heart & Stroke also funded my position and this research. I am grateful to every person who donated to these charities, without such selfless people no research would be possible.

I would particularly like to thank Dr Peter Henriksen, who has been invaluable as a supervisor. He has supported me in clinical medicine, in research and in all manner of problems I encountered during this time. He has gone far beyond the usual remit

of a supervisor to help me, and without these interventions I may well have left clinical medicine. As an academic, he is a researcher of the highest intelligence and creativity. As a friend and colleague, he has proven himself to be a man of integrity, generosity and the highest character. I hope and pray for the best for him and his family.

Chapter 1: MYOCARDIAL INFLAMMATION FOLLOWING ISCHAEMIA-REPERFUSION INJURY

1.1 OVERVIEW

Ischemia-reperfusion injury occurs when blood flow is restored to organs and tissues that have sustained a period of interrupted blood supply. This occurs following therapies for acute myocardial infarction, and during cardiac surgery. Inflammation follows in order to remove necrotic cellular debris and allow tissue remodelling. Excessive inflammation may follow reperfusion therapy, and can have detrimental effects on healing and left ventricular remodelling (Nahrendorf et al., 2010). Mechanisms of cell and tissue injury include a neutrophil-mediated post-ischaemic inflammatory response and activation of cellular death pathways following reperfusion (Hansen, 1995). Protecting organs from ischaemia-reperfusion injury to improve clinical outcome is a high priority. Despite intense research efforts and huge promise from pre-clinical and early phase clinical trials, there are currently no effective therapies that can limit this injurious response.

With the aim of improving outcomes following acute myocardial infarction, novel drugs are increasingly focusing on optimisation of myocardial repair and regeneration, and include anti-inflammatory interventions (Bonvini et al., 2005, Frangogiannis, 2006, Gonzalez et al., 2011, Steffens et al., 2009). There is therefore a need for non-invasive methods to assess *in vivo* myocardial inflammation following myocardial infarction both to define the healing process and to measure the potential efficacy of novel therapeutic interventions. Such interventions include targeting the neutrophil mediated inflammatory cascade.

1.2 MYOCARDIAL INFARCTION

Coronary atherosclerosis is responsible for the initiation of acute myocardial infarction with plaque rupture leading to acute coronary thrombosis and myocardial infarction. Current treatment in the acute phase involves re-establishing vessel patency by percutaneous coronary intervention supported by anti-thrombotic therapy. Thereafter, statins, angiotensin-converting enzyme inhibitors and beta-blockade all have prognostic benefit but no treatments have been successfully developed to target post-infarction inflammatory pathways.

Necrotic cardiac muscle elicits an inflammatory cascade that serves to clear the infarct of dead cells and matrix debris. Human cardiac muscle has negligible regenerative capacity and ultimately inflammation leads to replacement of damaged tissue with a fibrotic scar. Enhancing reparative mechanisms following the inflammatory reaction to myocardial infarction may reduce cardiac myocyte injury, attenuate adverse remodelling and improve clinical outcome. A better understanding of the early post-infarct healing phase will also facilitate cell therapy strategies to engraft stem cells or stimulate regeneration. In order to achieve this goal, we must better characterise the inflammatory processes that follow infarction and myocardial necrosis in humans.

1.2.1 TROPONIN BIOLOGY AND KINETICS

Troponin is a protein complex involved in cardiac muscle contraction, and is used in clinical practice to detect myocardial infarction. There are a number of forms of troponin. Cardiac troponin T (cTnT) and troponin I (cTnI) are derived from genes specific to the myocardium (Coudrey, 1998, Katus et al., 1992) whereas troponin C

(cTnC) is present in both cardiac and skeletal muscle with no specific isoform for cardiac tissue (Coudrey, 1998). Whilst most of the cardiac troponin complex (troponin I, T and C) is bound within the cytoskeletal structure of the cardiac myocyte, approximately 7% and 3.5% of troponin T and I respectively is present within the cytosolic pool (Katus et al., 1991, Wu et al., 1998). There are also important differences in the size of troponin I and T with troponin T being twice the size (37 kiloDaltons [kDa]) of troponin I (22 kDa) (Mair et al., 1992).

Wu *et al* showed that there remains significant differences in the release of troponin following acute myocardial injury (Wu et al., 1998). Following acute myocardial infarction troponin was released in three forms; a ternary complex (cTn T-I-C), a binary complex (cTn I-C) and free troponin T (Wu et al., 1998). Wu et al also showed significant heterogeneity in the cross-reactivities of antibodies to various forms of troponin I reflecting the assay differences in absolute troponin I measurements between assays (Wu et al., 1998).

1.2.2 MYOCARDIAL CELLULAR INFLAMMATION POST INFARCTION

Inflammation within the infarcted myocardium is associated with induction of endothelial adhesion molecules and enhanced permeability of the microvasculature. Up regulation of chemokines including interleukin (IL)-8 and monocyte chemoattractant protein (MCP)-1 attracts neutrophils and monocytes to the site of injury (Hammond et al., 1995, Kumar et al., 1997). Early reperfusion therapy amplifies this inflammatory cell influx and accelerates the healing response through proliferative and maturation phases. Neutrophil adhesion to endothelium of infarcted myocardium occurs within minutes of reperfusion (Weyrich et al., 1995). Ischaemic

cardiomyocytes are further injured by adherent neutrophils that release reactive oxygen species and destructive proteases including human neutrophil elastase (HNE) and proteinase 3 (Borregaard and Cowland, 1997). HNE has a wide range of substrates including matrix components elastin, fibronectin, and collagen types III and IV (Lee and Downey, 2001, Si-Tahar et al., 1997). Activated neutrophils also occlude microvessels and increase endothelial permeability contributing to myocardial oedema. Capillary plugging and obstruction by activated neutrophils contributes to failure of microvascular perfusion and increased infarct size within the 'no-reflow' zone. Neutrophil depletion reduces this phenomenon and infarct size following reperfusion in pre-clinical models (Romson et al., 1983b).

Recruitment of monocytes into the infarcted myocardium is followed by maturation and differentiation into macrophages: a process dependent on growth factors such as macrophage-colony stimulating factor (M-CSF) (Okazaki et al., 2007, Yano et al., 2006). Macrophages have multiple roles within the infarct including (i) phagocytic clearance of dead cells and debris, (ii) production of growth factors and cytokines that stimulate fibroblast growth and angioneogenesis, and (iii) matrix turnover through the production of matrix metalloproteases and their inhibitors (Lambert et al., 2008). Macrophages are resident within 24 hours of infarction and persist for up to 4 weeks. During this period, macrophages regulate infarct healing with the initial development of granulation tissue and subsequent scar formation. Murine studies suggest that distinct monocyte subsets regulate these different processes. Monocytes arriving within the first 3 days mature into macrophages that scavenge necrotic debris through inflammatory mediator expression, proteolysis and phagocytosis. Monocytes arriving later on give rise to macrophages which promote reparative processes such as angioneogenesis and extracellular matrix deposition (Nahrendorf et

al., 2007a). Apoptosis is the primary mechanism determining longevity of neutrophils within sites of inflammation and infarction. Engulfment and clearance of apoptotic neutrophils by macrophages produces potent anti-inflammatory signals including release of transforming growth factor (TGF)-β. Combined with clearance of pro-inflammatory matrix fragments, these processes drive the switch to tissue repair and resolution of the post-infarct inflammatory response.

MCP-1 expression is increased in ischaemic myocardium following reperfusion and this accounts for a substantial proportion of the monocyte chemotactic activity (Kumar et al., 1997). MCP-1 knockout mice exhibit delayed macrophage infiltration in the healing infarct with a prolonged inflammatory phase and delayed replacement of injured cardiomyocytes with granulation tissue (Dewald et al., 2005). The MCP-1 deficient mice have similar size infarcts but attenuated remodelling compared to wild types. MCP-1 mRNA levels are increased 40-fold within non-infarcted myocardium (Hayashidani et al., 2003) and blockade of MCP-1 signalling with a deletion mutant of MCP-1 markedly reduced macrophage infiltration both within the infarct and non-infarcted myocardium. Widespread myocardial inflammatory cell infiltration beyond the non-infarcted zone has been observed in human autopsy specimens (Abbate et al., 2004). Blockade of MCP-1 signalling is associated with improved survival rates and reduced left ventricular dilatation as well as reduced tumour necrosis factor (TNF)-α gene expression in the non-infarcted myocardium. These studies indicate that macrophage activity outside the infarct zone may contribute to adverse myocardial remodelling following myocardial infarction.

The inflammatory response to myocardial infarction is necessarily complex to coordinate the development of a healing scar from infarcted tissue. The role of the

macrophage differs depending on differentiation and location within the myocardium. Therapeutic manipulation of this healing process will only come from understanding mechanisms and targeting reparative pathways. Indiscriminate immunosuppressive therapy in this setting may result in harm as observed in trials with methylprednisolone in acute myocardial infarction (Mannisi et al., 1987).

1.3 CORONARY ARTERY BYPASS SURGERY

Over 300 000 coronary artery bypass graft (CABG) operations are performed each year in the United States of America (Diodato and Chedrawy, 2014). Myocardial inflammation and injury follows surgery. During coronary artery bypass graft surgery, the myocardium receives an immediate ischaemic insult that is exacerbated by post-ischaemic reperfusion inflammatory responses leading to increased myocardial injury. Coronary artery bypass graft surgery can therefore be used as a clinical model of myocardial infarction and inflammation (Steuer et al., 2004c, Anselmi et al., 2004).

1.3.1 MYOCARDIAL INFLAMMATION POST CARDIAC SURGERY

Cardiopulmonary bypass (CPB) contributes to systemic and coronary inflammation (Zahler et al., 1999, Paparella et al., 2002). Inflammatory cytokines depress cardiac function after CPB (te Velthuis et al., 1995) and plasma IL-6 and IL-8 concentrations in the postoperative period correlate with myocardial injury and apoptosis (Wan et al., 2002). Although elevations in circulating markers of cellular inflammation are seen to rise during CPB, in vivo cellular infiltration into the myocardium has not been demonstrated (Ascione et al., 2000).

Plasma cTnI concentrations increase in all patients undergoing CABG surgery (van Gaal et al., 2011). The magnitude of cTnI concentration increase correlates with major adverse cardiac events within 30 days as well as long-term mortality (Nesher et al., 2008, Croal et al., 2006). However cardiac magnetic resonance (CMR) evidence of myocardial necrosis is only evident in a minority, suggesting that cTnI

release may result from additional mechanisms such as post ischaemia-reperfusion inflammation (Noora et al., 2005). It has been demonstrated that concentrations below the 99th centile detected with this assay provide major prognostic information in patients with non ST-elevation myocardial infarction (Shah et al., 2015a). The components for defining a myocardial infarction include the presence of symptoms, electrocardiographic evidence of myocardial ischaemia and / or biomarker evidence of myocardial necrosis. This definition has not substantially changed from the initial MONICA World Health Organisation (WHO) statement. What has, however, changed significantly over the last few decades is our ability to measure and quantify myocardial necrosis.

1.4 ROLE OF THE ENDOGENOUS ELASTASE IN CARDIOVASCULAR INFLAMMATION AND INJURY

1.4.1 NEUTROPHIL-DERIVED ELASTASES AND VASCULAR INFLAMMATION

Neutrophils lead the early phase of the inflammatory response gathering at sites of inflammation, and transmigrating through the endothelium to release granule contents and generate oxygen-derived free radicals that serve the host defence by providing microbicidal activity. Human neutrophil elastase (HNE) and proteinase-3 are amongst the contents of neutrophil azurophilc granules (Borregaard and Cowland, 1997). These enzymes degrade components of the extracellular matrix and the list of substrates for HNE is extensive (Lee and Downey, 2001) including fibrin, fibronectin, collagen, the glycoprotein IIb/IIIa receptor (Si-Tahar et al., 1997), elastin and cadherins (Carden et al., 1998) (Figure 1.1).

Figure 1.1 Inflammatory effects of HNE and proteinase 3.

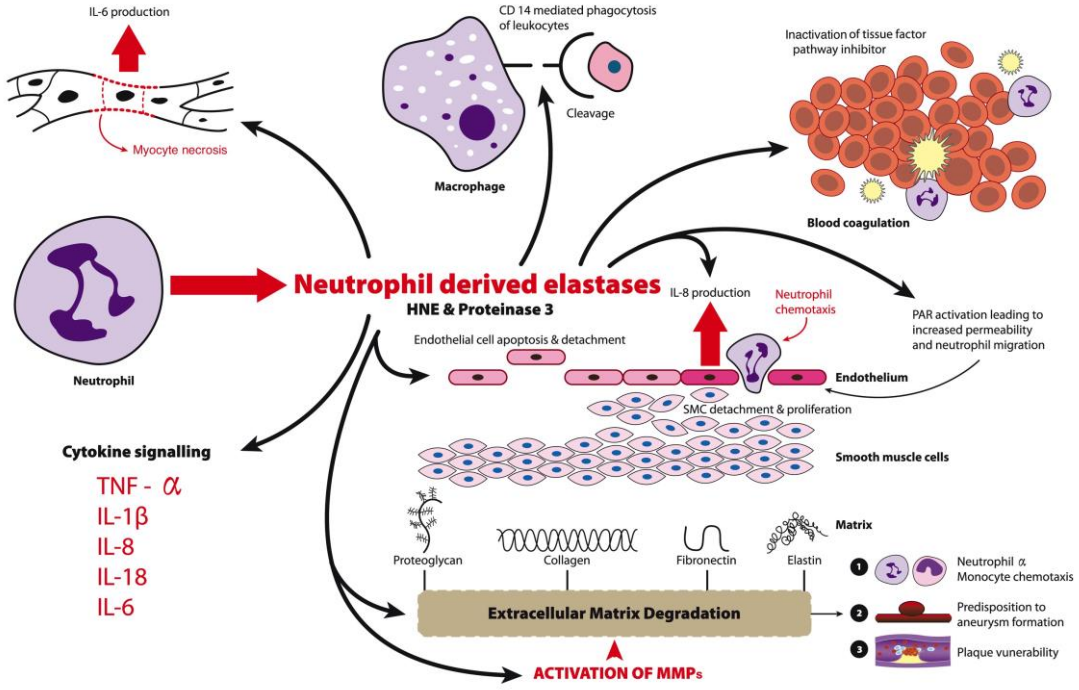

HNEs' action on extracellular matrix components exposes recognition sites that bind cellular integrin and tyrosine kinase receptors. These signals direct the cellular response to injury. Recognition of elastin-derived fragments by the elastin receptor results in migration and chemotaxis of monocytes and vascular smooth muscle cells (Robert et al., 1998, Houghton et al., 2006).

Endothelial cells are susceptible to detachment when cultured with activated neutrophils or HNE (Westlin and Gimbrone Jr, 1993). Anchorage of cells to the extracellular matrix is necessary for survival and cleavage of matrix components and cadherins responsible for adhesion results in apoptosis (Frisch and Francis, 1994, Mtairag et al., 2002). HNE is joined by the matrix metalloproteinase (MMP) and the cathepsin family of proteases in modulating endothelial extracellular matrix degradation during acute inflammation (Garcia-Touchard et al., 2005). There is considerable overlap of substrates between these protease families leading to apparent redundancy. HNE is distinct in having both a broad range of substrates and the ability to be released rapidly and in high concentration from neutrophil granules at sites of inflammation. By contrast, many of the extracellular MMP and cathepsin proteases are regulated by gene expression and MMPs are activated in a cascade of proteolytic steps (Chakraborti et al., 2003). HNE also modulates the activity of vascular extracellular proteases. It directly activates MMPs and inactivates their inhibitors (tissue inhibitors of metalloproteases: TIMPs) (Okada and Nakanishi, 1989, Okada et al., 1988). A complex interplay between extracellular proteases that share common substrates occurs during inflammatory endothelial injury. HNE's broad ranging activity and modulating activity over other proteolytic pathways suggest a central role at the onset of the proteolytic cascade in pathologies where neurophil degranulation is present.

1.4.2 MODULATION OF THROMBOSIS AND FIBRINOLYSIS AND POTENTIAL INVOLVEMENT IN ACUTE CORONARY SYNDROMES

The capacity of HNE to degrade components of the coagulation and fibrinolytic pathways has been demonstrated *in vitro*. Cleavage of plasminogen activator inhibitor type -1 (PAI-1) shortens clot lysis time *in vitro* (Wu et al., 1995). Plasminogen is degraded to miniplasminogen by HNE. This plasminogen fragment is more readily activated and the resulting miniplasmin retains fibrinolytic activity but may be relatively resistant to inhibition by α-2 antiplasmin (Duboscq et al., 1997). More recently, the role of neutrophil-derived elastases in thrombus formation has been demonstrated in knockout mice (Massberg et al., 2010). Compared to wild type mice the animals deficient in neutrophil elastase had markedly reduced fibrin formation in response to chemical injury on intravital videomicroscopy. The mechanism involved proteolytic inactivation of an endogenous anticoagulant, tissue factor pathway inhibitor (TFPI). TFPI and neutophil elastase were observed to co-localise on the external surface of neutrophils in nucleosomes facilitating TFPI degradation. The formation and externalisation of nucleosomes is increased by neutrophil interaction with activated platelets. The combination of human neutrophils and platelets generates pro-coagulant activity measured by the production of active factor X and this was markedly reduced in the presence of HNE inhibitors (Massberg et al., 2010). These observations point to a hitherto unappreciated role for neutrophils and HNE in triggering coagulation and stabilising thrombus formation. Massberg *et al* suggested an innate immunity role for neutrophil elastase generated thrombosis promoting retention of invading pathogens within liver microvessels (Massberg et al., 2010). This work demonstrated the capability of neutrophils to promote thrombus

formation in larger vessels in the absence of infection. The circulating neutrophil count is associated with clinical events including myocardial infarction (Madjid et al., 2004). Neutrophils from patients with acute coronary syndromes exhibit evidence of activation and degranulation (Buffon et al., 2002). Together these finding suggest a more direct pro-thrombotic role for neutrophils in coronary disease.

1.4.3 REGULATION OF INFLAMMATORY SIGNALLING

HNE and proteinase-3 modulate cytokine signaling. HNE and Proteinase-3 can proteolytically activate or process the inflammatory cytokines TNF-α, IL-1β, IL-8 and IL-18 (Carroll et al., 2005, Coeshott et al., 1999, Padrines et al., 1994, Sugawara et al., 2001). HNE is capable of degrading IL-1β and TNF-α possibly acting as a negative regulator of inflammation. Chemerin is a chemoattractant protein that promotes recruitment of antigen presenting cells such as macrophages and dendritic cells (Wittamer et al., 2003). HNE activates chemerin from prochemerin by proteolytically cleaving its C-terminal peptide. This provides one mechanism whereby initial infiltration of neutrophils may orchestrate subsequent antigen presenting cell recruitment at inflammatory sites (Wittamer et al., 2005).

HNE mediated cleavage of the CD14 receptor on monocytes and fibroblasts reduces responsiveness and TNF-α production in response to LPS (Nemoto et al., 2000) as well as impairing recognition and clearance of apoptotic cells by phagocytosis (Vandivier et al., 2002). HNE mediated cleavage of the complement receptor 1 from the surface of erythrocytes generates a fragment that acts as an inhibitor of complement (Sadallah et al., 1999). These findings indicate divergent effects on inflammatory signalling and may reflect changing roles for neutrophil derived

elastases depending on variables such as local concentration, stage of inflammation and signalling context.

HNE stimulates production of the neutrophil chemokine IL-8 and augments endothelial cell production of IL-8 in response to other stimuli such as lipopolysaccharide (Henriksen et al., 2004b). The observation that HNE stimulates cytokine production from a variety of cell types has raised the possibility of receptor interaction. Devaney *et al* demonstrated that HNE up-regulation of IL-8 mRNA and protein was dependent on expression of the toll-like receptor 4 in a kidney cell line (Devaney et al., 2003). HNE and proteinase-3 also activate the protease activated receptors (PAR) (Uehara et al., 2003, Uehara et al., 2002) that influence a wide range of physiological responses including platelet activation, intimal hyperplasia and the maintenance of vascular tone and barrier function (Leger et al., 2006). Activation of PAR-1, PAR-2 and PAR-4 stimulates IL-6, IL-8 and prostaglandin E2 release (Asokananthan et al., 2002). Selective activation of PAR-1 and PAR-2 by HNE results in increased epithelial permeability and transepithelial migration of neutrophils. This effect is blocked by PAR antagonists and is not related to cleavage of gap junctions (Chin et al., 2008). Recently, HNE has been shown to activate PAR-2 through cleavage of the N-terminus (Ramachandran et al., 2011). This results in selective activation of downstream MAP kinase signaling pathways, and PAR-2 dependent calcium signaling is silenced. This recent observation of interaction with specific cell surface receptors indicates the potential for discriminate signaling by HNE.

1.5 NEUTROPHIL ELASTASE ACTIVITY REGULATION

1.5.1 ENDOGENOUS INHIBITORS

Neutrophil derived elastases have wide ranging inflammatory effects on a broad range of substrates. Endogenous serine protease inhibitors (serpins) block activity by complexing with the elastase molecule. α1-antitrypsin (α1-PI) is the major circulating serpin produced in the liver with inhibitory activity against HNE. α1-PI is present at saturating levels within the circulation providing systemic inhibitory activity against HNE. Elafin and secretory leucocyte protease inhibitor (SLPI) are serpins produced locally at sites of inflammation by epithelial cells in response to inflammatory stimuli such as TNF-α and HNE. The ability to raise this local defence of 'alarm' antiproteases illustrates the extent to which epithelial tissues have evolved mechanisms to respond to, and contain, neutrophil-mediated inflammation (Sallenave, 2000b). Cardiovascular tissues do not express these alarm antiproteases and are more vulnerable to HNE mediated injury as a result.

HNE can evade high local concentrations of inhibitors through a series of mechanisms. Large quantities of oxidants and proteases released by leukocytes recruited to the site of inflammation can overwhelm and inactivate protease inhibitors. Adhesion of neutrophils to the extracellular matrix leads to the compartmentalisation of the released proteases between the neutrophil and matrix, and this microenvironment excludes the large circulating protease inhibitors such as α1-PI (Korkmaz et al., 2005). A large proportion of the serine proteases released from azurophil granules bind to the plasma membrane with catalytic activity preserved. Owen and colleagues suggested that this tight binding of extracellular neutrophil serine proteases to the cell membrane makes them inaccessible, and

therefore resistant, to circulating, high-molecular-weight, endogenous inhibitors such as α1-PI (Owen et al., 1995). Surface bound HNE is inhibited by small molecule inhibitors including SLPI suggesting a specific locale for alarm antiproteases to control HNE (Owen et al., 1995). This local antiprotease shield is not present within the cardiovascular system and strategies to introduce or mimic it will reduce HNE mediated tissue injury and inflammation.

1.5.2 POTENTIAL CLINICAL APPLICATION OF BIOLOGICAL AND SYNTHETIC INHIBITORS OF HNE

Endogenous and synthetic small molecule inhibitors have been developed to combat the pro-inflammatory activity of HNE. Clinical studies with elastase inhibitors have focussed on inflammatory lung disease.

SLPI belongs to the same family of four disulphide core proteins as elafin. It shares many properties including inhibition of HNE and interference with lipopolysaccharide signalling, transcription factor NF-κB activation and TNF-α production. Delivery of recombinant SLPI was protective in rat and murine models of ischaemia reperfusion injury (Lentsch et al., 1999). A clinical study examining the effect of aerosolised SLPI in cystic fibrosis patients demonstrated reduced elastase activity, IL-8 and neutrophil levels in treated patients (McElvaney et al., 1992). α1-PI is regarded as the major inhibitor of HNE in the lung and intravenous formulations derived from human plasma (Prolastin; Talecris Corporation, Aralast; Alpha Therapeutic Corporation and Zemaira; CSL Behring) have been trialled in patients with α1-antitrypsin deficiency with minimal impact on disease progression (Silverman and Sandhaus, 2009). DX-890 (Depelstat; Dyax Corporation/Debiopharm) is a potent HNE inhibitor derived from human inter-α-

inhibitor. It may have application as an aerosol elastase inhibitor in the treatment of cystic fibrosis.

Several synthetic neutrophil elastase inhibitors have been developed. Preclinical studies have shown promise in demonstrating reduced neutrophil elastase injury and inflammation but clinical translation has been frustrated by lack of efficacy and concerns over toxicity. Sivelestat (Ono Pharmaceutical) is a low molecular weight reversible competitive inhibitor of HNE. In observational studies, administration was associated with reduced mortality in critically ill patients and attenuated pulmonary dysfunction in patients with acute respiratory distress syndrome (Hoshi et al., 2005, Okayama et al., 2006). In prospective double-blinded controlled trials, it has been shown to reduce IL-8 production and reduce acute lung injury after cardiopulmonary bypass, and reduce duration of ventilation in intensive care (Ryugo et al., 2006, Tamakuma et al., 2004). The only multi-centre double-blind placebo-controlled trial of sivelestat failed to show a decrease in mortality or reduced ventilator requirement in critically ill patients (Zeiher et al., 2004). ONO-6818 (Ono Pharmaceutical) is a non-peptide selective neutrophil elastase inhibitor that reduced IL-8 production and complement activation in a simulated cardiac bypass circuit (Yoshimura et al., 2003). Clinical studies in patients with lung disease were halted because of liver injury associated with the drug. Mr889 is a less potent, reversible and slow-binding competitive inhibitor of HNE developed by Medea Research. Clinical evaluation demonstrated the drug to be safe but ineffective in modifying biochemical markers of lung destruction (Luisetti et al., 1996).

1.6 MODIFICATION OF INFLAMMATION BY ELAFIN

1.6.1 ELAFIN AS A POTENT ENDOGENOUS INHIBITOR OF NEUTROPHIL ELASTASE

Elafin is an endogenous inhibitor of human neutrophil elastase (HNE) and proteinase-3 that was first isolated from psoriatic skin and human bronchial secretions.(Wiedow et al., 1990, Sallenave and Ryle, 1991b). Cloning of elafin cDNA indicates that initial transcription produces a protein of 117 amino acid residues, which undergoes intracellular cleavage of an N-terminal hydrophobic signal sequence to produce pro-elafin (Molhuizen et al., 1993, Sallenave and Silva, 1993, Schalkwijk et al., 1999). The pro-elafin protein is composed of 2 domains: a C-terminus consisting of 57 amino acids and an N-terminus consisting of 60 amino acids also known as the cementoin domain (Francart et al., 1997, Nara et al., 1994). The N-terminus contains VKGQ sequences that provide the substrate for transglutaminase, with glutamine and lysine acting as acyl donors and acceptors in formation of isopeptide inter-protein cross-links (Nara et al., 1994). Transglutaminisation allows elafin to be cross-linked to the extracellular matrix where it may persist as a tissue bound inhibitor of HNE. Sumi *et al* demonstrated elafin immunoreactivity within the intima of human coronary arteries in association with transglutaminase (Sumi et al., 2002). The C-terminus is responsible for the elastase inhibition. It has a four-disulphide core and shows structural similarity with the whey acidic protein (WAP) family (Nara et al., 1994, Tsunemi et al., 1996). This combination of a transglutaminase substrate area and a WAP/four-disulphide core has similarities with other proteins that have been named “trappins” (Schalkwijk et al., 1999). Elafin has 40% sequence homology with SLPI and is more specific in its spectrum of activity exhibiting potent inhibition of HNE and proteinase-3. It has

equilibrium dissociation constants for these enzymes of 0.8 x 10^{-10} M and 1.2 x 10^{-10} M respectively (Zani et al., 2004).

1.6.2 TISSUE DISTRIBUTION AND REGULATION OF ELAFIN

Elafin is secreted constitutively by the squamous epithelium of the skin, with expression raised in inflammatory skin conditions such as psoriasis (Wiedow et al., 1990, Nara et al., 1994). It has also been isolated in other epithelia such as sweat glands, hair follicles, tongue, tonsils, gingiva, epiglottis, esophageal lining, the vagina, the pharynx (Pfundt et al., 2000), submandibular glands (Lee et al., 2002), trachea, stomach, intestine (Nara et al., 1994), and mammaries (Zhang et al., 1995). More recently leucocyte expression has been identified within human endometrial neutrophils and alveolar macrophages of the respiratory system (King et al., 2003, Sallenave et al., 1993). The detection of elafin within human coronary arteries in association with atherosclerosis raises the question over whether it has originated from infiltrating inflammatory cells or free protein entering from the circulation.

IL-1β and TNF-α together with HNE are major inducers of elafin expression in human airway epithelial cells and keratinocytes (Sallenave et al., 1994, Pfundt et al., 2000). Regulation by these inflammatory cytokines highlights the role elafin may play in the early orchestration of the inflammatory response as an ‘alarm’ antiprotease secreted by local cells.

1.6.3 INHIBITION OF INFLAMMATORY CYTOKINE PRODUCTION

It has been demonstrated that there is attenuated inflammatory cytokine production by human endothelial cells and macrophages following elafin overexpression using adenoviral vectors (Henriksen et al., 2004b). Endothelial cell IL-8 production was reduced in response to bacterial lipopolysaccharide (LPS), TNF-α and oxidised low-density lipoprotein, a key inflammatory stimulus and driver of atherosclerotic plaque development. Overexpression in monocyte-differentiated human macrophages reduced TNF-α production in response to low concentrations of LPS (Henriksen et al., 2004b). SLPI has similar properties reducing TNF-α and matrix metalloprotease production in response to LPS (Jin et al., 1997, Zhu et al., 1999). An intracellular mechanism was suggested by the finding that transfection of a non-secreted form of SLPI but not addition of recombinant SLPI to cultured macrophages suppresses the response to LPS (Zhu et al., 1999). NF-κB upregulates many inflammatory genes associated with the inflammatory response including IL-8 and TNF-α. Overexpression or incubation of elafin and SLPI with monocytes reduces LPS responsiveness (Butler et al., 2006, Henriksen et al., 2004b). This effect is seen in association with reduced proteolytic degradation of NF-κBs' inhibitory subunits IκBα and IκBβ suggesting an action by elafin and SLPI on the ubiquitin-proteosome pathway (Figure 1.2).

Figure 1.2 Elafins' effects on inflammation

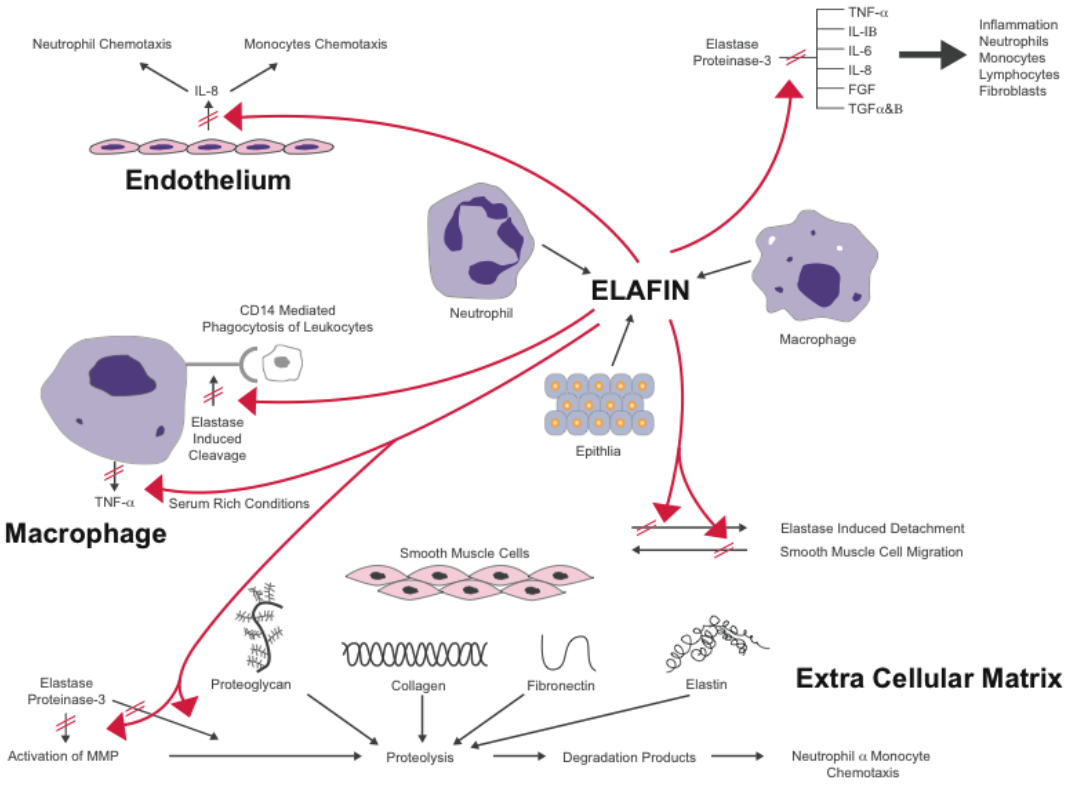

1.7 NEUTROPHIL MEDIATED INJURY AS A POTENTIAL TARGET FOR ATTENUATION OF INFLAMMATION

1.7.1 NEUTROPHIL-MEDIATED ISCHEMIA-REPERFUSION INJURY

The role of the neutrophil in myocardial-reperfusion injury following myocardial infarction has been reviewed by Hansen and Jordan *et al* (Jordan et al., 1999, Hansen, 1995). Cardiomyocyte injury is exacerbated following reperfusion and neutrophils are pivotal mediators determining post-ischemic inflammatory reperfusion injury. Neutrophils accumulate within the reperfused myocardium releasing HNE and reactive oxygen species that further effect microvascular and myocardial injury. Preclinical studies have demonstrated that neutrophil depletion or inhibition of neutrophil elastase attenuates post-ischemic inflammatory reperfusion injury within the myocardium (Romson et al., 1983a, Tiefenbacher et al., 1997).

Plasma HNE and myeloperoxidase concentrations increase following myocardial infarction providing evidence of neutrophil activation (Dinerman and Mehta, 1990, Mocatta et al., 2007). Neutrophils are activated by a vast array of mediators released from endothelial cells, mast cells and myocytes within the myocardium following ischemia. The complement fragment C5a, IL-8 and platelet activating factor act as chemoattractants and stimulate adherence to the endothelium. TNF-α released from mast cells and IL-6 from ischemic cardiomyocytes further stimulate neutrophil superoxide production, transendothelial migration and degranulation (Richter et al., 1990).

Coronary occlusion without reperfusion is associated with infarction and restricted infiltration of neutrophils into the border area of the infarcted zone over 24 hours (Reimer et al., 1989). The goal of therapy in acute myocardial infarction is timely

restoration of perfusion and whereas this reduces infarct size, it is associated with accelerated accumulation of neutrophils within the reperfused myocardium (Dreyer et al., 1991, Zhao et al., 2001). Neutrophil adhesion to the endothelium occurs within minutes of reperfusion (Sheridan et al., 1996, Murohara et al., 1994). Release of proteases and reactive oxygen species cause cardiomyocyte necrosis. Neutrophils also occlude microvessels and cause changes in endothelial permeability that contribute to myocardial oedema (Engler et al., 1983). Capillary plugging and obstruction by activated neutrophils contributes to failure of microvascular perfusion and increased infarct size within the "no-reflow" zone. Neutrophil depletion reduced this phenomenon and infarct size in a pre-clinical model (Litt et al., 1989). Neutrophil mediated inflammation generates production of further chemokines and adhesion molecule expression that amplify inflammatory cell recruitment. The goal of therapy is both to reduce neutrophil-mediated injury and to break the vicious cycle of further neutrophil recruitment.

Administration or over-expression of elafin was associated with reduced infarct size and neutrophil infiltration in several models of ischemia-reperfusion injury. Tiefenbacher *et al* investigated cardiac reperfusion injury in a rat model inducing repeated ischemia and reperfusion with ligation of the left coronary artery (Tiefenbacher et al., 1997). The animal received a bolus of recombinant elafin by tail vein injection prior to ischemia. Myocardial function measured by systolic fractional thickening was better in animals receiving elafin or a synthetic elastase inhibitor. Systolic fractional thickening of the myocardium measured by pulsed Doppler was reduced by 50% in the controls compared to 22% in elafin treated animals. Mice expressing human elafin under the control of the preproendothelin promoter exhibit better cardiac function compared to littermates following myocardial infarction. Left

ventricular dimensions in diastole were significantly increased in the wild-type mice (mean 4.75 mm) compared to sham operated mice (mean 3.95 mm). Elafin expressing mice had some increase in cavity size (mean 4.30 mm), which was not significantly different from sham operated mice. Elafin expressing mice had reduced infarct expansion and less scar thinning. The increases in myocardial tissue elastase and matrix metalloprotease activity following infarction were effectively suppressed in elafin transgenic animals compared to wild type littermates (Ohta et al., 2004b). Tissue myeloperoxidase content can be used as a measure of neutrophil infiltration. In the rat myocardial infarction model myeloperoxidase levels increased 14-fold in control animals compared to only a 3-fold rise in elafin treated animals (Tiefenbacher et al., 1997). Similar reductions in neutrophil infiltration were observed in the elafin transgenic mice and following elafin administration prior to arterial ligation in a rodent limb ischemia model (Crinnion et al., 1994). In the latter study, elafin attenuated the acceleration in neutrophil infiltration (myeloperoxidase content) following reperfusion and was associated with reduced myocyte necrosis.

Elafin administration or overexpression was consistently associated with reduced myocyte death and preserved function following ischemia and reperfusion across different models. The reduction in neutrophil infiltration suggests that elafin interrupts the positive feedback loop signaling further neutrophil recruitment during reperfusion. This may be through combined direct inhibitory action on HNE and proteinase 3 mediated tissue injury and suppression of the potent neutrophil chemokine IL-8.

1.8 THERAPEUTIC APPLICATION OF ELAFIN IN CARDIOVASCULAR DISEASE

Elafin augmentation protects the cardiovascular system from a range of diseases characterized by neutrophil-mediated inflammation (Figure 1.3). Elafin provides the endothelium and myocardium with protection against the damaging effects of neutrophil-derived elastases. This suggests that intravenous elafin administration or gene overexpression can provide inhibition by reaching elastase enzyme that is not suppressed by the high circulating concentrations of larger molecular weight elastase inhibitors. Elafin attenuates disease progression in chronic injury models including atherosclerosis and pulmonary hypertension (Zaidi et al., 2002b) and provides survival benefit in a murine model of viral myocarditis (Zaidi et al., 1999). The neutrophil does not have a prominent role in these pathologies indicating alternative mechanisms for elafin's effect beyond inhibition of elastase through suppressing NF-κB activation or modulating the adaptive immune response. Recombinant elafin has very low toxicity with short plasma and activity half-lives. It is possible to maintain circulating activity with intravenous infusion and this approach is used routinely with antithrombotic drugs in acute coronary syndrome patients. Translating the efficacy of elafin in pre-clinical models to diseases, such as acute myocardial infarction, will depend on achieving adequate concentrations of active protein at the site of tissue injury. In most pre-clinical models, elafin is delivered before or at the point of vascular injury. This advantageous position is not generally feasible in the clinic. The complexities of human disease over animal models have seen many promising therapies for ischemia reperfusion fail at translation (Bolli et al., 2004).

Figure 1.3 Elafins' effects on cardiovascular pathologies.

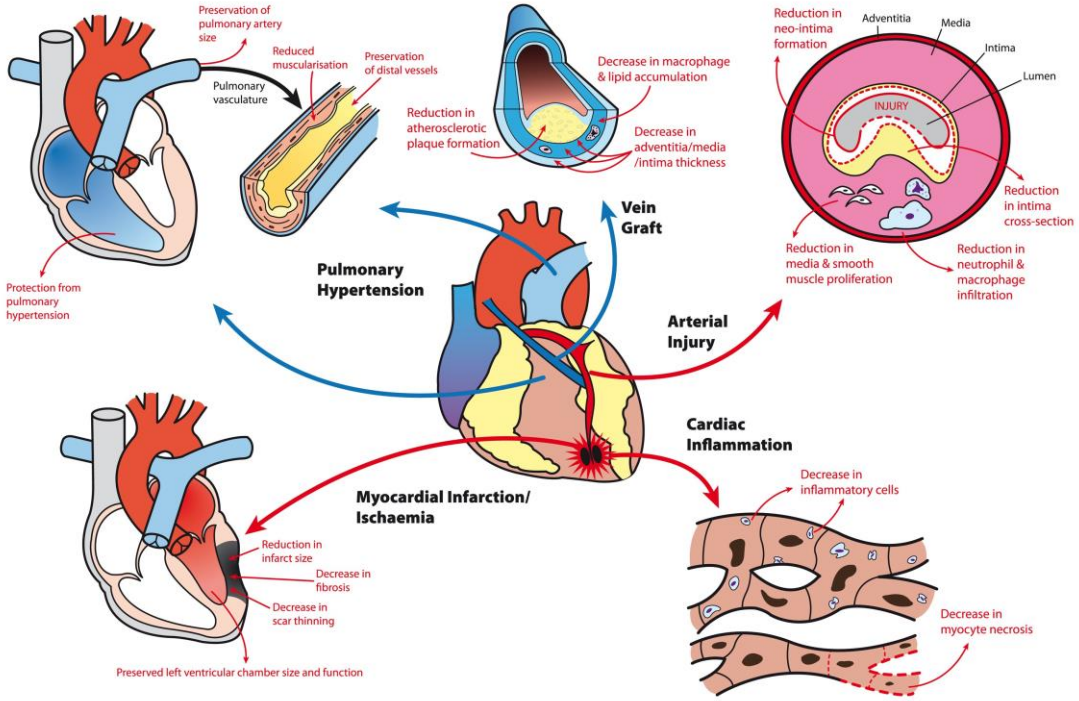

1.9 MAGNETIC RESONANCE IMAGING OF THE MYOCARDIUM

Magnetic resonance imaging (MRI) is a well-established clinical imaging modality offering excellent soft tissue contrast and spatial resolution, whilst avoiding ionizing radiation. Standard gadolinium-based contrast agents are paramagnetic and are infused into the blood pool with variable organ extraction rates, although subsequent extravasation and redistribution can be used to identify the interstitial and extracellular spaces. Gadolinium is commonly used as an MRI contrast agent after acute myocardial infarction (MI) to identify areas of tissue infarction and fibrosis (Lima et al., 1995, Schelbert et al., 2010). Tissue oedema and rupture of cell membranes with consequent diffusion of gadolinium into the inter- and intra-cellular spaces (Lima et al., 1995) results in a "delayed gadolinium enhancement" effect in infarcted regions. This is also known as late gadolinium enhancement (LGE). Recent interest has turned to novel agents that provide additional structural and functional cellular information. Such 'smart' contrast agents include iron oxide nanoparticles.

1.10 IMAGING INFLAMMATION USING ULTRASMALL SUPERPARAMAGNETIC PARTICLES OF IRON OXIDE

Particles of iron oxide are divided into classes based on their size (Table 1-1). Ultrasmall superparamagnetic particles of iron oxide (USPIOs) consist of nanoparticles with a diameter of <50 nm and include ferumoxtran-10 (Sinerem, Guerbet) and ferumoxytol (Rienso, Takeda; Feraheme, AMAG Pharmaceuticals). USPIOs can be used as a blood pool contrast agent but it is their ability to be taken up by inflammatory cells that has distinguished them (Christen et al., 2012). Cellular uptake of USPIOs occurs through a variety of mechanisms. Phagocytosis and receptor-mediated endocytosis are important for uptake of larger particles, whilst smaller particles are internalized by pinocytosis. Although the avidity of macrophage uptake is strongly influenced by particle size and charge, the surface coating is particularly important (Saito et al., 2012, Tsuchiya et al., 2013). As a result of their smaller size, USPIOs are less readily recognized by phagocytic cells and persist in the circulation for longer than other iron particles (plasma half-life 14-30 h in humans) (Landry et al., 2005, Hunt et al., 2005). They are capable of passing through capillary walls, to be taken up by tissue-resident macrophages and neutrophils (Ruehm et al., 2001b, Dousset et al., 1999, Gellissen et al., 1999a). These characteristics allow USPIOs to detect and highlight cellular inflammation within tissues using MRI.

Table 1-1 Iron oxide nanoparticle preparations

Particle	Size (Diameter)	Plasma Half-life (h)	Application
Microparticles of iron oxide (MPIOs)	1 μm	1-2 min	Readily endocytosed and detected with MRI (Shapiro et al., 2005b). Need immediate scan following infusion. Can be combined with ligands for cellular targets allowing molecular imaging (McAteer et al., 2011). Large size means they remain in the blood pool and are suitable for endovascular imaging t (Yang et al., 2010).
Superparamagnetic particles of iron oxide (SPIOs)	80-150 nm	2-3 h	Ferumoxide (Endorem, Guerbet, France) and ferucarbotran (Resovist, Bayer-Schering Pharma, Germany). Recognised by cells of the reticuloendothelial system. Have been used for oncological imaging including liver studies where they are taken up by Kuppfer cells in normal tumour-free liver .(Margolis et al., 2007) Mesenchymal stem cell, monocyte/macrophage labelling (Richards et al., 2012a).
Ultrasmall SPIO (USPIOs)	<50 nm	Ferumxytol: 9-15 h Ferumoxtran -10: 25-30 h	Ferumoxtran-10 (Sinerem, Guerbet, France) and ferumoxytol (Rienso, Takeda, United Kingdom).
Very small superparamagnetic iron oxide particles (VSOPs)	<10 nm	1 h	Alternative blood pool agents with longer circulating half-life than gadolinium based agents (Schnorr et al., 2012, Wagner et al., 2011). Potential as cell tracking agents (Ludwig et al., 2013).

Figure 1.4 USPIO concentrating in lysosome in macrophage.

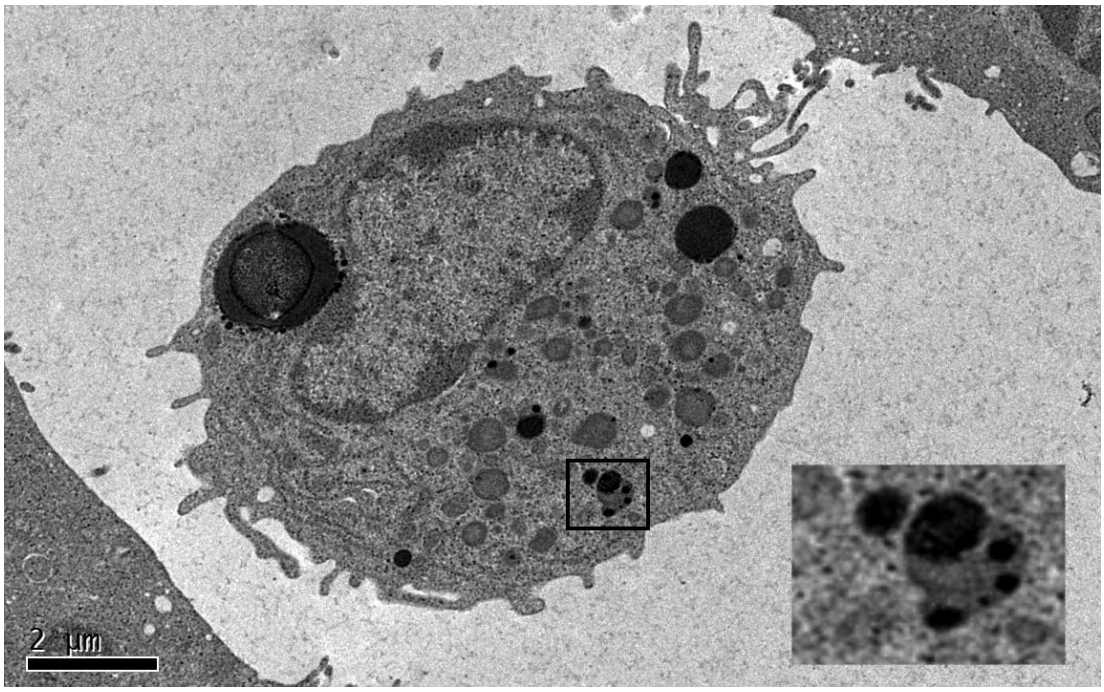

Image from animal study, see “Nanoparticle enhanced MRI scanning to detect cellular inflammation in experimental chronic renal allograft rejection” in 6.1.1.1.1.1.1.1Appendix G: (page 505).

1.10.1 IMAGING METHODOLOGY

USPIOs induce local magnetic field inhomogeneities that shorten T2 and T2* relaxations times resulting in a signal deficit on magnetic resonance images. USPIOs also have a T1 shortening effect, particularly at low concentrations, and appear bright on T1 weighted images.

A range of approaches have been used to evaluate USPIO accumulation in tissues. Most simply, images may be qualitatively assessed for signal deficits. However this approach is subjective, and signal deficits due to calcification or other artefacts may be misinterpreted. Manually drawn regions of interest have been used to allow comparison of signal intensity of the target tissue with that of control tissue although discrete focal areas of USPIO accumulation, and thus focal inflammation, may be missed.

Tissue properties, such as the presence of oedema or haemorrhage, can alter image intensities on T2* sequences, and so pre- and post-contrast images need to be compared to delineate the impact of USPIO accumulation. This requires accurate co-registration of these paired scans and adjustments for differences in baseline intensity. A specific region of interest (ROI) map can be drawn and subsequently transferred to each subsequent co-registered image, thus ensuring the signal intensity can be compared for identical sample regions in different scans from the same patient.

Rather than assessing focal image brightness at a single echo time, the T2* time constant can be calculated from the exponential decay curve using multiple echo times (Figure 1.5). This method provides greater reproducibility, broad applicability throughout the field of view, and independence from T1 effects and a range of imaging variables. In the presence of USPIO, the T2* relaxation rate is increased

thus giving a lower T2* value, or higher R2* value (R2* is the inverse of T2*, R2* = 1/T2*). Calculation of these values permits the generation of T2* or R2* maps indicative of USPIO accumulation (Figure 1.6).

Figure 1.5 Creation of T2* map from multiple echo times.

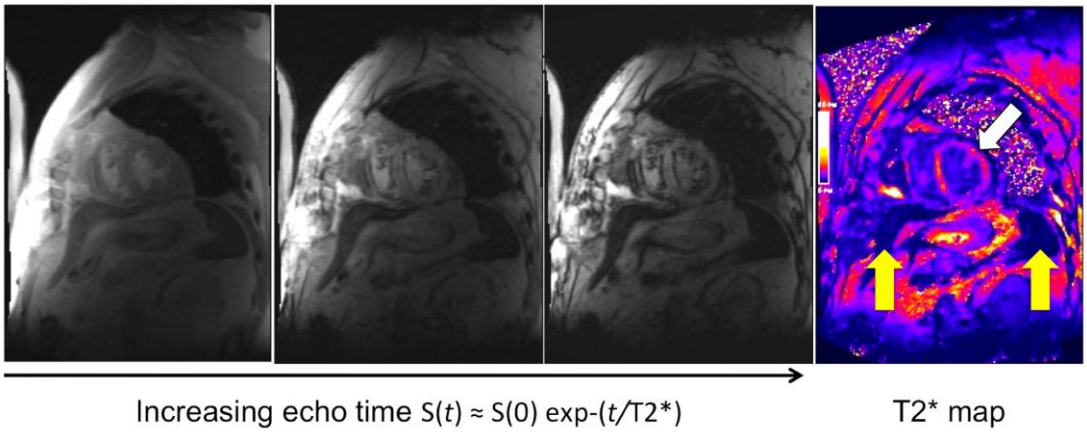

Figure 1.6 T2* decay curve and time constant with and without USPIO.

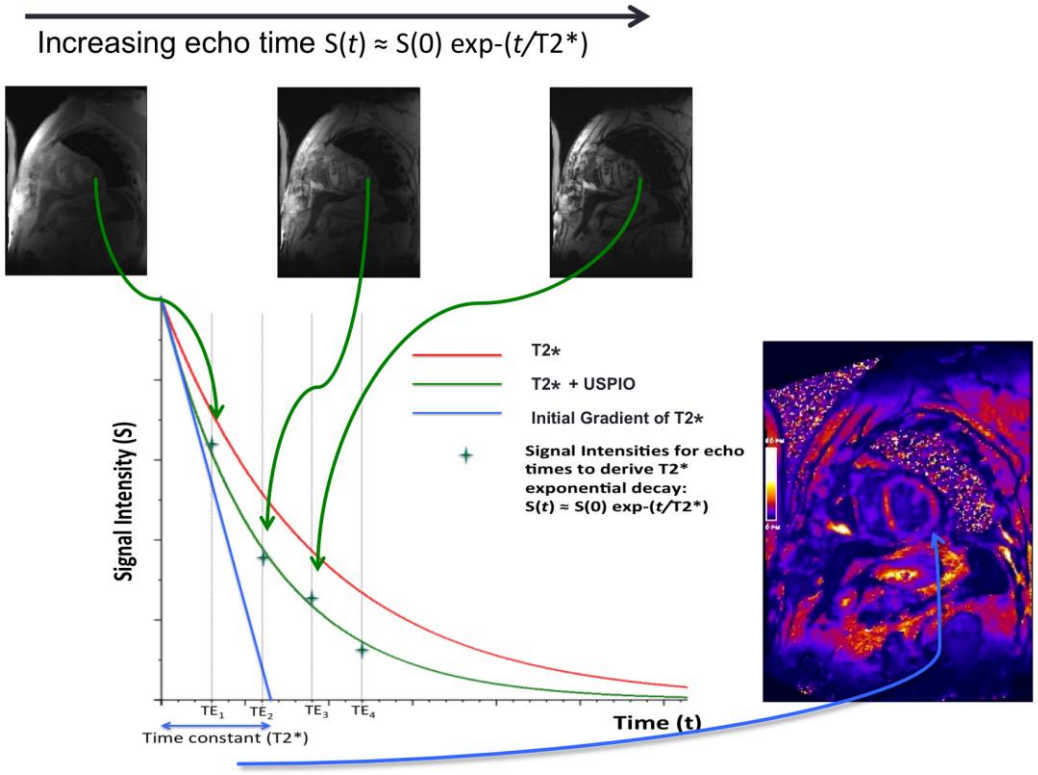

Various authors have used different techniques to calculate USPIO uptake in tissues, and have reported results using T2, T2* or R2*. This can cause confusion since higher values infer diminished USPIO uptake in T2/T2* weighted images, but higher uptake in R2* maps. Therefore for simplicity, imaging techniques can be described but results reported in terms of "increased USPIO uptake", or increased R2* value (indicating increased USPIO uptake). In order to account for native R2* values, various authors have used the delta increase in R2* value from successive scans, or factor increase. When pre-USPIO scans have not been performed, it must be assumed that non-inflamed tissue has similar R2* values to pre-USPIO native R2* values.

Finally, it must be noted that USPIO also shorten T1, and so cause signal enhancement of T1 weighted imaging (Small et al., 1993). However, at high concentration USPIO can cause signal loss with such imaging limiting its use with T1 weighted sequences (Fananapazir et al., 2014).

1.10.2 Assessing myocardial inflammation.

The USPIO NC100150 (Clariscan; Nycomed Imaging, Oslo, Norway) has been evaluated as a blood pool contrast agent in a porcine model of MI, and does identify areas of non-perfused myocardium (Bjerner et al., 2000). This agent was again studied as a blood pool agent in a rodent model of reperfusion after MI (Krombach et al., 2002). USPIO T1-weighted hyper-enhancement was larger than the area of infarction after reperfusion, but was smaller than the area at risk. Thus UPSIO seemed to estimate the spatial extent of microvascular injury, with associated leakage into the extravascular space.

Monocytes infiltrate the myocardium following infarction or reperfusion injury, and differentiate into macrophages as described above. They are initially involved in a pro-inflammatory response, whereas monocytes arriving later promote reparative processes (Nahrendorf et al., 2007a). Non-invasive imaging using USPIO enhancement may provide insights into the dynamics of inflammatory cell recruitment in the peri-infarct region, and is ideally suited to evaluate future therapies aimed at modifying the inflammatory process.

Several rodent models of MI have demonstrated excellent histological co-localisation of USPIOs with macrophages within infarcted myocardium (Montet-Abou et al., 2010). Moreover anti-inflammatory interventions reduce USPIO uptake within the infarct zone and this corresponds to lower macrophage infiltration on histology. Thus USPIO-enhanced MRI tracks myocardial inflammation following MI and can be used to assess response to therapeutic intervention.

Allograft rejection is a potential complication of cardiac transplantation with patients requiring life-long monitoring including invasive cardiac biopsy. It is a condition where myocardial inflammation causes significant clinical injury. During transplant rejection, antigen presenting cells stimulate lymphocytes to release cytokines that recruit and activate macrophages that are the main effector cells (Suzuki et al., 2010). Macrophage and monocyte infiltration correlate with rejection in biopsies from cardiac transplant recipients (Lones et al., 1995). Rodents with allografts undergoing rejection exhibit large USPIO uptake in the myocardium, with rodents treated with anti-rejection treatment exhibiting an intermediate reduction in uptake (Penno et al., 2007). This is mirrored by myocardial macrophage count that is largest in the allograft group, reduced in the treatment group and smallest in controls. Indeed,

higher USPIO accumulation is identified with increasing rejection grade (Wu et al., 2009). USPIO-enhanced MRI indicates a heterogeneous distribution of the inflammatory change throughout the myocardium. This underlines the limitations of single-site endomyocardial biopsy, widely regarded as the gold standard for diagnosing rejection. USPIO-enhanced MRI may therefore prove to be a more sensitive method to monitor graft status with the additional advantage that it is non-invasive. However translational studies in man are now awaited.

1.11 SUMMARY

Inflammation occurs following acute myocardial infarction due to ischaemic-reperfusion injury. Inflammation within the infarcted myocardium is associated with induction of endothelial adhesion molecules and enhanced permeability of the microvasculature. Up regulation of chemokines including interleukin (IL)-8 and monocyte chemoattractant protein (MCP)-1 attracts neutrophils and monocytes to the site of injury. Recruitment of monocytes into the infarcted myocardium is followed by maturation and differentiation into macrophages: a process dependent on growth factors such as macrophage-colony stimulating factor (M-CSF). Early reperfusion therapy amplifies this inflammatory cell influx and accelerates the healing response through proliferative and maturation phases.

During coronary artery bypass graft (CABG) surgery and cardiopulmonary bypass, coronary blood flow is interrupted and the heart is put into circulatory arrest. This also causes ischemia-reperfusion injury. This is exacerbated by adverse neutrophil-mediated myocardial inflammation and injury (Vinten-Johansen, 2004, Butler et al., 1993, Wakayama et al., 2007). CABG surgery therefore represents a programmed clinical model of ischemia-reperfusion injury that lends itself to testing the efficacy of potential therapeutic interventions (Hausenloy et al., 2007).

Iron oxide particles can be used as a contrast medium in magnetic resonance imaging since they alter the T2* relaxation time of tissues in which they accumulate. Ultrasmall superparamagnetic particles of iron oxide (USPIO) are taken up by cells of the liver, spleen, bone marrow and lymph nodes. As a result of their small size (approximately 30 nm) they extravasate freely through capillaries and are phagocytosed by tissue-resident inflammatory cells of the reticuloendothelial system (Ruehm et al., 2001b). These cells are predominately macrophages (Dousset et al.,

1999, Gellissen et al., 1999a). T2*-weighted MRI has been validated as a method of detecting hepatic and myocardial iron accumulation in patients with thalassemia and transfusion-related iron overload. This method could be adapted for the detection of focal USPIO accumulation (Anderson et al., 2001, Westwood et al., 2005), and thus assess myocardial inflammation in the myocardium.

Elafin is an endogenous anti-inflammatory protein that was first isolated in the search for inhibitors of neutrophil elastase activity in the lung and skin (Sallenave and Ryle, 1991a, Wiedow et al., 1991). It has inhibitory activity against both human neutrophil elastase and proteinase-3 as well as suppressing production of inflammatory cytokines such as interleukin-8 (IL-8) and tumor necrosis factor alpha (TNF-α) (Henriksen et al., 2004b). Elafin is produced locally at sites of inflammation, raising a local defence of 'alarm' antiproteases in order to contain and inhibit neutrophil-mediated inflammation (Sallenave, 2000a). Cardiovascular tissues do not express elafin or other neutrophil elastase inhibitors, and are therefore more vulnerable to neutrophil-mediated injury. Elafin augmentation therefore may protect the cardiovascular system from a range of conditions characterized by neutrophil elastase-mediated inflammation and injury.

1.12 AIM AND HYPOTHESES

The aim of this thesis is firstly to perform a proof-of-concept study to investigate the feasibility of using USPIO enhanced cardiac MRI to identify and assess myocardial cellular inflammation. This technique will then be utilised in conjunction with blood and conventional MRI markers of inflammation and injury to assess the impact of anti-inflammatory Elafin in a randomised controlled trial of patients undergoing coronary artery bypass surgery. The detailed characterisation of myocardial injury occurring during CABG surgery provided by this study will be used to assess the performance of the current universal definition of Type V myocardial infarction.

The following novel hypothesis will be addressed:

1. Changes in R2* in USPIO enhanced MRI scans will detect cellular inflammation post myocardial infarction.
2. Myocardial injury post coronary artery bypass surgery can be assessed with blood markers of inflammation and infarction.
3. Elafin, the neutrophil elastase inhibitor, can modify post coronary artery bypass surgery myocardial injury and inflammation
4. Cellular inflammation post coronary artery bypass surgery can be detected and assessed using USPIO enhanced MRI scanning.

Chapter 2: METHODS

2.1 ETHICAL AND REGULATORY CONSIDERATIONS

The studies were undertaken with the approval of the Scotland A Research Ethics Committee and Lothian Local Research Ethics Committee 03 (REC 10/S1 103/50), who approved the use of the MRI contrast agent ferumoxytol (Feraheme, AMAG Pharmaceuticals) to investigate patients.

The Elafin Myocardial Protection from Ischemia Reperfusion (EMPIRE) randomised controlled clinical trial was performed with the approval of the national research ethics committee (11/MRE00/5), under a Clinical Trial Authorization (27586/0015/001-0001) from the Medicine and Healthcare products Regulatory Authority (MHRA, United Kingdom). The Medicines and Healthcare Products Regulatory Agency (MHRA) approved the use of the MRI contrast agent ferumoxytol (Rienso, Takeda; Feraheme, AMAG Pharmaceuticals) to investigate patients. All studies were conducted in accordance with the Declaration of Helsinki.

2.2 SUBJECT RECRUITMENT

All participants gave written informed consent before participating in the study. An information sheet was provided and participants' general practitioners were informed in writing (Appendix C: page 320).

2.2.1 PATIENTS WITH MYOCARDIAL INFARCTION

Patients who had suffered an acute ST-elevation myocardial infarction were approached to take part in the proof of concept study investigating if USPIO could detect myocardial cellular inflammation. Patients were identified in the coronary care unit at the Royal Infirmary of Edinburgh. Inclusion criteria were age 18-80 years, recent (within 48 hours) myocardial infarction defined by the universal definition of myocardial infarction and plasma troponin I concentration in excess of 10 μg/L at 12 hours from the onset of chest pain (Thygesen et al., 2007a). Exclusion criteria were known critical stenosis (≥95%) of left main stem, ongoing symptoms of unstable angina, atrial fibrillation, heart failure (Killip class ≥II), hepatic failure (Childs-Pugh grade B or C) or renal failure (estimated glomerular filtration rate <25 mL/min), contraindication to magnetic resonance imaging, past history of systemic iron overload or hemochromatosis, and patients with known allergy to dextran- or iron-containing compounds.

2.2.2 HEALTHY VOLUNTEERS

Healthy volunteers (aged >18 years) were recruited by local advertisement through the Edinburgh Heart Centre. Volunteers were excluded from participation in the study on the same criteria outlined in section 2.2.1.

2.2.3 PATIENTS UNDERGOING CORONARY ARTERY BYPASS SURGERY: THE EMPIRE STUDY

The Elafin Myocardial Protection from Ischemia RepErfusion injury (EMPIRE) study examined the effect of Elafin, an endogenous neutrophil elastase inhibitor on myocardial injury occurring during coronary artery bypass surgery. The full study protocol is attached in 5.1.1.1.1.1.1.1Appendix D: (page 373). Consecutive patients referred for elective CABG surgery were recruited from two clinics at Edinburgh Heart Centre. Patients were 18 years or older, and were referred for isolated CABG surgery requiring 2 or more grafts. Exclusion criteria included patients with recent myocardial infarction (within 1 month of surgery), emergency or concomitant valve surgery, significant renal impairment (estimated glomerular filtration rate <40 mL/min), severe respiratory disease (maintenance corticosteroid therapy or forced expiratory volume in one second <50% predicted), severe left ventricular impairment (ejection fraction <40%), contraindication to magnetic resonance scanning, treatment for chronic inflammatory disease, women of child-bearing potential and inability to provide consent. For analysis of USPIO uptake in the myocardium, patients who had evidence of acute graft or coronary artery occlusion peri-operatively were excluded since this would not be representative of standard patients undergoing CABG surgery.

All participants gave written informed consent before participating in the study. An information sheet was provided and participants' general practitioners were informed in writing (5.1.1.1.1.1.1.1Appendix D: page 362).

2.3 BLOOD SAMPLING AND TESTING

2.3.1 VENEPUNCTURE

Venesection was performed on a peripheral vein using standard aseptic technique. Whole venous blood (up to 240 mL) was obtained from a vein in the antecubital fossa using a 17-21 gauge needle. In the post-operative period, an arterial or centrally placed cannula was available for blood sampling.

2.3.2 ASSAYS

The prototype ARCHITECT *STAT* high sensitive Troponin-I (TnI) assay (Abbott Diagnostics, Abbott Park, IL) is a two-step assay in which plasma TnI is bound by an anti-TnI antibody (amino acids 24-40)-coated paramagnetic microparticles and then sandwiched with an acridinium-labeled anti-TnI antibody (amino acids 41-49). The limit of detection and limit of quantification are 1.0 and 4.1 pg/mL respectively. The mean±SD of an apparently healthy population (n=300) is 1.58±3.07 pg/mL and the 99th percentile was determined to be 16.8 pg/mL with the 10% co-efficient of varation (CV) determined as <5.5 pg/mL. Within run, between run, between day and total precision (CV) ranged respectively from 1.9-6.2%, 0.0-4.2%, 0.0-3.2% and 2.4-7.0%. The age specific 99th centile upper reference limit (URL) were 34 ng/L (men) and 16 ng/L (women) (Shah et al., 2015c).

Plasma concentrations of high-sensitive C-reactive protein (hsCRP), interleukin (IL)-6, IL-8, myeloperoxidase and elastase were quantified using enzyme-linked immunosorbant assays (ELISAs; R&D Systems, U.K.; Elastase ELISA, Cambridge Biosciences, U.K.). Plasma elastase activity and serum Elafin concentrations were measured by the Department of Dermatology, University of Kiel, Germany. Samples of plasma for Elafin concentration and elastase activity were sent to Proteo Biotech

AG for analysis. The quantification method was propriety information, therefore validation data was not available. However, Elafin concentration and elastase activity were not used for primary and secondary endpoints nor post hoc analysis.

2.4 ELAFIN

2.4.1 STUDY DRUG IDENTIFICATION

Elafin CAS number: 820211-82-3. "Recombinant human Elafin" is produced in yeast with a structure identical to the 57 amino acid human form and with 95% purity. It was prepared and infused as aqueous solution in 0.9% saline.

Amino acid sequence (SwissProt accession number: P19957):

Ala-Gln-Glu-Pro-Val-Lys-Gly-Pro-Val-Ser-Thr-Lys-Pro-Gly-Ser-Cys-Pro-Ile-Ile-Leu-Ile-Arg-Cys-Ala-Met-Leu-Asn-Pro-Pro-Asn-Arg-Cys-Leu-Lys-Asp-Thr-Asp-Cys-Pro-Gly-Ile-Lys-Lys-Cys-Cys-Glu-Gly-Ser-Cys-Gly-Met-Ala-Cys-Phe-Val-Pro-Gln

2.4.2 STUDY DRUG MANUFACTURER

Elafin, the investigational medicinal product, was manufactured, packaged and labelled by Eurogentac S.A. (Biologics, Liege Science Park, 4102 Seraing, Belgium) as a subcontractor of Proteo Biotech AG in accordance with Good Manufacturing Practice (GMP) guidelines.

2.4.3 LABELLING

The pharmacy department at the Royal Infirmary of Edinburgh and the research nurses within the Welcome Trust Clinical Research Facility shared the responsibility for the preparation of 200 mg of Elafin in 250 mL of 0.9% saline or matched placebo 0.9% saline solution, as well as labelling the infusion for blinding the study to investigators and participants.

2.4.4 STORAGE

The study drug was kept in the pharmacy department as per product label.

2.4.5 STUDY DRUG PREPERATION AND ADMINISTRATION

Intravenous recombinant human Elafin (Proteo Biotech AG, Germany) 200 mg was prepared and infused as aqueous solution of 250 mL 0.9% saline.

Intravenous Elafin 200 mg causes complete inhibition of plasma elastase activity for 2 hours and >50% inhibition for 8 hours (Bellemare et al., 2008). This dosage regime was selected to cover the increased elastase activity following CABG that peaks at the time of weaning from cardiopulmonary bypass and has returned to baseline by 6-7 hours. The study drug was administered to the patient through a central venous cannula over a period of 30 minutes. The intravenous infusion was started at first skin incision and completed at least 20 minutes before cardiopulmonary bypass commenced.

2.4.6 RANDOMISATION

Patients were randomised (1:1) to receive Elafin or matched placebo by Edinburgh Clinical Trials Unit to ensure allocation concealment. No member of the clinical team or research team had randomisation information. Subsequent clinical management and trial protocol investigation were identical. Communication of randomisation to the pharmacy department was web-based.

The minimisation technique incorporated the following binary criteria:

- Age; ≥ 65 or < 65 years
- Sex; male or female
- Diabetes Mellitus; present or absent
- Extent of coronary artery disease; 2 or 3 vessel coronary disease
- Estimated glomerular filtration rate (eGFR mL/min); 40- 59 or ≥60
- Surgeon; Surgeon 1 or Surgeon 2

2.5 PLACEBO

Placebo consisted of 250 mL of 0.9% saline. Identical to the study drug, this was administered to the patient through a central venous cannula over a period of 30 minutes. The intravenous infusion was started at first skin incision and completed at least 20 minutes before cardiopulmonary bypass commenced.

2.6 PARTICIPANT COMPLIANCE

Responsibility for infusion was with the anaesthetic team. Timing and dose was noted on anaesthetic chart as per usual clinical practice. This information was entered into the study database.

2.7 OVERDOSE

From previous studies, a dose of 400 mg was not associated with any relevant safety concerns. The only side effects of nausea and headache were attributed to the investigational procedure. The study drug infusion was prepared with no other source of Elafin being available for clinicians or the research team to administer additional amounts. Therefore each patient did not receive more than 200 mg of Elafin.

2.8 ADDITIONAL OUTCOMES

The following data was collected as expected events in the care of patients post coronary bypass surgery, but not reported as adverse events related to the study. They were included in the primary or secondary end point analysis.

Postoperative complications related to coronary artery bypass surgery between 0 (time of first skin incision) and 48 hours including;

- Wound infection; sternotomy and vein harvest sites
- Respiratory complications; chest infection, pleural effusion requiring drainage
- Administration of antibiotics for any infection
- Atrial fibrillation (sustained for more than 5 minutes)
- Stroke
- Renal function measured by creatinine/GFR
- Low cardiac output syndrome and inotrope requirement
- Red blood cell transfusion
- Re-operation for bleeding

Death was reported as a serious complication of CABG surgery, and registered as an adverse event.

The patient was quoted an individualised risk of these complications within the cardiothoracic surgery using the Euroscore algorithm (Nashef et al., 1999).

2.9 CARDIAC MAGNETIC RESONANCE

2.9.1 CONTRAST AGENTS - GADOLINIUM

Gadolinium is commonly used as an MRI contrast agent after acute myocardial infarction (MI) to identify areas of tissue infarction and fibrosis (Lima et al., 1995, Schelbert et al., 2010). Tissue oedema and rupture of cell membranes with consequent diffusion of gadolinium into the inter- and intra-cellular spaces (Lima et al., 1995) results in a "delayed gadolinium enhancement" effect in infarcted regions. Intravenous administration of gadolinium contrast agent (0.1 mmol/kg; Gadovist, Bayer Plc, Germany) was used to quantify infarct mass.

2.9.2 CONTRAST AGENTS - ULTRASMALL SUPERPARAMAGNETIC PARTICLES OF IRON OXIDE

Ultrasmall superparamagnetic particles of iron oxide (USPIOs) consist of nanoparticles with a diameter of <50 nm. USPIOs can be used as a blood pool contrast agent but it is their ability to be taken up by inflammatory cells that has distinguished them (Christen et al., 2012). Ferumoxytol (Rienso, Takeda; Feraheme, AMAG Pharmaceuticals) was used to investigate inflammatory cell infiltration of the myocardium. Each vial contained 510 mg of elemental iron in 17 mL (30 mg/mL).

2.9.3 IMAGING METHODOLOGY

USPIOs induce local magnetic field inhomogeneities that shorten T2 and T2* relaxation times resulting in a signal deficit on magnetic resonance images. USPIOs

also have a T1 shortening effect, particularly at low concentrations, and appear bright on T1 weighted images.

Manually drawn regions of interest were used to quantify USPIO uptake in areas of interest, such as the infarct zone. Pan-myocardial USPIO uptake was assessed by creating regions of interest covering the entire heart. Specific methods are detailed below.

Tissue properties, such as the presence of oedema or haemorrhage, can alter image intensities on T2* sequences, and so pre- and post-contrast images were used to delineate the impact of USPIO accumulation. This required accurate co-registration of these paired scans. A specific region of interest (ROI) map was drawn and transferred to each subsequent co-registered image, thus ensuring accurate comparison of identical sample regions in different scans from the same patient.

The T2* time constant was calculated from the exponential decay curve using multiple echo times. In the presence of USPIO, the T2* relaxation rate is increased thus giving a lower T2* value, or higher R2* value (R2* is the inverse of T2*, R2* = 1/T2* and represents the rate constant). Calculation of these values permits the generation of T2* or R2* maps indicative of USPIO accumulation. R2* maps and values were used since the higher the USPIO accumulation, the higher the R2* value. In order to account for native R2* values, we used the delta increase in R2* value from successive scans.

2.9.4 CINE AND LATE ENHANCEMENT IMAGING

Magnetic resonance imaging was performed using a combination of body matrix and spine coil matrix coil elements of a 3-Tesla Verio scanner (Siemens Medical, Germany). Standard cardiac breath-held ECG-gated true-FISP sequences were used to acquire vertical long axis, horizontal long axis and short axis views of the heart to determine cardiac ejection fraction and mass.

Breath-held inversion recovery sequences in the short-axis, and horizontal and vertical long-axis planes were used to acquire late enhancement images 10-15 min following an intravenous administration of gadolinium contrast agent (0.1 mmol/kg; Gadovist, Bayer Plc, Germany). Optimal TI was determined on a slice-by-slice basis using standard late enhancement protocols. The inversion recovery late enhancement short axis slices were acquired with the same slice position as the short axis T2*-weighted slices (see below).

2.9.5 USPIO SCANNING PROTOCOL

USPIO imaging was performed using established T2*-weighted multi-gradient-echo sequences, breath-held and cardiac-gated after a volumetric shim had been applied over the entire heart volume. Standard cardiac slice width (6 mm width with 4 mm gap) and echo times (2.1-17.1 ms range) with matrix size of 256x115. The in-plane resolution differed as required for larger or smaller objects, generally a field of view of 400x300 was used with an in-plane resolution of 2.6x1.6. Quantitative analysis of USPIO accumulation was achieved by calculation of T2* relaxation times before and after administration of USPIO.(Richards et al., 2011a). In order to optimise image analysis and prevent degradation due to “T2*-blooming” artefacts, USPIO images

were quantitatively analysed using a susceptibility gradient mapping post-processing technique previously used in SPIO imaging to quantitate USPIO accumulation using changes in calculated T2* relaxation times (Dahnke et al., 2008).

The inversion recovery late enhancement short axis slices were acquired with the same slice position as the short axis T2*-weighted slices. The T2*-weighted short-axis acquisitions included views of abdominal organs including through the liver and spleen, and allowed quantification of USPIO uptake within the reticuloendothelial system via changes in these tissues' R2* value.

2.9.6 Timing Of USPIO MRI Scans

Each patient underwent baseline cardiac magnetic resonance imaging, and USPIO was infused immediately after. USPIO enhanced scan were performed as closed to 24 hours after the baseline scan as possible.

2.9.7 Analysis Of Ejection Fraction And Volume Of Infarction

Quantification of left ventricular mass, ejection fraction and late gadolinium enhancement infarct size were determined using established protocols and dedicated cardiac analysis software by two trained independent blinded observers. Late enhancement analysis was performed using QMass software (Medis medical imaging systems, Netherlands), allowing quantification of infarct size using the full-width, half-maximum criterion. The change in mass of infarcted tissue was determined by the difference in LGE from the preoperative and first postoperative CMR scans. The infarct size was given in mass unless specifically stated. The absolute change in

ejection fraction from pre to post surgery was calculated and an arbitrary value of 5% change was used to categorize patients into increased, decreased or no change.

2.9.8 USPIO ENHANCED MRI IMAGE PREPERATION

Baseline and post-USPIO T2*-weighted multi-gradient-echo images for each patient were spatially co-registered using ANALYZE software (AnalyzeDirect Software, United States). The four echoes (TE = 2.13, 4.27, 6.41, 8.55 ms) in a multi-echo T2*-weighted sequence were combined to generate a T2* map, in which the data represented the T2* value (S(t) = S(0)exp- (t/T2*)) for each voxel. This was achieved using in-house software developed in Matlab (Mathworks, US). The T2* value is the decay constant for the exponential decay of signal intensity with time. In the presence of USPIO, the signal decays more rapidly due to local field inhomogeneities and the T2* value is reduced. A 3x3 voxel Gaussian filter was applied to the individual echoes to reduce noise. By minimising the sum of the squares of errors between the data and an exponential function, the decay constant (i.e. T2*) was obtained. An experimentally determined threshold for the co-efficient of determination (r2>0.85) was used to exclude data that did not have an acceptable exponential decay when SI was plotted against echo time. The inverse of T2*, R2*, was then calculated to assess USPIO uptake. In our laboratory, we have previously assessed the repeatability of the measurement of the R2* value by comparing data from two T2*W sequences (run 1 *versus* run 2) performed in quick succession without moving the patient. This was performed on a voxel-by-voxel basis with a total of 32,936 data points, of which 1.2% were affected by artifact and discarded. Using the Bland and Altman method, (Bland and Altman, 1986) there was no

evidence of mean difference (0.99±21.9 s^{-1}) with a coefficient of repeatability of 42.9 s^{-1}.

The transformation matrix of the co-registration was then applied to the subsequent T2*-weighted echoes and R2* was calculated on a voxel-by-voxel basis to generate co-registered R2* ‘maps’ at baseline, and subsequent scans. The late enhancement short-axis images were also spatially co-registered with the R2* images for each visit in case of lack of reproducibility of patient breath-holding between scans.

2.10 Study Protocols for the Assessment Of Cellular Inflammation Following Acute Myocardial Infarction (Chapter 3)

This study investigated the feasibility of using USPIO enhance CMR to detect myocardial inflammation following myocardial infarction (Chapter 3: page 89).

2.10.1 Subjects

This study was an open-label pilot proof-of-concept study in 16 patients who suffered a recent myocardial infarction defined by the universal definition of myocardial infarction (Thygesen et al., 2007a). For inclusion & exclusion criteria, see section 2.1.3. Healthy volunteers, to define the R2* changes following USPIO administration in normal tissues, were recruited via local advertising.

All patients suffered an acute ST-elevation myocardial infarction. One patient in each group received thrombolytic therapy with tenecteplase, followed by percutaneous coronary angioplasty and stent placement. One patient in the control group re-perfused spontaneously followed by percutaneous coronary angioplasty and stent placement. All other patients were treated by primary percutaneous coronary intervention.

All patients gave written informed consent and the study was conducted with the approval of the local research ethics committee.

2.10.2 ULTRASMALL SUPERPARAMAGNETIC PARTICLES OF IRON OXIDE

Intravenous infusion of USPIO was performed immediately following the initial baseline magnetic resonance scan. USPIO (Ferumoxytol; Advanced Magnetics Inc, Cambridge, MA) was administered via a peripheral venous cannula at a dose of 4 mg/kg at a rate of up to 1 mL/s. Hemodynamic and electrocardiographic monitoring was conducted throughout.

2.10.3 MAGNETIC RESONANCE IMAGING

Sequential imaging was performed at baseline (24-72 h after admission), and 24 and 48 h thereafter. In 10 patients, USPIO was administered immediately after the baselines scan. Six patients received no infusion and acted as control subjects. Magnetic resonance imaging was performed as per 2.9.5.

2.10.4 IMAGE ANALYSIS

Late enhancement analysis was performed using QMass software (Medis medical imaging systems, Netherlands), allowing quantification of infarct size and location for correlation with USPIO-related signal changes.

Baseline, and 24 and 48 hours T2*-weighted multi-gradient-echo images for each patient were spatially co-registered using ANALYZE software (AnalyzeDirect Software, United States) as described in section 2.4.8. Subsequently, R2* maps were generated and used for analysis.

The late enhancement short-axis images were also spatially co-registered with the R2* images for each visit in case of lack of reproducibility of patient breath-holding between scans. Regions of interests (ROIs) were selected on the late enhancement images and applied to the co-registered R2* maps corresponding to: (i) micro-vascular obstruction if present, (ii) infarct area (defined by late gadolinium enhancement), (iii) peri-infarct area (adjacent to late gadolinium enhancement), (iv) myocardium remote from the infarct zone (distant from late gadolinium enhancement), (v) skeletal muscle, (vi) blood pool, (vii) liver and (viii) spleen (Figure 2.1). The ROIs were mapped to the first T2* echo before being applied to R2* maps to ensure there was coherence to the corresponding areas on all 3 scans, and no overlap with the blood pool or extra-cardiac structures. Two investigators created and quantified ROIs for all scans independently in order to assess reproducibility of the technique.

Figure 2.1 Object map creation

Following registration with late gadolinium enhancement (LGE) images, an "object map" (OM) was defined from regions of interest of specific tissues and subsections: skeletal muscle (light blue), spleen (dark blue), liver (yellow), blood pool (lilac) and heart subdivided into areas of infarction (red), peri-infarction (white) and remote myocardium (green). The object map was spatially co-registered with the R2* map (R2*) to measure specific R2* values (R2*+OM).

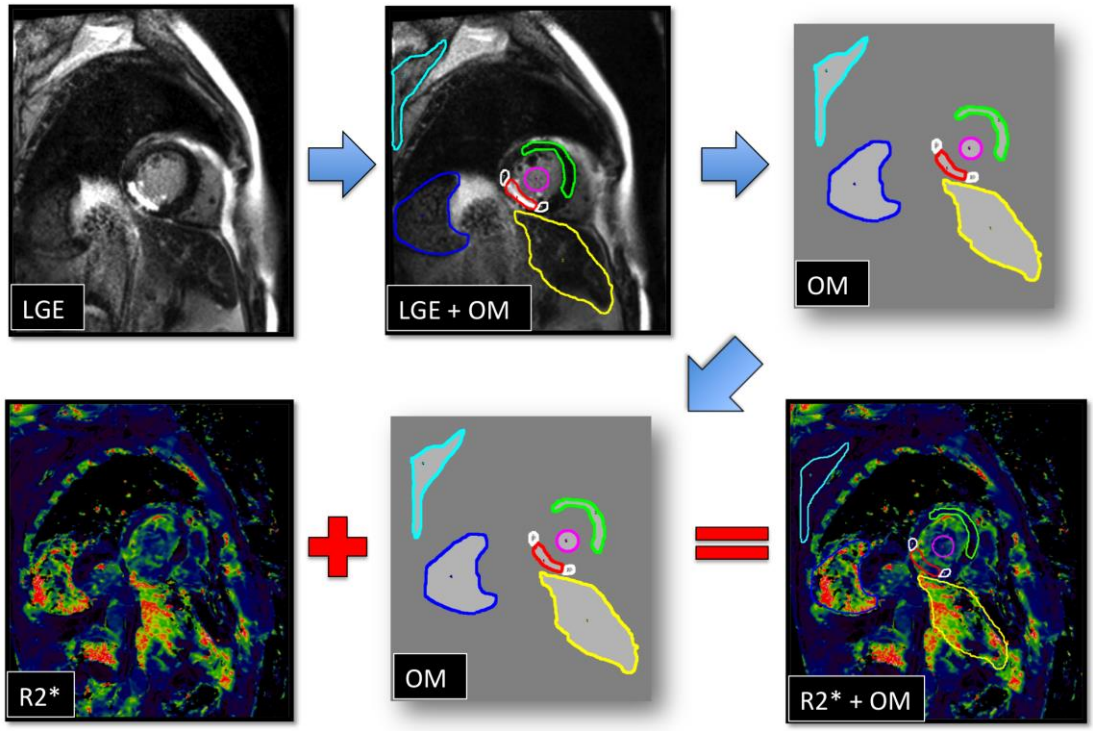

2.10.5 Data And Statistical Analysis For Chapter 3

All statistical analysis was performed with GraphPad Prism version 4.00 (GraphPad Software, San Diego California USA), except the Intraclass Correlation (ICC) which was performed with SPSS (IBM Version 20.0.0, USA) using a one-way random effects model. Repeatability was assessed by the method of Bland and Altman and coefficient of repeatability defined as twice the standard deviation of the mean of the differences (Bland and Altman, 1986). Patient characteristics were compared using unpaired non-parametric Mann-Whitney test. R2* values at baseline, 24 hours and 48 hours for each ROI were compared using repeated measure one-way ANOVA (Friedman test). If significant, Dunn's multiple comparison post-test was performed comparing R2* value at baseline to 24 hours, and baseline to 48 hours. Statistical significance was defined as two-sided $P<0.05$.

2.11 ELAFIN MYOCARDIAL PROTECTION FROM ISCHEMIA REPERFUSION (EMPIRE) TRIAL – CHAPTERS 4, 5 & 6

This study investigated whether Elafin, a neutrophil elastase inhibitor, could reduce myocardial inflammation following cardiac surgery (Chapter 4: page 118). As sub-studies, detection of cellular inflammation by USPIO enhanced CMR in the myocardium and other organs following surgery, and its modulation by Elafin was investigated (Chapter 5: page 143). Myocardial injury & inflammation following surgery was analysed with detection and of type 5 myocardial (Chapter 6: page 178).

2.11.1 CLINICAL STUDY AND RECRUITMENT

Myocardial inflammation and injury (see Chapter 6: page 178) was characterised as a sub-study of the "Elafin Myocardial Protection from Ischemia Reperfusion" (EMPIRE, ISRCTN 82061264) randomized controlled clinical trial (see Chapter 4: page 118)(Alam et al., 2015). This investigated the effect of Elafin, a neutrophil elastase inhibitor, on myocardial injury during on-pump CABG surgery. As a further substudy of the EMPIRE trial, cellular inflammation was investigated using USPIO (Chapter 5: page 143).

Patients referred for elective CABG surgery were recruited at Edinburgh Heart Centre between June 2011 and September 2013. Key inclusion & exclusion criteria are described in section 2.2.3, page 64.

2.11.2 CORONARY ARTERY BYPASS GRAFT SURGERY

Routine clinical monitoring included an arterial line, central venous line, urinary catheter, electrocardiogram and trans-esophageal echocardiography. Anaesthesia included opiate analgesia, induction with propofol and muscle relaxation with a non-depolarizing agent. The trachea was intubated and mechanical ventilation commenced. General anaesthesia was maintained with isoflurane propofol infusion during bypass. Surgical approach was via a median sternotomy and cardiopulmonary bypass was started after heparin administration with a non-pulsatile flow and a membrane oxygenator. Cardioprotection was provided by cold-blood cardioplegia (1:4), which was administered antegradely, after cross-clamping the aorta, into the coronary arteries or by cross clamp fibrillation. Where possible the left internal mammary artery was used for grafting. Other conduits were chosen from saphenous vein, radial artery or the right internal mammary artery. After grafting, cardiopulmonary bypass was discontinued and protamine was given to reverse the heparin. Patients received usual postoperative care within the intensive care unit.

2.11.3 ELECTROCARDIOGRAM

An ECG was performed prior to surgery, and then immediately post-surgery, 24 hours, 48 hours and at discharge. Additional ECGs were performed only if clinically indicated. Ischemia or infarction by ECG was defined as at least 2 mm ST deviation in the chest leads or 1 mm in the limb leads, development of new pathological Q waves or new bundle branch block. Other ECG categories included T-wave inversion (TWI) with no signs of ischemia or infarction, concave ST elevation with or without PR segment depression and no changes.

2.11.4 BLOOD BIOMARKERS

Blood samples were taken at baseline (time 0 hours, skin incision) and at 2, 6, 24 and 48 h post-operatively. Stored plasma samples were analysed using the high-sensitive troponin I assay. Plasma concentrations of high-sensitive C-reactive protein (hsCRP), interleukin IL-6, IL-8, tumour necrosis factor (TNF)-α, myeloperoxidase and elastase were quantified.

2.11.5 CARDIAC MAGNETIC RESONANCE IMAGING

Each patient underwent cardiac magnetic resonance imaging thrice: baseline CMR was performed 6 weeks before surgery. The first post-operative CMR was performed from 5 days after surgery, and a further USPIO enhances scan performed 24 hours after this. Patients were scanned as described in section 2.4. Quantification of left ventricular mass, ejection fraction and late gadolinium enhancement infarct size were determined using established protocols and dedicated cardiac analysis software by two trained independent blinded observers.

Healthy volunteers underwent CMR at baseline and 24 hours post USPIO infusion. In addition, there was USPIO enhanced scanning carried out immediately after infusion. Ex-vivo blood was scanned pre-USPIO infusion, 1 hour post USPIO infusion and 24 hours post infusion.

2.11.6 Development Of USPIO Uptake Analysis Protocols

The inflammation following CABG surgery may not be confined to areas of new infarction, and would be expected to be distributed diffusely in the myocardium. In order to develop a robust technique to analyse USPIO enhanced scans, the myocardium was divided into the standard 17-segment model and a R2* value calculated for each segment (Cerqueira et al., 2002). After calculating the increase in R2* value between the second and third scans, three methods for USPIO uptake quantification where used. Firstly, a pan-myocardial R2* value calculated from the mean of all segments. Secondly, since inflammation in the myocardium was likely to be non-uniform, a mean of the highest three segments was also calculated. Thirdly, the sum of the R2* values for the highest three segments was calculated for comparison. Since the apex of the myocardium is relatively thin and difficult to apply ROIs to accurately, these three methods of analysis were repeated excluding the apex.

Finally the median, 25^{th} & 75^{th} percentile of the R2* increase per segment of myocardium for healthy volunteers (from chapter 3) was calculated (non-parametric data). An increase in R2* over the 75^{th} percentile was arbitrarily defined as significant USPIO uptake in the study population. The number of "segments with significant USPIO uptake" was calculated for each patient.

2.11.7 DATA AND STATISTICAL ANALYSIS FOR CHAPTER 4

Recruitment power calculations were based on a study of patients in a U.K. centre undergoing remote ischemic preconditioning before coronary artery bypass surgery (Hausenloy et al., 2007). Mean area under the troponin T release curve in control patients was 36.12 µg/L (s.d. 26.08) and 20.58 µg/L (s.d. 9.58) in treated patients. No contemporary AUC data were available for cTnI release in this patient group but the measurements are equivalent in terms of quantifying myocardial injury. With a sample size of 80 patients we had 90% power to detect this 40 % difference with a significance level of 5%, using a t-test with unequal variances and allowing for 4 dropouts in each arm.

The primary outcome variable was the 48-h area under the curve (AUC) for plasma cTnI concentration. It was analysed using a generalized linear model, including terms for the treatment allocation and the variables on which the randomization was minimised. Log transformations were applied as the data were skewed, and the results have been unlogged and presented as geometric means. Secondary outcome measures involving area under the curve (hs-CRP, IL-6, IL-8, myeloperoxidase and elastase) were analysed similarly, taking log transformation if the data were skewed. Left ventricular ejection fraction and mass were analysed using QMass software (Medis medical imaging systems, Netherlands). The change in volume of infarction from preoperative and first postoperative magnetic resonance scans was categorized as increased, no change or reduced according to detection threshold based on inter-observer variability. Post hoc analyses of individual time points used Wilcoxon tests.

The primary analysis included all randomized patients on an intention-to-treat basis regardless of compliance with allocated treatment, and post randomization events. A

secondary pre-specified exploratory analysis of AUC cTnI release excluded patients who had myocardial infarction or a cardiac arrest resulting in loss of cardiac output for >1 min. Type V myocardial infarction was defined according to the third universal definition (Thygesen et al., 2012b). Finally, post hoc, we examined treatment effect for each time point using the high-sensitive cTnI assay.

2.11.8 Data And Statistical Analysis For Chapter 5

Parametric data was presented as mean with 95% confidence intervals, and non-parametric data as median with inter-quartile range as appropriate. Categorical data were compared using the Pearson's chi-square test. Parametric R2* data were analysed with unpaired t-test, and non-parametric with the Mann-Whitney U-test as appropriate. Multiple comparisons for USPIO uptake were compared using Kruskal-Wallis. If significant, Dunn's multiple comparison post-test was performed comparing R2* value across groups. Statistical significance was defined as two-sided $P<0.05$.

2.11.9 Data And Statistical Analysis For Chapter 6

Chapter 4 reports that Elafin had no significant effect on primary and secondary outcome measures with the exceptions of increased circulating Elafin concentrations and a reduction in circulating elastase activity in Elafin treated patients. In chapter 6, data from patients in placebo and active treatment arms were aggregated to provide an assessment of myocardial injury post CABG surgery.

Plasma hs-cTnI, hs-CRP, IL-6, IL-8 and MPO concentrations at each time point were

expressed as median [inter-quartile range], mean ± standard error of mean or mean (95% confidence intervals) as appropriate. Forty-eight hour area-under-the-curve (AUC) was calculated for plasma hs-cTnI, hsCRP and cytokines.

The change in mass of infarcted tissue was determined by the difference in LGE from the preoperative and first postoperative CMR scans. This was categorized as increased, no change or reduced according to detection threshold based on inter-observer variability *and* agreement between both independent analysers. The absolute change in ejection fraction from pre to post surgery was calculated and an arbitrary value of 5% change was used to categorize patients into increased, decreased or no change.

Categorical data were compared using the Pearson's chi-square test. Non-parametric R2* data were analysed with the Mann-Whitney U-test. Multiple comparisons for USPIO uptake were compared using Kruskal-Wallis. If significant, Dunn's multiple comparison post-test was performed comparing R2* value across groups. Statistical significance was defined as two-sided $P<0.05$.

Chapter 3: Ultrasmall Superparamagnetic Particles Of Iron Oxide Detect Cellular Inflammation In Patients With Acute Myocardial Infarction

3.1 Summary

Inflammation following acute myocardial infarction has detrimental effects on reperfusion, myocardial remodelling and ventricular function. Magnetic resonance imaging using ultrasmall superparamagnetic particles of iron oxide (USPIO) can detect cellular inflammation in tissues. We designed a proof of concept study to explore its utilisation in acute myocardial infarction in humans.

Sixteen patients within five days of ST-segment elevation myocardial infarction underwent 3 sequential magnetic resonance scans at -1, 24 and 48 hours following no infusion (controls; n=6) or intravenous infusion of USPIO (n=10; 4 mg/kg). T2*-weighted multi-gradient-echo sequences were acquired and R2* values calculated for specific regions of interest.

In the control group, R2* remained constant in all tissues throughout all scans with excellent repeatability (bias of -0.208, s^{-1}, coefficient of repeatability of 26.96, s^{-1}; intra-class coefficient 0.989). Consistent with uptake by the reticuloendothelial system, R2* increased in the liver (84±49.5 to 319±70.0 s^{-1}; $p<0.001$) but was unchanged in skeletal muscle (54±8.4 to 67.0±9.5 s^{-1}; $p>0.05$) 24 hours after USPIO administration. In the myocardial infarct, R2* increased from 41.0±12.0 (baseline) to 155±45.0 ($p<0.001$) and 124±35.0 s^{-1} ($p<0.05$) at 24 and 48 hours respectively.

Following acute myocardial infarction, USPIO uptake occurs within the infarct zone. This technique is as a potential method of assessing cellular myocardial inflammation and left ventricular remodelling that may have a range of applications in patients with myocardial infarction and other inflammatory cardiac conditions.

3.2 INTRODUCTION

Inflammation occurs in the acutely infarcted myocardium in order to remove necrotic cellular debris and allow tissue remodelling. Excessive inflammation may follow reperfusion therapy, and can have detrimental effects on healing and left ventricular remodelling (Nahrendorf et al., 2010). With the aim of improving outcomes following acute myocardial infarction, novel drugs are increasingly focusing on optimisation of myocardial repair and regeneration, and include anti-inflammatory interventions (Bonvini et al., 2005, Frangogiannis, 2006, Gonzalez et al., 2011, Steffens et al., 2009). There is therefore a need for non-invasive methods to assess *in vivo* myocardial inflammation following myocardial infarction both to define the healing process and to measure the potential efficacy of novel therapeutic interventions. As such, this method could be utilised to detect myocardial inflammation post CABG surgery and assess modulation by Elafin (Chapter 6: page 178).

Magnetic resonance imaging is ideally suited for the serial examination of the heart as it is non-invasive, does not involve ionizing radiation and has excellent soft tissue contrast and spatial resolution. Cardiac magnetic resonance, using T2-weighted imaging, has previously been used to detect myocardial oedema associated with myocardial infarction as it may help delineate the “area at risk” from the infarcted region (Garcia-Dorado et al., 1993). However there are major differences in the diagnostic performance of oedema imaging and there have been conflicting results regarding its utility as a prognostic marker or guide to therapeutic intervention (Viallon et al., 2012) (Eitel et al., 2010, Larose et al., 2010). One explanation for this is that magnetic resonance imaging of oedema does not directly assess the more dynamic cellular inflammatory processes.

Iron oxide particles can be used as a contrast medium in magnetic resonance imaging since they alter the T2* relaxation time of tissues in which they accumulate. USPIO are taken up by cells of the liver, spleen, bone marrow and lymph nodes. As a result of their small size (approximately 30 nm) they extravasate freely through capillaries and are taken up by tissue-resident inflammatory cells of the reticuloendothelial system (Ruehm et al., 2001b). These cells are predominately macrophages, but neutrophils may also take up USPIOs (Dousset et al., 1999, Gellissen et al., 1999a). It has been established that USPIOs can be used to assess vascular cellular inflammation in patients with abdominal aortic aneurysms (Richards et al., 2011a). Histological examination of aneurysm tissue confirmed co-localization and uptake of USPIO in areas with macrophage infiltration and mural USPIO uptake was associated with a 3-fold increase in the rate of abdominal aortic aneurysm expansion (Richards et al., 2011a). T2*-weighted MRI has been validated as a method of detecting hepatic and myocardial iron accumulation in patients with thalassemia and transfusion-related iron overload, and this method could be adapted for the detection of focal USPIO accumulation (Anderson et al., 2001, Westwood et al., 2005).

We hypothesised that we could use USPIO to track inflammatory cell infiltration within the myocardium of patients who had recently sustained an acute myocardial infarction. The aims of the study were therefore to investigate the proof-of-principle that USPIO could be used to assess cellular myocardial inflammation following acute myocardial infarction in humans. Healthy volunteers were also scanned non-contemporaneously in order to investigate the changes in R2* values in normal tissues and in the bloods pool.

3.3 RESULTS

3.3.1 USPIO UPTAKE IN HEALTHY VOLUNTEERS

There were 10 healthy volunteers (mean age 26±5 years, 5 male and 5 female) who completed the scanning protocol.

3.3.1.1 MYOCARDIUM

The mean R2* increase was 41.2±11.3 (95% CI 33.1 to 49.3) s^{-1}. The median increase was 41.2 [interquartile range 32.6 to 50.7] s^{-1} (Table 3-1). As such a "segments with significant USPIO uptake increase" was defined as an R2* increase over 50 s^{-1}.

Table 3-1 R2* values of myocardium in healthy volunteers

	R2* Value Pre-USPIO (s^{-1})	R2* Value Post-USPIO (s^{-1})	R2* Value 24 hours Post-USPIO (s^{-1})
Number of values	10	10	10
25% Percentile	39.9	121.0	80.7
Median	42.7	132.4	85.3
75% Percentile	48.2	152.8	99.4
Mean	44.2	133.6	88.4
Std. Deviation	5.6	23.6	11.9
Std. Error of Mean	1.8	7.5	3.8
Lower 95% CI of mean	40.2	116.7	79.9
Upper 95% CI of mean	48.3	150.5	97.0

3.3.1.2 OTHER ORGANS

R2* increase 24 hours post USPIO infusion of other organs are given in Table 3-2.

Table 3-2 R2* increase of various tissues in healthy volunteers

	Liver	Smooth Muscle	Spleen	Renal	Bone Marrow
Mean R2* (s^{-1})	229	19.7	311	58.9	272
Std. Deviation (s^{-1})	25.2	17.9	93.0	10.3	83.8
Std. Error of Mean (s^{-1})	8.0	5.7	29.4	3.3	26.5

3.3.1.3 USPIO & IRON THE IN BLOOD POOL

In healthy volunteers mean R2* values rose in the blood pool from 14.5±6.7 s^{-1} to 294.2±40.1 s^{-1} immediately post USPIO infusion, and 89.5±13.6 s^{-1} 24 hours post infusion (Table 3-3). There was a correlation with R2* increase in the myocardium and the blood pool (r=0.76, p=0.01). Skeletal muscle was used as a marker of blood pool perfusion, and R2* rose from 49.6±5.2 s^{-1} to 69.2±16.11 s^{-1}. There was a correlation with skeletal muscle R2* increase and that of the myocardium (r=0.68, p=0.03) (Figure 3.1). Ex vivo blood mean R2* value rose from 148.0±38.5 s^{-1} to 264.0±76.0 s^{-1} immediately post USPIO infusion, and 111.0±45.3 s^{-1} 24 hours post infusion (Figure 3.2).

Figure 3.1 Correlation between R2* increase in the myocardium, skeletal muscle or blood pool in healthy volunteers.

Skeletal muscle – left

Blood pool - right

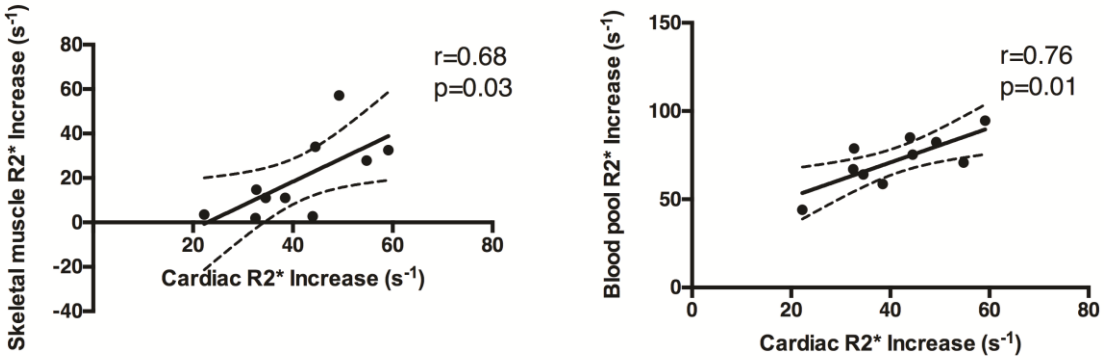

Figure 3.2 R2* Increase in myocardium *in vivo* & *ex vivo* blood & increase in iron content

R2* - left y-axis

Iron content - Right y-axis

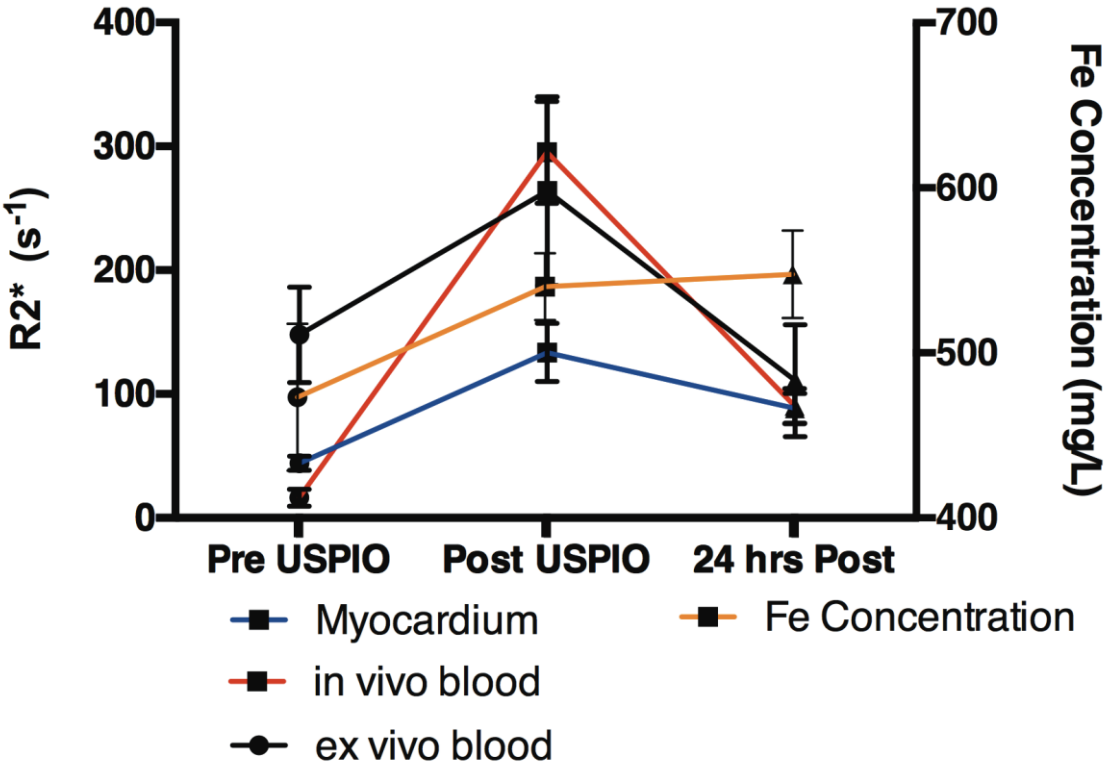

Table 3-3 Serum iron concentration and R2* values in *ex vivo* & *in vivo* blood and the myocardium of healthy volunteers.

	Baseline to 1 hour	**Correlation between Fe Concentration**	**1 hour to 24 hours**	**Correlation between Fe Concentration**
Fe Concentration Increase (mg/l)	50.3 ± 16.8		8.7 ± 27.6	
Ex vivo Blood R2* increase (s^{-1})	142.0 ± 73.3	Nil p=0.80	-180.0 ± 73.8	Nil p=0.50
In vivo Blood R2* increase (s^{-1})	277.7 ± 42.8	Nil p=0.30	-200.3 ± 35.2	Nil p=0.78
Myocardial R2* increase (s^{-1})	88.6 ± 26.3	Nil p=0.69	-32.6 ± 18.5	Nil p=0.57

Five healthy volunteers had iron concentration of blood measured at each time point. Mean values were 473.1 mg/l at baseline, 540.1mg/l 1-hour post infusion, and 547.6 mg/l 24 hours post infusion. There was no correlation with iron concentration and change in R2* values at any time course in ex vivo & in vivo blood or the myocardium (Table 3-3).

3.3.2 Completion Of Protocol For Patients With Myocardial Infarction

All patients sustained an acute myocardial infarction with a substantial area of myocardial necrosis (Table 3-4). All patients underwent three scans (baseline, and 24 and 48 h) including T2*-weighted multi-gradient-echo sequences and late gadolinium enhancement. Late enhancement reconfirmed myocardial infarction in all patients.

Table 3-4 Characteristics of trial participants.

CAD – coronary artery disease; SD – standard deviation.

	USPIO	CONTROL	p Value
Number	10	6	
Age (yr (range))	52 (38-65)	55 (48-65)	0.5622
Male	10	5	0.1824
Risk Factors			
Hypercholesterolemia	5	2	0.5153
Hypertension	4	0	0.7897
Family History of CAD	6	3	0.6963
Diabetes Mellitus	0	0	1.0
Current Smoker (Ex-smoker)	4 (2)	3 (1)	0.6963
Myocardial Infarction			
Symptoms to reperfusion time (min; mean±SD)	300±218	181±92	0.2198
Plasma Troponin I concentration (μg/L)	33.04±15.5	45.27±10.63	0.1120
Infarct Volume (mL (95% confidence intervals))	35.1 (8.0, 62.2)	43.2 (14.9, 71.7)	0.1471
Site of Infarction			
Anterior Infarct	3	3	0.4237
Lateral Infarct	1	3	0.0736
Inferior Infarct	6	0	0.0164
Left Ventricular Variables			
Ejection Fraction (%, mean±SD)	54±15	48 ±11	0.5622
Myocardial Mass (g, mean±SD)	76±19	67± 15	0.3676
Timing of Scanning			
Reperfusion to Baseline Scan (h (mean±SD))	49±30	44±16	0.8749
Reperfusion to Scan 2 (h (mean±SD))	73±30	68±17	0.9578
Reperfusion to Scan 3 (h (mean±SD))	95±30	92±38	0.7925
USPIO Infusion to Scan 2 (h (mean±SD))	22±2	NA	
USPIO Infusion to Scan 3 (h (mean±SD))	44±3	NA	

3.3.3 REPEATABILITY

Data from patients who did not receive USPIO administration were used to assess any potential changes in R2* attributable to acute myocardial infarction alone. There were no changes in R2* value within the myocardium or the infarct zone itself (Figure 3.3, Figure 3.4; Table 3-5; $p>0.05$). Similar findings were also observed in other organs such as the liver, spleen and skeletal muscle. Moreover, we were able to demonstrate excellent repeatability for the assessment of R2* value with a mean bias of -0.208,s^{-1}, coefficient of repeatability of 26.96 s^{-1} and intra-class coefficient 0.989 (Figure 3.5).

Figure 3.3 Tissue R2* Values

R2* value in regions of interest from the different tissues in control patients (blue) and patients who received an infusion of ultrasmall supraparamagnetic particles of iron oxide (USPIO; red). Asterisk denotes a significant increase from baseline.

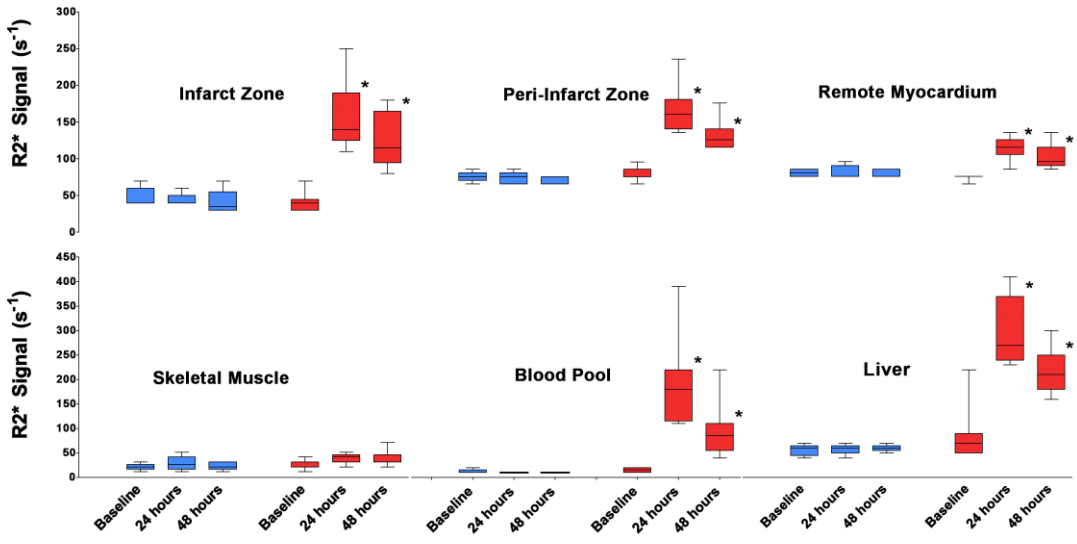

Figure 3.4 Comparison of R2* colour maps in patients with myocardial infarction

(i) Baseline and (ii) 24 hours after no infusion (3A, upper panels) or after an infusion of ultrasmall supraparamagnetic particles of iron oxide (USPIO; 3B, lower panels). R2* values did not change in the liver (blue) or myocardium (remote myocardium, green; infarct, red; microvascular obstruction, purple) of the control patient (3A iii) but did rise in the patient who received USPIOs (3B iii).

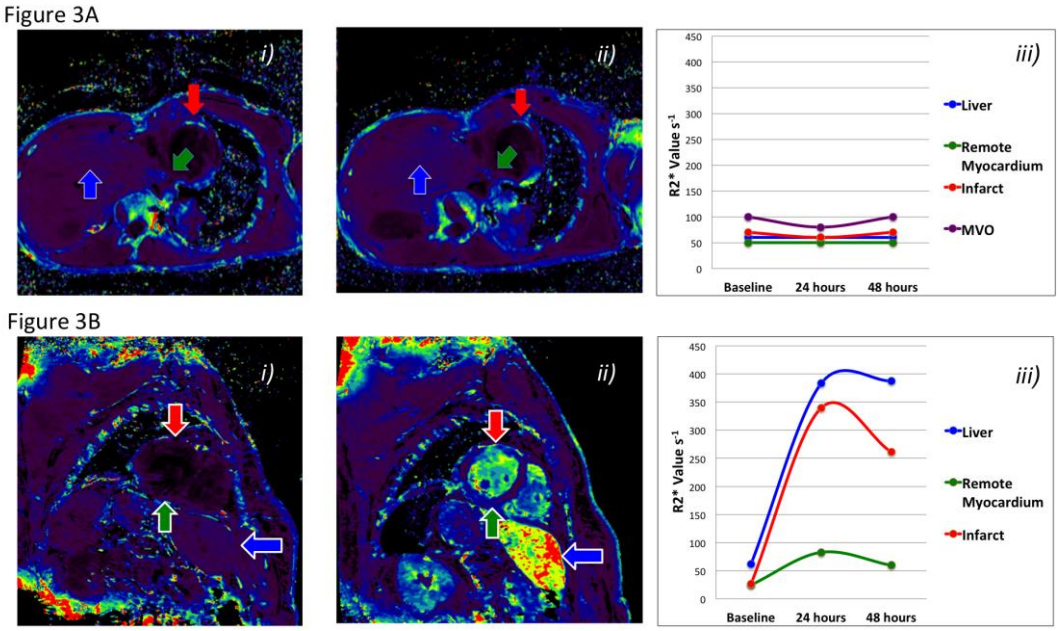

Figure 3.5 Bland-Altman plot - Differences versus average of R2* values in all patients.

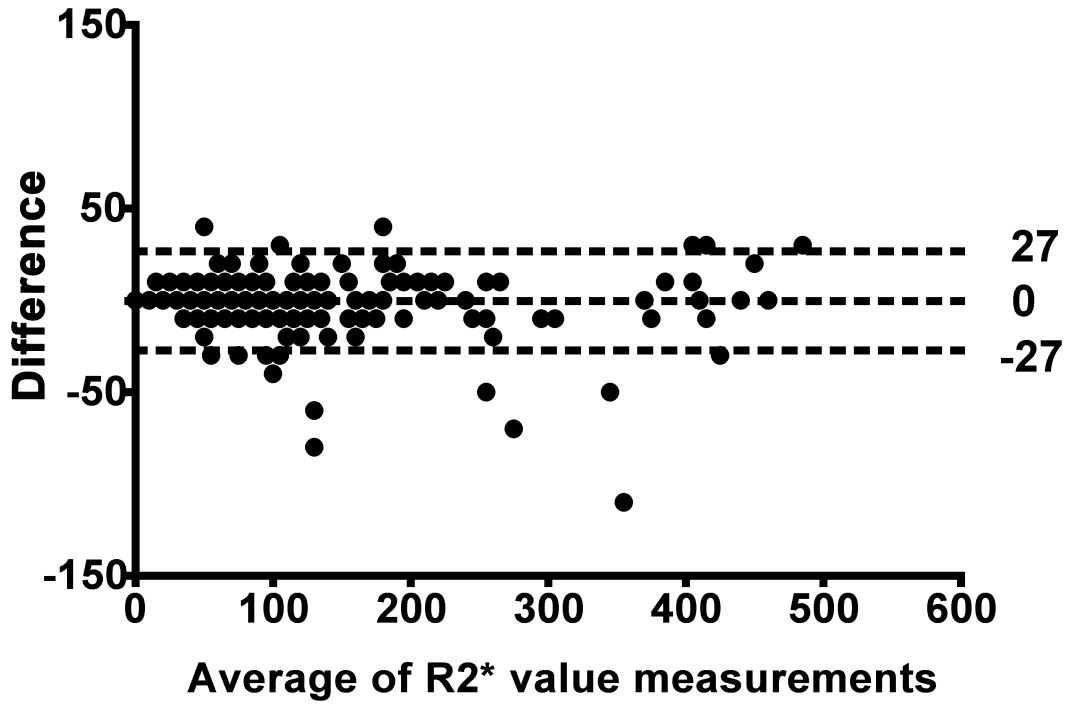

Table 3-5 R2* value (s^{-1}) in infarct region of interest (ROI) of control patients

		Baseline	Day 2	Day 3
Micro-Vascular Obstruction (When present)	**Mean**	63.3	53.33	66.7
	S.D.	32.2	23.1	30.6
	Min, Max	40, 100	40, 80	40, 100
Infarct ROI	**Mean**	45.0	43.33	41.7
	S.D.	13.8	8.2	14.7
	Min, Max	30, 70	40, 60	30, 70
Peri-Infarct ROI	**Mean**	40.0	38.3	36.7
	S.D.	6.3	7.5	5.2
	Min, Max	30, 50	30, 50	30, 40
Remote Myocardium ROI	**Mean**	43.3	41.7	43.3
	S.D.	5.2	4.1	5.2
	Min, Max	40, 50	40, 50	40, 50
Liver ROI	**Mean**	56.7	58.3	56.7
	S.D.	10.3	9.8	8.2
	Min, Max	40, 70	40, 70	40, 60
Skeletal Muscle	**Mean**	51.67	51.67	51.67
	S.D.	75.3	75.3	9.8
	Min, Max	40, 60	40, 60	40, 70
Spleen	**Mean**	68.3	75.0	70.0
	S.D.	28.6	37.8	32.3
	Min, Max	40, 100	40, 120	40, 120

3.3.4 EFFECT OF USPIO ADMINISTRATION

All patients tolerated the infusions well with no significant adverse events or arrhythmia. In the area of myocardial infarction, R2* increased from 41.0±12.0 s^{-1} at baseline to 155±45.0 ($p<0.001$) and 124±35.0 s^{-1} ($p<0.05$) at 24 and 48 h respectively following USPIO administration (Figure 3.3, Figure 3.4, Table 3-6).

Table 3-6 R2* value (s^{-1}) in regions of interest (ROI) of patients receiving USPIO.

		Baseline	Day 2	Day 3
Micro-Vascular Obstruction (When Present)	**Mean**	66.7	173.3	143.3
	S.D.	55.1	68.1	41.6
	Min, Max	30, 130	120, 250	100, 190
Infarct ROI	**Mean**	41.0	155.0	124.0
	S.D.	12.0	45.0	35.0
	Min, Max	30, 70	110, 250	80, 180
Peri-Infarct ROI	**Mean**	43.0	130.0	95.0
	S.D.	8.2	30.2	19.0
	Min, Max	30, 60	100, 200	80, 140
Remote Myocardium ROI	**Mean**	39.0	80.0	67.0
	S.D.	3.2	14.9	15.7
	Min, Max	30, 40	50, 100	50, 100
Liver ROI	**Mean**	84.0	319.0	243.0
	S.D.	49.5	70.0	63.6
	Min, Max	50, 220	230, 420	160, 370
Skeletal Muscle	**Mean**	54.0	67.0	65.0
	S.D.	8.4	9.5	14.2
	Min, Max	40, 70	50, 80	50, 100
Spleen	**Mean**	65.0	293.0	250.0
	S.D.	23.7	172.1	162.6
	Min, Max	20, 100	10, 500	10, 460

continued

Bone Marrow (Ribs)	**Mean**	247.0	276.0	274.0
	S.D.	92.6	140.4	164.9
	Min, Max	80, 360	100, 500	60, 570

3.3.5 NON-SPECIFIC EFFECTS OF USPIO

To determine whether there was a non-specific effect of USPIO enhancing R2* values in muscle, we assessed regions of interest within skeletal muscle. We were able to confirm that there was no change in R2* value of skeletal muscle (Figure 3.4, Figure 3.5, Table 3-6). Given that USPIO are taken up by cells of the reticuloendothelial system, both the liver and spleen were expected to develop marked changes in R2* values and act as positive controls. In the liver, there was a large increase in R2* from 84.0±49.5 s^{-1} at baseline to 319±70.0 ($p<0.001$) and 243.0±63.6 s^{-1} ($p<0.001$) at 24 and 48 h respectively following USPIO administration. A similar pattern was also seen in the spleen (Figure 3.6). The remote non-infarcted myocardium also demonstrated an increase from a baseline of 39.0±3.2 to 80.0±14.9 ($p<0.001$) and 67.0±15.7 s^{-1} ($p<0.05$) at 24 and 48 h respectively (Figure 3.3, Figure 3.4, Table 3-6).

Figure 3.6 Medullary and extramedullary R2* value post myocardial infarction

There is a significant increase in R2* value of hepatic and splenic tissues at 24 hours, that later fall. The R2* value of rib bone marrow does not increase significantly.

* P<0.05 versus baseline

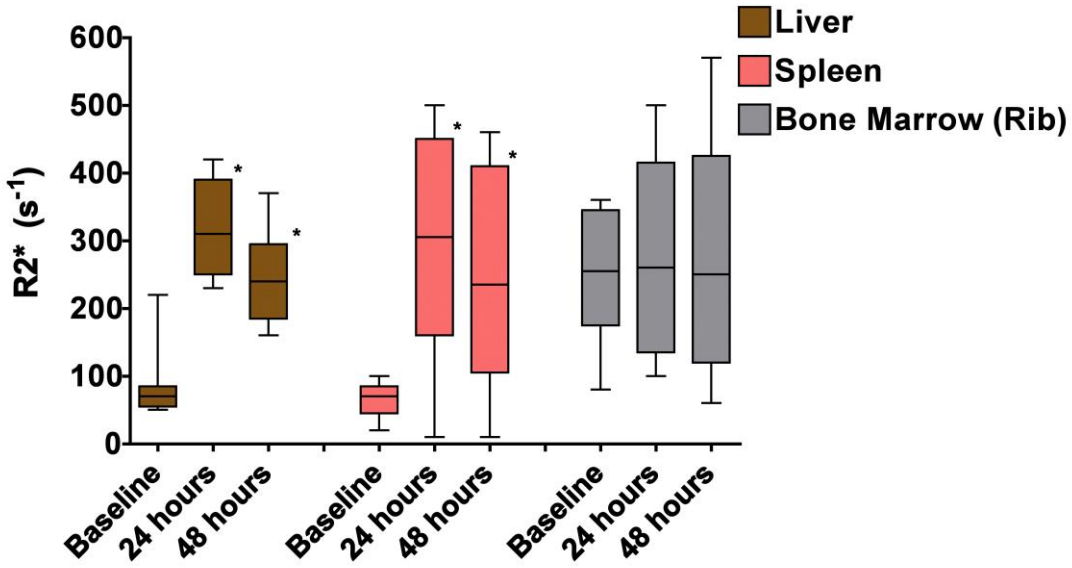

3.4 DISCUSSION

For the first time, we have demonstrated that USPIO are taken up into the myocardium of patients with a recent myocardial infarction. The increase of R2* by USPIO was highest within infarcted tissue, although we did observe a more modest increase within myocardium remote from the site of infarction. This suggests early macrophage and inflammatory cell infiltration predominantly occurs within the infarcted myocardium but appears to be associated with a more global influx of these cells that extends beyond the area at risk. However no histological quantification of macrophage infiltration was performed, and so the degree of inflammation cannot be correlated to MRI changes. Our preliminary findings need further confirmation in larger cohorts but this technique does appear to hold major promise in the investigation of myocardial inflammation following myocardial infarction and could be applied to other inflammatory cardiac diseases such as cardiac sarcoidosis, myocarditis or transplant rejection.

There was no correlation between the iron content of blood and the R2* value in the blood pool of healthy volunteers. Only 10 healthy volunteers were scanned, and half of these had the iron content analysed. Therefore it is possible the lack of correlation was due to an insufficient sample size. However, a CMR sequence would be susceptible to flow and motion artefact from a moving blood pool. The T2* sequence utilised to detect USPIO accumulation depends on static field non-uniformity within each voxel including magnetic susceptibility effects in the patient. In this study, the iron within haemoglobin itself exacerbated by the iron load from USPIOs would have affected this susceptibility. This would in turn be affected by the patients' heart rate, rhythm, systolic and diastolic function. All these factors would make determining the blood pool signal by sampling the ventricular cavity highly variable

and inaccurate. This accounts for the different R2* values at baseline and after USPIO infusion in healthy volunteers as compared to CABG patients, as well as the disparate R2* values in ex-vivo and in vivo blood. However there was a correlation between cardiac R2* increase and that of the blood pool, suggesting some of the increase seen in the study was due to organ perfusion by USPIO.

USPIO are actively taken up by inflammatory phagocytic cells, especially macrophages. They have been used to explore a number of inflammatory conditions including atherosclerotic plaques and abdominal aortic aneurysms (Kooi et al., 2003b, Trivedi et al., 2006b) (Richards et al., 2011a). Histological examination of excised clinical tissue has confirmed co-localisation of USPIO with macrophages (Kooi et al., 2003b, Trivedi et al., 2006b, Schmitz et al., 2001, Ruehm et al., 2001b). More specifically, pre-clinical models have demonstrated the uptake of magnetic nanoparticles into macrophages of infarcted myocardium by both fluorescence microscopy and immunohistochemistry (Sosnovik et al., 2007). We were unable to obtain tissue confirmation of USPIO uptake into macrophages in our cohort of patients. It is possible that other cell types with phagocytic capacity such as neutrophils may contribute to the increase in R2* value (Gellissen et al., 1999a). However, we have no reason to believe that uptake would differ from previous studies and, indeed, phagocytosis into macrophages is 4-6 times greater with ferumoxytol than with ferumoxtran-10, a previously used USPIO agent (Yancy et al., 2005). Moreover, we have demonstrated that organs of the reticuloendothelial system, such as the liver and spleen, demonstrate marked increases in R2* consistent with monocyte and macrophage uptake.

We found that there was an increase in R2* in the remote myocardium and this finding is intriguing. It has been demonstrated that increased numbers of macrophages in the myocardium remote from the area of infarction both in murine models and autopsies of patients who have died from myocardial infarction (Lee et al., 2012). Expression of cytokines is not confined to the infarct or peri-infarct zone, but is also expressed by myocardium remote from the infarct (Irwin et al., 1999). Furthermore, when myocardial infarction is induced in an abdominal heterotopic transplanted rodent heart, the native heart demonstrates a decrease in left ventricular (LV) fractional shortening and increased in LV end-diastolic dimension accompanied by increased TNF-α (Nakamura et al., 2003). Thus the post-infarct inflammatory process may induce cytokine production and inflammatory cell infiltration in remote "normal myocardium". This is reflected by our finding of an almost three-fold increase in R2* in remote myocardium. It is possible that increased macrophage infiltration is not a post- or peri-mortem artefact but a real pathophysiological phenomenon (Lee et al., 2012). However there is no histo-pathological confirmation or remote macrophage infiltration. USPIOs persist in the circulation with a plasma half-life of 14-30 h in humans (Landry et al., 2005, Hunt et al., 2005). At 24 hours post infusion, there would be circulating USPIO capable of increasing R2* when perfusing the myocardium. This was also seen in the healthy volunteer (Table 3-1, page 94).

R2* was decreasing in myocardial, splenic and hepatic tissues by 48 h post-infusion. The decrease in R2* in the blood pool is to be expected given efficient USPIO uptake by reticuloendothelial cells leading to rapid clearance (Yancy et al., 2005). However pre-clinical findings suggest that monocyte tissue residence in infarcted myocardium is brief despite high recruitment rates (Leuschner et al., 2012).

Consistent with this study, we found evidence of high extra-medullary activity in terms of high USPIO uptake in the liver and spleen in contrast with minimal uptake in the bone marrow (Figure 3.6). However, post hoc analysis of bone marrow uptake was performed using a ROI in the ribs since CMR protocols to scan extra-medullary sites had not been planned. As such analysis is liable to error. The decrease in R2* value in the splenic tissues at 48 hours may represent mobilisation of the splenic reservoir of monocytes (Swirski et al., 2009b, Nahrendorf et al., 2010). In addition, the decrease in tissue R2* will reflect clearance of extravasated particles by phagocytic cells through efflux of USPIO laden inflammatory cells. The time course of monocyte and macrophage recruitment into the myocardium is unclear from our study and would require USPIO administration at differing time points following myocardial infarction. This would help define the peak influx and time course of macrophage trafficking into the myocardium.

We have applied this technique to patients who have recently sustained a myocardial infarction. However, this approach could be applied to other cardiac conditions that involve intense inflammatory processes. This could include viral myocarditis, giant cell myocarditis, anthracycline-induced cardiotoxicity and sarcoidosis. Indeed, it may also have a role in detecting cardiac transplant rejection in a non-invasive manner. However, this needs further careful validation in well phenotyped clinical subgroups.

Limitations to our study included the lack of histo-pathological confirmation of macrophage uptake. However we performed the same scanning protocol on a rodent model of infarction, and obtained myocardial tissue for histological analysis (6.1.1.1.1.1.1.1Appendix G: , page 497). This confirmed USPIO were taken up by monocytes infiltrating the infarcted myocardium. Other limitations are the longer

reperfusion time in the USPIO group potentially resulting in more inflammation and the injection of USPIOs at variable time points post MI. However, given the previous evidence that USPIO are taken up by macrophages, our study provides proof of principle that cellular inflammation may be tracked post myocardial infarction.

In conclusion, we have demonstrated for the first time that USPIO is taken up by the infarct tissue in patients with recent myocardial infarction and by the peri-infarct myocardium to a lesser degree. Given previous pre-clinical and clinical studies, this is likely to correspond to cellular inflammation. This represents a novel non-invasive method to further study cardiac inflammation and therapeutic interventions. It may also provide prognostic information or provide a diagnostic tool for the investigation of inflammatory cardiac conditions such as myocarditis and transplant rejection, as well as a potential biomarker for therapeutic interventions targeted at improving left ventricular remodelling following infarction.

Chapter 4: PERI-OPERATIVE ELAFIN FOR ISCHEMIA-REPERFUSION INJURY DURING CORONARY ARTERY BYPASS GRAFT SURGERY: A RANDOMISED CONTROLLED TRIAL

4.1 SUMMARY

Elafin is a potent endogenous neutrophil elastase inhibitor that protects against myocardial inflammation and injury in pre-clinical models of ischemic-reperfusion injury. We investigated whether Elafin could inhibit myocardial ischemia-reperfusion injury induced during coronary artery bypass graft (CABG) surgery.

In a randomised double blind placebo controlled parallel group clinical trial, 87 patients undergoing CABG surgery were randomized 1:1 to intravenous Elafin 200 mg or saline placebo after induction of anaesthesia and prior to sternotomy. Myocardial injury was measured with area under the curve (AUC) troponin I release over 48 h and quantification of macro-infarction by magnetic resonance imaging. Post-ischemic inflammation was measured by plasma markers including AUC high-sensitive c-reactive protein (hs-CRP), and myeloperoxidase (MPO).

Elafin infusion was safe and resulted in >3000-fold increase in plasma Elafin concentrations with associated >50% inhibition of elastase activity in the first 24 h. AUC myocardial injury was not significantly reduced by Elafin (ratio of geometric means (Elafin/placebo) of 48h AUC troponin I 0.74 (95% CI 0.47 to 1.15), P=0.18) although post-hoc analysis of highly sensitive assay revealed a lower troponin I concentration at 6 hours in Elafin treated patients (median 2.4 *versus* 4.1 μg/L, P=0.035). Elafin had no effect on macro-infarction (Elafin, 7/34 versus placebo, 5/35 patients) or markers of inflammation: mean differences for AUC hs-CRP of 499

mg/L/48-h (95% CI -207 to 1205, *P*=0.16), and AUC MPO of 238 ng/mL/48-h (95% CI -235 to 711, *P*=0.320).

There was no strong evidence that neutrophil elastase inhibition with a single dose Elafin treatment reduced myocardial injury and inflammation following CABG-induced ischemia-reperfusion injury.

4.2 INTRODUCTION

Ischemia-reperfusion injury occurs when blood flow is restored to organs and tissues that have sustained a period of interrupted blood supply. This occurs following therapies for acute myocardial infarction and ischemic stroke, and is a necessary consequence of solid organ transplantation. Mechanisms of cell and tissue injury include a neutrophil-mediated post-ischemic inflammatory response and activation of cellular death pathways following reperfusion (Hansen, 1995). Protecting organs from ischemia-reperfusion injury to improve clinical outcome is a high priority. Despite intense research efforts and huge promise from pre-clinical and early phase clinical trials, there are currently no effective therapies that can limit this injurious response.

Coronary artery bypass graft (CABG) surgery improves symptoms and survival, and remains the treatment of choice for patients with complex multi-vessel coronary artery disease. During CABG and cardiopulmonary bypass, coronary blood flow is interrupted and the heart is put into circulatory arrest. This causes ischemia-reperfusion injury that is exacerbated by adverse neutrophil-mediated myocardial inflammation and injury (Vinten-Johansen, 2004, Butler et al., 1993, Wakayama et al., 2007). CABG surgery therefore represents a programmed clinical model of ischemia-reperfusion injury that lends itself to testing the efficacy of potential therapeutic interventions (Hausenloy et al., 2007).

Elafin is an endogenous anti-inflammatory protein that was first isolated in the search for inhibitors of neutrophil elastase activity in the lung and skin (Sallenave and Ryle, 1991a, Wiedow et al., 1991). It has inhibitory activity against both human neutrophil elastase and proteinase-3 as well as suppressing production of

inflammatory cytokines such as IL-8 and TNF-α (Henriksen et al., 2004b). Elafin is produced locally at sites of inflammation, raising a local defence of 'alarm' antiproteases in order to contain and inhibit neutrophil-mediated inflammation (Sallenave, 2000a). Cardiovascular tissues do not express elafin or other neutrophil elastase inhibitors, and are therefore more vulnerable to neutrophil-mediated injury.

Augmentation of human elafin has consistently demonstrated impressive protective effects in rodent models of ischemic and inflammatory elastase-mediated vascular injury. Elafin infusion reduced muscular injury and neutrophil recruitment in the rat ischemic hind-limb and myocardial ischemia–reperfusion injury models (Crinnion et al., 1994, Tiefenbacher et al., 1997). Transgenic mice overexpressing human elafin under the control of the vascular pre-proendothelin promoter have relatively preserved left ventricular size and function following myocardial infarction (Ohta et al., 2004a). Compared to wild-type littermates, these animals are also protected from viral myocarditis and hypoxia-induced pulmonary hypertension, and exhibit less restenosis following wire induced carotid artery denudation (Zaidi et al., 1999, Zaidi et al., 2002a, Zaidi et al., 2000a). Elafin augmentation therefore protects the cardiovascular system from a range of conditions characterized by neutrophil elastase-mediated inflammation and injury.

The purpose of the Elafin Myocardial Protection from Ischemia Reperfusion (EMPIRE) randomized controlled clinical trial was to provide proof-of-concept that Elafin treatment could reduce myocardial ischemia-reperfusion inflammation and injury in patients undergoing CABG surgery.

4.3 RESULTS

4.3.1 PATIENT CHARACTERISTICS AND INTRA-OPERATIVE DETAILS

A total of 189 patients were screened for recruitment of whom 29 were excluded, 79 declined to participate, 88 patients gave informed consent and 1 died before surgery leaving 87 patients to undergo randomisation (Figure 4.1). In 85 of the 87 patients, the trial infusion was administered as planned. Patient characteristics and intra-operative details are shown in Table 4-1. Full data to calculate area under the curve for cTnI (primary outcome) was obtained in 83 patients (95%). Data quality was similarly good for all secondary end-points with missing data evenly balanced across the treatment arms.

Figure 4.1 Patient flow chart

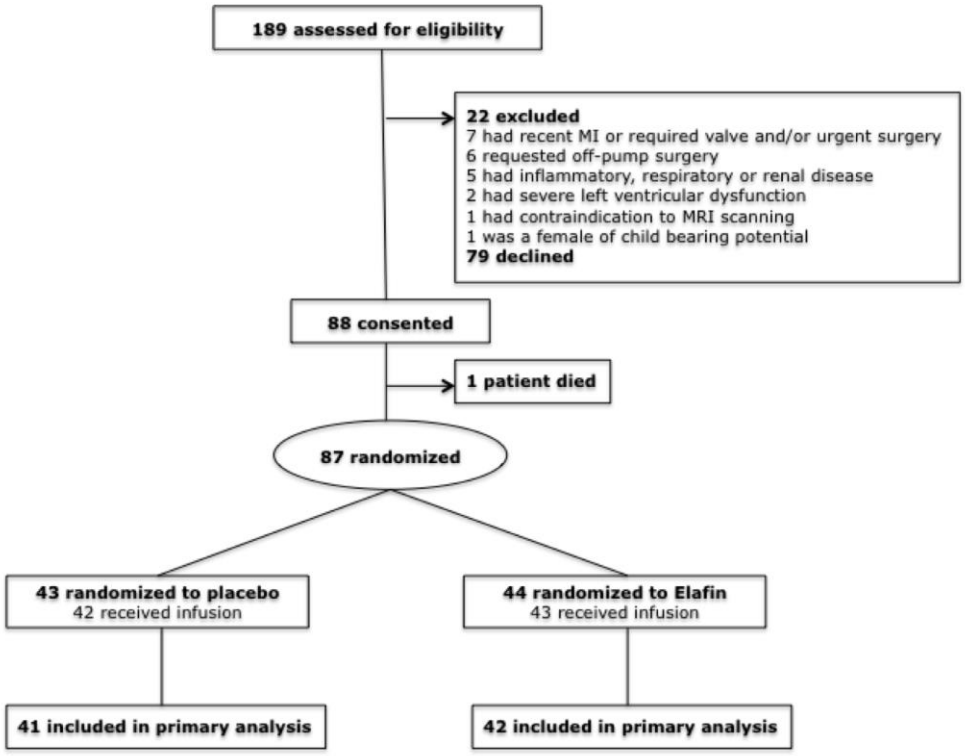

Table 4-1 Baseline characteristics and intra-operative details by treatment group. Data are number of patients (%) or mean ± SD

	Placebo	**Elafin**
Baseline characteristics		
Age	63.6 ± 8.4	63.9 ± 7.7
2-vessel coronary disease	12 (27.9)	11 (25.0)
3-vessel coronary disease	31 (72.1)	33 (75.0)
Creatinine (mg/dl)	0.92 ± 0.18	0.94 ± 0.23
Diabetes Mellitus	9 (20.9)	11 (25.0)
Surgeon A	16 (37.2)	18 (40.9)
Surgeon B	27 (62.8)	26 (59.1)
Male Gender	36 (83.7)	38 (86.4)
EuroSCORE	2.21 ± 1.73	2.64 ± 2.06
Intra-operative details		
Number of bypass grafts		
One	1	2
Two	19	14
Three	14	22
Four	9	5
Five	0	1
Cardiopulmonary bypass time (min)	77 ± 26	78 ± 26
Cross clamp time (min)	45 ± 15	47 ± 16

4.3.2 ELAFIN AND ELASTASE ACTIVITY

Elafin infusion resulted >3000-fold higher plasma concentrations (31.1±9.6 *versus* 0.01±0.07 μg/mL for placebo). This increase in plasma Elafin concentration was reflected in a marked reduction in plasma elastase activity (4.28±5.13 *versus* 9.66±9.21units/mL; Figure 4.2).

Figure 4.2 Perioperative plasma Elafin concentration (A) and plasma elastase activity (B) between groups.

Data are median plus interquartile range from the first skin incision (time 0 hours) to 24 hours. Placebo group n = 41; Elafin group, n = 43.

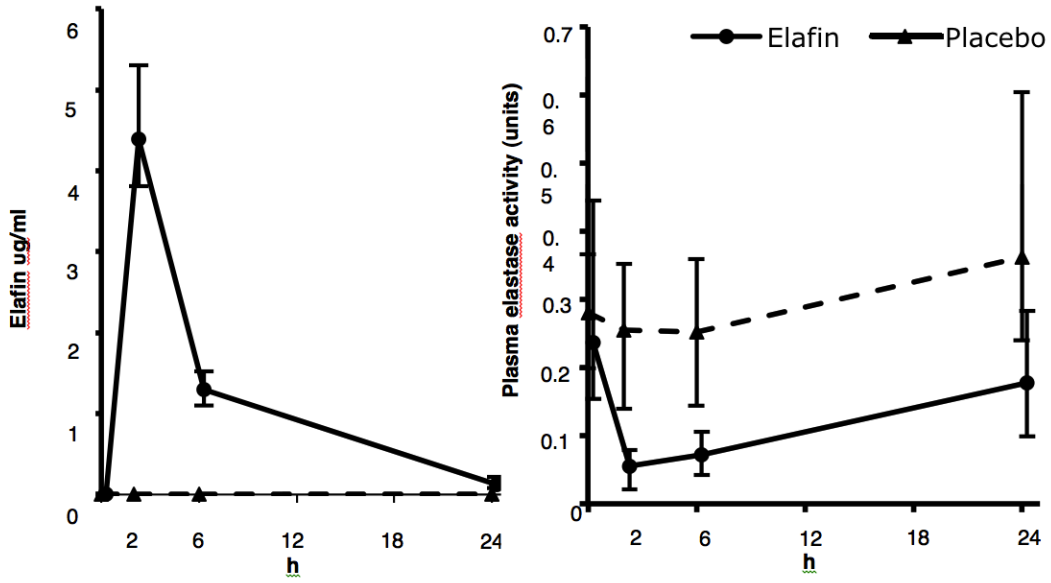

4.3.3 TROPONIN I

There was no significant change in troponin I concentrations over the first 48 hours in Elafin treated patients (adjusted ratio of geometric means (Elafin/placebo) 0.74, 95% CI 0.47 to 1.15, $P = 0.18$). There remained no evidence of a difference in a pre-specified secondary analysis where 3 patients who sustained a clinical myocardial infarction or had a cardiac arrest were excluded from analysis (adjusted ratio of geometric means 0.76, 95% CI 0.50 to 1.14, $P = 0.17$). Post-hoc analysis using the high-sensitivity assay demonstrated significant reduction of plasma cTnI concentrations in Elafin-treated patients at 6 hours (median 2.4 *versus* placebo 4.1 μg/L, $P = 0.035$; Figure 4.3, Table 4-2).

Figure 4.3 Myocardial injury.

Cardiac troponin I (cTnI) release following coronary artery bypass graft surgery between treatment groups from first skin incision (time 0 hours) to 48 hours. Data are median plus interquartile range. Placebo group, n= 42; Elafin group, n = 44.

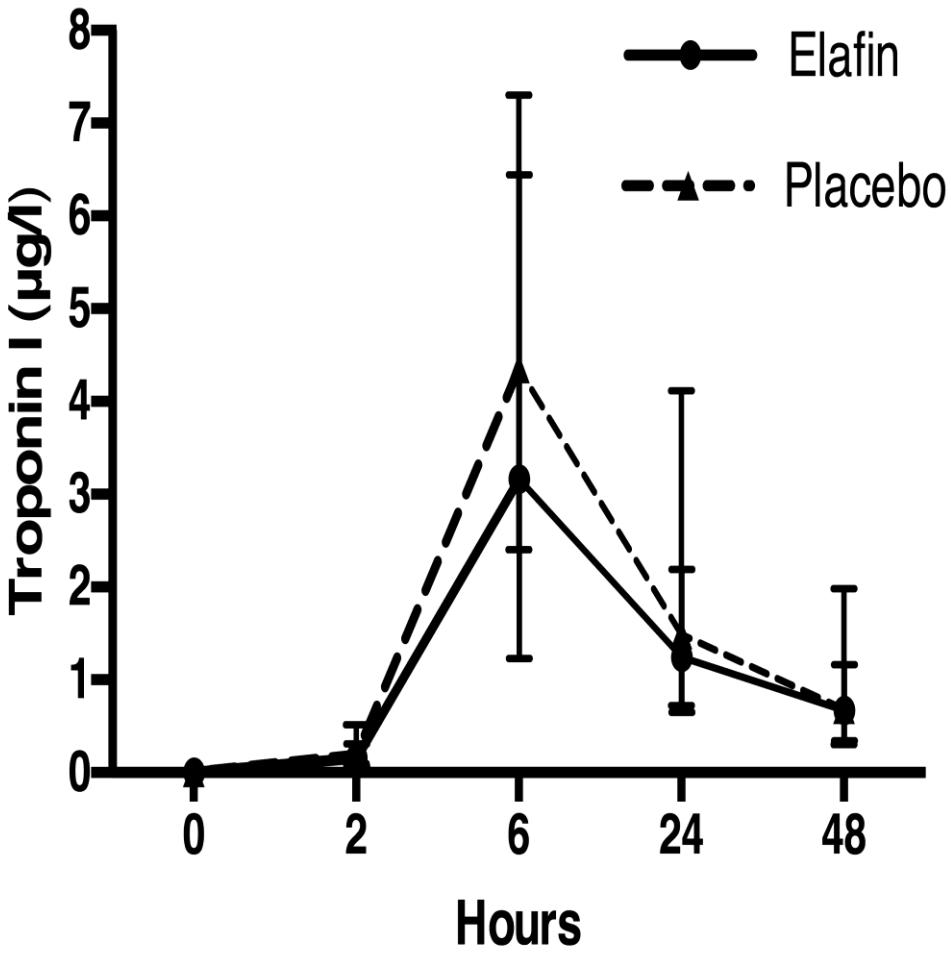

Table 4-2 Post-hoc analysis of plasma cardiac troponin I (cTnI) concentration to 48 hours.

(μg/L, median and interquartile range, high-sensitive assay)

Time (hours)	**Placebo** (n = 43)	**Elafin** (n = 44)	*P* *Wilcoxon*
0	0.00 (0.0, 0.0)	0.00 (0.0, 0.0)	*0.861*
2	0.08 (0.0, 0.2)	0.07 (0.0, 0.1)	0.228
6	4.07 (2.0, 6.4)	2.41 (1.0, 4.6)	0.035
24	1.02 (0.6, 3.9)	1.08 (0.5, 2.3)	0.421
48	0.53 (0.2, 1.9)	0.47 (0.2, 1.2)	0.648

4.3.4 CMR

Data from pre and post-operative scans were available for 34 (77.3%) Elafin and 35 (81.4%) placebo treated patients (Table 4-3). There was no difference in post-operative left ventricular mass or left ventricular ejection fraction. The intra-class correlation coefficient for late gadolinium enhancement was 0.99 and the coefficient of repeatability 1.78 mL (1.87 g) giving a threshold of 1.8 mL (1.9 g) for an increase in late gadolinium enhancement. The incidence of increased myocardial infarction volume was similar between treatment groups.

Table 4-3 Magnetic resonance imaging analysis of postoperative ejection fraction, left ventricular mass and infarct volume.

	Placebo (n =35)	**Elafin**(n =34)
Change in ejection fraction (percentage points)	-0.62±6.2	-2.4± 6.3
Change in LV mass (g)	1.2±3.8	2.0±3.8
Change in infarct volume (%)		
Reduced volume	2.9	0
No Change	82.9	79.4
Increased volume	14.3	20.6

4.3.5 HUMORAL INFLAMMATORY MARKERS

There was no effect on peak myeloperoxidase concentrations (mean difference 54.73 ng/L, 95% CI -60.0 to 169.5, $p = 0.35$) but peak elastase concentration was reduced (mean difference -168.4 ng/mL, 95% CI; -323.4 to -13.47ng/mL, $P = 0.03$; Figure 4.2). In contrast, there was no effect on the 48-hour AUC for plasma elastase concentration (mean difference -524.0 ng/mL/48-h, 95% CI -1239 to 191.3ng/mL/48-h,$P = 0.15$). Although all inflammatory markers rose following CABG surgery ($P < 0.001$ for all), there was no treatment effect of Elafin ($p > 0.05$ for all; Figure 4.4).

Figure 4.4 Perioperative hsCRP (A) and inflammatory cytokines IL-6 (B) and IL-8 (C) release between groups.

Data are median plus interquartile range. Placebo group, n= 42; Elafin group, n = 44

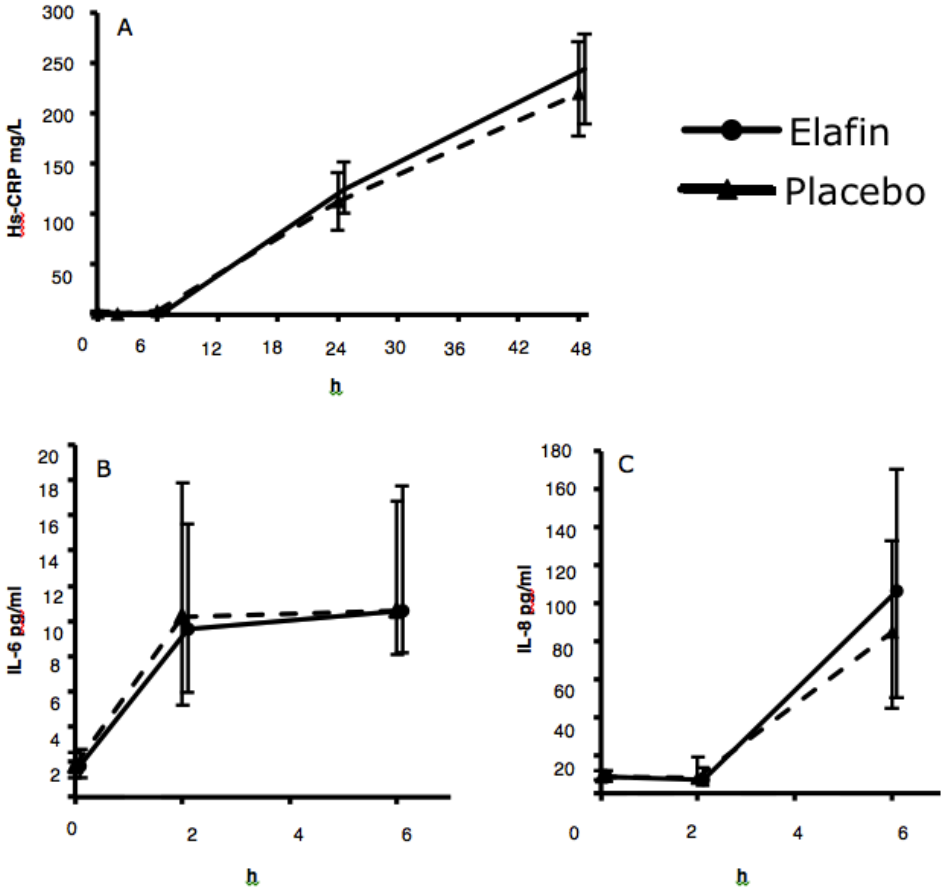

4.3.6 CLINICAL OUTCOMES

Median duration of stay in the intensive care unit was 24 and 23 h for patients treated with Elafin and placebo respectively (HR 1.25, 95% CI; 0.81 to 1.94 $P = 0.32$). Clinical outcomes and the incidence of perioperative complications in the first 48 hours were also similar (in Figure 4.4).

Table 4-4 Post-operative complications and outcomes by treatment.

Data are number of patients (%) or mean ± SD.

	Placebo		**Elafin**	
Post-operative complications and outcomes (48 hours)				
Death	0	(0)	0	(0)
Stroke	0	(0)	0	(0)
Myocardial infarction	0	(0)	1	(2.3)
Inotrope or balloon pump support for > 24h	10	(27.3)	12	(23.3)
Red cell transfusion post-op	12	(27.9)	12	(27.3)
Re-operation for bleeding	2	(4.7)	1	(2.3)
Respiratory complications	3	(7.0)	5	(11.4)
Antibiotic administration	2	(4.7)	4	(9.1)
Atrial fibrillation	4	(9.3)	3	(6.8)
Serum creatinine (mg/dl)				
24 hours	0.90 ± 0.32		0.87 ± 0.32	
48 hours	0.96 ± 0.48		0.88 ± 0.42	

4.4 DISCUSSION

This is the first Phase 2 clinical trial investigating the effect of Elafin, an endogenous neutrophil elastase inhibitor, on myocardial ischemia-reperfusion injury in patients undergoing CABG surgery. Despite achieving >3000-fold increase in plasma concentrations sufficient to more than halve plasma elastase activity, it was not possible to demonstrate a clear evidence of beneficial effect of human recombinant Elafin. Specifically, it was not possible to attenuate the systemic inflammatory response nor conclusively detect a reduction in two very sensitive, complementary and gold-standard measures of myocardial injury: AUC for plasma cTnI concentrations and late gadolinium enhancement on magnetic resonance imaging. However, Elafin was safe and well tolerated in this high-risk clinical population and post-hoc analysis indicated reduced myocardial injury at 6 hours raising the possibility that more extensive treatment effect would have been seen with multiple doses or bolus and infusion.

All patients in this trial exhibited evidence of myocardial injury demonstrated by cTnI release. This was associated with a marginal reduction in left ventricular ejection fraction detected on post-operative MRI imaging. Small increases in delayed gadolinium enhancement indicative of new myocardial infarction were detected in a fifth of patients in keeping with sub-clinical myocardial injury and infarction that follows circulatory arrest and ischemia-reperfusion during CABG surgery. The current MRI results contrast with an earlier study reporting increased infarct volume in 78% of patients undergoing planned CABG (Steuer et al., 2004b). A key difference that may explain this discrepancy is the detailed patient characterization in our study with availability of pre-operative MRI scans allowing

identification of small areas of pre-existing infarct that would be missed by using clinical history, echocardiography or ECGs to screen for pre-existing infarction.

The data indicate that with single bolus administration, Elafin does not confer clinically meaningful myocardial protection in the context of CABG surgery. This result was not changed in a secondary analysis excluding patients that had sustained clinical events thought to be unrelated to study drug that would have contributed to large additional cTnI elevations.

cTnI by high sensitivity assay may have provided more accurate data given its' limit of detection of 4.1 pg/mL, and analysis of all samples was performed as a batch at the same time. The reason it was not used for the primary endpoint was that it was not available until the end of the study and was therefore not included in the secondary endpoint. Although post hoc analysis identified a reduction in plasma cTnI concentrations at 6 hours in Elafin treated patients, the overall absence of a convincing beneficial effect conflicts with pre-clinical ischemia-reperfusion studies where Elafin infusion was associated with a 27%-reduction in myocardial infarct size and improved left ventricular performance. Our clinical CABG model allows recapitulation of a key condition in pre-clinical models where Elafin is administered up front or expressed in tissues prior to the onset of cardiopulmonary bypass and ischemic tissue injury. However, despite this, we were unable to demonstrate clear efficacy despite using two complementary and highly sensitive measures of myocardial injury.

Elafin is one of several agents targeting inflammatory pathways that have been investigated in ischemia-reperfusion injury during cardiac surgery without success. Pexelizumab, a recombinant, single-chain anti-C5 monoclonal antibody, was studied

in 2 multi-center, randomised clinical trials of patients undergoing CABG surgery with or without valve surgery on cardiopulmonary bypass. There was no difference in the primary outcome of death or myocardial infarction between the Pexelizumab and placebo treatment groups (Verrier et al., 2004). Failure of treatment effect with Elafin and Pexelizumab may reflect different mechanisms responsible for myocardial injury during CABG. Myocardial ischemia and necrosis undoubtedly occur during CABG surgery and the magnitude of cTnI release is correlated with subsequent morbidity and mortality (Croal et al., 2006). Mechanism of ischemia in preclinical models commonly involves complete interruption of coronary blood flow with a ligature to the beating heart. In CABG surgery the heart is in a dormant state of circulatory arrest with protective cardioplegia and the impact of blood flow interruption is less severe. Despite evidence of neutrophil mediated inflammatory injury post-CABG, it may be activation of cellular survival pathways within cardiomyocytes that determines the outcome of ischemia-reperfusion in this setting. Pharmacological manipulation of the Na^+-H^+ exchanger with cariporide reduces lethal intracellular calcium accumulation following ischemia reperfusion and was associated with reduced perioperative myocardial infarction in two large studies (Boyce et al., 2003, Mentzer et al., 2008). Further development of this treatment was limited by an excess mortality from stroke but these studies do illustrate the therapeutic potential of blocking cell death pathways. Elafin treatment was associated with substantial (> 50%) inhibition of circulating elastase activity following CABG surgery and the data therefore indicate that neutrophil-derived elastase injury is not a prominent cause of myocardial injury in this setting.

The patients did have evidence of neutrophil activation and degranulation with increased plasma concentrations of the primary granule contents, elastase and

myeloperoxidase. This is in keeping with other studies that have demonstrated increased expression of neutrophil cell surface adhesion molecules (CD18 and CD 11b) and elevated elastase concentrations peaking at the end of cardiopulmonary bypass (Hill et al., 1995, Ninomiya et al., 2003). Peak elastase concentrations were reduced in Elafin-treated patients although there was no demonstrable effect on peak myeloperoxidase concentrations. This discrepancy is explained by differences in the origin of these two neutrophil primary granule proteins. Circulating human neutrophil elastase is derived largely from acute neutrophil degranulation. A pool of neutrophil-derived myeloperoxidase is transcytosed and bound to the subendothelial matrix (Baldus et al., 2001). This contributes to the circulating pool and is released following heparin administration during cardiopulmonary bypass (Rudolph et al., 2013).

Elafin mediated reductions in elastolytic activity and myeloperoxidase staining (as a marker of neutrophil infiltration) have been consistent findings in pre-clinical models. Elafin infusion produced impressive reductions in myocardial inflammation and necrosis in rabbits undergoing heterotopic cardiac transplantation (Cowan et al., 1996). This was associated with a marked attenuation of myocardial elastolytic activity in transplanted hearts. Transgenic mice over-expressing full-length human elafin under the control of the vascular pre-proendothelin promoter exhibit complete inhibition of tissue elastolytic activity following acute myocardial infarction and carotid arterial wire denudation (Ohta et al., 2004a, Zaidi et al., 2000a). These favorable treatment effects consistently occurred with reduced tissue myeloperoxidase content in keeping with less neutrophil recruitment. It was not possible to access myocardial tissue for assessment of neutrophil infiltration and elastolytic activity but the significant reduction in peak elastase concentration leaves

open the possibility of an Elafin effect on neutrophil activation and degranulation which if present was not large enough to translate into a reduction in AUC elastase at 6 hours.

The EMPIRE patients exhibited increased IL-8 and IL-6 production and increased levels of circulating hs-CRP in keeping with a post-ischemic inflammatory response following CABG. A systemic inflammatory response follows CABG surgery driven both by major surgical insult and contact activation of blood with artificial surfaces of the extracorporeal circuit (Day and Taylor, 2005). Belief that magnitude of this response may drive clinical outcome has led to trials examining interventions to reduce post-operative inflammation. Peak and AUC hs-CRP, IL-6 and IL-8 release were similar between treatment groups. This result for Elafin contrasts with previous work indicating broad ranging anti-inflammatory activity in human endothelial cells and monocyte-derived macrophages. It has been demonstrated that overexpression of elafin reduced production of IL-8 and TNF-α by cultured human endothelial cells and monocyte derived macrophages respectively in response to inflammatory stimuli (Henriksen et al., 2004b). Elafin effect was mediated by reduced NF-κB regulated gene transcription through inhibition of degradation of the inhibitory IκBα subunit. This work has been replicated by others using a human myelomonocytic cell line with the same recombinant Elafin used in the EMPIRE study (Butler et al., 2006). These *in vitro* findings suggested the potential of Elafin to work beyond neutralisation of elastase in suppressing inflammatory cytokine pathways. The failure of Elafin to suppress IL-8 production during CABG surgery may indicate that additional inflammatory pathways are active or that despite impacting on circulating elastase activity, Elafin is not reaching or is not active in the subcellular space between neutrophils and their target tissue. Large quantities of oxidants and

proteases released by neutrophils recruited to the site of inflammation can overwhelm and inactivate protease inhibitors. Adhesion of neutrophils to the extracellular matrix and release of elastase in association with neutrophil extracellular traps may compartmentalize the protease between the neutrophil and matrix and this microenvironment excludes larger circulating protease inhibitors such as α1-PI (Owen et al., 1995).

ONO-6818 and Sivelestat are synthetic inhibitors of elastase that reduced IL-8 production in models of a cardiopulmonary bypass circuit using human blood (Yoshimura et al., 2003, Matsuzaki et al., 2005) Aprotinin a serine protease inhibitor with broad ranging inhibitory activity provided proof of principle that pharmacological intervention can reduce inflammatory cytokine production in CABG patients. Aprotinin infusion led to a 5-fold fall in peak IL-8 release at the end of cardiopulmonary bypass and 4-fold reduction in IL-6 at 4 h in CABG patients (Isbir et al., 2001, Tassani et al., 2000). Clinical use of this drug was halted following evidence of serious renal, cardiac and cerebral events in a large observational study of 4374 patients (Mangano et al., 2006). Elafin infusion was safe. There were no drug related adverse events in this high-risk surgical group and no evidence of excessive bleeding, cardiovascular complications or renal dysfunction. Given lack of a conclusive therapeutic effect on myocardial injury and post-ischemic inflammation it is not surprising that the exploratory clinical endpoint of post-operative ITU stay was no different between treatment groups.

In conclusion, despite the body of work indicating therapeutic potential from several groups using different models, species and modes of augmentation, Elafins' promise as a therapeutic agent to attenuate myocardial ischemia-reperfusion injury and

inflammation was not translated in this first phase II study. Post-hoc analysis identified reduced cTnI concentrations at 6 h in Elafin treated patients and it is possible that a bigger dose would have conferred protection out to 48 hours. Elafin was safe and lack of treatment effect was seen despite achieving high plasma Elafin concentrations and halving of circulating elastase activity.

Chapter 5: Assessment Of Cellular Inflammation Post Coronary Bypass Grafting Surgery – Empire Sub-study

5.1 Summary

Very little is known about myocardial inflammation following CABG surgery. In Chapter 3: (page 89) it was established that CMR enhanced USPIO can identify cellular inflammation in the infarct zone post ST-elevation infarction. The work in this chapter investigated if this technique could be used in the post CABG surgery setting, and whether Elafin reduced cellular inflammation as assessed by USPIO enhanced scanning.

The work presented in this chapter pertains to a sub-study of EMPIRE, the randomised double blind placebo controlled parallel group clinical trial described in Chapter 6:. 54 patients undergoing CABG surgery were randomized 1:1 to intravenous Elafin 200 mg or saline placebo after induction of anesthesia and prior to sternotomy and underwent USPIO infusion and CMR scanning within 14 days of surgery. Quantitative analysis of USPIO accumulation was achieved by calculation of T2* relaxation times before and after administration of USPIO. A variety of analysis techniques were explored. Plasma inflammatory biomarkers and hs-cTnI was tested in all patients.

USPIO-defined cellular myocardial inflammation following coronary artery bypass surgery ranged from levels seen in healthy volunteers to those associated with type 1 myocardial infarction (median 80.2 [IQR 67.4 to 104.8] /s). Although there was an

increased pan-myocardial uptake of USPIO, focal inflammation was best detected by taking the average of the top 3 R2* values in a 17-segment model. Macrophage recruitment into the myocardium correlated weakly with hsCRP, but there was no correlation with hs-cTnI or CPB time. There was no treatment effect of Elafin detected by USPIO enhanced CMR.

Inflammatory markers rise post CABG surgery, and cellular inflammation can be detected by USPIO CMR. Humoral and cellular inflammation was co-ordinated, however the magnitude of myocardial inflammation was not dependent on degree of myocardial injury (hs-cTnI) or ischemia time. Elafin did not attenuate cellular inflammation as assessed by USPIO.

5.2 INTRODUCTION

During coronary artery bypass graft surgery, the myocardium receives an immediate ischaemic insult that is exacerbated by post-ischaemic reperfusion inflammatory responses leading to increased myocardial injury. Inflammation within the infarcted myocardium is associated with induction of endothelial adhesion molecules and enhanced permeability of the microvasculature. Up regulation of chemokines including interleukin IL-8 and monocyte chemoattractant protein (MCP)-1 attracts neutrophils and monocytes to the site of injury. Early reperfusion therapy amplifies this inflammatory cell influx and accelerates the healing response through proliferative and maturation phases. Neutrophil adhesion to the endothelium of infarcted myocardium occurs within minutes of reperfusion. Ischaemic cardiomyocytes are further injured by adherent neutrophils that release reactive oxygen species and destructive proteases including HNE and proteinase 3. HNE has a wide range of substrates including matrix components elastin, fibronectin, and collagen types III and IV. Activated neutrophils also occlude microvessels and increase endothelial permeability contributing to myocardial oedema. Capillary plugging and obstruction by activated neutrophils contributes to failure of microvascular perfusion and increased infarct size within the ‘no-reflow’ zone.

Non-invasive techniques to assess inflammation in the myocardium are limited. Inflammatory cells have high glycolytic activity, and the glucose component of ^{18}F-fluorodeoxyglucose (^{18}F-FDG) can cross cell membranes to become phosphorylated and trapped. This can then be imaged using positron emission tomography (PET). This has been utilised to assess myocardial inflammation associated with sarcoidosis (Skali et al., 2013). Although this technique is sensitive, it relies on suppression of glucose uptake in normal myocardium. This is both difficult and unreliable in clinical

practice. Clinical CMR has been utilised by using water sensitive T2 sequences to identify oedema, but will only identify this consequence of inflammation rather than the cellular infiltration (Friedrich and Marcotte, 2013). Pre-clinical studies have utilised direct labelling of white cells, but have not yet been developed for clinical practice (Riou et al., 2002). Non-invasive imaging of cellular infiltration would allow early identification and quantification of the pathological process and identify patients suitable for modulation of inflammation. The efficacy of therapeutic interventions could also be monitored with such a technique and potentially provide prognostic information.

In preclinical studies Elafin delivery and gene overexpression is associated with reduced myocardial injury and preserved left ventricular function following ischaemia and infarction. This effect is associated with reduced neutrophil infiltration and elastase activity at the site of injury. Activated neutrophils facilitate monocyte recruitment. Granule contents including LL-37, azurocidin and human neutrophil peptides 1-3 have direct chemotactic activity on monocytes. Neutrophil-derived proteases induce chemokine, MCP-1 and IL-8 production from endothelial cells and their effects on matrix components produce degradation products with chemotactic activity for monocytes (Richardson et al., 1976, Postlethwaite and Kang, 1976, Norris et al., 1982).

As discussed in Chapter 3:(page 89), USPIO have the capacity to extravasate through capillaries and be taken up by tissue inflammatory cells of the reticuloendothelial system (Ruehm et al., 2001a). These cells are predominately macrophages, but neutrophils have also been shown to take up USPIOs (Dousset et al., 1999, Gellissen et al., 1999b). This model of USPIO-enhanced MRI can highlight areas of

inflammation in models of vertebral osteomyelitis, aortic atherosclerosis, arthritis-induced hyperperfusion, autoimmune encephalomyelitis, nephritis and nephropathy, cerebral ischaemia, renal ischaemia (Bierry et al., 2008, Dousset et al., 1999, Ruehm et al., 2001a, Hauger et al., 2000, Rausch et al., 2001b, Lutz et al., 2006, Jo et al., 2003b). USPIOs can be used to assess cellular vascular inflammation in patients with abdominal aortic aneurysms (Richards et al., 2011b). Histological examination of aneurysm tissue confirmed co-localization and uptake of USPIOs in areas with macrophage infiltration and this was associated with a 3-fold increase in the rate of abdominal aortic aneurysm expansion.

The data presented in Chapter 4: established proof-of-concept that USPIOs can be used to image the myocardium in patients having sustained a recent acute myocardial infarction. The data demonstrates that there is a marked and clear uptake of USPIOs in the week following acute myocardial infarction and there is a 2-3 fold increase in the R2* value in the infarct and peri-infarct area. As a negative control, little or no change in the R2* value was observed in the myocardium remote from the site of ischaemia or skeletal muscle.

In this chapter, USPIO enhanced CMR scanning was used to demonstrate cellular inflammation in the myocardium post CABG surgery, and to investigate if Elafin reduce neutrophil mediated post-ischaemic myocardial injury. We investigated four different protocols for analysing R2* signal change in the myocardium.

In post hoc analysis, we investigated USPIO uptake in other tissues. We recorded R2* signal change in the kidney, skeletal muscle and organs of the reticuloenothelial system and examined variation in R2* with Elafin treatment in these organs.

5.3 METHODS

See Chapter 2: (page 62).

5.4 RESULTS

5.4.1 COMPLETION OF SCANNING PROTOCOL

In total, 54 patients underwent USPIO infusion and CMR scanning within 14 days of surgery. USPIO infusion was well tolerated, with only 1 patient reporting muscle cramps after administration. 2 patients had ECG evidence of acute graft or coronary artery occlusion post surgery, and were excluded. Therefore 52 patients had available data for USPIO analysis, and these were compared with 10 contemporaneous healthy volunteers (Chapter 3, mean age 26±5 years, 5 male and 5 female) for reference. The data from Chapter 3:(page 89) analysing the infarct zone of patients who had experienced type 1 myocardial infarction are also provided for comparison (Alam et al., 2012d).

5.4.2 USPIO UPTAKE: ELAFIN VS PLACEBO

5.4.2.1 MYOCARDIUM

As described in chapter 2 (page 84), three methods of data analysis were employed (Table 5-1, Table 5-2, Figure 5.1).

Table 5-1 USPIO uptake from all myocardial segments

	Mean pan-myocardial R2* Value (s^{-1})		Mean R2* increase for highest 3 segments (s^{-1})		Sum of 3 segments with highest R2* increase (s^{-1})	
	PLACEBO	ELAFIN	PLACEBO	ELAFIN	PLACEBO	ELAFIN
Number of values	24	28	24	28	24	28
25% Percentile	38.2	38.9	55.3	53.6	166.0	160.8
Median	47.4	53.1	64.5	73.5	193.4	220.4
75% Percentile	58.6	67.7	76.9	92.6	230.6	277.9
Mean	49.3	56.0	66.9	76.3	200.7	228.9
Std. Deviation	18.4	20.6	20.5	28.2	61.4	84.5
Std. Error of Mean	3.8	3.9	4.2	5.3	12.5	16.0
Lower 95% CI of mean	41.6	48.0	58.3	65.4	174.8	196.1
Upper 95% CI of mean	57.1	64.0	76.0	87.2	227	261.6

Table 5-2 USPIO uptake from all myocardial segments excluding the apex

	Mean pan-myocardial R2* Value (s^{-1})		**Mean R2* increase for highest 3 segments (s^{-1})**		**Sum of 3 segments with highest R2* increase (s^{-1})**	
	PLACEBO	ELAFIN	PLACEBO	ELAFIN	PLACEBO	ELAFIN
Number of values	24	28	24	28	24	28
25% Percentile	38.2	38.9	55.3	53.6	166.0	160.8
Median	47.4	53.1	64.5	73.5	193.4	220.4
75% Percentile	58.6	67.7	76.9	92.6	230.6	277.9
Mean	49.3	56.0	66.9	76.3	200.7	228.9
Std. Deviation	18.4	20.6	20.5	28.2	61.4	84.5
Std. Error of Mean	3.8	3.9	4.2	5.3	12.5	16.0
Lower 95% CI of mean	41.6	48.0	58.3	65.4	174.8	196.1
Upper 95% CI of mean	57.1	64.0	75.5	87.2	226.6	261.6

Figure 5.1 Myocardial USPIO uptake

Box-and-whisker plots of USPIO uptake as an average of all segments (left), average of the 3 segments with the highest uptake (centre) and the sum of the 3 highest segments. The upper panel includes data from all 17 segments, the bottom panel excludes data from the apex.

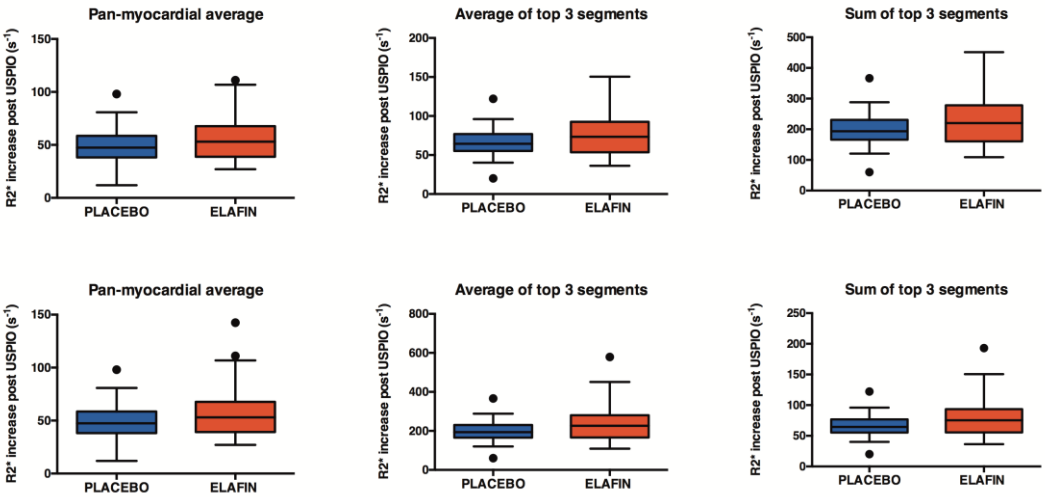

Patients receiving placebo had a median pan-myocardial R2* signal of 52.0 [interquartile range 41.5 to 60.4] s^{-1}. This was not significantly different to patients receiving Elafin: 57.8 [interquartile range 49.3 to 71.1] s^{-1} (p=0.20). There was no difference between placebo and Elafin groups if only scans performed within 7 days of surgery were analysed; placebo 78.5 [interquartile range 65.6 to 101.0] s^{-1}, Elafin 86.8 [73.5 interquartile range to 102.7] s^{-1} (p=0.44). Similarly, there was no significant difference when excluding the cardiac apex; placebo median R2* increase 47.4 [interquartile range 38.2 to 58.6] s^{-1}, Elafin 53.1 [interquartile range 38.9 to 67.7] s^{-1} (p=0.27).

Using the average for the three segments with the highest R2* increase, there was no difference between placebo and Elafin groups; placebo median 74.4 [interquartile range 65.8 to 87.4] s^{-1}, Elafin 87.5 [interquartile range 74.0 to 113.8] s^{-1} (p=0.10). There was no difference between placebo and Elafin groups if only scans performed within 7 days of surgery were analysed; placebo 84.1 [interquartile range 70.1 to 113.2] s^{-1}, Elafin 88.3 [81.9 interquartile range to 109.7] s^{-1} (p=0.51). There was also no difference when excluding the apex; placebo median 64.5 [interquartile range 55.3 to 76.9] s^{-1}, Elafin 73.5 [interquartile range 53.6 to 92.6] s^{-1} (p=0.10).

Using the sum for the three segments with the highest R2* increase, there was no difference between placebo and Elafin groups; placebo median 221.8 [interquartile range 191.9 to 260.4] s^{-1}, Elafin 262.6 [interquartile range 222.1 to 341.4] s^{-1} (p=0.07). There was also no difference when excluding the apex; placebo median 193.4 [interquartile range 166.0 to 230.6] s^{-1}, Elafin 220.4 [interquartile range 160.8 to 277.9] s^{-1} (p=0.24).

The mean number of "segments with significant USPIO uptake" was 9.1 (95% CI -7.0 to 11.1) in the placebo group. This was not significantly different to the Elafin group; 8.9 (95% CI 6.8 to 10.9), $p = 0.94$.

5.4.2.2 SKELETAL MUSCLE AND RETICULOENDOTHELIAL SYSTEM UPTAKE

There was no significant difference in R2* increase in skeletal muscle between elafin and placebo groups (p=0.22) (Table 5-3). Similarly, there was no significant difference in tissues of the reticuloendothelial system (Table 5-4).

Table 5-3 R2* increase in skeletal muscle post CABG (Elafin vs Placebo).

The data was normally distributed.

	Elafin	Placebo	p value
Mean (s^{-1})	15.1	20.9	0.22
Std. Deviation	20.2	18.0	
Std. Error of Mean	3.5	3.2	
Lower 95% CI of mean	8.4	14.4	
Upper 95% CI of mean	22.2	27.4	

Table 5-4 Increase in R2* in the reticuloendothelial system (Elafin vs Placebo).

The data was not normally distributed.

	Elafin	Placebo		Elafin	Placebo		Elafin	Placebo	
	Liver	Liver	p value	Spleen	Spleen	p value	Bone marrow	Bone marrow	p value
25% Percentile	193	194		243	273		75.5	47.2	
Median (s^{-1})	236	228	0.81	298	309	0.48	178	176	0.61
75% Percentile	270	268		362	369		265	238	

5.4.2.3 KIDNEYS

Post-hoc analysis of renal USPIO uptake showed that in the Elafin group, R2* increased non-significantly from 79.9±19.7 s^{-1} to 95.10±36.6 s^{-1} (p=0.07). When only scans performed within a week of surgery were analysed, the R2* increase in the placebo group was significantly higher than the elafin group; 99.9±35.6 s^{-1} versus 77.6±19.3s^{-1} respectively (p=0.03)

The renal R2* increase in healthy volunteers was 64±15.8 s^{-1}. Compared to the study population there was no significant difference compared to the Elafin group (p>0.1), but the placebo group had a larger R2* increase (p<0.001) (Figure 5.2). This was true for scans performed both with 7 days or 14 days of surgery.

There was no significant difference in the absolute post-operative creatinine clearance, nor in the change in creatinine clearance from pre to post surgery between Elafin and placebo groups; p=0.98 and p=0.73 respectively (Table 5-5, Table 5-6).

Table 5-5 Change in creatinine levels and creatinine clearance pre and post CABG surgery in Elafin group.

	Baseline creatinine (µmol/L)	24 hour post-surgery creatinine (µmol/L)	48 hour post-surgery creatinine (µmol/L)	Pre-surgery creatinine clearance (ml/min)	Post-surgery peak creatinine (µmol/L)	Post-surgery creatinine clearance (ml/min)	Change in creatinine clearance (ml/min)
25% Percentile	61.5	60.0	60.0	94.0	64.5	78.5	0.0
Median	72.0	69.0	68.0	126.1	76.0	109.6	-11.7
75% Percentile	84.0	85.0	87.5	149.8	96.5	129.5	-23.8
Mean	74.4	76.5	78.1	125.8	89.9	109.3	-16.5
Std. Deviation	16.0	28.5	37.9	37.3	46.1	32.5	-32.3
Std. Error of Mean	2.4	4.3	5.7	6.3	7.6	5.5	-5.5

Table 5-6 Change in creatinine levels and creatinine clearance pre and post CABG surgery in Placebo group.

	Baseline creatinine (µmol/L)	24 hour post-surgery creatinine (µmol/L)	48 hour post-surgery creatinine (µmol/L)	Pre-surgery creatinine clearance (ml/min)	Post-surgery peak creatinine (µmol/L)	Post-surgery creatinine clearance (ml/min)	Change in creatinine clearance (ml/min)
25% Percentile	66.0	61.8	63.0	90.8	73.0	80.0	-0.6
Median	74.5	71.5	72.0	104	85.0	89.4	12.3
75% Percentile	86.3	81.5	89.0	124	99.5	112	21.9
Mean	76.7	76.8	82.8	109	92.0	93.4	15.7
Std. Deviation	14.9	24.7	34.3	30.8	32.4	26.0	26.3
Std. Error of Mean	2.3	3.8	5.3	5.2	5.3	4.4	4.4

Figure 5.2 Increase in R2* values in renal tissue

Mean and 95% confidence intervals. Blue – CABG patients receiving placebo. Red – CABG patients receiving Elafin. Green – Healthy volunteers.

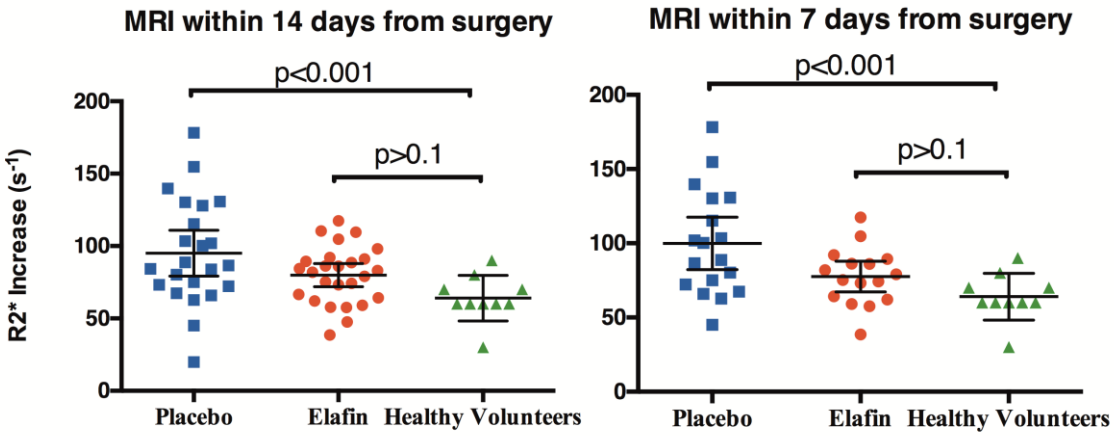

5.4.3 USPIO UPTAKE: POOLED RESULTS

5.4.3.1 MYOCARDIAL UPTAKE POST CABG SURGERY

Since there was no demonstrable treatment effect of Elafin, data from both arms of the study were combined to assess post-CABG surgery inflammation. Patients undergoing CABG had increased pan-myocardial R2* (median 54.8 [interquartile range 43.8 to 68.4] s^{-1} versus 41.2 [32.6 to 50.4] s^{-1} in healthy volunteers, $p<0.05$) (Figure 5.3). It was also increased in the highest 3 of the 17 segments (median 80.2 [67.4 to 104.8] s^{-1} versus 58.7 [48.8 to 68.6] s^{-1} in healthy volunteers, $p<0.0001$) and was similar to patients who had sustained type 1 myocardial infarction (109.5 [87.5 to 128.3] s^{-1}, $p=0.41$). Figure 5.4 provides comparison of the R2* increase compared to infarcted myocardium, healthy myocardium and to skeletal muscle.

Figure 5.3 Left – Pan-myocardium R2* increase in healthy volunteers (n=10) and post-coronary artery bypass graft (CABG) surgery.

Median and inter-quartile range.

Right - Tukey box plot comparing R2* increase in the myocardium of (a) patients with acute myocardial infarction (remote from the site of infarction), (b) healthy volunteers, (c) patients post-CABG surgery (pan-myocardial average), (d) patients post-CABG surgery (average of 3 highest values from 17 segment model), and (e) patients with acute myocardial infarction (site of infarction).

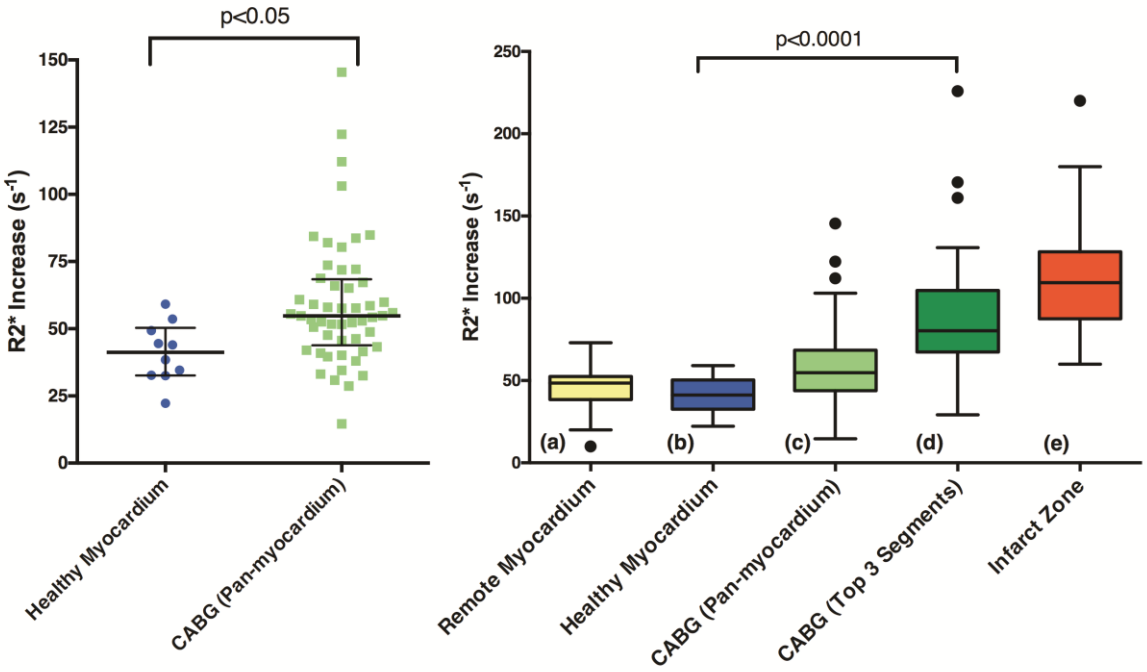

Figure 5.4 R2* increase in the myocadium of patients suffering MI, undergoing CABG surgery and healthy volunteers compared to skeletal muscle uptake.

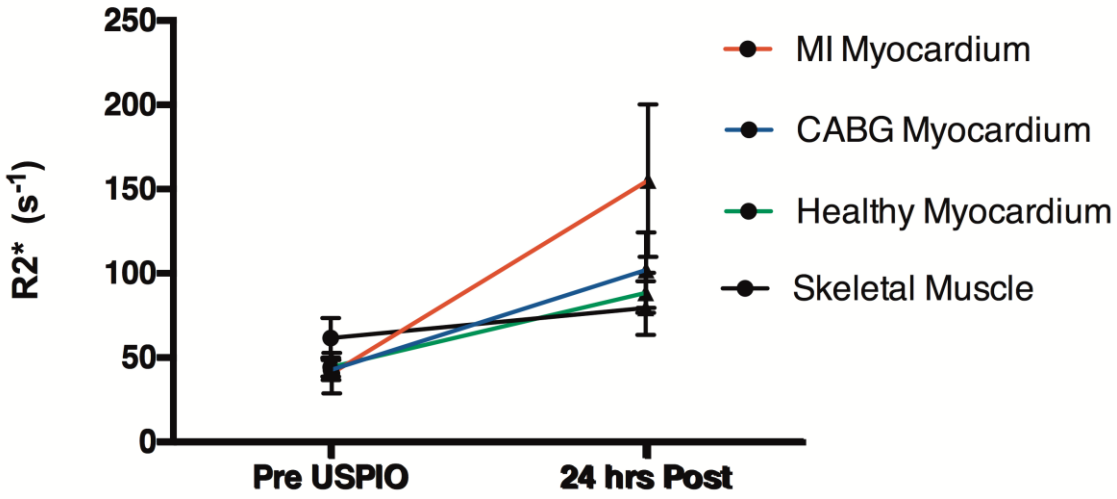

Using data from the healthy volunteers, a significant increase in the myocardial segments with USPIO uptake could be defined by the upper 95% confidence interval (>49 s^{-1} increase in R2*), or by the 75% percentile (>51s^{-1} increase in R2*). The median number of segments with significant USPIO uptake was higher in the post surgical group (9.5 [interquartile range 5 to 13]) compared to healthy volunteers (3.5 [interquartile range 0 to 6.75], p=0.005) (Figure 5.5) regardless of the definition used.

Figure 5.5 Number of myocardial segments with significant USPIO uptake.

Left – CABG patients (red). Right – Healthy volunteers (green).

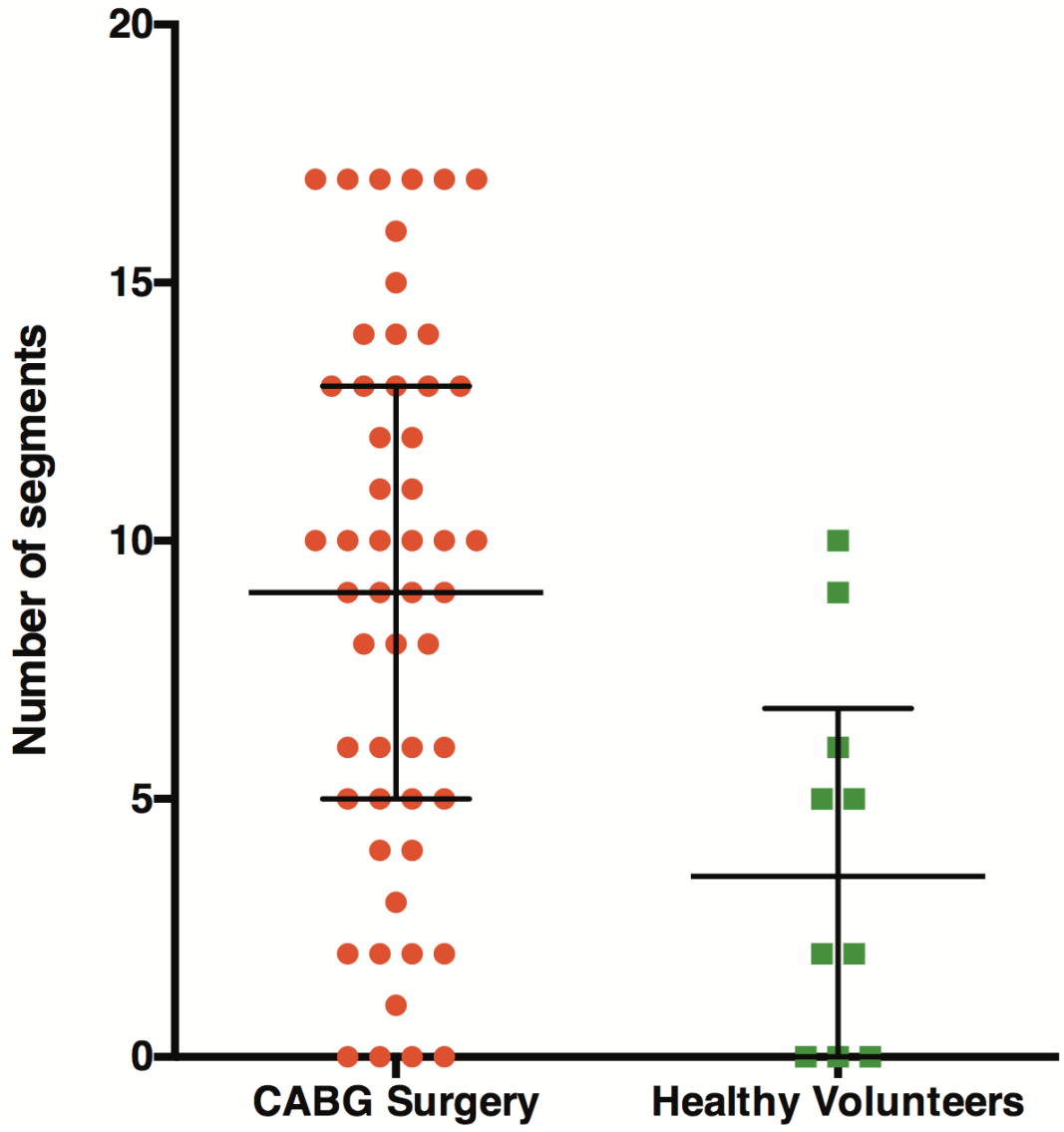

R2* increase correlated with plasma hsCRP concentrations in CABG surgery patients (Figure 5.6; r=0.3, p=0.03) but not with cTnI release (r=0.15, p=0.15) or CPB time (r=0.00, p=0.49).

Figure 5.6 hsCRP vs R2* increase in the myocardium.

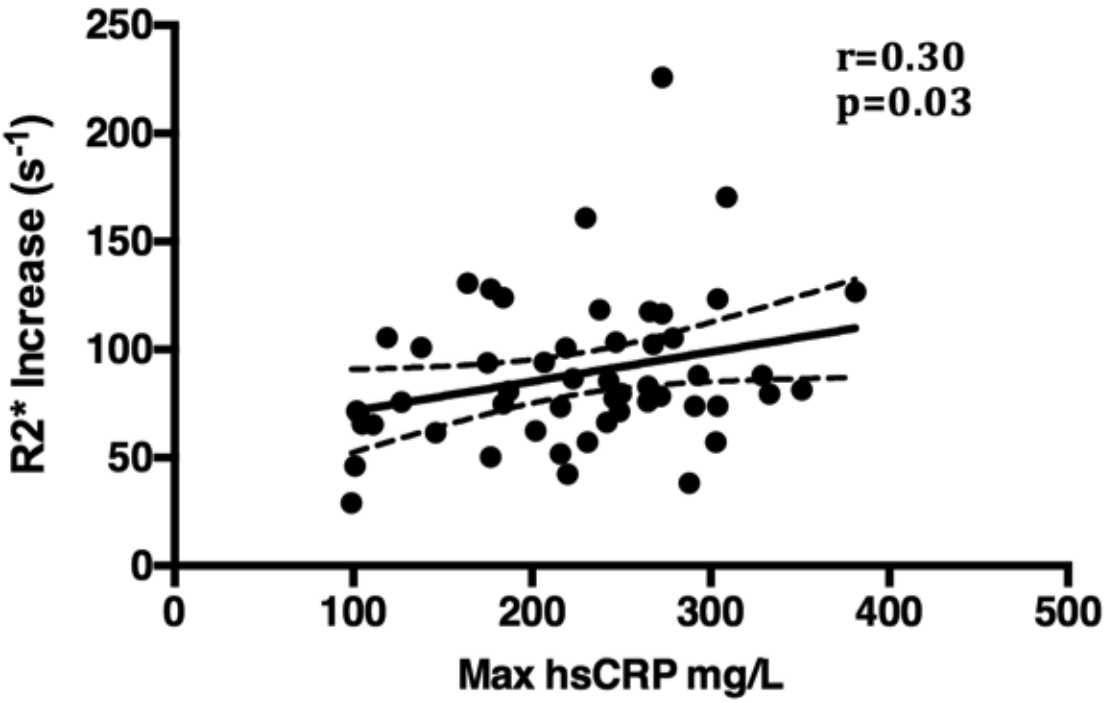

5.4.3.2 SKELETAL MUSCLE AND RETICULOENDOTHELIAL SYSTEM.

In patients undergoing CABG surgery, there was a small increase in skeletal muscle R2* from median 60.1 [interquartile range 52.3 to 70.1.] s^{-1} to 76.2 [interquartile range 67.0 to 87.9] s^{-1} (Table 5-7). The absolute blood pool R2* value rose from 29.9±14.0 s^{-1} to 126.9±49.6 s^{-1}.

Increase in R2* in the reticuloendothelial system is shown in **Table 5-8**. The spleen R2* value rose greatly from 63.7 [interquartile range 45.5 to 84.7] s^{-1} to 367.7 [interquartile range 317.3 to 422.9] s^{-1}. Bone marrow R2* also rose from 314.0 [interquartile range 276.4 to 348.2] s^{-1} to 515.5 [interquartile range 440.2 to 561.9] s^{-1}.

Table 5-7 Increase in R2* from pre to post surgery in skeletal muscle.

	CABG	Healthy Volunteers	
	Skeletal Muscle	**Skeletal Muscle**	**p value**
Mean (s^{-1})	18.1	19.7	0.81
Std. Deviation	18.7	17.9	
Std. Error of Mean	2.4	5.7	
Lower 95% CI of mean	13.3	6.9	
Upper 95% CI of mean	22.9	32.4	

Table 5-8 Increase in R2*in the reticuloendothelial system in CABG patients compared to healthy

P values have been given for parametric or non-parametric tests as appropriate.

	CABG	HV		CABG	HV		CABG	HV	
	Liver	Liver	p value	Spleen	Spleen	p value	Bone Marrow	Bone Marrow	p value
25% Percentile	193	215		259	265		63.8	233	
Median R2* (s^{-1})	232	221	0.88	306	290		175	275	0.01
75% Percentile	269	252		371	415		240	301	
Mean R2* (s^{-1})	228	229		304	311	0.84	177	272	
Std. Deviation	51.9	25.2		90.2	93.0		139	83.8	
Lower 95% CI of mean	215	210		281	244		142	212	
Upper 95% CI of mean	241	247		328	377		213	331	

CABG – Coronary Artery Bypass Grafting, HV – Healthy Volunteers.

There was no significant increase in the splenic R2* values of cardiac patients compared to healthy volunteers (290.0 [interquartile range 265.4 to 414.5] s^{-1}, p=0.83). However the bone marrow rise in healthy volunteers was significantly higher (275.0 [interquartile range 232.8 to 301.0] s^{-1}, p=0.01).

5.5 DISCUSSION

In this chapter, USPIO contrast was used for the first time to assess in vivo myocardial inflammation following CABG surgery in a randomised controlled trial examining myocardial protection and anti-inflammatory effects of Elafin. We found no significant difference in cellular inflammatory cell infiltration between patients treated with Elafin and those receiving placebo. Even when only scans performed within 7 days of surgery were analysed to mitigate the effects of resolving inflammation, no difference was detected. This was consistent with systemic biomarker results reported in Chapter 4:.

The average pan-myocardial USPIO uptake was higher in patients following CABG surgery than that of healthy myocardium from controls. However it would be expected that inflammation would not be uniform throughout the heart following CABG surgery given variation in the distribution and severity of coronary disease and surgical factors. Using the average USPIO uptake in the three segments with the highest uptake, a 2-fold increase was identified compared to the pan-myocardial values. Macrophage recruitment into the myocardium correlated weakly with hsCRP suggesting an association with humoral and cellular inflammation. However there was no correlation with hs-cTnI or CPB time indicating that the magnitude of myocardial inflammation was not dependent on degree of myocardial injury or ischemia time. The determinants and the sequelae of higher levels of cellular inflammation post-CABG surgery require further study.

Four separate methods for USPIO analysis were examined. A pan-myocardial R2* increase was demonstrated post CABG surgery. This approach would be expected to miss focal areas of inflammation. Consequently the average USPIO uptake from the

three highest segments was preferred. This method is more sensitive for detecting focal inflammation, and averaging three segments diminishes the possibility of false positives resulting from artefact or blood pooling. Summing the three highest segments did not appear to provide any further advantage. The number of segments with significantly increased USPIO uptake was greater in the post CABG population compared to healthy volunteer myocardium. This approach holds promise and could be used to better describe regional variations in myocardial inflammation. In this study the R2* value determining a significant increase was taken arbitrarily, as > 75^{th} percentile from a population of 10 healthy volunteers. A larger study form matched controls could be used to determine a more robust value before instituting this method.

Skeletal muscle was used as a marker of blood perfusion since it can be assumed that perfusion at rest would be relatively constant. Indeed, R2* increase was 19.7±17.9 s^{-1} in healthy volunteers compared to 17.0±20.5 s^{-1} in CABG patients. There was a correlation between skeletal muscle and cardiac R2* increase in the healthy volunteers, confirming he contribution of USPIO blood perfusion. However there was no such correlation in CABG patients. This combined with the significantly larger increase in R2* values, in both patients undergoing CABG surgery or suffering myocardial infarction, indicated that USPIO accumulation in the myocardium of CABG patients was more than simply perfusion (Figure 5.4).

We found no difference in the Elafin and placebo groups in terms of USPIO uptake in skeletal muscle. The inflammatory insult does prime and release neutrophils systemically, followed by a decrease in circulation suggesting sequestration (Botha et al., 1995). Furthermore, endothelial induction of ICAM-1 and VCAM-1 during CPB initiates extravascular movement of neutrophils and monocytes (Patel et al., 2002). However there is complex kinetics of inflammatory cells following surgery that is reflected in different cell phenotypes and dynamic cytokine release (Pillay et al., 2007). Differing amounts of neutrophil infiltration is seen in various organs following systemic inflammation caused by trauma (Nuytinck et al., 1988). It is likely that inflammatory cell infiltration occurs predominately at sites of tissue injury, ischaemia-reperfusion and infarction caused by emboli or thrombosis. Therefore skeletal muscle is unlikely to be significantly infiltrated by monocytes following systemic inflammatory response of surgery. There was also no difference in hepatic uptake, and this may reflect avid uptake by Kupffer cells regardless of inflammatory status. There was also no difference in the spleen or bone marrow despite the role these tissues play in systemic inflammation. The spleen has been identified as a reservoir of monocytes following myocardial infarction (Swirski et al., 2009a). Pre-clinical models have shown pro-inflammatory monocytes are released by the spleen to take up residence with the infarcted myocardial infarction and potentially develop into macrophages (Nahrendorf et al., 2007b). However we did not demonstrate a significant difference in USPIO uptake in the spleen post cardiac surgery compared to healthy volunteers. Patients were scanned at least five days following surgery and key changes in inflammatory cell activity may have subsided by then. The healthy volunteers provide a reference but were not matched for age or

other co-morbidity and these factors may contribute to the USPIO signal in the spleen. Although there was a lower R2* increase in the spleens of patients with myocardial infarction studied in chapter 3 ($259.0 \pm 145\ s^{-1}$) suggesting monocyte release, this was not significant. This may have been due to the varied times from infarction to scanning (73±30 hours). Nahrendorf et al demonstrated a change in the prevailing subsets of monocytes at day five following infarction, from cells responsible for inflammation to those having attenuated inflammatory and pro-angiogenic properties. When pooling data for all patients undergoing surgery, even though the bone marrow of CABG patients demonstrated lower USPIO uptake overall, there was a large overlap with values from healthy volunteers. Cardiac surgery has been shown to release bone marrow resident progenitor cells (Dotsenko et al., 2010). CD14++ monocyte leave the bone marrow and differentiate into different subsets in cardiovascular disease (Zawada et al., 2012, Dutta and Nahrendorf, 2015). The overall reduction in bone marrow USPIO uptake demonstrated may reflect depletion of these progenitor cells.

Acute kidney injury (AKI) complicates up to 30 % of patients following cardiac surgery (Parolari et al., 2012). The 30-day mortality of patients who develop a 0 to 44.2 μmol/L or >44.2 μmol/L rise in serum creatinine is 2.77 or 18.64-fold higher, respectively, than patients without a change in serum creatinine (Lassnigg et al., 2004). However, creatinine is an insensitive marker of renal injury since it will not be higher than the normal range until 50% of the renal function is lost (Najafi, 2014, Bagshaw and Gibney, 2008). As such the lack of correlation between creatinine and renal inflammation detected by USPIO may have been due to lack of an adequate biomarker. AKI associated with cardiac surgery is caused by a combination of factors including sympathetic nervous system induced vasoconstriction,

hypoperfusion, atheroembolism, formation of reactive oxygen species and systemic inflammation. All these processes lead to leucocyte recruitment and renal infiltration by neutrophils, macrophages and lymphocytes (O'Neal et al., 2016). During cardiac surgery in particular, there are macro and micro emboli generated by aortic cannulation and cross-clamping that can lead to kidney injury (Sreeram et al., 2004). Although maintaining that mean arterial pressures on CPB >70 mmHg leads to higher intraoperative creatinine clearances, this does not seem to change postoperative renal function as compared with pressures between 50 and 60 mmHg (Urzua et al., 1992).

Elevated inflammatory biomarkers are associated with post cardiac surgery acute renal injury and mortality (Zhang et al., 2015). Elafin is produced from epithelial surfaces including the kidney. For this reason we examined renal USPIO signal post hoc in CABG surgery patients. Serum creatinine increased post CABG surgery and there was no difference in renal function between Elafin and placebo treated groups.

There was decreased renal USPIO uptake in patients treated with Elafin compared to placebo. This was evident in patients who had CMR scanning within 7 days of surgery, with a non-significant decrease when patients with later scan dates were included in the analysis. This finding is consistent with renal infiltration with monocytes, with inflammation decreasing with time. Compared to healthy volunteers, renal R2* values were increased in placebo but not Elafin treated when including all patients scanned within 14 days of surgery. Neutrophils are central to renal ischaemia-reperfusion injury (Welbourn et al., 1991, Okusa, 2002), and there is massive infiltration in the cortex and outer medulla (Willinger et al., 1992). Neurophil elastase is a potent enzyme involved in inflammation and damage of renal

tissue (Oda et al., 1997). Sivelestat, a synthetic neutrophil elastase inhibitor, attenuates sepsis related kidney injury in rats (Li et al., 2016). Neutrophil activation and infiltration leads to monocyte recruitment (Soehnlein et al., 2009). Reducing monocyte/macrophage accumulation in the renal parenchyma reduces ischaemia-reperfusion injury (Nagata et al., 2016). The post-hoc analysis was consistent with the possibility that Elafin inhibition of neutrophil elastase reduced the inflammatory cascade in kidneys, ultimately reducing monocyte/macrophage tissue residence. This was not reflected in changes in creatinine levels, the only available measure of glomerular filtration rate between placebo and Elafin groups. As previously stated, creatinine is an inadequate measure of acute kidney injury. Neutrophil gelatinase-associated lipocalin (NGAL), cystatin C, KIM-1, and IL-18 rise within 6 hours of cardiac surgery and correlate with AKI and precede elevation in creatinine levels (Boldt and Wolf, 2008, Cruz et al., 2010, Haase et al., 2009, Ristikankare et al., 2010). Blood NGAL levels can be detected in response to ischemic injury and its' early appearance is independent of glomerular filtration rate, and so would have been a superior biomarker to detect subtle AKI associated with renal inflammation. Plasma volume, fluid administration, nephrotoxic drugs and blood pressure affect creatinine levels and renal function separately. Since these factors were not controlled, a correlation between renal inflammation and AKI may have been missed in this study. We were not able to obtain tissue for histological confirmation of monocyte or macrophage infiltration, and so the significance of the increased USPIO uptake remains uncertain. However we did perform a separate pre-clinical study in a allograft model of transplant rejection and renal inflammation (Appendix G:). This study confirmed USPIO localisation within macrophages within the kidneys that can be detected by MRI.

One significant limitation is that USPIO-enhanced scans were carried out at later time points (5 to 14 days post-surgery), this may have hindered our ability to identify some of the correlations with our early (first 48 hours) biomarker assessments.

In conclusion, for the first time we identified differing levels of inflammatory cell infiltrate into the myocardium post CABG. This varied from none to levels similar to infarcted myocardial tissues, and the cause and consequences of this requires further study. Elafin did not attenuate the cellular infiltration into the myocardium post CABG surgery, but did appear to reduce inflammation in renal tissue. There was also evidence of a reduction in cell population in the bone marrow post surgery, which was possible evidence of monocyte progenitor cell egress. USPIO enhanced CMR holds major promise in the non-invasive assessment of myocardial inflammation post surgery.

Chapter 6: Myocardial Inflammation, Injury And Infarction During On-Pump Coronary Artery Bypass Graft Surgery

6.1 Summary

Myocardial inflammation and injury occur during CABG surgery. We aimed to characterise these processes during routine CABG surgery, and to inform the diagnosis of type 5 myocardial infarction.

We pooled data from the EMPIRE study (Chapter 4: page 118) to assess 85 patients with stable coronary artery disease who underwent elective CABG surgery. Myocardial inflammation, injury and infarction were assessed using plasma inflammatory biomarkers, high-sensitivity cardiac troponin I (hs-cTnI) and CMR using late gadolinium enhancement LGE.

Systemic humoral inflammatory biomarkers (myeloperoxidase, interleukin-6, interleukin-8 and c-reactive protein) increased in the post-operative period with C-reactive protein concentrations plateauing by 48 h (median area under the curve (AUC) 7,530 [interquartile range (IQR) 6,088 to 9,027] mg/L/48h). Plasma hs-cTnI concentrations rose by ≥50-fold from baseline and exceeded 10-fold the upper limit of normal in all patients. Two distinct patterns of peak cTnI release were observed at 6 and 24 h. After CABG surgery, new LGE was seen in 20% (n=18) of patients although clinical peri-operative type 5 myocardial infarction was diagnosed in only 9% (n=8). LGE was associated with the delayed 24-h peak in hs-cTnI and its magnitude correlated with AUC plasma hs-cTnI concentrations ($r=0.33$, $p<0.01$) but not systemic inflammation, myocardial inflammation or bypass time. Patients

undergoing CABG surgery invariably have plasma hs-cTnI concentrations >10-fold the 99th centile upper limit of normal that is not attributable to inflammatory or ischemic injury alone. Peri-operative type 5 myocardial infarction is often unrecognised and is associated with a delayed 24-h peak in plasma hs-cTnI concentrations. Inflammatory markers rise post CABG surgery and this model can be used to assess the effect of anti-inflammatory agents such as Elafin.

6.2 INTRODUCTION

Over 300,000 coronary artery bypass graft (CABG) operations are performed each year in the United States of America (Diodato and Chedrawy, 2014). Cardiopulmonary bypass (CPB) during these procedures is known to induce systemic and myocardial inflammation (Zahler et al., 1999, Paparella et al., 2002). Inflammatory cytokines such a tumour necrosis factor alpha (TNF-α) depress cardiac function after CPB (te Velthuis et al., 1995), whereas elevations of IL-6 and IL-8 are proportional to levels of myocardial injury and apoptosis (Wan et al., 2002). Elevated cardiac troponin concentrations have been identified in up to 100% of patients undergoing CABG (van Gaal et al., 2011). However, corresponding CMR evidence of myocardial necrosis is evident in only 28% of patients, suggesting that troponin release may reflect reversible injury resulting from other processes such as inflammation or ischemia-reperfusion injury rather than infarction (Noora et al., 2005). The identification of clinically relevant peri-operative myocardial injury and infarction can be challenging but is important because it predicts short, medium and long-term mortality (Onorati et al., 2005, Croal et al., 2006).

The universal definition of myocardial infarction defines procedural (type 5) MI as a >10-fold elevation above the 99th centile of cardiac troponin within 48 hours of CABG surgery accompanied by new pathological Q waves or left bundle branch block, angiographically documented new graft or new native coronary artery occlusion, or imaging evidence of new loss of viable myocardium or new regional wall motion abnormality (Thygesen et al., 2012a). Elevation of plasma cardiac troponin concentration is required but in the absence of these other clinical features, is insufficient to make the diagnosis of type 5 MI.

The latest generation of high-sensitivity cardiac troponin I (cTnI) assays have been widely adopted since the introduction of the third universal definition of MI. These assays have defined normal plasma concentrations in healthy populations and can identify at-risk patients presenting with chest pain and very small elevations in cTnI concentration that would pass undetected by older contemporary assays (Shah et al., 2015b). This increased sensitivity may have consequences for the identification and diagnosis of myocardial infarction in patients undergoing CABG surgery.

Using a comprehensive panel of blood and imaging biomarkers, we explored the relationship between perioperative myocardial inflammation and infarction in order to characterise this injury

6.3 RESULTS

6.3.1 RECRUITMENT AND BASELINE CHARACTERISTICS

Consecutive patients were assessed for eligibility and 53% consented to participate. A total of 189 patients were screened for recruitment of whom 29 were excluded, 79 declined to participate, 88 patients gave informed consent and 1 died before surgery leaving 87 patients to undergo randomisation (Figure 6.1 Study flow diagram). In 85 of the 87 patients, the trial infusion was administered as planned. Patient characteristics and intra-operative details are shown in Table 6-1. Pre-existing (previously unidentified) myocardial infarction was common with 27% (21/79) of patients having pre-operative LGE. Two patients died in the early post-operative period from graft failure and cardiac arrest and a further 6 patients were diagnosed with a MI by the clinical team based on ECG changes and troponin release giving a total of 8 (9%) patients who were clinically diagnosed with type 5 myocardial infarction. Unrecognised type 5 myocardial infarction was identified in a further 10 patients (total of 18; 21%) with new LGE on CMR.

Figure 6.1 Study flow diagram

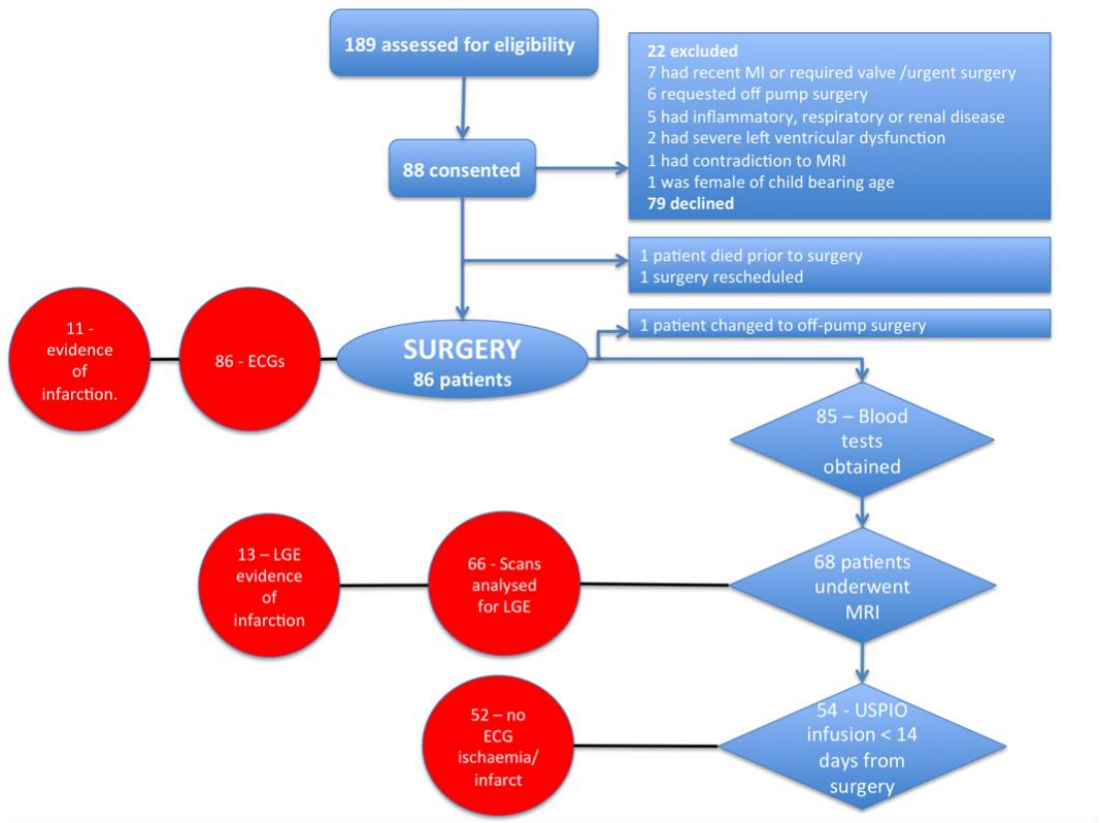

Table 6-1 Baseline patient characteristics.

Mean±SD or n (%)

Age (years)	63±8
2-vessel coronary disease	23 (26%)
3-vessel coronary disease	64 (74%)
Creatinine (mg/dL)	0.90±0.21
Creatinine Clearance (mL/min)	117±35
Diabetes Mellitus	20 (23%)
Surgeon A	34 (39%)
Surgeon B	53 (61%)
Male Gender	74 (85%)
EuroSCORE	2.4±190
Clinically diagnosed previous MI	32/87 (37%)
Clinical diagnosis of previous MI without LGE	7/79 (9%)
LGE without previous clinically recognized MI	21/79 (27%)
Intra-operative details	
Number of bypass grafts	
One	3
Two	33
Three	36
Four	14
Five	1
Cardiopulmonary bypass time (min)	78±24
Cross clamp time (min)	46±15

Overall 25.3% of patients required intra-aortic balloon pump counterpulsation, inotropes or vasoactive support in the first 48 hours, 33% required red cell transfusion, and 31% developed atrial fibrillation prior to discharge (Table 6-2).

Table 6-2 Clinical outcomes.

Mean±SD or n (%)

	<48 h		**In-hospital**	
Post-operative complications and outcomes				
Death	0	(0)	2	(0)
Stroke	0	(0)	0	(0)
Clinically diagnosed Myocardial infarction	1	(2.3)	8	(9)
Inotrope or balloon pump support for > 24h	22	(25.3)	22	(25.3)
Red cell transfusion post-op	24	(27.6)	29	(33.3)
Re-operation for bleeding	3	(3.4)	3	(3.4)
Antibiotic administration	6	(6.9)	33	(37.9)
Atrial fibrillation	7	(8)	27	(31)
Peak serum creatinine (mg/dL)	1.00±0.41		1.03±0.45	
Peak creatinine clearance (mL/min)	101.9±33.2		101.4±30.3	

6.3.2 HUMORAL INFLAMMATION

Systemic inflammatory markers rose following surgery (Table 6-3, Figure 6.2 Perioperative cytokine, high-sensitivity c-reactive protein (hsCRP) concentrations and circulating white blood cell (WBC) count.with IL-6 and MPO peaking at 2 h, and IL-8 and TNF-α continuing to rise at 6 hours. Plasma hsCRP concentrations rose steeply at 6 h and continued to rise at 48 hours. There was no correlation between cytokines and LGE on CMR. There was weak correlation between AUC hsCRP release and hs-TnI ($r=-0.27$, $p=0.01$).

Table 6-3 Cardiac troponin and cytokine concentrations.

Median (inter-quartile range). hs-TnI – Troponin I by high sensitivity assay. hs-CRP – C-reactive protein by high sensitivity assay. AUC – area under the curve

	0 h	2 h	6 h	24 h	48 h	AUC
hs-TnI (ng/l or ng/l/48h)	3.5 (2, 9.6)	76.5 (35.6, 163.6)	3222 (1413, 5607)	1043 (5344, 2948)	5210 (2302, 1342)	74480 (35100, 164100)
hs-CRP protein (mg/L)	2.00 (0.5, 3.00)	1.00 (0.50, 2.00)	2.00 (1.00, 3.00)	121 (96.0, 148)	236 (182, 279)	7530 (6088, 9027)
Interleukin-6 (pg/mL)	1.80 (1.10, 2.60)	10.0 (5.75, 15.6)	10.5 (8.15, 17.7)			55.8 (43.3, 80.5)
Interleukin-8 (pg/mL)	8.90 (6.28, 11.7)	7.60 (4.95, 16.9)	93.8 (45.9, 148)			240 (121, 411)
Tumour necrosis factor-α (pg/mL)	4.50 (4.50, 7.30)	4.50 (4.50, 11.5)	7.10 (4.50, 14.25)			37.3 (27.0, 66.7)
Myeloperoxidase (ng/mL)	75.6 (45.6, 150)	532 (383, 743)	194 (112, 350)			2175 (1588, 2889)

Figure 6.2 Perioperative cytokine, high-sensitivity c-reactive protein (hsCRP) concentrations and circulating white blood cell (WBC) count.

Mean ± SEM.

IL-6 - Interleukin-6. IL-8 - Interleukin-8. TNF-α – Tumour necrosis factor alpha. MPO - Myeloperoxidase

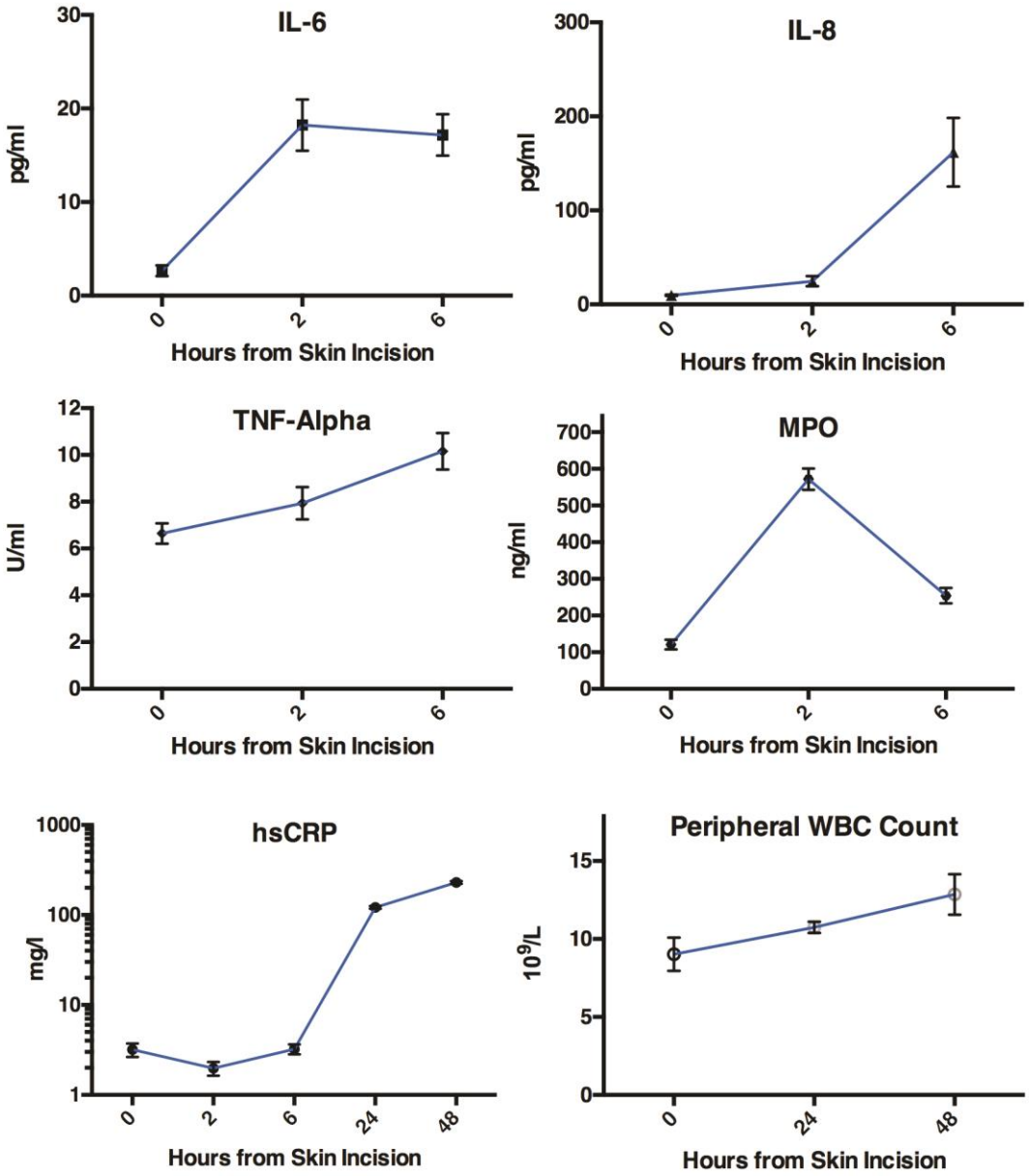

6.3.3 MYOCARDIAL INJURY

Complete cTnI profiles over 48 h were available in 84 patients. Plasma cTnI concentrations peaked at 6 h (median 3,220 [1,410 to 5,610] ng/L; Figure 6.3) with almost all patients demonstrating >100-fold (median 760 [151 to 1623] fold) increase from baseline to 6 h and all patients exhibiting >10-fold (median 102 [55 to 206] fold) elevation above the 99th centile URL. Patients without new LGE had lower increases (median 83 [11 to 161] fold) compared to patients with new LGE (median 174 [91 to 248] fold, p=0.04; Figure 6.3).

Figure 6.3 Perioperative high-sensitivity cardiac troponin.

Mean ± SD and fold increase from baseline (top left). Hs-cTnI concentration fold increase above 99th centile upper reference limit (URL) according to the presence of new late-gadolinium enhancement (top right). Perioperative hs-cTnI profiles of all patients (bottom)

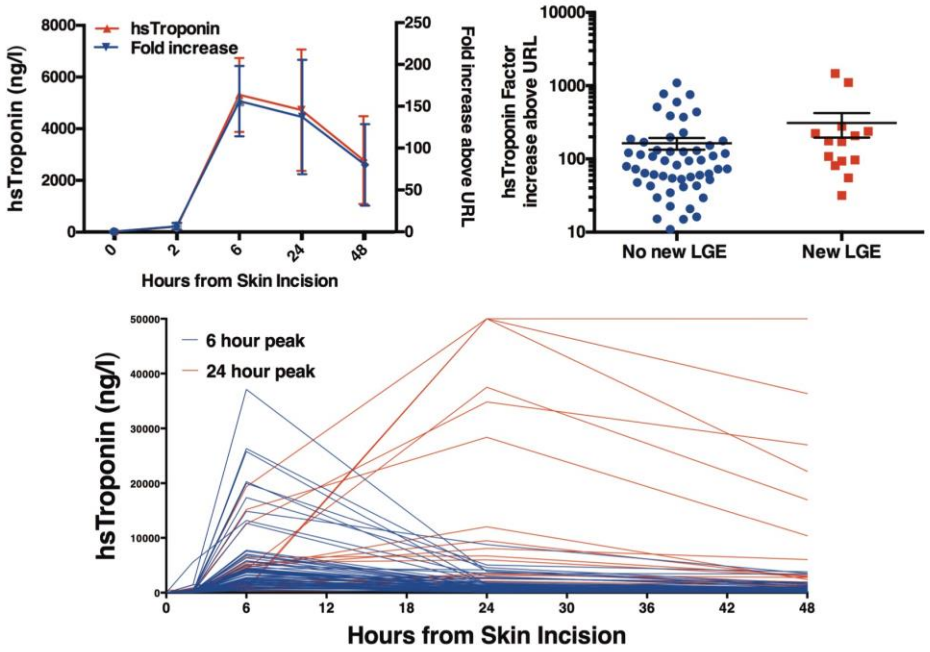

Two patterns of cTnI release were noted in the post-operative period with peak concentrations at 6 (n= 67) or 24 h (n=18; Figure 6.3). Median AUC for hs-cTnI release was 74,478 [35,100 to 164,100] ng/L/48 h. There was no correlation between cTnI AUC and cardiopulmonary bypass (r=0.14, p=0.11) or cross clamp time (r=0.02 p=0.43).

6.3.4 MYOCARDIAL INFARCTION

6.3.4.1 ELECTROCARDIOGRAM

Eleven (13 %) patients developed new ST-change/new bundle branch block/new Q-waves consistent with myocardial infarction (Figure 6.4). The majority of patients had no ECG changes (n=41, 48%) or non-specific pericarditic change (n=19, 22%) and T wave inversion (n=14, 16%). Patients with ECG evidence of infarction exhibited a cTnI peak at 24 h: 6 hour mean, 6,124 ng/L (95% CI 1,758 to 10,490) and 24 hour mean 23,410 ng/L (95% CI 8,530 to 38,300). Patients without specific ECG changes of infarction (n=74) had peak cTnI concentrations at 6 h: 6 hour mean 5,186 (95% confidence intervals 3,635, 6,738) ng/L and 24 hour mean 1,905 (95% confidence intervals 1,353, 2,458) ng/L.

Figure 6.4 Troponin versus CMR & ECG changes.

Perioperative high-sensitivity cardiac troponin concentration (mean ± SEM) according to new late gadolinium enhancement (left) and ECG changes (right). Post-operative evidence of infarction on ECG (bottom).

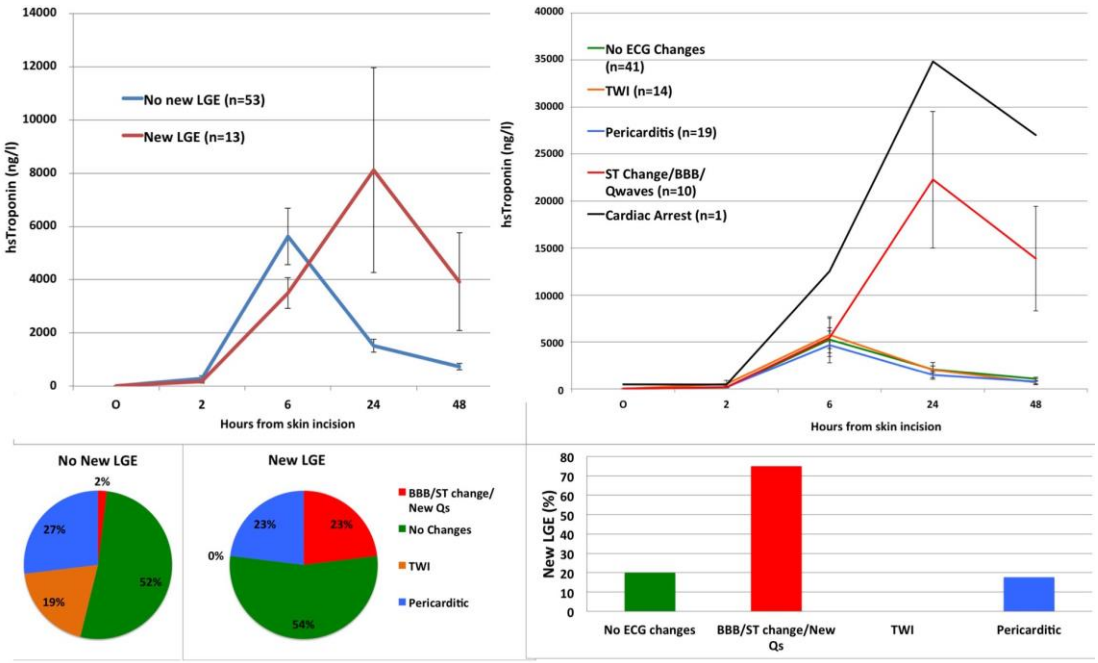

Overall, 7/11 (64%) of patients with an ECG suggesting infarction had a rise in cTnI concentration between 6 and 24 h. In patients with no evidence of infarction on ECG, only 11/74 (15%) had a rise in cTnI concentration between 6 and 24 h. Thus ECG analysis provided a positive predictive value of a late troponin peak of 64% (95% confidence intervals 31% to 89%) and a negative predictive value of 85% (95% confidence intervals 75% to 92%). An ECG demonstrating infarction was 23% sensitive and 98% specific for the formation of LGE.

6.3.4.2 CARDIAC MAGNETIC RESONANCE

Assessment of late gadolinium enhancement was available in 66 of 68 patients who underwent both pre- and post-operative CMR. Thirteen patients developed new LGE distributed by ECG category as follows; 3/4 (75%) with ST-change/new bundle branch block/new Q-waves, 7/35 (20%) with no ECG changes, 3/17 (18%) with pericarditic changes and 0/10 (0%) with T wave inversion (Figure 6.4). Infarct volume by LGE correlated with AUC for cTnI ($r=0.33$, $p<0.01$). For left ventricular function, 8/68 (12%) of patients had at least 5% increase in ejection fraction, 20/68 (29%) had a decrease and 40/68 (59%) had no change (Figure 6.5).

There was a correlation between hsTnI release and LGE ($p<0.01$, $r=0.33$), and between hsTnI and maximum hsCRP levels ($p=0.01$, $r=0.26$) (Figure 6.6)

Figure 6.5 Change in ejection fraction

(Median and IQR)

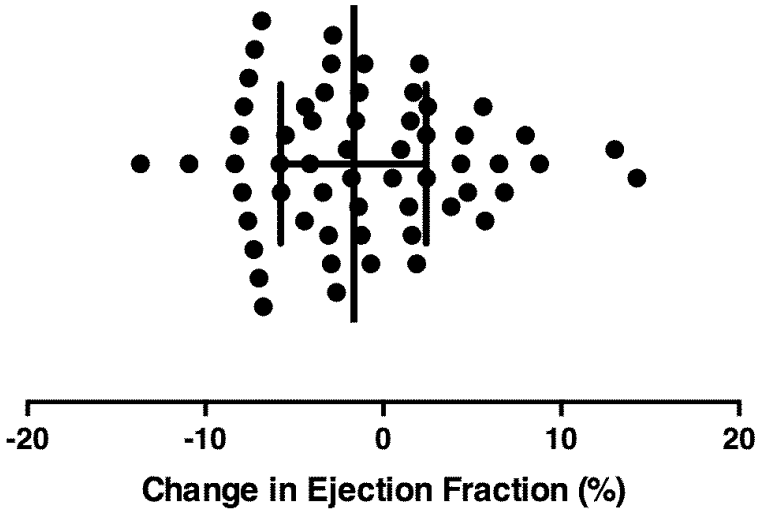

Figure 6.6 Associations between area under the curve high-sensitivity cardiac troponin I and LGE & maximum hs-CRP

(line of best fit and 95% confidence intervals)

LGE – left

hs-CRP - right

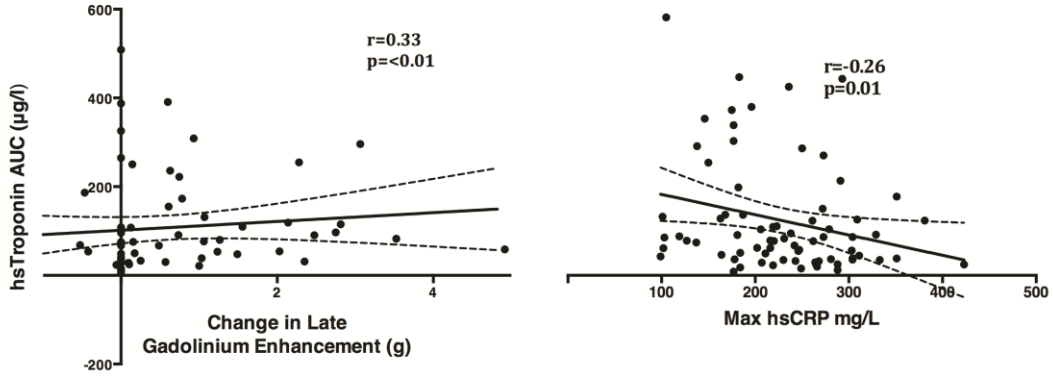

Peak plasma cTnI concentration occurred at 24 hours in patients with new LGE: 6-hour mean 3,655 (95% confidence intervals 2,228 to 5,081) ng/L and 24-hour mean 9,073 (95% confidence intervals 5106 to 18,660) ng/L. By contrast, patients without new LGE had a peak cTnI concentration at 6 hours of 5,487 (95% confidence intervals 3,390 to 7,585) ng/L compared to a mean of 1,545 (95% confidence intervals 1,060 to 2,031) ng/L at 24 hours. Overall 6/13 (46%) of patients with new LGE had a rise in cTnI concentration between 6 and 24 hours compared to 5/52 (10%) in patients without LGE ($p<0.01$). A rise in troponin release after 6 hours was 46% sensitive (95% CI 19 to 75) and 90% specific (95% confidence intervals 79 to 97) for detecting new LGE. The positive predictive value was 55% (95% confidence intervals 23.38 to 83.25) and the negative predictive value 87% (95% confidence intervals 75.10 to 94.63) respectively.

6.4 DISCUSSION

This study was performed on a highly characterised and phenotyped population using the current gold standard techniques to detect myocardial injury and infarction (Shah et al., 2015b). Patients undergoing CABG surgery invariably have plasma hs-cTnI concentrations >10-fold the 99th centile that is not attributable to inflammatory or ischemic injury alone. Peri-operative type 5 myocardial infarction is often unrecognised and is associated with a delayed 24-hour peak in plasma hs-cTnI concentrations.

Using the latest generation high-sensitivity assay, cTnI release was found to be >10-fold the upper limit of normal (99th centile) in all patients following CABG surgery. Importantly, two patterns of release were identified with an early 6 hour peak and a more delayed 24 hour peak. These peaks reflect perioperative myocardial injury and infarction respectively as demonstrated by late gadolinium enhancement on cardiac magnetic resonance imaging. There appears to be no single discriminatory threshold for troponin concentration that could reliably discriminate clinically overt myocardial infarction. The data indicate that the profile, rather than peak, of troponin release may be more important when attempting to distinguish between myocardial injury and type 5 MI.

All patients in the study exhibited at least 50-fold rise from baseline troponin and all but 4 had at least 100-fold increase. Many factors contribute to myocardial injury in the perioperative period including manipulation of the heart during on-pump surgery, cardioplegia, ischemia and patients specific factors including severity of underlying coronary artery disease and myocardial function. The average increase in cTnI

concentration from baseline was nearly 2,000. The third universal definition for type 5 myocardial infarction occurring during CABG surgery stipulates a cardiac marker elevation of ≥10-fold the upper limit of normal (99th centile). In this study, all patients undergoing on-pump surgery fulfil this criterion and this threshold is therefore unhelpful and has no value. This leads to the questions of whether a higher single threshold should be employed or whether alternative criteria looking at the profile of cTnI release may be more discriminatory.

The data do not support the approach of increasing troponin threshold to provide greater discrimination. For example, increasing the threshold to >100-fold 99th centile would have excluded 64% of patients with LGE proven macro-infarction and included 43% of patients without. The data support the findings by other groups that multiple time-point sampling to detect a late rise in troponin concentration is more discriminatory for type 5 myocardial infarction (Selvanayagam et al., 2005, Pegg et al., 2011, Lim et al., 2011). Selvanayagam et al demonstrated a late peak in troponin levels in patients with new LGE compared to those without (20.3±11.9 versus 11.3±11.0 hours) (Selvanayagam et al., 2005). Both Pegg et al and Lim et al demonstrated that subjects with new LGE showed a trend for continuous increase of troponin up to 24 hours whereas those without new LGE showed peaks at 6 to 12 hours (Lim et al., 2011, Pegg et al., 2011). In this study there were also two distinct cTnI concentration peaks at 6 and 24 hours. Patients with ECG or LGE evidence of infarction were much more likely to have a peak cTnI at 24 hours compared to those without. An ECG demonstrating infarction was highly specific (98%) for detecting the formation of LGE. However both ECG and cTnI profile in isolation had relatively low sensitivity for such detection. This may be because greater volume of infarction must occur in order to cause a change in the electrical or biochemical

profile. The data from this study suggest that the most effective and practical method for diagnosing type 5 myocardial infarction involves cTnI testing at 6 and 24 hours combined with ECG evidence of infarction.

A previous study reported new LGE in up to 78% of patients undergoing CABG surgery, but the investigators did not perform pre-operative CMR (Steuer et al., 2004a). In this study, LGE was identified in 27% of pre-operative MRI scans in patients with no prior clinical history of myocardial infarction suggesting the presence of sub-clinical infarction is common even in stable patients. Consistent with the work in this chapter, Pegg and colleagues also reported pre-existing LGE from preoperative scans in 8/40 (20%) of patients participating in a study of a novel hybrid method of on-pump beating heart CABG surgery (Pegg et al., 2011).

Although it might have been anticipated that the magnitude of myocardial injury would correlate with CPB time, there was no association with AUC cTnI release. Furthermore there was no correlation with inflammatory cytokine release or myocardial inflammation. This suggests that injury is not mediated by inflammation alone. Other processes influence the cTnI injury such as microemboli, surgical manipulation of the heart and patient specific factors. The data also confirm that substantial cTnI release occurs in the perioperative period without imaging evidence of infarction and new scar formation consistent with reversible myocardial injury.

The study has some limitations. Some patients had difficulty lying flat and breath-holding in the MRI scanner for post-operative scans. This sometimes resulted in reduced scan quality. Since the CMR scans were carried out at later time points (5 to 14 days post-surgery), this may have hindered the ability to identify some of the correlations with our early (first 48 hours) biomarker assessments.

In conclusion, all patients undergoing CABG surgery demonstrate >10-fold elevation above the 99th centile of cardiac troponin indicating the current universal definition of type 5 myocardial infarction lacks specificity. A peak hs-cTnI at 6 hours following CABG appears to be related to the surgical process and non-specific myocardial injury whilst a continuing increase at 24 hours suggesting myocardial infarction. We would suggest cTnI sampling at 6 and 24 hours post CABG surgery together with ECG assessment for the routine detection and diagnosis of type 5 MI.

Differing levels of humoral markers of inflammation post CABG surgery occurred and did not correlate directly with the length of CPB or hs-cTnI release, except for a weak correlation between hsCRP and hs-cTnI.

Chapter 7: CONCLUSIONS AND FUTURE DIRECTIONS

7.1 BACKGROUND

7.1.1 MYOCARDIAL INFARCTION

Cardiovascular disease is the commonest cause of premature death in the United Kingdom and accounts for 30% of all deaths among men and 22% among women. The single largest cause of death is acute myocardial infarction (http://www.bts.org.uk/transplantation/heart/, 2015).

Coronary atherosclerosis is responsible for the initiation of acute myocardial infarction with plaque rupture leading to acute coronary thrombosis and myocardial infarction. Current treatment in the acute phase involves re-establishing vessel patency by percutaneous coronary intervention supported by anti-thrombotic therapy. Thereafter, statins, angiotensin-converting enzyme inhibitors and beta-blockade all have prognostic benefit but no treatments have been successfully developed to target post-infarction inflammatory pathways.

Necrotic cardiac muscle elicits an inflammatory cascade that serves to clear the infarct of dead cells and matrix debris. Human cardiac muscle has negligible regenerative capacity and ultimately inflammation leads to replacement of damaged tissue with a fibrotic scar. Enhancing reparative mechanisms following the inflammatory reaction to myocardial infarction may reduce cardiomyocyte injury, attenuate adverse remodelling and improve clinical outcome. A better understanding of the early post-infarct healing phase will also facilitate cell therapy strategies that

engraft stem cells or stimulate regeneration. In order to achieve this goal, we must better characterise the inflammatory processes that follow infarction and myocardial necrosis in humans.

7.1.2 MYOCARDIAL INFLAMMATION FOLLOWING ISCHAEMIA AND INFARCTION

(i) Neutrophils and Human Neutrophil Elastase

Inflammation within the infarcted myocardium is associated with induction of endothelial adhesion molecules and enhanced permeability of the microvasculature. Up regulation of chemokines, including IL-8 and MCP-1, attracts neutrophils and monocytes to the site of injury. Early reperfusion therapy amplifies this inflammatory cell influx and accelerates the healing response through proliferative and maturation phases. Neutrophil adhesion to endothelium of infarcted myocardium occurs within minutes of reperfusion. Ischaemic cardiomyocytes are further injured by adherent neutrophils that release reactive oxygen species and destructive proteases including HNE and proteinase 3. HNE has a wide range of substrates including matrix components elastin, fibronectin, and collagen types III and IV. Activated neutrophils also occlude microvessels and increase endothelial permeability contributing to myocardial oedema. Preclinical studies have demonstrated that neutrophil depletion or inhibition of neutrophil elastase attenuates post-ischemic inflammatory reperfusion injury within the myocardium (Romson et al., 1983a, Tiefenbacher et al., 1997).

(ii) Monocyte-derived Macrophages

Recruitment of monocytes into the infarcted myocardium is followed by maturation and differentiation into macrophages. Macrophages have multiple roles within the infarct including (i) phagocytic clearance of dead cells and debris, (ii) production of growth factors and cytokines that stimulate fibroblast growth and angioneogenesis, and (iii) matrix turnover through the production of matrix metalloproteases and their inhibitors. Macrophages are resident within 24 hours of infarction and persist for up to 4 weeks. During this period, macrophages regulate infarct healing with the initial development of granulation tissue and subsequent scar formation. Monocytes arriving within the first 3 days mature into macrophages that scavenge necrotic debris through inflammatory mediator expression, proteolysis and phagocytosis while monocytes arriving later on give rise to macrophages which promote reparative processes such as angioneogenesis and extracellular matrix deposition (Nahrendorf et al., 2007a).

MCP-1 expression is increased in ischaemic myocardium following reperfusion and this accounts for a substantial proportion of the monocyte chemotactic activity (Kumar et al., 1997). Macrophage activity outside the infarct zone may contribute to adverse myocardial remodelling following myocardial infarction. The role of the macrophage differs depending on differentiation and location within the myocardium. Therapeutic manipulation of this healing process will only come from understanding mechanisms and targeting reparative pathways. Indiscriminate immunosuppressive therapy in this setting may result in harm as observed in trials with methylprednisolone in acute myocardial infarction.

7.1.3 MAGNETIC RESONANCE IMAGING IN TRACKING CELLULAR INFLAMMATION

Iron oxide particles can be used as a contrast medium in magnetic resonance imaging since they can alter the magnetic properties and relaxation of tissues after application of radiofrequency pulses. Such contrast media consist of an iron oxide core within a dextran coat. They can be classified as "ultrasmall superparamagnetic iron oxide particles" (USPIOs) which are under 30 nm in diameter (Lawaczeck et al., 2004). USPIOs are taken up by cells of the liver, spleen, bone marrow and lymph nodes. They have the capacity to extravasate through capillaries and be phagocytosed by tissue inflammatory cells of the reticuloendothelial system (Ruehm et al., 2001a). These cells are predominately macrophages, but neutrophils have also been shown to take up USPIOs (Dousset et al., 1999, Gellissen et al., 1999b). This model of USPIO-enhanced MRI can highlight areas of inflammation in models of vertebral osteomyelitis, aortic atherosclerosis, arthritis-induced hyperperfusion, autoimmune encephalomyelitis, nephritis and nephropathy, cerebral ischaemia and renal ischaemia (Bierry et al., 2008, Dousset et al., 1999, Ruehm et al., 2001a, Hauger et al., 2000, Rausch et al., 2001b, Lutz et al., 2006, Jo et al., 2003b). Therefore we hypothesised that USPIO enhanced CMR could identify and assess cellular inflammation of the myocardium.

7.1.4 CORONARY ARTERY BYPASS SURGERY

During coronary artery bypass graft surgery, the myocardium receives an immediate ischaemic insult that is exacerbated by post-ischaemic reperfusion inflammatory responses leading to increased myocardial injury. Coronary artery bypass graft

surgery can therefore be used as a clinical model of myocardial infarction and inflammation (Steuer et al., 2004c, Anselmi et al., 2004).

7.1.5 ELAFIN

Elafin inhibits destructive and inflammatory neutrophil derived proteases. Beyond this elafin inhibits inflammatory cytokines and modulates the innate and adaptive immune systems. Elafin is expressed within epithelial tissues that have evolved mechanisms to adapt and repair from neutrophil mediated injury. In preclinical studies elafin delivery and gene overexpression is associated with reduced myocardial injury and preserved left ventricular function following ischaemia and infarction. This effect is associated with reduced neutrophil infiltration and elastase activity at the site of injury. Activated neutrophils facilitate monocyte recruitment. Granule contents including LL-37, azurocidin and human neutrophil peptides 1-3 have direct chemotactic activity on monocytes. Neutrophil-derived proteases induce chemokine, MCP-1 and IL-8 production from endothelial cells and their effects on matrix components produce degradation products with chemotactic activity for monocytes (Richardson et al., 1976, Postlethwaite and Kang, 1976, Norris et al., 1982). As such, elafin has a marked potential for the treatment of cardiovascular disease including acute myocardial infarction. Therefore, we hypothesised that elafin will reduce perioperative ischaemic myocardial injury and inflammation in patients undergoing elective coronary artery bypass graft surgery.

7.2 SUMMARY OF THESIS FINDINGS

7.2.1 CHANGES IN R2* IN USPIO ENHANCED MRI SCANS DETECT CELLULAR INFLAMMATION POST MYOCARDIAL INFARCTION

We demonstrated for the first time that USPIOs are taken up by the infarct tissue in patients with recent myocardial infarction and by the peri-infarct myocardium to a lesser degree. Given previous pre-clinical and clinical studies, this is likely to correspond to cellular inflammation. This represents a novel non-invasive method to further study cardiac inflammation and therapeutic interventions. It may also provide prognostic information or provide a diagnostic tool for the investigation of inflammatory cardiac conditions such as myocarditis and transplant rejection, as well as a potential biomarker for therapeutic interventions targeted at improving left ventricular remodelling following infarction.

7.2.2 MYOCARDIAL INJURY POST CORONARY ARTERY BYPASS SURGERY CAN BE ASSESSED WITH BLOOD MARKERS OF INFLAMMATION AND INFARCTION.

All patients undergoing CABG surgery demonstrated >10-fold elevation above the 99th centile of cardiac troponin indicating the current universal definition of type 5 myocardial infarction lacks specificity. A peak hs-TnI at 6 hours following CABG surgery appears to be related to the surgical process and non-specific myocardial injury whilst a continuing increase at 24 hours suggesting myocardial infarction. We would suggest troponin sampling at 6 and 24 hours post CABG surgery together with ECG assessment for the routine detection and diagnosis of type 5 MI.

Differing levels of humoral makers inflammation post CABG surgery occurred, and did not correlate directly with the length of CPB or hs-TnI release. However the marked elevation of IL-6, IL-8, TNF-alpha, MPO and hsCRP following surgery indicated that CABG surgery can be used as a model of programmed cardiac injury and inflammation.

7.2.3 ELAFIN, THE NEUTROPHIL ELASTASE INHIBITOR, DID NOT MODIFY POST CORONARY ARTERY BYPASS SURGERY MYOCARDIAL INJURY AND INFLAMMATION

Despite the body of work indicating therapeutic potential from several groups using different models, species and modes of augmentation, Elafin's promise as a therapeutic agent to attenuate myocardial ischemia-reperfusion injury and inflammation was not translated in this first phase II study. Post-hoc analysis identified reduced cTnI concentrations at 6 hours in Elafin treated patients and it is possible that repeated dosing would have conferred protection out to 48 hours. Elafin was safe and lack of treatment effect was seen despite achieving high plasma Elafin concentrations and halving of circulating elastase activity.

7.2.4 CELLULAR INFLAMMATION POST CORONARY ARTERY BYPASS SURGERY CAN BE DETECTED AND ASSESSED USING USPIO ENHANCED MRI SCANNING.

For the first time we identified differing levels of inflammatory cell infiltrate into the myocardium post CABG. This varied from none to levels similar to infarcted myocardial tissues, and the cause and consequences of this requires further study. Elafin did not attenuate the cellular infiltration into the myocardium post CABG surgery, but did appear to reduce inflammation in renal tissue. There was also

evidence of a reduction in cell population in the bone marrow post surgery, which was possible evidence of monocyte progenitor cell egress. USPIO enhanced CMR holds major promise in the non-invasive assessment of myocardial inflammation post surgery.

7.3 FUTURE DIRECTIONS

7.3.1 PROPOSED CONTINUATION OF RESEARCH FROM CHAPTER 3

7.3.1.1 IRON NANOPARTICLE ENHANCED MRI IN THE ASSESSMENT OF MYOCARDIAL INFARCTION (IRNMAN) TRIAL

We have established uptake of USPIOs in the penumbra and infarct zone of the myocardium in patients with a recent myocardial infarction. In an investigation already underway, we aim to establish the time course and determinants of cellular tissue inflammation. This is the first clinical study to examine the ability of USPIOs to image myocardial inflammation following acute myocardial infarction.

Using ferumoxytol (Rienso) as a USPIO contrast agent for magnetic resonance imaging at 3 tesla, we aim to conduct a clinical study to examine the utility of this novel contrast agent to image myocardial inflammation after myocardial infarction.

7.3.1.1.1 HYPOTHESIS

We hypothesise that the myocardial accumulation of ultrasmall superparamagnetic particles of iron oxide within phagocytic inflammatory cells will:

i. Occur within and adjacent to areas of acute myocardial infarction.
ii. Occur early and be proportional to the extent of infarction and the degree of systemic inflammation.

7.3.1.1.2 EXPECTED VALUE OF RESULTS

We propose to describe, characterise and identify the determinants of USPIO uptake using the clinical model of acute myocardial infarction. This will be the first description of this 'smart contrast agent' in the setting of acute myocardial infarction and, if successful, this technique has many major potential benefits and ramifications. First, it may assist in risk stratifying patients who may have an adverse outcome. For example, intense and persistent USPIO uptake may be associated with adverse remodelling and progression to heart failure. Second, it will provide a method of assessing the inflammatory and reparative processes following infarction. This may be a useful biomarker to assess the impact of therapeutic interventions.

For further details please refer to Appendix H: .

7.3.2 PROPOSED CONTINUATION OF RESEARCH FROM CHAPTER 4

7.3.2.1 ELAFIN IN THE MODULATION OF CARDIOVASCULAR INFLAMMATION

We showed that a single administration of Elafin prior to on-pump coronary artery bypass surgery did not result in attenuation of injury inflammation as measured troponin release or cytokine profiles. Inflammatory cascades are activated via multiple mechanisms, with overlap between substrates for different enzymes. Such redundancy in tissues inflammatory pathways may mean that inhibition of one pathway cannot modulate the overall acute response to injury. However, post hoc analysis did reveal that troponin levels were reduced at 6 hours albeit without statistical correction for multiple time-point analysis. As described in section 1.6 (page 39) Elafin has anti-inflammatory effect through receptor interaction as well as enzyme activity. Elafin levels began to rise, with elastaste activity increasing at 2 hours post skin incision. It is possible that more sustained HNE suppression and Elafin plasma levels may have resulted in significant attenuation of myocardial injury and inflammation.

7.3.2.1.1 HYPOTHESIS

Using the same model of cardiac inflammation and methods, repeated doses of Elafin to ensure sustained plasma levels and complete suppression of HNE will result in significant reduction in myocardial inflammation and injury.

7.3.2.1.2 EXPECTED VALUE OF RESULTS

If the anti-inflammatory effect of Elafin can be demonstrated in the above model of inflammation, it could be studied as a therapeutic intervention in more severe forms of cardiac inflammation. This would include type 1 myocardial infarction, valvular heart surgery and myocarditis.

7.3.3 PROPOSED CONTINUATION OF RESEARCH FROM CHAPTER 5

We have established that USPIOs can be used to assess cellular inflammation in patients with acute myocardial infarction (Chapter 3:) and post CABG surgery (Chapter 5:, Figure 7.1). This technique can be utilised to detect inflammation in pathologies causing myocarditis.

Figure 7.1 Comparison of myocardial R2* values post surgery, infarction and in controls.

Post cardiac surgery (green) compared to infarct (red) and non-infarct areas (blue) in patients with acute myocardial infarction. The myocardium of healthy volunteers is shown in yellow.

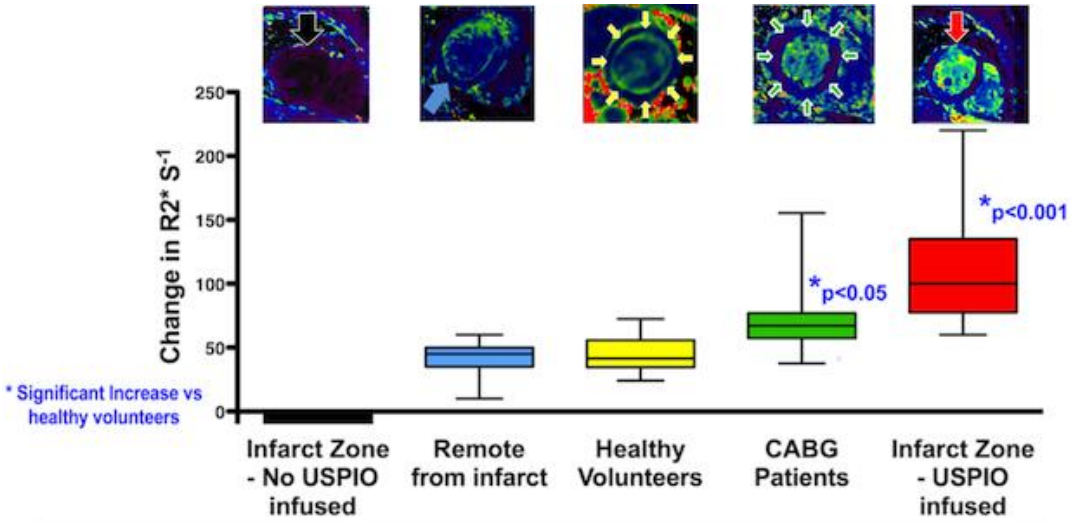

7.3.3.1 DETECTION OF CELLULAR INFLAMMATION WITH FERUMOXYTOL IN THE HEART: 'DECIFER-HEART' TRIAL

7.3.3.1.1 CARDIAC TRANSPLANTATION

Approximately 150 people per year receive a cardiac transplant in the United Kingdom (http://www.bts.org.uk/transplantation/heart/, 2015)(http://www.bts.org.uk/transplantation/heart/, 2015) (http://www.bts.org.uk/transplantation/heart/, 2015). Up to 21 to 30 per cent of recipients are treated for rejection during the first year after transplantation (Hertz et al., 2009). All patients therefore require lifetime immunosuppression and careful follow-up to assess for rejection. However no reliable non-invasive method of assessment exists for its detection or surveillance of at-risk patients (Christen et al., 2010). During cardiac transplant rejection, antigen presenting cells stimulate lymphocytes to release cytokines which recruit and activate macrophages that are the main effector cells (Suzuki et al., 2010). In clinical specimens, macrophages and monocytes have been recognised as a correlate of humoral rejection in cardiac transplant recipients (Lones et al., 1995).

Iron oxide particles have been used to assess heart transplant rejection in pre-clinical models (Kanno et al., 2001, Johansson et al., 2002, Penno et al., 2007). In a rodent model, Kanno and colleagues showed that T2 signal intensity decreased 24 hours after iron oxide particle administration in untreated allografts compared to isografts. Moreover, signal intensity in rejecting allografts returned to baseline after treatment with cyclosporin for seven days. Immunohistochemistry confirmed accumulation of iron oxide containing macrophages in areas of graft rejection. Thus there is great potential in the translational use of iron oxide particles in the clinical assessment of cardiac transplant recipients.

7.3.3.1.2 MYOCARDITIS

Acute myocarditis comprises a wide clinical spectrum from sub-clinical disease to severe heart failure. Its causes include infectious, toxic iatrogenic (often by chemotherapeutic agents) and autoimmune conditions although often no cause can be identified (Meybohm et al., 2009, Marchant et al., 2012). Currently biopsy is often considered the gold standard in diagnosis, although it is prone to sample error and clinically indicated in only a few scenarios (Cooper et al., 2007). Although in some cases cardiac MRI can reveal a 'typical' pattern of myocarditis based on T2 oedema imaging, the sensitivity and specificity is unclear and not yet established. The diagnostic yield is therefore limited.

Monocytes and macrophages are intimately involved in myocarditis (Sagar et al., 2012). In pre-clinical models of myocarditis, monocytes differentiate into macrophages at sites of inflammation and exhibit a T-helper 1 (Th1)-type cytokine/chemokine profile suggesting they play an important role in the pathogenesis of myocarditis (Baba et al., 2006). Thus, iron oxide particles are ideally suited to target cellular inflammation in the myocardium and diagnose the condition with greater sensitivity then current techniques.

7.3.3.1.3 CARDIAC SARCOIDOSIS

The incidence of sarcoidosis varies: 3 to 20 per 100 000 for white and 35 to 80 per 100 000 for black individuals (Rybicki and Iannuzzi, 2007). There is cardiac involvement in up to 27% of sarcoid cases (Silverman et al., 1978) and complications include atrial and ventricular arrhythmias, congestive cardiac failure and sudden cardiac death (Silverman et al., 1978, Roberts et al., 1977, Kandolin et al., 2011, Banba et al., 2007, Yazaki et al., 2001). The diagnosis is challenging and, although histology is the gold standard method, obtaining a tissue biopsy is invasive and

subject to sampling error. The role of imaging techniques such as magnetic resonance imaging remains ill defined, and there is a need for improved accuracy with greater sensitivity and specificity to diagnose the condition and guide therapeutic intervention.

The core inflammatory cells of sarcoid granulomas include monocytes and macrophages (Mitchell et al., 1977) and an imaging technique targeting these cells would be ideally placed to establish the diagnosis and to assess disease activity.

7.3.3.1.4 HYPOTHESIS

USPIO-enhanced magnetic resonance imaging can be utilised for the diagnosis and characterisation of cardiac conditions associated with myocardial inflammation.

Primary Objective: To non-invasively image myocardial accumulation of ultrasmall superparamagnetic particles of iron oxide (USPIOs) by an increase in R2* values (compared to controls) within the myocardium of patients with:

i. Cardiac transplantation
ii. Acute myocarditis
iii. Active cardiac sarcoidosis

Secondary Objectives:

i. Does treatment or recovery from these inflammatory myocardial conditions reduce or halt uptake of USPIOs as assessed by reduction in R2* values.
ii. Do systemic inflammatory markers correlate with R2* values

iii. Do patients with higher R2* values have worse outcomes assessed by deterioration in ejection fraction, increase in medications or increase in late gadolinium enhancement.

7.3.3.1.5 EXPECTED VALUE OF RESULTS

USPIO enhanced MRI could be used an a diagnostic and/or monitoring tool is the clinical care of conditions associated with inflammation of the myocardium.

For further details please refer to 5.1.1.1.1.1.1.1Appendix H:

7.3.3.2 DETECTION & MODULATION OF INFLAMMATION IN RENAL TISSUE

We established that USPIO accumulation occurs in renal tissue post CABG surgery and can be assessed with R2* CMR imaging. In the context of pre-clinical studies, it can be assumed this represents concentration within macrophages. We also confirmed this using transplantation as a model of renal inflammation in Appendix G: (page 505). Furthermore, there was reduced USPIO accumulation in patients treated with Elafin compared to placebo or healthy volunteers suggesting an anti-inflammatory treatment effect. However, this was post hoc analysis in a subset of patients. Therefore, this finding could be confirmed with clinical studies.

We have established that on-pump cardiac surgery is associated with a systemic inflammatory response. Acute kidney injury (AKI) complicates up to 30 % of patients following cardiac surgery (Parolari et al., 2012). AKI associated with cardiac surgery is caused by a combination of factors including sympathetic nervous system induced vasoconstriction, hypoperfusion, atheroembolism, formation of reactive oxygen species and systemic inflammation. All these processes lead to leucocyte

recruitment and renal infiltration by neutrophils, macrophages and lymphocytes (O'Neal et al., 2016).

The role of monocytes and macrophages in chronic renal allograft damage has been well established (Magil, 2009). Monocytes and macrophages are known to play a role in chronic renal allograft damage (Dang et al., 2012), and are key promotors of fibrosis in other organs, such as the liver (Duffield et al., 2005, Ramachandran et al., 2012).

7.3.3.2.1 HYPOTHESIS

Using USPIO enhanced MRI, renal inflammation can be;

A. i) Assessed post cardiac surgery and correlated to markers of renal injury such as plasm and urinary NGAL.

   ii) Modulated by Elafin administration with complete HNE inhibition in the first 24 hours post cardiac surgery

B. Assessed in chronic renal allograft rejection and correlated to biopsy specimens.

7.3.3.2.2 EXPECTED VALUE OF RESULTS

USPIO enhanced MRI could be used an a diagnostic and/or monitoring tool is the clinical care of conditions associated with inflammation of renal tissues.

7.3.4 PROPOSED CONTINUATION OF RESEARCH IN CHAPTER 6

We established that there are 2 peaks of troponin release post cardiac surgery at 6 hours and 24 hours post skin incision. Using late gadolinium enhancement and ECG assessment, we showed a troponin peak at 24 hour indicated myocardial infarction. A peak at 6 hours was due to cardiac injury associated with cardiac surgery. This finding needs to be confirmed in a larger registry of patients undergoing cardiac surgery.

7.3.4.1 HYPOTHESIS

A rising troponin at 24 hours post cardiac troponin is caused my myocardial infarction independent of cardiac injury associated with cardiac surgery and confers an adverse prognosis. Such myocardial infarction can be treated with dual anti-platelet therapy.

Primary Objective: To measure plasma troponin concentrations at 6 hours and 24 hours post cardiac surgery. Patients will be divided into 2 cohorts:

i) Troponin peak within 24 hours from cardiac surgery

ii) Troponin peak after 24 hours from cardiac surgery

The cohorts will be followed up long-term for the incidence of fatal and non-fatal myocardial infarction, stroke, hospital admission for heart failure and all cause death.

Secondary Objectives: If there are adverse outcomes for patients with a late troponin peak, a study can be set-up in which patients are randomised to dual anti-platelet therapy or standard care. The primary end-point would be the incidence of fatal and non-fatal myocardial infarction, stroke, hospital admission for heart failure

and all cause death. Gastro-intestinal haemorrhage and haemorrhagic stroke would be safety end-points.

7.3.4.2 EXPECTED VALUE OF RESULTS

By using troponin to identifying patients with an adverse prognosis post cardiac surgery, the diagnostic methodology of a type 5 myocardial infarction could be established. Such patients can then be better treated to improve clinical outcomes.

REFERENCES

ABBATE, A., BONANNO, E., MAURIELLO, A., BUSSANI, R., BIONDI-ZOCCAI, G. G., LIUZZO, G., LEONE, A. M., SILVESTRI, F., DOBRINA, A., BALDI, F., PANDOLFI, F., BIASUCCI, L. M., BALDI, A., SPAGNOLI, L. G. & CREA, F. 2004. Widespread myocardial inflammation and infarct-related artery patency. *Circulation,* 110**,** 46-50.

ALAM, S. R., LEWIS, S. C., ZAMVAR, V., PESSOTTO, R., DWECK, M. R., KRISHAN, A., GOODMAN, K., OATEY, K., HARKESS, R., MILNE, L., THOMAS, S., MILLS, N. M., MOORE, C., SEMPLE, S., WIEDOW, O., STIRRAT, C., MIRSADRAEE, S., NEWBY, D. E. & HENRIKSEN, P. A. 2015. Perioperative elafin for ischaemia-reperfusion injury during coronary artery bypass graft surgery: a randomised-controlled trial. *Heart,* 101**,** 1639-45.

ALAM, S. R., SHAH, A. S., RICHARDS, J., LANG, N. N., BARNES, G., JOSHI, N., MACGILLIVRAY, T., MCKILLOP, G., MIRSADRAEE, S., PAYNE, J., FOX, K. A., HENRIKSEN, P., NEWBY, D. E. & SEMPLE, S. I. 2012. Ultrasmall superparamagnetic particles of iron oxide in patients with acute myocardial infarction: early clinical experience. *Circulation. Cardiovascular imaging,* 5**,** 559-65.

ANDERSON, L. J., HOLDEN, S., DAVIS, B., PRESCOTT, E., CHARRIER, C. C., BUNCE, N. H., FIRMIN, D. N., WONKE, B., PORTER, J., WALKER, J. M. & PENNELL, D. J. 2001. Cardiovascular T2-star (T2*) magnetic resonance for the early diagnosis of myocardial iron overload. *European Heart Journal,* 22**,** 2171-2179.

ANSELMI, A., ABBATE, A., GIROLA, F., NASSO, G., BIONDI-ZOCCAI, G. G. L., POSSATI, G. & GAUDINO, M. 2004. Myocardial ischemia, stunning, inflammation, and apoptosis during cardiac surgery: a review of evidence. *European Journal of Cardio-thoracic Surgery,* 25**,** 304-311.

ASCIONE, R., LLOYD, C. T., UNDERWOOD, M. J., LOTTO, A. A., PITSIS, A. A. & ANGELINI, G. D. 2000. Inflammatory response after coronary revascularization with or without cardiopulmonary bypass. *The Annals of Thoracic Surgery,* 69**,** 1198-204.

ASOKANANTHAN, N., GRAHAM, P. T., FINK, J., KNIGHT, D. A., BAKKER, A. J., MCWILLIAM, A. S., THOMPSON, P. J. & STEWART, G. A. 2002. Activation of protease-activated receptor PAR-1, PAR-2, and PAR-4 stimulates IL-6, IL-8, and prostaglandin E2 release from human respiratory epithelial cells. *The Journal of Immunology,* 168**,** 3577.

BABA, T., ISHIZU, A., IWASAKI, S., SUZUKI, A., TOMARU, U., IKEDA, H., YOSHIKI, T. & KASAHARA, M. 2006. CD4+/CD8+ macrophages infiltrating at inflammatory sites: a population of monocytes/macrophages with a cytotoxic phenotype. *Blood,* 107**,** 2004-12.

BAGSHAW, S. M. & GIBNEY, R. T. 2008. Conventional markers of kidney function. *Crit Care Med,* 36**,** S152-8.

BALDUS, S., EISERICH, J. P., MANI, A., CASTRO, L., FIGUEROA, M., CHUMLEY, P., MA, W., TOUSSON, A., WHITE, C. R., BULLARD, D. C., BRENNAN, M. L., LUSIS, A. J., MOORE, K. P. & FREEMAN, B. A. 2001.

Endothelial transcytosis of myeloperoxidase confers specificity to vascular ECM proteins as targets of tyrosine nitration. *J Clin Invest,* 108**,** 1759-70.

BANBA, K., KUSANO, K. F., NAKAMURA, K., MORITA, H., OGAWA, A., OHTSUKA, F., OGO, K. O., NISHII, N., WATANABE, A., NAGASE, S., SAKURAGI, S. & OHE, T. 2007. Relationship between arrhythmogenesis and disease activity in cardiac sarcoidosis. *Heart Rhythm,* 4**,** 1292-9.

BIERRY, G., JEHL, F., BOEHM, N., ROBERT, P., PRÈVOST, G., DIETEMANN, J. L., DESAL, H. & KREMER, S. 2008. Macrophage Activity in Infected Areas of an Experimental Vertebral Osteomyelitis Model: USPIO-enhanced MR ImagingóFeasibility Study1. *Radiology,* 248**,** 114.

BJERNER, T., ERICSSON, A., WIKSTROM, G., JOHANSSON, L., NILSSON, S., AHLSTROM, H. & HEMMINGSSON, A. 2000. Evaluation of nonperfused myocardial ischemia with MRI and an intravascular USPIO contrast agent in an ex vivo pig model. *J Magn Reson Imaging,* 12**,** 866-72.

BLAND, J. M. & ALTMAN, D. G. 1986. Statistical methods for assessing agreement between two methods of clinical measurement. *Lancet,* 1**,** 307-10.

BOLDT, J. & WOLF, M. 2008. Identification of renal injury in cardiac surgery: the role of kidney-specific proteins. *J Cardiothorac Vasc Anesth,* 22**,** 122-32.

BOLLI, R., BECKER, L., GROSS, G., MENTZER JR, R., BALSHAW, D. & LATHROP, D. A. 2004. Myocardial protection at a crossroads: the need for translation into clinical therapy. *Circulation Research,* 95**,** 125.

BONVINI, R. F., HENDIRI, T. & CAMENZIND, E. 2005. Inflammatory response post-myocardial infarction and reperfusion: a new therapeutic target? *European Heart Journal Supplements,* 7**,** I27-I36.

BORREGAARD, N. & COWLAND, J. B. 1997. Granules of the human neutrophilic polymorphonuclear leukocyte. *Blood,* 89**,** 3503.

BOTHA, A. J., MOORE, F. A., MOORE, E. E., SAUAIA, A., BANERJEE, A. & PETERSON, V. M. 1995. Early neutrophil sequestration after injury: a pathogenic mechanism for multiple organ failure. *J Trauma,* 39**,** 411-7.

BOYCE, S. W., BARTELS, C., BOLLI, R., CHAITMAN, B., CHEN, J. C., CHI, E., JESSEL, A., KEREIAKES, D., KNIGHT, J., THULIN, L. & THEROUX, P. 2003. Impact of sodium-hydrogen exchange inhibition by cariporide on death or myocardial infarction in high-risk CABG surgery patients: results of the CABG surgery cohort of the GUARDIAN study. *J Thorac Cardiovasc Surg,* 126**,** 420-7.

BUFFON, A., BIASUCCI, L. M., LIUZZO, G., D'ONOFRIO, G., CREA, F. & MASERI, A. 2002. Widespread coronary inflammation in unstable angina. *The New England journal of medicine,* 347**,** 5-12.

BUTLER, J., PARKER, D., PILLAI, R., WESTABY, S., SHALE, D. J. & ROCKER, G. M. 1993. Effect of cardiopulmonary bypass on systemic release of neutrophil elastase and tumor necrosis factor. *J Thorac Cardiovasc Surg,* 105**,** 25-30.

BUTLER, M. W., ROBERTSON, I., GREENE, C. M., O'NEILL, S. J., TAGGART, C. C. & MCELVANEY, N. G. 2006. Elafin prevents lipopolysaccharide-induced AP-1 and NF- B activation via an effect on the ubiquitin-proteasome pathway. *Journal of Biological Chemistry,* 281**,** 34730.

CARDEN, D., XIAO, F., MOAK, C., WILLIS, B. H., ROBINSON-JACKSON, S. & ALEXANDER, S. 1998. Neutrophil elastase promotes lung microvascular injury and proteolysis of endothelial cadherins. *American Journal of Physiology-Heart and Circulatory Physiology,* 275**,** H385.

CARROLL, T. P., GREENE, C. M., TAGGART, C. C., BOWIE, A. G., O'NEILL, S. J. & MCELVANEY, N. G. 2005. Viral inhibition of IL-1-and neutrophil elastase-induced inflammatory responses in bronchial epithelial cells. *The Journal of Immunology,* 175**,** 7594.

CERQUEIRA, M. D., WEISSMAN, N. J., DILSIZIAN, V., JACOBS, A. K., KAUL, S., LASKEY, W. K., PENNELL, D. J., RUMBERGER, J. A., RYAN, T. & VERANI, M. S. 2002. Standardized myocardial segmentation and nomenclature for tomographic imaging of the heart. A statement for healthcare professionals from the Cardiac Imaging Committee of the Council on Clinical Cardiology of the American Heart Association. *Circulation,* 105**,** 539-42.

CHAKRABORTI, S., MANDAL, M., DAS, S., MANDAL, A. & CHAKRABORTI, T. 2003. Regulation of matrix metalloproteinases: an overview. *Molecular and Cellular Biochemistry,* 253**,** 269-285.

CHIN, A. C., LEE, W. Y., NUSRAT, A., VERGNOLLE, N. & PARKOS, C. A. 2008. Neutrophil-mediated activation of epithelial protease-activated receptors-1 and-2 regulates barrier function and transepithelial migration. *The Journal of Immunology,* 181**,** 5702.

CHRISTEN, T., NI, W., QIU, D., SCHMIEDESKAMP, H., BAMMER, R., MOSELEY, M. & ZAHARCHUK, G. 2012. High-resolution cerebral blood volume imaging in humans using the blood pool contrast agent ferumoxytol. *Magn Reson Med*.

CHRISTEN, T., SHIMIZU, K. & LIBBY, P. 2010. Advances in imaging of cardiac allograft rejection. *Current Cardiovascular Imaging Reports,* 3**,** 99-105.

COESHOTT, C., OHNEMUS, C., PILYAVSKAYA, A., ROSS, S., WIECZOREK, M., KROONA, H., LEIMER, A. H. & CHERONIS, J. 1999. Converting enzyme-independent release of tumor necrosis factor and IL-1 from a stimulated human monocytic cell line in the presence of activated neutrophils or purified proteinase 3. *Proceedings of the National Academy of Sciences of the United States of America,* 96**,** 6261.

COOPER, L. T., BAUGHMAN, K. L., FELDMAN, A. M., FRUSTACI, A., JESSUP, M., KUHL, U., LEVINE, G. N., NARULA, J., STARLING, R. C., TOWBIN, J. & VIRMANI, R. 2007. The role of endomyocardial biopsy in the management of cardiovascular disease: a scientific statement from the American Heart Association, the American College of Cardiology, and the European Society of Cardiology Endorsed by the Heart Failure Society of America and the Heart Failure Association of the European Society of Cardiology. *Eur Heart J,* 28**,** 3076-93.

COUDREY, L. 1998. The troponins. *Archives of internal medicine,* 158**,** 1173-80.

COWAN, B., BARON, O., CRACK, J., COULBER, C., WILSON, G. J. & RABINOVITCH, M. 1996. Elafin, a serine elastase inhibitor, attenuates post-cardiac transplant coronary arteriopathy and reduces myocardial necrosis in rabbits afer heterotopic cardiac transplantation. *J Clin Invest,* 97**,** 2452-68.

CRINNION, J., HOMER-VANNIASINKAM, S., HATTON, R., PARKIN, S. & GOUGH, M. 1994. Role of neutrophil depletion and elastase inhibition in modifying skeletal muscle reperfusion injury. *Cardiovascular Surgery (London, England),* 2**,** 749.

CROAL, B. L., HILLIS, G. S., GIBSON, P. H., FAZAL, M. T., EL-SHAFEI, H., GIBSON, G., JEFFREY, R. R., BUCHAN, K. G., WEST, D. &

CUTHBERTSON, B. H. 2006. Relationship between postoperative cardiac troponin I levels and outcome of cardiac surgery. *Circulation,* 114**,** 1468-75.

CRUZ, D. N., RONCO, C. & KATZ, N. 2010. Neutrophil gelatinase-associated lipocalin: a promising biomarker for detecting cardiac surgery-associated acute kidney injury. *J Thorac Cardiovasc Surg,* 139**,** 1101-6.

DAHNKE, H., LIU, W., HERZKA, D., FRANK, J. A. & SCHAEFFTER, T. 2008. Susceptibility gradient mapping (SGM): a new postprocessing method for positive contrast generation applied to superparamagnetic iron oxide particle (SPIO)-labeled cells. *Magn Reson Med,* 60**,** 595-603.

DAY, J. R. & TAYLOR, K. M. 2005. The systemic inflammatory response syndrome and cardiopulmonary bypass. *Int J Surg,* 3**,** 129-40.

DEVANEY, J. M., GREENE, C. M., TAGGART, C. C., CARROLL, T. P., O'NEILL, S. J. & MCELVANEY, N. G. 2003. Neutrophil elastase up-regulates interleukin-8 via toll-like receptor 4. *FEBS letters,* 544**,** 129-132.

DEWALD, O., ZYMEK, P., WINKELMANN, K., KOERTING, A., REN, G., ABOU-KHAMIS, T., MICHAEL, L. H., ROLLINS, B. J., ENTMAN, M. L. & FRANGOGIANNIS, N. G. 2005. CCL2/monocyte chemoattractant protein-1 regulates inflammatory responses critical to healing myocardial infarcts. *Circulation Research,* 96**,** 881.

DINERMAN, J. L. & MEHTA, J. L. 1990. Endothelial, platelet and leukocyte interactions in ischemic heart disease: insights into potential mechanisms and their clinical relevance. *Journal of the American College of Cardiology,* 16**,** 207-222.

DIODATO, M. & CHEDRAWY, E. G. 2014. Coronary artery bypass graft surgery: the past, present, and future of myocardial revascularisation. *Surgery research and practice,* 2014**,** 726158.

DOTSENKO, O., XIAO, Q., XU, Q. & JAHANGIRI, M. 2010. Bone marrow resident and circulating progenitor cells in patients undergoing cardiac surgery. *Ann Thorac Surg,* 90**,** 1944-51.

DOUSSET, V., DELALANDE, C., BALLARINO, L., QUESSON, B., SEILHAN, D., COUSSEMACQ, M., THIAUDIÈRE, E., BROCHET, B., CANIONI, P. & CAILLÈ, J. M. 1999. In vivo macrophage activity imaging in the central nervous system detected by magnetic resonance. *Magnetic resonance in medicine,* 41**,** 329-333.

DREYER, W., MICHAEL, L., WEST, M., SMITH, C., ROTHLEIN, R., ROSSEN, R., ANDERSON, D. & ENTMAN, M. 1991. Neutrophil accumulation in ischemic canine myocardium. Insights into time course, distribution, and mechanism of localization during early reperfusion. *Circulation,* 84**,** 400.

DUBOSCQ, C., GENOUD, V., PARBORELL, M. F. & KORDICH, L. C. 1997. Impaired clot lysis by rt-PA catalyzed mini-plasminogen activation. *Thrombosis Research,* 86**,** 505-513.

DUTTA, P. & NAHRENDORF, M. 2015. Monocytes in myocardial infarction. *Arterioscler Thromb Vasc Biol,* 35**,** 1066-70.

EITEL, I., DESCH, S., FUERNAU, G., HILDEBRAND, L., GUTBERLET, M., SCHULER, G. & THIELE, H. 2010. Prognostic significance and determinants of myocardial salvage assessed by cardiovascular magnetic resonance in acute reperfused myocardial infarction. *J Am Coll Cardiol,* 55**,** 2470-9.

ENGLER, R., SCHMID-SCHÖNBEIN, G. & PAVELEC, R. 1983. Leukocyte capillary plugging in myocardial ischemia and reperfusion in the dog. *The American Journal of Pathology,* 111**,** 98.

FANANAPAZIR, G., MARIN, D., SUHOCKI, P. V., KIM, C. Y. & BASHIR, M. R. 2014. Vascular artifact mimicking thrombosis on MR imaging using ferumoxytol as a contrast agent in abdominal vascular assessment. *J Vasc Interv Radiol,* 25**,** 969-76.

FRANCART, C., DAUCHEZ, M., ALIX, A. J. P. & LIPPENS, G. 1997. Solution structure of R-elafin, a specific inhibitor of elastase. *Journal of Molecular Biology,* 268**,** 666-677.

FRANGOGIANNIS, N. G. 2006. Targeting the inflammatory response in healing myocardial infarcts. *Curr Med Chem,* 13**,** 1877-93.

FRIEDRICH, M. G. & MARCOTTE, F. 2013. Cardiac magnetic resonance assessment of myocarditis. *Circ Cardiovasc Imaging,* 6**,** 833-9.

FRISCH, S. M. & FRANCIS, H. 1994. Disruption of epithelial cell-matrix interactions induces apoptosis. *The Journal of Cell Biology,* 124**,** 619.

GARCIA-DORADO, D., OLIVERAS, J., GILI, J., SANZ, E., PEREZ-VILLA, F., BARRABES, J., CARRERAS, M. J., SOLARES, J. & SOLER-SOLER, J. 1993. Analysis of myocardial oedema by magnetic resonance imaging early after coronary artery occlusion with or without reperfusion. *Cardiovasc Res,* 27**,** 1462-9.

GARCIA-TOUCHARD, A., HENRY, T. D., SANGIORGI, G., SPAGNOLI, L. G., MAURIELLO, A., CONOVER, C. & SCHWARTZ, R. S. 2005. Extracellular proteases in atherosclerosis and restenosis. *Arteriosclerosis, Thrombosis, and Vascular Biology,* 25**,** 1119.

GELLISSEN, J., AXMANN, C., PRESCHER, A., BOHNDORF, K. & LODEMANN, K. P. 1999a. Extra- and intracellular accumulation of ultrasmall superparamagnetic iron oxides (USPIO) in experimentally induced abscesses of the peripheral soft tissues and their effects on magnetic resonance imaging. *Magn Reson Imaging,* 17**,** 557-67.

GONZALEZ, A., RAVASSA, S., BEAUMONT, J., LOPEZ, B. & DIEZ, J. 2011. New targets to treat the structural remodeling of the myocardium. *J Am Coll Cardiol,* 58**,** 1833-43.

HAASE, M., BELLOMO, R., DEVARAJAN, P., MA, Q., BENNETT, M. R., MOCKEL, M., MATALANIS, G., DRAGUN, D. & HAASE-FIELITZ, A. 2009. Novel biomarkers early predict the severity of acute kidney injury after cardiac surgery in adults. *Ann Thorac Surg,* 88**,** 124-30.

HAMMOND, M., LAPOINTE, G. R., FEUCHT, P. H., HILT, S., GALLEGOS, C. A., GORDON, C. A., GIEDLIN, M. A., MULLENBACH, G. & TEKAMP-OLSON, P. 1995. IL-8 induces neutrophil chemotaxis predominantly via type I IL-8 receptors. *The Journal of Immunology,* 155**,** 1428.

HANSEN, P. R. 1995. Role of neutrophils in myocardial ischemia and reperfusion. *Circulation,* 91**,** 1872.

HAUGER, O., DELALANDE, C., DEMINIËRE, C., FOUQUERAY, B., OHAYON, C., GARCIA, S., TRILLAUD, H., COMBE, C. & GRENIER, N. 2000. Nephrotoxic Nephritis and Obstructive Nephropathy: Evaluation with MR Imaging Enhanced with Ultrasmall Superparamagnetic Iron OxideóPreliminary Findings in a Rat Model1. *Radiology,* 217**,** 819.

HAUSENLOY, D. J., MWAMURE, P. K., VENUGOPAL, V., HARRIS, J., BARNARD, M., GRUNDY, E., ASHLEY, E., VICHARE, S., DI SALVO,

C., KOLVEKAR, S., HAYWARD, M., KEOGH, B., MACALLISTER, R. J. & YELLON, D. M. 2007. Effect of remote ischaemic preconditioning on myocardial injury in patients undergoing coronary artery bypass graft surgery: a randomised controlled trial. *Lancet,* 370**,** 575-9.

HAYASHIDANI, S., TSUTSUI, H., SHIOMI, T., IKEUCHI, M., MATSUSAKA, H., SUEMATSU, N., WEN, J., EGASHIRA, K. & TAKESHITA, A. 2003. Anti-monocyte chemoattractant protein-1 gene therapy attenuates left ventricular remodeling and failure after experimental myocardial infarction. *Circulation,* 108**,** 2134.

HENRIKSEN, P. A., HITT, M., XING, Z., WANG, J., HASLETT, C., RIEMERSMA, R. A., WEBB, D. J., KOTELEVTSEV, Y. V. & SALLENAVE, J. M. 2004. Adenoviral gene delivery of elafin and secretory leukocyte protease inhibitor attenuates NF- B-dependent inflammatory responses of human endothelial cells and macrophages to atherogenic stimuli. *The Journal of Immunology,* 172**,** 4535.

HERTZ, M. I., AURORA, P., CHRISTIE, J. D., DOBBELS, F., EDWARDS, L. B., KIRK, R., KUCHERYAVAYA, A. Y., RAHMEL, A. O., ROWE, A. W., STEHLIK, J. & TAYLOR, D. O. 2009. Scientific Registry of the International Society for Heart and Lung Transplantation: introduction to the 2009 Annual Reports. *J Heart Lung Transplant,* 28**,** 989-92.

HILL, G. E., ALONSO, A., SPURZEM, J. R., STAMMERS, A. H. & ROBBINS, R. A. 1995. Aprotinin and methylprednisolone equally blunt cardiopulmonary bypass-induced inflammation in humans. *J Thorac Cardiovasc Surg,* 110**,** 1658-62.

HOSHI, K., KUROSAWA, S., KATO, M., ANDOH, K., SATOH, D. & KAISE, A. 2005. Sivelestat, a neutrophil elastase inhibitor, reduces mortality rate of critically ill patients. *Tohoku J Exp Med,* 207**,** 143-8.

HOUGHTON, A. M. G., QUINTERO, P. A., PERKINS, D. L., KOBAYASHI, D. K., KELLEY, D. G., MARCONCINI, L. A., MECHAM, R. P., SENIOR, R. M. & SHAPIRO, S. D. 2006. Elastin fragments drive disease progression in a murine model of emphysema. *Journal of Clinical Investigation,* 116**,** 753.

http://www.bts.org.uk/TRANSPLANTATION/HEART/ 2015. BHF CVD Statistics Factsheet - UK. *BHF Centre on Population Approaches for Non-Communicable Disease Prevention*.

HUNT, M. A., BAGO, A. G. & NEUWELT, E. A. 2005. Single-dose contrast agent for intraoperative MR imaging of intrinsic brain tumors by using ferumoxtran-10. *AJNR Am J Neuroradiol,* 26**,** 1084-8.

IRWIN, M. W., MAK, S., MANN, D. L., QU, R., PENNINGER, J. M., YAN, A., DAWOOD, F., WEN, W. H., SHOU, Z. & LIU, P. 1999. Tissue expression and immunolocalization of tumor necrosis factor-alpha in postinfarction dysfunctional myocardium. *Circulation,* 99**,** 1492-8.

ISBIR, C. S., DOGAN, R., DEMIRCIN, M., YAYLIM, I. & PASAOGLU, I. 2001. Aprotinin reduces the IL-8 after coronary artery bypass grafting. *Cardiovasc Surg,* 9**,** 403-6.

JIN, F., NATHAN, C., RADZIOCH, D. & DING, A. 1997. Secretory leukocyte protease inhibitor: a macrophage product induced by and antagonistic to bacterial lipopolysaccharide. *Cell,* 88**,** 417-426.

JO, S. K., HU, X., KOBAYASHI, H., LIZAK, M., MIYAJI, T., KORETSKY, A. & STAR, R. A. 2003. Detection of inflammation following renal ischemia by magnetic resonance imaging. *Kidney International,* 64**,** 43-51.

JOHANSSON, L., JOHNSSON, C., PENNO, E., BJORNERUD, A. & AHLSTROM, H. 2002. Acute cardiac transplant rejection: detection and grading with MR imaging with a blood pool contrast agent--experimental study in the rat. *Radiology,* 225**,** 97-103.

JORDAN, J. E., ZHAO, Z. Q. & VINTEN-JOHANSEN, J. 1999. The role of neutrophils in myocardial ischemiañreperfusion injury. *Cardiovascular Research,* 43**,** 860.

KANDOLIN, R., LEHTONEN, J. & KUPARI, M. 2011. Cardiac sarcoidosis and giant cell myocarditis as causes of atrioventricular block in young and middle-aged adults. *Circ Arrhythm Electrophysiol,* 4**,** 303-9.

KANNO, S., WU, Y. J., LEE, P. C., DODD, S. J., WILLIAMS, M., GRIFFITH, B. P. & HO, C. 2001. Macrophage accumulation associated with rat cardiac allograft rejection detected by magnetic resonance imaging with ultrasmall superparamagnetic iron oxide particles. *Circulation,* 104**,** 934-8.

KATUS, H. A., LOOSER, S., HALLERMAYER, K., REMPPIS, A., SCHEFFOLD, T., BORGYA, A., ESSIG, U. & GEUSS, U. 1992. Development and in vitro characterization of a new immunoassay of cardiac troponin T. *Clinical chemistry,* 38**,** 386-93.

KATUS, H. A., REMPPIS, A., SCHEFFOLD, T., DIEDERICH, K. W. & KUEBLER, W. 1991. Intracellular compartmentation of cardiac troponin T and its release kinetics in patients with reperfused and nonreperfused myocardial infarction. *The American journal of cardiology,* 67**,** 1360-7.

KING, A. E., CRITCHLEY, H. O. D., SALLENAVE, J. M. & KELLY, R. W. 2003. Elafin in human endometrium: an antiprotease and antimicrobial molecule expressed during menstruation. *Journal of Clinical Endocrinology & Metabolism,* 88**,** 4426.

KOOI, M. E., CAPPENDIJK, V. C., CLEUTJENS, K. B. J. M., KESSELS, A. G. H., KITSLAAR, P. J. E. H. M., BORGERS, M., FREDERIK, P. M., DAEMEN, M. J. A. P. & VAN ENGELSHOVEN, J. M. A. 2003. Accumulation of ultrasmall superparamagnetic particles of iron oxide in human atherosclerotic plaques can be detected by in vivo magnetic resonance imaging. *Circulation,* 107**,** 2453-8.

KORKMAZ, B., ATTUCCI, S., JOURDAN, M. L., JULIANO, L. & GAUTHIER, F. 2005. Inhibition of neutrophil elastase by 1-protease inhibitor at the surface of human polymorphonuclear neutrophils. *The Journal of Immunology,* 175**,** 3329.

KROMBACH, G. A., WENDLAND, M. F., HIGGINS, C. B. & SAEED, M. 2002. MR imaging of spatial extent of microvascular injury in reperfused ischemically injured rat myocardium: value of blood pool ultrasmall superparamagnetic particles of iron oxide. *Radiology,* 225**,** 479-86.

KUMAR, A. G., BALLANTYNE, C. M., MICHAEL, L. H., KUKIELKA, G. L., YOUKER, K. A., LINDSEY, M. L., HAWKINS, H. K., BIRDSALL, H. H., MACKAY, C. R. & LAROSA, G. J. 1997. Induction of monocyte chemoattractant protein-1 in the small veins of the ischemic and reperfused canine myocardium. *Circulation,* 95**,** 693.

LAMBERT, J. M., LOPEZ, E. F. & LINDSEY, M. L. 2008. Macrophage roles following myocardial infarction. *International Journal of Cardiology,* 130**,** 147-158.

LANDRY, R., JACOBS, P. M., DAVIS, R., SHENOUDA, M. & BOLTON, W. K. 2005. Pharmacokinetic study of ferumoxytol: a new iron replacement therapy in normal subjects and hemodialysis patients. *Am J Nephrol,* 25**,** 400-10.

LAROSE, E., RODES-CABAU, J., PIBAROT, P., RINFRET, S., PROULX, G., NGUYEN, C. M., DERY, J. P., GLEETON, O., ROY, L., NOEL, B., BARBEAU, G., ROULEAU, J., BOUDREAULT, J. R., AMYOT, M., DE LAROCHELLIERE, R. & BERTRAND, O. F. 2010. Predicting late myocardial recovery and outcomes in the early hours of ST-segment elevation myocardial infarction traditional measures compared with microvascular obstruction, salvaged myocardium, and necrosis characteristics by cardiovascular magnetic resonance. *J Am Coll Cardiol,* 55**,** 2459-69.

LASSNIGG, A., SCHMIDLIN, D., MOUHIEDDINE, M., BACHMANN, L. M., DRUML, W., BAUER, P. & HIESMAYR, M. 2004. Minimal changes of serum creatinine predict prognosis in patients after cardiothoracic surgery: a prospective cohort study. *J Am Soc Nephrol,* 15**,** 1597-605.

LAWACZECK, R., MENZEL, M. & PIETSCH, H. 2004. Superparamagnetic iron oxide particles: contrast media for magnetic resonance imaging. *Applied Organometallic Chemistry,* 18**,** 506-513.

LEE, S., HIROSE, S., PARK, S., CHI, J., CHUNG, S. & MORI, M. 2002. Elafin expression in human fetal and adult submandibular glands. *Histochemistry and Cell Biology,* 117**,** 423-430.

LEE, W. L. & DOWNEY, G. P. 2001. Leukocyte elastase. Physiological functions and role in acute lung injury. *American Journal of Respiratory and Critical Care Medicine,* 164**,** 896.

LEE, W. W., MARINELLI, B., VAN DER LAAN, A. M., SENA, B. F., GORBATOV, R., LEUSCHNER, F., DUTTA, P., IWAMOTO, Y., UENO, T., BEGIENEMAN, M. P., NIESSEN, H. W., PIEK, J. J., VINEGONI, C., PITTET, M. J., SWIRSKI, F. K., TAWAKOL, A., DI CARLI, M., WEISSLEDER, R. & NAHRENDORF, M. 2012. PET/MRI of Inflammation in Myocardial Infarction. *J Am Coll Cardiol,* 59**,** 153-63.

LEGER, A. J., COVIC, L. & KULIOPULOS, A. 2006. Protease-activated receptors in cardiovascular diseases. *Circulation,* 114**,** 1070.

LENTSCH, A. B., YOSHIDOME, H., WARNER, R. L., WARD, P. A. & EDWARDS, M. J. 1999. Secretory leukocyte protease inhibitor in mice regulates local and remote organ inflammatory injury induced by hepatic ischemia/reperfusion. *Gastroenterology,* 117**,** 953-61.

LEUSCHNER, F., RAUCH, P. J., UENO, T., GORBATOV, R., MARINELLI, B., LEE, W. W., DUTTA, P., WEI, Y., ROBBINS, C., IWAMOTO, Y., SENA, B., CHUDNOVSKIY, A., PANIZZI, P., KELIHER, E., HIGGINS, J. M., LIBBY, P., MOSKOWITZ, M. A., PITTET, M. J., SWIRSKI, F. K., WEISSLEDER, R. & NAHRENDORF, M. 2012. Rapid monocyte kinetics in acute myocardial infarction are sustained by extramedullary monocytopoiesis. *J Exp Med,* 209**,** 123-37.

LI, G., JIA, J., JI, K., GONG, X., WANG, R., ZHANG, X., WANG, H. & ZANG, B. 2016. The neutrophil elastase inhibitor, sivelestat, attenuates sepsis-related kidney injury in rats. *Int J Mol Med,* 38**,** 767-75.

LIM, C. C., CUCULI, F., VAN GAAL, W. J., TESTA, L., ARNOLD, J. R., KARAMITSOS, T., FRANCIS, J. M., DIGBY, J. E., ANTONIADES, C., KHARBANDA, R. K., NEUBAUER, S., WESTABY, S. & BANNING, A. P. 2011. Early diagnosis of perioperative myocardial infarction after coronary

bypass grafting: a study using biomarkers and cardiac magnetic resonance imaging. *The Annals of Thoracic Surgery,* 92**,** 2046-53.

LIMA, J. A., JUDD, R. M., BAZILLE, A., SCHULMAN, S. P., ATALAR, E. & ZERHOUNI, E. A. 1995. Regional heterogeneity of human myocardial infarcts demonstrated by contrast-enhanced MRI. Potential mechanisms. *Circulation,* 92**,** 1117-25.

LITT, M. R., JEREMY, R. W., WEISMAN, H. F., WINKELSTEIN, J. A. & BECKER, L. C. 1989. Neutrophil depletion limited to reperfusion reduces myocardial infarct size after 90 minutes of ischemia. Evidence for neutrophil-mediated reperfusion injury. *Circulation,* 80**,** 1816.

LONES, M. A., CZER, L. S., TRENTO, A., HARASTY, D., MILLER, J. M. & FISHBEIN, M. C. 1995. Clinical-pathologic features of humoral rejection in cardiac allografts: a study in 81 consecutive patients. *J Heart Lung Transplant,* 14**,** 151-62.

LUDWIG, A., POLLER, W. C., WESTPHAL, K., MINKWITZ, S., LATTIG-TUNNEMANN, G., METZKOW, S., STANGL, K., BAUMANN, G., TAUPITZ, M., WAGNER, S., SCHNORR, J. & STANGL, V. 2013. Rapid binding of electrostatically stabilized iron oxide nanoparticles to THP-1 monocytic cells via interaction with glycosaminoglycans. *Basic Res Cardiol,* 108**,** 328.

LUISETTI, M., STURANI, C., SELLA, D., MADONINI, E., GALAVOTTI, V., BRUNO, G., PEONA, V., KUCICH, U., DAGNINO, G., ROSENBLOOM, J., STARCHER, B. & GRASSI, C. 1996. MR889, a neutrophil elastase inhibitor, in patients with chronic obstructive pulmonary disease: a double-blind, randomized, placebo-controlled clinical trial. *Eur Respir J,* 9**,** 1482-6.

LUTZ, A. M., GˆPFERT, K., JOCHUM, W., NANZ, D., FRˆHLICH, J. M. & WEISHAUPT, D. 2006. USPIO enhanced MR imaging for visualization of synovial hyperperfusion and detection of synovial macrophages: Preliminary results in an experimental model of antigen induced arthritis. *Journal of Magnetic Resonance Imaging,* 24**,** 657-666.

MADJID, M., AWAN, I., WILLERSON, J. T. & CASSCELLS, S. W. 2004. Leukocyte count and coronary heart disease:: Implications for risk assessment. *Journal of the American College of Cardiology,* 44**,** 1945-1956.

MAIR, J., DIENSTL, F. & PUSCHENDORF, B. 1992. Cardiac troponin T in the diagnosis of myocardial injury. *Critical reviews in clinical laboratory sciences,* 29**,** 31-57.

MANGANO, D. T., TUDOR, I. C. & DIETZEL, C. 2006. The risk associated with aprotinin in cardiac surgery. *N Engl J Med,* 354**,** 353-65.

MARCHANT, D. J., BOYD, J. H., LIN, D. C., GRANVILLE, D. J., GARMAROUDI, F. S. & MCMANUS, B. M. 2012. Inflammation in myocardial diseases. *Circ Res,* 110**,** 126-44.

MARGOLIS, D. J., HOFFMAN, J. M., HERFKENS, R. J., JEFFREY, R. B., QUON, A. & GAMBHIR, S. S. 2007. Molecular imaging techniques in body imaging. *Radiology,* 245**,** 333-56.

MASSBERG, S., GRAHL, L., VON BRUEHL, M. L., MANUKYAN, D., PFEILER, S., GOOSMANN, C., BRINKMANN, V., LORENZ, M., BIDZHEKOV, K., KHANDAGALE, A. B., KONRAD, I., KENNERKNECHT, E., REGES, K., HOLDENRIEDER, S., BRAUN, S., REINHARDT, C., SPANNAGL, M., PREISSNER, K. T. & ENGELMANN,

B. 2010. Reciprocal coupling of coagulation and innate immunity via neutrophil serine proteases. *Nat Med,* 16**,** 887-96.

MATSUZAKI, K., HIRAMATSU, Y., HOMMA, S., SATO, S., SHIGETA, O. & SAKAKIBARA, Y. 2005. Sivelestat reduces inflammatory mediators and preserves neutrophil deformability during simulated extracorporeal circulation. *Ann Thorac Surg,* 80**,** 611-7.

MCATEER, M. A., VON ZUR MUHLEN, C., ANTHONY, D. C., SIBSON, N. R. & CHOUDHURY, R. P. 2011. Magnetic resonance imaging of brain inflammation using microparticles of iron oxide. *Methods Mol Biol,* 680**,** 103-15.

MCELVANEY, N. G., NAKAMURA, H., BIRRER, P., HEBERT, C. A., WONG, W. L., ALPHONSO, M., BAKER, J. B., CATALANO, M. A. & CRYSTAL, R. G. 1992. Modulation of airway inflammation in cystic fibrosis. In vivo suppression of interleukin-8 levels on the respiratory epithelial surface by aerosolization of recombinant secretory leukoprotease inhibitor. *J Clin Invest,* 90**,** 1296-301.

MENTZER, R. M., JR., BARTELS, C., BOLLI, R., BOYCE, S., BUCKBERG, G. D., CHAITMAN, B., HAVERICH, A., KNIGHT, J., MENASCHE, P., MYERS, M. L., NICOLAU, J., SIMOONS, M., THULIN, L. & WEISEL, R. D. 2008. Sodium-hydrogen exchange inhibition by cariporide to reduce the risk of ischemic cardiac events in patients undergoing coronary artery bypass grafting: results of the EXPEDITION study. *Ann Thorac Surg,* 85**,** 1261-70.

MEYBOHM, P., GRUENEWALD, M., ALBRECHT, M., ZACHAROWSKI, K. D., LUCIUS, R., ZITTA, K., KOCH, A., TRAN, N., SCHOLZ, J. & BEIN, B. 2009. Hypothermia and postconditioning after cardiopulmonary resuscitation reduce cardiac dysfunction by modulating inflammation, apoptosis and remodeling. *PLoS One,* 4**,** e7588.

MITCHELL, D. N., SCADDING, J. G., HEARD, B. E. & HINSON, K. F. 1977. Sarcoidosis: histopathological definition and clinical diagnosis. *J Clin Pathol,* 30**,** 395-408.

MOCATTA, T. J., PILBROW, A. P., CAMERON, V. A., SENTHILMOHAN, R., FRAMPTON, C. M., RICHARDS, A. M. & WINTERBOURN, C. C. 2007. Plasma concentrations of myeloperoxidase predict mortality after myocardial infarction. *Journal of the American College of Cardiology,* 49**,** 1993-2000.

MOLHUIZEN, H., ALKEMADE, H., ZEEUWEN, P., DE JONGH, G., WIERINGA, B. & SCHALKWIJK, J. 1993. SKALP/elafin: an elastase inhibitor from cultured human keratinocytes. Purification, cDNA sequence, and evidence for transglutaminase cross-linking. *Journal of Biological Chemistry,* 268**,** 12028.

MONTET-ABOU, K., DAIRE, J. L., HYACINTHE, J. N., JORGE-COSTA, M., GROSDEMANGE, K., MACH, F., PETRI-FINK, A., HOFMANN, H., MOREL, D. R., VALLEE, J. P. & MONTET, X. 2010. In vivo labelling of resting monocytes in the reticuloendothelial system with fluorescent iron oxide nanoparticles prior to injury reveals that they are mobilized to infarcted myocardium. *Eur Heart J,* 31**,** 1410-20.

MTAIRAG, E. M., HOUARD, X., RAIS, S., PASQUIER, C., OUDGHIRI, M., JACOB, M. P., MEILHAC, O. & MICHEL, J. B. 2002. Pharmacological potentiation of natriuretic peptide limits polymorphonuclear neutrophil-vascular cell interactions. *Arteriosclerosis, Thrombosis, and Vascular Biology,* 22**,** 1824.

MUROHARA, T., BUERKE, M. & LEFER, A. M. 1994. Polymorphonuclear leukocyte-induced vasocontraction and endothelial dysfunction. Role of selectins. *Arteriosclerosis, Thrombosis, and Vascular Biology,* 14**,** 1509.

NAGATA, Y., FUJIMOTO, M., NAKAMURA, K., ISOYAMA, N., MATSUMURA, M., FUJIKAWA, K., UCHIYAMA, K., TAKAKI, E., TAKII, R., NAKAI, A. & MATSUYAMA, H. 2016. Anti-TNF-alpha Agent Infliximab and Splenectomy Are Protective Against Renal Ischemia-Reperfusion Injury. *Transplantation,* 100**,** 1675-82.

NAHRENDORF, M., PITTET, M. J. & SWIRSKI, F. K. 2010. Monocytes: protagonists of infarct inflammation and repair after myocardial infarction. *Circulation,* 121**,** 2437.

NAHRENDORF, M., SWIRSKI, F. K., AIKAWA, E., STANGENBERG, L., WURDINGER, T., FIGUEIREDO, J. L., LIBBY, P., WEISSLEDER, R. & PITTET, M. J. 2007a. The healing myocardium sequentially mobilizes two monocyte subsets with divergent and complementary functions. *J Exp Med,* 204**,** 3037-47.

NAHRENDORF, M., SWIRSKI, F. K., AIKAWA, E., STANGENBERG, L., WURDINGER, T., FIGUEIREDO, J. L., LIBBY, P., WEISSLEDER, R. & PITTET, M. J. 2007b. The healing myocardium sequentially mobilizes two monocyte subsets with divergent and complementary functions. *The Journal of Experimental Medicine,* 204**,** 3037.

NAJAFI, M. 2014. Serum creatinine role in predicting outcome after cardiac surgery beyond acute kidney injury. *World J Cardiol,* 6**,** 1006-21.

NAKAMURA, H., UMEMOTO, S., NAIK, G., MOE, G., TAKATA, S., LIU, P. & MATSUZAKI, M. 2003. Induction of left ventricular remodeling and dysfunction in the recipient heart after donor heart myocardial infarction: new insights into the pathologic role of tumor necrosis factor-alpha from a novel heterotopic transplant-coronary ligation rat model. *J Am Coll Cardiol,* 42**,** 173-81.

NARA, K., ITO, S., ITO, T., SUZUKI, Y., GHONEIM, M. A., TACHIBANA, S. & HIROSE, S. 1994. Elastase inhibitor elafin is a new type of proteinase inhibitor which has a transglutaminase-mediated anchoring sequence termed ìcementoinî. *Journal of Biochemistry,* 115**,** 441.

NASHEF, S. A., ROQUES, F., MICHEL, P., GAUDUCHEAU, E., LEMESHOW, S. & SALAMON, R. 1999. European system for cardiac operative risk evaluation (EuroSCORE). *Eur J Cardiothorac Surg,* 16**,** 9-13.

NEMOTO, E., SUGAWARA, S., TADA, H., TAKADA, H., SHIMAUCHI, H. & HORIUCHI, H. 2000. Cleavage of CD14 on human gingival fibroblasts cocultured with activated neutrophils is mediated by human leukocyte elastase resulting in down-regulation of lipopolysaccharide-induced IL-8 production. *J Immunol,* 165**,** 5807-13.

NESHER, N., ALGHAMDI, A. A., SINGH, S. K., SEVER, J. Y., CHRISTAKIS, G. T., GOLDMAN, B. S., COHEN, G. N., MOUSSA, F. & FREMES, S. E. 2008. Troponin after cardiac surgery: a predictor or a phenomenon? *Ann Thorac Surg,* 85**,** 1348-54.

NINOMIYA, M., MIYAJI, K. & TAKAMOTO, S. 2003. Influence of PMEA-coated bypass circuits on perioperative inflammatory response. *Ann Thorac Surg,* 75**,** 913-7; discussion 917-8.

NOORA, J., RICCI, C., HASTINGS, D., HILL, S. & CYBULSKY, I. 2005. Determination of troponin I release after CABG surgery. *J Card Surg,* 20**,** 129-35.

NORRIS, D. A., CLARK, R., SWIGART, L. M., HUFF, J., WESTON, W. & HOWELL, S. 1982. Fibronectin fragment (s) are chemotactic for human peripheral blood monocytes. *The Journal of Immunology,* 129**,** 1612.

NUYTINCK, H. K., OFFERMANS, X. J., KUBAT, K. & GORIS, J. A. 1988. Whole-body inflammation in trauma patients. An autopsy study. *Arch Surg,* 123**,** 1519-24.

O'NEAL, J. B., SHAW, A. D. & BILLINGS, F. T. T. 2016. Acute kidney injury following cardiac surgery: current understanding and future directions. *Crit Care,* 20**,** 187.

ODA, T., HOTTA, O., TAGUMA, Y., KITAMURA, H., SUDO, K., HORIGOME, I., CHIBA, S., YOSHIZAWA, N. & NAGURA, H. 1997. Involvement of neutrophil elastase in crescentic glomerulonephritis. *Hum Pathol,* 28**,** 720-8.

OHTA, K., NAKAJIMA, T., CHEAH, A. Y., ZAIDI, S. H., KAVIANI, N., DAWOOD, F., YOU, X. M., LIU, P., HUSAIN, M. & RABINOVITCH, M. 2004a. Elafin-overexpressing mice have improved cardiac function after myocardial infarction. *Am J Physiol Heart Circ Physiol,* 287**,** H286-92.

OHTA, K., NAKAJIMA, T., CHEAH, A. Y. L., ZAIDI, S. H. E., KAVIANI, N., DAWOOD, F., YOU, X. M., LIU, P., HUSAIN, M. & RABINOVITCH, M. 2004b. Elafin-overexpressing mice have improved cardiac function after myocardial infarction. *American Journal of Physiology-Heart and Circulatory Physiology,* 287**,** H286.

OKADA, Y. & NAKANISHI, I. 1989. Activation of matrix metalloproteinase 3 (stromelysin) and matrix metalloproteinase 2 ('gelatinase') by human neutrophil elastase and cathepsin G. *FEBS letters,* 249**,** 353-356.

OKADA, Y., WATANABE, S., NAKANISHI, I., KISHI, J., HAYAKAWA, T., WATOREK, W., TRAVIS, J. & NAGASE, H. 1988. Inactivation of tissue inhibitor of metalloproteinases by neutrophil elastase and other serine proteinases. *FEBS letters,* 229**,** 157-160.

OKAYAMA, N., KAKIHANA, Y., SETOGUCHI, D., IMABAYASHI, T., OMAE, T., MATSUNAGA, A. & KANMURA, Y. 2006. Clinical effects of a neutrophil elastase inhibitor, sivelestat, in patients with acute respiratory distress syndrome. *J Anesth,* 20**,** 6-10.

OKAZAKI, T., EBIHARA, S., ASADA, M., YAMANDA, S., SAIJO, Y., SHIRAISHI, Y., EBIHARA, T., NIU, K., MEI, H. & ARAI, H. 2007. Macrophage colony-stimulating factor improves cardiac function after ischemic injury by inducing vascular endothelial growth factor production and survival of cardiomyocytes. *American Journal of Pathology,* 171**,** 1093.

OKUSA, M. D. 2002. The inflammatory cascade in acute ischemic renal failure. *Nephron,* 90**,** 133-8.

ONORATI, F., DE FEO, M., MASTROROBERTO, P., CRISTODORO, L., PEZZO, F., RENZULLI, A. & COTRUFO, M. 2005. Determinants and prognosis of myocardial damage after coronary artery bypass grafting. *Ann Thorac Surg,* 79**,** 837-45.

OWEN, C. A., CAMPBELL, M. A., SANNES, P. L., BOUKEDES, S. S. & CAMPBELL, E. J. 1995. Cell surface-bound elastase and cathepsin G on human neutrophils: a novel, non-oxidative mechanism by which neutrophils

focus and preserve catalytic activity of serine proteinases. *The Journal of Cell Biology,* 131**,** 775.

PADRINES, M., WOLF, M., WALZ, A. & BAGGIOLINI, M. 1994. Interleukin-8 processing by neutrophil elastase, cathepsin G and proteinase-3. *FEBS letters,* 352**,** 231-235.

PAPARELLA, D., YAU, T. M. & YOUNG, E. 2002. Cardiopulmonary bypass induced inflammation: pathophysiology and treatment. An update. *Eur J Cardiothorac Surg,* 21**,** 232-44.

PAROLARI, A., PESCE, L. L., PACINI, D., MAZZANTI, V., SALIS, S., SCIACOVELLI, C., ROSSI, F., ALAMANNI, F. & MONZINO RESEARCH GROUP ON CARDIAC SURGERY, O. 2012. Risk factors for perioperative acute kidney injury after adult cardiac surgery: role of perioperative management. *Ann Thorac Surg,* 93**,** 584-91.

PATEL, K. D., CUVELIER, S. L. & WIEHLER, S. 2002. Selectins: critical mediators of leukocyte recruitment. *Semin Immunol,* 14**,** 73-81.

PEGG, T. J., MAUNSELL, Z., KARAMITSOS, T. D., TAYLOR, R. P., JAMES, T., FRANCIS, J. M., TAGGART, D. P., WHITE, H., NEUBAUER, S. & SELVANAYAGAM, J. B. 2011. Utility of cardiac biomarkers for the diagnosis of type V myocardial infarction after coronary artery bypass grafting: insights from serial cardiac MRI. *Heart,* 97**,** 810-6.

PENNO, E., JOHANSSON, L., AHLSTROM, H. & JOHNSSON, C. 2007. Ultrasmall iron oxide particle contrast agent and MRI can be used to monitor the effect of anti-rejection treatment. *Transplantation,* 84**,** 374-9.

PFUNDT, R., WINGENS, M., BERGERS, M., ZWEERS, M., FRENKEN, M. & SCHALKWIJK, J. 2000. TNF- and serum induce SKALP/elafin gene expression in human keratinocytes by a p38 MAP kinase-dependent pathway. *Archives of Dermatological Research,* 292**,** 180-187.

PILLAY, J., HIETBRINK, F., KOENDERMAN, L. & LEENEN, L. P. 2007. The systemic inflammatory response induced by trauma is reflected by multiple phenotypes of blood neutrophils. *Injury,* 38**,** 1365-72.

POSTLETHWAITE, A. & KANG, A. H. 1976. Collagen-and collagen peptide-induced chemotaxis of human blood monocytes. *The Journal of Experimental Medicine,* 143**,** 1299.

RAMACHANDRAN, R., MIHARA, K., CHUNG, H., RENAUX, B., LAU, C. S., MURUVE, D. A., DEFEA, K. A., BOUVIER, M. & HOLLENBERG, M. D. 2011. Neutrophil Elastase Acts as a Biased Agonist for Proteinase-activated Receptor-2 (PAR2). *Journal of Biological Chemistry,* 286**,** 24638.

RAUSCH, M., SAUTER, A., FRˆHLICH, J., NEUBACHER, U., RAD¸, E. W. & RUDIN, M. 2001. Dynamic patterns of USPIO enhancement can be observed in macrophages after ischemic brain damage. *Magnetic Resonance in Medicine,* 46**,** 1018-1022.

REIMER, K. A., MURRY, C. E. & RICHARD, V. J. 1989. The role of neutrophils and free radicals in the ischemic-reperfused heart: why the confusion and controversy? *Journal of Molecular and Cellular Cardiology,* 21**,** 1225.

RICHARDS, J. M., SEMPLE, S. I., MACGILLIVRAY, T. J., GRAY, C., LANGRISH, J. P., WILLIAMS, M., DWECK, M., WALLACE, W., MCKILLOP, G., CHALMERS, R. T., GARDEN, O. J. & NEWBY, D. E. 2011a. Abdominal aortic aneurysm growth predicted by uptake of ultrasmall superparamagnetic particles of iron oxide: a pilot study. *Circ Cardiovasc Imaging,* 4**,** 274-81.

RICHARDS, J. M., SHAW, C. A., LANG, N. N., WILLIAMS, M. C., SEMPLE, S. I., MACGILLIVRAY, T. J., GRAY, C., CRAWFORD, J. H., ALAM, S. R. & ATKINSON, A. P. 2012. In Vivo Mononuclear Cell Tracking Using Superparamagnetic Particles of Iron OxideClinical Perspective Feasibility and Safety in Humans. *Circulation: Cardiovascular Imaging,* 5**,** 509-517.

RICHARDS, J. M. J., SEMPLE, S. I., MACGILLIVRAY, T. J., GRAY, C., LANGRISH, J. P., WILLIAMS, M., DWECK, M., WALLACE, W., MCKILLOP, G. & CHALMERS, R. T. A. 2011b. Abdominal Aortic Aneurysm Growth Predicted by Uptake of Ultrasmall Superparamagnetic Particles of Iron Oxide: A Pilot Study. *Circulation: Cardiovascular Imaging*.

RICHARDSON, D., PEPPER, D. & KAY, A. 1976. Chemotaxis for Human Monocytes by Fibrinogen derived Peptides. *British Journal of Haematology,* 32**,** 507-514.

RICHTER, J., NG-SIKORSKI, J., OLSSON, I. & ANDERSSON, T. 1990. Tumor necrosis factor-induced degranulation in adherent human neutrophils is dependent on CD11b/CD18-integrin-triggered oscillations of cytosolic free Ca2+. *Proceedings of the National Academy of Sciences,* 87**,** 9472.

RIOU, L. M., RUIZ, M., SULLIVAN, G. W., LINDEN, J., LEONG-POI, H., LINDNER, J. R., HARRIS, T. D., BELLER, G. A. & GLOVER, D. K. 2002. Assessment of myocardial inflammation produced by experimental coronary occlusion and reperfusion with 99mTc-RP517, a new leukotriene B4 receptor antagonist that preferentially labels neutrophils in vivo. *Circulation,* 106**,** 592-8.

RISTIKANKARE, A., POYHIA, R., KUITUNEN, A., SKRIFVARS, M., HAMMAINEN, P., SALMENPERA, M. & SUOJARANTA-YLINEN, R. 2010. Serum cystatin C in elderly cardiac surgery patients. *Ann Thorac Surg,* 89**,** 689-94.

ROBERT, L., ROBERT, A. & JACOTOT, B. 1998. Elastin-elastase-atherosclerosis revisited. *Atherosclerosis,* 140**,** 281-295.

ROBERTS, W. C., MCALLISTER, H. A., JR. & FERRANS, V. J. 1977. Sarcoidosis of the heart. A clinicopathologic study of 35 necropsy patients (group 1) and review of 78 previously described necropsy patients (group 11). *Am J Med,* 63**,** 86-108.

ROMSON, J. L., HOOK, B. G., KUNKEL, S. L., ABRAMS, G., SCHORK, M. & LUCCHESI, B. 1983a. Reduction of the extent of ischemic myocardial injury by neutrophil depletion in the dog. *Circulation,* 67**,** 1016.

ROMSON, J. L., HOOK, B. G., KUNKEL, S. L., ABRAMS, G. D., SCHORK, M. A. & LUCCHESI, B. R. 1983b. Reduction of the extent of ischemic myocardial injury by neutrophil depletion in the dog. *Circulation,* 67**,** 1016-23.

RUDOLPH, T. K., SCHAPER, N., KLINKE, A., DEMIR, C., GOLDMANN, B., LAU, D., KOSTER, R., HELLMICH, M., MEINERTZ, T., BALDUS, S. & RUDOLPH, V. 2013. Liberation of vessel-adherent myeloperoxidase reflects plaque burden in patients with stable coronary artery disease. *Atherosclerosis,* 231**,** 354-8.

RUEHM, S. G., COROT, C., VOGT, P., KOLB, S. & DEBATIN, J. F. 2001a. Magnetic resonance imaging of atherosclerotic plaque with ultrasmall superparamagnetic particles of iron oxide in hyperlipidemic rabbits. *Circulation,* 103**,** 415.

RUEHM, S. G., COROT, C., VOGT, P., KOLB, S. & DEBATIN, J. F. 2001b. Magnetic resonance imaging of atherosclerotic plaque with ultrasmall superparamagnetic particles of iron oxide in hyperlipidemic rabbits. *Circulation,* 103**,** 415-22.

RYBICKI, B. A. & IANNUZZI, M. C. 2007. Epidemiology of sarcoidosis: recent advances and future prospects. *Semin Respir Crit Care Med,* 28**,** 22-35.

RYUGO, M., SAWA, Y., TAKANO, H., MATSUMIYA, G., IWAI, S., ONO, M., HATA, H., YAMAUCHI, T., NISHIMURA, M., FUJINO, Y. & MATSUDA, H. 2006. Effect of a polymorphonuclear elastase inhibitor (sivelestat sodium) on acute lung injury after cardiopulmonary bypass: findings of a double-blind randomized study. *Surg Today,* 36**,** 321-6.

SADALLAH, S., HESS, C., MIOT, S., SPERTINI, O., LUTZ, H. & SCHIFFERLI, J. A. 1999. Elastase and metalloproteinase activities regulate soluble complement receptor 1 release. *European Journal of Immunology,* 29**,** 3754-3761.

SAGAR, S., LIU, P. P. & COOPER, L. T., JR. 2012. Myocarditis. *Lancet,* 379**,** 738-47.

SAITO, S., TSUGENO, M., KOTO, D., MORI, Y., YOSHIOKA, Y., NOHARA, S. & MURASE, K. 2012. Impact of surface coating and particle size on the uptake of small and ultrasmall superparamagnetic iron oxide nanoparticles by macrophages. *Int J Nanomedicine,* 7**,** 5415-21.

SALLENAVE, J. & SILVA, A. 1993. Characterization and gene sequence of the precursor of elafin, an elastase-specific inhibitor in bronchial secretions. *American Journal of Respiratory Cell and Molecular Biology,* 8**,** 439.

SALLENAVE, J., SILVA, A., MARSDEN, M. & RYLE, A. 1993. Secretion of mucus proteinase inhibitor and elafin by Clara cell and type II pneumocyte cell lines. *American Journal of Respiratory Cell and Molecular Biology,* 8**,** 126.

SALLENAVE, J. M. 2000a. The role of secretory leukocyte proteinase inhibitor and elafin (elastase-specific inhibitor/skin-derived antileukoprotease) as alarm antiproteinases in inflammatory lung disease. *Respir Res,* 1**,** 87-92.

SALLENAVE, J. M. & RYLE, A. P. 1991a. Purification and characterization of elastase-specific inhibitor. Sequence homology with mucus proteinase inhibitor. *Biol Chem Hoppe Seyler,* 372**,** 13-21.

SALLENAVE, J. M., SHULMANN, J., CROSSLEY, J., JORDANA, M. & GAULDIE, J. 1994. Regulation of secretory leukocyte proteinase inhibitor (SLPI) and elastase-specific inhibitor (ESI/elafin) in human airway epithelial cells by cytokines and neutrophilic enzymes. *American Journal of Respiratory Cell and Molecular Biology,* 11**,** 733.

SCHALKWIJK, J., WIEDOW, O. & HIROSE, S. 1999. The trappin gene family: proteins defined by an N-terminal transglutaminase substrate domain and a C-terminal four-disulphide core. *Biochemical Journal,* 340**,** 569.

SCHELBERT, E. B., HSU, L. Y., ANDERSON, S. A., MOHANTY, B. D., KARIM, S. M., KELLMAN, P., ALETRAS, A. H. & ARAI, A. E. 2010. Late gadolinium-enhancement cardiac magnetic resonance identifies postinfarction myocardial fibrosis and the border zone at the near cellular level in ex vivo rat heart. *Circ Cardiovasc Imaging,* 3**,** 743-52.

SCHMITZ, S. A., TAUPITZ, M., WAGNER, S., WOLF, K. J., BEYERSDORFF, D. & HAMM, B. 2001. Magnetic resonance imaging of atherosclerotic plaques

using superparamagnetic iron oxide particles. *J Magn Reson Imaging,* 14**,** 355-61.

SCHNORR, J., TAUPITZ, M., SCHELLENBERGER, E. A., WARMUTH, C., FAHLENKAMP, U. L., WAGNER, S., KAUFELS, N. & WAGNER, M. 2012. Cardiac magnetic resonance angiography using blood-pool contrast agents: comparison of citrate-coated very small superparamagnetic iron oxide particles with gadofosveset trisodium in pigs. *Rofo,* 184**,** 105-12.

SELVANAYAGAM, J. B., PIGOTT, D., BALACUMARASWAMI, L., PETERSEN, S. E., NEUBAUER, S. & TAGGART, D. P. 2005. Relationship of irreversible myocardial injury to troponin I and creatine kinase-MB elevation after coronary artery bypass surgery: insights from cardiovascular magnetic resonance imaging. *Journal of the American College of Cardiology,* 45**,** 629-31.

SHAH, A. S., ANAND, A., SANDOVAL, Y., LEE, K. K., SMITH, S. W., ADAMSON, P. D., CHAPMAN, A. R., LANGDON, T., SANDEMAN, D., VASWANI, A., STRACHAN, F. E., FERRY, A., STIRZAKER, A. G., REID, A., GRAY, A. J., COLLINSON, P. O., MCALLISTER, D. A., APPLE, F. S., NEWBY, D. E. & MILLS, N. L. 2015a. High-sensitivity cardiac troponin I at presentation in patients with suspected acute coronary syndrome: a cohort study. *Lancet,* 386**,** 2481-8.

SHAH, A. S., GRIFFITHS, M., LEE, K. K., MCALLISTER, D. A., HUNTER, A. L., FERRY, A. V., CRUIKSHANK, A., REID, A., STODDART, M., STRACHAN, F., WALKER, S., COLLINSON, P. O., APPLE, F. S., GRAY, A. J., FOX, K. A., NEWBY, D. E. & MILLS, N. L. 2015c. High sensitivity cardiac troponin and the under-diagnosis of myocardial infarction in women: prospective cohort study. *BMJ,* 350**,** g7873.

SHAPIRO, E. M., SKRTIC, S. & KORETSKY, A. P. 2005. Sizing it up: cellular MRI using micron-sized iron oxide particles. *Magn Reson Med,* 53**,** 329-38.

SHERIDAN, F. M., COLE, P. G. & RAMAGE, D. 1996. Leukocyte adhesion to the coronary microvasculature during ischemia and reperfusion in an in vivo canine model. *Circulation,* 93**,** 1784.

SI-TAHAR, M., PIDARD, D., BALLOY, V., MONIATTE, M., KIEFFER, N., DORSSELAER, A. V. & CHIGNARD, M. 1997. Human neutrophil elastase proteolytically activates the platelet integrin aIIbb3 through cleavage of the carboxyl terminus of the aIIb subunit heavy chain. Involvement in the potentiation of platelet. *Journal of Biological Chemistry,* 272**,** 11636-11647.

SILVERMAN, E. K. & SANDHAUS, R. A. 2009. Clinical practice. Alpha1-antitrypsin deficiency. *N Engl J Med,* 360**,** 2749-57.

SILVERMAN, K. J., HUTCHINS, G. M. & BULKLEY, B. H. 1978. Cardiac sarcoid: a clinicopathologic study of 84 unselected patients with systemic sarcoidosis. *Circulation,* 58**,** 1204-11.

SKALI, H., SCHULMAN, A. R. & DORBALA, S. 2013. 18F-FDG PET/CT for the assessment of myocardial sarcoidosis. *Curr Cardiol Rep,* 15**,** 352.

SMALL, W. C., NELSON, R. C. & BERNARDINO, M. E. 1993. Dual contrast enhancement of both T1- and T2-weighted sequences using ultrasmall superparamagnetic iron oxide. *Magn Reson Imaging,* 11**,** 645-54.

SOEHNLEIN, O., LINDBOM, L. & WEBER, C. 2009. Mechanisms underlying neutrophil-mediated monocyte recruitment. *Blood,* 114**,** 4613-23.

SOSNOVIK, D. E., NAHRENDORF, M., DELIOLANIS, N., NOVIKOV, M., AIKAWA, E., JOSEPHSON, L., ROSENZWEIG, A., WEISSLEDER, R. &

NTZIACHRISTOS, V. 2007. Fluorescence tomography and magnetic resonance imaging of myocardial macrophage infiltration in infarcted myocardium in vivo. *Circulation,* 115**,** 1384-91.

SREERAM, G. M., GROCOTT, H. P., WHITE, W. D., NEWMAN, M. F. & STAFFORD-SMITH, M. 2004. Transcranial Doppler emboli count predicts rise in creatinine after coronary artery bypass graft surgery. *J Cardiothorac Vasc Anesth,* 18**,** 548-51.

STEFFENS, S., MONTECUCCO, F. & MACH, F. 2009. The inflammatory response as a target to reduce myocardial ischaemia and reperfusion injury. *Thromb Haemost,* 102**,** 240-7.

STEUER, J., BJERNER, T., DUVERNOY, O., JIDEUS, L., JOHANSSON, L., AHLSTROM, H., STAHLE, E. & LINDAHL, B. 2004a. Visualisation and quantification of peri-operative myocardial infarction after coronary artery bypass surgery with contrast-enhanced magnetic resonance imaging. *Eur Heart J,* 25**,** 1293-9.

SUGAWARA, S., UEHARA, A., NOCHI, T., YAMAGUCHI, T., UEDA, H., SUGIYAMA, A., HANZAWA, K., KUMAGAI, K., OKAMURA, H. & TAKADA, H. 2001. Neutrophil proteinase 3-mediated induction of bioactive IL-18 secretion by human oral epithelial cells. *The Journal of Immunology,* 167**,** 6568.

SUMI, Y., INOUE, N., AZUMI, H., SENO, T., OKUDA, M., HIRATA, K., KAWASHIMA, S., HAYASHI, Y., ITOH, H. & YOKOYAMA, M. 2002. Expression of tissue transglutaminase and elafin in human coronary artery:: Implication for plaque instability. *Atherosclerosis,* 160**,** 31-39.

SUZUKI, J., ISOBE, M., MORISHITA, R. & NAGAI, R. 2010. Characteristics of chronic rejection in heart transplantation: important elements of pathogenesis and future treatments. *Circ J,* 74**,** 233-9.

SWIRSKI, F. K., NAHRENDORF, M., ETZRODT, M., WILDGRUBER, M., CORTEZ-RETAMOZO, V., PANIZZI, P., FIGUEIREDO, J. L., KOHLER, R. H., CHUDNOVSKIY, A., WATERMAN, P., AIKAWA, E., MEMPEL, T. R., LIBBY, P., WEISSLEDER, R. & PITTET, M. J. 2009b. Identification of splenic reservoir monocytes and their deployment to inflammatory sites. *Science,* 325**,** 612-6.

TAMAKUMA, S., OGAWA, M., AIKAWA, N., KUBOTA, T., HIRASAWA, H., ISHIZAKA, A., TAENAKA, N., HAMADA, C., MATSUOKA, S. & ABIRU, T. 2004. Relationship between neutrophil elastase and acute lung injury in humans. *Pulm Pharmacol Ther,* 17**,** 271-9.

TASSANI, P., AUGUSTIN, N., BARANKAY, A., BRAUN, S. L., ZACCARIA, F. & RICHTER, J. A. 2000. High-dose aprotinin modulates the balance between proinflammatory and anti-inflammatory responses during coronary artery bypass graft surgery. *J Cardiothorac Vasc Anesth,* 14**,** 682-6.

TE VELTHUIS, H., JANSEN, P. G., OUDEMANS-VAN STRAATEN, H. M., STURK, A., EIJSMAN, L. & WILDEVUUR, C. R. 1995. Myocardial performance in elderly patients after cardiopulmonary bypass is suppressed by tumor necrosis factor. *J Thorac Cardiovasc Surg,* 110**,** 1663-9.

THYGESEN, K., ALPERT, J. S., JAFFE, A. S., SIMOONS, M. L., CHAITMAN, B. R., WHITE, H. D., KATUS, H. A., APPLE, F. S., LINDAHL, B., MORROW, D. A., CLEMMENSEN, P. M., JOHANSON, P., HOD, H., UNDERWOOD, R., BAX, J. J., BONOW, J. J., PINTO, F., GIBBONS, R. J., FOX, K. A., ATAR, D., NEWBY, L. K., GALVANI, M., HAMM, C. W.,

URETSKY, B. F., STEG, P. G., WIJNS, W., BASSAND, J. P., MENASCHE, P., RAVKILDE, J., OHMAN, E. M., ANTMAN, E. M., WALLENTIN, L. C., ARMSTRONG, P. W., JANUZZI, J. L., NIEMINEN, M. S., GHEORGHIADE, M., FILIPPATOS, G., LUEPKER, R. V., FORTMANN, S. P., ROSAMOND, W. D., LEVY, D., WOOD, D., SMITH, S. C., HU, D., LOPEZ-SENDON, J. L., ROBERTSON, R. M., WEAVER, D., TENDERA, M., BOVE, A. A., PARKHOMENKO, A. N., VASILIEVA, E. J., MENDIS, S., BAUMGARTNER, H., CECONI, C., DEAN, V., DEATON, C., FAGARD, R., FUNCK-BRENTANO, C., HASDAI, D., HOES, A., KIRCHHOF, P., KNUUTI, J., KOLH, P., MCDONAGH, T., MOULIN, C., POPESCU, B. A., REINER, Z., SECHTEM, U., SIRNES, P. A., TORBICKI, A., VAHANIAN, A., WINDECKER, S., MORAIS, J., AGUIAR, C., ALMAHMEED, W., ARNAR, D. O., BARILI, F., BLOCH, K. D., BOLGER, A. F., BOTKER, H. E., BOZKURT, B., BUGIARDINI, R., CANNON, C., DE LEMOS, J., EBERLI, F. R., ESCOBAR, E., HLATKY, M., JAMES, S., KERN, K. B., MOLITERNO, D. J., MUELLER, C., NESKOVIC, A. N., PIESKE, B. M., SCHULMAN, S. P., STOREY, R. F., TAUBERT, K. A., VRANCKX, P. & WAGNER, D. R. 2012a. Third universal definition of myocardial infarction. *J Am Coll Cardiol,* 60**,** 1581-98.

THYGESEN, K., ALPERT, J. S. & WHITE, H. D. 2007. Universal definition of myocardial infarction. *Eur Heart J,* 28**,** 2525-38.

TIEFENBACHER, C., EBERT, M., NIROOMAND, F., BATKAI, S., TILLMANNS, H., ZIMMERMANN, R. & KÜBLER, W. 1997. Inhibition of elastase improves myocardial function after repetitive ischaemia and myocardial infarction in the rat heart. *Pflugers Archiv European Journal of Physiology,* 433**,** 563-570.

TRIVEDI, R. A., MALLAWARACHI, C., U-KING-IM, J.-M., GRAVES, M. J., HORSLEY, J., GODDARD, M. J., BROWN, A., WANG, L., KIRKPATRICK, P. J., BROWN, J. & GILLARD, J. H. 2006. Identifying inflamed carotid plaques using in vivo USPIO-enhanced MR imaging to label plaque macrophages. *Arterioscler Thromb Vasc Biol,* 26**,** 1601-6.

TSUCHIYA, K., NITTA, N., SONODA, A., OTANI, H., TAKAHASHI, M., MURATA, K., SHIOMI, M., TABATA, Y. & NOHARA, S. 2013. Atherosclerotic imaging using 4 types of superparamagnetic iron oxides: new possibilities for mannan-coated particles. *Eur J Radiol,* 82**,** 1919-25.

TSUNEMI, M., MATSUURA, Y., SAKAKIBARA, S. & KATSUBE, Y. 1996. Crystal structure of an elastase-specific inhibitor elafin complexed with porcine pancreatic elastase determined at 1.9 A resolution. *Biochemistry,* 35**,** 11570-11576.

UEHARA, A., MURAMOTO, K., TAKADA, H. & SUGAWARA, S. 2003. Neutrophil serine proteinases activate human nonepithelial cells to produce inflammatory cytokines through protease-activated receptor 2. *The Journal of Immunology,* 170**,** 5690.

UEHARA, A., SUGAWARA, S., MURAMOTO, K. & TAKADA, H. 2002. Activation of human oral epithelial cells by neutrophil proteinase 3 through protease-activated receptor-2. *The Journal of Immunology,* 169**,** 4594.

URZUA, J., TRONCOSO, S., BUGEDO, G., CANESSA, R., MUNOZ, H., LEMA, G., VALDIVIESO, A., IRARRAZAVAL, M., MORAN, S. & MENESES, G. 1992. Renal function and cardiopulmonary bypass: effect of perfusion pressure. *J Cardiothorac Vasc Anesth,* 6**,** 299-303.

VAN GAAL, W. J., ARNOLD, J. R., TESTA, L., KARAMITSOS, T., LIM, C. C., PONNUTHURAI, F. A., PETERSEN, S., FRANCIS, J. M., SELVANAYAGAM, J., SAYEED, R., WEST, N., WESTABY, S., NEUBAUER, S. & BANNING, A. P. 2011. Myocardial injury following coronary artery surgery versus angioplasty (MICASA): a randomised trial using biochemical markers and cardiac magnetic resonance imaging. *EuroIntervention,* 6**,** 703-10.

VANDIVIER, R. W., FADOK, V. A., HOFFMANN, P. R., BRATTON, D. L., PENVARI, C., BROWN, K. K., BRAIN, J. D., ACCURSO, F. J. & HENSON, P. M. 2002. Elastase-mediated phosphatidylserine receptor cleavage impairs apoptotic cell clearance in cystic fibrosis and bronchiectasis. *Journal of Clinical Investigation,* 109**,** 661-670.

VERRIER, E. D., SHERNAN, S. K., TAYLOR, K. M., VAN DE WERF, F., NEWMAN, M. F., CHEN, J. C., CARRIER, M., HAVERICH, A., MALLOY, K. J., ADAMS, P. X., TODARO, T. G., MOJCIK, C. F., ROLLINS, S. A. & LEVY, J. H. 2004. Terminal complement blockade with pexelizumab during coronary artery bypass graft surgery requiring cardiopulmonary bypass: a randomized trial. *JAMA,* 291**,** 2319-27.

VIALLON, M., MEWTON, N., THUNY, F., GUEHRING, J., O'DONNELL, T., STEMMER, A., BI, X., RAPACCHI, S., ZUEHLSDORFF, S., REVEL, D. & CROISILLE, P. 2012. T2-weighted cardiac MR assessment of the myocardial area-at-risk and salvage area in acute reperfused myocardial infarction: Comparison of state-of-the-art dark blood and bright blood T2-weighted sequences. *J Magn Reson Imaging,* 35**,** 328-39.

VINTEN-JOHANSEN, J. 2004. Involvement of neutrophils in the pathogenesis of lethal myocardial reperfusion injury. *Cardiovasc Res,* 61**,** 481-97.

WAGNER, M., WAGNER, S., SCHNORR, J., SCHELLENBERGER, E., KIVELITZ, D., KRUG, L., DEWEY, M., LAULE, M., HAMM, B. & TAUPITZ, M. 2011. Coronary MR angiography using citrate-coated very small superparamagnetic iron oxide particles as blood-pool contrast agent: initial experience in humans. *J Magn Reson Imaging,* 34**,** 816-23.

WAKAYAMA, F., FUKUDA, I., SUZUKI, Y. & KONDO, N. 2007. Neutrophil elastase inhibitor, sivelestat, attenuates acute lung injury after cardiopulmonary bypass in the rabbit endotoxemia model. *Ann Thorac Surg,* 83**,** 153-60.

WAN, S., YIM, A. P., WONG, C. K., ARIFI, A. A., YIP, J. H., NG, C. S., WAYE, M. M. & LAM, C. W. 2002. Expression of FHL2 and cytokine messenger RNAs in human myocardium after cardiopulmonary bypass. *Int J Cardiol,* 86**,** 265-72.

WELBOURN, C. R., GOLDMAN, G., PATERSON, I. S., VALERI, C. R., SHEPRO, D. & HECHTMAN, H. B. 1991. Pathophysiology of ischaemia reperfusion injury: central role of the neutrophil. *Br J Surg,* 78**,** 651-5.

WESTLIN, W. & GIMBRONE JR, M. 1993. Neutrophil-mediated damage to human vascular endothelium. Role of cytokine activation. *The American Journal of Pathology,* 142**,** 117.

WESTWOOD, M. A., FIRMIN, D. N., GILDO, M., RENZO, G., STATHIS, G., MARKISSIA, K., VASILI, B. & PENNELL, D. J. 2005. Intercentre reproducibility of magnetic resonance T2* measurements of myocardial iron in thalassaemia. *Int J Cardiovasc Imaging,* 21**,** 531-8.

WEYRICH, A. S., BUERKE, M., ALBERTINE, K. H. & LEFER, A. M. 1995. Time course of coronary vascular endothelial adhesion molecule expression during reperfusion of the ischemic feline myocardium. *J Leukoc Biol,* 57**,** 45-55.

WIEDOW, O., LUADEMANN, J. & UTECHT, B. 1991. Elafin is a potent inhibitor of proteinase 3. *Biochem Biophys Res Commun,* 174**,** 6-10.

WIEDOW, O., SCHRÖDER, J., GREGORY, H., YOUNG, J. & CHRISTOPHERS, E. 1990. Elafin: an elastase-specific inhibitor of human skin. Purification, characterization, and complete amino acid sequence. *Journal of Biological Chemistry,* 265**,** 14791.

WILLINGER, C. C., SCHRAMEK, H., PFALLER, K. & PFALLER, W. 1992. Tissue distribution of neutrophils in postischemic acute renal failure. *Virchows Arch B Cell Pathol Incl Mol Pathol,* 62**,** 237-43.

WITTAMER, V., BONDUE, B., GUILLABERT, A., VASSART, G., PARMENTIER, M. & COMMUNI, D. 2005. Neutrophil-mediated maturation of chemerin: a link between innate and adaptive immunity. *J Immunol,* 175**,** 487-93.

WITTAMER, V., FRANSSEN, J. D., VULCANO, M., MIRJOLET, J. F., LE POUL, E., MIGEOTTE, I., BREZILLON, S., TYLDESLEY, R., BLANPAIN, C., DETHEUX, M., MANTOVANI, A., SOZZANI, S., VASSART, G., PARMENTIER, M. & COMMUNI, D. 2003. Specific recruitment of antigen-presenting cells by chemerin, a novel processed ligand from human inflammatory fluids. *J Exp Med,* 198**,** 977-85.

WU, A. H., FENG, Y. J., MOORE, R., APPLE, F. S., MCPHERSON, P. H., BUECHLER, K. F. & BODOR, G. 1998. Characterization of cardiac troponin subunit release into serum after acute myocardial infarction and comparison of assays for troponin T and I. American Association for Clinical Chemistry Subcommittee on cTnI Standardization. *Clinical chemistry,* 44**,** 1198-208.

WU, K., URANO, T., IHARA, H., TAKADA, Y., FUJIE, M., SHIKIMORI, M., HASHIMOTO, K. & TAKADA, A. 1995. The cleavage and inactivation of plasminogen activator inhibitor type 1 by neutrophil elastase: the evaluation of its physiologic relevance in fibrinolysis. *Blood,* 86**,** 1056.

WU, Y. L., YE, Q., SATO, K., FOLEY, L. M., HITCHENS, T. K. & HO, C. 2009. Noninvasive evaluation of cardiac allograft rejection by cellular and functional cardiac magnetic resonance. *JACC Cardiovasc Imaging,* 2**,** 731-41.

YANCY, A. D., OLZINSKI, A. R., HU, T. C., LENHARD, S. C., ARAVINDHAN, K., GRUVER, S. M., JACOBS, P. M., WILLETTE, R. N. & JUCKER, B. M. 2005. Differential uptake of ferumoxtran-10 and ferumoxytol, ultrasmall superparamagnetic iron oxide contrast agents in rabbit: critical determinants of atherosclerotic plaque labeling. *J Magn Reson Imaging,* 21**,** 432-42.

YANG, Y., YANASAK, N., SCHUMACHER, A. & HU, T. C. 2010. Temporal and noninvasive monitoring of inflammatory-cell infiltration to myocardial infarction sites using micrometer-sized iron oxide particles. *Magn Reson Med,* 63**,** 33-40.

YANO, T., MIURA, T., WHITTAKER, P., MIKI, T., SAKAMOTO, J., NAKAMURA, Y., ICHIKAWA, Y., IKEDA, Y., KOBAYASHI, H. & OHORI, K. 2006. Macrophage colony-stimulating factor treatment after myocardial infarction attenuates left ventricular dysfunction by accelerating infarct repair. *Journal of the American College of Cardiology,* 47**,** 626-634.

YAZAKI, Y., ISOBE, M., HIROE, M., MORIMOTO, S., HIRAMITSU, S., NAKANO, T., IZUMI, T. & SEKIGUCHI, M. 2001. Prognostic determinants of long-term survival in Japanese patients with cardiac sarcoidosis treated with prednisone. *Am J Cardiol,* 88**,** 1006-10.

YOSHIMURA, Y., HIRAMATSU, Y., SATO, Y., HOMMA, S., ENOMOTO, Y., JIKUYA, T. & SAKAKIBARA, Y. 2003. ONO-6818, a novel, potent neutrophil elastase inhibitor, reduces inflammatory mediators during simulated extracorporeal circulation. *Ann Thorac Surg,* 76**,** 1234-9.

ZAHLER, S., MASSOUDY, P., HARTL, H., HAHNEL, C., MEISNER, H. & BECKER, B. F. 1999. Acute cardiac inflammatory responses to postischemic reperfusion during cardiopulmonary bypass. *Cardiovasc Res,* 41**,** 722-30.

ZAIDI, S. H., HUI, C. C., CHEAH, A. Y., YOU, X. M., HUSAIN, M. & RABINOVITCH, M. 1999. Targeted overexpression of elafin protects mice against cardiac dysfunction and mortality following viral myocarditis. *J Clin Invest,* 103**,** 1211-9.

ZAIDI, S. H., YOU, X. M., CIURA, S., HUSAIN, M. & RABINOVITCH, M. 2002a. Overexpression of the serine elastase inhibitor elafin protects transgenic mice from hypoxic pulmonary hypertension. *Circulation,* 105**,** 516-21.

ZAIDI, S. H., YOU, X. M., CIURA, S., O'BLENES, S., HUSAIN, M. & RABINOVITCH, M. 2000. Suppressed smooth muscle proliferation and inflammatory cell invasion after arterial injury in elafin-overexpressing mice. *J Clin Invest,* 105**,** 1687-95.

ZAIDI, S. H. E., YOU, X. M., CIURA, S., HUSAIN, M. & RABINOVITCH, M. 2002b. Overexpression of the serine elastase inhibitor elafin protects transgenic mice from hypoxic pulmonary hypertension. *Circulation,* 105**,** 516-521.

ZANI, M. L., NOBAR, S. M., LACOUR, S. A., LEMOINE, S., BOUDIER, C., BIETH, J. G. & MOREAU, T. 2004. Kinetics of the inhibition of neutrophil proteinases by recombinant elafin and pre elafin (trappin 2) expressed in Pichia pastoris. *European Journal of Biochemistry,* 271**,** 2370-2378.

ZAWADA, A. M., ROGACEV, K. S., SCHIRMER, S. H., SESTER, M., BOHM, M., FLISER, D. & HEINE, G. H. 2012. Monocyte heterogeneity in human cardiovascular disease. *Immunobiology,* 217**,** 1273-84.

ZEIHER, B. G., ARTIGAS, A., VINCENT, J. L., DMITRIENKO, A., JACKSON, K., THOMPSON, B. T. & BERNARD, G. 2004. Neutrophil elastase inhibition in acute lung injury: results of the STRIVE study. *Crit Care Med,* 32**,** 1695-702.

ZHANG, M., ZOU, Z., MAASS, N. & SAGER, R. 1995. Differential expression of elafin in human normal mammary epithelial cells and carcinomas is regulated at the transcriptional level. *Cancer Research,* 55**,** 2537.

ZHANG, W. R., GARG, A. X., COCA, S. G., DEVEREAUX, P. J., EIKELBOOM, J., KAVSAK, P., MCARTHUR, E., THIESSEN-PHILBROOK, H., SHORTT, C., SHLIPAK, M., WHITLOCK, R., PARIKH, C. R. & CONSORTIUM, T.-A. 2015. Plasma IL-6 and IL-10 Concentrations Predict AKI and Long-Term Mortality in Adults after Cardiac Surgery. *J Am Soc Nephrol,* 26**,** 3123-32.

ZHAO, Z. Q., VELEZ, D. A., WANG, N. P., HEWAN-LOWE, K. O., NAKAMURA, M., GUYTON, R. A. & VINTEN-JOHANSEN, J. 2001.

Progressively developed myocardial apoptotic cell death during late phase of reperfusion. *Apoptosis,* 6**,** 279-290.

ZHU, J., NATHAN, C. & DING, A. 1999. Suppression of macrophage responses to bacterial lipopolysaccharide by a non-secretory form of secretory leukocyte protease inhibitor. *Biochimica et Biophysica Acta (BBA)-Molecular Cell Research,* 1451**,** 219-223.

Appendix A: ELAFIN REVIEW PAPER

Journal: Biochemical Pharmacology

DOI: 10.1016/j.bcp.2011.11.003

Published: November 15th 2011

ROLE OF THE ENDOGENOUS ELASTASE INHIBITOR, ELAFIN, IN CARDIOVASCULAR INJURY

FROM EPITHELIUM TO ENDOTHELIUM

Authors:

Dr Shirjel R. Alam MBChB MRCP MRCS MRCA BSE (For communication)

Cardiology Research Fellow, Centre for Cardiovascular Sciences,

University of Edinburgh, 47 Little France Crescent. Edinburgh. EH16 4TJ

0131 242 9300

s.r.alam-1@sms.ed.ac.uk

Professor David E. Newby BA BSc PhD BM DM DSc FRCP FRSE FMedSci FESC FACC

Consultant Cardiologist & British Heart Foundation John Wheatley Chair of Cardiology.

Centre for Cardiovascular Sciences,

University of Edinburgh, 47 Little France Crescent. Edinburgh. EH16 4TJ

Dr Peter A. Henriksen BSc MBChB PhD FRCP

Consultant Cardiologist

Honorary Senior Lecturer

Royal Infirmary of Edinburgh, 47 Little France Crescent. Edinburgh. EH16 4TJ

Abbreviations:

HNE – Human Neutrophil Elastase.

PAR – Protease Activated Receptor.

MMP - Matrix Metalloproteinase.

TIMP - Tissue Inhibitors of Metalloproteases.

PAI-1 – Plasminogen Activator Inhibitor type -1.

TFPI - Tissue Factor Pathway Inhibitor.

α1-PI - α1-antitrypsin.

SLPI - Secretory Leucocyte Protease Inhibitor.

WAP - Whey Acidic Protein.

LPS – Lipopolysaccharide.

EMPIRE - Elafin Myocardial Protection from Ischaemia Reperfusion.

ABSTRACT

Neutrophils and neutrophil-derived elastases play a major role in the regulation of vascular injury and inflammation, such as ischemia-reperfusion injury. Elafin is an endogenous inhibitor of neutrophil-derived elastases with numerous anti-inflammatory functions that include modulation of inflammatory cytokine release as well as innate and adaptive immunity. It is produced by epithelial tissues including the skin and respiratory system that have adapted to respond to the microbial and chemical insults that lead to inflammation. The production of peptides like elafin with multi-faceted anti-inflammatory activity is an important part of this adaptation. Although not directly expressed within the cardiovascular system itself, pre-clinical studies have suggested therapeutic benefit of elafin in cardiovascular disease.

The aim of this review is to highlight the role of neutrophil-derived elastases in vascular inflammation and injury. We will discuss the beneficial effects of elafin inhibition of neutrophil elastase and its extended anti-inflammatory activity in pre-clinical models of inflammatory vascular injury.

1. INTRODUCTION

1.1 Neutrophil-derived elastases and vascular inflammation

Extracellular matrix turnover

Neutrophils lead the early phase of the inflammatory response gathering at sites of inflammation, and transmigrating through the endothelium to release granule contents and generate oxygen-derived free radicals that serve the host defence by

providing microbicidal activity. Human neutrophil elastase (HNE) and proteinase-3 are amongst the contents of neutrophil azurophilc granules (Borregaard and Cowland, 1997). These enzymes degrade components of the extracellular matrix and the list of substrates for HNE is extensive (Lee and Downey, 2001) including fibrin, fibronectin, collagen, the glycoprotein IIb/IIIa receptor (Si-Tahar et al., 1997), elastin and cadherins (Carden et al., 1998). Figure 1 illustrates the effects of HNE and proteinase 3 within the vasculature.

HNE's action on extracellular matrix components exposes recognition sites that bind cellular integrin and tyrosine kinase receptors. These signals direct the cellular response to injury. Recognition of elastin-derived fragments by the elastin receptor results in migration and chemotaxis of monocytes and vascular smooth muscle cells (Robert et al., 1998, Houghton et al., 2006).

Endothelial cells are susceptible to detachment when cultured with activated neutrophils or HNE (Westlin and Gimbrone Jr, 1993). Anchorage of cells to the extracellular matrix is necessary for survival and cleavage of matrix components and cadherins responsible for adhesion results in apoptosis (Frisch and Francis, 1994, Mtairag et al., 2002). HNE is joined by the matrix metalloproteinase (MMP) and the cathepsin family of proteases in modulating endothelial extracellular matrix degradation during acute inflammation (Garcia-Touchard et al., 2005). There is considerable overlap of substrates between these protease families leading to apparent redundancy. HNE is distinct in having both a broad range of substrates and the ability to be released rapidly and in high concentration from neutrophil granules at sites of inflammation. By contrast, many of the extracellular MMP and cathepsin proteases are regulated by gene expression and MMPs are activated in a cascade of

proteolytic steps (Chakraborti et al., 2003). HNE also modulates the activity of vascular extracellular proteases. It directly activates MMPs and inactivates their inhibitors (tissue inhibitors of metalloproteases: TIMPs) (Okada and Nakanishi, 1989, Okada et al., 1988). A complex interplay between extracellular proteases that share common substrates occurs during inflammatory endothelial injury. HNE's broad ranging activity and modulating activity over other proteolytic pathways suggest a central role at the onset of the proteolytic cascade in pathologies where neurophil degranulation is present. HNE has a central role alongside MMPs and cysteine proteases in atherosclerotic aneurysm development. Thrombus is present over the surface of larger aneurysms providing an active interface for neutrophil recruitment and activation. The thrombus from abdominal aortic aneurysms is rich in HNE particularly within the luminal compartment This contributes to aneurysm growth by preventing in-growth of smooth muscle cells and re-colonisation by circulating progenitors (Fontaine et al., 2004). Thrombus is continuously turning over and together with neutrophil recruitment provides a supply of HNE, plasmin and activated MMPs. These proteases permeate to the abluminal side of the thrombus to contribute to expansive arterial wall modelling

1.2 Modulation of thrombosis and fibrinolysis

The capacity of HNE to degrade components of the coagulation and fibrinolytic pathways has been demonstrated *in vitro*. Cleavage of plasminogen activator inhibitor type -1 (PAI-1) shortens clot lysis time *in vitro* (Wu et al., 1995). Plasminogen is degraded to miniplasminogen by HNE. This plasminogen fragment is more readily activated and the resulting miniplasmin retains fibrinolytic activity but

may be relatively resistant to inhibition by α-2 antiplasmin (Duboscq et al., 1997). More recently, the role of neutrophil-derived elastases in thrombus formation has been demonstrated in knockout mice (Massberg et al., 2010). Compared to wild type mice the animals deficient in neutrophil elastase had markedly reduced fibrin formation in response to chemical injury on intravital videomicroscopy. The mechanism involved proteolytic inactivation of an endogenous anticoagulant, tissue factor pathway inhibitor (TFPI). TFPI and neutophil elastase were observed to co-localise on the external surface of neutrophils in nucleosomes facilitating TFPI degradation. The formation and externalisation of nucleosomes is increased by neutrophil interaction with activated platelets. The combination of human neutrophils and platelets generates pro-coagulant activity measured by the production of active factor X and this was markedly reduced in the presence of HNE inhibitors (Massberg et al., 2010). These observations point to a hitherto unappreciated role for neutrophils and HNE in triggering coagulation and stabilising thrombus formation. Massberg *et al* suggested an innate immunity role for neutrophil elastase generated thrombosis promoting retention of invading pathogens within liver microvessels (Massberg et al., 2010). This work demonstrated the capability of neutrophils to promote thrombus formation in larger vessels in the absence of infection. The circulating neutrophil count is associated with clinical events including myocardial infarction (Madjid et al., 2004). Neutrophils from patients with acute coronary syndromes exhibit evidence of activation and degranulation (Buffon et al., 2002). Together these finding suggest a more direct pro-thrombotic role for neutrophils in coronary disease.

1.3 Regulation of inflammatory signalling

HNE and proteinase-3 modulate cytokine signaling. HNE and Proteinase-3 can proteolytically activate or process the inflammatory cytokines TNF-α, IL-1β, IL-8 and IL-18 (Carroll et al., 2005, Coeshott et al., 1999, Padrines et al., 1994, Sugawara et al., 2001). HNE is capable of degrading IL-1β and TNF-α possibly acting as a negative regulator of inflammation. Chemerin is a chemoattractant protein that promotes recruitment of antigen presenting cells such as macrophages and dendritic cells (Wittamer et al., 2003). HNE activates chemerin from prochemerin by proteolytically cleaving its C-terminal peptide. This provides one mechanism whereby initial infiltration of neutrophils may orchestrate subsequent antigen presenting cell recruitment at inflammatory sites (Wittamer et al., 2005).

HNE mediated cleavage of the CD14 receptor on monocytes and fibroblasts reduces responsiveness and TNF-α production in response to LPS (Nemoto et al., 2000) as well as impairing recognition and clearance of apoptotic cells by phagocytosis (Vandivier et al., 2002). HNE mediated cleavage of the complement receptor 1 from the surface of erythrocytes generates a fragment that acts as an inhibitor of complement (Sadallah et al., 1999). These findings indicate divergent effects on inflammatory signalling and may reflect changing roles for neutrophil derived elastases depending on variables such as local concentration, stage of inflammation and signalling context.

HNE stimulates production of the neutrophil chemokine IL-8 and augments endothelial cell production of IL-8 in response to other stimuli such as lipopolysaccharide (Henriksen et al., 2004b). The observation that HNE stimulates cytokine production from a variety of cell types has raised the possibility of receptor

interaction. Devaney *et al* demonstrated that HNE up-regulation of IL-8 mRNA and protein was dependent on expression of the toll-like receptor 4 in a kidney cell line (Devaney et al., 2003). HNE and proteinase-3 also activate the protease activated receptors (PAR) (Uehara et al., 2003, Uehara et al., 2002) that influence a wide range of physiological responses including platelet activation, intimal hyperplasia and the maintenance of vascular tone and barrier function (Leger et al., 2006). Activation of PAR-1, PAR-2 and PAR-4 stimulates IL-6, IL-8 and prostaglandin E2 release (Asokananthan et al., 2002). Selective activation of PAR-1 and PAR-2 by HNE results in increased epithelial permeability and transepithelial migration of neutrophils. This effect is blocked by PAR antagonists and is not related to cleavage of gap junctions (Chin et al., 2008). Recently, HNE has been shown to activate PAR-2 through cleavage of the N-terminus (Ramachandran et al., 2011). This results in selective activation of downstream MAP kinase signaling pathways, and PAR-2 dependent calcium signaling is silenced. This recent observation of interaction with specific cell surface receptors indicates the potential for discriminate signaling by HNE.

1.4 Antimicrobial actions of HNE

Neutrophil elastase deficient mice are susceptible to bacterial and fungal infection. (Belaaouaj et al., 2000a, Tkalcevic et al., 2000). HNE has direct antimicrobial action against gram-negative bacteria such as *Escherichia coli* by degrading the bacterium's outer membrane protein A (Belaaouaj et al., 2000a). Flagella are bacterial components with strong pro-inflammatory activity on epithelial and inflammatory cells. Degradation of flagellin the structural component of flagella in *Pseudomonas*

aeruginosa by HNE results in loss of this virulence factor's stimulatory activity (Belaaouaj et al., 2000b, Belaaouaj et al., 1998, Hirche et al., 2008). HNE cleaves other virulence factors of enterobacteria and has direct antifungal activity against *Candida albicans* and *Aspergillus fumigatus* (Reeves et al., 2002, Tkalcevic et al., 2000). Antimicrobial activity of HNE and proteinase-3 against gram-positive bacteria was recently demonstrated with direct *in vitro* killing activity on *Streptococcus pneumoniae* (Standish and Weiser, 2009).

Cathelicidins are antimicrobial peptides that are stored and released from the lysosomes of neutrophils. HNE and proteinase 3 regulate the activity of cathelicidins by proteolytic release of the antimicrobial C-terminal fragment (Lehrer and Ganz, 2002). Neutrophil derived elastases can therefore affect microbial killing by direct and indirect mechanisms.

1.5 Neutrophil elastase activity is regulated by endogenous inhibitors

Neutrophil derived elastases have wide ranging inflammatory effects on a broad range of substrates. Endogenous serine protease inhibitors (serpins) block activity by complexing with the elastase molecule. α1-antitrypsin (α1-PI) is the major circulating serpin produced in the liver with inhibitory activity against HNE. α1-PI is present at saturating levels within the circulation providing systemic inhibitory activity against HNE. Elafin and secretory leucocyte protease inhibitor (SLPI) are serpins produced locally at sites of inflammation by epithelial cells in response to inflammatory stimuli such as TNF-α and HNE. The ability to raise this local defence

of ‘alarm’ antiproteases illustrates the extent to which epithelial tissues have evolved mechanisms to respond to, and contain, neutrophil-mediated inflammation (Sallenave, 2000b). Cardiovascular tissues do not express these alarm antiproteases and are more vulnerable to HNE mediated injury as a result.

HNE can evade high local concentrations of inhibitors through a series of mechanisms. Large quantities of oxidants and proteases released by leukocytes recruited to the site of inflammation can overwhelm and inactivate protease inhibitors. Adhesion of neutrophils to the extracellular matrix leads to the compartmentalisation of the released proteases between the neutrophil and matrix, and this microenvironment excludes the large circulating protease inhibitors such as α1-PI (Korkmaz et al., 2005). A large proportion of the serine proteases released from azurophil granules bind to the plasma membrane with catalytic activity preserved. Owen and colleagues suggested that this tight binding of extracellular neutrophil serine proteases to the cell membrane makes them inaccessible, and therefore resistant, to circulating, high-molecular-weight, endogenous inhibitors such as α1-PI (Owen et al., 1995). Surface bound HNE is inhibited by small molecule inhibitors including SLPI suggesting a specific locale for alarm antiproteases to control HNE (Owen et al., 1995). This local antiprotease shield is not present within the cardiovascular system and strategies to introduce or mimic it will reduce HNE mediated tissue injury and inflammation. Sections 2, 3 & 4 will examine the therapeutic potential of elafin in diseases characterised by neutrophil mediated vascular injury.

1.6 Clinical application of biological and synthetic inhibitors of HNE

Endogenous and synthetic small molecule inhibitors have been developed to combat the pro-inflammatory activity of HNE. Clinical studies with elastase inhibitors have focussed on inflammatory lung disease.

SLPI belongs to the same family of four disulphide core proteins as elafin. It shares many properties including inhibition of HNE and interference with lipopolysaccharide signalling, transcription factor NF-κB activation and TNF-α production. Delivery of recombinant SLPI was protective in rat and murine models of ischaemia reperfusion injury (Lentsch et al., 1999). A clinical study examining the effect of aerosolised SLPI in cystic fibrosis patients demonstrated reduced elastase activity, IL-8 and neutrophil levels in treated patients (McElvaney et al., 1992). α1-PI is regarded as the major inhibitor of HNE in the lung and intravenous formulations derived from human plasma (Prolastin; Talecris Corporation, Aralast; Alpha Therapeutic Corporation and Zemaira; CSL Behring) have been trialled in patients with α1-antitrypsin deficiency with minimal impact on disease progression (Silverman and Sandhaus, 2009). DX-890 (Depelstat; Dyax Corporation/Debiopharm) is a potent HNE inhibitor derived from human inter-α-inhibitor. It may have application as an aerosol elastase inhibitor in the treatment of cystic fibrosis.

Several synthetic neutrophil elastase inhibitors have been developed. Preclinical studies have shown promise in demonstrating reduced neutrophil elastase injury and inflammation but clinical translation has been frustrated by lack of efficacy and concerns over toxicity. Sivelestat (Ono Pharmaceutical) is a low molecular weight reversible competitive inhibitor of HNE. In observational studies, administration was

associated with reduced mortality in critically ill patients and attenuated pulmonary dysfunction in patients with acute respiratory distress syndrome (Hoshi et al., 2005, Okayama et al., 2006). In prospective double-blinded controlled trials, it has been shown to reduce IL-8 production and reduce acute lung injury after cardiopulmonary bypass, and reduce duration of ventilation in intensive care (Ryugo et al., 2006, Tamakuma et al., 2004). The only multi-centre double-blind placebo-controlled trial of sivelestat failed to show a decrease in mortality or reduced ventilator requirement in critically ill patients (Zeiher et al., 2004). ONO-6818 (Ono Pharmaceutical) is a non-peptide selective neutrophil elastase inhibitor that reduced IL-8 production and complement activation in a simulated cardiac bypass circuit (Yoshimura et al., 2003). Clinical studies in patients with lung disease were halted because of liver injury associated with the drug. Mr889 is a less potent, reversible and slow-binding competitive inhibitor of HNE developed by Medea Research. Clinical evaluation demonstrated the drug to be safe but ineffective in modifying biochemical markers of lung destruction (Luisetti et al., 1996).

2. ELAFIN

2.1 Elafin is a potent endogenous inhibitor of neutrophil elastase

Elafin is an endogenous inhibitor of human neutrophil elastase (HNE) and proteinase-3 that was first isolated from psoriatic skin and human bronchial secretions.(Wiedow et al., 1990, Sallenave and Ryle, 1991b). Cloning of elafin cDNA indicates that initial transcription produces a protein of 117 amino acid residues, which undergoes intracellular cleavage of an N-terminal hydrophobic

signal sequence to produce pro-elafin (Molhuizen et al., 1993, Sallenave and Silva, 1993, Schalkwijk et al., 1999). The pro-elafin protein is composed of 2 domains: a C-terminus consisting of 57 amino acids and an N-terminus consisting of 60 amino acids also known as the cementoin domain (Francart et al., 1997, Nara et al., 1994). The N-terminus contains VKGQ sequences that provide the substrate for transglutaminase, with glutamine and lysine acting as acyl donors and acceptors in formation of isopeptide inter-protein cross-links (Nara et al., 1994). Transglutaminisation allows elafin to be cross-linked to the extracellular matrix where it may persist as a tissue bound inhibitor of HNE. Sumi *et al* demonstrated elafin immunoreactivity within the intima of human coronary arteries in association with transglutaminase (Sumi et al., 2002). The C-terminus is responsible for the elastase inhibition. It has a four-disulphide core and shows structural similarity with the whey acidic protein (WAP) family (Nara et al., 1994, Tsunemi et al., 1996). This combination of a transglutaminase substrate area and a WAP/four-disulphide core has similarities with other proteins that have been named “trappins” (Schalkwijk et al., 1999). Elafin has 40% sequence homology with SLPI and is more specific in its spectrum of activity exhibiting potent inhibition of HNE and proteinase-3. It has equilibrium dissociation constants for these enzymes of 0.8×10^{-10} M and 1.2×10^{-10} M respectively (Zani et al., 2004).

2.2 Tissue distribution and regulation of elafin

Elafin is secreted constitutively by the squamous epithelium of the skin, with expression raised in inflammatory skin conditions such as psoriasis (Wiedow et al., 1990, Nara et al., 1994). It has also been isolated in other epithelia such as sweat

glands, hair follicles, tongue, tonsils, gingiva, epiglottis, esophageal lining, the vagina, the pharynx (Pfundt et al., 2000), submandibular glands (Lee et al., 2002), trachea, stomach, intestine (Nara et al., 1994), and mammaries (Zhang et al., 1995). More recently leucocyte expression has been identified within human endometrial neutrophils and alveolar macrophages of the respiratory system (King et al., 2003, Sallenave et al., 1993). The detection of elafin within human coronary arteries in association with atherosclerosis raises the question over whether it has originated from infiltrating inflammatory cells or free protein entering from the circulation.

IL-1β and TNF-α together with HNE are major inducers of elafin expression in human airway epithelial cells and keratinocytes (Sallenave et al., 1994, Pfundt et al., 2000). Regulation by these inflammatory cytokines highlights the role elafin may play in the early orchestration of the inflammatory response as an ‘alarm’ antiprotease secreted by local cells.

3 Extended anti-inflammatory roles of elafin

3.3 Inhibition of inflammatory cytokine production

Our group demonstrated attenuated inflammatory cytokine production by human endothelial cells and macrophages following elafin overexpression using adenoviral vectors (Henriksen et al., 2004b). Endothelial cell IL-8 production was reduced in response to bacterial lipopolysaccharide (LPS), TNF-α and oxidised low-density lipoprotein, a key inflammatory stimulus and driver of atherosclerotic plaque development. Overexpression in monocyte-differentiated human macrophages reduced TNF-α production in response to low concentrations of LPS (Henriksen et

al., 2004b). SLPI has similar properties reducing TNF-α and matrix metalloprotease production in response to LPS (Jin et al., 1997, Zhu et al., 1999). An intracellular mechanism was suggested by the finding that transfection of a non-secreted form of SLPI but not addition of recombinant SLPI to cultured macrophages suppresses the response to LPS (Zhu et al., 1999). In search of an intracellular target, we and others have identified the transcription factor NF-κB. NF-κB upregulates many inflammatory genes associated with the inflammatory response including IL-8 and TNF-α. Overexpression or incubation of elafin and SLPI with monocytes reduces LPS responsiveness (Butler et al., 2006, Henriksen et al., 2004b). This effect is seen in association with reduced proteolytic degradation of NF-κB's inhibitory subunits IκBα and IκBα suggesting an action by elafin and SLPI on the unbiquitin-proteosome pathway.

3.4 Innate and adaptive immunity functions

Elafin forms part of the complex antimicrobial defence screen on mucosal and epithelial surfaces. Elafin has direct antimicrobial activity against *Staphlylococcus aureus* and *Pseudomonas aeruginosa* (Simpson et al., 1999). It is possible the positive charge of elafin allows it to disrupt the anionic membrane of bacteria directly and this mechanism has been proposed for other cationic antimicrobial peptides. The interaction of elafin with LPS is complex. When preincubated together, the elafin-LPS complex increases cytokine production from inflammatory cells suggesting that elafin is priming the innate immune response (McMichael et al., 2005). This facilitates recognition of bacterial invasion on epithelial surfaces where concentrations of elafin are high allowing complexes to form prior to signalling. This

contrasts with the inhibitory effects of elafin on LPS signalling described above and the reduced production of TNF-α in response to systemic LPS administration observed in elafin expressing mice (Sallenave et al., 2003). Cleavage of the surface receptor CD14 by HNE impedes apoptotic cell recognition and tethering by macrophages. Our group demonstrated that adenoviral overexpression of elafin in human macrophages prevents CD14 cleavage and preserved apoptotic cell tethering (Henriksen et al., 2004a). This rescues these cells from an HNE induced pro-inflammatory to anti-inflammatory phenotype favouring apoptotic cell recognition and clearance (Savill et al., 2002).

Elafin favours the development of a Th1-type immune response. Overexpression in transgenic mice or delivery using adenoviral vectors was associated with increased numbers and activation of antigen presenting dendritic cells (Roghanian et al., 2006). Cytokine and antibody analysis from pulmonary cells, serum and bronchial washings suggested that immunity was biased toward a type 1 response with production of IL-12, IFN-γ and IgG2a antibody. Clinically, this finding is supported by high concentrations of elafin in bronchoalveolar lavage from farmer's lung and psoriatic skin (Tremblay et al., 1996, Schalkwijk et al., 1993). Both conditions are characterised by a vigorous type-1 immune response.

4. NEUTROPHIL MEDIATED CARDIOVASCULAR INJURY: THE ROLE OF HNE AND THERAPEUTIC POTENTIAL OF ELAFIN

The earlier sections outlined the pro-inflammatory actions of HNE that serve to initiate and sustain inflammatory tissue injury. Elafin is a potent endogenous inhibitor of HNE with multifaceted anti-inflammatory roles. Production of elafin in

response to inflammatory injury represents a mechanism whereby epithelial tissues have evolved to contain and repair neutrophil-mediated injury. The following sections will outline the prominent role of neutrophils and HNE in cardiovascular pathologies including myocardial infarction and arterial inflammation. We will discuss the substantial evidence from pre-clinical studies (summarised in table 1) indicating a therapeutic role for elafin in models of vascular injury.

4.1 Neutrophil-mediated ischemia-reperfusion injury

The role of the neutrophil in myocardial-reperfusion injury following myocardial infarction has been reviewed by Hansen and Jordan *et al* (Jordan et al., 1999, Hansen, 1995). Cardiomyocyte injury is exacerbated following reperfusion and neutrophils are pivotal mediators determining post-ischemic inflammatory reperfusion injury. Neutrophils accumulate within the reperfused myocardium releasing HNE and reactive oxygen species that further effect microvascular and myocardial injury. Preclinical studies have demonstrated that neutrophil depletion or inhibition of neutrophil elastase attenuates post-ischemic inflammatory reperfusion injury within the myocardium (Romson et al., 1983a, Tiefenbacher et al., 1997).

Plasma HNE and myeloperoxidase concentrations increase following myocardial infarction providing evidence of neutrophil activation (Dinerman and Mehta, 1990, Mocatta et al., 2007). Neutrophils are activated by a vast array of mediators released from endothelial cells, mast cells and myocytes within the myocardium following ischemia. The complement fragment C5a, IL-8 and platelet activating factor act as

chemoattractants and stimulate adherence to the endothelium. TNF-α released from mast cells and IL-6 from ischemic cardiomyocytes further stimulate neutrophil superoxide production, transendothelial migration and degranulation (Richter et al., 1990).

Coronary occlusion without reperfusion is associated with ischemia and restricted infiltration of neutrophils into the border area of the infarcted zone over 24 hours (Reimer et al., 1989). The goal of therapy in acute myocardial infarction is timely restoration of perfusion and whereas this reduces infarct size, it is associated with accelerated accumulation of neutrophils within the reperfused myocardium (Dreyer et al., 1991, Zhao et al., 2001). Neutrophil adhesion to the endothelium occurs within minutes of reperfusion (Sheridan et al., 1996, Murohara et al., 1994). Release of proteases and reactive oxygen species cause cardiomyocyte necrosis. Neutrophils also occlude microvessels and cause changes in endothelial permeability that contribute to myocardial edema (Engler et al., 1983). Capillary plugging and obstruction by activated neutrophils contributes to failure of microvascular perfusion and increased infarct size within the “no-reflow” zone. Neutrophil depletion reduced this phenomenon and infarct size in a pre-clinical model (Litt et al., 1989). Neutrophil mediated inflammation generates production of further chemokines and adhesion molecule expression that amplify inflammatory cell recruitment. The goal of therapy is both to reduce neutrophil-mediated injury and to break the vicious cycle of further neutrophil recruitment.

Administration or over-expression of elafin was associated with reduced infarct size and neutrophil infiltration in several models of ischemia-reperfusion injury.

Tiefenbacher *et al* investigated cardiac reperfusion injury in a rat model inducing repeated ischemia and reperfusion with ligation of the left coronary artery (Tiefenbacher et al., 1997). The animal received a bolus of recombinant elafin by tail vein injection prior to ischemia. Myocardial function measured by systolic fractional thickening was better in animals receiving elafin or a synthetic elastase inhibitor. Systolic fractional thickening of the myocardium measured by pulsed Doppler was reduced by 50% in the controls compared to 22% in elafin treated animals. Mice expressing human elafin under the control of the preproendothelin promoter exhibit better cardiac function compared to littermates following myocardial infarction. Left ventricular dimensions in diastole were significantly increased in the wild-type mice (mean 4.75 mm) compared to sham operated mice (mean 3.95 mm). Elafin expressing mice had some increase in cavity size (mean 4.30 mm) which was not significantly different from sham operated mice. Elafin expressing mice had reduced infarct expansion and less scar thinning. The increases in myocardial tissue elastase and matrix metalloprotease activity following infarction were effectively suppressed in elafin transgenic animals compared to wild type littermates (Ohta et al., 2004b). Tissue myeloperoxidase content can be used as a measure of neutrophil infiltration. In the rat myocardial infarction model myeloperoxidase levels increased 14-fold in control animals compared to only a 3-fold rise in elafin treated animals (Tiefenbacher et al., 1997). Similar reductions in neutrophil infiltration were observed in the elafin transgenic mice and following elafin administration prior to arterial ligation in a rodent limb ischemia model (Crinnion et al., 1994). In the latter study, elafin attenuated the acceleration in neutrophil infiltration (myeloperoxidase content) following reperfusion and was associated with reduced myocyte necrosis.

Elafin administration or overexpression was consistently associated with reduced myocyte death and preserved function following ischemia and reperfusion across different models. The reduction in neutrophil infiltration suggests that elafin interrupts the positive feedback loop signaling further neutrophil recruitment during reperfusion. This may be through combined direct inhibitory action on HNE and proteinase 3 mediated tissue injury and suppression of the potent neutrophil chemokine IL-8.

4.2 Neutrophil elastase-mediated inflammation of the vessel wall

Endothelial function is compromised by neutrophil-mediated injury. Loss of permeability barrier leads to edema and hemorrhage and loss of antithrombotic activity is conducive to platelet adhesion and fibrin deposition. These effects manifest in diverse diseases that share neutrophil-mediated injury including the adult respiratory distress syndrome, vasculitides and disseminated intravascular coagulation. Activated endothelial cells release platelet activating factor and IL-8 facilitating paracrine activation and degranulation of neutrophils. HNE stimulates IL-8 production directly and augments endothelial cell production in response to other stimuli such as lipopolysaccharide (Henriksen et al., 2004b). HNE activation of endothelial PAR receptors (described above) may signal thrombus formation and neutrophil adhesion through mobilisation and secretion of Weibel-Palade bodies, which harbor vWF multimers and the P-selectin adhesion molecule (Hattori et al., 1989).

The neutrophil is not a prevalent cell type within atherosclerotic plaque. Nevertheless an expanding body of evidence implicates neutrophils and HNE in the development

of arterial wall inflammation. Macrophage and endothelial cell localisation of HNE mRNA was identified by *in situ* hybridisation within human atheroma (Dollery et al., 2003). HNE colocalised with macrophages at the plaque shoulder. This region is characterised by a paucity of smooth muscle cells and is prone to rupture through mechanisms involving excess proteolytic activity. This work demonstrated HNE production by human endothelial cells and peripheral blood-derived monocytes suggesting the intriguing possibility that these cell types may contribute directly to elastase activity within the arterial wall. Neutrophils are activated in patients the acute coronary syndromes (Buffon et al., 2002) and are observed infiltrating ruptured plaques and areas of endothelial erosion responsible for thrombosis in human coronary specimens (Naruko et al., 2002). It is possible that HNE is assimilated into the plaque from degranulating neutrophils. The phenomenon of neutrophil-derived proteins accumulating in the subendothelial space of atheromatous vessels has been demonstrated for myeloperoxidase which is taken up by endothelial cells through transcytosis (Baldus et al., 2003, Daugherty et al., 1994).

Rabinovitch's group have demonstrated that augmentation of elafin by delivery of recombinant protein or overexpression using transgenic mice or vectors has therapeutic benefit in models of inflammatory vessel wall injury(Zaidi et al., 2000b). Neutrophil recruitment and elastase activity increase within the arterial wall following balloon angioplasty (Barolet et al., 2001, Okamoto et al., 2001). Two episodes of balloon angioplasty 3 weeks apart were used in a double injury model in rabbit carotid arteries (Barolet et al., 2001). There was an 8-fold increase in elastase activity peaking 1 week after the second balloon injury. The elastase activity was associated with a 25 kDa protein that was inhibited by elafin suggesting neutrophil elastase. Using a liposome vector, human elafin cDNA was transfected into the

carotid arteries following the second balloon injury. Elafin transgene expression was evident at 48 hours and suppressed the rise in elastase activity by 90% compared with controls. This was associated with reduced restenosis and a 43% reduction in intimal cross-sectional area in elafin-transfected arteries. Wire induced carotid injury in transgenic mice expressing elafin produced similar findings (Zaidi et al., 2000b). Elafin transgenic animals exhibited almost complete suppression of elastase activity in response to wire injury. Wild-type mice had a doubling in the cross sectional arterial medial area at 10 days. This was taken as a measure of restenosis and reflects matrix deposition, cellular migration and proliferation. There was no significant difference in the medial area between non-injured wild-type and injured elafin transgenic mice. These changes were seen in association with reduced neutrophil infiltration and lower deposition of the matrix protein tenascin-C. Tenascin-C signals vascular smooth muscle cell proliferation (Jones et al., 1997), a key feature of arterial restenosis following angioplasty. Venous grafts are used as conduits in coronary bypass surgery. They are susceptible to rapid atherosclerotic degeneration and this was modelled in the rabbit with an interposition jugular venous graft inserted into the carotid artery (O'Blenes et al., 2000). Liposomal transfection of elafin cDNA resulted in reduced elastase activity, neutrophil infiltration within the graft and a 50% reduction in neointimal formation compared to mock transfected control grafts. This model was used to study the effects of elafin on chronic atherosclerotic plaque development. Following 3 months of high cholesterol feed, the rabbit interposition venous grafts developed marked intimal plaque with high lipid and macrophage content. The plaque size was reduced in elafin-transfected grafts by 40% and lipid content was reduced by 50%.

These findings indicate a prominent role for neutrophil elastase in acute arterial inflammation. Overexpression of human elafin cDNA in the arterial wall (rodents do not produce elafin) was associated with a reduction in elastase activity, neutrophil infiltration and injury response in the form of restenosis in response to mechanical injury. The observation that elafin overexpression reduced atherosclerotic plaque development in a chronic model of hyperlipidemic rabbits raises the possibility that additional anti-inflammatory actions of elafin may be at work reducing inflammatory cytokine production.

5. THERAPEUTIC APPLICATION OF ELAFIN IN CARDIOVASCULAR DISEASE

Elafin augmentation protects the cardiovascular system from a range of diseases characterized by neutrophil-mediated inflammation (Figure 2). Elafin provides the endothelium and myocardium with protection against the damaging effects of neutrophil-derived elastases. This suggests that intravenous elafin administration or gene overexpression can provide inhibition by reaching elastase enzyme that is not suppressed by the high circulating concentrations of larger molecular weight elastase inhibitors. Elafin attenuates disease progression in chronic injury models including atherosclerosis and pulmonary hypertension (Zaidi et al., 2002b) and provides survival benefit in a murine model of viral myocarditis (Zaidi et al., 1999). The neutrophil does not have a prominent role in these pathologies indicating alternative

mechanisms for elafin's effect beyond inhibition of elastase through suppressing NF-κB activation or modulating the adaptive immune response. Recombinant elafin has very low toxicity with short plasma and activity half-lives. It is possible to maintain circulating activity with intravenous infusion and this approach is used routinely with antithrombotic drugs in acute coronary syndrome patients. Translating the efficacy of elafin in pre-clinical models to diseases, such as acute myocardial infarction, will depend on achieving adequate concentrations of active protein at the site of tissue injury. In most pre-clinical models, elafin is delivered before or at the point of vascular injury. This advantageous position is not generally feasible in the clinic. The complexities of human disease over animal models have seen many promising therapies for ischemia reperfusion fail at translation (Bolli et al., 2004). The EMPIRE study (Elafin Myocardial Protection from Ischaemia Reperfusion: EudraCT no. 2010-019527-58) will recapitulate some of the conditions of pre-clinical studies to demonstrate whether elafin can attenuate myocardial ischemia-reperfusion injury and inflammation in patients undergoing coronary bypass surgery. Patients will receive an elafin infusion prior to going onto cardiopulmonary bypass and the effects on myocardial injury will be quantified by troponin release within the first 48 h after surgery and infarct volume measured with cardiac magnetic resonance scanning. Post-operative inflammatory cytokine response will also be examined. This study aims to provide proof-of-principle for elafin's therapeutic potential in cardiovascular disease.

6. CONCLUSION

Elafin inhibits destructive and inflammatory neutrophil derived proteases. Beyond this elafin inhibits inflammatory cytokines and modulates the innate and adaptive immune systems. Elafin is expressed within epithelial tissues that have evolved mechanisms to adapt and repair from neutrophil mediated injury. Elafin administration in preclinical studies of inflammatory vascular injury limits tissue destruction and preserves organ function. As such it may provide a therapeutic option in the clinical setting. The EMPIRE trial is currently underway to investigate this.

LEGEND

Graphical Abstract: Pre-clinical studies indicate the therapeutic potential of the human neutrophil elastase inhibitor "elafin" in inflammatory cardiovascular pathology

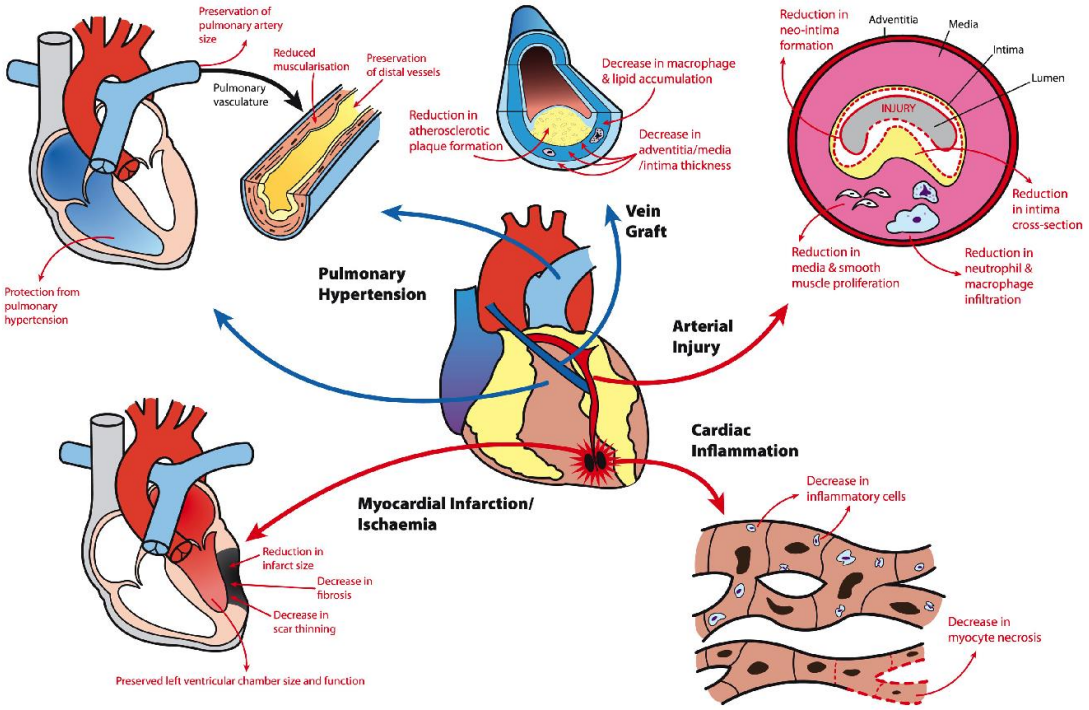

Figure 1: Actions of neutrophil-derived elastases: Human neutrophil elastase and proteinase 3

Activated neutrophils release HNE and proteinase 3 leading to endothelial disruption and extracellular matrix degradation. These processes contribute to aneurysm development and disruption of vulnerable atherosclerotic plaques. HNE and proteinase-3 modulate the activity of TNF-α, IL-1β, IL-8 and IL-18 by proteolytic cleavage. HNE activation of protease activated receptors (PAR) activation may contribute to changes in endothelial permeability and migration of neutrophils. HNE stimulates production of IL-8 production from endothelial cells and induces IL-6 release from necrotic myocardium. HNE cleavage of the CD14 receptor on macrophages impedes resolution of inflammation by preventing recognition and clearance of apoptotic cells. HNE also promotes thrombosis by inactivating tissue factor pathway inhibitor.

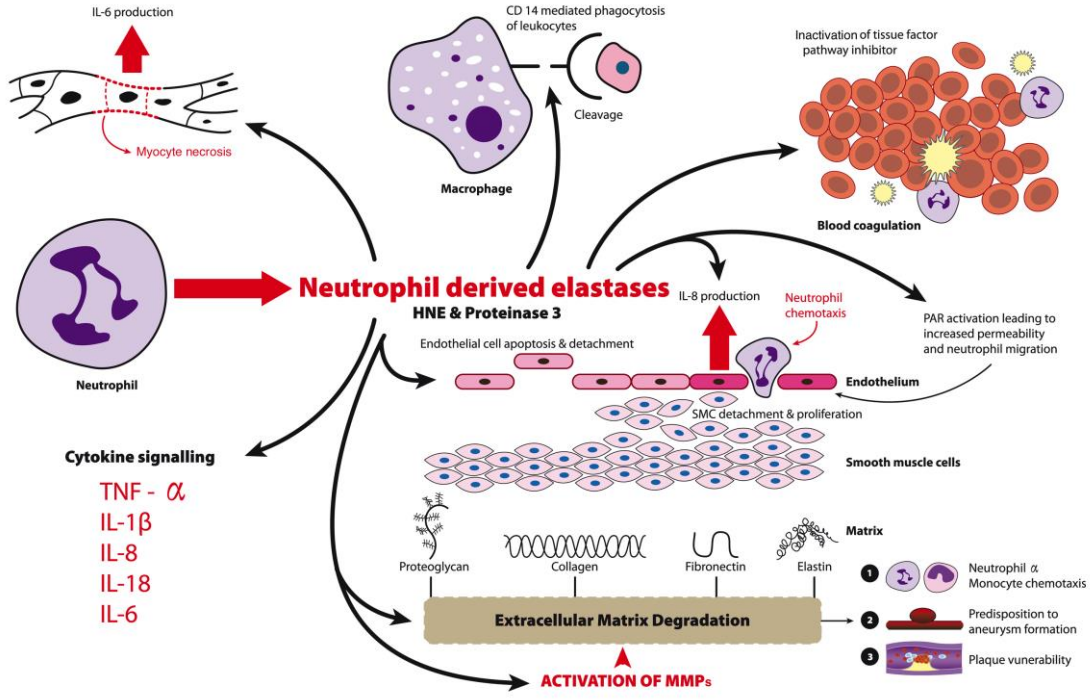

Figure 2: Cardiovascular effects of Elafin

Elafin administration or gene overexpression has demonstrated beneficial effects in a series of vascular injury models. Clockwise from top-right these are arterial injury and balloon angioplasty, myocarditis, myocardial ischaemia and infarction, pulmonary hypertension and vein graft degeneration. Elafin treatment is associated with consistent findings of reduced elastase activity, tissue injury and inflammatory cell infiltration in these models.

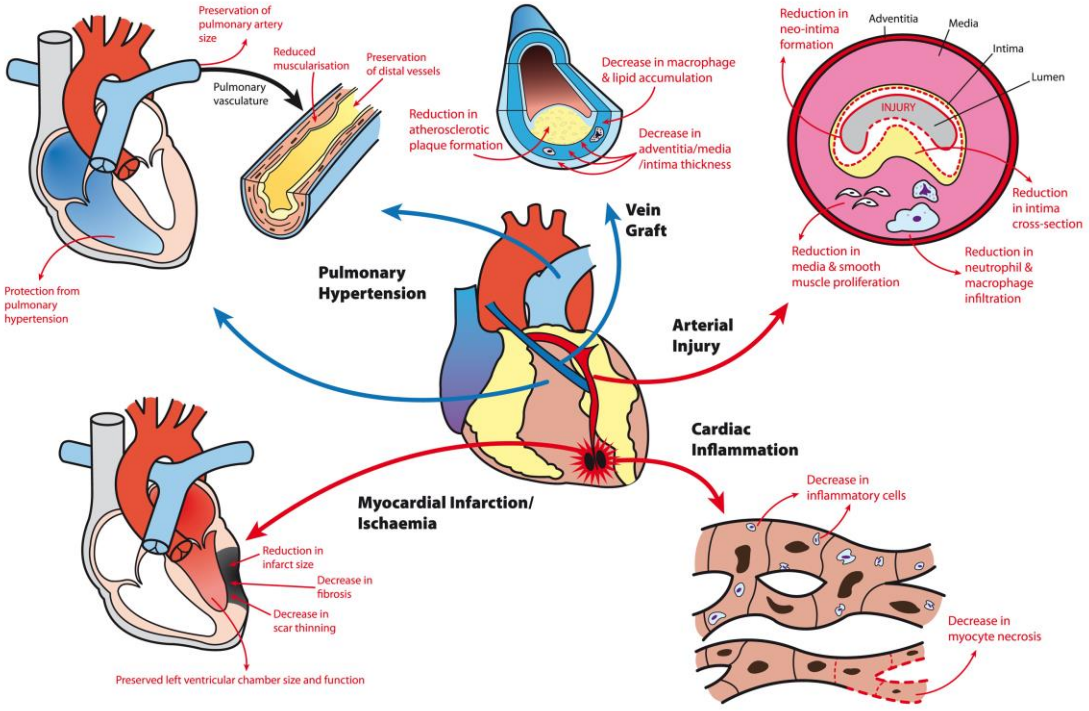

REFERENCES

[1] Borregaard N, Cowland JB. Granules of the human neutrophilic polymorphonuclear leukocyte. Blood 1997;89:3503.

[2] Lee WL, Downey GP. Leukocyte elastase. Physiological functions and role in acute lung injury. American Journal of Respiratory and Critical Care Medicine 2001;164:896.

[3] Si-Tahar M, Pidard D, Balloy V, Moniatte M, Kieffer N, Dorsselaer AV, et al. Human neutrophil elastase proteolytically activates the platelet integrin aIIbb3 through cleavage of the carboxyl terminus of the aIIb subunit heavy chain. Involvement in the potentiation of platelet. Journal of Biological Chemistry 1997;272:11636-47.

[4] Carden D, Xiao F, Moak C, Willis BH, Robinson-Jackson S, Alexander S. Neutrophil elastase promotes lung microvascular injury and proteolysis of endothelial cadherins. American Journal of Physiology-Heart and Circulatory Physiology 1998;275:H385.

[5] Robert L, Robert A, Jacotot B. Elastin-elastase-atherosclerosis revisited. Atherosclerosis 1998;140:281-95.

[6] Houghton AMG, Quintero PA, Perkins DL, Kobayashi DK, Kelley DG, Marconcini LA, et al. Elastin fragments drive disease progression in a murine model of emphysema. Journal of Clinical Investigation 2006;116:753.

[7] Westlin W, Gimbrone Jr M. Neutrophil-mediated damage to human vascular endothelium. Role of cytokine activation. The American Journal of Pathology 1993;142:117.

[8] Frisch SM, Francis H. Disruption of epithelial cell-matrix interactions induces apoptosis. The Journal of Cell Biology 1994;124:619.

[9] Mtairag EM, Houard X, Rais S, Pasquier C, Oudghiri M, Jacob MP, et al. Pharmacological potentiation of natriuretic peptide limits polymorphonuclear neutrophil-vascular cell interactions. Arteriosclerosis, Thrombosis, and Vascular Biology 2002;22:1824.

[10] Garcia-Touchard A, Henry TD, Sangiorgi G, Spagnoli LG, Mauriello A, Conover C, et al. Extracellular proteases in atherosclerosis and restenosis. Arteriosclerosis, Thrombosis, and Vascular Biology 2005;25:1119.

[11] Chakraborti S, Mandal M, Das S, Mandal A, Chakraborti T. Regulation of matrix metalloproteinases: an overview. Molecular and Cellular Biochemistry 2003;253:269-85.

[12] Okada Y, Nakanishi I. Activation of matrix metalloproteinase 3 (stromelysin) and matrix metalloproteinase 2 ('gelatinase') by human neutrophil elastase and cathepsin G. FEBS letters 1989;249:353-6.

[13] Okada Y, Watanabe S, Nakanishi I, Kishi J, Hayakawa T, Watorek W, et al. Inactivation of tissue inhibitor of metalloproteinases by neutrophil elastase and other serine proteinases. FEBS letters 1988;229:157-60.

[14] Fontaine V, Touat Z, Mtairag EM, Vranckx R, Louedec L, Houard X, et al. Role of leukocyte elastase in preventing cellular re-colonization of the mural thrombus. American Journal of Pathology 2004;164:2077.

[15] Wu K, Urano T, Ihara H, Takada Y, Fujie M, Shikimori M, et al. The cleavage and inactivation of plasminogen activator inhibitor type 1 by neutrophil elastase: the evaluation of its physiologic relevance in fibrinolysis. Blood 1995;86:1056.

[16] Duboscq C, Genoud V, Parborell MF, Kordich LC. Impaired clot lysis by rt-PA catalyzed mini-plasminogen activation. Thrombosis Research 1997;86:505-13.

[17] Massberg S, Grahl L, von Bruehl ML, Manukyan D, Pfeiler S, Goosmann C, et al. Reciprocal coupling of coagulation and innate immunity via neutrophil serine proteases. Nat Med 2010;16:887-96.

[18] Madjid M, Awan I, Willerson JT, Casscells SW. Leukocyte count and coronary heart disease:: Implications for risk assessment. Journal of the American College of Cardiology 2004;44:1945-56.

[19] Buffon A, Biasucci LM, Liuzzo G, D'ONOFRIO G, Crea F, Maseri A. Widespread coronary inflammation in unstable angina. The New England journal of medicine 2002;347:5-12.

[20] Carroll TP, Greene CM, Taggart CC, Bowie AG, O'Neill SJ, McElvaney NG. Viral inhibition of IL-1-and neutrophil elastase-induced inflammatory

responses in bronchial epithelial cells. The Journal of Immunology 2005;175:7594.

[21] Coeshott C, Ohnemus C, Pilyavskaya A, Ross S, Wieczorek M, Kroona H, et al. Converting enzyme-independent release of tumor necrosis factor and IL-1 from a stimulated human monocytic cell line in the presence of activated neutrophils or purified proteinase 3. Proceedings of the National Academy of Sciences of the United States of America 1999;96:6261.

[22] Padrines M, Wolf M, Walz A, Baggiolini M. Interleukin-8 processing by neutrophil elastase, cathepsin G and proteinase-3. FEBS letters 1994;352:231-5.

[23] Sugawara S, Uehara A, Nochi T, Yamaguchi T, Ueda H, Sugiyama A, et al. Neutrophil proteinase 3-mediated induction of bioactive IL-18 secretion by human oral epithelial cells. The Journal of Immunology 2001;167:6568.

[24] Wittamer V, Franssen JD, Vulcano M, Mirjolet JF, Le Poul E, Migeotte I, et al. Specific recruitment of antigen-presenting cells by chemerin, a novel processed ligand from human inflammatory fluids. J Exp Med 2003;198:977-85.

[25] Wittamer V, Bondue B, Guillabert A, Vassart G, Parmentier M, Communi D. Neutrophil-mediated maturation of chemerin: a link between innate and adaptive immunity. J Immunol 2005;175:487-93.

[26] Nemoto E, Sugawara S, Tada H, Takada H, Shimauchi H, Horiuchi H. Cleavage of CD14 on human gingival fibroblasts cocultured with activated neutrophils is mediated by human leukocyte elastase resulting in down-regulation of lipopolysaccharide-induced IL-8 production. J Immunol 2000;165:5807-13.

[27] Vandivier RW, Fadok VA, Hoffmann PR, Bratton DL, Penvari C, Brown KK, et al. Elastase-mediated phosphatidylserine receptor cleavage impairs apoptotic cell clearance in cystic fibrosis and bronchiectasis. Journal of Clinical Investigation 2002;109:661-70.

[28] Sadallah S, Hess C, Miot S, Spertini O, Lutz H, Schifferli JA. Elastase and metalloproteinase activities regulate soluble complement receptor 1 release. European Journal of Immunology 1999;29:3754-61.

[29] Henriksen PA, Hitt M, Xing Z, Wang J, Haslett C, Riemersma RA, et al. Adenoviral gene delivery of elafin and secretory leukocyte protease inhibitor

attenuates NF- B-dependent inflammatory responses of human endothelial cells and macrophages to atherogenic stimuli. The Journal of Immunology 2004;172:4535.

[30] Devaney JM, Greene CM, Taggart CC, Carroll TP, O'Neill SJ, McElvaney NG. Neutrophil elastase up-regulates interleukin-8 via toll-like receptor 4. FEBS letters 2003;544:129-32.

[31] Uehara A, Muramoto K, Takada H, Sugawara S. Neutrophil serine proteinases activate human nonepithelial cells to produce inflammatory cytokines through protease-activated receptor 2. The Journal of Immunology 2003;170:5690.

[32] Uehara A, Sugawara S, Muramoto K, Takada H. Activation of human oral epithelial cells by neutrophil proteinase 3 through protease-activated receptor-2. The Journal of Immunology 2002;169:4594.

[33] Leger AJ, Covic L, Kuliopulos A. Protease-activated receptors in cardiovascular diseases. Circulation 2006;114:1070.

[34] Asokananthan N, Graham PT, Fink J, Knight DA, Bakker AJ, McWilliam AS, et al. Activation of protease-activated receptor PAR-1, PAR-2, and PAR-4 stimulates IL-6, IL-8, and prostaglandin E2 release from human respiratory epithelial cells. The Journal of Immunology 2002;168:3577.

[35] Chin AC, Lee WY, Nusrat A, Vergnolle N, Parkos CA. Neutrophil-mediated activation of epithelial protease-activated receptors-1 and-2 regulates barrier function and transepithelial migration. The Journal of Immunology 2008;181:5702.

[36] Ramachandran R, Mihara K, Chung H, Renaux B, Lau CS, Muruve DA, et al. Neutrophil Elastase Acts as a Biased Agonist for Proteinase-activated Receptor-2 (PAR2). Journal of Biological Chemistry 2011;286:24638.

[37] Belaaouaj A, Kim KS, Shapiro SD. Degradation of outer membrane protein A in Escherichia coli killing by neutrophil elastase. Science 2000;289:1185-8.

[38] Tkalcevic J, Novelli M, Phylactides M, Iredale JP, Segal AW, Roes J. Impaired immunity and enhanced resistance to endotoxin in the absence of neutrophil elastase and cathepsin G. Immunity 2000;12:201-10.

[39] Belaaouaj A, Kim KS, Shapiro SD. Degradation of outer membrane protein A in Escherichia coli killing by neutrophil elastase. Science 2000;289:1185.

[40] Belaaouaj A, McCarthy R, Baumann M, Gao Z, Ley TJ, Abraham SN, et al. Mice lacking neutrophil elastase reveal impaired host defense against gram negative bacterial sepsis. Nature Medicine 1998;4:615-8.

[41] Hirche TO, Benabid R, Deslee G, Gangloff S, Achilefu S, Guenounou M, et al. Neutrophil elastase mediates innate host protection against Pseudomonas aeruginosa. The Journal of Immunology 2008;181:4945-54.

[42] Reeves EP, Lu H, Jacobs HL, Messina CG, Bolsover S, Gabella G, et al. Killing activity of neutrophils is mediated through activation of proteases by K+ flux. Nature 2002;416:291-7.

[43] Standish AJ, Weiser JN. Human neutrophils kill Streptococcus pneumoniae via serine proteases. The Journal of Immunology 2009;183:2602.

[44] Lehrer RI, Ganz T. Cathelicidins: a family of endogenous antimicrobial peptides. Curr Opin Hematol 2002;9:18-22.

[45] Sallenave JM. The role of secretory leukocyte proteinase inhibitor and elafin (elastase-specific inhibitor/skin-derived antileukoprotease) as alarm antiproteinases in inflammatory lung disease. Respiratory Research 2000;1:87-92.

[46] Korkmaz B, Attucci S, Jourdan ML, Juliano L, Gauthier F. Inhibition of neutrophil elastase by 1-protease inhibitor at the surface of human polymorphonuclear neutrophils. The Journal of Immunology 2005;175:3329.

[47] Owen CA, Campbell MA, Sannes PL, Boukedes SS, Campbell EJ. Cell surface-bound elastase and cathepsin G on human neutrophils: a novel, non-oxidative mechanism by which neutrophils focus and preserve catalytic activity of serine proteinases. The Journal of Cell Biology 1995;131:775.

[48] Lentsch AB, Yoshidome H, Warner RL, Ward PA, Edwards MJ. Secretory leukocyte protease inhibitor in mice regulates local and remote organ inflammatory injury induced by hepatic ischemia/reperfusion. Gastroenterology 1999;117:953-61.

[49] McElvaney NG, Nakamura H, Birrer P, Hebert CA, Wong WL, Alphonso M, et al. Modulation of airway inflammation in cystic fibrosis. In vivo suppression of interleukin-8 levels on the respiratory epithelial surface by aerosolization of recombinant secretory leukoprotease inhibitor. J Clin Invest 1992;90:1296-301.

[50] Silverman EK, Sandhaus RA. Clinical practice. Alpha1-antitrypsin deficiency. N Engl J Med 2009;360:2749-57.

[51] Hoshi K, Kurosawa S, Kato M, Andoh K, Satoh D, Kaise A. Sivelestat, a neutrophil elastase inhibitor, reduces mortality rate of critically ill patients. Tohoku J Exp Med 2005;207:143-8.

[52] Okayama N, Kakihana Y, Setoguchi D, Imabayashi T, Omae T, Matsunaga A, et al. Clinical effects of a neutrophil elastase inhibitor, sivelestat, in patients with acute respiratory distress syndrome. J Anesth 2006;20:6-10.

[53] Ryugo M, Sawa Y, Takano H, Matsumiya G, Iwai S, Ono M, et al. Effect of a polymorphonuclear elastase inhibitor (sivelestat sodium) on acute lung injury after cardiopulmonary bypass: findings of a double-blind randomized study. Surg Today 2006;36:321-6.

[54] Tamakuma S, Ogawa M, Aikawa N, Kubota T, Hirasawa H, Ishizaka A, et al. Relationship between neutrophil elastase and acute lung injury in humans. Pulm Pharmacol Ther 2004;17:271-9.

[55] Zeiher BG, Artigas A, Vincent JL, Dmitrienko A, Jackson K, Thompson BT, et al. Neutrophil elastase inhibition in acute lung injury: results of the STRIVE study. Crit Care Med 2004;32:1695-702.

[56] Yoshimura Y, Hiramatsu Y, Sato Y, Homma S, Enomoto Y, Jikuya T, et al. ONO-6818, a novel, potent neutrophil elastase inhibitor, reduces inflammatory mediators during simulated extracorporeal circulation. Ann Thorac Surg 2003;76:1234-9.

[57] Luisetti M, Sturani C, Sella D, Madonini E, Galavotti V, Bruno G, et al. MR889, a neutrophil elastase inhibitor, in patients with chronic obstructive pulmonary disease: a double-blind, randomized, placebo-controlled clinical trial. Eur Respir J 1996;9:1482-6.

[58] Wiedow O, Schröder J, Gregory H, Young J, Christophers E. Elafin: an elastase-specific inhibitor of human skin. Purification, characterization, and complete amino acid sequence. Journal of Biological Chemistry 1990;265:14791.

[59] Sallenave JM, Ryle AP. Purifkation and Characterization of Elastase-Specific Inhibitor. Sequence Homology with Mucus Proteinase Inhibitor. Biological Chemistry Hoppe-Seyler 1991;372:13-22.

[60] Molhuizen H, Alkemade H, Zeeuwen P, De Jongh G, Wieringa B, Schalkwijk J. SKALP/elafin: an elastase inhibitor from cultured human keratinocytes. Purification, cDNA sequence, and evidence for transglutaminase cross-linking. Journal of Biological Chemistry 1993;268:12028.

[61] Sallenave J, Silva A. Characterization and gene sequence of the precursor of elafin, an elastase-specific inhibitor in bronchial secretions. American Journal of Respiratory Cell and Molecular Biology 1993;8:439.

[62] Schalkwijk J, Wiedow O, Hirose S. The trappin gene family: proteins defined by an N-terminal transglutaminase substrate domain and a C-terminal four-disulphide core. Biochemical Journal 1999;340:569.

[63] Francart C, Dauchez M, Alix AJP, Lippens G. Solution structure of R-elafin, a specific inhibitor of elastase. Journal of Molecular Biology 1997;268:666-77.

[64] Nara K, Ito S, Ito T, Suzuki Y, Ghoneim MA, Tachibana S, et al. Elastase inhibitor elafin is a new type of proteinase inhibitor which has a transglutaminase-mediated anchoring sequence termed ìcementoinî. Journal of Biochemistry 1994;115:441.

[65] Sumi Y, Inoue N, Azumi H, Seno T, Okuda M, Hirata K, et al. Expression of tissue transglutaminase and elafin in human coronary artery:: Implication for plaque instability. Atherosclerosis 2002;160:31-9.

[66] Tsunemi M, Matsuura Y, Sakakibara S, Katsube Y. Crystal structure of an elastase-specific inhibitor elafin complexed with porcine pancreatic elastase determined at 1.9 A resolution. Biochemistry 1996;35:11570-6.

[67] Zani ML, Nobar SM, Lacour SA, Lemoine S, Boudier C, Bieth JG, et al. Kinetics of the inhibition of neutrophil proteinases by recombinant elafin and pre elafin (trappin 2) expressed in Pichia pastoris. European Journal of Biochemistry 2004;271:2370-8.

[68] Pfundt R, Wingens M, Bergers M, Zweers M, Frenken M, Schalkwijk J. TNF- and serum induce SKALP/elafin gene expression in human keratinocytes by a p38 MAP kinase-dependent pathway. Archives of Dermatological Research 2000;292:180-7.

[69] Lee S, Hirose S, Park S, Chi J, Chung S, Mori M. Elafin expression in human fetal and adult submandibular glands. Histochemistry and Cell Biology 2002;117:423-30.

[70] Zhang M, Zou Z, Maass N, Sager R. Differential expression of elafin in human normal mammary epithelial cells and carcinomas is regulated at the transcriptional level. Cancer Research 1995;55:2537.

[71] King AE, Critchley HOD, Sallenave JM, Kelly RW. Elafin in human endometrium: an antiprotease and antimicrobial molecule expressed during menstruation. Journal of Clinical Endocrinology & Metabolism 2003;88:4426.

[72] Sallenave J, Silva A, Marsden M, Ryle A. Secretion of mucus proteinase inhibitor and elafin by Clara cell and type II pneumocyte cell lines. American Journal of Respiratory Cell and Molecular Biology 1993;8:126.

[73] Sallenave JM, Shulmann J, Crossley J, Jordana M, Gauldie J. Regulation of secretory leukocyte proteinase inhibitor (SLPI) and elastase-specific inhibitor (ESI/elafin) in human airway epithelial cells by cytokines and neutrophilic enzymes. American Journal of Respiratory Cell and Molecular Biology 1994;11:733.

[74] Jin F, Nathan C, Radzioch D, Ding A. Secretory leukocyte protease inhibitor: a macrophage product induced by and antagonistic to bacterial lipopolysaccharide. Cell 1997;88:417-26.

[75] Zhu J, Nathan C, Ding A. Suppression of macrophage responses to bacterial lipopolysaccharide by a non-secretory form of secretory leukocyte protease inhibitor. Biochimica et Biophysica Acta (BBA)-Molecular Cell Research 1999;1451:219-23.

[76] Butler MW, Robertson I, Greene CM, O'Neill SJ, Taggart CC, McElvaney NG. Elafin prevents lipopolysaccharide-induced AP-1 and NF- B activation via an effect on the ubiquitin-proteasome pathway. Journal of Biological Chemistry 2006;281:34730.

[77] Simpson A, Maxwell A, Govan J, Haslett C, Sallenave JM. Elafin (elastase-specific inhibitor) has anti-microbial activity against gram-positive and gram-negative respiratory pathogens. FEBS letters 1999;452:309-13.

[78] McMichael JW, Roghanian A, Lu J, Ramage R, Sallenave JM. The antimicrobial antiproteinase elafin binds to lipopolysaccharide and modulates

macrophage responses. American Journal of Respiratory Cell and Molecular Biology 2005;32:443-52.

[79] Sallenave JM, Cunningham G, James R, McLachlan G, Haslett C. Regulation of pulmonary and systemic bacterial lipopolysaccharide responses in transgenic mice expressing human elafin. Infection and Immunity 2003;71:3766.

[80] Henriksen PA, Devitt A, Kotelevtsev Y, Sallenave JM. Gene delivery of the elastase inhibitor elafin protects macrophages from neutrophil elastase-mediated impairment of apoptotic cell recognition. FEBS letters 2004;574:80-4.

[81] Savill J, Dransfield I, Gregory C, Haslett C. A blast from the past: clearance of apoptotic cells regulates immune responses. Nature Reviews Immunology 2002;2:965-75.

[82] Roghanian A, Williams SE, Sheldrake TA, Brown TI, Oberheim K, Xing Z, et al. The antimicrobial/elastase inhibitor elafin regulates lung dendritic cells and adaptive immunity. American Journal of Respiratory Cell and Molecular Biology 2006;34:634.

[83] Tremblay GM, Sallenave JM, Israel-Assayag E, Cormier Y, Gauldie J. Elafin/elastase-specific inhibitor in bronchoalveolar lavage of normal subjects and farmer's lung. American Journal of Respiratory and Critical Care Medicine 1996;154:1092.

[84] Schalkwijk J, Van Vlijmen I, Alkemade J, De Jongh G. Immunohistochemical localization of SKALP/elafin in psoriatic epidermis. Journal of Investigative Dermatology 1993;100:390-3.

[85] Jordan JE, Zhao ZQ, Vinten-Johansen J. The role of neutrophils in myocardial ischemiañreperfusion injury. Cardiovascular Research 1999;43:860.

[86] Hansen PR. Role of neutrophils in myocardial ischemia and reperfusion. Circulation 1995;91:1872.

[87] Romson JL, Hook BG, Kunkel SL, Abrams G, Schork M, Lucchesi B. Reduction of the extent of ischemic myocardial injury by neutrophil depletion in the dog. Circulation 1983;67:1016.

[88] Tiefenbacher C, Ebert M, Niroomand F, Batkai S, Tillmanns H, Zimmermann R, et al. Inhibition of elastase improves myocardial function after repetitive

ischaemia and myocardial infarction in the rat heart. Pflugers Archiv European Journal of Physiology 1997;433:563-70.

[89] Dinerman JL, Mehta JL. Endothelial, platelet and leukocyte interactions in ischemic heart disease: insights into potential mechanisms and their clinical relevance. Journal of the American College of Cardiology 1990;16:207-22.

[90] Mocatta TJ, Pilbrow AP, Cameron VA, Senthilmohan R, Frampton CM, Richards AM, et al. Plasma concentrations of myeloperoxidase predict mortality after myocardial infarction. Journal of the American College of Cardiology 2007;49:1993-2000.

[91] Richter J, Ng-Sikorski J, Olsson I, Andersson T. Tumor necrosis factor-induced degranulation in adherent human neutrophils is dependent on CD11b/CD18-integrin-triggered oscillations of cytosolic free Ca2+. Proceedings of the National Academy of Sciences 1990;87:9472.

[92] Reimer KA, Murry CE, Richard VJ. The role of neutrophils and free radicals in the ischemic-reperfused heart: why the confusion and controversy? Journal of Molecular and Cellular Cardiology 1989;21:1225.

[93] Dreyer W, Michael L, West M, Smith C, Rothlein R, Rossen R, et al. Neutrophil accumulation in ischemic canine myocardium. Insights into time course, distribution, and mechanism of localization during early reperfusion. Circulation 1991;84:400.

[94] Zhao ZQ, Velez DA, Wang NP, Hewan-Lowe KO, Nakamura M, Guyton RA, et al. Progressively developed myocardial apoptotic cell death during late phase of reperfusion. Apoptosis 2001;6:279-90.

[95] Sheridan FM, Cole PG, Ramage D. Leukocyte adhesion to the coronary microvasculature during ischemia and reperfusion in an in vivo canine model. Circulation 1996;93:1784.

[96] Murohara T, Buerke M, Lefer AM. Polymorphonuclear leukocyte-induced vasocontraction and endothelial dysfunction. Role of selectins. Arteriosclerosis, Thrombosis, and Vascular Biology 1994;14:1509.

[97] Engler R, Schmid-Schönbein G, Pavelec R. Leukocyte capillary plugging in myocardial ischemia and reperfusion in the dog. The American Journal of Pathology 1983;111:98.

[98] Litt MR, Jeremy RW, Weisman HF, Winkelstein JA, Becker LC. Neutrophil depletion limited to reperfusion reduces myocardial infarct size after 90

minutes of ischemia. Evidence for neutrophil-mediated reperfusion injury. Circulation 1989;80:1816.

[99] Ohta K, Nakajima T, Cheah AYL, Zaidi SHE, Kaviani N, Dawood F, et al. Elafin-overexpressing mice have improved cardiac function after myocardial infarction. American Journal of Physiology-Heart and Circulatory Physiology 2004;287:H286.

[100] Crinnion J, Homer-Vanniasinkam S, Hatton R, Parkin S, Gough M. Role of neutrophil depletion and elastase inhibition in modifying skeletal muscle reperfusion injury. Cardiovascular Surgery (London, England) 1994;2:749.

[101] Hattori R, Hamilton K, Fugate R, McEver R, Sims P. Stimulated secretion of endothelial von Willebrand factor is accompanied by rapid redistribution to the cell surface of the intracellular granule membrane protein GMP-140. Journal of Biological Chemistry 1989;264:7768.

[102] Dollery CM, Owen CA, Sukhova GK, Krettek A, Shapiro SD, Libby P. Neutrophil elastase in human atherosclerotic plaques: production by macrophages. Circulation 2003;107:2829.

[103] Naruko T, Ueda M, Haze K, van der Wal AC, van der Loos CM, Itoh A, et al. Neutrophil infiltration of culprit lesions in acute coronary syndromes. Circulation 2002;106:2894.

[104] Baldus S, Heeschen C, Meinertz T, Zeiher AM, Eiserich JP, Munzel T, et al. Myeloperoxidase serum levels predict risk in patients with acute coronary syndromes. Circulation 2003;108:1440.

[105] Daugherty A, Dunn JL, Rateri DL, Heinecke JW. Myeloperoxidase, a catalyst for lipoprotein oxidation, is expressed in human atherosclerotic lesions. Journal of Clinical Investigation 1994;94:437.

[106] Zaidi SHE, You XM, Ciura S, O'Blenes S, Husain M, Rabinovitch M. Suppressed smooth muscle proliferation and inflammatory cell invasion after arterial injury in elafin-overexpressing mice. Journal of Clinical Investigation 2000;105:1687-730.

[107] Barolet AW, Nili N, Cheema A, Robinson R, Natarajan MK, O'Blenes S, et al. Arterial elastase activity after balloon angioplasty and effects of elafin, an elastase inhibitor. Arteriosclerosis, Thrombosis, and Vascular Biology 2001;21:1269.

[108] Okamoto E, Couse T, De Leon H, Vinten-Johansen J, Goodman RB, Scott NA, et al. Perivascular inflammation after balloon angioplasty of porcine coronary arteries. Circulation 2001;104:2228-35.

[109] Jones PL, Cowan KN, Rabinovitch M. Tenascin-C, proliferation and subendothelial fibronectin in progressive pulmonary vascular disease. The American journal of pathology 1997;150:1349.

[110] O'Blenes SB, Zaidi SH, Cheah AY, McIntyre B, Kaneda Y, Rabinovitch M. Gene transfer of the serine elastase inhibitor elafin protects against vein graft degeneration. Circulation 2000;102:III289-95.

[111] Zaidi SHE, You XM, Ciura S, Husain M, Rabinovitch M. Overexpression of the serine elastase inhibitor elafin protects transgenic mice from hypoxic pulmonary hypertension. Circulation 2002;105:516-21.

[112] Zaidi SH, Hui CC, Cheah AY, You XM, Husain M, Rabinovitch M. Targeted overexpression of elafin protects mice against cardiac dysfunction and mortality following viral myocarditis. J Clin Invest 1999;103:1211-9.

[113] Bolli R, Becker L, Gross G, Mentzer Jr R, Balshaw D, Lathrop DA. Myocardial protection at a crossroads: the need for translation into clinical therapy. Circulation Research 2004;95:125.

[114] http://www.clinicaltrialsregister.eu/ctr-search/ Search for 2010-019527-58. Accessed 26/10/2011.

Appendix B: USPIO REVIEW PAPER

Journal: Journal of Cardiovascular Magnetic Resonance

DOI: 10.1186/s12968-015-0183-4

Published: 18th September 2015

Vascular and Plaque Imaging with Ultrasmall Superparamagnetic Particles of Iron Oxide

Shirjel R Alam MD,[1,2] Colin Stirrat MD,[1,2] Jennifer Richards MD,[1] Saeed Mirsadraee MD PhD,[3,4] Scott I K Semple PhD,[3] George Tse MD,[5] *Peter Henriksen MD PhD,[1,2] *David E Newby MD PhD [1,2]

[1]Centre of Cardiovascular Science, University of Edinburgh
[2]Department of Cardiology, Royal Infirmary of Edinburgh
[3]Clinical Research Imaging Centre, University of Edinburgh
[4]Department of Radiology, Royal Infirmary of Edinburgh
[5]MRC Centre for Inflammation Research, The University of Edinburgh, Edinburgh

*Equal contribution

Corresponding Author

Shirjel R Alam MB ChB MRCP(Ed), MRCS(Ed), MRCA
Centre for Cardiovascular Science,
The University of Edinburgh,
The Chancellor's Building,
Little France Crescent,
Edinburgh EH16 5SA

Support: Dr Shirjel Alam was supported by a Scholarship grant from the British Heart Foundation.

KEY WORDS: USPIO, Nanoparticles, MRI, Cardiovascular Imaging, inflammation, macrophage.

Abstract

Magnetic Resonance Imaging (MRI) has become a primary tool for non-invasive assessment of cardiovascular anatomy, pathology and function. Existing contrast agents have been utilised for the identification of infarction, fibrosis, perfusion deficits and for angiography. Novel USPIO contrast agents that are taken up by inflammatory cells can detect cellular inflammation non-invasively using MRI, potentially aiding the diagnosis of inflammatory medical conditions, guiding their treatment and giving insight into their pathophysiology. In this review we describe the utilization of ultrasmall superparamagnetic particles of iron oxide as a novel contrast agent in vascular disease.

Introduction

Inflammation is central to many cardiovascular pathophysiological processes including atherosclerosis, myocardial infarction and heart failure. Macrophages are key mediators of these inflammatory pathways, initiating both destructive and reparative processes (Nahrendorf et al., 2010). Quantification and characterization of tissue macrophage activity may therefore assist in our understanding of the pathogenesis of cardiovascular disease and help determine disease severity and prognosis, as well as providing a biomarker to assess the efficacy of established or novel therapeutic interventions.

Magnetic resonance imaging (MRI) is a well-established clinical imaging modality offering excellent soft tissue contrast and spatial resolution, whilst avoiding ionizing radiation. Standard gadolinium-based contrast agents are paramagnetic and are infused into the blood pool with variable organ extraction rates, although subsequent extravasation and redistribution can be used to identify the interstitial and extracellular spaces. Gadolinium is commonly used as an MRI contrast agent after acute myocardial infarction (MI) to identify areas of tissue infarction and fibrosis (Lima et al., 1995, Schelbert et al., 2010). Tissue oedema and rupture of cell membranes with consequent diffusion of gadolinium into the inter- and intra-cellular spaces (Lima et al., 1995) results in a “delayed gadolinium enhancement” effect in infarcted regions. Recent interest has turned to novel agents that provide additional structural and functional cellular information. Such ‘smart’ contrast agents include iron oxide nanoparticles.

Iron Oxide Nano-Particles

Particles of iron oxide are divided into classes based on their size (Table 1). In this review, we will focus on ultrasmall superparamagnetic particles of iron oxide (USPIOs) that consist of nanoparticles with a diameter of <50 nm and include ferumoxtran-10 (Sinerem, Guerbet) and ferumoxytol (Rienso, Takeda; Feraheme, AMAG Pharmaceuticals). Although Rienso had been authorised for use in European Union, Takeda since has withdrawn it. However Feraheme is clinically available in the United States for the treatment of iron deficiency anemia in adult patients with chronic kidney disease (CKD).

Ferumoxytol is well tolerated by patients with chronic kidney disease and iron deficiency anaemia, and had a similar overall treatment-related adverse event rate to oral iron (Spinowitz et al., 2008). This safety data is further supported by additional retrospective observational data from three large haemodialysis clinics in the United States involving more than 8,600 patients and more than 33,300 administered doses of ferumoxytol (Schiller et al., 2011, Sharma et al., 2011). The only contraindications to use are known hypersensitivity or iron overload. Therefore there is little to limit widespread clinical use as an imaging agent.

USPIOs can be used as a blood pool contrast agent but it is their ability to be taken up by inflammatory cells that has distinguished them (Christen et al., 2013). Cellular uptake of USPIOs occurs through a variety of mechanisms. Phagocytosis and receptor-mediated endocytosis are important for uptake of larger particles, whilst smaller particles are internalized by pinocytosis. Although the avidity of macrophage

uptake is strongly influenced by particle size and charge, the surface coating is particularly important (Saito et al., 2012, Tsuchiya et al., 2013). As a result of their smaller size, USPIOs are less readily recognized by phagocytic cells and persist in the circulation for longer than other iron particles (plasma half-life 14-30 h in humans) (Landry et al., 2005, Hunt et al., 2005). They are capable of passing through capillary walls, to be taken up by tissue-resident macrophages and neutrophils (Figure 1) (Ruehm et al., 2001b, Dousset et al., 1999, Gellissen et al., 1999a). These characteristics allow USPIOs to detect and highlight cellular inflammation within tissues using MRI.

Imaging Methodology

USPIOs induce local magnetic field inhomogeneities that shorten T2 and T2* relaxations times resulting in a signal deficit on magnetic resonance images. USPIOs also have a T1 shortening effect, particularly at low concentrations, and appear bright on T1 weighted images. The T1 shortening effect mainly depends on the strength of the magnetic field, and is higher in lower field strength.

A range of approaches have been used to evaluate USPIO accumulation in tissues. Most simply, images may be qualitatively assessed for signal deficits. However this approach is subjective, and signal deficits due to calcification or other artefacts may be misinterpreted. Manually drawn regions of interest have been used to allow comparison of signal intensity of the target tissue with that of control tissue although discrete focal areas of USPIO accumulation, and thus focal inflammation, may be missed.

Tissue properties, such as the presence of oedema or haemorrhage, can alter image

intensities on T2* sequences, and so pre- and post-contrast images need to be compared to delineate the impact of USPIO accumulation. This requires accurate co-registration of these paired scans and adjustments for differences in baseline intensity. A specific region of interest (ROI) map can be drawn and subsequently transferred to each subsequent co-registered image, thus ensuring the signal intensity can be compared for identical sample regions in different scans from the same patient.

Rather than assessing focal image brightness at a single echo time, the T2* time constant can be calculated from the exponential decay curve using multiple echo times (Figure 2). This method provides greater reproducibility, broad applicability throughout the field of view, and independence from T1 effects and a range of imaging variables. In the presence of USPIO, the T2* relaxation rate is increased thus giving a lower T2* value, or higher R2* value (R2* is the inverse of T2*, R2* = 1/T2*). Calculation of these values permits the generation of T2* or R2* maps indicative of USPIO accumulation (Figure 3).

Various authors have used different techniques to calculate USPIO uptake in tissues, and have reported results using T2, T2* or R2*. This can cause confusion since higher values infer diminished USPIO uptake in T2/T2* weighted images, but higher uptake in R2* maps. For the purposes of this paper, imaging techniques will be described but results reported in terms of "increased USPIO uptake." In order to account for native R2* values, various authors have used the delta increase in R2* value from successive scans, or factor increase. When pre-USPIO scans have not been performed, it must be assumed that non-inflamed tissue has similar R2* values

to pre-USPIO native R2* values.

Finally, it must be noted that USPIO imaging can be affected by artefact. USPIO also shorten T1, and so cause signal enhancement of T1 weighted imaging (Small et al., 1993). However, at high concentration USPIO can cause signal loss with such imaging limiting its use with T1 weighted sequences (Fananapazir et al., 2014). The superparamagnetic nature of the particles means that they generate strong local magnetic field inhomogeneities, and it is this magnetic susceptibility that is being imaged by MRI. However this can cause loss of distinction of anatomical borders and distort normal tissues ("blooming artefact"). USPIO will accumulate in the reticulo-endothelial system including the liver and spleen. This accumulation can affect neighbouring structures, and care must be taken not mistake blooming artefact for USPIO uptake.

Cardiovascular Applications

Atherosclerotic Plaque

Given the central role of macrophage biology in the pathogenesis of atherosclerosis, USPIOs have an obvious application in the investigation of atherosclerotic disease. In pre-clinical studies, uptake of USPIOs is demonstrable within numerous atherosclerotic models including aortic plaques of hyperlipidemic rabbits (Schmitz et al., 2000, Schmitz et al., 2002) and mice (Sigovan et al., 2010) as well as the neointimal hyperplasia following balloon injury (Ruehm et al., 2001b, Hyafil et al., 2006), and is proportional to plaque macrophage content.

Modulation of inflammation within atherosclerotic plaques can be assessed by USPIO imaging (Morris et al., 2008). P38 Mitogen-activated protein kinase (MAPK) is an inflammatory signalling pathway activated by angiotensin II in various vascular cell types (Herlaar and Brown, 1999, Ju et al., 2002). Angiotensin II infusion leads to macrophage accumulation and UPSIO uptake in atherosclerotic plaques of mice (Morris et al., 2008, Brasier et al., 2002) that can be inhibited by co-administration of a p38 MAPK pathway inhibitor. Interestingly, this effect was predominantly manifested by a reduction in USPIO uptake by macrophages rather than a reduction in macrophage numbers, suggesting an effect on macrophage activity rather than recruitment. In contrast, the angiotensin II type 1 receptor antagonist, irbesartan, decreased both USPIO uptake and macrophage content in the apolipoprotein E deficient mouse model (Sigovan et al., 2012).

USPIO uptake occurs in human carotid atherosclerotic plaques and appears to correlate with the number of iron-laden macrophages on histology (Trivedi et al., 2006a). Consistent with the inflammatory cell infiltrate associated with vulnerable plaques, 75% of ruptured or rupture-prone lesions show USPIO uptake compared to only 7% of apparently stable lesions. Determining the overall macrophage burden is challenging because of a number of factors. There is a curvilinear relationship between area of signal intensity reduction and USPIO concentration. Signal intensity is also dependent on density of particle accumulation, and a heterogeneous population of macrophages would be expected to have differing degrees of USPIO uptake. The amount of USPIO infused, and by extrapolation perfusion of target tissue, will also determine the magnitude of MRI changes (Lutz et al., 2005).

USPIO uptake and inflammation does not correlate with plaque volume or the degree of luminal stenosis (Tang et al., 2008b), and as already stated USPIO maybe useful in investigating USPIO activity in contrast to concentration (Brasier et al., 2002). This raises the possibility of using USPIO uptake to monitor disease activity in carotid stenosis rather than using conventional anatomical measurements. For instance, statins reduce inflammation within atherosclerotic plaques as well as systemic markers of inflammation (Ridker et al., 2001, Tahara et al., 2006) and this has been assessed using USPIO uptake. The ATHEROMA study (Atorvastatin THerapy: Effects on Reduction Of Macrophage Activity) compared the effect of high-dose (80 mg daily) versus low-dose (10 mg daily) atorvastatin on plaque inflammation (Tang et al., 2009). Patients underwent UPSIO-enhanced MRI at baseline, 6 weeks and 12 weeks of therapy. Although there were no differences in USPIO uptake over the course of the study in the low-dose group, there was a reduction in USPIO uptake in the high-dose group at both 6 and 12 weeks. This correlated with a reduction in LDL cholesterol and a reduction in micro-emboli count on trans-cranial Doppler (Patterson et al., 2011).

Abdominal Aortic Aneurysms

Macrophages are intimately involved in the development, expansion and ultimately rupture of abdominal aortic aneurysms. Preliminary evidence of USPIO uptake in human abdominal aortic aneurysms (AAA) has been described (Sadat et al., 2011, Howarth et al., 2007). In a pilot study, we demonstrated that just under half of patients with AAA had focal mural uptake of USPIOs. The aneurysm expansion rate was three-fold higher in patients with USPIO uptake in the aneurysm wall (0.66

versus 0.22 cm/year) (Richards et al., 2011a). Histology of tissue excised at the time of elective surgical repair confirmed co-localization of USPIOs with CD68 immunostaining for macrophages. Thus USPIO-enhanced MRI appears to identify those patients with more rapid disease progression requiring earlier preventative surgical or endovascular intervention to prevent rupture.

Cerebrovascular Disease

Stroke results from an acute disruption to the cerebral blood supply leading to tissue ischemia and eventually necrosis. Inflammatory cells are recruited to the infarct zone, but may extend the injury by interacting with "at risk" cells in the penumbra of the infarct (Braun et al., 1996, del Zoppo et al., 2000). In a murine model of middle cerebral artery occlusion, USPIO uptake is detected in this penumbra region of infarction (Rausch et al., 2001a, Wiart et al., 2007). By 7 days the USPIO is confined to the infarct itself, and histology confirms a large population of iron-containing macrophages in the infarcted tissue consistent with migration of macrophages from the penumbra. Further work has indicated that in the setting of established stroke, USPIO leaks through the injured blood-brain barrier accounting for the initial accumulation at the periphery of the infarct and intravascular trapping rather than macrophage uptake (Desestret et al., 2009). In addition there is widespread uptake resulting from leakage of USPIO into the cerebro-spinal fluid with delivery of nanoparticals to more remote areas. Thus the application of USPIO in such settings is limited although it is possible to track focal USPIO uptake associated with macrophage/microglial infiltration 6 days after cerebral ischaemia, identifying a subacute pathological process (Yang et al., 2014, Yang et al., 2013).

Clinical studies have utilized ferumoxtran-10 in patients 4-5 days after stroke, with imaging at 24-36 hours and repeated 48-72 hours later (Saleh et al., 2004). T1- and T2/T2*-weighted imaging reveals parenchymal enhancement that increases between the 2 scans, corresponding to the expected macrophage distribution. These USPIO induced changes do not correspond to conventional gadolinium-enhanced changes, suggesting they occurred independently of blood-brain-barrier breakdown. It could be speculated that these changes may have been due to differences in blood pooling effects due to perfusion changes rather than USPIO inflammatory cell uptake. It would be expected that ischemic volume would correlate with inflammatory burden and MRI changes if USPIOs were being taken up by inflammatory cells. Nighoghossian et al found no such correlation six days after stroke (Nighoghossian et al., 2007) although the study had a number of limitations including imperfect timing of the scans and the completion of only 5 patients using the more sensitive T2* imaging protocol.

Despite these limitations, a pre-clinical model of the investigation of anti-inflammatory medication in the treatment of stroke has major potential (Marinescu et al., 2013). Using a murine model, the anti-inflammatory agent minocycline can be evaluated after middle cerebral artery occlusion (Marinescu et al., 2013). Minocycline treatment reduced USPIO uptake within the infarct, and was associated with reductions in infarct size, blood-brain barrier permeability and microglia/macrophage counts.

Future Applications

The application of USPIOs to study myocardial inflammation has translational application where the pathology involves substantial monocyte influx into the plaque or tissue (Alam et al., 2012c) (Table 2).

Targeted Iron Oxide Particles

Conjugating iron oxide particles with antibodies allows targeted imaging. Pre-clinical imaging to date has employed 9.4 Tesla MRI. This would be more sensitive in detecting USPIO than clinical MRI systems (1.5 or 3-tesla). In addition, injected unconjugated USPIOs injected directly into the blood stream concentrate within macrophages resulting in high local distribution. It remains to be seen if antibody-labelled USPIOs will be sufficiently concentrated at their target site to allow detection in clinical MRI systems. Specific subsets of monocytes or other cell types could be tracked with successful application of this method. This would allow delineation of the temporal dynamics of cellular and immunological processes by repeated scanning. This has been demonstrated in a pre-clinical model of cerebral ischaemia using USPIOs grafted with a specific peptide targeting vascular cellular adhesion molecule-1 (VCAM-1) . This study indicated the potential of VCAM-1 to assess vascular injury.

E-selectin is an adhesion molecule between the endothelium and leukocytes that plays a critical role in the pathogenesis of inflammation (Kansas, 1996). An E-selectin monoclonal antibody-USPIO conjugate has been used to track vascular inflammation in a murine model of contact hypersensitivity (Reynolds et al., 2006).

More recently, USPIOs have been conjugated with a scavenger receptor to identify inflammation in atherosclerotic plaques (Segers et al., 2013).

Another potential confounding factor is that macrophages of different subsets or with different activation status take up USPIO at different rates. This could result in false positive or negative MRI enhancement. Direct labeling of cells with USPIO would avoid this error but published data are limited. Although directly labeling of macrophages with USPIO and delivery through the carotid artery has been successful in producing T2* hypo-enhancement after transient ischaemia, it is associated with increased mortality in a rat model (Riou et al., 2013).

USPIO cell labelling and monitoring cell trafficking

The ability to track cells non-invasively *in vivo* would be a valuable technique with a number of potential applications that include inflammatory cell tracking and evaluation of engraftment of cells administered as part of cell-based therapies.

USPIOs can be used to label cells *in vitro* for subsequent *in vivo* tracking. Smooth muscle cells labelled with iron nanoparticles can be imaged when directly injected into either healthy or infarcted myocardium in a pre-clinical model (Riviere et al., 2005). This technique can be utilized to label human aortic smooth muscle cells incorporated into tissue engineered vascular grafts and implanted into mice (Nelson et al., 2008). We have also demonstrated that cell tracking can be achieved in vivo in humans using similar approaches with the larger SPIOs (Richards et al., 2012b)

Summary

USPIOs are taken up by macrophages, and can be identified *in vivo* by MRI scanning. T2 and T2*-weighted scanning provide a sensitive method of assessing USPIO accumulation.

USPIO-enhanced magnetic resonance imaging is a promising method for assessing inflammatory processes associated with a range of cardiovascular diseases including those affecting the atherosclerotic plaque and large arteries. Potential clinical applications are under evaluation and include assessing the effects of novel pharmacological agents and *in vivo* cell tracking to determine the fate of cells administered as part of cell therapy.

ABBREVIATIONS

CABG	-	Coronary Artery Bypass Grafting
FDG-PET	-	Fluorodeoxyglucose-Positron Emission Tomography
MAPK	-	Mitogen-activated protein kinase
MCP-1	-	Monocyte Chemotactic Protein-1
MI	-	Myocardial Infarction
MRI	-	Magnetic Resonance Imaging
RAS	-	Renin-Angiotensin System
ROI	-	Region of Interest
SPIO	-	Super-paramagnetic Iron Oxide
TNF-α	-	Tumour Necrosis Factor Alpha
USPIO	-	Ultrasmall Super-paramagnetic Iron Oxide
VCAM-1	-	Vascular cell adhesion molecule 1

Acknowledgements

The authors are supported by grants from the British Heart Foundation (RE/08/001 and FS/12/83), Medical Research Council (G1001339), National Institute for Health Research (EME 11/20/03), Chest Heart and Stroke Scotland (R11/A135) and Chief Scientist Office (ETM/266). DEN is supported by the British Heart Foundation (CH/09/002). PAH is supported by NHS Research Scotland Fellowship.

Conflict of Interest Disclosures

None.

Contributions

SA conceived and wrote the review paper. GT provided figure 1, SS provided figure 2. CA, JR, SM,PH and DN reviewed and edited the paper. All authors read and approved the manuscript.

References

1. Nahrendorf M, Pittet MJ, Swirski FK. Monocytes: protagonists of infarct inflammation and repair after myocardial infarction. Circulation. 2010; **121**(22): 2437.

2. Lima JA, Judd RM, Bazille A, Schulman SP, Atalar E, Zerhouni EA. Regional heterogeneity of human myocardial infarcts demonstrated by contrast-enhanced MRI. Potential mechanisms. Circulation. 1995; **92**(5): 1117-25.

3. Schelbert EB, Hsu LY, Anderson SA, Mohanty BD, Karim SM, Kellman P, et al. Late gadolinium-enhancement cardiac magnetic resonance identifies postinfarction myocardial fibrosis and the border zone at the near cellular level in ex vivo rat heart. Circ Cardiovasc Imaging. 2010; **3**(6): 743-52.

4. Spinowitz BS, Kausz AT, Baptista J, Noble SD, Sothinathan R, Bernardo MV, et al. Ferumoxytol for treating iron deficiency anemia in CKD. J Am Soc Nephrol. 2008; **19**(8): 1599-605.

5. Schiller B, Bhat P, Sharma A, Li Z, Fortin G, McLaughlin J, et al. Safety of Feraheme¬Æ(Ferumoxytol) in hemodialysis patients at 3 dialysis chains over a 1-year period. J Am Soc Nephrol. 2011; **22**: 477A-8A.

6. Sharma A, Bhat P, Schiller B, Fortin G, McLaughlin J, Li Z, et al. Efficacy of Feraheme¬Æ(Ferumoxytol) administration on target hemoglobin levels and other iron parameters across 3 dialysis chains. J Am Soc Nephrol. 2011; **22**: 485A.

7. Christen T, Ni W, Qiu D, Schmiedeskamp H, Bammer R, Moseley M, et al. High-resolution cerebral blood volume imaging in humans using the blood pool contrast agent ferumoxytol. Magnetic Resonance in Medicine. 2013; **70**(3): 705-10.

8. Saito S, Tsugeno M, Koto D, Mori Y, Yoshioka Y, Nohara S, et al. Impact of surface coating and particle size on the uptake of small and ultrasmall superparamagnetic iron oxide nanoparticles by macrophages. Int J Nanomedicine. 2012; **7**: 5415-21.

9. Tsuchiya K, Nitta N, Sonoda A, Otani H, Takahashi M, Murata K, et al. Atherosclerotic imaging using 4 types of superparamagnetic iron oxides: new possibilities for mannan-coated particles. Eur J Radiol. 2013; **82**(11): 1919-25.

10. Landry R, Jacobs PM, Davis R, Shenouda M, Bolton WK. Pharmacokinetic study of ferumoxytol: a new iron replacement therapy in normal subjects and hemodialysis patients. Am J Nephrol. 2005; **25**(4): 400-10.

11. Hunt MA, Bago AG, Neuwelt EA. Single-dose contrast agent for intraoperative MR imaging of intrinsic brain tumors by using ferumoxtran-10. AJNR Am J Neuroradiol. 2005; **26**(5): 1084-8.

12. Ruehm SG, Corot C, Vogt P, Kolb S, Debatin JF. Magnetic resonance imaging of atherosclerotic plaque with ultrasmall superparamagnetic particles of iron oxide in hyperlipidemic rabbits. Circulation. 2001; **103**(3): 415-22.

13. Dousset V, Delalande C, Ballarino L, Quesson B, Seilhan D, Coussemacq M, et al. In vivo macrophage activity imaging in the central nervous system detected by magnetic resonance. Magnetic resonance in medicine. 1999; **41**(2): 329-33.

14. Gellissen J, Axmann C, Prescher A, Bohndorf K, Lodemann KP. Extra- and intracellular accumulation of ultrasmall superparamagnetic iron oxides (USPIO) in experimentally induced abscesses of the peripheral soft tissues and their effects on magnetic resonance imaging. Magn Reson Imaging. 1999; **17**(4): 557-67.

15. Small WC, Nelson RC, Bernardino ME. Dual contrast enhancement of both T1- and T2-weighted sequences using ultrasmall superparamagnetic iron oxide. Magn Reson Imaging. 1993; **11**(5): 645-54.

16. Fananapazir G, Marin D, Suhocki PV, Kim CY, Bashir MR. Vascular artifact mimicking thrombosis on MR imaging using ferumoxytol as a contrast agent in abdominal vascular assessment. J Vasc Interv Radiol. 2014; **25**(6): 969-76.

17. Schmitz SA, Coupland SE, Gust R, Winterhalter S, Wagner S, Kresse M, et al. Superparamagnetic iron oxide-enhanced MRI of atherosclerotic plaques in Watanabe hereditable hyperlipidemic rabbits. Invest Radiol. 2000; **35**(8): 460-71.

18. Schmitz SA, Taupitz M, Wagner S, Coupland SE, Gust R, Nikolova A, et al. Iron-oxide-enhanced magnetic resonance imaging of atherosclerotic plaques: postmortem analysis of accuracy, inter-observer agreement, and pitfalls. Invest Radiol. 2002; **37**(7): 405-11.

19. Sigovan M, Bessaad A, Alsaid H, Lancelot E, Corot C, Neyran B, et al. Assessment of age modulated vascular inflammation in ApoE-/- mice by USPIO-enhanced magnetic resonance imaging. Invest Radiol. 2010; **45**(11): 702-7.

20. Hyafil F, Laissy JP, Mazighi M, Tchetche D, Louedec L, Adle-Biassette H, et al. Ferumoxtran-10-enhanced MRI of the hypercholesterolemic rabbit aorta:

relationship between signal loss and macrophage infiltration. Arterioscler Thromb Vasc Biol. 2006; **26**(1): 176-81.

21. Morris JB, Olzinski AR, Bernard RE, Aravindhan K, Mirabile RC, Boyce R, et al. p38 MAPK inhibition reduces aortic ultrasmall superparamagnetic iron oxide uptake in a mouse model of atherosclerosis: MRI assessment. Arterioscler Thromb Vasc Biol. 2008; **28**(2): 265-71.

22. Herlaar E, Brown Z. p38 MAPK signalling cascades in inflammatory disease. Mol Med Today. 1999; **5**(10): 439-47.

23. Ju H, Nerurkar S, Sauermelch CF, Olzinski AR, Mirabile R, Zimmerman D, et al. Sustained activation of p38 mitogen-activated protein kinase contributes to the vascular response to injury. J Pharmacol Exp Ther. 2002; **301**(1): 15-20.

24. Brasier AR, Recinos A, 3rd, Eledrisi MS. Vascular inflammation and the renin-angiotensin system. Arterioscler Thromb Vasc Biol. 2002; **22**(8): 1257-66.

25. Sigovan M, Kaye E, Lancelot E, Corot C, Provost N, Majd Z, et al. Anti-Inflammatory Drug Evaluation in ApoE-/- Mice by Ultrasmall Superparamagnetic Iron Oxide-Enhanced Magnetic Resonance Imaging. Invest Radiol. 2012; **47**(9): 546-52.

26. Trivedi RA, Mallawarachi C, JM UK-I, Graves MJ, Horsley J, Goddard MJ, et al. Identifying inflamed carotid plaques using in vivo USPIO-enhanced MR imaging to label plaque macrophages. Arterioscler Thromb Vasc Biol. 2006; **26**(7): 1601-6.

27. Lutz AM, Weishaupt D, Persohn E, Goepfert K, Froehlich J, Sasse B, et al. Imaging of macrophages in soft-tissue infection in rats: relationship between ultrasmall superparamagnetic iron oxide dose and MR signal characteristics. Radiology. 2005; **234**(3): 765-75.

28. Tang TY, Howarth SP, Miller SR, Graves MJ, JM UK-I, Li ZY, et al. Correlation of carotid atheromatous plaque inflammation using USPIO-enhanced MR imaging with degree of luminal stenosis. Stroke. 2008; **39**(7): 2144-7.

29. Ridker PM, Rifai N, Clearfield M, Downs JR, Weis SE, Miles JS, et al. Measurement of C-reactive protein for the targeting of statin therapy in the primary prevention of acute coronary events. N Engl J Med. 2001; **344**(26): 1959-65.

30. Tahara N, Kai H, Ishibashi M, Nakaura H, Kaida H, Baba K, et al. Simvastatin attenuates plaque inflammation: evaluation by fluorodeoxyglucose positron emission tomography. J Am Coll Cardiol. 2006; **48**(9): 1825-31.

31. Tang TY, Howarth SP, Miller SR, Graves MJ, Patterson AJ, JM UK-I, et al. The ATHEROMA (Atorvastatin Therapy: Effects on Reduction of Macrophage Activity) Study. Evaluation using ultrasmall superparamagnetic iron oxide-enhanced magnetic resonance imaging in carotid disease. J Am Coll Cardiol. 2009; **53**(22): 2039-50.

32. Patterson AJ, Tang TY, Graves MJ, Muller KH, Gillard JH. In vivo carotid plaque MRI using quantitative T2* measurements with ultrasmall superparamagnetic iron oxide particles: a dose-response study to statin therapy. NMR Biomed. 2011; **24**(1): 89-95.

33. Sadat U, Taviani V, Patterson AJ, Young VE, Graves MJ, Teng Z, et al. Ultrasmall superparamagnetic iron oxide-enhanced magnetic resonance imaging of abdominal aortic aneurysms--a feasibility study. Eur J Vasc Endovasc Surg. 2011; **41**(2): 167-74.

34. Howarth SP, Tang TY, Graves MJ, JM UK-I, Li ZY, Walsh SR, et al. Non-invasive MR imaging of inflammation in a patient with both asymptomatic carotid atheroma and an abdominal aortic aneurysm: a case report. Ann Surg Innov Res. 2007; **1**: 4.

35. Richards JM, Semple SI, MacGillivray TJ, Gray C, Langrish JP, Williams M, et al. Abdominal aortic aneurysm growth predicted by uptake of ultrasmall superparamagnetic particles of iron oxide: a pilot study. Circ Cardiovasc Imaging. 2011; **4**(3): 274-81.

36. Braun JS, Jander S, Schroeter M, Witte OW, Stoll G. Spatiotemporal relationship of apoptotic cell death to lymphomonocytic infiltration in photochemically induced focal ischemia of the rat cerebral cortex. Acta Neuropathol. 1996; **92**(3): 255-63.

37. del Zoppo G, Ginis I, Hallenbeck JM, Iadecola C, Wang X, Feuerstein GZ. Inflammation and stroke: putative role for cytokines, adhesion molecules and iNOS in brain response to ischemia. Brain Pathol. 2000; **10**(1): 95-112.

38. Rausch M, Sauter A, Frohlich J, Neubacher U, Radu EW, Rudin M. Dynamic patterns of USPIO enhancement can be observed in macrophages after ischemic brain damage. Magn Reson Med. 2001; **46**(5): 1018-22.

39. Wiart M, Davoust N, Pialat JB, Desestret V, Moucharrafie S, Cho TH, et al. MRI monitoring of neuroinflammation in mouse focal ischemia. Stroke. 2007; **38**(1): 131-7.

40. Desestret V, Brisset JC, Moucharrafie S, Devillard E, Nataf S, Honnorat J, et al. Early-stage investigations of ultrasmall superparamagnetic iron oxide-induced signal change after permanent middle cerebral artery occlusion in mice. Stroke. 2009; **40**(5): 1834-41.

41. Yang YM, Feng X, Yin le K, Li CC, Jia J, Du ZG. Comparison of USPIO-enhanced MRI and Gd-DTPA enhancement during the subacute stage of focal cerebral ischemia in rats. Acta radiologica. 2014; **55**(7): 864-73.

42. Yang YM, Feng XY, Yin le K, Li CC, Li AN, Jia J, et al. In vivo USPIO-enhanced MR signal characteristics of secondary degeneration in the ipsilateral substantia nigra after middle cerebral artery occlusion at 3T. J Neuroradiol. 2013; **40**(3): 198-203.

43. Saleh A, Schroeter M, Jonkmanns C, Hartung HP, Modder U, Jander S. In vivo MRI of brain inflammation in human ischaemic stroke. Brain. 2004; **127**(Pt 7): 1670-7.

44. Nighoghossian N, Wiart M, Cakmak S, Berthezene Y, Derex L, Cho TH, et al. Inflammatory response after ischemic stroke: a USPIO-enhanced MRI study in patients. Stroke. 2007; **38**(2): 303-7.

45. Marinescu M, Chauveau F, Durand A, Riou A, Cho TH, Dencausse A, et al. Monitoring therapeutic effects in experimental stroke by serial USPIO-enhanced MRI. European Radiology. 2013; **23**(1): 37-47.

46. Alam SR, Shah AS, Richards J, Lang NN, Barnes G, Joshi N, et al. Ultrasmall superparamagnetic particles of iron oxide in patients with acute myocardial infarction: early clinical experience. Circ Cardiovasc Imaging. 2012; **5**(5): 559-65.

47. Kansas GS. Selectins and their ligands: current concepts and controversies. Blood. 1996; **88**(9): 3259-87.

48. Reynolds PR, Larkman DJ, Haskard DO, Hajnal JV, Kennea NL, George AJ, et al. Detection of vascular expression of E-selectin in vivo with MR imaging. Radiology. 2006; **241**(2): 469-76.

49. Segers FM, den Adel B, Bot I, van der Graaf LM, van der Veer EP, Gonzalez W, et al. Scavenger receptor-AI-targeted iron oxide nanoparticles for in vivo MRI detection of atherosclerotic lesions. Arterioscler Thromb Vasc Biol. 2013; **33**(8): 1812-9.

50. Riou A, Chauveau F, Cho TH, Marinescu M, Nataf S, Nighoghossian N, et al. MRI assessment of the intra-carotid route for macrophage delivery after transient cerebral ischemia. NMR in biomedicine. 2013; **26**(2): 115-23.
51. Riviere C, Boudghene FP, Gazeau F, Roger J, Pons JN, Laissy JP, et al. Iron oxide nanoparticle-labeled rat smooth muscle cells: cardiac MR imaging for cell graft monitoring and quantitation. Radiology. 2005; **235**(3): 959-67.
52. Nelson GN, Roh JD, Mirensky TL, Wang Y, Yi T, Tellides G, et al. Initial evaluation of the use of USPIO cell labeling and noninvasive MR monitoring of human tissue-engineered vascular grafts in vivo. FASEB J. 2008; **22**(11): 3888-95.
53. Richards JM, Shaw CA, Lang NN, Williams MC, Semple SI, MacGillivray TJ, et al. In vivo mononuclear cell tracking using superparamagnetic particles of iron oxide: feasibility and safety in humans. Circ Cardiovasc Imaging. 2012; **5**(4): 509-17.
54. Shapiro EM, Skrtic S, Koretsky AP. Sizing it up: cellular MRI using micron-sized iron oxide particles. Magnetic Resonance in Medicine. 2005; **53**(2): 329-38.
55. McAteer MA, von Zur Muhlen C, Anthony DC, Sibson NR, Choudhury RP. Magnetic resonance imaging of brain inflammation using microparticles of iron oxide. Methods Mol Biol. 2011; **680**: 103-15.
56. Yang Y, Yanasak N, Schumacher A, Hu TC. Temporal and noninvasive monitoring of inflammatory-cell infiltration to myocardial infarction sites using micrometer-sized iron oxide particles. Magn Reson Med. 2010; **63**(1): 33-40.
57. Boutry S, Brunin S, Mahieu I, Laurent S, Vander Elst L, Muller RN. Magnetic labeling of non-phagocytic adherent cells with iron oxide nanoparticles: a comprehensive study. Contrast media & molecular imaging. 2008; **3**(6): 223-32.
58. Margolis DJ, Hoffman JM, Herfkens RJ, Jeffrey RB, Quon A, Gambhir SS. Molecular imaging techniques in body imaging. Radiology. 2007; **245**(2): 333-56.
59. Richards JM, Shaw CA, Lang NN, Williams MC, Semple SI, MacGillivray TJ, et al. In Vivo Mononuclear Cell Tracking Using Superparamagnetic Particles of Iron OxideClinical Perspective Feasibility and Safety in Humans. Circulation: Cardiovascular Imaging. 2012; **5**(4): 509-17.
60. Di Marco M, Sadun C, Port M, Guilbert I, Couvreur P, Dubernet C. Physicochemical characterization of ultrasmall superparamagnetic iron oxide particles (USPIO) for biomedical application as MRI contrast agents. International journal of nanomedicine. 2007; **2**(4): 609-22.

61. Taupitz M, Wagner S, Schnorr J, Kravec I, Pilgrimm H, Bergmann-Fritsch H, et al. Phase I clinical evaluation of citrate-coated monocrystalline very small superparamagnetic iron oxide particles as a new contrast medium for magnetic resonance imaging. Investigative Radiology. 2004; **39**(7): 394-405.
62. Schnorr J, Taupitz M, Schellenberger EA, Warmuth C, Fahlenkamp UL, Wagner S, et al. Cardiac magnetic resonance angiography using blood-pool contrast agents: comparison of citrate-coated very small superparamagnetic iron oxide particles with gadofosveset trisodium in pigs. Rofo. 2012; **184**(2): 105-12.
63. Wagner M, Wagner S, Schnorr J, Schellenberger E, Kivelitz D, Krug L, et al. Coronary MR angiography using citrate-coated very small superparamagnetic iron oxide particles as blood-pool contrast agent: initial experience in humans. J Magn Reson Imaging. 2011; **34**(4): 816-23.
64. Ludwig A, Poller WC, Westphal K, Minkwitz S, Lattig-Tunnemann G, Metzkow S, et al. Rapid binding of electrostatically stabilized iron oxide nanoparticles to THP-1 monocytic cells via interaction with glycosaminoglycans. Basic Res Cardiol. 2013; **108**(2): 328.
65. Herborn CU, Vogt FM, Lauenstein TC, Dirsch O, Corot C, Robert P, et al. Magnetic resonance imaging of experimental atherosclerotic plaque: comparison of two ultrasmall superparamagnetic particles of iron oxide. J Magn Reson Imaging. 2006; **24**(2): 388-93.
66. Kooi ME, Cappendijk VC, Cleutjens KB, Kessels AG, Kitslaar PJ, Borgers M, et al. Accumulation of ultrasmall superparamagnetic particles of iron oxide in human atherosclerotic plaques can be detected by in vivo magnetic resonance imaging. Circulation. 2003; **107**(19): 2453-8.
67. Tang TY, Howarth SP, Miller SR, Graves MJ, JM UK-I, Trivedi RA, et al. Comparison of the inflammatory burden of truly asymptomatic carotid atheroma with atherosclerotic plaques contralateral to symptomatic carotid stenosis: an ultra small superparamagnetic iron oxide enhanced magnetic resonance study. J Neurol Neurosurg Psychiatry. 2007; **78**(12): 1337-43.
68. Tang TY, Howarth SP, Miller SR, Graves MJ, JM UK-I, Li ZY, et al. Comparison of the inflammatory burden of truly asymptomatic carotid atheroma with atherosclerotic plaques in patients with asymptomatic carotid stenosis undergoing coronary artery bypass grafting: an ultrasmall superparamagnetic iron

oxide enhanced magnetic resonance study. Eur J Vasc Endovasc Surg. 2008; **35**(4): 392-8.

69. Rausch M, Baumann D, Neubacher U, Rudin M. In-vivo visualization of phagocytotic cells in rat brains after transient ischemia by USPIO. NMR Biomed. 2002; **15**(4): 278-83.

70. Marinescu M, Chauveau F, Durand A, Riou A, Cho TH, Dencausse A, et al. Monitoring therapeutic effects in experimental stroke by serial USPIO-enhanced MRI. Eur Radiol. 2012.

71. Krombach GA, Wendland MF, Higgins CB, Saeed M. MR imaging of spatial extent of microvascular injury in reperfused ischemically injured rat myocardium: value of blood pool ultrasmall superparamagnetic particles of iron oxide. Radiology. 2002; **225**(2): 479-86.

72. Montet-Abou K, Daire JL, Hyacinthe JN, Jorge-Costa M, Grosdemange K, Mach F, et al. In vivo labelling of resting monocytes in the reticuloendothelial system with fluorescent iron oxide nanoparticles prior to injury reveals that they are mobilized to infarcted myocardium. Eur Heart J. 2010; **31**(11): 1410-20.

73. Kanno S, Wu YJ, Lee PC, Dodd SJ, Williams M, Griffith BP, et al. Macrophage accumulation associated with rat cardiac allograft rejection detected by magnetic resonance imaging with ultrasmall superparamagnetic iron oxide particles. Circulation. 2001; **104**(8): 934-8.

Figures

Figure 1: Murine blood monocyte in peripheral circulation 48 hours after infusion of USPIO. Inlay (bottom right – magnified form black box) demonstrates USPIO within lysosome.

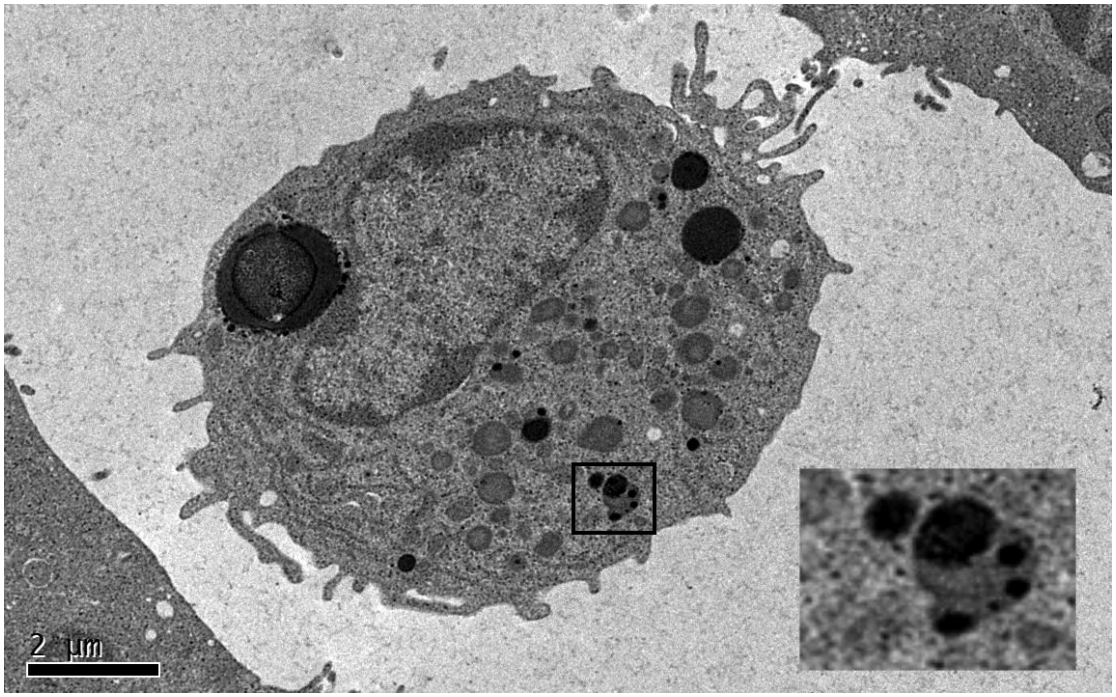

Figure 2: Theoretical T2* exponential decay curves. The T2* curve can be plotted using signal intensities from a region of interest (green crosses) for specific echo times (TEs). In this case, a line of best fit is plotted using the known equation for T2* decay. A T2* map is created from these derived T2* values giving pixel-by-pixel measurements of T2* reported in units of milliseconds, rather than signal intensity of raw images. The red curve describes the decay from pre-USPIO tissue, and the green curved indicated a faster decay due to presence of USPIO. The blue line describes the time constant, T2*.

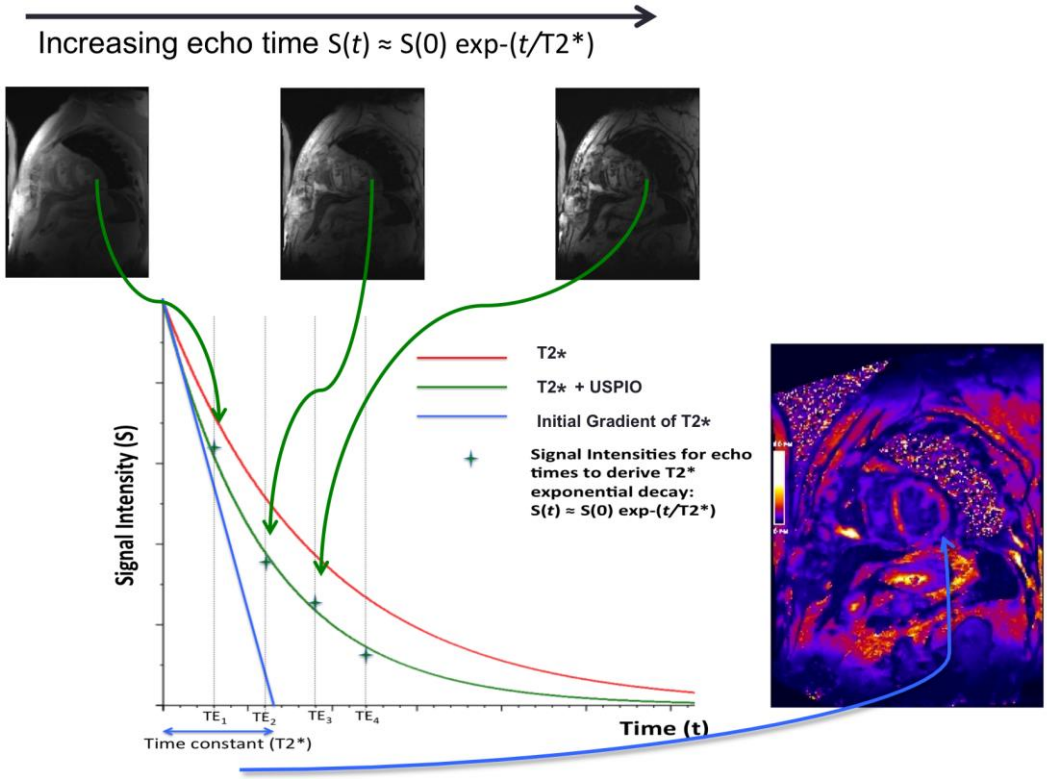

Figure 3: Cardiac T2* Imaging. Multiple images obtained from increasing echo time points (3 time points shown from the left) can be combined to create a T2* map (final image on the right). This map includes the spleen and liver (yellow arrows) and the myocardium (white arrow). These tissues are dark indicating low T2* values consistent with higher USPIO uptake.

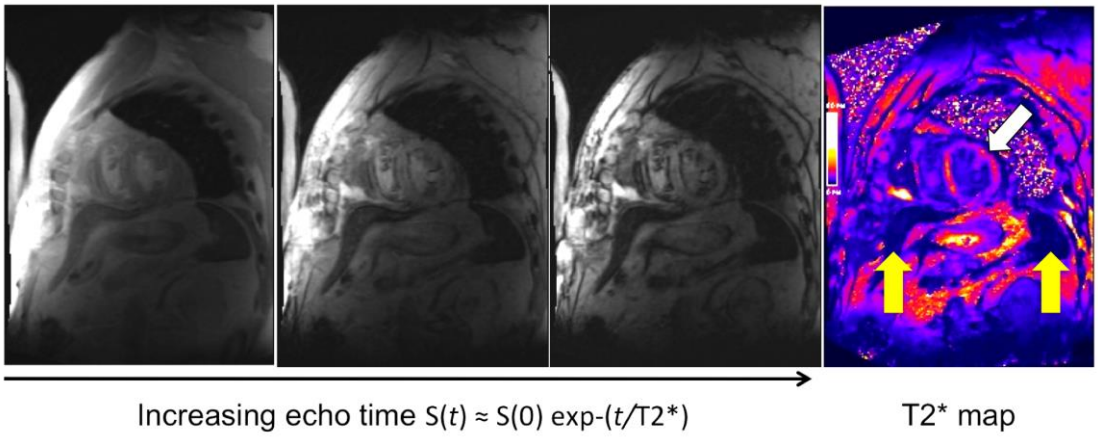

Table 1: Iron oxide nanoparticle preparations

Particle	Size (Diameter)	Plasma Half-life (h)	Application
Microparticles of iron oxide (MPIOs)	1-6 µm (Shapiro et al., 2005a)	1-2 min	Readily endocytosed and detected with MRI.(Shapiro et al., 2005a) Need immediate scan following infusion. Can be combined with ligands for cellular targets allowing molecular imaging (McAteer et al., 2011). Large size means they remain in the blood pool and are suitable for endovascular imaging t (Yang et al., 2010).
Superparamagnetic particles of iron oxide (SPIOs)	65-150 nm (Boutry et al., 2008)	2-3 h	Ferumoxide (Endorem, Guerbet, France) and ferucarbotran (Resovist, Bayer-Schering Pharma, Germany). Recognised by cells of the reticuloendothelial system. Have been used for oncological imaging including liver studies where they are taken up by Kuppfer cells in normal tumour-free liver .(Margolis et al., 2007) Mesenchymal stem cell,

			monocyte/macrophage labelling (Richards et al., 2012a).
Ultrasmall SPIO (USPIOs)	<50 nm (Di Marco et al., 2007)	Ferumoxytol : 9-15 h Ferumoxtran -10: 25-30 h	Ferumoxtran-10 (Sinerem, Guerbet, France) and ferumoxytol (Rienso, Takeda, United Kingdom).
Very small superparamagnetic iron oxide particles (VSOPs)	<10 nm (Taupitz et al., 2004)	1 h	Alternative blood pool agents with longer circulating half-life than gadolinium based agents (Schnorr et al., 2012, Wagner et al., 2011). Potential as cell tracking agents (Ludwig et al., 2013).

Table 2: USPIO in cardiovascular disease.

Target	Model & USPIO Preparation	Imaging Findings
Atherosclerotic Plaques	Ferumoxtran-10 imaging of rabbit aorta (Ruehm et al., 2001b).	UPSIOs identified within aortic atherosclerotic plaques. They are taken up by macrophages.
	Ferumoxtran-10 & ferumoxytol in rabbit aorta (Herborn et al., 2006).	Both USPIO preparations could lidentified within atherosclerotic inflammation. The peak signal for imaging was 2-3 days after ferumoxytol injection, compared to 4-5 days with ferumoxtran-10.
	$ApoE^{-/-}$ mice infused with angiotensin II, or angiotensin II and a p38 MAPK inhibitor with ferumoxtran-10 imaging (Morris et al., 2008).	The angiotensin II treated animals had the greatest USPIO uptake corresponding with macrophage infiltration. The angiotensin II/p38 MAPK inhibitor group had lower USPIO uptake, which was no different to untreated controls. Modulation of inflammatory cell activity within atherosclerotic plaque could be monitored with USPIO contrast.
	$ApoE^{-/-}$ mice treated with irbesartan were compared to non-treated mice using P904 USPIO (Sigovan et al., 2012). *in vivo* USPIO labelled macrophages compared to *in vitro* USPIO labelling macrophages.	Irbesartan treatment resulted in decreased USPIO uptake compared to controls, which was associated with a significant reduction in macrophage-covered area. The use of *in vitro* labelled macrophages did not produce a significant difference in T2* values despite a difference in macrophage accumulation at histology.
Carotid Atherosclerosis	Human carotid plaques using ferumoxtran-10 (Kooi	USPIOs taken up by macrophages could be identified in human atherosclerotic plaques. High risk plaques

	et al., 2003a).	took up USPIO more avidly.
	Ferumoxtran-10 uptake within carotid plaques of patients with symptomatic and asymptomatic disease. (Tang et al., 2007).	There was more USPIO signal in "contralateral asymptomatic plaques" compared to "truly asymptomatic" patients. Patients with stroke disease have a higher inflammatory burden within non-culprit carotid artery plaques compared with the plaques from asymptomatic patients.
	Comparison of carotid plaques of patients awaiting CABG to asymptomatic patients using ferumoxtran-10 (Tang et al., 2008a).	Higher USPIO uptake within the CABG group. The plaques of the CABG patients exhibited a USPIO related signal of i 16.4% compared to 8.4% in asymptomatic patients. Patients awaiting CABG had higher inflammatory plaque burden.
	The ATHEROMA study (Atorvastatin THerapy: Effects on Reduction Of Macrophage Activity) to investigate the effects of high-dose versus low-dose statin with ferumoxtran-10 imaging (Tang et al., 2009, Patterson et al., 2011).	Significant reduction in USPIO uptake in the high-dose atorvastatin group at 6 and 12 weeks. This correlated with favourable reductions in LDL cholesterol and micro-emboli count. Quantitative T2* values showed a highly significant reduction in USPIO-related signal over the course of follow-up. Modulation of plaque inflammation by statins can be monitored by USPIO imaging.
Stroke	Murine model of middle cerebral artery occlusion using ferumoxtran-10 (Rausch et al., 2001a).	48 hours after stroke, USPIO signal identified within peri-infarct zone. Histology confirmed a large population of iron containing macrophages in the infarcted tissue.
	Murine model with ferumoxtran-10 and T2-	Disruption of the blood brain barrier leads to leakage of USPIO into the CSF, limiting the specificity of

	weighted imaging with multiple scanning points in the first 72 hours after stroke (Wiart et al., 2007).	inflammatory cell imaging.
	Spatio-temporal distribution of ferumoxtran-10 was monitored in a rat model of transient cerebral infarction using T1- and T2-weighted MRI sequences(Rausch et al., 2002).	Maximum USPIO related signal occurred on day 2. The technique was successful in achieving non-invasive imaging of inflammation associated with transient ischaemia, but was not sensitive enough to identify increased macrophage infiltration at later time points.
	Murine model to investigate the effects of anti-inflammatory minocycline after middle cerebral artery occlusion using P904 (Marinescu et al., 2012).	Treatment reduced infarct size, blood-brain barrier permeability and microglia/macrophage counts. This correlated with decreased R2* value (and USPIO uptake) on imaging as well as tissue iron content.
	Ferumoxtran-10 administered to patients 4-5 days after suffering a stroke with imaging performed 24-36 hours and 48-72 hours later (Saleh et al., 2004).	T1 weighted imaging revealed parenchymal enhancement that increased between the 2 scans, corresponding to the expected macrophage distribution. T2/T2* weighted imaging revealed increased USPIO enhancement between scans, which the authors interpreted as blood pool effect. These USPIO induced changes did not correspond to conventional gadolinium enhanced changes, suggesting they occurred independent of blood-brain-barrier breakdown.
Myocardial Infarction	USPIO agent NC100150 as a blood pool agent in a	Hyperenhancement of the myocardium by UPSIO was compared to infarct size. USPIO T1-weighted hyper-

	rodent model of reperfusion after MI (Krombach et al., 2002).	enhancement was larger than infarction area after reperfusion, but smaller than area at risk. UPSIO corresponded with micro vascular injury and was associated with leakage into the extravascular space.
	Montet-Abou et al studied fluorescent iron oxide nanoparticles (5-20nm) in a rodent MI model (Montet-Abou et al., 2010).	Rats with a sham operation and those with MI but not given USPIO did not have significant change in USPIO uptake. The MI group given USPIO had a significant increase in USPIO uptake over the 3 days, with excellent correlation of monocytes/macrophages on histology. CD-68 immuno-staining confirmed co-localisation of fluorescent USPIO particles within macrophages. Rats treated with anti-inflammatory medication showed reduced USPIO signal. This corresponded with less monocyte/macrophage infiltration confirming that USPIO can track inflammation and response to therapeutic intervention within infarcted myocardium.
	Ferumoxytol in human myocardial infarction (Alam et al., 2012c).	USPIO uptake increased significantly in the infarct zone and also in the peri-infarct and remote myocardium to lesser extents.
Cardiac Transplant	Synthesised dextran coated USPIO to investigate macrophage accumulation in a rodent cardiac allograft rejection model [72,] (Kanno et al., 2001).	Control rodents did not have significant USPIO uptake at baseline. Allograft rodents exhibited large USPIO uptake which was reduced by immunosuppression.. Corresponding macrophage counts were greatest in the allograft group and reduced by immunosuppressive treatment indicating that USPIOs can be used to monitor transplant rejection.

APPENDICES

Appendix C: USPIO To Detect Cellular Inflammation In Patients With Acute Myocardial Infarction

Consent form for active group (Figure 1)

Figure 1: Consent form - Active Group

FERUMOXYTOL FOR MAGNETIC RESONANCE IMAGING OF MYOCARDIAL INFARCTION

CONSENT FORM

Please initial box

1. I confirm that I have read and understand the information sheet dated 22nd September 2010 (Version 2.0) for the above study and have had the opportunity to ask questions. ☐
2. I understand that my participation is voluntary and that I am free to withdraw at any time, without giving any reason, without my medical care or legal rights being affected. ☐
3. I agree for up to 175 mL of blood to be taken over the course of the study. ☐
4. I agree to having up to six MRI scans over a one month period. ☐
5. I agree for notice to be sent to my General Practitioner about my participation in this study and the provision of any clinically significant information. ☐
6. I agree to take part in the above study. ☐

Name of Patient	Date	Signature
Name of Person taking consent (if different from researcher)	Date	Signature
Researcher	Date	Signature

Volunteer Ref No:

GP INFORMATION - ACTIVE GROUP (FIGURE 2)

Figure 2: GP Letter - Active Group

Cardiovascular Research
Chancellor's Building
Royal Infirmary of Edinburgh
EDINBURGH
EH16 4SU

Dr. Name
Address
Address
Post code

Dear Dr

Re: Patient Name, Address (DOB):

The above named patient has agreed to participate in a clinical research study entitled "Ferumoxytol for Magnetic Resonance Imaging of Myocardial Infarction". I enclose a copy of the information sheet. This study is being conducted by Dr Ninian Lang (Clinical Lecturer in Cardiology, University of Edinburgh) and Professor David Newby (British Heart Foundation Professor in Cardiology, University of Edinburgh).

The inclusion criteria for the study comprise: Presentation with myocardial infarction (*either* 'ST-elevation' myocardial infarction *or* 'non-ST-elevation' myocardial infarction, troponin I ≥ 10 IU/mL at 12 hours after the onset of chest pain and age 18 – 80 years inclusive. Exclusion criteria include known critical (≤95%) left main stem coronary artery disease, continued symptoms of angina at rest or minimal exertion, atrial fibrillation, symptomatic heart failure; Killip Class ≥2, hepatic failure (Childs-Pugh grade B or C) or renal failure (estimated glomerular filtration rate <25 mL/min). Patients with a contraindication to magnetic resonance imaging, a past history of systemic iron overload/haemochromatosis and those with known allergy to dextran- or iron-containing compounds will also be excluded.

We will notify you of any clinically significant information arising from your patient's participation in this study. Should you require any further information please do not hesitate to contact myself or Dr Ninian Lang on telephone number 0131 536 1000, e-mail ninianlang@gmail.com.

Yours sincerely,

Dr Shirjel Alam
Research Fellow in Cardiology
Enc.

PATIENT INFORMATION – ACTIVE GROUP

FERUMOXYTOL FOR MAGNETIC RESONANCE IMAGING OF MYOCARDIAL INFARCTION

Participant Information Sheet

You are being invited to participate in a clinical research study. Before you decide it is important for you to understand why the research is being done and what it will involve. Please feel free to discuss it with friends, relatives and your GP if you wish. You are welcome to ask us any questions you may have. You may also contact the independent advisor for the study, Dr Cruden, who is a doctor in the Cardiology Department who is not directly involved in the study. Dr Cruden's contact details can be found at the bottom of this information sheet. Take time to decide whether or not you wish to take part.

This study is being conducted at the Royal Infirmary of Edinburgh by Dr S Alam (Research Fellow in Cardiology), Dr. N Lang (Clinical Lecturer in Cardiology) and Professor D Newby (Professor of Cardiology).

Thank you for taking the time to read this information sheet.

What is the purpose of the study?

This study will make use of new heart scanning techniques to look at inflammation in the heart after a heart attack. An approved treatment for people with anaemia is to give an infusion of microscopic particles of iron called ferumoxytol. However, there is also evidence that the tiny particles of iron are taken up by cells involved with inflammation and can be seen using magnetic resonance imaging (MRI). We aim to perform MRI scans of the heart before and after administering ferumoxytol to assess whether this a useful technique to assess the amount of inflammation after a heart attack. Using blood tests, we will also examine the amount of inflammation in the body as a whole. Another group of patients will undergo MRI scanning of the heart after heart attack but will not receive ferumoxytol. This will allow us to compare non-specific MRI changes after a heart attack with the changes that are specifically highlighted by ferumoxytol.

Why have I been chosen?

You have been chosen because you have had a heart attack and are recovering well. Twelve participants will be recruited for this part of the study.

Do I have to take part?

It is up to you to decide whether or not to take part. If you do decide to take part you will be given this information sheet to keep and be asked to sign a consent form. You are still free to withdraw at any time and without giving a reason. You will not benefit directly from this study. However, the information we get from this study

may help us to understand and develop new treatments for conditions such as heart attacks, heart failure and strokes.

What will happen to me if I take part?

One to three days after your admission to hospital we will perform an MRI scan of your heart. We will also scan the upper part of your abdomen to look for changes in the liver and spleen that normally contain a lot of cells involved in inflammation and may also take up the ferumoxytol. The MRI scan involves lying on a flat bed and passing through the tube-shaped scanner. This scanner does not use x-rays. In order for us to look in more detail at the part of the heart that has been affected by the heart attack, we will administer an agent called 'gadolinium' through a vein before the scan. Gadolinium is in routine clinical use. The scan should take about forty-five minutes in total.

Shortly after the scan we will administer the microscopic iron particles, known as ferumoxytol (the trade name is *Feraheme*). Ferumoxytol is approved for use in the treatment of anaemia and is safely used at the same dose that we propose to give. It has also been used in MRI scanning at this dose but has not been used after heart attack in this way. It will be given through a vein in your arm. Your blood pressure, heart rhythm, temperature and oxygen levels will be monitored during, and for at least one hour after, the infusion. The infusion itself will take less than a minute.

Twenty-four hours and forty-eight hours after the infusion, you will undergo another MRI scan of the heart and upper abdomen. You will also be invited to return for another scan at 4 days, 1 week and 1 month after the infusion. However, if you were not keen to undergo these further scans (for example due to travel constraints) then

we would still be able to include you as a participant to undergo the scans in the first 48 hours.

Immediately after each MRI scan and immediately after the infusion of ferumoxytol we will take a blood test (25 mL; approx. 2 tablespoonsful). This will be used to measure components in the blood that indicate levels of inflammation throughout the body. Therefore, over the course of the study we will take a maximum of approximately 175 mL blood (less than half the volume that would be given in a routine blood donation) and we will perform a maximum of six MRI scans.

All of the procedures will take place either in the Coronary Care Unit, Cardiology Ward, Clinical Research Facility or the Clinical Research Imaging centre at the Royal Infirmary of Edinburgh. None of the procedures should interfere with your routine care after a heart attack and your date of discharge from the hospital should not be affected.

Any expenses you incur (for example travel expenses) will be reimbursed.

Figure 1. Chain of events. There would also be 3 optional MRI scans 96 hours, 1 week and 1 month after the first can if your are willing to participate

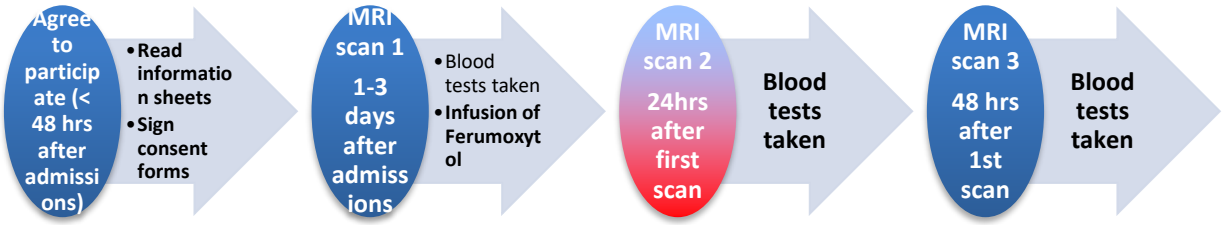

CORE STUDY SCANS

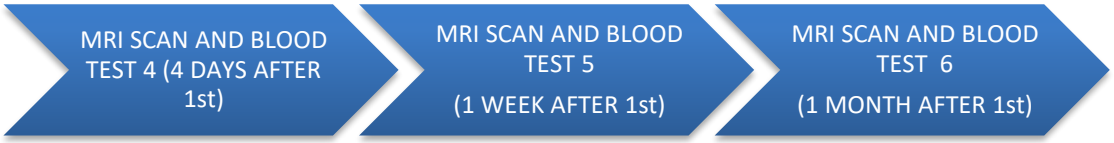

OPTIONAL SCANS

Figure 2. Line diagram showing process of events during scans 1, 3, 4, 5 and 6.

Figure 3. Line diagram showing process of events during scan 2 (ferumoxytol infusion)

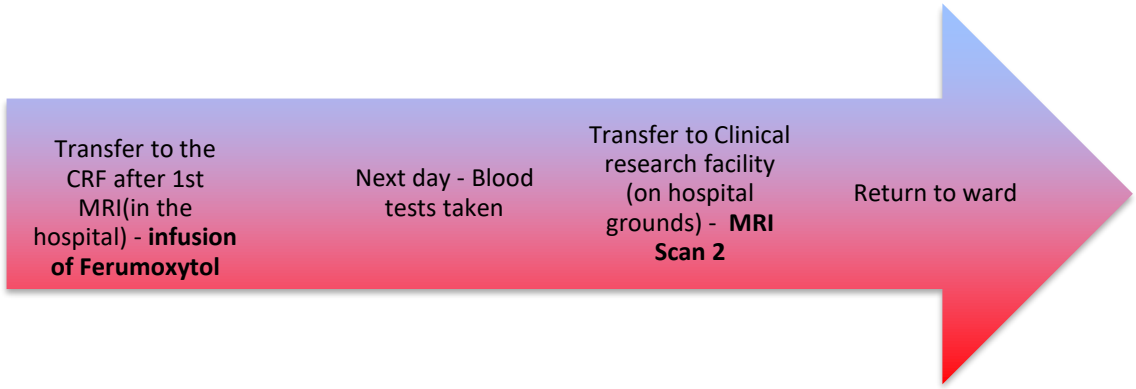

What are the side effects of any treatment received when taking part?

Taking the amount of blood that we plan should not harm you in any way. Taking blood should not be associated with any more than mild discomfort at the needle site. The injection of ferumoxytol should not be painful and has not been associated with any significant side effects. However, there is always a possibility of allergic reactions and we will monitor carefully for these at the time of the administration of ferumoxytol and afterwards and would treat you as necessary. People who have a past history of allergies to iron-containing compounds or 'dextran' (a component of ferumoxytol) would be excluded from participation. The iron particles will be degraded by your body and removed by your liver. Because we will be giving extra iron, people with a history of conditions associated with abnormally high quantities of iron in the body will be excluded from taking part.

Because MRI scanners use strong magnets, we will complete a detailed safety questionnaire before you enroll in the study to check that there is no reason why it would be unsafe for you to have a scan. People with metal joint replacements,

pacemakers or a history of eye injury involving metal (such as from shrapnel or welding) will not be able to take part. Patients who have had brain surgery with the implantation of metalwork will also have to be excluded. MRI scanners do not use x-rays and therefore are not associated with the risks of radiation associated with other imaging methods including CT scans. Other than the risk associated with MRI in people with metal implants, there are no known risks from MRI scanning. The MRI scanner is noisy, so you will wear special headphones to reduce the noise.

It is unlikely that this study should cause you any side effects. If you are concerned about the way you are feeling at any stage during course of the study you should contact Dr Lang or Professor Newby. Dr Lang's contact details can be found at the bottom of this information sheet. Professor Newby can be contacted by telephoning the Royal Infirmary of Edinburgh (0131 242 1000).

What are the possible benefits of taking part?

Taking part in this study will not affect your normal medical care. This study is not intended to benefit you personally. It may help us to discover new treatments for people who have had a heart attack, stroke or have impaired heart pumping action. However, this is just one step in a long series of experiments.

What if something abnormal is found in my scans?

As part of your study we will obtain pictures of your heart. We expect to be able to see the area of the heart attack and are interested to see whether the ferumoxytol can also be seen there. Our research studies are designed to improve our knowledge of the heart after a heart attack. They are not designed for other purposes. After your scan, a specialist will examine these pictures (this will not be done on the day of your study). Other changes either related or unrelated to your heart attack may be seen but you should be aware that because our pictures are taken for a specific research purpose, not all abnormalities that might be detected by other MRI scans are necessarily seen. On rare occasions, we might find an abnormality that is significant and which should be investigated further. If we find such a significant abnormality in your heart, we will contact the Consultant Cardiologist directly involved in your ongoing clinical care. Although a significant abnormality is unlikely, you should be aware that if such an abnormality is detected and you are informed, then this may have consequences for your treatment.

Is there anything else that I may be asked to do?

If, following you heart attack, you undergo a heart bypass operation we would seek your permission to obtain a small biopsy specimen (about 1 mm x 2 mm in size) from the heart muscle at the region of the previous heart attack. We would use this to compare what the cells and/or ferumoxytol look like under the microscope in comparison to the MRI pictures. A Consultant Cardiac Surgeon involved with the study would perform this procedure. This procedure has been safely performed around the world many times before and is associated with only a small risk of

bleeding from the heart muscle but this would be carefully monitored and treated at the time of the operation if felt to be necessary. Consent to providing this biopsy specimen is not required for participation in the study and you can complete the rest of the study in the normal fashion if you do not wish a biopsy to be taken.

Will my GP be informed?

We would like to inform your General Practitioner of your participation in this study. We will notify your General Practitioner, and also the Consultant Cardiologist in charge of your ongoing care, should any clinically relevant material come to light during the study.

What if new information becomes available?

Sometimes during the course of a research project, new information becomes available about the treatment being studied. If this happens, your research doctor will tell you about it and discuss with you whether you want to continue in the study. If you decide to continue in the study you will be asked to sign an updated consent form.

Also, on receiving new information your research doctor might consider it to be in your best interests to withdraw you from the study. This will be explained to you.

What if something goes wrong?

If you are harmed by taking part in this research project, there are no special compensation arrangements. If you are harmed due to someone's negligence, then you may have grounds for legal action but you may have to pay for it.

Will my taking part in this study be kept confidential?

All the information collected about you during the course of the research will be kept strictly confidential. Any information about you which leaves the hospital will have your name and address removed so that you cannot be recognised from it.

What will happen to the results of the research study?

We aim to complete this research by 2012. Once we have analysed all of the results, we will write a paper that will be submitted for publication in one of the medical research journals. You will not be personally identified in any report/publication. If you would like a copy of the paper, please contact Dr. Lang at the address below.

Who is organising and funding the research?

The research is being performed by doctors employed by The University of Edinburgh. Your doctors will not be paid for including you in this study.

Who has reviewed the study?

The study has been reviewed by the South East Scotland Research Ethics Committee.

Where can I obtain further information about the study?

Further information about the study can be obtained from Dr. Ninian Lang who will arrange to meet you. In addition you can discuss the study with Dr. Nicholas Cruden. He is another doctor who works in the hospital but is not involved with the study and acts an independent advisor.

Thank you once again for taking the time to read this information sheet.

Contact for further information

Dr Ninian Lang
(Principal Investigator)
Lecturer in Cardiology
Cardiovascular Research Unit
University of Edinburgh
Chancellor's Building
49 Little France Crescent
EDINBURGH
EH16 4SB
Tel: 0131 242 1000

Dr Nicholas Cruden
(Independent Advisor)
Consultant Cardiologist
Royal Infirmary of Edinburgh
49 Little France Crescent
EDINBURGH
EH16 4SU
Tel 0131 242 1000

CONSENT FORM FOR CONTROL GROUP (FIGURE 3)

FERUMOXYTOL FOR MAGNETIC RESONANCE IMAGING OF MYOCARDIAL INFARCTION

CONSENT FORM

Please initial box

1. I confirm that I have read and understand the information sheet dated 1st November 2010 (Version 2.0) for the above study and have had the opportunity to ask questions. ☐
2. I understand that my participation is voluntary and that I am free to withdraw at any time, without giving any reason, without my medical care or legal rights being affected. ☐
3. I agree for up to 150 mL of blood to be taken over the course of the study. ☐
4. I agree to having up to six MRI scans over a one month period. ☐
5. I agree for notice to be sent to my General Practitioner about my participation in this study and the provision of any clinically significant information. ☐
6. I agree to take part in the above study. ☐

Name of Patient	Date	Signature
Name of Person taking consent (if different from researcher)	Date	Signature
Researcher	Date	Signature

Volunteer Ref No:

7.4 GP INFORMATION FOR CONTROL GROUP (FIGURE 4)

Cardiovascular Research
Chancellor's Building
Royal Infirmary of Edinburgh
EDINBURGH
EH16 4SU

Dr. Name
Address
Address
Post code

Dear Dr

Re: Patient Name, Address (DOB):

The above named patient has agreed to participate in a clinical research study entitled "Ferumoxytol for Magnetic Resonance Imaging of Myocardial Infarction". I enclose a copy of the information sheet. This study is being conducted by Dr Ninian Lang (Clinical Lecturer in Cardiology, University of Edinburgh) and Professor David Newby (British Heart Foundation Professor in Cardiology, University of Edinburgh).

The inclusion criteria for the study comprise: Presentation with myocardial infarction (*either* 'ST-elevation' myocardial infarction *or* 'non-ST-elevation' myocardial infarction, troponin I ≥ 10 IU/mL at 12 hours after the onset of chest pain and age 18 – 80 years inclusive. Exclusion criteria include known critical (≤95%) left main stem coronary artery disease, continued symptoms of angina at rest or minimal exertion, atrial fibrillation, symptomatic heart failure; Killip Class ≥2, hepatic failure (Childs-Pugh grade B or C) or renal failure (estimated glomerular filtration rate <25 mL/min). Patients with a contraindication to magnetic resonance imaging, a past history of systemic iron overload/haemochromatosis and those with known allergy to dextran- or iron-containing compounds will also be excluded.

We will notify you of any clinically significant information arising from your patient's participation in this study. Should you require any further information please do not hesitate to contact myself or Dr Ninian Lang on telephone number 0131 536 1000, e-mail ninianlang@gmail.com.

Yours sincerely,

Dr Shirjel Alam
Research Fellow in Cardiology

PATIENT INFORMATION – CONTROL GROUP

FERUMOXYTOL FOR MAGNETIC RESONANCE IMAGING OF MYOCARDIAL INFARCTION

Participant Information Sheet

You are being invited to participate in a clinical research study. Before you decide it is important for you to understand why the research is being done and what it will involve. Please feel free to discuss it with friends, relatives and your GP if you wish. You are welcome to ask us any questions you may have. You may also contact the independent advisor for the study, Dr Cruden, who is a doctor in the Cardiology Department who is not directly involved in the study. Dr Cruden's contact details can be found at the bottom of this information sheet. Take time to decide whether or not you wish to take part.

This study is being conducted at the Royal Infirmary of Edinburgh by Dr S Alam (Research Fellow in Cardiology), Dr. N Lang (Clinical Lecturer in Cardiology) and Professor D Newby (Professor of Cardiology).

Thank you for taking the time to read this information sheet.

What is the purpose of the study?

We are conducting a study giving a preparation of microscopic iron particles (called ferumoxytol) to patients after a heart attack. We aim to assess whether this will help to highlight the inflammation in the heart seen using magnetic resonance imaging (MRI).

However, to understand what are specific effects of ferumoxytol and not just the effects of the heart attack itself we need to conduct similar scans of patients who have had a heart attack but have not been administered ferumoxytol. We will compare the scans of patients in the two groups.

Participants in this part of the study will act as a 'control' group and will not receive ferumoxytol.

Why have I been chosen?

You have been chosen because you have had a heart attack and are recovering well. Six participants will be recruited for this part of the study.

Do I have to take part?

It is up to you to decide whether or not to take part. If you do decide to take part you will be given this information sheet to keep and be asked to sign a consent form. You are still free to withdraw at any time and without giving a reason. You will not

benefit directly from this study. However, the information we get from this study may help us to understand and develop new treatments for conditions such as heart attacks, heart failure and strokes.

What will happen to me if I take part?

One to three days after your admission to hospital we will perform an MRI scan of your heart. We will also scan the upper part of your abdomen to look at the liver and spleen that normally contain a lot of cells involved in inflammation. The MRI scan involves lying on a flat bed and passing through the tube-shaped scanner. This scanner does not use x-rays. In order for us to look in more detail at the part of the heart that has been affected by the heart attack, we will administer an agent called 'gadolinium' through a vein before the scan. Gadolinium is in routine clinical use. The scan should take about forty-five minutes in total.

Twenty-four hours and forty-eight hours after the first scan, you will undergo another MRI scan of the heart and upper abdomen. You will also be invited to return for another scan at 4 days, 1 week and 1 month after the first scan. However, if you were not keen to undergo these further scans (for example due to travel constraints) then we would still be able to include you as a participant to undergo the scans in the first 48 hours.

Immediately after each MRI scan we will take a blood test (25 mL; approx. 2 tablespoonsful). This will be used to measure components in the blood that indicate levels of inflammation throughout the body. Therefore, over the course of the study we will take a maximum of approximately 150 mL blood (less than half the volume

that would be given in a routine blood donation) and we will perform a maximum of six MRI scans.

All of the procedures will take place either in the Coronary Care Unit, Cardiology Ward, Clinical Research Facility or the Clinical Research Imaging centre at the Royal Infirmary of Edinburgh. None of the procedures should interfere with your routine care after a heart attack and your date of discharge from the hospital should not be affected.

Any expenses you incur (for example travel expenses) will be reimbursed.

Figure 1. Flow diagram showing chain of events. There would also be 3 optional MRI scans 96 hours, 1 week and 1 month after the first can if your are willing to participate

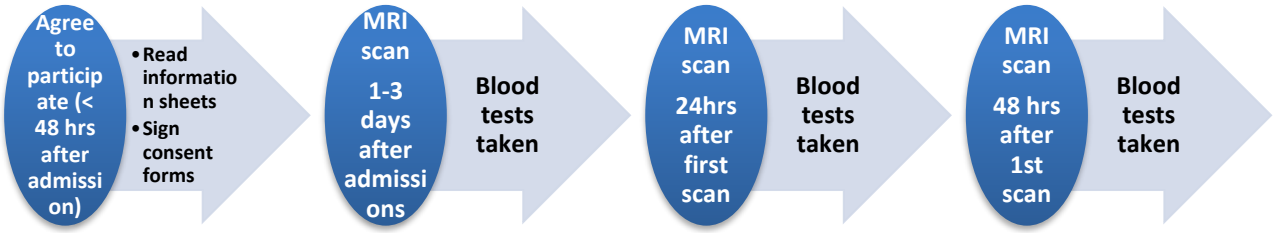

CORE STUDY SCANS

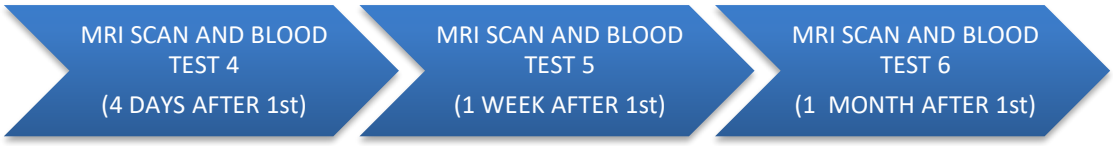

OPTIONAL SCANS

Figure 2. Line diagram showing process of events during all MRI

What are the side effects of any treatment received when taking part?

Taking the amount of blood that we plan should not harm you in any way. Taking blood should not be associated with any more than mild discomfort at the needle site.

Because MRI scanners use strong magnets, we will complete a detailed safety questionnaire before you enroll in the study to check that there is no reason why it would be unsafe for you to have a scan. People with metal joint replacements, pacemakers or a history of eye injury involving metal (such as from shrapnel or welding) will not be able to take part. Patients who have had brain surgery with the implantation of metalwork will also have to be excluded. MRI scanners do not use x-rays and therefore are not associated with the risks of radiation associated with other imaging methods including CT scans. Other than the risk associated with MRI in people with metal implants, there are no known risks from MRI scanning. The MRI scanner is noisy, so you will wear special headphones to reduce the noise.

People with a history of any condition associated with abnormally high levels of iron in the body will not be eligible to take part.

It is unlikely that this study should cause you any side effects. If you are concerned about the way you are feeling at any stage during course of the study you should contact Dr Lang or Professor Newby. Dr Lang's contact details can be found at the bottom of this information sheet. Professor Newby can be contacted by telephoning the Royal Infirmary of Edinburgh (0131 242 1000).

What are the possible benefits of taking part?

Taking part in this study will not affect your normal medical care. This study is not intended to benefit you personally. It may help us to discover new treatments for people who have had a heart attack, stroke or have impaired heart pumping action. However, this is just one step in a long series of experiments.

What if something abnormal is found in my scans?

As part of your study we will obtain pictures of your heart, liver and spleen. Our research studies are designed to improve our knowledge of the heart after a heart attack. They are not designed for other purposes. After your scan, a specialist will examine these pictures (this will not be done on the day of your study). Other changes either related or unrelated to your heart attack may be seen but you should be aware that because our pictures are taken for a specific research purpose, not all abnormalities that might be detected by other MRI scans are necessarily seen. On rare occasions, we might find an abnormality that is significant and which should be investigated further. If we find such a significant abnormality in your heart, we will contact the Consultant Cardiologist directly involved in your ongoing clinical care. Although a significant abnormality is unlikely, you should be aware that if such an abnormality is detected and you are informed, then this may have consequences for your treatment.

Will my GP be informed?

We would like to inform your General Practitioner of your participation in this study. We will notify your General Practitioner, and also the Consultant Cardiologist in

charge of your ongoing care, should any clinically relevant material come to light during the study.

What if new information becomes available?

Sometimes during the course of a research project, new information becomes available about the treatment being studied. If this happens, your research doctor will tell you about it and discuss with you whether you want to continue in the study. If you decide to continue in the study you will be asked to sign an updated consent form.

Also, on receiving new information your research doctor might consider it to be in your best interests to withdraw you from the study. This will be explained to you.

What if something goes wrong?

If you are harmed by taking part in this research project, there are no special compensation arrangements. If you are harmed due to someone's negligence, then you may have grounds for legal action but you may have to pay for it.

Will my taking part in this study be kept confidential?

All the information collected about you during the course of the research will be kept strictly confidential. Any information about you which leaves the hospital will have your name and address removed so that you cannot be recognised from it.

What will happen to the results of the research study?

We aim to complete this research by 2012. Once we have analysed all of the results, we will write a paper that will be submitted for publication in one of the medical research journals. You will not be personally identified in any report/publication. If you would like a copy of the paper, please contact Dr. Lang at the address below.

Who is organising and funding the research?

The research is being performed by doctors employed by The University of Edinburgh. Your doctors will not be paid for including you in this study.

Who has reviewed the study?

The study has been reviewed by the South East Scotland Research Ethics Committee.

Where can I obtain further information about the study?

Further information about the study can be obtained from Dr. Ninian Lang who will arrange to meet you. In addition you can discuss the study with Dr. Nicholas Cruden. He is another doctor who works in the hospital but is not involved with the study and acts an independent advisor.

Thank you once again for taking the time to read this information sheet.

Contact for further information

Dr Ninian Lang
(Principal Investigator)
Lecturer in Cardiology
Cardiovascular Research Unit
University of Edinburgh
Chancellor's Building
49 Little France Crescent
EDINBURGH
EH16 4SB
Tel: 0131 242 1000

Dr Nicholas Cruden
(Independent Advisor)
Consultant Cardiologist
Royal Infirmary of Edinburgh
49 Little France Crescent
EDINBURGH
EH16 4SU
Tel 0131 242 1000

APPENDICES

STUDY PROTOCOL

RESEARCH PROTOCOL

ASSESSMENT OF FERUMOXYTOL AS A NOVEL CONTRAST AGENT FOR MAGNETIC RESONANCE IMAGING OF MYOCARDIAL INFARCTION

Cardiovascular disease is the commonest cause of premature death in the United Kingdom and accounts for thirty percent of all deaths among men and twenty two percent among women. The single largest cause of death is acute myocardial infarction.(2004)

In the context of myocardial infarction, activation of inflammatory cascades is maximal and seen as a ripe target for novel therapeutic strategies currently in clinical development. The development of a robust, non-invasive imaging method to highlight active myocardial inflammation is overdue. Such a technique would not only provide valuable clinical information would also be a valuable tool with which to assess the therapeutic utility of novel anti-inflammatory cardiac therapies.

The Role of Inflammatory Cells in Myocardial Infarction

After myocardial infarction, the myocardium subtended by the critically stenotic or occluded coronary artery consists of heterogeneous tissue that may recover immediately, be stunned or be apoptotic/necrotic. Indeed recruitment of inflammatory cells, including mononuclear leucocytes, into the myocardium from circulating blood may initiate and maintain processes of inflammation, wound

healing and the clearance of cellular debris.(Frantz et al., 2009) These interactions are complex and incompletely understood. However, a fine balance appears to exist between the benefits afforded by inflammatory mechanisms in wound healing and ventricular remodelling versus the potential deleterious effects of uncontrolled inflammation including infarct expansion.

Magnetic Resonance Imaging of Myocardial Inflammation

Magnetic resonance imaging is ideally suited for the serial examination of disease progression as it is non-invasive, does not require ionizing radiation and has excellent spatial resolution.

Ferumoxytol *(Feraheme, Advanced Magnetics, Inc., Cambridge, MA)* was originally developed for the treatment of iron-deficiency anaemia in patients with chronic kidney disease but it has also gained data supporting its use as a magnetic resonance imaging contrast agent. It consists of a suspension of ultrasmall superparamagnetic particles of iron oxide (USPIO) with an ultrasmall core (~7 nm) and a semi-synthetic carbohydrate coating giving an overall particle size of 30 nm. The size of the particle prevents any early redistribution outside the vascular space and therefore it has received specific assessment for blood pool imaging where its plasma elimination half-life is approximately 10-14 hours in humans. During this period it allows first-pass and equilibrium phase imaging of the vasculature and causes a marked increase in signal-to-noise ratio in T1-weighted MR images. Indeed, it allows a greater window of time for imaging than provided by conventional gadolinium-chelates which rapidly distribute into the extra-vascular space (Prince et al., 2003).

Although their small size allows USPIOs to escape immediate recognition by phagocytic cells, clearance of the particles is via phagocytosis by macrophages and, therefore, after the initial blood-pool effects have peaked, signal changes (particularly on T2- and T2*-weighted imaging) may be observed in the reticulo-endothelial system. Capitalising on these effects, USPIOs have been used in the diagnosis of diseases of the liver, spleen and lymph nodes.

Ferumoxytol has been proposed for use in the imaging of active atherosclerosis. Other USPIOs, such as ferumoxtran-10 *(Sinerem, Guerbet Laboratories, France),* have been demonstrated to be useful for the detection of carotid atheroma. In clinical studies with ferumoxtran-10, T2*-weighted MRI signal decrease has been demonstrated within the carotid plaques of patients prior to endarterectomy. Furthermore, USPIO signal effect correlates with the propensity for plaque rupture. Indeed, histology post surgery confirmed the presence of intracellular USPIO in plaque macrophages (Kooi et al., 2003b, Trivedi et al., 2006b). These magnetic resonance and histologic observations are consistent with findings in the aortae of hyperlipidaemic rabbits administered ferumoxtran-10 (Schmitz et al., 2001, Ruehm et al., 2001b).

Herborn and colleagues examined the utility of ferumoxytol (*Feraheme)* for imaging atheroma in the aortae of hyperlipidaemic rabbits using a 1.5T MR scanner.(Herborn et al., 2006) Susceptibility artefacts were detectable in the aortic wall at day 2 to 3 post administration of contrast. Signal voids were observed as a result of T2/T2* effects and were more homogenous than seen in similar animals administered ferumoxtran-10. Histology revealed the accumulation of iron particles under the endothelium and into the medial layer of diseased vessels (Herborn et al., 2006).

Ferumoxytol has been administered safely as a bolus dose of 4 mgFe/kg for use as an MRI contrast agent in man (Ersoy et al., 2004, Li et al., 2007, Li et al., 2005, Prince et al., 2003, Neuwelt et al., 2007). Most of these studies have examined and confirmed its utility as a blood-pool contrast agent. However, it has also been assessed for its use in lymph node imaging for cancer staging. In a study of patients with prostate cancer, ferumoxytol was administered at 4 mgFe/kg and imaging performed at baseline, 5, 8 and 24 hours post dose using a 1.5 T scanner. Maximum signal to noise ratio was observed in lymph nodes at 24 hours on T2*-weighted MR imaging (Harisinghani et al., 2007).

The utility of USPIOs, including ferumoxytol, for imaging myocardial infarction and inflammation has not been assessed but, given the effects seen in atheroma imaging, more marked effects would be expected given the potentially larger area and more aggressive inflammation associated with myocardial infarction. Furthermore, clinical studies examining USPIO magnetic resonance effects have primarily been in scanners limited to a magnetic field strength of 1.5 Tesla and susceptibility effects would be expected to be greater in newer, more powerful clinical scanners with a field strength of 3 Tesla.

AIMS AND HYPOTHESES

Using ferumoxtran (Feraheme) as a USPIO contrast agent for magnetic resonance imaging at 3 Tesla, we aim to conduct the first clinical study to examine the utility of

this novel contrast agent to image myocardial inflammation after myocardial infarction.

We will test the following hypotheses in patients who have suffered recent acute myocardial infarction.

1) Intravenous injection of ferumoxytol accumulates at the site of myocardial infarction and this can be visualised by magnetic resonance imaging.

2) The spatial extent of the MRI signal change evoked by ferumoxytol in the myocardium is proportional to the volume of infarcted myocardium (as assessed by a gadolinium late-enhancement study).

3) Myocardial MRI signal change evoked by ferumoxytol is positively correlated with blood markers of systemic inflammation.

METHODS

Study Population

This study will be open-label and non-randomised. We will perform this pilot, proof-of-concept study in 18 patients who have suffered a myocardial infarction.

Stable patients who are eligible for inclusion will be approached up to 48 hours after admission and asked to consider participation.

Inclusion Criteria:

- Presentation with myocardial infarction (*either* 'ST-elevation' myocardial infarction *or* 'non-ST-elevation' myocardial infarction
- Troponin I ≥ 10 IU/mL at 12 hours after the onset of chest pain
- Age 18 – 80 years inclusive

Exclusion Criteria:

- Known critical (≥95%) left main stem coronary artery disease
- Continued symptoms of angina at rest or minimal exertion
- Atrial fibrillation
- Symptomatic heart failure; Killip Class ≥2.
- Hepatic failure (Childs-Pugh grade B or C) or renal failure (estimated glomerular filtration rate <25 mL/min)
- Contraindication to magnetic resonance imaging
- Past history of systemic iron overload/haemochromatosis
- Patients with known allergy to dextran- or iron-containing compounds

Study Groups

Group 1 – Ferumoxytol

Twelve subjects will be recruited to receive ferumoxytol and to undergo imaging and assessments outlined below.

Group 2 – Control

Six subjects will be recruited to undergo the same study procedures as those in Group 1 but will not receive ferumoxytol. This group will allow us to control for any non-specific effects of myocardial infarction upon the MRI signal parameters assessed. For example, it will allow us to control for the potential confounding effect of intra-myocardial micro-haemorrhage associated with myocardial infarction.

Administration

Ferumoxytol will be supplied by Advanced Magnetics, Inc., Cambridge, MA. As supplied, each vial contains 510 mg of elemental iron in 17 mL (30 mg/mL). It will be administered via a peripheral venous cannula at a dose of 4 mgFe/kg body weight at a rate of up to 1 mL/sec. This dose has been safely administered before and equates to 8% of total body iron for males and 9.5% for females, or about the same amount of iron as is contained in 1-2 units of blood.

Administration of ferumoxytol will be immediately after the first ‘baseline’ cardiac MR scan (see below). Administration will be performed by a member of the research team or a qualified research nurse, either in the Clinical Research Facility, Coronary Care Unit or Cardiology ward at the Royal Infirmary of Edinburgh.

Non-invasive physiological monitoring (continuous ECG monitoring, oxygen saturation probe, non-invasive blood pressure, temperature and nurse observation) will be performed during ferumoxytol administration. If, on clinical grounds, the patient is due for discharge the same day, they will be observed for at least one hour following the administration of ferumoxytol prior to discharge.

Magnetic Resonance Imaging

Magnetic resonance imaging will be performed using a dedicated clinical research Siemens 3T Verio MRI scanner at the Clinical Research Imaging Centre at the Queen's Medical Research Institute, University of Edinburgh. Data will be acquired using a body matrix coil.

Standard cardiac imaging breath-held ECG-gated sequences will be used to acquire 2-chamber, 4-chamber, long axis and short axis views of the heart. USPIO imaging will be performed using established $T2^*$-weighted multi-echo gradient-echo sequences, breath-held and cardiac gated. Scan parameters (such as echo time to dictate degree of $T2^*$-weighting) will require a degree of optimisation for USPIO imaging of the myocardium at 3T (high concentrations of USPIO will require reduction in echo times). The use of multi-echo sequence allows a quantitative analysis of USPIO accumulation through calculation of T2* relaxation times before and after administration of USPIO. Therefore, it is anticipated that scanning of the first few patients will constitute a scanning protocol optimisation phase. In order to optimise image analysis of $T2^*$-weighted images (and prevent analysis degradation due to "$T2^*$-blooming" artefacts, USPIO images will be quantitatively analysed using a susceptibility gradient mapping post-processing technique previously used in SPIO imaging to quantitate USPIO accumulation using changes in calculated T2* relaxation

times.(Liu et al., 2008) We have recently employed this technique to quantify T2*-weighted signal change post-ferumoxytol-10 administration in patients with abdominal aortic aneurysm.(Richards et al., 2010)

Imaging will be performed at baseline (24 – 72 hours after admission) prior to administration of ferumoxytol. Subsequent imaging will be performed 24 and 48 hours after the administration of ferumoxytol. Volunteers will also be invited to return for scanning at 96 hours, 96 hours, one week and one month post ferumoxytol, but this will not be a mandatory feature of the protocol.

Immediately prior to the baseline T2*-weighted scan, a breath-held inversion recovery sequence will be used to acquire delayed enhancement images after a delay of 10-15 minutes following an intravenous administration of 0.2 mmol/kg of MR gadolinium contrast agent. Standard cardiac MR acquisition parameters will be used for these acquisitions. Delayed enhancement analysis will be performed using QMass software (Medis medical imaging systems, Netherlands), allowing quantification of infarct size and location for correlation with SPIO-related signal changes.

An additional T2*-weighted acquisition will be acquired axially through the liver for each time point to allow quantification of non-specific ferumoxytol uptake within the reticulo-endothelial system via changes in hepatic and splenic tissue T2*.

The investigator performing image analysis will be blinded to the subject's study group.

Systemic Markers of Inflammation

Prior to each MRI scan, approximately 25 mL peripheral venous blood will be obtained from each volunteer for the measurement of systemic markers of

inflammation. These will include high sensitivity C-reactive protein (hsCRP), interleukin-6 (IL-6), interleukin-8 (IL-8), tumour necrosis factor alpha (TNFα) and full blood count for differential leucocyte count. Platelet function assays will also be performed. This will allow the evaluation of any correlation of myocardial signal change, putatively reflecting local myocardial inflammation, with markers of systemic inflammation.

Myocardial Tissue Collection

Patients who undergo coronary artery bypass grafting will be asked whether they consent to left ventricular 'Tru-Cut' core biopsy of a small area of infarcted myocardium at the time of surgery. This tissue sample would allow the direct histological assessment of the presence of intra-myocardial iron/mononuclear cells.

Figure 5: Timing for cardiac magnetic resonance scanning and ferumoxytol administration.

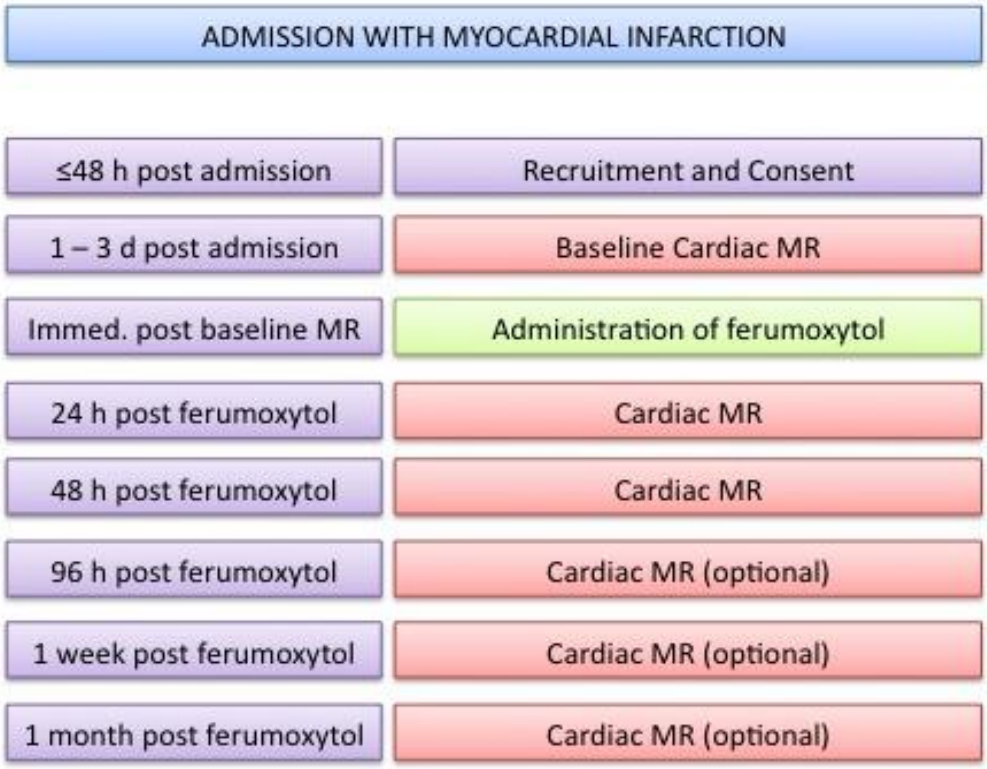

REFERENCES

2004. *Coronary heart disease statistics: factsheet* [Online]. Available: http://www.heartstats.org [Accessed].

ERSOY, H., JACOBS, P., KENT, C. K. & PRINCE, M. R. 2004. Blood pool MR angiography of aortic stent-graft endoleak. *AJR Am J Roentgenol,* 182**,** 1181-6.

FRANTZ, S., BAUERSACHS, J. & ERTL, G. 2009. Post-infarct remodelling: contribution of wound healing and inflammation. *Cardiovasc Res,* 81**,** 474-81.

HARISINGHANI, M., ROSS, R. W., GUIMARAES, A. R. & WEISSLEDER, R. 2007. Utility of a new bolus-injectable nanoparticle for clinical cancer staging. *Neoplasia,* 9**,** 1160-5.

HERBORN, C. U., VOGT, F. M., LAUENSTEIN, T. C., DIRSCH, O., COROT, C., ROBERT, P. & RUEHM, S. G. 2006. Magnetic resonance imaging of experimental atherosclerotic plaque: comparison of two ultrasmall superparamagnetic particles of iron oxide. *J Magn Reson Imaging,* 24**,** 388-93.

KOOI, M. E., CAPPENDIJK, V. C., CLEUTJENS, K. B. J. M., KESSELS, A. G. H., KITSLAAR, P. J. E. H. M., BORGERS, M., FREDERIK, P. M., DAEMEN, M. J. A. P. & VAN ENGELSHOVEN, J. M. A. 2003. Accumulation of ultrasmall superparamagnetic particles of iron oxide in human atherosclerotic plaques can be detected by in vivo magnetic resonance imaging. *Circulation,* 107**,** 2453-8.

LI, W., SALANITRI, J., TUTTON, S., DUNKLE, E. E., SCHNEIDER, J. R., CAPRINI, J. A., PIERCHALA, L. N., JACOBS, P. M. & EDELMAN, R. R. 2007. Lower extremity deep venous thrombosis: evaluation with ferumoxytol-enhanced MR imaging and dual-contrast mechanism--preliminary experience. *Radiology,* 242**,** 873-81.

LI, W., TUTTON, S., VU, A. T., PIERCHALA, L., LI, B. S. Y., LEWIS, J. M., PRASAD, P. V. & EDELMAN, R. R. 2005. First-pass contrast-enhanced magnetic resonance angiography in humans using ferumoxytol, a novel ultrasmall superparamagnetic iron oxide (USPIO)-based blood pool agent. *J Magn Reson Imaging,* 21**,** 46-52.

LIU, W., DAHNKE, H., JORDAN, E. K., SCHAEFFTER, T. & FRANK, J. A. 2008. In vivo MRI using positive-contrast techniques in detection of cells labeled with superparamagnetic iron oxide nanoparticles. *NMR in biomedicine,* 21**,** 242-50.

NEUWELT, E. A., VÁRALLYAY, C. G., MANNINGER, S., SOLYMOSI, D., HALUSKA, M., HUNT, M. A., NESBIT, G., STEVENS, A., JEROSCH-HEROLD, M., JACOBS, P. M. & HOFFMAN, J. M. 2007. The potential of ferumoxytol nanoparticle magnetic resonance imaging, perfusion, and angiography in central nervous system malignancy: a pilot study. *Neurosurgery,* 60**,** 601-11; discussion 611-2.

PRINCE, M. R., ZHANG, H. L., CHABRA, S. G., JACOBS, P. & WANG, Y. 2003. A pilot investigation of new superparamagnetic iron oxide as a contrast agent for cardiovascular MRI. *Journal of X-Ray Science and Technology*, 11**,** 231-240.

RICHARDS, J. M., SEMPLE, S. I., MACGILLIVRAY, T. J., GRAY, C., LANGRISH, J. P., WILLIAMS, M., DWECK, M., WALLACE, W., MCKILLOP, G., CHALMERS, R. T. A., GARDEN, O. J. & NEWBY, D. E. 2010. Abdominal aortic aneurysm growth predicted by uptake of ultrasmall superparamagnetic particles of iron oxide

.

RUEHM, S. G., COROT, C., VOGT, P., KOLB, S. & DEBATIN, J. F. 2001. Magnetic resonance imaging of atherosclerotic plaque with ultrasmall superparamagnetic particles of iron oxide in hyperlipidemic rabbits. *Circulation,* 103**,** 415-22.

SCHMITZ, S. A., TAUPITZ, M., WAGNER, S., WOLF, K. J., BEYERSDORFF, D. & HAMM, B. 2001. Magnetic resonance imaging of atherosclerotic plaques using superparamagnetic iron oxide particles. *J Magn Reson Imaging,* 14**,** 355-61.

TRIVEDI, R. A., MALLAWARACHI, C., U-KING-IM, J.-M., GRAVES, M. J., HORSLEY, J., GODDARD, M. J., BROWN, A., WANG, L.,

Appendix D: EMPIRE TRIAL

CONSENT FORM (FIGURE 1)

Figure 1: EMPIRE Study - Consent Form

NHS Lothian

The effect of elafin in coronary artery bypass surgery
Consent Form

		Patient's initials
1.	I confirm that I have read the information sheet dated *23rd November 2010* for the above study. I have had the opportunity to consider the information, ask questions and have had these answered satisfactorily.	☐
2.	I understand that my participation is voluntary and I am free to withdraw at any time without giving any reason, without my medical treatment or legal rights being affected.	☐
3.	I agree to have blood taken for the study at 6 extra sampling points from routine clinical care (approximately 175 mL).	☐
4.	I agree to undergo 3 cardiac MRI scans.	☐
5.	I understand that my medical notes and data collected during the study may be looked at by the individuals carrying out the research, regulatory authorities or NHS Lothian Trust, where it is relevant to my taking part in this research. I give permission for these individuals to have access to my medical records for the purpose of research.	☐
6.	If I withdraw from the study, I agree any data already collected may be used as part of the results of the trial.	☐
7.	I agree to my GP being informed about my participation in the study.	☐
6.	I agree to take part in the study.	☐

Name of patient	date	signature
_____	_____	_____
Name of person taking consent	date	signature
_____	_____	_____

GP LETTER (FIGURE 2)

Figure 2 EMPIRE Study - GP Letter

Cardiovascular Research
Chancellor's Building
Royal Infirmary of Edinburgh
EDINBURGH
EH16 4SU

Date

Dr. Name
Address
Address
Post code

Dear Dr

Re: Patient *Name, Address (DOB):*

The above named patient has agreed to participate in a clinical research study entitled "The effect of elafin in coronary artery bypass surgery". I enclose a copy of the information sheet. This study is being conducted by Dr Shirjel Alam (Reseach Fellow in Cardiology, University of Edinburgh) and Dr Peter Henriksen (Consultant in Cardiology, NHS Lothian & University of Edinburgh).

We will notify you of any clinically significant information arising from your patient's participation in this study. Should you require any further information please do not hesitate to contact myself or Dr Nicholas Crudenon telephone number 0131 242 1843.

Yours sincerely,

Dr Shirjel Alam
Research Fellow in Cardiology

EMPRIRE STUDY – PATIENT INFORMATION

Participant Information Sheet

The effect of elafin in coronary artery bypass surgery

You are being invited to take part in a research study. Before you decide whether or not to take part, it is important for you to understand why the research is being done and what it will involve. Please take time to read the following information carefully. Talk to others about the study if you wish. Contact us if there is anything that is not clear or if you would like more information. Take time to decide whether or not you wish to take part.

What is the purpose of the study?

Heart muscle cells are susceptible to injury and death following interruption of blood flow e.g. after a heart attack. One of the treatments for this is coronary heart bypass surgery although this treatment can cause a very mild form of heart injury. We can assess this injury by taking blood samples and measuring for a specific marker, troponin and this provides a helpful model to study drugs that may reduce heart injury

Neutrophils are blood cells that contribute to heart injury by releasing destructive enzymes (elastases). Humans produce a protein called elafin that reduces neutrophil elastase injury. Extensive research from different international centres indicates that elafin has a therapeutic role in diseases of the arteries and heart muscle. We believe that administering elafin to patients undergoing bypass surgery will reduce neutrophil mediated heart injury and therefore help patients recover more quickly from surgery

We intend to study heart injury and inflammation using blood tests and cardiac magnetic resonance imaging (CMRI): a detailed heart scan. We are aiming to recruit 80 patients into the study.

Why have I been asked to take part?

You have been asked to take part as you have been referred for coronary artery bypass surgery at the Edinburgh Heart Centre.

Do I have to take part?

No, it is up to you to decide whether or not to take part. If you do decide to take part you will be given this information sheet to keep and be asked to sign a consent form. If you decide to take part you are still free to withdraw at any time and without giving a reason. Deciding not to take part, or withdrawing from the study, will not affect the healthcare that you receive.
What is the drug being tested?

Elafin is a protein that is naturally produced within the body. The drug is produced using molecular biology techniques from yeast. Elafin has been given to healthy volunteers and patients undergoing surgery. No significant toxicity or side effects have been identified.

What will happen if I take part?

If you agree to take part you will be asked to sign a consent form recognising that you have read this information leaflet and have agreed to participate in the trial.
If you consent to participating in the trial you will receive the following additional tests over and above your routine clinical care.

CMRI heart scan

You will attend for **3 CMRI heart scans** on separate days. The first will be conducted around 7 days **before** your operation. The second and third scans will be conducted on consecutive days between day 5 and day 9 **after** the operation. These scans are performed in the MRI scanner in the Clinical Research Imaging Centre

(CRIC) within the University of Edinburgh's Queen's Medical Research Institute on the Little France site

The MRI scan involves lying on a flat bed and passing through the tube-shaped scanner. This scanner does not use x-rays. In order for us to look in more detail at the heart we will administer an agent called 'gadolinium' through a vein in your arm before the scan. Gadolinium is in routine clinical use. The scan should take about forty-five minutes in total.

After the second scan, we will administer microscopic iron particles, known as ferumoxytol (the trade name is Feraheme). Ferumoxytol is approved for use in the treatment of anaemia and is safely used at the same dose that we propose to give. It has also been used in MRI scanning at this dose but has not been used after bypass surgery in this way. It will be given through a vein in your arm. Your blood pressure, heart rhythm, temperature and oxygen levels will be monitored during, and for at least one hour after, the infusion. The infusion itself will take less than a minute.

Twenty-four hours after the ferumoxytol infusion, you will undergo the final MRI scan of the heart

The research team will arrange these scans, keep you informed and offer reimbursement for travel and food.

All of the procedures will take place either in the cardiothoracic surgery units, Clinical Research Facility or the Clinical Research Imaging centre at the Royal Infirmary of Edinburgh. None of the procedures should interfere with your routine care after a heart attack and your date of discharge from the hospital should not be affected.

Blood tests and drug administration

On the day of surgery you will be allocated at random to receive either the study drug (Elafin) or placebo (saline) during the operation. The research team, surgical

team and you will not know which of these treatments is given. This is standard process for clinical trials and means that you will not know whether you received the drug or placebo.
During and after surgery blood tests will be taken from a plastic cannula that has inserted as part of your routine care during the operation. These blood tests will be used to measure heart muscle injury and inflammation. If you participate in the study a small amount of extra blood will be taken for analysis (around 40 mls in total). The blood will not be stored after the study is finished.

What are the possible benefits of taking part?

You may not get a direct benefit from taking part in this study. The CMRI heart scan will assess your heart function very closely and it is possible that findings from this may help the surgical and medical teams looking after you.
We expect that Elafin will assist with healing and recovery after the operation, although it may not. We believe that elafin's action may translate into a more rapid post-operative recovery and we will be measuring this in the clinical trial.

What are the possible disadvantages and risks of taking part?

It is not thought that there are many disadvantages. Previous studies with elafin in humans including healthy volunteers and surgical patients have suggested that it is a drug with no specific toxicity or side effects. With any drug there is a possible low risk of allergic reaction and you will be monitored for this as part of the trial.

There is a similar low risk of reactions to the contrast agents given for the MRI study. The injection of ferumoxytol should not be painful and has not been associated with any significant side effects. However, we will monitor carefully for these at the time of the administration of ferumoxytol and afterwards and would treat you as necessary. People who have a past history of allergies to iron-containing compounds or 'dextran' (a component of ferumoxytol) would be excluded from

participation. The iron particles will be degraded by your body and removed by your liver. Because we will be giving extra iron, people with a history of conditions associated with abnormally high quantities of iron in the body will be excluded from taking part.

Because MRI scanners use strong magnets, we will complete a detailed safety questionnaire before you enroll in the study to check that there is no reason why it would be unsafe for you to have a scan. People with metal joint replacements, pacemakers or a history of eye injury involving metal (such as from shrapnel or welding) will not be able to take part. Patients who have had brain surgery with the implantation of metalwork will also have to be excluded. MRI scanners do not use x-rays and therefore are not associated with the risks of radiation associated with other imaging methods including CT scans. Other than the risk associated with MRI in people with metal implants, there are no known risks from MRI scanning. The MRI scanner is noisy, so you will wear special headphones to reduce the noise.

What if something abnormal is found in my scans?

As part of your study we will obtain pictures of your heart. We expect to be able to see areas of mild heart injury and are interested to see whether the ferumoxytol can also be seen in these areas. Our research studies are designed to improve our knowledge of the heart after heart muscle injury following bypass surgery. They are not designed for other purposes. After your scan, a specialist will examine these pictures (this will not be done on the day of your study). Other changes either related or unrelated to your heart may be seen but you should be aware that because our pictures are taken for a specific research purpose, not all abnormalities that might be detected by other MRI scans are necessarily seen. On rare occasions, we might find an abnormality that is significant and which should be investigated further. If we find such a significant abnormality in your heart, we will contact the Consultant Surgeon directly involved in your ongoing clinical care. Although a significant abnormality is unlikely, you should be aware that if such an abnormality is detected and you are informed, then this may have consequences for your treatment.

What happens when the study is finished?

Your involvement will finish following the final post-operative MRI scan. You will continue with routine care including follow-up clinics with your surgeon and cardiologist. We can provide a summary of the trial results to patients who participate on request. If you would like this please let the person taking your consent know.

Will my taking part in the study be kept confidential?

All the information we collect during the course of the research will be kept confidential and there are strict laws which safeguard your privacy at every stage. Your name will be removed from the data so that you cannot be recognised from it.

Will my GP be informed?

We would like to inform your General Practitioner of your participation in this study. We will notify your General Practitioner, and also the Consultant Surgeon in charge of your ongoing care, should any clinically relevant material come to light during the study.

What if new information becomes available?

Sometimes during the course of a research project, new information becomes available about the treatment being studied. If this happens, your research doctor will tell you about it and discuss with you whether you want to continue in the study. If you decide to continue in the study you will be asked to sign an updated consent form.

Also, on receiving new information your research doctor might consider it to be in your best interests to withdraw you from the study. This will be explained to you.

What will happen to the results of the study?

At the end of the research we will complete analysis of the information collected from the blood tests and CMRI scans. We will publish this data in peer-reviewed international journals. A positive result in this trial will pave the way to further clinical studies examining the therapeutic benefit of elafin in coronary bypass surgery and other diseases including heart attack and organ transplantation.

Who is organising the research and why?

The study is being led by Dr Peter Henriksen a Consultant Cardiologist at Edinburgh Heart Centre. Dr Henriksen has been researching the protective effects of elafin on the heart and blood vessels. The value and importance of this study has been recognised by the Medical Research Council who have agreed to fund it after rigorous peer-review.

Who has reviewed the study?

The study proposal has been reviewed by 7 independent clinical trial experts in the field and a dedicated research board within the Medical Research Council. The study has been reviewed by the South East Scotland Research Ethics Committee. NHS management approval has also been obtained

If you have any further questions about the study please contact:

Dr Shirjel Alam ***Mobile: 07813955996***
Email: s.r.alam@sms.ed.ac.uk
Dr Peter Henriksen ***Mobile 07747603492***
Email: peter.henriksen@luht.scot.nhs.uk

If you would like to discuss this study with someone *independent* of the study please contact:

Dr Nicholas Cruden

Consultant Cardiologist

Edinburgh Heart Centre

Royal Infirmary of Edinburgh

Little France

EH16 4SA

Phone: 0131-242-1843

If you wish to make a complaint at any stage please contact NHS Lothian:

NHS Lothian Complaints Team

2nd Floor

Waverley Gate

2-4 Waterloo Place

Edinburgh

EH1 3EG

Tel: 0131 465 5708

TRIAL PROTOCOL

Study Protocol

EMPIRE

Elafin **M**yocardial **P**rotection from **I**schaemia **R**ep**E**rfusion injury

A randomised trial to investigate the effect of Elafin on myocardial injury and inflammation in coronary artery bypass surgery

Sponsor	University of Edinburgh and NHS Lothian Health Board
Funder	Medical Research Council and Chest Heart and Stroke, Scotland
Funding Reference	G1001339 (MRC) and R11/A135 (CHSS)
Chief Investigator	Dr Peter Henriksen
EudraCT Number	2010-019527-58
CTA Number	27586/0015/001-0001
MREC Number	11/MRE00/5
ISRCTN Number	ISRCTN82061264

Protocol Approval

Insert study title: Elafin Myocardial Protection from Ischaemia RepErfusion injury

EudraCT number: 2010-019527-58

Signatures

Chief Investigator	Signature	Date

Trial Statistician	Signature	Date

List Of Abbreviations

Coronary artery bypass surgery	CABG
Edinburgh Clinical Trials Unit	ECTU
Cardiac magnetic resonance imaging	CMRI
Ultra-small superparamagnetic particles of iron oxide	USPIO
highly sensitive C-reactive protein	hsCRP
Estimated glomerular filtration rate	eGFR
Electrocardiogram	ECG
Medicines and Healthcare products Regulatory Agency	MHRA
Interleukin 8	IL-8
Tumour necrosis factor α	TNF-α
Interleukin 6	IL-6

SUMMARY

Professional: During coronary artery bypass graft surgery, the myocardium receives an immediate ischaemic insult, exacerbated by post-ischaemic inflammatory responses following reperfusion that lead to increased myocardial injury. Elafin is a potent endogenous anti-elastase with wide ranging anti-inflammatory properties that inhibit destructive post-ischaemic inflammatory pathways. We hypothesise that elafin will reduce perioperative ischaemic myocardial injury and systemic inflammation in elective coronary artery bypass graft surgery. Myocardial injury will be quantified over the first 48 hours using serial measurements of plasma troponin I concentrations. Subsequent myocardial infarct volume will be quantified by cardiac magnetic resonance imaging (CMRI). CMRI will also be used to detect inflammatory macrophage activity within the infarcted myocardium. This proof-of-concept study will establish whether elafin has cardioprotective effects in a clinical model of predictable myocardial injury. It has implications for the treatment of ischaemic heart disease, myocardial infarction and other diseases of ischaemic origin.

Lay: Heart muscle cells are susceptible to injury and death following interruption of blood flow. A mild form of injury occurs during coronary artery bypass surgery. Certain white blood cells contribute to this heart injury by releasing enzymes that break down the tissues. Elafin is a naturally occurring protein that can potentially reduce heart injury by blocking these harmful enzymes. We believe that administering elafin to patients undergoing coronary artery bypass surgery will

reduce heart injury and potentially improve patient outcome. This study sets out to determine whether elafin can indeed benefit patients in this setting.

INTRODUCTION

BACKGROUND

Post-ischaemic inflammatory myocardial injury: the role of neutrophil elastase

Myocardial injury characterised by myocardial troponin release occurs in all patients undergoing coronary artery bypass graft surgery.[1;2] Elevated postoperative plasma troponin concentrations are closely correlated with worse clinical outcomes and mortality. Ischaemic myocardial injury is an immediate result of coronary blood flow interruption during cardiopulmonary bypass. Cardiomyocyte injury is exacerbated following reperfusion and neutrophils are pivotal mediators determining post-ischaemic inflammatory reperfusion injury.[3] Neutrophils accumulate within the reperfused myocardium and release cytotoxic elastases and reactive oxygen species that further affect microvascular and myocardial injury. Preclinical studies have demonstrated that neutrophil depletion or inhibition of neutrophil elastase attenuates post-ischaemic inflammatory reperfusion injury within the myocardium.[4-6]

Interaction between neutrophil mediated injury and macrophage infiltration

Inflammation is characterised by initial recruitment of neutrophils preceding a second wave of monocytes to the site of injury or infection. Leucocytosis including neutrophilia and monocytosis predicts prognosis following acute myocardial infarction.[7] Neutrophil mediated injury facilitates monocyte infiltration.[8;9] Neutrophil derived granule proteins including cathelicidin LL-37 and defensins exhibit

chemotactic activity for monocytes and neutrophil depletion reduces monocyte recruitment following inflammatory injury.[10;11] Data from murine models indicate that monocytes infiltrate the infarcted myocardium and persist as tissue differentiated macrophages where they orchestrate the reparatory response through processes such as extracellular matrix turn over and removal of apoptotic cardiomyocytes.[12] Following myocardial infarction, patients with monocytosis display more left ventricular dilatation and are more likely to develop post-infarct aneurysms.[13] Clinical and experimental evidence from the lung and kidney indicate a central role for macrophages in coordinating the reparatory response to inflammatory tissue injury. Relatively little is known about the role of macrophages following myocardial infarction in humans.

Systemic inflammatory response following CABG

Plasma myeloperoxidase and elastase concentrations can be used as circulating markers of neutrophil activation following coronary bypass graft surgery.[14] A systemic inflammatory response follows surgical trauma, tissue ischaemia and exposure of circulating blood to the cardiopulmonary bypass circuit.[15] This can be measured with plasma markers including highly sensitive C-reactive protein (hsCRP) and inflammatory cytokines (IL-6, IL-8 and TNF-α).[16] Higher plasma IL-6 and IL-8 concentrations are associated with a complicated postoperative course including weight gain, greater oxygen requirement and trends toward worsening renal function.

RATIONALE FOR STUDY

Vascular injury is reduced by administration of elafin

Elafin is a multifaceted anti-inflammatory molecule directly inhibiting destructive neutrophil elastases and reducing inflammatory cytokine production.[17] We have demonstrated a reduction in cytotoxicity and IL-8 production from human endothelial cells incubated with neutrophil elastase when elafin is added to the culture medium.[18] Elafin overexpression reduces inflammatory IL-8 and TNF-α production in human endothelial cells and macrophages exposed to bacterial lipopolysaccharide. This effect is mediated through a mechanism involving diminished activation of the NF-κB transcription pathway possibly through a direct action of elafin on the ubiquitin-proteosome degradation pathway.[18;19] Elafin has protective effects in a range of acute vascular injury models. Elafin infusion reduced skeletal muscle infarction and neutrophil recruitment quantified by muscle myeloperoxidase content in a rat ischaemic hind limb model.[20] Elafin delivery was associated with a 27 % reduction in myocardial infarct size (% area at risk) compared to placebo in rats.[5] The same study demonstrated better myocardial function following repetitive ischaemia reperfusion with a 22% reduction in echocardiographic fractional thickening in elafin treated animals compared to 50% drop in controls. Elafin gene overexpression led to preserved left ventricular function in a murine model of myocardial infarction.[6] Work within our own institution on the same elafin transgenic mice has further characterised the phenotype and demonstrated diminished post-infarct failure with reduced pulmonary oedema and markedly reduced plasma atrial natriuretic peptide concentrations. Elafin is therefore

well suited to addressing the neutrophil mediated inflammatory tissue injury occurring post cardiac surgery.

Coronary bypass surgery provides a controlled vascular injury model

Elective coronary artery bypass graft surgery provides a clinical model of predictable and programmed ischaemic myocardial injury and systemic inflammatory activation. It is suited to the study of interventions targeted at reducing ischaemic myocardial and tissue injury.[2;21;22]

Therefore in this study, CABG surgery will provide an ideal vehicle for the assessment of elafin as an anti-inflammatory cardioprotective agent in humans for the first time.

STUDY OBJECTIVES

OBJECTIVES

Primary Objective

To demonstrate that perioperative Elafin administration reduces post-ischaemic inflammatory myocardial injury following coronary artery bypass graft surgery.

Secondary Objectives

To examine the infiltration of macrophages into the myocardium following ischaemic myocardial injury using advanced CMRI techniques

ENDPOINTS AND OUTCOMES

Primary Endpoint

The primary endpoint will be area under the curve for plasma troponin I concentration profile over the first 48 h.

Secondary Endpoints

The effect of Elafin on myocardial injury and inflammation will be further quantified by comparing infarct volume and macrophage infiltration before and after surgery.

Infarct volume and macrophage infiltration will be quantified using MRI together with late gadolinium enhancement and accumulation of ultra-small superparamagnetic particles of iron oxide (USPIO) respectively. USPIO contrast acts as a cellular marker through the detection of macrophage-mediated inflammation within tissues.[23;24]

Elafin's effect on inflammatory activation will be assessed by comparing peak and area under the curve of plasma hsCRP and cytokine (IL-6, TNF-α and IL-8) concentrations.

Neutrophil activation will be assessed by measuring the white cell and neutrophil differential counts and measuring peak and area under the curve of plasma myeloperoxidase and elastase concentrations.

Postoperative intensive therapy unit (ITU) stay will be recorded from the end of the operation (as documented on the anaesthetic chart) until the ITU team consider the patient fit for ‘step down’ either to cardiothoracic high dependency unit (HDU) or general surgical ward. It will be measured hours.

Additional outcomes

The following data will be collected as expected events in the care of patients post coronary bypass surgery, but NOT reported as adverse events related to the study. They will not be included in the primary or secondary end point analysis.

- Serum Elafin concentration and plasma elastase activity (0 to 24 h)
- Postoperative complications related to coronary artery bypass surgery between 0 (time of first skin incision) and 48 h including;
- Wound infection; sternotomy and vein harvest sites
- Respiratory complications; chest infection, pleural effusion requiring drainage
- Administration of antibiotics for any infection
- Atrial fibrillation (sustained for more than 5 minutes)
- Stroke

- Renal function measured by creatinine/GFR
- Low cardiac output syndrome and inotrope requirement
- Red blood cell transfusion
- Re-operation for bleeding

STUDY DESIGN

This is a single centre randomised placebo-controlled trial. The use of matched placebo treatment that is identical in appearance to the active treatment means that patients, administering clinicians, surgeons and theatre staff, and those collecting data and assessing endpoints will all be blinded to the allocated treatment. Patients will be given information about the trial to take away and the research team will contact them by telephone to find out if they are willing to participate. Consent and recruitment will occur on the day of the preoperative MRI scan. The study will run for 3 years with the intention of recruiting 80 patients within 2.5 years.

Patients will be randomised to either Elafin or matched placebo control the day before surgery. Randomisation will include a minimisation technique that will incorporate age, sex, extent of coronary artery disease, presence of left ventricular dysfunction, presence of diabetes mellitus, surgeon and estimated glomerular filtration rate. This will be performed by Edinburgh Clinical Trials Unit (ECTU) to ensure allocation concealment.

Coronary artery bypass surgery and anaesthesia

All patients will have general anaesthesia. Routine monitoring will include arterial line, central venous line, urinary catheter and electrocardiogram (ECG). Surgical approach will be via a median sternotomy and, where possible, use the left internal mammary artery. All patients will be put on a cardiopulmonary bypass circuit and the surgical protocol will be no different to patients not in the trial. Other conduits will be chosen from saphenous vein, radial artery or the right internal mammary artery (depending on coronary anatomy and surgeon preference). Patients will receive usual postoperative care within the intensive care unit. Patients in both treatment arms will receive standard medications during anaesthesia, surgery and during the postoperative period. No drug interactions have been identified with Elafin and no specific rescue treatment is available.

Elafin and placebo administration

A 200 mg dose of Elafin in 250 mL of normal saline or normal saline placebo will be prepared in the hospital and delivered to the theatre suite by the clinical research nurse or pharmacist. The drug will be administered to the patient through a central venous cannula over a period of 30 min. Investigators and theatre staff will be blinded to the study drug. The intravenous infusion will begin at time 0 h: the time of the first skin incision. Administration will therefore be complete by 20 min before cardiopulmonary bypass commences. The period of just over 48h between the start of Elafin or placebo infusion will be considered the treatment phase.

Cardiac MRI scanning

Each patient will require 3 visits for MRI scanning- preoperative (visit 1), day 7±2 (visit 2- prior to USPIO administration) then 24 h post-USPIO administration (visit 3). Patients will have visit 1 within a period of 6 weeks prior to coronary artery bypass surgery. Visit 2 will be conducted no sooner than 5 days after surgery to examine for delayed enhancement and myocardial infarction using gadolinium contrast. In the event of clinical circumstance dictating a delay in the patient receiving the post-operative scans, these will be performed as close to this timeframe as possible. Reasons and the extent of any delay will be recorded. After the 2nd MRI scan patients will receive an infusion of Feraheme. The infusion will take less than 1 minute and patients will have their blood pressure recorded prior and 1 hr post infusion. Patients will be imaged using a dedicated research 3T Siemens Verio scanner using the phased array body matrix. ECG-gating will be obtained using the Siemens on-line ECG gating system, with a MEDRAD VERIS monitor for gating backup. Total imaging time per cardiac scan per patient will be approximately 40 minutes. Analysis of late gadolinium enhancement infarct size and USPIO/inflammation assessment will be determined using established departmental protocols and dedicated cardiac analysis software by two independent blinded observers trained in cardiac MRI analysis. Discrepancies will be discussed so that a single value can be entered into the study database. The follow up phase will continue up until completion of the third postoperative MRI. All MRI images

obtained for the study will have a clinical report supervised by Dr Graham McKillop, Consultant Radiologist, Royal Infirmary of Edinburgh.

Blood sampling

Blood samples will be taken at baseline (defined as up to 4 hours before the first skin incision, time 0 h) and at 2, 6, 24 and 48 h after this time. The baseline and 2-h intra-operative samples will be taken by the theatre staff and collected by the clinical research nurse. The 6, 24 and 48-h samples will be taken on the ward by either the nursing staff or clinical research nurse. Samples taken at baseline, 2 and 6 hours will represent additional blood sampling to the routine care of the patient if they were not in the research study. Troponin I will be measured by the Abbot Architect assay. This Troponin I assay has been chosen because it has the greatest accuracy and precision of all Troponin assays at low concentrations, Using this assay will also enable samples to be handled by the clinical laboratories at the Royal Infirmary of Edinburgh ensuring robust analysis. Blood sampling will be conducted through an arterial line. Plasma concentrations of TNF-α, interleukins (IL-6, IL-8), myeloperoxidase and elastase will be quantified at each time point out to 6 h using enzyme-linked immunosorbant assays (ELISA; R&D Systems). Serum hsCRP concentrations will be quantified at each time point out to 48 hours. Plasma elastase activity and serum Elafin concentrations will be measured from baseline to 24 by the University Kiel (Department of Dermatologie, Laboratory of Prof. Wiedow). The intended measurement techniques have been used for analysis of Elafin and Elastase

in the past two Elafin studies. The methods have been tested repeatedly and reliably over years, but they are however, research assays and no formally validated methods.

STUDY POPULATION

NUMBER OF PARTICIPANTS

We will recruit 80 patients referred for coronary artery bypass surgery into this study, 40 into each treatment group.

The only site involved will be the Royal Infirmary of Edinburgh, with a 12-30 month recruitment period.

INCLUSION CRITERIA

Patients 18 years or older, who are referred for coronary artery bypass graft surgery requiring 2 or more grafts will be approached for consent to enter the study during visits to the cardiothoracic surgery outpatient clinic.

EXCLUSION CRITERIA

The following exclusion criteria will apply: Recent myocardial infarction (a recorded troponin elevation within 1 month of surgery), emergency surgery, concomitant

valve or aortic surgery, re-intervention or re-do surgery, chronic renal failure (estimated glomerular filtration rate <40 mL/min), severe respiratory disease (maintenance corticosteroid therapy or forced expiratory volume in one second (FEV_1) < 50% predicted), severe left ventricular dysfunction (ejection fraction less than 30%), contraindication to MRI scanning or a history of chronic inflammatory illness requiring immunosuppressive treatment such as inflammatory joint disease, connective tissue disorder. Woman with child-bearing potential will not be enrolled into the trial (woman who have experienced menarche, are pre-menopausal, have not been sterilised or who are currently pregnant). Patients unable to give informed consent will not be approached.

People with a contraindication to feraheme will be excluded from having the final MRI scan but will not be excluded from the study.

PARTICIPANT SELECTION AND ENROLMENT

SCREENING FOR ELIGIBILITY

Initial screening will be performed using information from the detailed clinic referral letter.

IDENTIFYING PARTICIPANTS

Patients referred for coronary artery bypass grafting to clinics at the Royal Infirmary of Edinburgh will be given information about the research study and invited to participate. The cardiothoracic surgeons involved in the patients' care and the research nurse will identify potentially suitable patients from the surgical referrals. The cardiothoracic surgical team will invite suitable patients to participate at surgical clinic. Suitable patients awaiting coronary bypass surgery on the ward will be identified by the research nurse and physicians on the research team.

CONSENTING PARTICIPANTS

The research study will be explained by the cardiothoracic surgeon or research nurse at the cardiothoracic surgical clinic and the patient will be invited to participate. Patients will be given information on the research study to take away after the initial visit. They will be contacted by telephone within 24 hours and if they agree to take part they will be booked in for a preoperative MRI visit during which full written consent will be obtained by physicians on the research team, the research nurse or a deputy.

INELIGIBLE AND NON-RECRUITED PARTICIPANTS

There are no particular arrangements for follow up or assessment of ineligible patients or patients that decline to participate.

RANDOMISATION

After enrolment in the study and the baseline MRI scan, patients will be randomised (1:1) to receive an infusion of Elafin or matched placebo. Elafin or placebo will be prepared and dispensed by the pharmacy department or Clinical Research Facility, who will have received randomisation instructions, on the day of surgery. No member of the clinical team or research team will have randomisation information. Subsequent clinical management and trial protocol investigation will be identical.

Randomisation will be performed by the Edinburgh Clinical Trials Unit (ECTU) to ensure allocation concealment, and by minimisation technique that will incorporate the following binary criteria:

- Age; ≥ 65 or < 65 years
- Sex; male or female
- Diabetes Mellitus; present or absent
- Extent of coronary artery disease; 2 or 3 vessel coronary disease
- Presence of significant left ventricular dysfunction (estimated ejection fraction less than 40% or echocardiographic evidence of left ventricular impairment); present or absent
- Estimated glomerular filtration rate (eGFR mL/min); 40- 59 or ≥60
- Surgeon; Mr Renzo Pessotto or Mr Vipin Zamvar
- Communication of randomisation to the pharmacy department will be web-based.

Treatment Allocation

A 200 mg dose of Elafin in 250 mL of normal saline or matched saline placebo will be prepared and infused through a central venous cannula. The infusion will start at the time of skin incision (time 0), and last 30 minutes. The infusion will be complete at least 20 minutes prior to commencement of cardio-pulmonary bypass circulation.

Emergency Unblinding Procedures

In case of a medical emergency, when the study drug assignment is needed to make treatment decisions for the patient, the clinical team may unblind the patient's drug assignment by contacting the study investigators (Dr Alam, Dr Henriksen or Professor Newby). If unblinding is deemed necessary, the study investigators will contact the pharmacy department, Clinical Research Facility or the pharmacist on call who will keep details of the randomisation and will be able to unblind the allocation if necessary.

The Academic and Clinical Central Office of Research and Development (ACCORD) will be notified immediately of adverse events and the need to unblind study allocation. The circumstances leading to the breaking of the code will be fully documented, in the investigator’s study files, in the study database and in the patient’s source documentation.

Premature Withdrawal

Patients are free to withdraw from the study at any point, but where possible we will try to obtain a complete set of blood samples from each time point to enable a full intention-to-treat analysis on the primary end-point. Consent will include the option for data already collected prior to withdrawal (i.e. results of blood tests or MRI scans) to be included in the study. Where patients withdraw from the study prior to coronary bypass surgery the reason for withdrawal will be noted and a further patient will be recruited.

Some patients may be unable to comply with MRI scanning. The reason for this will be recorded (e.g. claustrophobia, booking error, unable to travel etc). Patients without scans will continue to be followed up as per protocol and will remain in the primary analysis.

Emergency stopping criteria and rescue treatments

The Elafin infusion is delivered over a short window of 30 mins when the patient is anaesthetised prior to going onto cardiopulmonary bypass. No specific toxicity is expected. In the unlikely event that the cardiothoracic surgical team feel that a significant change in the patient's condition may be related to the study they will make a clinical decision to stop the study drug infusion. No specific rescue treatment is available for Elafin.

INVESTIGATIONAL MEDICINAL PRODUCT AND PLACEBO

STUDY DRUG

Study Drug Identification

Elafin CAS number: 820211-82-3. “Recombinant human Elafin” is produced in yeast with a structure identical to the 57 amino acid human form and with 95% purity. It will be prepared and infused as aqueous solution in 0.9% saline.

Amino acid sequence (SwissProt accession number: P19957):

Ala-Gln-Glu-Pro-Val-Lys-Gly-Pro-Val-Ser-Thr-Lys-Pro-Gly-Ser-Cys-Pro-Ile-Ile-Leu-Ile-Arg-Cys-Ala-Met-Leu-Asn-Pro-Pro-Asn-Arg-Cys-Leu-Lys-Asp-Thr-Asp-Cys-Pro-Gly-Ile-Lys-Lys-Cys-Cys-Glu-Gly-Ser-Cys-Gly-Met-Ala-Cys-Phe-Val-Pro-Gln

Study Drug Manufacturer

Elafin, the investigational medicinal product, is manufactured, packaged and labelled by Eurogentac S.A. (Biologics, Liege Science Park, 4102 Seraing, Belgium) as a subcontractor of Proteo Biotech AG in accordance with current Good Manufacturing Practice (GMP) guidelines.

Marketing Authorisation Holder

Elafin is an Investigational Medicinal Phase II product without Marketing Authorisation

Labelling and Packaging

Vial labelling:

Recombinant human Elafin

Vol: 5ml, conc. 10 mg/mL in 0,9% sodium chloride

Concentrate for solution for infusion

Route of administration: i.v. infusion 0.9% sodium chloride

Ch.B. M-HPI-P02/50

Sponsor: Proteo Biotech AG, Am Kiel-Kanal 44, D-24106 Kiel

Box Labelling

Proteo Biotech rec. human ELAFIN, 50 mg/vial

Content: ... vials

Ch.B. M-HPI-P02/50

Retest date: 08/27/2012

Concentrate for solution for infusion

Route of administration: i.v. infusion 0.9% sodium chloride

Dosage according to leaflet enclosed

Storage: -20°C

Medicine for clinical trial use only

Keep out of reach of children

SPONSOR: Proteo Biotech AG

Am Kiel-Kanal 44

D-24106 Kiel

phone +49 431 8888 462

The pharmacy department at the Royal Infirmary of Edinburgh and the research nurses within the Welcome Trust Clinical Research Facility will share the

responsibility for the preparation of 200 mg of Elafin in 250 mL of 0.9% saline or matched placebo 0.9% saline solution, as well as labelling the infusion for blinding the study to investigators and participants.

Storage

The study drug will be kept in the pharmacy department as per product label.

Summary of Product Characteristics

Elafin is an unlicensed trial medication and so no “summary of product characteristic” is available. There are no contra-indications or side-effects expected.

PLACEBO

Placebo will consist of 250 mL of 0.9% saline to be infused via a peripheral intra-venous cannula.

DOSING REGIME

Elafin 200 mg in 250 mL 0.9% saline will be administered. The infusion will last 30 min with administration starting at the time of skin incision and ending prior to onset of cardio-pulmonary bypass circulation.

DOSE CHANGES

No dose changes envisioned.

PARTICIPANT COMPLIANCE

Responsibility for infusion will be with the anaesthetic team, with timing and dose noted on anaesthetic chart as per usual clinical practice. This information will be entered into the study database.

OVERDOSE

From previous studies, a dose of 400 mg was not associated with any relevant safety concerns. The only side effects of nausea and headache were attributed to the investigational procedure. The study drug infusion will be prepared with no other source of Elafin being available for clinicians or the research team to administer additional amounts. Therefore each patient will not receive more than 200 mg of Elafin.

OTHER MEDICATIONS

Permitted Medications

Any other medication necessary for clinical care can be taken, with no specific restrictions placed due to the study.

Prohibited Medications

Any other medication necessary for clinical care can be taken, with no specific restrictions placed due to the study.

STUDY ASSESSMENTS

The patient will undergo standard monitoring during cardiac surgery and the subsequent cardiac intensive care unit stay. No additional safety assessment will be required due to the intensity of monitoring during this time.

The study assessments are outlined below, and will also include measurement of length of stay in cardiac intensive care. The beginning of this period will be the end of surgery as noted on the anaesthetic chart, until the time the responsible consultant deems the patient fit for discharge to the HDU or general ward.

DATA COLLECTION

Figure 1.1 & **Figure 1.2** provides an outline of data collection from blood sampling and CMRI. Each patient will undergo blood sampling at 5 time points to measure Troponin I. hsCRP will be measured at each time point out to 48 h. IL-6, IL-8, TNF-α, myeloperoxidase and elastase concentrations will be measured at each time point

out to 6 h. Serum Elafin concentration and plasma elastase activity will be measured out to 24 h. Each patient will attend for 1 preoperative and 2 postoperative CMRIs. Myocardial infarct volume and USPIO signal will be analysed and recorded by the Wellcome Trust Clinical Research Facility Imaging Core. Blood samples will be collected by nursing staff employed in the cardiothoracic unit. Quantification of troponin I will be made in a reference laboratory Abbot Architecture assay using the supplier's commercial kits. Data collection will be performed by the research nurse and trial research fellow.

Figure 1.1 Blood Sampling and MRI Time points

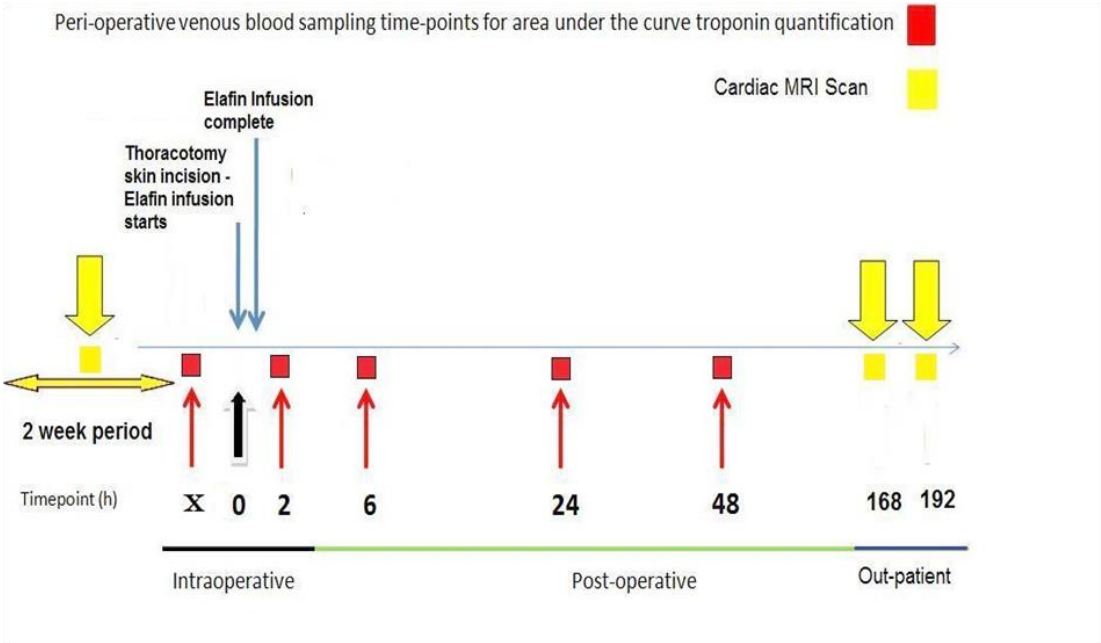

Figure 1.2: Blood Sampling Time Points

TIME POINTS (HOURS POST SKIN INCISION)	TESTS
6 week period pre-surgery	Cardiac MRI scan
Baseline ('X' = up to 4 hours before skin incision)	IL-6, 1L-8, TNF-α, elastase, elastase activity, Myeloperoxidase, hsCRP, Troponin I, Elafin
0 (Skin incision)	
2	IL-6, 1L-8, TNF-α, elastase, elastase activity, Myeloperoxidase, hsCRP, Troponin I, Elafin
6	IL-6, 1L-8, TNF-α, elastase, elastase activity, Myeloperoxidase, hsCRP, Troponin I, Elafin
24	hsCRP, , Troponin I, elastase activity, Elafin
48	hsCRP, Troponin I
168	Cardiac MRI scan
192	Cardiac MRI scan

STATISTICS AND DATA ANALYSIS

SAMPLE SIZE CALCULATION

We will recruit 80 patients into the study, 40 into each group. A recent study of patients in a U.K. centre undergoing coronary artery bypass surgery indicated a mean area under the troponin T release curve in control patients of36.12 µg/L (s.d. 26.08) and in treated patients the value was 20.58 (s.d. 9.58)[2]. No contemporary data are available on Troponin I release in this patient group but the measurements are equivalent in terms of quantifying myocardial injury. The troponin I assay used in the EMPIRE study has greater accuracy and precision than assays for troponin T. Our calculations (based on Troponin T release) assume a 90% power, a significance level of 5%, use a t-test with unequal variances and allow for 4 dropouts in each arm. Additional quantification of infarct size will be conducted with MRI. The expected mean infarct volume in control patients is 4.4g (s.d. 5.5] and in Elafin treated patients we estimate a mean of 1.4g (s.d. 1.7).[25] With our proposed sample size of 80 patients we will have 85% power to detect this difference, at a significance level of 5% (allowing for drop out)

In a double blind randomised controlled trial of high dose aprotinin in 20 patients undergoing cardiopulmonary bypass surgery, IL-6 production was reduced by 58% in the aprotinin treated group.[22] This study suggests that the proposed study size is adequately powered to detect moderate changes in troponin I and inflammatory cytokine production.

PROPOSED ANALYSES

The primary outcome variable is the area under the curve for plasma troponin I concentration from the end of the infusion to 48 hours post infusion. It will be analysed using a generalised linear model, including terms for the treatment allocation and the variables on which the randomisation minimised. Other secondary outcomes involving area under the curve will be analysed similarly.

The volume of infarction from cardiac MRI on the first postoperative scan will be analysed using analysis of covariance, with terms for the volume identified on the preoperative MRI scan, treatment allocation and the variables on which the randomisation minimised. Other secondary outcomes that are measured at baseline and follow up will be analysed similarly. If any variable does not fulfil the distributional assumptions for the techniques described above, another suitable technique will be used. Every effort will be made to complete an intention-to-treat analysis. Patients will be analysed in the groups they were assigned at randomisation, regardless of the treatment actually received. Full follow-up data will be obtained wherever possible. Where data are missing the reason will be recorded to obtain information on the missingness mechanism.

There are no pre-planned subgroup analyses.

A full statistical analysis plan will be written separately. This will include a plan on how missing data will be dealt with, using the guidance available at http://missingdata.lshtm.ac.uk/.

ADVERSE EVENTS

The Investigator is responsible for the detection and documentation of events meeting the criteria and definitions detailed below. All adverse events (AEs) that occur after intervention begins must be reported in detail. In the case of an AE, the investigator will initiate the appropriate treatment according to their medical judgment. Participants with AEs present at the last visit must be followed up until resolution of the event.

Participants should be instructed to contact their Investigator at any time after consenting to join the trial if any symptoms develop. All adverse events (AEs) that occur after joining the trial must be reported in detail in the CRF. In the case of an AE, the Investigator should initiate the appropriate treatment according to their medical judgment. Participants with AEs present at the last visit must be followed up.

ADVERSE EFFECTS ASSOCIATED WITH ELAFIN ADMINISTRATION

The tolerability and safety of intravenous Elafin at 20-400 mg in humans was studied in a single-ascending-dose double-blind randomised placebo-controlled Phase I clinical trial performed on healthy male subjects. In this trial Elafin elicited no severe adverse events. Clinical adverse events were generally mild, showed no obvious correlation with a particular Elafin dose and resolved spontaneously without any sequelae. Elafin had no significant effect on vital signs, ECG, and safety laboratory

values. Headache and nausea reported in some patients was thought to be due to frequent blood sampling rather than Elafin administration.

ADVERSE EFFECTS ASSOCIATED WITH CARDIAC MRI, GADOLINIUM AND USPIO CONTRAST ADMINISTRATION

Ultra-small SPIOs (USPIOs), with particle sizes in the range 10-30 nm escape immediate recognition by the reticulo-endothelial system having a circulatory half-life of approximately 16 hours. Current preparations are biodegradable, safe for clinical administration and used in routine clinical practice to treat iron deficiency anaemia in patients undergoing regular renal dialysis treatment. Feraheme will be the USPIO used in the study.[24] Patients can feel nauseas, constipated, dizzy, suffer hypotension, pruritus, back pain or general gastrointestinal upset when taking Feraheme.

MRI confers no use of ionising radiation, and is not associated with any adverse outcome. The only risk is in patients with magnetic internal or external magnetic material interacting with the magnetic field of the MRI machine. Patient will fill in a safety questionnaire, and be screened by research staff as well as the scanning radiographers prior to scanning. Any patients with possible magnetic material will be excluded from scanning. Patients can feel claustrophobic and anxious as well as suffer muscle aches from prolonged positioning in the MRI scanner.

Gadolinum is the contrast agent used in MRI scanning. It has been used for 15 years and has an incidence of less than 1 in 1000 of hypersensitivity or allergic reaction. Patients will be screened for previous reactions to gadolinium, and be excluded if present. Full resuscitation equipment will be available, and the scan will be supervised by trained medical staff. Gadolinium can increase the risk of nephrogenic system fibrosis in people with severe renal insufficiency, but only patients with an eGFR >40 will be included in the study. Gadovist will be the preparation of gadolinium used in the study. Patients can suffer from nausea, headache, dizziness or local injection site pain when gadovist is infused.

ADVERSE EFFECTS AND COMPLICATIONS OF CABG SURGERY

CABG surgery is associated with risks of perioperative morbidity and mortality. Patients would require careful titration of analgesia for discomfort relating to the sternotomy in the postoperative period. The following are common complications in the immediate postoperative period (0-48h) with mild to moderate severity, and will not be reported as adverse events but as additional outcomes:

Atrial fibrillation

Superficial infection of sternotomy wound and vein harvest site

Respiratory tract infection

Administration of antibiotics for infection in the first 48 h.

Renal function measured by Creatinine/GFR

Pleural effusion requiring percutaneous drainage

Requirement for red blood cell transfusion

The following are serious complications of CABG surgery, which will not be reported as adverse events but as additional outcomes during the period of 0-48h post surgery:

Stroke

Myocardial infarction

Inotrope support for low cardiac output state

Repeat surgery for bleeding.

The following is a serious complication of CABG surgery, which will reported as an adverse event.

Death

The patient is quoted an individualised risk of these complications within our unit using the Euroscore algorithm.[26]

DEFINITIONS

An **adverse event** (AE) is any untoward medical occurrence in a clinical trial subject who is administered a medicinal product, which does not have a causal relationship with the treatment.

An **adverse reaction** (AR) is any untoward or unintended response to an investigational medicinal product related to any dose administered.

An **unexpected adverse reaction** (UAR) is an adverse reaction that is not consistent with the product information in the Elafin brochure.

A **serious adverse event** (SAE), **serious adverse reaction** (SAR) or **suspected unexpected serious adverse reaction** (SUSAR) is any AE, AR or UAR that at any dose:

results in death;

is life threatening (i.e. the subject was at risk of death at the time of the event; it does not refer to an event which hypothetically might have caused death if it were more severe);

requires hospitalisation or prolongation of existing hospitalisation;

results in persistent or significant disability or incapacity;

or is a congenital anomaly/birth defect

Note: Hospitalisations for treatment planned prior to randomisation and hospitalisation for elective treatment of a pre-existing condition will not be considered as an AE. Complications occurring during such hospitalisation will be AEs.

DETECTING AEs AND SAEs

All AEs and SAEs must be recorded from the time a participant undergoes the first MRI scan, until the last MRI visit ends (or discharge from hospital if the patient does not undergo MRI scanning after surgery).

The Investigator will ask about the occurrence of AEs/SAEs at every visit during the study. Open-ended and non-leading verbal questioning of the participant will be used to enquire about AE/SAE occurrence. Participants will also be asked if they have been admitted to hospital, had any accidents, used any new medicines or changed concomitant medication regimens. If there is any doubt as to whether a clinical observation is an AE, the event should be recorded.

RECORDING AEs AND SAEs

When an AE/SAE occurs, it is the responsibility of the Investigator to review all documentation (e.g. hospital notes, laboratory and diagnostic reports) related to the event. The Investigator should then record all relevant information in the CRF and on the SAE form (if the AE meets the criteria of serious).

Information to be collected includes dose, type of event, onset date, Investigator assessment of severity and causality, date of resolution as well as treatment required, investigations needed and outcome. MedDRA will be used to code all AEs.

EVALUATION OF AEs AND SAEs

Seriousness, causality, severity and expectedness should be evaluated as though the participant is taking active drug. Where cases are considered serious plus possibly, probably or definitely related to drug and unexpected (i.e. SUSARs) the investigator team will make a decision regarding unblinding.

Assessment of Seriousness

The Investigator should make an assessment of seriousness as defined in Section 10.1.

Assessment of Causality

The Investigator will make an assessment of whether the AE/SAE is likely to be related to treatment according to the following definitions. All AEs/SAEs judged as having a reasonable suspected causal relationship (e.g. possibly, probably, definitely) to the study drug will be considered as ARs/SARs. All AEs/SAEs judged as being related (e.g. possibly, probably, definitely) to an interaction between the study drug

and concomitant or rescue/escape drugs, or any AE/SAE that cannot be attributed to only the study drug or the concomitant or rescue/escape drugs will also be considered to be ARs/SARs .

Unrelated: where an event is not considered to be related to the study drug.

Possibly: although a relationship to the study drug cannot be completely ruled out, the nature of the event, the underlying disease, concomitant medication or temporal relationship make other explanations possible.

Probably: the temporal relationship and absence of a more likely explanation suggest the event could be related to the study drug.

Definitely: The known effects of the study drug or its therapeutic class, or based on challenge testing, suggest that study drug is the most likely cause.

Alternative causes such as natural history of the underlying disease, other risk factors and the temporal relationship of the event to the treatment should be considered and investigated. The blind should not be broken for the purpose of making this assessment.

Assessment of Severity

The Investigator will make an assessment of severity for each AE/SAE and record this on the CRF according to one of the following categories:

Mild: an event that is easily tolerated by the participant, causing minimal discomfort and not interfering with every day activities.

Moderate: an event that is sufficiently discomforting to interfere with normal everyday activities.

Severe: an event that prevents normal everyday activities.

Note: the term ‘severe’, used to describe the intensity, should not be confused with ‘serious’ which is a regulatory definition based on participant/event outcome or action criteria. For example, a headache may be severe but not serious, while a minor stroke is serious but may not be severe.

Assessment of Expectedness

If an event is judged to be an AR/SAR, the evaluation of expectedness should be made based on knowledge of the reaction and the relevant product information documented in the product literature.

REPORTING OF SAEs/SARs/SUSARs

Once the Investigator becomes aware that an SAE has occurred in a study participant, they will report the information to the ACCORD office within 24 hours. The SAE form will be completed as thoroughly as possible with all available details of the event, signed by a member of the Investigator team. If the Investigator does

not have all information regarding an SAE, they will not wait for this additional information before notifying ACCORD. The form will be updated when the additional information is received.

The SAE report must provide an assessment of causality and expectedness at the time of the initial report to ACCORD according to Sections 10.4.2, Assessment of Causality and 10.4.4, Assessment of Expectedness.

The SAE form should be transmitted by fax to the ACCORD central office on 0131 242 9447 or may be transmitted by hand to the office.

The SAE form will also be sent to Proteo Biotech AG on +49 (431) 8888463.

Events listed in section 2.2.3 will not be reported as adverse events however, will be recorded.

REGULATORY REPORTING REQUIREMENTS

The University of Edinburgh is responsible for Pharmacovigilance reporting on behalf of the Co-Sponsors (University of Edinburgh and Lothian Health Board).

The University of Edinburgh has a legal responsibility to notify the regulatory competent authority and the relevant ethics committee (main Research Ethics Committee (REC) that approved the trial). Fatal or life threatening SUSARs will be reported no later than 7 calendar days and all other SUSARs will be reported no later than 15 calendar days after ACCORD is first aware of the reaction.

An Annual Safety Report will be submitted to the regulatory competent authority and the main REC listing all SARs and SUSARs.

A copy of the annual safety report will also be sent to Proteo Biotech AG.

FOLLOW UP PROCEDURES

After initially recording an AE or recording and reporting an SAE, the Investigator will follow each participant‘s medical progress. Follow up information on an SAE should be reported to the ACCORD office.

AEs still present in participants at the last study visit should be monitored until resolution of the event or until no longer medically indicated.

PREGNANCY

Woman of child bearing potential (including pregnant woman) will not be enrolled into the trial.

TRIAL MANAGEMENT AND OVERSIGHT ARRANGEMENTS

PROJECT MANAGEMENT GROUP

The trial will be coordinated by a Project Management Group, consisting of the Trial Investigators, Trial Research Fellow, Trial Research Nurse, Trial Manager and Data Manager.

TRIAL MANAGEMENT

A Trial Manager and Trial Research Fellow will oversee the study and will be accountable to the Chief Investigator. The Trial Manager will be responsible for checking the CRFs for completeness, plausibility and consistency. Any queries will be resolved by the Investigator or delegated member of the trial team.

A Delegation Log will be prepared, detailing the responsibilities of each member of staff working on the trial.

CENTRAL TRIAL OFFICE

The Central Trial Office is based in the Edinburgh Clinical Trials Unit. The office will be responsible for randomisation, collection of data in collaboration with the research nurses, data processing and analysis.

Publication and dissemination of the study results will be coordinated by “Trial Research Fellow,” in collaboration with the Chief Investigator and other Investigators.

TRIAL STEERING COMMITTEE

A Trial Steering Committee (TSC) will consist of an independent cardiologist, cardiothoracic surgeon and clinical academic together with the trial management group Dr Peter Henriksen, Professor Newby, Dr Shirjel Alam, and the trial manager. Responsibility for calling and organising trial steering committee meetings will lie with the principal investigator, and at least one meeting will be convened midway through the trial.

DATA MONITORING COMMITTEE

An independent Data Monitoring Committee (DMC) will be established to oversee the safety of subjects in the trial. This will include an independent statistician, cardiologist and clinical pharmacologist. At least one meeting will be convened, which will take place after 40 trial participants have completed.

INSPECTION OF RECORDS

Principal Investigators and institutions involved in the study will permit trial related monitoring, audits, REC review, and regulatory inspection(s). In the event of an audit, the Investigator agrees to allow the Sponsors, representatives of the Sponsors or regulatory authorities direct access to all study records and source documentation.

STUDY MONITORING

The ACCORD (joint office for University of Edinburgh and Lothian Health Board) Clinical Trials Monitor or an appointed local monitor will visit the Edinburgh study site prior to the start of the study and during the course of the study.

RISK ASSESSMENT

This will be carried out by the ACCORD Clinical Trials Monitor to provide risk assessment analysis and will follow an agreed plan as agreed by the sponsor. An independent risk assessment will also be carried out by the ACCORD Quality Assurance to determine if an audit(s) should be performed before/during/after the study.

Potential Risks

There were no specific toxicities identified from a phase I trial. There is theoretical risk of anaphylaxis, and extravasations of the infusion via a central venous cannula. There are very low risks associated with MRI scanning and the use of Feraheme and gadolinium contrast (see section 10.2).

Minimising Risk

The patient will be invasively monitored by the anaesthetic, surgical and nursing staff during the operation (when Elafin/placebo is being infused) and in the subsequent cardiac intensive care stay.

GOOD CLINICAL PRACTICE MODULE

ETHICAL CONDUCT OF THE STUDY

The study will be conducted in accordance with the principles of the International Conference on Harmonisation Tripartite Guideline for Good Clinical Practice (ICH GCP).

A favourable ethical opinion will be obtained from the appropriate REC and local R&D approval will be obtained prior to commencement of the study.

REGULATORY COMPLIANCE THE STUDY

The study will not commence until a Clinical Trial Authorisation (CTA) is obtained from the MHRA. The protocol and study conduct will comply with the Medicines for Human Use (Clinical Trials) Regulations 2004, and any relevant amendments.

INVESTIGATOR RESPONSIBILITIES

The Investigator is responsible for the overall conduct of the study at the site and compliance with the protocol and any protocol amendments. In accordance with the principles of ICH GCP, the following areas listed in this section are also the

responsibility of the Investigator. Responsibilities may be delegated to an appropriate member of study site staff. Delegated tasks will be documented on a delegation log and signed by those named on the list.

Informed Consent

The Investigator is responsible for ensuring informed consent is obtained before any protocol specific procedures are carried out. The decision of a participant to participate in clinical research is voluntary and should be based on a clear understanding of what is involved.

Participants will receive adequate oral and written information –participant information and informed consent forms will be provided. The oral explanation to the participant will be performed by the Investigator or designated person, and must cover all the elements specified in the participant information sheet/informed consent.

The participant must be given every opportunity to clarify any points they do not understand and, if necessary, ask for more information. The participant will be given sufficient time to consider the information provided. It will be emphasised that the participant may withdraw their consent to participate at any time without loss of benefits to which they otherwise would be entitled.

The participant should be informed and agree to their medical records being inspected by regulatory authorities but understand that their name will not be disclosed outside the hospital.

The Investigator or delegated member of the trial team and the participant will sign and date the informed consent form(s) to confirm that consent has been obtained. The participant should receive a copy of this document and a copy filed in the Investigator Site File (ISF).

Study Site Staff

The Investigator will be familiar with the IMP, protocol and the study requirements. It is the Investigator's responsibility to ensure that all staff assisting with the study are adequately informed about the IMP, protocol and their trial related duties.

Data Recording

The Investigator is responsible for the quality of the data recorded in the CRF.

Investigator Documentation

Prior to beginning the study, each Investigator will provide the following documents to ECTU, including but not limited to:

An original signed Investigator's Declaration (as part of the Clinical Trial Agreement documents);

Curriculum vitae (CV), signed and dated by the Investigator indicating that it is accurate and current.

ECTU will ensure all other documents required by ICH GCP are retained in a Trial Master File and that appropriate documentation is available in local ISFs.

GCP Training

All study staff will hold evidence of appropriate GCP training or undergo GCP training. This should be updated every two years throughout the trial.

Confidentiality

All laboratory specimens, evaluation forms, reports, and other records will be identified in a manner designed to maintain participant confidentiality. All records will be kept in a secure storage area with limited access. Clinical information will not be released without the written permission of the participant, except as necessary for monitoring and auditing by the Sponsor, its designee, Regulatory Authorities, or the REC. The Investigator and study site staff involved with this study may not disclose or use for any purpose other than performance of the study, any data, record, or other unpublished, confidential information disclosed to those individuals for the purpose

of the study. Prior written agreement from the Sponsor or its designee must be obtained for the disclosure of any said confidential information to other parties.

Data Protection

All Investigators and study site staff involved with this study will comply with the requirements of the Data Protection Act 1998 with regard to the collection, storage, processing and disclosure of personal information and will uphold the Act's core principles. Access to collated participant data will be restricted to those clinicians treating the participants.

Computers used to collate the data will have limited access measures via user names and passwords.

Published results will not contain any personal data that could allow identification of individual participants.

STUDY CONDUCT RESPONSIBILITIES

PROTOCOL AMENDMENTS

Any changes in research activity, except those necessary to remove an apparent, immediate hazard to the participant, must be reviewed and approved by the Chief Investigator. Amendments to the protocol must be submitted in writing to the appropriate REC, Regulatory Authority and local R&D for approval prior to participants being enrolled into an amended protocol.

PROTOCOL VIOLATIONS AND DEVIATIONS

The Investigator should not implement any deviation from the protocol without agreement from the Chief Investigator and appropriate REC, Regulatory Authority and R&D approval except where necessary to eliminate an immediate hazard to trial participants.

In the event that an Investigator needs to deviate from the protocol, the nature of and reasons for the deviation should be recorded in the CRF. If this necessitates a subsequent protocol amendment, this should be submitted to the REC, Regulatory Authority and local R&D for review and approval if appropriate.

STUDY RECORD RETENTION

All study documentation will be kept for 15 years.

END OF STUDY

The end of study is defined as the last participant's last visit.

The Investigators and/or the trial steering committee have the right at any time to terminate the study for clinical or administrative reasons.

The end of the study will be reported to the REC and Regulatory Authority within 90 days, or 15 days if the study is terminated prematurely. The Investigators will inform participants and ensure that the appropriate follow up is arranged for all involved.

A summary report of the study will be provided to the REC and Regulatory Authority within 1 year of the end of the study.

CONTINUATION OF DRUG FOLLOWING THE END OF STUDY

The study drug will not be continued at the end of the study. The efficacy of the medication surrounds its ability to attenuate cardiac injury and inflammation at the time of cardiac bypass.

REPORTING, PUBLICATIONS AND NOTIFICATION OF RESULTS

AUTHORSHIP POLICY

Ownership of the data arising from this study resides with the study team. On completion of the study, the study data will be analysed and tabulated, and a clinical study report will be prepared in accordance with ICH guidelines.

PUBLICATION

The clinical study report will be used for publication and presentation at scientific meetings. Investigators have the right to publish orally or in writing the results of the study.

Summaries of results will also be made available to Investigators for dissemination within their clinics (where appropriate and according to their discretion).

REFERENCES

(1) Croal BL, Hillis GS, Gibson PH, Fazal MT, El-Shafei H, Gibson G et al. Relationship between postoperative cardiac troponin I levels and outcome of cardiac surgery. *Circulation* 2006; 114(14):1468-1475.

(2) Hausenloy DJ, Mwamure PK, Venugopal V, Harris J, Barnard M, Grundy E et al. Effect of remote ischaemic preconditioning on myocardial injury in patients undergoing coronary artery bypass graft surgery: a randomised controlled trial. *Lancet* 2007; 370(9587):575-579.

(3) Hansen PR. Role of neutrophils in myocardial ischemia and reperfusion. *Circulation* 1995; 91(6):1872-1885.

(4) Romson JL, Hook BG, Kunkel SL, Abrams GD, Schork MA, Lucchesi BR. Reduction of the extent of ischemic myocardial injury by neutrophil depletion in the dog. *Circulation* 1983; 67(5):1016-1023.

(5) Tiefenbacher CP, Ebert M, Niroomand F, Batkai S, Tillmanns H, Zimmermann R et al. Inhibition of elastase improves myocardial function after repetitive ischaemia and myocardial infarction in the rat heart. *Pflugers Arch* 1997; 433(5):563-570.

(6) Ohta K, Nakajima T, Cheah AY, Zaidi SH, Kaviani N, Dawood F et al. Elafin-overexpressing mice have improved cardiac function after myocardial infarction. *Am J Physiol Heart Circ Physiol* 2004; 287(1):H286-H292.

(7) Mariani M, Fetiveau R, Rossetti E, Poli A, Poletti F, Vandoni P et al. Significance of total and differential leucocyte count in patients with acute myocardial infarction treated with primary coronary angioplasty. *Eur Heart J* 2006; 27(21):2511-2515.

(8) Doherty DE, Downey GP, Worthen GS, Haslett C, Henson PM. Monocyte retention and migration in pulmonary inflammation. Requirement for neutrophils. *Lab Invest* 1988; 59(2):200-213.

(9) Soehnlein O, Zernecke A, Eriksson EE, Rothfuchs AG, Pham CT, Herwald H et al. Neutrophil secretion products pave the way for inflammatory monocytes. *Blood* 2008; 112(4):1461-1471.

(10) Territo MC, Ganz T, Selsted ME, Lehrer R. Monocyte-chemotactic activity of defensins from human neutrophils. *J Clin Invest* 1989; 84(6):2017-2020.

(11) Soehnlein O, Zernecke A, Eriksson EE, Rothfuchs AG, Pham CT, Herwald H et al. Neutrophil secretion products pave the way for inflammatory monocytes. *Blood* 2008; 112(4):1461-1471.

(12) Nahrendorf M, Swirski FK, Aikawa E, Stangenberg L, Wurdinger T, Figueiredo JL et al. The healing myocardium sequentially mobilizes two monocyte subsets with divergent and complementary functions. *J Exp Med* 2007; 204(12):3037-3047.

(13) Maekawa Y, Anzai T, Yoshikawa T, Asakura Y, Takahashi T, Ishikawa S et al. Prognostic significance of peripheral monocytosis after reperfused acute

myocardial infarction:a possible role for left ventricular remodeling. *J Am Coll Cardiol* 2002; 39(2):241-246.

(14) Faymonville ME, Pincemail J, Duchateau J, Paulus JM, Adam A, Deby-Dupont G et al. Myeloperoxidase and elastase as markers of leukocyte activation during cardiopulmonary bypass in humans. *J Thorac Cardiovasc Surg* 1991; 102(2):309-317.

(15) Day JR, Taylor KM. The systemic inflammatory response syndrome and cardiopulmonary bypass. *Int J Surg* 2005; 3(2):129-140.

(16) Quaniers JM, Leruth J, Albert A, Limet RR, Defraigne JO. Comparison of inflammatory responses after off-pump and on-pump coronary surgery using surface modifying additives circuit. *Ann Thorac Surg* 2006; 81(5):1683-1690.

(17) Williams SE, Brown TI, Roghanian A, Sallenave JM. SLPI and elafin: one glove, many fingers. *Clin Sci (Lond)* 2006; 110(1):21-35.

(18) Henriksen PA, Hitt M, Xing Z, Wang J, Haslett C, Riemersma RA et al. Adenoviral gene delivery of elafin and secretory leukocyte protease inhibitor attenuates NF-kappa B-dependent inflammatory responses of human endothelial cells and macrophages to atherogenic stimuli. *J Immunol* 2004; 172(7):4535-4544.

(19) Butler MW, Robertson I, Greene CM, O'Neill SJ, Taggart CC, McElvaney NG. Elafin prevents lipopolysaccharide-induced AP-1 and NF-kappaB

activation via an effect on the ubiquitin-proteasome pathway. *J Biol Chem* 2006; 281(46):34730-34735.

(20) Crinnion JN, Homer-Vanniasinkam S, Hatton R, Parkin SM, Gough MJ. Role of neutrophil depletion and elastase inhibition in modifying skeletal muscle reperfusion injury. *Cardiovasc Surg* 1994; 2(6):749-753.

(21) Mentzer RM, Jr., Bartels C, Bolli R, Boyce S, Buckberg GD, Chaitman B et al. Sodium-hydrogen exchange inhibition by cariporide to reduce the risk of ischemic cardiac events in patients undergoing coronary artery bypass grafting: results of the EXPEDITION study. *Ann Thorac Surg* 2008; 85(4):1261-1270.

(22) Tassani P, Augustin N, Barankay A, Braun SL, Zaccaria F, Richter JA. High-dose aprotinin modulates the balance between proinflammatory and anti-inflammatory responses during coronary artery bypass graft surgery. *J Cardiothorac Vasc Anesth* 2000; 14(6):682-686.

(23) Trivedi RA, King-Im JM, Graves MJ, Cross JJ, Horsley J, Goddard MJ et al. In vivo detection of macrophages in human carotid atheroma: temporal dependence of ultrasmall superparamagnetic particles of iron oxide-enhanced MRI. *Stroke* 2004; 35(7):1631-1635.

(24) Bernd H, De KE, Gaillard S, Bonnemain B. Safety and tolerability of ultrasmall superparamagnetic iron oxide contrast agent: comprehensive analysis of a clinical development program. *Invest Radiol* 2009; 44(6):336-342.

(25) Steuer J, Bjerner T, Duvernoy O, Jideus L, Johansson L, Ahlstrom H et al. Visualisation and quantification of peri-operative myocardial infarction after coronary artery bypass surgery with contrast-enhanced magnetic resonance imaging. *Eur Heart J* 2004; 25(15):1293-1299.

(26) Roques F, Michel P, Goldstone AR, Nashef SA. The logistic EuroSCORE. *Eur Heart J* 2003; 24(9):881-882.

Appendix E: USPIO IN MYOCARDIAL INFARCTION PUBLICATION

Journal: Circulation: Cardiovascular Imaging

DOI: 10.1161/CIRCIMAGING.112.974907

Published: 8th August, 2012

ORIGINAL ARTICLE

ULTRASMALL SUPERPARAMAGNETIC PARTICLES OF IRON OXIDE IN PATIENTS WITH ACUTE MYOCARDIAL INFARCTION

EARLY CLINICAL EXPERIENCE

Shirjel R Alam MD,[1] Anoop S V Shah MD,[1] Jennifer Richards MD,[1,2] Ninian N Lang MD PhD,[1,3] Gareth Barnes MD,[1] Nikhil Joshi MD,[1] Tom MacGillivray PhD,[4] Graham McKillop MD,[4,5] Saeed Mirsadraee MD PhD,[4,5] John Payne MD,[6] Keith A A Fox MD,[1,3] Peter Henriksen MD PhD,[1,3] *David E Newby MD PhD,[1,3,4] *Scott I K Semple PhD.[1,4]

[1]Centre of Cardiovascular Science, University of Edinburgh

[2]Department of Vascular Surgery, Royal infirmary of Edinburgh

[3]Department of Cardiology, Royal Infirmary of Edinburgh

[4]Clinical Research Imaging Centre, University of Edinburgh

[5]Department of Radiology, Royal Infirmary of Edinburgh

[6] Scottish National Advanced Heart Failure Service, Golden Jubilee National Hospital

*Equal contribution

Corresponding Author

Shirjel R Alam MB ChB MRCP(Ed), MRCS(Ed), MRCA

Centre for Cardiovascular Science,

The University of Edinburgh,

The Chancellor's Building,

Little France Crescent,

Edinburgh EH16 5SA

s.r.alam@sms.ed.ac.uk

Tel: 0131 242 6515

Support: Dr Shirjel Alam was supported by a Scholarship grant from the British Heart Foundation.

Word count:	**2850**	**Figures and tables:**	3 figures & 1 table
			2 supplemental figures 2 tables
Abstract:	**250**	**References:**	**28**

Subject Codes: [4] [30] [124]

Abstract

Background: Inflammation following acute myocardial infarction has detrimental effects on reperfusion, myocardial remodelling and ventricular function. Magnetic resonance imaging using ultrasmall superparamagnetic particles of iron oxide (USPIO) can detect cellular inflammation in tissues, and we therefore explored its role in acute myocardial infarction in humans.

Methods: Sixteen patients within five days of ST-segment elevation myocardial infarction underwent 3 sequential magnetic resonance scans at -1, 24 and 48 h following no infusion (controls; n=6) or intravenous infusion of USPIO (n=10; 4 mg/kg). T2*-weighted multi-gradient-echo sequences were acquired and R2* values calculated for specific regions of interest.

Results: In the control group, R2* remained constant in all tissues throughout all scans with excellent repeatability (bias of -0.208, s^{-1}, coefficient of repeatability of 26.96, s^{-1}; intra-class coefficient 0.989). Consistent with uptake by the reticuloendothelial system, R2* increased in the liver (84±49.5 to 319±70.0 s^{-1}; $p<0.001$) but was unchanged in skeletal muscle (54±8.4 to 67.0±9.5 s^{-1}; $p>0.05$) 24 hours after USPIO administration. In the myocardial infarct, R2* increased from 41.0±12.0 (baseline) to 155±45.0 ($p<0.001$) and 124±35.0 s^{-1} ($p<0.05$) at 24 and 48 h respectively. A similar but lower magnitude response was seen in the remote myocardium from 39±3.2 to 80±14.9 ($p<0.001$) and 67.0±15.7 s^{-1} ($p<0.05$) respectively.

Conclusion: Following acute myocardial infarction, USPIO uptake occurs with the infarcted and remote myocardium. This technique holds major promise as a potential method of assessing cellular myocardial inflammation and left ventricular remodelling that may have a range of applications in patients with myocardial infarction and other inflammatory cardiac conditions.

Clinical Trial Registration Information:

http://clinicaltrials.gov/ct2/show/NCT01323296

Unique Identifier - NCT01323296
Other Study ID (NHS Research Ethic Committee) - 10/S1103/50

Key Words: Myocardial Infarction, Inflammation, Magnetic Resonance, USPIO

Introduction

Inflammation occurs in the acutely infarcted myocardium in order to remove necrotic cellular debris and allow tissue remodelling. Excessive inflammation may follow reperfusion therapy, and can have detrimental effects on healing and left ventricular remodelling.(Nahrendorf et al., 2010) With the aim of improving outcomes following acute myocardial infarction, novel drugs are increasingly focusing on optimisation of myocardial repair and regeneration, and include anti-inflammatory interventions.(Bonvini et al., 2005, Frangogiannis, 2006, Gonzalez et al., 2011, Steffens et al., 2009) There is therefore a need for non-invasive methods to assess *in vivo* myocardial inflammation following myocardial infarction both to define the healing process and to measure the potential efficacy of novel therapeutic interventions.

Magnetic resonance imaging is ideally suited for the serial examination of the heart as it is non-invasive, does not involve ionizing radiation and has excellent soft tissue contrast and spatial resolution. Cardiac magnetic resonance, using T2-weighted imaging, has previously been used to detect myocardial edema associated with myocardial infarction as it may help delineate the “area at risk” from the infarcted region.(Garcia-Dorado et al., 1993) However there are major differences in the diagnostic performance of edema imaging and there have been conflicting results regarding its utility as a prognostic marker or guide to therapeutic intervention.(Viallon et al., 2012) (Eitel et al., 2010, Larose et al., 2010) One explanation for this is that magnetic resonance imaging of edema does not directly assess the more dynamic cellular inflammatory processes.

Iron oxide particles can be used as a contrast medium in magnetic resonance imaging since they alter the T2* relaxation time of tissues in which they accumulate. Ultrasmall superparamagnetic particles of iron oxide (USPIO) are taken up by cells of the liver, spleen, bone marrow and lymph nodes. As a result of their small size (approximately 30 nm) they extravasate freely through capillaries and are phagocytosed by tissue-resident inflammatory cells of the reticuloendothelial system.(Ruehm et al., 2001b) These cells are predominately macrophages, but neutrophils may also take up USPIOs.(Dousset et al., 1999, Gellissen et al., 1999a) We have recently established that USPIOs can be used to assess vascular cellular inflammation in patients with abdominal aortic aneurysms.(Richards et al., 2011a) Histological examination of aneurysm tissue confirmed co-localization and uptake of USPIO in areas with macrophage infiltration and mural USPIO uptake was associated with a 3-fold increase in the rate of abdominal aortic aneurysm expansion.(Richards et al., 2011a) T2*-weighted MRI has been validated as a method of detecting hepatic and myocardial iron accumulation in patients with thalassemia and transfusion-related iron overload, and this method could be adapted for the detection of focal USPIO accumulation.(Anderson et al., 2001, Westwood et al., 2005)

We hypothesised that we could use USPIO to track inflammatory cell infiltration within the myocardium of patients who had recently sustained an acute myocardial infarction. The aims of the study were therefore to investigate the proof-of-principle that USPIO could be used to assess cellular myocardial inflammation following acute myocardial infarction in humans.

Methods

Subjects

This study was an open-label pilot proof-of-concept study in 16 patients who suffered a recent myocardial infarction. Inclusion criteria were age 18-80 years, recent (within 48 h) myocardial infarction defined by the universal definition of myocardial infarction and plasma troponin I concentration in excess of 10 µg/L at 12 h from the onset of chest pain (Thygesen et al., 2007a). Exclusion criteria were known critical stenosis (≥95%) of left main stem, ongoing symptoms of unstable angina, atrial fibrillation, heart failure (Killip class ≥II), hepatic failure (Childs-Pugh grade B or C) or renal failure (estimated glomerular filtration rate <25 mL/min), contraindication to magnetic resonance imaging, past history of systemic iron overload or hemochromatosis, and patients with known allergy to dextran- or iron-containing compounds.

All patients suffered an acute ST-elevation myocardial infarction. One patient in each group received thrombolytic therapy with tenecteplase, followed by percutaneous coronary angioplasty and stent placement. One patient in the control group re-perfused spontaneously followed by percutaneous coronary angioplasty and stent placement. All other patients were treated by primary percutaneous coronary intervention.

All patients gave written informed consent and the study was conducted with the approval of the local research ethics committee.

Ultrasmall superparamagnetic particles of iron oxide

Intravenous infusion of USPIO was performed immediately following the initial baseline magnetic resonance scan. USPIO (Ferumoxytol; Advanced Magnetics Inc, Cambridge, MA) was administered via a peripheral venous cannula at a dose of 4 mg/kg at a rate of up to 1 mL/s. Hemodynamic and electrocardiographic monitoring was conducted throughout.

Magnetic Resonance Imaging

Sequential imaging was performed at baseline (24-72 h after admission), and 24 and 48 h thereafter. In 10 patients, USPIO was administered immediately after the baseline scan. Six patients received no infusion and acted as control subjects. Magnetic resonance imaging was performed using a combination of body matrix and spine coil matrix coil elements of a 3-tesla Verio scanner (Siemens Medical, Germany). Standard cardiac breath-held ECG-gated true-FISP sequences were used to acquire vertical long axis, horizontal long axis and short axis views of the heart. USPIO imaging was performed using established T2*-weighted multi-gradient-echo sequences, breath-held and cardiac-gated after a volumetric shim had been applied over the entire heart volume. Standard cardiac slice width (6 mm width with 4 mm gap) and echo times (2.1-17.1 ms range) with matrix size of 256x115. The in-plane resolution differed as required for larger or smaller objects, generally a field of view of 400x300 was used with an in-plane resolution of 2.6x1.6. Quantitative analysis of USPIO accumulation was achieved by calculation of T2* relaxation times before and after administration of USPIO.(Richards et al., 2011a) In order to optimise image analysis and prevent degradation due to “T2*-blooming” artefacts, USPIO images

were quantitatively analysed using a susceptibility gradient mapping post-processing technique previously used in SPIO imaging to quantitate USPIO accumulation using changes in calculated T2* relaxation times.(Dahnke et al., 2008)

Immediately after the baseline T2*-weighted scan, breath-held inversion recovery sequences in the short-axis, and horizontal and vertical long-axis planes were used to acquire late enhancement images 10-15 min following an intravenous administration of gadolinium contrast agent (0.2 mmol/kg; Gadovist, Bayer Plc, Germany). Optimal TI was determined on a slice-by-slice basis using standard late enhancement protocols. The inversion recovery late enhancement short axis slices were acquired with the same slice position as the short axis T2*-weighted slices. The T2*-weighted short-axis acquisitions included views through the liver and spleen, and allowed quantification of USPIO uptake within the reticuloendothelial system via changes in these tissues' R2* value.

Image Analysis

Late enhancement analysis was performed using QMass software (Medis medical imaging systems, Netherlands), allowing quantification of infarct size and location for correlation with USPIO-related signal changes.

Baseline, and 24 and 48 h T2*-weighted multi-gradient-echo images for each patient were spatially co-registered using ANALYZE software (AnalyzeDirect Software, United States). The four echoes (TE = 2.13, 4.27, 6.41, 8.55 ms) in a multi-echo T2*-weighted sequence were combined to generate a T2* map, in which the data represented the T2* value (S(t) = S(0)exp- (t/T2*)) for each voxel. This was

achieved using in-house software developed in Matlab (Mathworks, US). The T2* value is the decay constant for the exponential decay of signal intensity with time. In the presence of USPIO, the signal decays more rapidly due to local field inhomogeneities and the T2* value is reduced. A 3x3 voxel Gaussian filter was applied to the individual echoes to reduce noise. By minimising the sum of the squares of errors between the data and an exponential function, the decay constant (i.e. T2*) was obtained. An experimentally determined threshold for the co-efficient of determination ($r2>0.85$) was used to exclude data that did not have an acceptable exponential decay when SI was plotted against echo time. The inverse of T2*, R2*, was then calculated to assess USPIO uptake. In our laboratory, we have previously assessed the repeatability of the measurement of the R2* value by comparing data from two T2*W sequences (run 1 *versus* run 2) performed in quick succession without moving the patient. This was performed on a voxel-by-voxel basis with a total of 32,936 data points, of which 1.2% were affected by artifact and discarded. Using the Bland and Altman method,[18] there was no evidence of mean difference ($0.99\pm21.9\ s^{-1}$) with a coefficient of repeatability of $42.9\ s^{-1}$.

The transformation matrix of the co-registration was then applied to the subsequent T2*-weighted echoes and R2* was calculated on a voxel-by-voxel basis to generate co-registered R2* 'maps' at baseline, and 24 and 48 h. The late enhancement short-axis images were also spatially co-registered with the R2* images for each visit in case of lack of reproducibility of patient breath-holding between scans. Regions of interests (ROIs) were selected on the late enhancement images and applied to the co-registered R2* maps corresponding to: (i) micro-vascular obstruction if present, (ii)

infarct area (defined by late gadolinium enhancement), (iii) peri-infarct area (adjacent to late gadolinium enhancement), (iv) myocardium remote from the infarct zone (distant from late gadolinium enhancement), (v) skeletal muscle, (vi) blood pool, (vii) liver and (viii) spleen (Figure 1). The ROIs were mapped to the first T2* echo before being applied to R2* maps to ensure there was coherence to the corresponding areas on all 3 scans, and no overlap with the blood pool or extra-cardiac structures. Two investigators created and quantified ROIs for all scans independently in order to assess reproducibility of the technique.

Statistical Analysis

All statistical analysis was performed with GraphPad Prism version 4.00 (GraphPad Software, San Diego California USA), except the Intraclass Correlation (ICC) which was performed with SPSS (IBM Version 20.0.0, USA) using a one-way random effects model. Repeatability was assessed by the method of Bland and Altman and coefficient of repeatability defined as twice the standard deviation of the mean of the differences.(Bland and Altman, 1986) Patient characteristics (Table 1) were compared using unpaired non-parametric Mann-Whitney test. R2* values at baseline, 24 hours and 48 hours for each ROI were compared using repeated measure one-way ANOVA (Friedman test). If significant, Dunn's multiple comparison post-test was performed comparing R2* value at baseline to 24 hours, and baseline to 48 hours. Statistical significance was defined as two-sided $P<0.05$.

Results

All patients sustained an acute myocardial infarction with a substantial area of myocardial necrosis (Table 1). All patients underwent three scans (baseline, and 24 and 48 h) including T2*-weighted multi-gradient-echo sequences and late gadolinium enhancement. Late enhancement reconfirmed myocardial infarction in all patients.

Repeatability

Data from patients who did not receive USPIO administration were used to assess any potential changes in R2* attributable to acute myocardial infarction alone. There were no changes in R2* value within the myocardium or the infarct zone itself (Figures 2 and 3; on-line data supplement Table S1; $p>0.05$). Similar findings were also observed in other organs such as the liver, spleen and skeletal muscle. Moreover, we were able to demonstrate excellent repeatability for the assessment of R2* value with a mean bias of -0.208,s^{-1}, coefficient of repeatability of 26.96 s^{-1} and intra-class coefficient 0.989 (on-line data supplement Figure S1).

Effect of USPIO Administration

All patients tolerated the infusions well with no significant adverse events or arrhythmia. In the area of myocardial infarction, R2* increased from 41.0±12.0 s^{-1} at baseline to 155±45.0 ($p<0.001$) and 124±35.0 s^{-1} ($p<0.05$) at 24 and 48 h respectively following USPIO administration (Figures 2 and 3). Although more modest, the

remote non-infarcted myocardium also demonstrated an increase from a baseline of 39.0±3.2 to 80.0±14.9 ($p<0.001$) and 67.0±15.7 s^{-1} ($p<0.05$) at 24 and 48 h respectively (Figures 2 and 3; online data supplement Table S2).

To determine whether there was a non-specific effect of USPIO enhancing R2* values in muscle, we assessed regions of interest within skeletal muscle. We were able to confirm that there was no change in R2* value of skeletal muscle (Figures 2 and 3; online data supplement Table S2). Given that USPIO are taken up by cells of the reticuloendothelial system, both the liver and spleen were expected to develop marked changes in R2* values and act as positive controls. In the liver, there was a large increase in R2* from 84.0±49.5 s^{-1} at baseline to 319±70.0 ($p<0.001$) and 243.0±63.6 s^{-1} ($p<0.001$) at 24 and 48 h respectively following USPIO administration. A similar pattern was also seen in the spleen (online data supplement Table S2).

Discussion

For the first time, we have demonstrated that USPIO are taken up into the myocardium of patients with a recent myocardial infarction. The increase of R2* by USPIO was highest within infarcted tissue, although we did observe a more modest increase within myocardium remote from the site of infarction. This suggests early macrophage and inflammatory cell infiltration predominantly occurs within the infarcted myocardium but appears to be associated with a more global influx of these cells that extends beyond the area at risk. However no histological quantification of macrophage infiltration was performed, and so the degree of inflammation cannot be correlated to MRI changes. Our preliminary findings need further confirmation in larger cohorts but this technique does appear to hold major promise in the investigation of myocardial inflammation following myocardial infarction and could be applied to other inflammatory cardiac diseases such as cardiac sarcoidosis, myocarditis or transplant rejection.

USPIO are actively taken up by inflammatory phagocytic cells, especially macrophages. They have been used to explore a number of inflammatory conditions including atherosclerotic plaques and abdominal aortic aneurysms.(Kooi et al., 2003b, Trivedi et al., 2006b) (Richards et al., 2011a) Histological examination of excised clinical tissue has confirmed co-localisation of USPIO with macrophages.(Kooi et al., 2003b, Trivedi et al., 2006b, Schmitz et al., 2001, Ruehm et al., 2001b) More specifically, pre-clinical models have demonstrated the uptake of magnetic nanoparticles into macrophages of infarcted myocardium by both fluorescence microscopy and immunohistochemistry.(Sosnovik et al., 2007) We

were unable to obtain tissue confirmation of USPIO uptake into macrophages in our cohort of patients. It is possible that other cell types with phagocytic capacity such as neutrophils may contribute to the increase in R2* value.(Gellissen et al., 1999a) However, we have no reason to believe that uptake would differ from previous studies and, indeed, phagocytosis into macrophages is 4-6 times greater with ferumoxytol than with ferumoxtran-10, a previously used USPIO agent.(Yancy et al., 2005) Moreover, we have demonstrated that organs of the reticuloendothelial system, such as the liver and spleen, demonstrate marked increases in R2* consistent with monocyte and macrophage uptake.

Data have also demonstrated increased numbers of macrophages in the myocardium remote from the area of infarction both in murine models and autopsies of patients who have died from myocardial infarction.(Lee et al., 2012) Expression of cytokines is not confined to the infarct or peri-infarct zone, but is also expressed by myocardium remote from the infarct.(Irwin et al., 1999) Furthermore, when myocardial infarction is induced in an abdominal heterotopic transplanted rodent heart, the native heart demonstrates a decrease in left ventricular (LV) fractional shortening and increased in LV end-diastolic dimension accompanied by increased TNF-α.(Nakamura et al., 2003) Thus the post-infarct inflammatory process may induce cytokine production and inflammatory cell infiltration in remote "normal myocardium". We found an almost three-fold increase in R2* in remote myocardium. However, this may have been to USPIO within the blood pool altering R2* when perfusing the myocardium. This does seem to be the case when imaging 24 hours post USPIO infusion (see Chapter 5: page 108). However, if imaging took

place after the blood pool of USPIO was cleared and the flux of monocytes in the myocardium had ceased, it would be possible to investigate the presence of tissue resident macrophages in the remote myocardium. Thus our technique has the potential, pending histo-pathological confirmation, to study macrophage infiltration and myocardial inflammation not just in the area of infarction but throughout the heart. This has potential applications as a method of assessing and monitoring left ventricular inflammation and remodelling following myocardial infarction.

R2* was decreasing in myocardial, splenic and hepatic tissues by 48 h post-infusion. The decrease in R2* in the blood pool is to be expected given efficient USPIO phagocytosis by reticuloendothelial cells leading to rapid clearance.(Yancy et al., 2005) However pre-clinical findings suggest that monocyte tissue residence in infarcted myocardium is brief despite high recruitment rates.(Leuschner et al., 2012) Consistent with this study, we found evidence of high extra-medullary activity in terms of high USPIO uptake in the liver and spleen in contrast with minimal uptake in the bone marrow (on-line data supplement Figure S2). The decrease in R2* value in the splenic tissues at 48 hours may represent mobilisation of the splenic reservoir of monocytes.(Swirski et al., 2009b, Nahrendorf et al., 2010) In addition, the decrease in tissue R2* will reflect clearance of extravasated particles by phagocytic cells through efflux of USPIO laden inflammatory cells. The time course of monocyte and macrophage recruitment into the myocardium is unclear from our study and would require USPIO administration at differing time points following myocardial infarction. This would help define the peak influx and time course of macrophage trafficking into the myocardium.

We have applied this technique to patients who have recently sustained a myocardial infarction. However, this approach could be applied to other cardiac conditions that involve intense inflammatory processes. This could include viral myocarditis, giant cell myocarditis, anthracycline-induced cardiotoxicity and sarcoidosis. Indeed, it may also have a role in detecting cardiac transplant rejection in a non-invasive manner. However, this needs further careful validation in well phenotyped clinical subgroups.

Limitations to our study included the lack of histo-pathological confirmation of macrophage uptake, the longer reperfusion time in the USPIO group potentially resulting in more inflammation and the injection of USPIOs at variable time points post MI. However, given the previous evidence that USPIO are taken up by macrophages, our study provides proof of principle that cellular inflammation may be tracked post myocardial infarction.

In conclusion, we have demonstrated for the first time that USPIO is taken up by the infarct tissue in patients with recent myocardial infarction, and by the peri-infarct and remote myocardium to a lesser degree. Given previous pre-clinical and clinical studies, this is likely to correspond to cellular inflammation. This represents a novel non-invasive method to further study cardiac inflammation and therapeutic interventions. It may also provide prognostic information or provide a diagnostic tool for the investigation of inflammatory cardiac conditions such as myocarditis and transplant rejection, as well as a potential biomarker for therapeutic interventions targeted at improving left ventricular remodelling following infarction.

Acknowledgements

We are grateful to the Wellcome Trust Clinical Research Facility and the Clinical Research Imaging Centre for their help with this study.

Funding Sources

This work and SA, SIKS, KAAF and DEN are supported by the British Heart Foundation (SS/CH/09/002, Centre of Research Excellence Award, CH/09/002). The Wellcome Trust Clinical Research Facility and the Clinical Research Imaging Centre are supported by NHS Research Scotland (NRS) through NHS Lothian. This work was supported by a research agreement with Siemens (Siemens Medical, Germany).

Conflict of Interest Disclosures

None.

References

1. Nahrendorf M, Pittet MJ, Swirski FK. Monocytes: Protagonists of infarct inflammation and repair after myocardial infarction. *Circulation*. 2010;121:2437
2. Bonvini RF, Hendiri T, Camenzind E. Inflammatory response post-myocardial infarction and reperfusion: A new therapeutic target? *European Heart Journal Supplements*. 2005;7:I27-I36
3. Frangogiannis NG. Targeting the inflammatory response in healing myocardial infarcts. *Curr Med Chem*. 2006;13:1877-1893
4. Gonzalez A, Ravassa S, Beaumont J, Lopez B, Diez J. New targets to treat the structural remodeling of the myocardium. *J Am Coll Cardiol*. 2011;58:1833-1843
5. Steffens S, Montecucco F, Mach F. The inflammatory response as a target to reduce myocardial ischaemia and reperfusion injury. *Thromb Haemost*. 2009;102:240-247
6. Garcia-Dorado D, Oliveras J, Gili J, Sanz E, Perez-Villa F, Barrabes J, Carreras MJ, Solares J, Soler-Soler J. Analysis of myocardial oedema by magnetic resonance imaging early after coronary artery occlusion with or without reperfusion. *Cardiovasc Res*. 1993;27:1462-1469
7. Viallon M, Mewton N, Thuny F, Guehring J, O'Donnell T, Stemmer A, Bi X, Rapacchi S, Zuehlsdorff S, Revel D, Croisille P. T2-weighted cardiac mr assessment of the myocardial area-at-risk and salvage area in acute reperfused myocardial infarction: Comparison of state-of-the-art dark blood and bright blood t2-weighted sequences. *J Magn Reson Imaging*. 2012;35:328-339
8. Eitel I, Desch S, Fuernau G, Hildebrand L, Gutberlet M, Schuler G, Thiele H. Prognostic significance and determinants of myocardial salvage assessed by cardiovascular magnetic resonance in acute reperfused myocardial infarction. *J Am Coll Cardiol*. 2010;55:2470-2479

9. Larose E, Rodes-Cabau J, Pibarot P, Rinfret S, Proulx G, Nguyen CM, Dery JP, Gleeton O, Roy L, Noel B, Barbeau G, Rouleau J, Boudreault JR, Amyot M, De Larochelliere R, Bertrand OF. Predicting late myocardial recovery and outcomes in the early hours of st-segment elevation myocardial infarction traditional measures compared with microvascular obstruction, salvaged myocardium, and necrosis characteristics by cardiovascular magnetic resonance. *J Am Coll Cardiol*. 2010;55:2459-2469

10. Ruehm SG, Corot C, Vogt P, Kolb S, Debatin JF. Magnetic resonance imaging of atherosclerotic plaque with ultrasmall superparamagnetic particles of iron oxide in hyperlipidemic rabbits. *Circulation*. 2001;103:415-422

11. Dousset V, Delalande C, Ballarino L, Quesson B, Seilhan D, Coussemacq M, ThiaudiÈre E, Brochet B, Canioni P, CaillÈ JM. In vivo macrophage activity imaging in the central nervous system detected by magnetic resonance. *Magnetic resonance in medicine*. 1999;41:329-333

12. Gellissen J, Axmann C, Prescher A, Bohndorf K, Lodemann KP. Extra- and intracellular accumulation of ultrasmall superparamagnetic iron oxides (uspio) in experimentally induced abscesses of the peripheral soft tissues and their effects on magnetic resonance imaging. *Magn Reson Imaging*. 1999;17:557-567

13. Richards JM, Semple SI, MacGillivray TJ, Gray C, Langrish JP, Williams M, Dweck M, Wallace W, McKillop G, Chalmers RT, Garden OJ, Newby DE. Abdominal aortic aneurysm growth predicted by uptake of ultrasmall superparamagnetic particles of iron oxide: A pilot study. *Circ Cardiovasc Imaging*. 2011;4:274-281

14. Anderson LJ, Holden S, Davis B, Prescott E, Charrier CC, Bunce NH, Firmin DN, Wonke B, Porter J, Walker JM, Pennell DJ. Cardiovascular t2-star (t2*) magnetic resonance for the early diagnosis of myocardial iron overload. *European Heart Journal*. 2001;22:2171-2179

15. Westwood MA, Firmin DN, Gildo M, Renzo G, Stathis G, Markissia K, Vasili B, Pennell DJ. Intercentre reproducibility of magnetic resonance t2* measurements of myocardial iron in thalassaemia. *Int J Cardiovasc Imaging*. 2005;21:531-538

16. Thygesen K, Alpert JS, White HD. Universal definition of myocardial infarction. *Eur Heart J*. 2007;28:2525-2538
17. Dahnke H, Liu W, Herzka D, Frank JA, Schaeffter T. Susceptibility gradient mapping (sgm): A new postprocessing method for positive contrast generation applied to superparamagnetic iron oxide particle (spio)-labeled cells. *Magn Reson Med*. 2008;60:595-603
18. Bland JM, Altman DG. Statistical methods for assessing agreement between two methods of clinical measurement. *Lancet*. 1986;1:307-310
19. Kooi ME, Cappendijk VC, Cleutjens KBJM, Kessels AGH, Kitslaar PJEHM, Borgers M, Frederik PM, Daemen MJAP, van Engelshoven JMA. Accumulation of ultrasmall superparamagnetic particles of iron oxide in human atherosclerotic plaques can be detected by in vivo magnetic resonance imaging. *Circulation*. 2003;107:2453-2458
20. Trivedi RA, Mallawarachi C, U-King-Im J-M, Graves MJ, Horsley J, Goddard MJ, Brown A, Wang L, Kirkpatrick PJ, Brown J, Gillard JH. Identifying inflamed carotid plaques using in vivo uspio-enhanced mr imaging to label plaque macrophages. *Arterioscler Thromb Vasc Biol*. 2006;26:1601-1606
21. Schmitz SA, Taupitz M, Wagner S, Wolf KJ, Beyersdorff D, Hamm B. Magnetic resonance imaging of atherosclerotic plaques using superparamagnetic iron oxide particles. *J Magn Reson Imaging*. 2001;14:355-361
22. Sosnovik DE, Nahrendorf M, Deliolanis N, Novikov M, Aikawa E, Josephson L, Rosenzweig A, Weissleder R, Ntziachristos V. Fluorescence tomography and magnetic resonance imaging of myocardial macrophage infiltration in infarcted myocardium in vivo. *Circulation*. 2007;115:1384-1391
23. Yancy AD, Olzinski AR, Hu TC, Lenhard SC, Aravindhan K, Gruver SM, Jacobs PM, Willette RN, Jucker BM. Differential uptake of ferumoxtran-10 and ferumoxytol, ultrasmall superparamagnetic iron oxide contrast agents in rabbit: Critical determinants of atherosclerotic plaque labeling. *J Magn Reson Imaging*. 2005;21:432-442

24. Lee WW, Marinelli B, van der Laan AM, Sena BF, Gorbatov R, Leuschner F, Dutta P, Iwamoto Y, Ueno T, Begieneman MP, Niessen HW, Piek JJ, Vinegoni C, Pittet MJ, Swirski FK, Tawakol A, Di Carli M, Weissleder R, Nahrendorf M. Pet/mri of inflammation in myocardial infarction. *J Am Coll Cardiol*. 2012;59:153-163

25. Irwin MW, Mak S, Mann DL, Qu R, Penninger JM, Yan A, Dawood F, Wen WH, Shou Z, Liu P. Tissue expression and immunolocalization of tumor necrosis factor-alpha in postinfarction dysfunctional myocardium. *Circulation*. 1999;99:1492-1498

26. Nakamura H, Umemoto S, Naik G, Moe G, Takata S, Liu P, Matsuzaki M. Induction of left ventricular remodeling and dysfunction in the recipient heart after donor heart myocardial infarction: New insights into the pathologic role of tumor necrosis factor-alpha from a novel heterotopic transplant-coronary ligation rat model. *J Am Coll Cardiol*. 2003;42:173-181

27. Leuschner F, Rauch PJ, Ueno T, Gorbatov R, Marinelli B, Lee WW, Dutta P, Wei Y, Robbins C, Iwamoto Y, Sena B, Chudnovskiy A, Panizzi P, Keliher E, Higgins JM, Libby P, Moskowitz MA, Pittet MJ, Swirski FK, Weissleder R, Nahrendorf M. Rapid monocyte kinetics in acute myocardial infarction are sustained by extramedullary monocytopoiesis. *J Exp Med*. 2012;209:123-137

28. Swirski FK, Nahrendorf M, Etzrodt M, Wildgruber M, Cortez-Retamozo V, Panizzi P, Figueiredo JL, Kohler RH, Chudnovskiy A, Waterman P, Aikawa E, Mempel TR, Libby P, Weissleder R, Pittet MJ. Identification of splenic reservoir monocytes and their deployment to inflammatory sites. *Science*. 2009;325:612-616

Table & Figure Legends

Table 1

Characteristics of trial participants.

Figure 1: Object map creation - Following registration with late gadolinium enhancement (LGE) images, an "object map" (OM) was defined from regions of interest of specific tissues and subsections: skeletal muscle (light blue), spleen (dark blue), liver (yellow), blood pool (lilac) and heart subdivided into areas of infarction (red), peri-infarction (white) and remote myocardium (green). The object map was spatially co-registered with the R2* map (R2*) to measure specific R2* values (R2*+OM).

Figure 2: Tissue R2* Values - R2* value in regions of interest from the different tissues in control patients (blue) and patients who received an infusion of ultrasmall supraparamagnetic particles of iron oxide (USPIO; red). Asterisk denotes a significant increase from baseline.

Figure 3: Comparison of R2* colour maps in patients with myocardial infarction at (i) baseline and (ii) 24 hours after no infusion (3A, upper panels) or after an infusion of ultrasmall supraparamagnetic particles of iron oxide (USPIO; 3B, lower panels). R2* values did not change in the liver (blue) or myocardium (remote myocardium, green; infarct, red; microvascular obstruction, purple) of the control patient (3A iii) but did rise in the patient who received USPIOs (3B iii).

Table & Figure Legends for Supplementary Data

Table S1:

R2* value (s^{-1}) in infarct region of interest (ROI) of control patients.

Table S2:

R2* value (s^{-1}) in infarct region of interest (ROI) of patients receiving ultrasmall superparamagnetic particles of iron oxide (USPIO).

Figure S1: Bland-Altman plot - Differences versus average of R2* values in all patients.

Figure S2: Medullary and extramedullary R2* value post myocardial infarction - There is a significant increase in R2* value of hepatic and splenic tissues at 24 hours, that later fall. The R2* value of rib bone marrow does not increase significantly. *P<0.05 versus baseline.

Table 1

	USPIO GROUP	**CONTROL GROUP**	**p Value**
Number	10	6	
Age (yr (range))	52 (38-65)	55 (48-65)	0.5622
Male	10	5	0.1824
WBC ($x10^9$/L)	9.3±2.6	12.7±3.9	0.0934
Risk Factors			
Hypercholesterolemia	5	2	0.5153
Hypertension	4	0	0.7897
Family History of	6	3	0.6963
Diabetes Mellitus	0	0	1.0
Current Smoker (Ex-smoker)	4 (2)	3 (1)	0.6963
Myocardial Infarction			
Time from symptoms to reperfusion (min; mean±SD)	300±218	181±92	0.2198
Plasma Troponin I concentration (µg/L)	33.04±15.5	45.27±10.63	0.1120
Infarct Volume (mL (95% confidence intervals))	35.1 (8.0, 62.2)	43.2 (14.9,71.7)	0.1471

Site of Infarction			
Anterior Infarct	3	3	0.4237
Lateral Infarct	1	3	0.0736
Inferior Infarct	6	0	0.0164
Left Ventricular Variables			
Ejection Fraction (%, mean±SD)	54±15	48 ±11	0.5622
Myocardial Mass (g, mean±SD)	76±19	67± 15	0.3676
Timing of Scanning			
Reperfusion to Baseline Scan (h (mean±SD))	49±30	44±16	0.8749
Reperfusion to Scan 2 (h (mean±SD))	73±30	68±17	0.9578
Reperfusion to Scan 3 (h (mean±SD))	95±30	92±38	0.7925
USPIO Infusion to Scan 2 (h (mean±SD))	22±2	NA	
USPIO Infusion to Scan 3 (h (mean±SD))	44±3	NA	

USPIO – Ultrasmall superparamagnetic particles of iron oxide; CAD – coronary artery disease; SD – standard deviation.

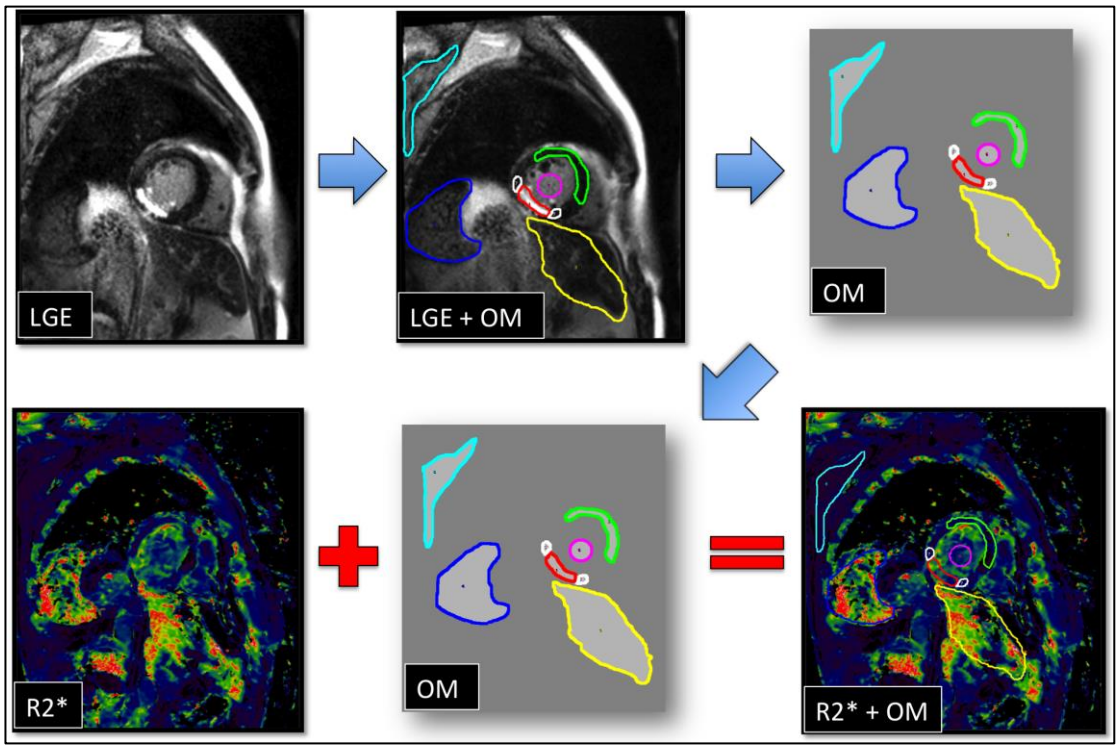

Figure 1

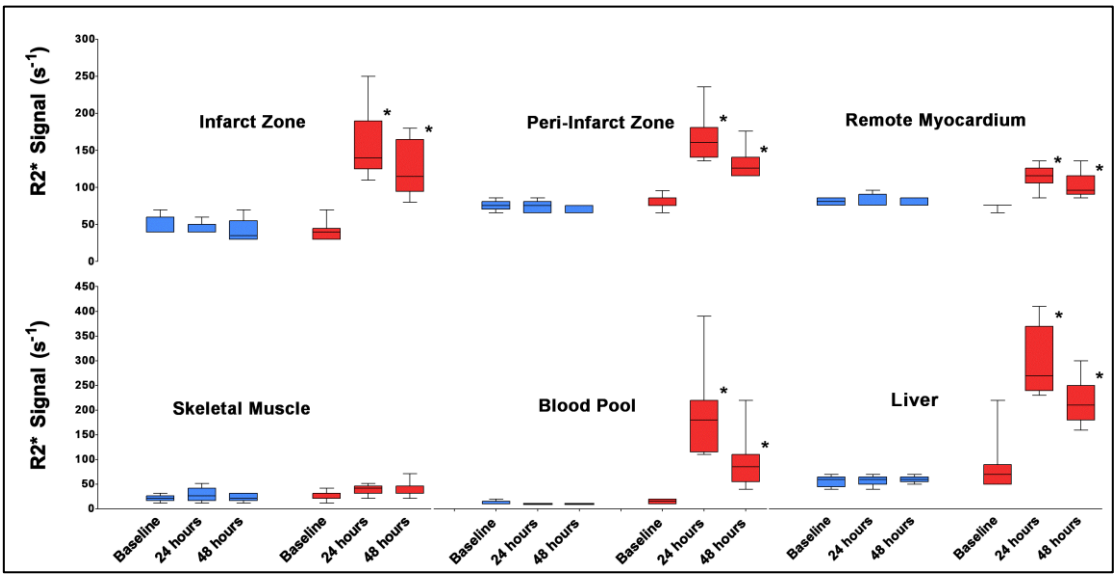
R2* Signal (s-1)
Infarct Zone
Peri-Infarct Zone
Remote Myocardium
Skeletal Muscle
Blood Pool
Liver
Baseline
24 hours
48 hours

Figure 2

Figure 3A

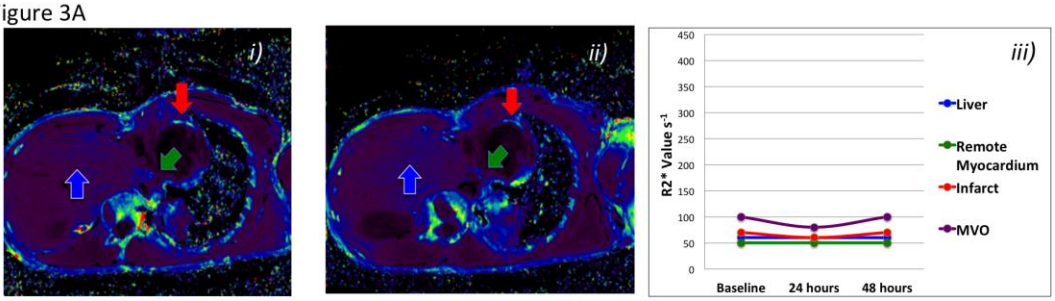

Figure 3B

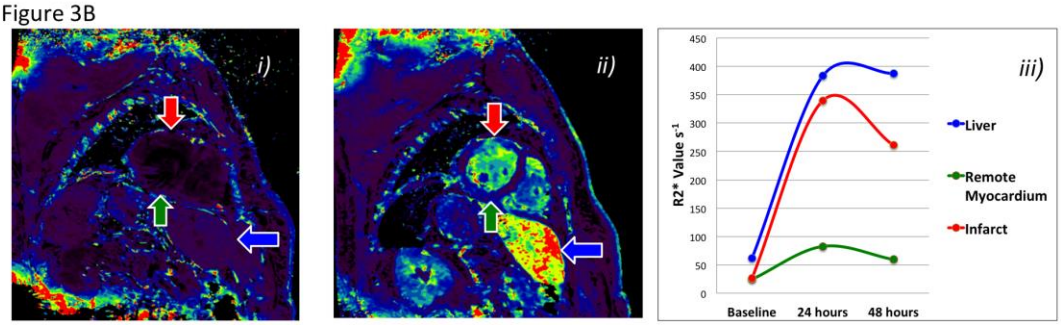

Figure 3

Appendix F: HEART PUBLICATION

Journal: Heart

DOI: 10.1136/heartjnl-2015-307745

Published: 26th August 2015

Perioperative Elafin for ischemia-reperfusion injury during coronary artery bypass graft surgery

A Randomized Controlled Trial

Alam S[1],Lewis SC[2], Zamvar V[3], Pessotto R[3], Dweck MR[1], Krishan A[2], Goodman K[2], Oatey K[2], Harkess R[2], Milne L[2], Thomas S[2], Mills NM[1], Moore C[3], Semple S[4], Wiedow O[5], Stirrat C[1], Mirsadraee S[4], Newby DE[1,4] and Henriksen PA[1]

Author information:

1. British Heart Foundation/Centre for Population Health Sciences, University of Edinburgh Centre for Cardiovascular Science, Edinburgh, UK.
2. Edinburgh Clinical Trials Unit, University of Edinburgh, Western General Hospital, Edinburgh, UK
3. Department of Cardio-thoracic Surgery, Edinburgh Royal Infirmary, Edinburgh, UK
4. Clinical Research Imaging Centre, University of Edinburgh, Edinburgh, UK
5. Department of Dermatology, University of Kiel, Kiel, Germany

Abstract

Background. Elafin is a potent endogenous neutrophil elastase inhibitor that protects against myocardial inflammation and injury in pre-clinical models of ischemic-reperfusion injury. We investigated whether Elafin could inhibit myocardial ischemia-reperfusion injury induced during coronary artery bypass graft (CABG) surgery.

Methods and Results. In a randomized double blind placebo controlled parallel group clinical trial, 87 patients undergoing CABG surgery were randomized 1:1 to intravenous Elafin 200 mg or saline placebo administered after induction of anesthesia and prior to sternotomy. Myocardial injury was measured as cardiac troponin I release over 48 h (area under the curve, AUC) and myocardial infarction identified with magnetic resonance imaging. Post-ischemic inflammation was measured by plasma markers including AUC high-sensitive C-reactive protein (hs-CRP), and myeloperoxidase (MPO).

Elafin infusion was safe and resulted in >3000-fold increase in plasma Elafin concentrations and >50% inhibition of elastase activity in the first 24 hours. This did not reduce myocardial injury over 48 hours (ratio of geometric means (Elafin/placebo) of AUC troponin I 0.74 (95% CI 0.47 to 1.15, *P*=0.18) although post-hoc analysis of the high-sensitive assay revealed lower troponin I concentrations at 6 hours in Elafin treated patients (median 2.4 *versus* 4.1 μg/L, *P*=0.035). Elafin had no effect on myocardial infarction (Elafin, 7/34 versus

placebo, 5/35 patients) or on markers of inflammation: mean differences for AUC hs-CRP of 499 mg/L/48-h (95% CI -207 to 1205, *P*=0.16), and AUC MPO of 238 ng/mL/48-h (95% CI -235 to 711, *P*=0.320).

Conclusion. There was no strong evidence that neutrophil elastase inhibition with a single-dose Elafin treatment reduced myocardial injury and inflammation following CABG-induced ischemia-reperfusion injury.

What is already known about this subject?

Ischaemia-reperfusion contributes to myocardial injury during cardiac surgery. Therapies to reduce injury remain elusive despite promise from pre-clinical studies. Elafin is an endogenous neutrophil elastase inhibitor with broad ranging anti-inflammatory activity. Elafin reduces myocardial injury and infarct size and is associated with better myocardial function in pre-clinical models of ischaemia-reperfusion injury.

What does this study add?

We investigated Elafin in myocardial ischemia-reperfusion injury induced during coronary artery bypass graft surgery. A single dose of Elafin was safe and reduced circulating elastase activity but did not attenuate ischaemia-reperfusion injury or post-operative inflammation following coronary artery bypass surgery.

How might this impact on clinical practice?

Elafin's promise as a therapeutic agent was not translated in this first phase 2 clinical trial. Post-hoc analysis revealed reduced myocardial injury at an early timpeoint in Elafin treated patients. Further studies with continuous infusion and alternative clinical models are needed to elucidate whether Elafin can confer protection form ischaemia-reperfusion injury.

Trial registration. EudraCT 2010-019527-58, ISRCTN82061264

Funding. Medical Research Council (U.K.) Developmental Clinical Studies grant G1001339 and Chest Heart and Stroke Scotland (U.K.) grant R11/A135. DEN is funded by the British Heart Foundation (CH/09/002). Proteo Biotech AG supported the study by supplying the Elafin required free of charge. The funders had no role in study design, data collection and analysis, decision to publish, or preparation of the manuscript. The content of this manuscript is solely the responsibility of the authors.

Introduction

Ischemia-reperfusion injury occurs when blood flow is restored to organs and tissues that have sustained a period of interrupted blood supply. This occurs following therapies for acute myocardial infarction and ischemic stroke, and is a necessary consequence of solid organ transplantation. Mechanisms of cell and tissue injury include a neutrophil-mediated post-ischemic inflammatory response and activation of cellular death pathways following reperfusion (Hansen, 1995). Protecting organs from ischemia-reperfusion injury to improve clinical outcome is a high priority. Despite intense research efforts and huge promise from pre-clinical and early phase clinical trials, there are currently no effective therapies that can limit this injurious response.

During coronary artery bypass graft (CABG) surgery and cardiopulmonary bypass, coronary blood flow is interrupted and the heart is put into circulatory arrest. This causes ischemia-reperfusion injury that is exacerbated by adverse neutrophil-mediated myocardial inflammation and injury (Vinten-Johansen, 2004, Butler et al., 1993, Wakayama et al., 2007). CABG surgery therefore represents a programmed clinical model of ischemia-reperfusion injury that lends itself to testing the efficacy of potential therapeutic interventions (Hausenloy et al., 2007).

Elafin is an endogenous anti-inflammatory protein that was first isolated in the search for inhibitors of neutrophil elastase activity in the lung and skin

(Sallenave and Ryle, 1991a, Wiedow et al., 1991). It has inhibitory activity against both human neutrophil elastase and proteinase-3 as well as suppressing production of inflammatory cytokines such as interleukin-8 (IL-8) and tumor necrosis factor alpha (TNF-α) (Henriksen et al., 2004b). Elafin is produced locally at sites of inflammation, raising a local defence of 'alarm' antiproteases in order to contain and inhibit neutrophil-mediated inflammation (Sallenave, 2000a). Cardiovascular tissues do not express elafin or other neutrophil elastase inhibitors, and are therefore more vulnerable to neutrophil-mediated injury.

Augmentation of human elafin has consistently demonstrated impressive protective effects in rodent models of ischemic and inflammatory elastase-mediated vascular injury. Elafin infusion reduced muscular injury and neutrophil recruitment in the rat ischemic hind-limb and myocardial ischemia–reperfusion injury models (Crinnion et al., 1994, Tiefenbacher et al., 1997). Transgenic mice overexpressing human elafin under the control of the vascular pre-proendothelin promoter have relatively preserved left ventricular size and function following myocardial infarction (Ohta et al., 2004a). Compared to wild-type littermates, these animals are also protected from viral myocarditis and hypoxia-induced pulmonary hypertension, and exhibit less restenosis following wire induced carotid artery denudation (Zaidi et al., 1999, Zaidi et al., 2002a, Zaidi et al., 2000a). Elafin augmentation therefore protects the cardiovascular system from a range of conditions characterized by neutrophil elastase-mediated inflammation and injury.

APPENDICES

The purpose of the Elafin Myocardial Protection from Ischemia Reperfusion (EMPIRE) randomized controlled clinical trial was to provide proof-of-concept that Elafin treatment could reduce myocardial ischemia-reperfusion inflammation and injury in patients undergoing CABG surgery.

Methods

This single center clinical trial was performed with the approval of the national research ethics committee (11/MRE00/5), in accordance with the Declaration of Helsinki (2000), under a Clinical Trial Authorization (27586/0015/001-0001) from the Medicine and Healthcare products Regulatory Authority (MHRA, United Kingdom), and the written informed consent of all participants.

Trial Population

Between June 2011 and September 2013, consecutive patients referred for elective CABG surgery were recruited from two clinics at Edinburgh Heart Centre. Patients were 18 years or older, and were referred for isolated CABG surgery requiring 2 or more grafts. Exclusion criteria included patients with recent myocardial infarction (within 1 month of surgery), emergency or concomitant valve surgery, significant renal impairment (estimated glomerular filtration rate <40 mL/min), severe respiratory disease (maintenance corticosteroid therapy or forced expiratory volume in one second <50% predicted), severe left ventricular impairment (ejection fraction <40%), contraindication to magnetic resonance scanning, treatment for chronic inflammatory disease, women of child-bearing potential and inability to provide consent.

Study drug and randomization

Intravenous recombinant human Elafin (Proteo Biotech AG, Germany) 200 mg or saline placebo was prepared and infused as aqueous solution of 250 mL 0.9% saline. Patients were randomized (1:1) to receive Elafin or matched placebo by Edinburgh Clinical Trials Unit to ensure allocation concealment. Randomization incorporated minimization for age, presence of diabetes mellitus, extent of coronary artery disease, renal function and surgeon A or B. To ensure blinding, study drugs were prepared by staff independent of the study investigators or clinical team responsible for the patients care.

Intravenous Elafin 200 mg causes complete inhibition of plasma elastase activity for 2 h and >50% inhibition for 6 h. This dosage regime was selected to cover the increased elastase release following CABG surgery that peaks at the time of weaning from cardiopulmonary bypass and has returned to baseline by 6-7 h. The study drug was administered to the patient through a central venous cannula over a period of 30 min. The intravenous infusion was started at first skin incision and completed at least 20 min before cardiopulmonary bypass commenced.

Anesthesia and coronary artery bypass surgery

General anesthesia was maintained with isoflurane and propofol infusion during bypass. Surgical approach was via a median sternotomy and cardiopulmonary bypass was started after heparin administration with a non-pulsatile flow and a membrane oxygenator. Cardioprotection was provided by cold-blood cardioplegia

(1:4), which was administered antegradely, after cross-clamping the aorta, into the coronary arteries or by cross clamp fibrillation.

Blood samples

Blood samples were taken at baseline (time 0, skin incision) and at 2, 6, 24 and 48 h post-operatively. Plasma cardiac troponin I (cTnI) concentrations were measured with the ARCHITECT*STAT* troponin I assay and ARCHITECT*STAT* high-sensitive troponin I assay (Abbott Laboratories, Abbott Park, IL) validated in our institution.(Mills et al., 2011, Mills et al., 2012). Plasma concentrations of high-sensitive C-reactive protein (hsCRP), interleukin (IL)-6, IL-8, myeloperoxidase and elastase were quantified using enzyme-linked immunosorbant assays (ELISAs; R&D Systems, U.K.; Elastase ELISA, Cambridge Biosciences, U.K.). Plasma elastase activity and serum Elafin concentrations were measured by the Department of Dermatology, University of Kiel, Germany.

Cardiac magnetic resonance imaging and analysis

Each patient underwent cardiac magnetic resonance imaging twice: within 6 weeks before surgery and from 5 days after surgery. Patients were scanned using a research-dedicated 3T Siemens Verio scanner (Siemens Medical, Germany). Quantification of left ventricular mass, ejection fraction and late gadolinium enhancement infarct size were determined using established protocols and dedicated cardiac analysis software by two trained independent blinded observers.

Statistical analysis

The primary outcome variable was the 48-h area under the curve (AUC) for plasma cTnI concentration. It was analyzed using a generalized linear model, including terms for the treatment allocation and the variables on which the randomization was minimised. Log transformations were applied as the data were skewed, and the results have been unlogged and presented as geometric means. Secondary outcome measures involving area under the curve (hs-CRP, IL-6, IL-8, myeloperoxidase and elastase) were analyzed similarly, taking log transformation if the data were skewed. Left ventricular ejection fraction and mass were analyzed using QMass software (Medis medical imaging systems, Netherlands). The change in volume of infarction from preoperative and first postoperative magnetic resonance scans was categorized as increased, no change or reduced according to detection threshold based on inter-observer variability. Post hoc analyses of individual time points used Wilcoxon tests.

The primary analysis included all randomized patients on an intention-to-treat basis regardless of compliance with allocated treatment, and post randomization events. A secondary pre-specified exploratory analysis of AUC cTnI release excluded patients who had myocardial infarction or a cardiac arrest resulting in loss of cardiac output for >1 min. Type V myocardial infarction was defined according to the third universal definition (Thygesen et al., 2012b). Finally, post hoc, we examined treatment effect for each time point using the high-sensitive cTnI assay.

Power calculations were based on a recent study of patients undergoing remote

ischemic preconditioning before coronary artery bypass surgery (Hausenloy et al., 2007). Mean cardiac troponin T release quantified as area under the curve was 36.12 μg/L (s.d. 26.08) and 20.58 μg/L (s.d. 9.58) in the control and treated patients respectively. No contemporary AUC data were available for cTnI release in this patient group but the measurements are equivalent in terms of quantifying myocardial injury. With a sample size of 80 patients we had 90% power to detect this 40 % difference in AUC cTnI with a significance level of 5%, using a t-test with unequal variances and allowing for 4 dropouts in each arm.

Results

A participant flow diagram is shown in Figure 1. In 85 of the 87 patients, the trial infusion was administered as planned. Patient characteristics and intra-operative details are shown in Table 1. Full data to calculate area under the curve for cTnI (primary outcome) was obtained in 83 patients (95%). Data quality was similarly good for all secondary end-points with missing data evenly balanced across the treatment arms.

Elafin infusion resulted in >3000-fold higher plasma concentrations (mean AUC at 24 h; 31.1±9.6 *versus* 0.01±0.07 μg/mL for placebo) that was associated with a marked reduction in plasma elastase activity (mean AUC at 24 h; 4.28±5.13 *versus* 9.66±9.21units/mL; Figure 2).

There was no change in mean AUC troponin concentrations over the first 48 h in Elafin treated patients (adjusted ratio of geometric means (Elafin/placebo) 0.74, 95% CI 0.47 to 1.15, $P = 0.18$; Figure 3). There remained no evidence of a difference in a pre-specified secondary analysis where 3 patients who sustained a clinical myocardial infarction or had a cardiac arrest were excluded from analysis. Post-hoc analysis using the high-sensitive assay demonstrated a reduction of plasma cTnI concentrations in Elafin-treated patients at 6 h (median 2.4 *versus* placebo 4.1 μg/L, $P = 0.035$; Table 2).

Data from pre and post-operative scans were available for 34 (77.3%) Elafin and 35 (81.4%) placebo treated patients (Table 3). There was no difference in post-

operative left ventricular mass, left ventricular ejection fraction. The intra-class correlation coefficient for late gadolinium enhancement was 0.99 and the coefficient of repeatability of 1.78 mL (1.87 g) giving a threshold of 1.8 mL (1.9 g) for an increase in late gadolinium enhancement. Using this threshold the incidence of increased myocardial infarction volume was 20.3% in Elafin and 14.3% in placebo treated patients.

There was no effect on peak myeloperoxidase concentrations (mean difference 54.73 ng/L, 95% CI -60.0 to 169.5, P = 0.35) but peak elastase concentration was reduced (mean difference -168.4 ng/mL, 95% CI; -323.4 to -13.47, P = 0.03; Figure 4). In contrast, there was no effect on the 6-h AUC for plasma elastase concentration (mean difference -524.0 ng/mL/48-h, 95% CI -1239 to 191.3,P = 0.15). Although hs-CRP, IL-6 and IL-8 concentrations rose following CABG surgery (P < 0.001 for all), there was no treatment effect of Elafin (mean differences for 48-h AUC hs-CRP of 499 mg/L/48-h, 95% CI -207 to 1205, P=0.16) and P > 0.05 for both IL-6 and IL-8; Figure 4).

Median duration of stay in the intensive care unit was 24 and 23 h for patients treated with Elafin and placebo respectively (HR 1.25, 95% CI; 0.81 to 1.94 P = 0.32). Clinical outcomes and the incidence of perioperative complications in the first 48 h were also similar (Table 4).

Discussion

This is the first phase 2 clinical trial investigating the effect of Elafin, an endogenous neutrophil elastase inhibitor, on myocardial ischemia-reperfusion injury in patients undergoing CABG surgery. Despite achieving >3000-fold increase in plasma concentrations sufficient to more than halve plasma elastase activity, we did not demonstrate clear evidence of beneficial effect of human recombinant Elafin in our patients. Specifically, we were unable to attenuate the systemic inflammatory response despite evidence of anti-inflammatory activity in preclinical disease models (Alam et al., 2012a). Nor could we conclusively detect a reduction in two very sensitive, complementary and gold-standard measures of myocardial injury: AUC for plasma cTnI concentrations and late gadolinium enhancement on magnetic resonance imaging despite pre-clinical studies with Elafin reducing myocardial inflammation and injury after myocardial infarction (Ohta et al., 2004b, Tiefenbacher et al., 1997). Differences between pre-clinical studies and the clinical CABG surgery model may have been responsible for different results. Elafin has never been tested in large animal models or in the setting of cardiopulmonary bypass surgery. The surgical population was relatively low risk and the use of isoflurane anaesthesia may provide cardioprotection (Kersten et al., 1997). Nevertheless, ischaemia-reperfusion injury in CABG surgery produced conditions where Elafin would be expected to exert a treatment effect: neutrophil activation, elastase release and heightened circulating elastase activity together with activation of inflammatory cytokine pathways.

Elafin was safe and well tolerated in this high-risk clinical setting and post-hoc analysis indicated reduced myocardial injury at 6 h raising the possibility that

more extensive treatment effect could have been seen with multiple doses or bolus and sustained infusions.

All patients in our trial exhibited evidence of myocardial injury demonstrated by cTnI release. This was associated with a marginal reduction in left ventricular ejection fraction detected on post-operative MRI imaging. Small increases in delayed gadolinium enhancement indicative of new myocardial infarction were detected in a fifth of patients in keeping with sub-clinical myocardial injury and infarction that follows circulatory arrest and ischemia-reperfusion during CABG surgery. The current MRI results contrast with an earlier study reporting increased infarct volume in 78% of patients undergoing planned CABG (Steuer et al., 2004b). A key difference that may explain this discrepancy is the detailed patient characterization in our study with availability of pre-operative MRI scans allowing identification of small areas of pre-existing infarct that would be missed by using clinical history, echocardiography or ECGs to screen for pre-existing infarction.

Our data indicate that with single bolus administration, Elafin does not confer myocardial protection in the first 48 h following CABG surgery. This result was unchanged in a secondary analysis excluding patients who had sustained clinical events thought to be unrelated to study drug that would have contributed to large additional cTnI elevations. The absence of a convincing beneficial effect conflicts with pre-clinical ischemia-reperfusion studies where Elafin infusion was associated with a 27% reduction in myocardial infarct size and improved left ventricular performance. Our clinical CABG model allows recapitulation of a key

condition in pre-clinical models where Elafin is administered up front or expressed in tissues prior to the onset of cardiopulmonary bypass and ischemic tissue injury. However, despite this, we were unable to demonstrate clear efficacy using two complementary and highly sensitive measures of myocardial injury. Post hoc analysis identified a reduction in plasma cTnI concentrations at 6 h in Elafin treated patients. Preclinical studies utilized continuous Elafin delivery by infusion or gene expression and the reduced cTnI concentration at an early post-operative time point raises the question whether continuous Elafin infusion following the bolus may have extended the treatment effect to 48 h.

Elafin is one of several agents targeting inflammatory pathways that have been investigated in ischemia-reperfusion injury during cardiac surgery without success. Pexelizumab, a recombinant, single-chain anti-C5 monoclonal antibody, was studied in 2 multicenter, randomized clinical trials of patients undergoing CABG surgery with or without valve surgery on cardiopulmonary bypass. There was no difference in the primary outcome of death or myocardial infarction between the Pexelizumab and placebo treatment groups (Verrier et al., 2004). Failure of treatment effect with Elafin and Pexelizumab may reflect different mechanisms responsible for myocardial injury during CABG. Myocardial ischemia and necrosis undoubtedly occur during CABG surgery and the magnitude of cTnI release is correlated with subsequent morbidity and mortality (Croal et al., 2006). Mechanism of ischemia in preclinical models commonly involves complete interruption of coronary blood flow with a ligature to the beating heart. In CABG surgery the heart is in a state of circulatory arrest with protective cardioplegia and the impact of blood flow interruption is less severe. Despite evidence of neutrophil mediated inflammatory injury post-CABG, it may be activation of

cellular survival pathways within cardiomyocytes that determines the outcome of ischemia-reperfusion in this setting. Ischemic pre-conditioning refers to resistance to acute myocardial ischemia reperfusion conferred by the application of brief repeated episodes of ischemia. This approach has been used successfully in CABG surgery to limit cardiac marker release (Hausenloy et al., 2007). We demonstrated substantial (>50%) inhibition of circulating elastase activity by Elafin following CABG surgery and our data therefore indicate that neutrophil-derived elastase injury is not a prominent cause of myocardial injury in this setting.

The patients in our study did have evidence of neutrophil activation and degranulation with increased plasma concentrations of the primary granule contents, elastase and myeloperoxidase. Peak elastase concentrations were reduced in Elafin-treated patients although there was no demonstrable effect on peak myeloperoxidase concentrations. This discrepancy is explained by differences in the origin of these two neutrophil primary granule proteins. Circulating human neutrophil elastase is derived largely from acute neutrophil degranulation. A pool of neutrophil-derived myeloperoxidase is transcytosed and bound to the subendothelial matrix (Baldus et al., 2001). This contributes to the circulating pool and is released following heparin administration during cardiopulmonary bypass (Rudolph et al., 2013).

Elafin mediated reductions in elastolytic activity and myeloperoxidase staining (as a marker of neutrophil infiltration) have been consistent findings in pre-clinical models. Elafin infusion produced impressive reductions in myocardial

inflammation and necrosis in rabbits undergoing heterotopic cardiac transplantation (Cowan et al., 1996). This was associated with a marked attenuation of myocardial elastolytic activity in transplanted hearts. Transgenic mice over-expressing full-length human elafin under the control of the vascular pre-proendothelin promoter exhibit complete inhibition of tissue elastolytic activity following acute myocardial infarction and carotid arterial wire denudation (Ohta et al., 2004a, Zaidi et al., 2000a). These favorable treatment effects consistently occurred with reduced tissue myeloperoxidase content in keeping with less neutrophil recruitment. We were not able to access myocardial tissue for assessment of neutrophil infiltration and elastolytic activity but the significant reduction in peak elastase concentration leaves open the possibility of an Elafin effect on neutrophil activation and degranulation which if present was not large enough to translate into a reduction in AUC elastase at 6 h.

The EMPIRE patients exhibited increased IL-8 and IL-6 production and increased levels of circulating hs-CRP in keeping with a post-ischemic inflammatory response following CABG surgery. A systemic inflammatory response follows CABG surgery driven both by major surgical insult and contact activation of blood with artificial surfaces of the extracorporeal circuit (Day and Taylor, 2005). Belief that the magnitude of this response may drive clinical outcome has led to trials examining interventions to reduce post-operative inflammation. Peak and AUC hs-CRP, IL-6 and IL-8 release were similar between treatment groups. This result for Elafin contrasts with previous work indicating broad ranging anti-inflammatory activity in human endothelial cells and monocyte-derived macrophages (Henriksen et al., 2004b). The failure of Elafin to suppress IL-8 production during CABG surgery may indicate that additional inflammatory

pathways are active or that despite impacting on circulating elastase activity, Elafin is not reaching or is not active in the subcellular space between neutrophils and their target tissue.

Given lack of a conclusive therapeutic effect on myocardial injury and post-ischemic inflammation it is not surprising that the exploratory clinical endpoint of post-operative ITU stay was no different between treatment groups. Elafin infusion was safe. There were no drug related adverse events in this high-risk surgical group and no evidence of excessive bleeding, cardiovascular complications or renal dysfunction.

In conclusion, despite the body of work indicating therapeutic potential from several groups using different models, species and modes of augmentation, Elafin's promise as a therapeutic agent to attenuate myocardial ischemia-reperfusion injury and inflammation was not translated in this first phase 2 clinical trial. Post-hoc analysis identified reduced cTnI concentrations at 6 h in Elafin treated patients and it is possible that a bigger dose could have conferred protection out to 48 h. Elafin was safe and lack of treatment effect was seen despite achieving high plasma Elafin concentrations and halving of circulating elastase activity.

References

1 Hansen PR. Role of neutrophils in myocardial ischemia and reperfusion. *Circulation* 1995;**91**:1872.

2 Vinten-Johansen J. Involvement of neutrophils in the pathogenesis of lethal myocardial reperfusion injury. *Cardiovasc Res* 2004;**61**:481-97.

3 Butler J, Parker D, Pillai R, et al. Effect of cardiopulmonary bypass on systemic release of neutrophil elastase and tumor necrosis factor. *J Thorac Cardiovasc Surg* 1993;**105**:25-30.

4 Wakayama F, Fukuda I, Suzuki Y, et al. Neutrophil elastase inhibitor, sivelestat, attenuates acute lung injury after cardiopulmonary bypass in the rabbit endotoxemia model. *Ann Thorac Surg* 2007;**83**:153-60.

5 Hausenloy DJ, Mwamure PK, Venugopal V, et al. Effect of remote ischaemic preconditioning on myocardial injury in patients undergoing coronary artery bypass graft surgery: a randomised controlled trial. *Lancet* 2007;**370**:575-9.

6 Sallenave JM, Ryle AP. Purification and characterization of elastase-specific inhibitor. Sequence homology with mucus proteinase inhibitor. *Biol Chem Hoppe Seyler* 1991;**372**:13-21.

7 Wiedow O, Luademann J, Utecht B. Elafin is a potent inhibitor of proteinase 3. *Biochem Biophys Res Commun* 1991;**174**:6-10.

8 Henriksen PA, Hitt M, Xing Z, et al. Adenoviral gene delivery of elafin and secretory leukocyte protease inhibitor attenuates NF- B-dependent inflammatory responses of human endothelial cells and macrophages to atherogenic stimuli. *The Journal of Immunology* 2004;**172**:4535.

9 Sallenave JM. The role of secretory leukocyte proteinase inhibitor and elafin (elastase-specific inhibitor/skin-derived antileukoprotease) as alarm antiproteinases in inflammatory lung disease. *Respir Res* 2000;**1**:87-92.

10 Crinnion J, Homer-Vanniasinkam S, Hatton R, et al. Role of neutrophil depletion and elastase inhibition in modifying skeletal muscle reperfusion injury. *Cardiovascular Surgery (London, England)* 1994;**2**:749.

11 Tiefenbacher C, Ebert M, Niroomand F, et al. Inhibition of elastase improves myocardial function after repetitive ischaemia and myocardial infarction in the rat heart. *Pflugers Archiv European Journal of Physiology* 1997;**433**:563-70.

12 Ohta K, Nakajima T, Cheah AY, et al. Elafin-overexpressing mice have improved cardiac function after myocardial infarction. *Am J Physiol Heart Circ Physiol* 2004;**287**:H286-92.

13 Zaidi SH, Hui CC, Cheah AY, et al. Targeted overexpression of elafin protects mice against cardiac dysfunction and mortality following viral myocarditis. *J Clin Invest* 1999;**103**:1211-9.

14 Zaidi SH, You XM, Ciura S, et al. Overexpression of the serine elastase inhibitor elafin protects transgenic mice from hypoxic pulmonary hypertension. *Circulation* 2002;**105**:516-21.

15 Zaidi SH, You XM, Ciura S, et al. Suppressed smooth muscle proliferation and inflammatory cell invasion after arterial injury in elafin-overexpressing mice. *J Clin Invest* 2000;**105**:1687-95.

16 Mills NL, Churchhouse AM, Lee KK, et al. Implementation of a sensitive troponin I assay and risk of recurrent myocardial infarction and death in patients with suspected acute coronary syndrome. *JAMA* 2011;**305**:1210-6.

17 Mills NL, Lee KK, McAllister DA, et al. Implications of lowering threshold of plasma troponin concentration in diagnosis of myocardial infarction: cohort study. *BMJ* 2012;**344**:e1533.

18 Thygesen K, Alpert JS, Jaffe AS, et al. Third universal definition of myocardial infarction. *J Am Coll Cardiol* 2012;**60**:1581-98.

19 Alam SR, Newby DE, Henriksen PA. Role of the endogenous elastase inhibitor, elafin, in cardiovascular injury: From epithelium to endothelium. *Biochem Pharmacol* 2012;**83**:695-704.

20 Ohta K, Nakajima T, Cheah AYL, et al. Elafin-overexpressing mice have improved cardiac function after myocardial infarction. *American Journal of Physiology-Heart and Circulatory Physiology* 2004;**287**:H286.

21 Kersten JR, Schmeling TJ, Pagel PS, et al. Isoflurane mimics ischemic preconditioning via activation of K(ATP) channels: reduction of myocardial infarct size with an acute memory phase. *Anesthesiology* 1997;**87**:361-70.

22 Steuer J, Bjerner T, Duvernoy O, et al. Visualisation and quantification of peri-operative myocardial infarction after coronary artery bypass surgery with contrast-enhanced magnetic resonance imaging. *Eur Heart J* 2004;**25**:1293-9.

23 Verrier ED, Shernan SK, Taylor KM, et al. Terminal complement blockade with pexelizumab during coronary artery bypass graft surgery requiring cardiopulmonary bypass: a randomized trial. *JAMA* 2004;**291**:2319-27.

24 Croal BL, Hillis GS, Gibson PH, et al. Relationship between postoperative cardiac troponin I levels and outcome of cardiac surgery. *Circulation* 2006;**114**:1468-75.

25 Baldus S, Eiserich JP, Mani A, et al. Endothelial transcytosis of myeloperoxidase confers specificity to vascular ECM proteins as targets of tyrosine nitration. *J Clin Invest* 2001;**108**:1759-70.

26 Rudolph TK, Schaper N, Klinke A, et al. Liberation of vessel-adherent myeloperoxidase reflects plaque burden in patients with stable coronary artery disease. *Atherosclerosis* 2013;**231**:354-8.

27 Cowan B, Baron O, Crack J, et al. Elafin, a serine elastase inhibitor, attenuates post-cardiac transplant coronary arteriopathy and reduces myocardial necrosis in rabbits afer heterotopic cardiac transplantation. *J Clin Invest* 1996;**97**:2452-68.

28 Day JR, Taylor KM. The systemic inflammatory response syndrome and cardiopulmonary bypass. *Int J Surg* 2005;**3**:129-40.

Figures

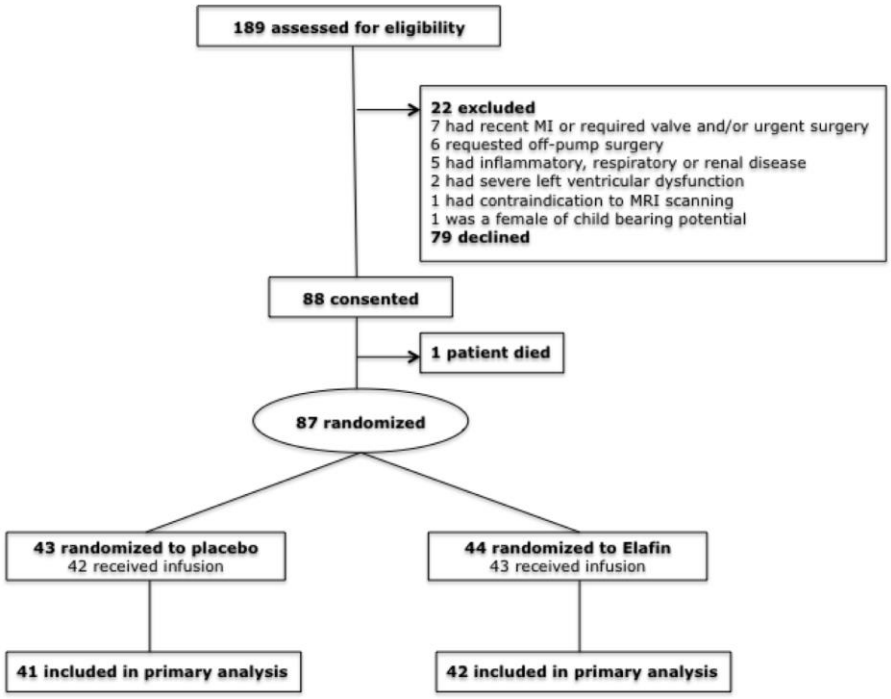

Figure 1: Trial flow diagram.

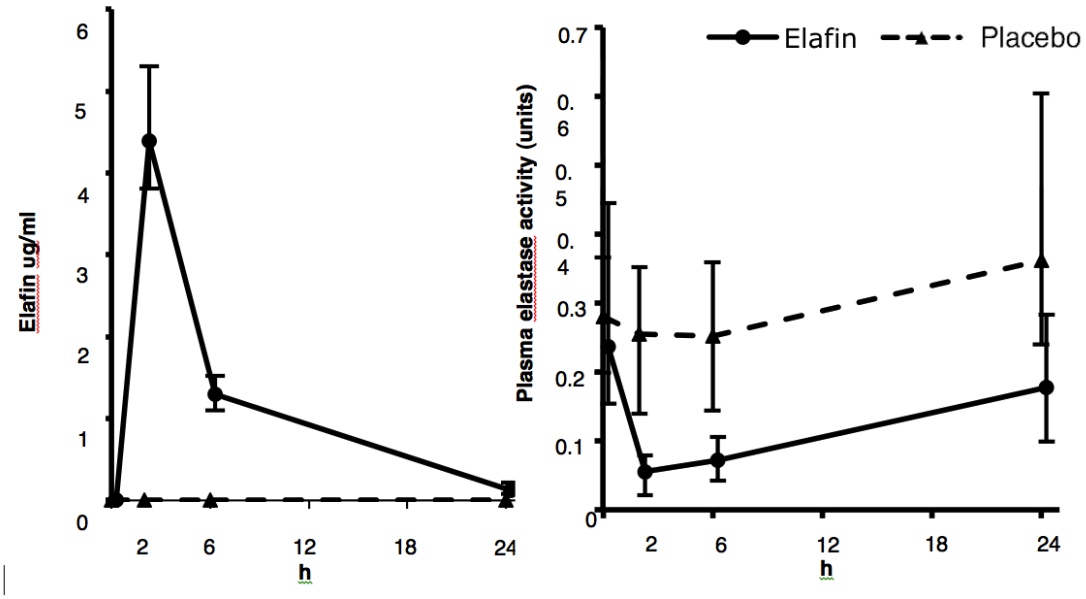

Figure 2: Perioperative plasma Elafin concentration (Left) and plasma elastase activity (Right) between groups. Data are median plus interquartile range from the first skin incision (time 0 h) to 24 h. Placebo group *n* = 41;Elafin group, *n* =43.

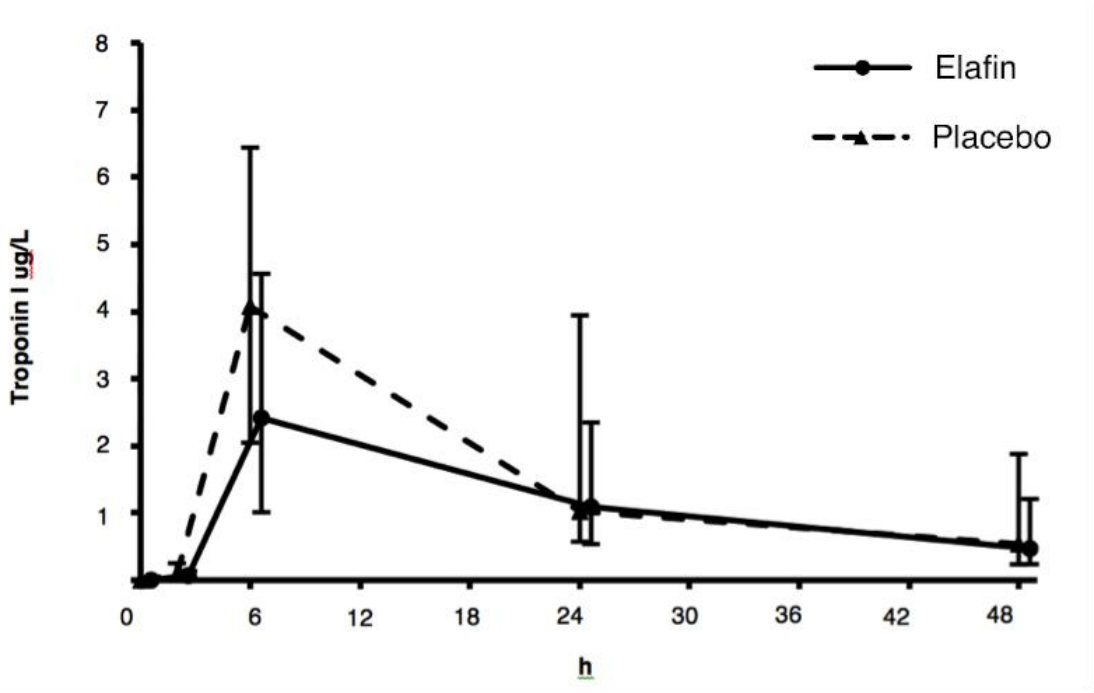

Figure 3: Myocardial injury. Cardiac troponin I (cTnI) release following coronary artery bypass graft surgery between treatment groups from first skin incision (time 0 h) to 48 h. Data are median plus interquartile range. Placebo group, *n*= 42; Elafin group, *n* = 44.

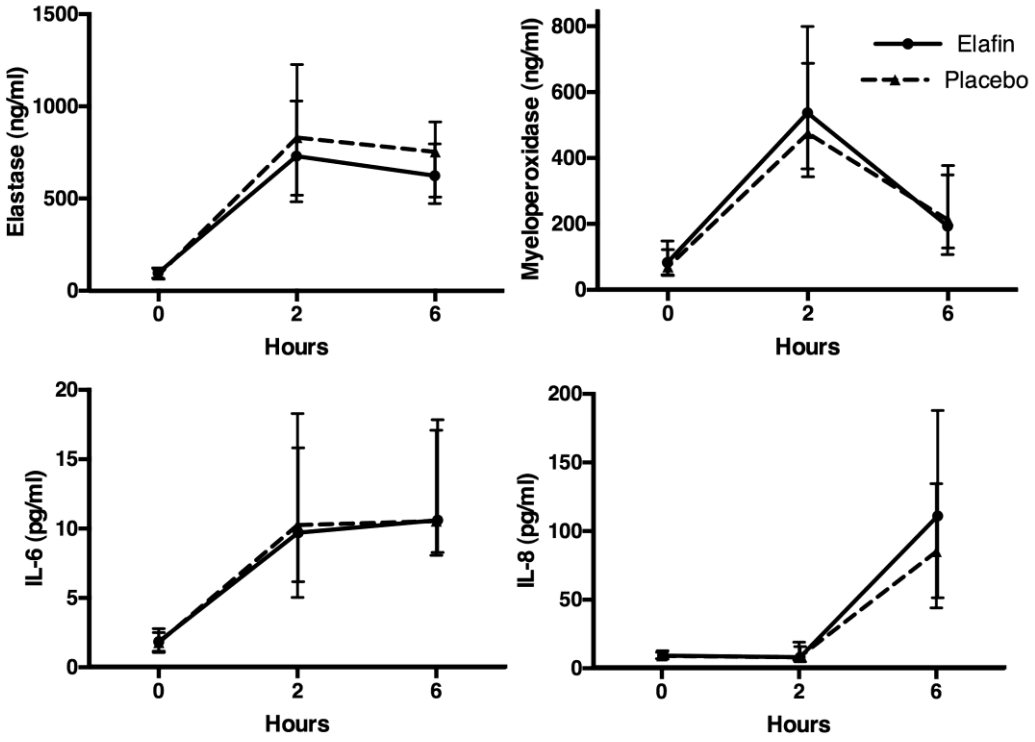

Figure 4: Perioperative circulating concentrations of neutrophil granule proteins elastase (top left), myeloperoxidase (top right), inflammatory cytokines IL-6 (bottom left) and IL-8 (bottom right) between treatment groups out to 6 h. Data are median plus interquartile range. Placebo group, *n*= 42; Elafin group, *n* = 44

Tables

	Placebo	**Elafin**
Baseline characteristics		
Age	63.6 ± 8.4	63.9 ± 7.7
2-vessel coronary disease	12 (27.9)	11 (25.0)
3-vessel coronary disease	31 (72.1)	33 (75.0)
Creatinine (mg/dl)	0.92 ± 0.18	0.94 ± 0.23
Diabetes Mellitus	9 (20.9)	11 (25.0)
Surgeon A	16 (37.2)	18 (40.9)
Surgeon B	27 (62.8)	26 (59.1)
Male Gender	36 (83.7)	38 (86.4)
EuroSCORE	2.21 ± 1.73	2.64 ± 2.06
Intra-operative details		
Number of bypass grafts		
One	1	2
Two	19	14
Three	14	22

Four	9	5
Five	0	1
Cardiopulmonary bypass time (min)	77 ± 26	78 ± 26
Cross clamp time (min)	45 ± 15	47 ± 16

Table 1: Baseline characteristics and intra-operative details by treatment group. Data are number of patients (%) or mean ± SD

Time (h)	**Placebo** (n = 43)	**Elafin** (n = 44)	*P* *Wilcoxon*
0	0.00 (0.0, 0.0)	0.00 (0.0, 0.0)	*0.861*
2	0.08 (0.0, 0.2)	0.07 (0.0, 0.1)	0.228
6	4.07 (2.0, 6.4)	2.41 (1.0, 4.6)	0.035
24	1.02 (0.6, 3.9)	1.08 (0.5, 2.3)	0.421
48	0.53 (0.2, 1.9)	0.47 (0.2, 1.2)	0.648

Table 2: Post-hoc analysis of plasma cardiac troponin I (cTnI) concentration (µg/L, median and interquartile range, high-sensitive assay) to 48 h.

	Placebo (n =35)	**Elafin**(n =34)
Change in ejection fraction (%)	-0.62±6.2	-2.4± 6.3
Change in LV mass (g)	1.2±3.8	2.0±3.8
Change in infarct volume (%)		
Reduced volume	2.9	0
No Change	82.9	79.4
Increased volume	14.3	20.6

Table 3: Magnetic resonance imaging analysis of postoperative ejection fraction, left ventricular mass and infarct volume.

	Placebo		**Elafin**	
Post-operative complications and outcomes (48 h)				
Death	0	(0)	0	(0)
Stroke	0	(0)	0	(0)
Myocardial infarction	0	(0)	1	(2.3)
Inotrope or balloon pump support for > 24h	10	(27.3)	12	(23.3)
Red cell transfusion post-op	12	(27.9)	12	(27.3)
Re-operation for bleeding	2	(4.7)	1	(2.3)
Respiratory complications	3	(7.0)	5	(11.4)
Antibiotic administration	2	(4.7)	4	(9.1)
Atrial fibrillation	4	(9.3)	3	(6.8)
Serum creatinine (mg/dl)				
24 hours	0.90 ± 0.32		0.87 ± 0.32	
48 hours	0.96 ± 0.48		0.88 ± 0.42	

Table 4: Post-operative complications and outcomes by treatment. Data are number of patients (%) or mean ± SD.

Figure Legends

Figure 1

Trial flow diagram.

Figure 2

Perioperative plasma Elafin concentration (A) and plasma elastase activity (B) between groups. Data are median plus interquartile range from the first skin incision (time 0 h) to 24 h. Placebo group *n* = 41;Elafin group, *n* =43.

Figure 3

Myocardial injury. Cardiac troponin I (cTnI) release following coronary artery bypass graft surgery between treatment groups from first skin incision (time 0 h) to 48 h. Data are median plus interquartile range. Placebo group, *n*= 42; Elafin group, *n* = 44

Figure 4

Figure 4: Perioperative circulating concentrations of neutrophil granule proteins elastase (top left), myeloperoxidase (top right), inflammatory cytokines IL-6

(bottom left) and IL-8 (bottom right) between treatment groups out to 6 h. Data are median plus interquartile range. Placebo group, *n*= 42; Elafin group, *n* = 44

Table Legends

Table 1

Baseline characteristics and intra-operative details by treatment group. Data are number of patients (%) or mean ± SD

Table 2

Post-hoc analysis of plasma cardiac troponin I (cTnI) concentration (μg/L, median and interquartile range, high-sensitive assay) to 48 h.

Table 3

Magnetic resonance imaging analysis of postoperative ejection fraction, left ventricular mass and infarct volume.

Table 4

Post-operative complications and outcomes by treatment. Data are number of patients (%) or mean ± SD.

Appendix G: ANIMAL STUDIES

USPIO ENHANCED CMR IN RODENT MODEL OF MYOCARDIAL INFARCTION

BACKGROUND

We have shown that USPIO uptake occurs in the infarcted region in myocardium of patients following MI. However histological confirmation of monocytes taking up the USPIO within this region is not available. Using a pre-clinical model of MI, we aimed to show that USPIO does indeed identify cellular inflammation. The animal work was carried out by Dr Gillian Gray (GG), and imaging by Maurits Jansen (MJ)(BHF/ University Centre for Cardiovascular Science, Queens Medical Research Institute, University of Edinburgh).

METHODS

Adult male Wistar rats (200-250 g; Charles River, Margate, UK) were used. All experiments were performed according to the guidelines of the Animals (Scientific Procedures) Act 1986 (U.K. Home Office) and the National Institutes of Health (NIH Publication No. 85-23, revised 1996) and were approved by the ethical review committee for animal research at the University of Edinburgh.

It was attempted to induce myocardial infarction in 3 rats by ligation of the left anterior descending artery as described previously (Gray et al., 2000). Adult male Wistar rats, 250–300 g (Charles River), were anaesthetised (isofluorane) and intubated via the mouth for ventilation. Buprenorphine analgesic was administered subcutaneously. The chest was opened by left thoracotomy and the heart exteriorised

for placement of a suture (5/0 silk suture (Ethicon Ltd, U.K.)) around the left anterior descending coronary artery. The heart will be placed back into the chest and the suture will be tightened around the artery for 30 minutes using a reversible snare then released for reperfusion.

Ferumoxytol was supplied by Advanced Magnetics Inc (Cambridge, MA) with each vial containing 510 mg of elemental iron in 17 mL (30 mg/mL). It was administered via a a tail vein injection (MJ) at a dose of 4 mg Fe/kg body weight at a rate of up to 1 mL/sec 24 hours prior to MRI scanning, so 4 days after MI.

4 days after infarction/reperfusion, the study rats received 4mg/kg Ferumoxytol by tail injection. After 24 hours, MRI (T2* - 4 echos) were performed to image the myocardium (**Figure 1**).

The rat were sacrificed by anaesthetic overdose immediately after imaging and the heart was rinsed in saline and placed into 10% phosphate buffered formalin for 24h, then into alcohol before processing and wax embedding. 5µm sections were cut for histological staining. Separate parallel sections will be stained using H&E for general visualisation of tissue structure, Prussian blue for detection of iron oxide and a general macrophage antibody (ED-1).

Figure 1: Flow chart of protocol.

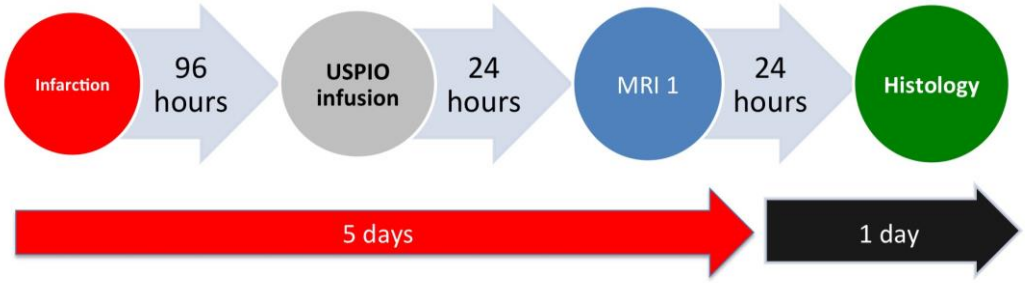

Magnetic resonance imaging was performed using our pre-clinical research 7T magnetic resonance imaging scanner (Edinburgh Preclinical Imaging, BRF, Chancellors Building, University of Edinburgh).

Standard cardiac imaging ECG-gated sequences were used. USPIO imaging was performed using $T2^*$-weighted cardiac gated echo gradient-echo sequences. Each echo will be acquired individually. Scan parameters (such as echo time to dictate degree of $T2^*$-weighting) required a degree of optimisation for USPIO imaging of the myocardium at 7T (high concentrations of USPIO will require reduction in echo times). The use of multi-echo sequence allowed a quantitative analysis of USPIO accumulation through calculation of T2* relaxation times before and after administration of USPIO. In order to optimise image analysis of $T2^*$-weighted images (and prevent analysis degradation due to "$T2^*$-blooming" artefacts) USPIO images was quantitatively analysed using a susceptibility gradient mapping post-processing technique previously used in patients with myocardial infarction.

Analysis was performed at the Clinical Research Imaging Centre. The first MRI scan acquired will be used as a baseline scan. The subsequent MRI scans will be registered and orientated to the baseline using ANALYZE software (AnalyzeDirect Software, United States). The myocardium will then be separated into infarct zone and remote myocardium.

RESULTS

Successful myocardial infarction was induced in 2 rats, and 1 rat survived 24 hours after the procedure. 4 mg/kg of USPIO was infused via rat tail injection. The rat then

underwent CMR with T2* sequences, and histological analysis of the myocardium (**Figure 2**).

Figure 2: There was USPIO uptake in the anterior myocardium corresponding to the infarct zone (left). There was a high level of ED-1 staining in the corresponding myocardium indicating monocyte infiltration (middle). This also corresponded to Prussian blue staining indicating iron accumulation (right).

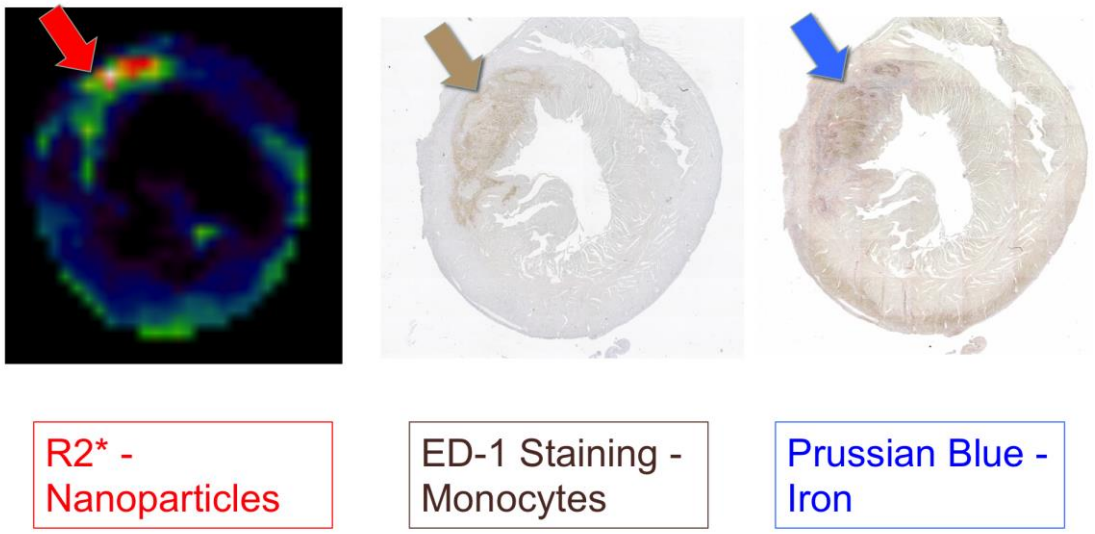

There was evidence of high USPIO uptake in the anterior myocardium corresponding to the distribution of the left anterior descending artery. R2* values 420 s-1 in this region. The same region had a high level of ED-1 antibody staining indicating high monocyte infiltration. The corresponding area also stained for Prussian Blue, with co-localisation indicating USPIO uptake by monocytes in the infarcted myocardium (**Figure 3**).

Figure 3: Monocytes in the infarcted myocardium stained with Prussian Blue.

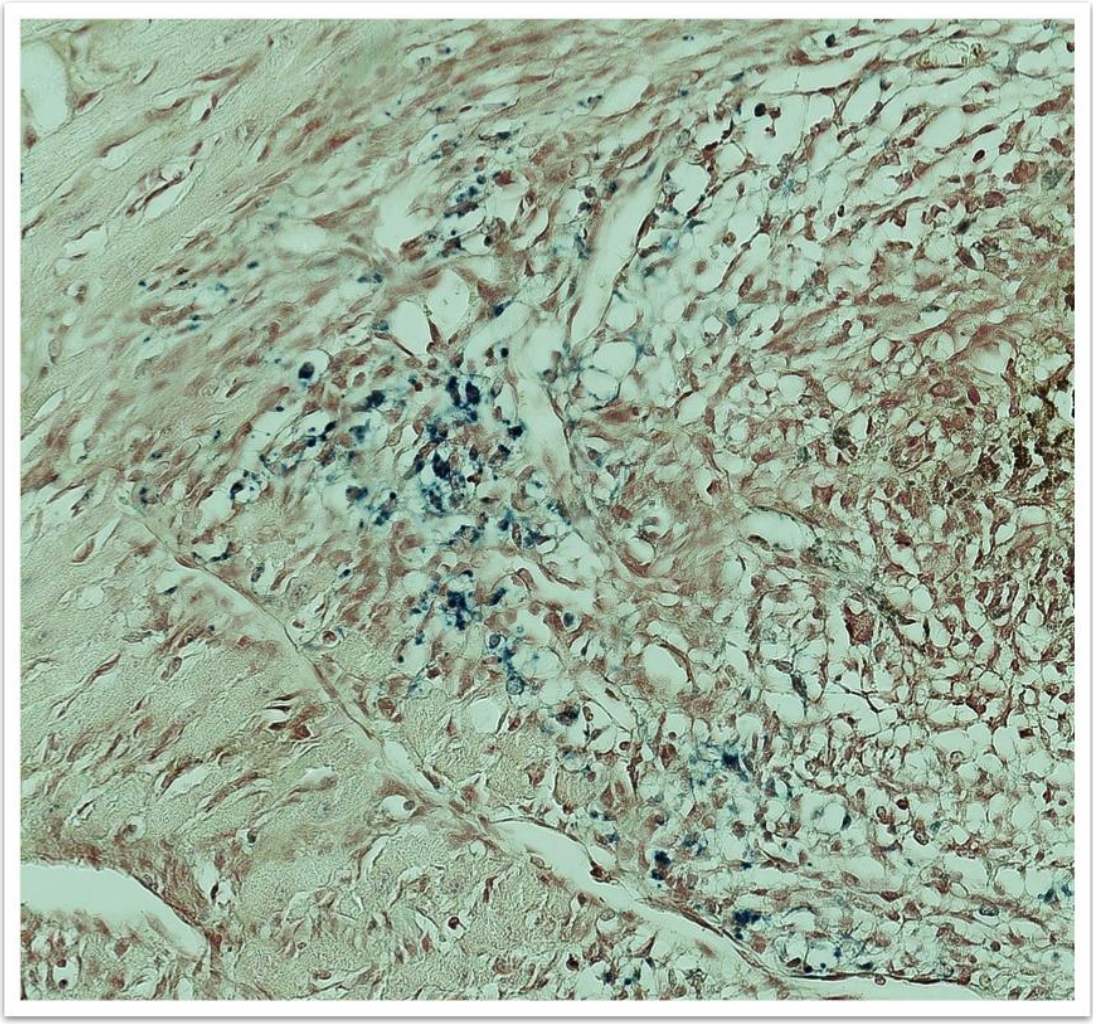

.

CONCLUSION

In this model of ischaemia-reperfusion in 1 rat, we demonstrated increased USPIO uptake by CMR that corresponded to monocyte infiltration. This provides further evidence of successful non-invasive detection of cellular inflammation in the post infarct myocardium in the clinical setting as performed in Chapter 3: Chapter 5:

NANOPARTICLE ENHANCED MRI SCANNING TO DETECT CELLULAR INFLAMMATION IN EXPERIMENTAL CHRONIC RENAL ALLOGRAFT REJECTION.

ABSTRACT

Objectves: We investigated whether ultrasmall paramagnetic particles of iron oxide (USPIO)-enhanced magnetic resonance imaging (MRI) can detect experimental chronic allograft damage in a murine renal allograft model.

Materials and Methods: Two cohorts of mice underwent renal transplantation with either a syngeneic isograft or allograft kidney. MRI scanning was performed prior to and 48 hours after USPIO infusion using T2*-weighted protocols. R2* values were calculated to indicate the degree of USPIO uptake. Native kidneys and skeletal muscle were imaged as reference tissues and renal explants analysed by histology and electron-microscopy.

Results: R2* values in the allograft group were higher compared to the isograft group when indexed to native kidney (median 1.24 (interquartile range: 1.12 to 1.36) versus 0.96 (0.92 to 1.04) , $P<0.01$). R2* values were also higher in the allograft transplant when indexed to skeletal muscle (6.24 (5.63 to 13.51)) compared to native kidney (2.91 (1.11 to 6.46) $P<0.05$). Increased R2* signal in kidney allograft was associated with macrophage and iron staining on histology. Internalised USPIO were identified within tissue resident macrophages on electron microscopy.

Conclusion: USPIO-enhanced MRI identifies macrophage infiltration within chronic renal damage. This technique offers the potential for non-invasive detection and monitoring of renal allograft refection following transplantation.

INTRODUCTION

Chronic allograft damage (CAD), characterised by interstitial fibrosis and tubular atrophy (IFTA), is the commonest cause of transplant failure following surgery. (Paul, 1999) The demand for organ transplantation is expanding and waiting lists for a kidney are likely to increase in coming years (Webb et al., 2010). Early identification of chronic allograft damage remains challenging but is crucial to allow intervention with immunosuppressive therapy. Renal biopsy remains the gold-standard for detecting allograft rejection but is associated with significant morbidity and mortality. The average complication rate is 7.4% with a life-threatening complication occurring in 1% (Korbet, 2002, Nankivell and Chapman, 2006). It would be advantageous to have a non-invasive imaging approach for the detection of acute rejection and IFTA. This would provide an alternative or adjunctive clinical assessment that may reduce the number of biopsies.

Current imaging techniques for monitoring allograft function involve the use of ultrasound to exclude ureteric obstruction or vascular compromise in the failing kidney. Measurement of vascular resistive index or the use of contrast-enhanced ultrasonography have been advocated, but have not been clinically validated

(Radermacher et al., 2003, Schwenger et al., 2006, Naesens et al., 2013). There is no imaging modality available to measure the development of graft fibrosis and current practice involves a biopsy when renal function deteriorates (Nankivell and Kuypers, 2011). The role of monocytes and macrophages in chronic renal allograft damage has been well established (Magil, 2009). Monocytes and macrophages are known to play a role in chronic renal allograft damage (Dang et al., 2012), and are key promotors of fibrosis in other organs, such as the liver (Duffield et al., 2005, Ramachandran et al., 2012). Several animal models of allograft rejection exhibit monocyte and macrophage infiltration in allograft tissue (Diamond et al., 1992, Hancock et al., 1993, Heemann et al., 1994, Azuma et al., 1994, Ziai et al., 2000), and these cells have a central role in human chronic allograft damage (Regele et al., 2002, Fahim et al., 2007). We have developed a model of chronic allograft damage: characterised by a single class II mismatch a kidney from C57BL/6^{BM12} (H-2B^{BM12}) donor is transplanted into a C57BL/6 (H-2B) recipient and leads to the progressive development of interstitial fibrosis and tubular atrophy (IFTA) over 4 to 8 weeks. The key role of macrophages in this model has been demonstrated when transplants were performed into galectin-3 knockout recipients on a C57Bl/6 background. This led to an alteration in macrophage phenotype with reduced numbers of YM1-expressing macrophages in the knockout group, and protection from IFTA (Dang et al., 2012).

Magnetic resonance imaging (MRI) offers detailed characterization of the kidney structure without using ionizing radiation and is suitable for monitoring renal allograft damage with repeated scanning. Iron oxide particles have been used as a contrast medium for MRI as they alter the T2* relaxation time of tissues in which

they accumulate (Alam et al., 2012b). Ultrasmall (approximately 30 nm), superparamagnetic particles of iron oxide (USPIO) extravasate freely through capillaries and are taken up by tissue-resident inflammatory cells of the reticuloendothelial system (Ruehm et al., 2001b). Available USPIOs include ferumoxytol (Rienso, Takeda; Feraheme, AMAG Pharmaceuticals), which is licensed for the treatment of anaemia caused by iron deficiency in patients with chronic kidney disease rather than as a contrast agent for MRI. Together with other groups, we have used USPIO as MRI conrast in clinical studies (Alam et al., 2012b, Sadat et al., 2012, Richards et al., 2011a, Tang et al., 2009).

Monocytes, macrophages and to a lesser extent neutrophils take up USPIOs, and accumulation in allograft rejection can be identified (Dousset et al., 1999, Gellissen et al., 1999a). MRI detected USPIO accumulation within the outer renal medulla in a model of renal ischaemia and this correlated histologically with USPIO uptake by macrophages (Jo et al., 2003a). USPIO have been used to investigate acute renal transplant rejection in pre-clinical models, however these effects may have been due to ischaemia reperfusion injury (Zhang et al., 2000, Ye et al., 2002). We hypothesized that they could be used to identify inflammation and fibrosis in a model of chronic renal allograft damage.

MATERIALS AND METHODS

Murine Model of Renal Transplantation

Two cohorts of C57BL/6 mice underwent renal transplantation. Syngeneic renal transplants (n=8) were performed between litter mates and allograft renal transplants from C57BL/6^{BM12} donors into C57Bl/6 recipients (n=10). Characterised by a single class II mHC mismatch, such kidneys develop chronic allograft damage over a progressive twelve-week period. The model is not transplant-dependent as the contralateral kidney is left in situ. The isograft transplanted kidney and the native non-transplanted kidney were available as controls for comparison with the allograft kidney. Mice were bred in-house in the Biomedical Research Resources, University of Edinburgh or purchased from Charles River. All animal experiments were performed under a project licence and in accordance with legislation in the Home Office Animal (Scientific Procedures) Act of 1986. Baseline MRI scanning was performed 4 weeks post transplant followed immediately by an infusion of USPIO by tail vein injection (4 mg/kg ferumoxytol; Rienso, Takeda). Repeat MRI scanning was performed 48 hours post infusion.

MR Imaging Protocols.

All MRI experiments were performed using a 7 Tesla horizontal bore NMR spectrometer (Agilent Technologies, Yarnton, UK), equipped with a high-performance gradient insert (60-mm inner diameter), maximum gradient strength 1000 mT/m. Mice were anaesthetised with 1.5% isofluorane in oxygen/air (50/50, 1 L/min) and placed in a cradle (Rapid Biomedical GmbH, Rimpar, Germany). The rectal temperature and respiration rate were monitored throughout the experiments, and body temperature was maintained at 37 °C with a heat fan. A 33-mm diameter

birdcage volume coil (Rapid Biomedical GmbH, Rimpar, Germany) was used for radio frequency transmission and signal reception. For anatomical assessment and to aid placement of the slice for the T2* mapping sequence, respiration-gated T2-weighted fast spin echo images (echo train length of 8) of 1-mm slice thickness in a coronal orientation were collected with the following parameters: repetition time (TR) ≈ 3000 ms depending on the respiration rate; effective echo time = 36 ms; 16 slices, field of view = 35 mm × 35 mm; matrix = 192 × 128, 2 signal averages. For T2* mapping and calculation of T2* relaxation times, image acquisition used a gradient echo, respiratory-gated pulse sequence (dummy pulses during respiratory movement) of 7 images weighted in T2* acquired consecutively; TE = 1.83, 3, 5, 7, 10, 12, 15 ms and a TR of 60 ms. The field of view was 35 x 35 mm and the acquisition matrix 192 × 128 (in-plane resolution = 0.182 × 0.273 mm). Slice thickness was 1-mm with 2 signal averages.

USPIO imaging was performed with T2*-weighted gradient-echo sequences using a 7 T MRI scanner. Quantitative analysis of USPIO accumulation was achieved by calculation of T2* relaxation times before and after administration of USPIO.(Alam et al., 2012b) In order to optimise image analysis and prevent degradation due to "T2*-blooming"lartefacts, images were quantitatively analysed using a susceptibility gradient mapping post-processing technique previously used in SPIO imaging to quantitate USPIO accumulation using changes in calculated T2* relaxation times.(Dahnke et al., 2008)

Image Analysis

The seven echoes in the multi-echo T2*-weighted sequence were combined to generate a T2* map, in which the data represented the T2* value ($S(t) = S(0)\exp-(t/T2^*)$) for each voxel. This was achieved using in-house software developed in Matlab (Mathworks, US). The T2* value is the decay constant for the exponential decay of signal intensity with time. In the presence of USPIO, the signal decays more rapidly due to local field inhomogeneities and the T2* value is reduced. By minimising the sum of the squares of errors between the data and an exponential function, the decay constant (i.e. T2* in ms) was obtained. An experimentally determined threshold for the co-efficient of determination ($r^2>0.85$) was used to exclude data that did not have an acceptable exponential decay when SI was plotted against echo time. The inverse of T2*, R2*, was then calculated to assess USPIO uptake. The greater the accumulation of USPIO in tissues, the greater the R2* value. R2* values were obtained from baseline and 48-hour scans using ANALYZE software (AnalyzeDirect Software, United States). Regions of interest were drawn on parenchyma, and pre-USPIO scans compared to post-USPIO scans. A semi-quantitative analysis was made from the increase in R2* value. To correct for differences in blood pool USPIO concentration, due to infusion errors or difference in blood volume, the transplanted kidney R2* increase was indexed to the native kidney R2* increase. To provide a value of translational value to clinical medicine, where a normal healthy native kidney will not be present, the renal R2* increase was also indexed to skeletal muscle R2* increase.

APPENDICES

Allograft Injury - Histology

Kidneys were divided and fixed fresh frozen or in methyl carnoy's solution and embedded in paraffin. Tissue sections were stained with haematoxylin-eosin to allow histological analysis, and reveal presence of inflammatory infiltrate.(Qi et al., 2008, Jabs et al., 2003)

Allograft Injury - Cellular Infiltrate

Macrophage infiltration was identified by F4/80+ (Abcam, Cambridge, UK) staining by immunohistochemistry using paraffin embedded tissue sections. Light microscopy was performed and images obtained and quantified by computer-assisted image analysis of 10 sequentially selected non-overlapping fields of renal cortex and medulla and expressed as the percentage of tissue surface area positive for staining.

Electron microscopy

For transmission electron microscopy, samples were fixed in 3% glutaraldehyde in 0.1M sodium cacodylate buffer, pH 7.3, for 2 h then post-fixed in 1% osmium tetroxide in 0.1M sodium cacodylate for 45 min. Samples were then dehydrated and embedded in araldite resin. Ultrathin 60-nm sections were cut from selected areas, stained in uranyl acetate and lead citrate then viewed in a Philips CM120 transmission electron microscope, images obtained with a Gatan Orius CCD camera.

Statistical Analysis

Statistical analysis was performed with GraphPad Prism version 4.00 (GraphPad Software, San Diego California USA). Grafts were compared with native kidneys using paired two-tailed non-parametric t-tests (Wilcoxon matched-pairs signed rank test). Isograft and allograft kidneys were compared using non-paired two-tailed non-parametric t-tests (Mann Whitney test). Statistical significance was taken as a two-sided $P<0.05$.

RESULTS

One allograft and 2 isograft recipients sustained infarction of the transplanted kidney. This left 9 allograft mice and 6 isograft mice for analysis.

Change in R2* values in allograft and isograft kidneys

Illustrative MRI scans with R2* signal derived colour maps of USPIO uptake in allograft and isograft kidneys are shown in **Figures 6 & 7**. Increased R2* signal and USPIO uptake is indicated by green and red colour.

Baseline R2* values were similar in native (median (interquartile range), 42.8 (38.5 to 50.5) ms^{-1})and allograft kidneys (44.2 (39.6 to 52.8) ms^{-1}). USPIO administration increased R2* values in both isograft and allograft kidneys. The increase in R2* value at 48 h was greater in allograft kidneys (30.15 (14.0 to 68.0) ms^{-1}) compared to native kidney (15.7 (4.5 to 26.8) ms^{-1}, $P < 0.01$). In contrast, the increased R2* signal in isograft kidneys at 48h (23.24 ms^{-1} (7.53 to 71.2) ms^{-1}) was no different to native kidney (26.4 ms^{-1} (3.71 to 86.9) ms^{-1}), $P = 0.58$).

Figure 6: Transplanted kidney (white arrows) compared to native kidney (yellow arrows) for allograft.

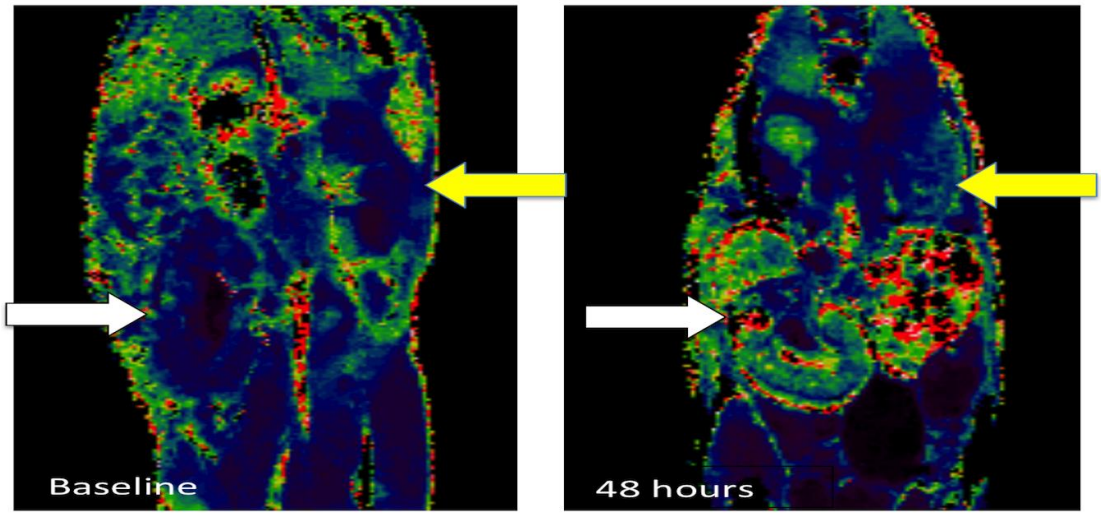

Figure 7: Transplanted kidney (white arrows) compared to native kidney (yellow arrows) for isograft.

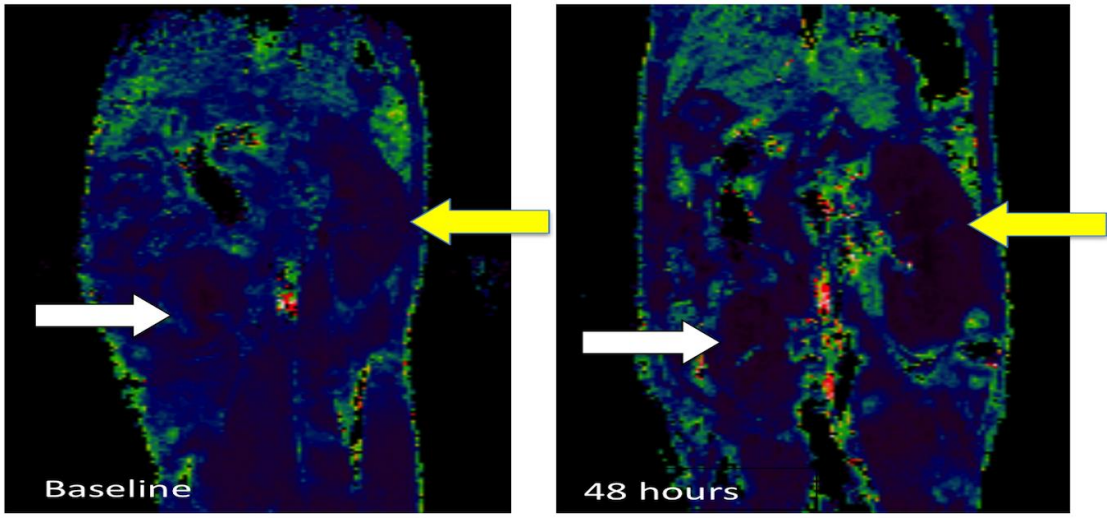

R2* value increases indexed for changes in native kidney and skeletal muscle are shown in **Figure 8**. Median increase (interquartile range), indexed for native kidney, was greater in allografts 1.24 (1.12 to 1.36) compared to isografts 0.96 (0.92 to 1.04), $P < 0.01$, Figure 2A. A similar result was obtained following indexing for skeletal muscle R2* increase (Figure 2B). The median increase in R2* value indexed to skeletal was greater in the allograft kidney 6.24 (5.63 to 13.51) compared to native kidney 2.91 (1.11 to 6.46), $P < 0.05$. The corresponding skeletal muscle indexed signals were similar in isograft 3.83 (0.78 to 6.24) and native kidneys 3.63 (1.00 to 5.33) and significantly lower than the allograft signal, $P < 0.05$.

Figure 8: Increase in R2* value from baseline to 48 hours for transplanted kidney indexed to native kidney (A) and skeletal muscle (B).

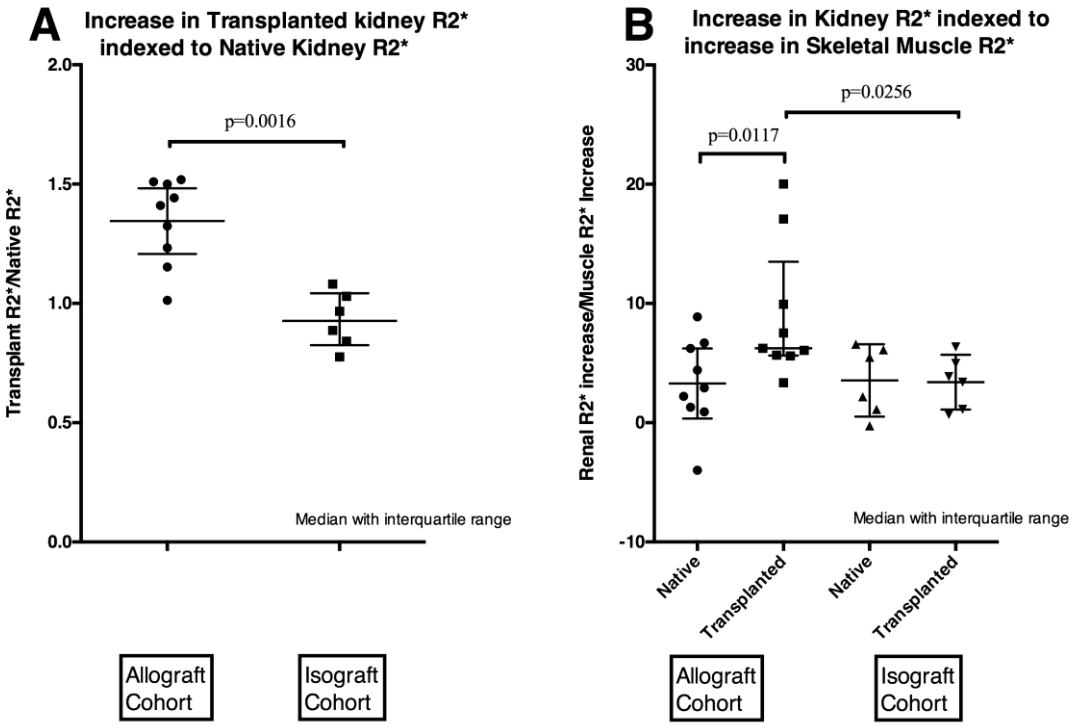

Histology and Electron Microscopy

F4/80 staining confirmed heavy macrophage resident cells in the allograft kidneys (2.70±0.84 percentage area staining) with very few cells in in the isograft kidneys (0.52±0.44 percentage area staining), (**Figures 9 & 10**). Iron staining with Prussian blue demonstrated deposition in allograft tissue with none in the isograft tissue. The reticulo-endothelial tissue of the spleen was also rich in monocyte and iron staining. Electron microscopy confirmed monocyte/macrophage USPIO uptake within the renal tissue (**Figure 11**).

Figure 9: F4/80 staining (top panel) for monocyte derived macrophages in the spleen and allograft and isograft (hollow arrows). Prussian blue staining (bottom panel) comparing iron deposition in the spleen, allograft tissue and isograft (sold black arrows).

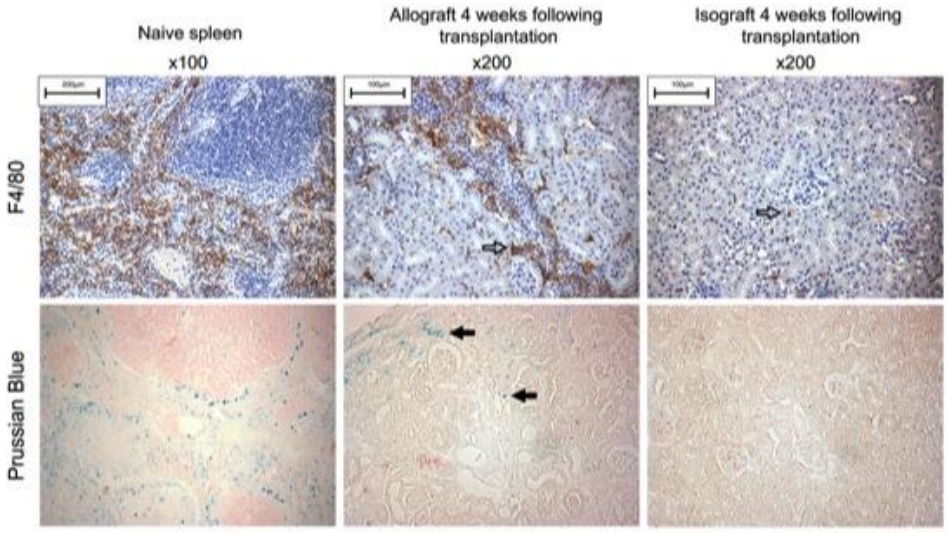

Figure 10: Histological monocyte count in allograft, isograft and non-transplanted native kidneys.

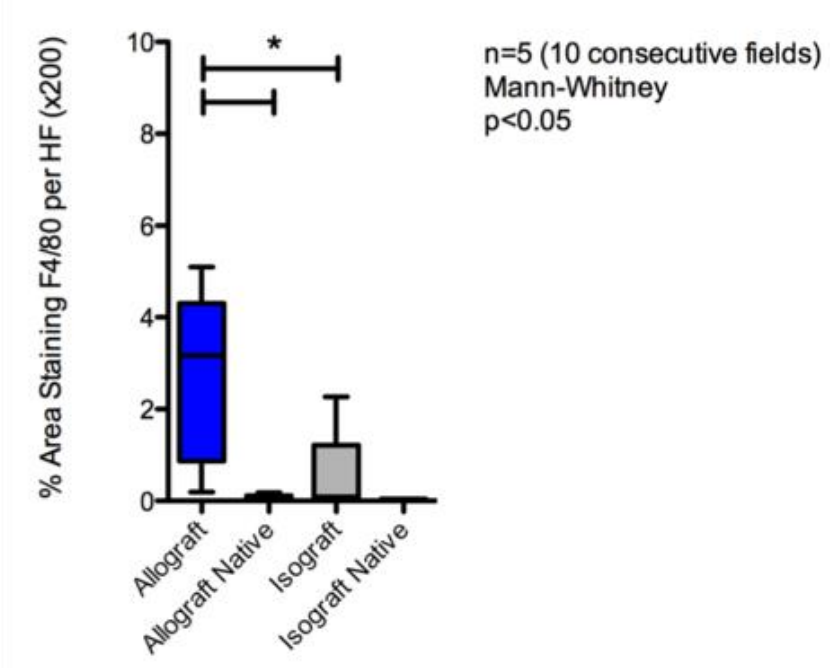

Figure 11: Electron microscopy of macrophages in renal allograft tissue. The inlay (top right - magnification from black box) demonstrates USPIO within lysosomes.

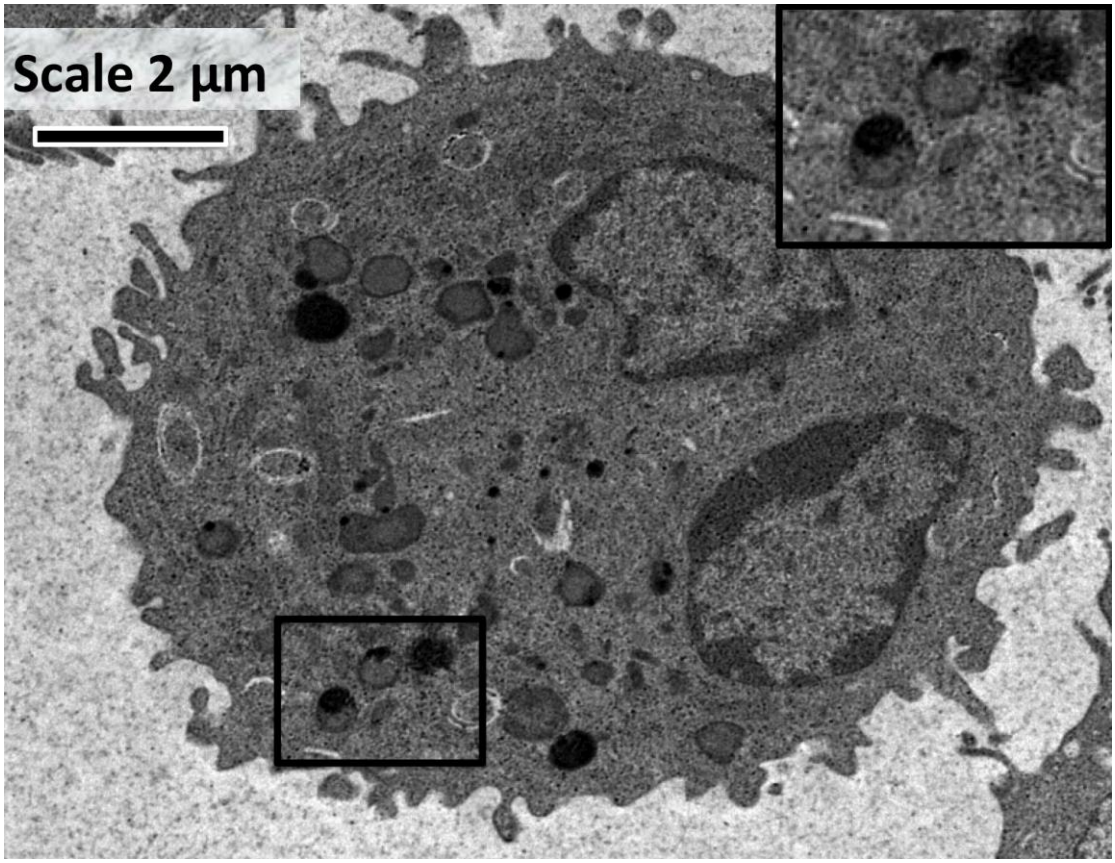

DISCUSSION

We have shown for the first time that USPIO-enhanced MRI can detect macrophage infiltration in a model of chronic inflammatory allograft damage. The prospect of non-invasive detection and monitoring of CAD, without resorting to renal biopsy, would be a significant advance in the management of renal transplant patients.

In this study the allograft USPIO signal was significantly increased compared to the native kidney. This direct comparison would be not feasible in a clinical study where the native kidney would be diseased or absent. Additionally human pathological factors may impact on the USPIO related signal. USPIO has a circulating half life of 18-30 hours and persistence of particles in the circulation will affect the tissue R2* value due to perfusion (Landry et al., 2005). In this study differences in blood volume and organ perfusion, due to surgical blood loss or physiological variation related to inflammation and rejection, may contribute to the blood pool related signal in each animal. To address this problem we indexed USPIO signal to skeletal muscle and native kidney. These findings on non-invasive imaging were associated with greatly increased macrophage infiltration and USPIO iron staining in allografts compared to isografts. We were able to further demonstrate macrophage USPIO uptake on scanning electron microscopy confirming that the USPIO signal on MRI was related to the macrophage infiltration in CAD.

It was not possible to be certain about the mechanism of cell labeling and distribution of USPIO within renal tissue. As a result of their smaller size, USPIOs are less readily recognized by phagocytic cells and persist in the circulation for longer than other iron particles (plasma half-life 14-30 h in humans) (Landry et al., 2005, Hunt et al., 2005). They are capable of passing through capillary walls, to be taken up through pinocytosis by tissue-resident macrophages and neutrophils (Ruehm et al., 2001b, Dousset et al., 1999, Gellissen et al., 1999a). Extravasated USPIO may remain in the interstitial space or be taken up by resident macrophages. Circulating USPIO may also be taken up by monocytes that subsequently infiltrate the kidney. These processes (monocyte uptake, USPIO blood extravasation and resident macrophage uptake) may have different kinetics and could all contribute to the increased USPIO signal in allografts. The study aim was to provide proof of principle that allograft rejection can be detected non-invasively with contrast MRI but this approach could be used to further dissect out CAD mechanisms.

Significant advances have been made in the management of acute rejection as modern immunosuppressive agents target primarily T lymphocytes. However, the rate of CAD characterized by interstitial fibrosis remains relatively constant, giving rise to the loss of 4% renal transplants per year. Work from our own group has demonstrated that modification of macrophage biology can protect against fibrosis in this model of CAD and the role of macrophages in renal and liver fibrosis has been well established (Dang et al., 2012, Henderson et al., 2008, Duffield et al., 2005, Ramachandran et al., 2012). Examination of macrophage phenotype was beyond the

remit of this study, which focused primarily on imaging, but would be of interest to determine whether the macrophages were predominantly YM1-expressing pro-fibrotic phenotype.

One limitation of the study is that imaging was performed at 4 weeks post-transplant, when there was already histological evidence of fibrosis and, as the model is not transplant dependent, it is not possible to ascertain whether deterioration in renal function had already occurred. However this is a proof of principle investigation to determine the feasibility of such an approach, and subsequent work will require imaging at earlier time points and correlating with renal function.

Blooming artefact associated with T2*/R2* imaging with MRI is another potential limitation. These distortions can be erroneously included in the region of interest covering the renal tissue leading to falsely high R2* readings. In our study, this was particularly evident when the spleen laden with USPIO could distort the values in the neighbouring transplanted kidney. Care was taken to avoid drawing regions of interest over such areas. In addition, T2*/R2* imaging identifies areas or tissue edema or hemorrhage in other organs, and as such the differing R2* values of baseline scans may have been due to differing amounts of edema (Ghugre et al., 2011). Finally, the relationship between R2* value and iron accumulation is non-linear, and so absolute increase in R2* value may not be directly proportional to increased inflammation (Patterson et al., 2011). The technique is semi-quantitive and so increasing values do indicate an increase in the number of monocytes or macrophages in a tissue, or an increase in activity. There was a range of values in the

allograft group, suggesting a differing amount of inflammation in the different allografts. As the mechanism of rejection in this model of CAD is multifaceted a single measurement at 4 weeks is expected to have variation given that this model develops gradual histological injury up to 12 weeks and beyond (Tse et al., 2013).

The USPIO agent Ferumoxytol is used as an intravenous iron supplementation agent for patients with end stage renal failure. It has an good safety profile and is an ideal agent for investigation of transplant rejection in patients (Schiller et al., 2014). Further translational studies are needed to identify if there is a R2* threshold value which would identify a level of excessive inflammation requiring alteration of therapy.

In conclusion, we have developed an MRI technique for detecting inflammation in a model of chronic renal allograft damage. The protocol employs USPIO contrast that is compatible with patients who have renal dysfunction. This non-invasive approach for the detection of changes of CAD offers the possibility of avoiding renal biopsy in some patients. Translational studies are required to assess its applicability in clinical practice.

Acknowledgements

The study was funded by a grant from the Royal College of Surgeons of Edinburgh (SRG/13/064), and GT was funded through a clinical training fellowship from Kidney Research UK (TF4/2012). The authors are supported by grants from the British Heart Foundation (RE/08/001 and FS/12/83), Medical Research Council (G1001339), National Institute for Health Research (EME 11/20/03), Chest Heart and Stroke Scotland (R11/A135) and Chief Scientist Office (ETM/266). DEN is supported by the British Heart Foundation (CH/09/002). PAH is supported by NHS Research Scotland Fellowship.

REFERENCES

http://www.bts.org.uk/transplantation/heart/.

www.clinicaltrialsregister.eu/ctr-search/ *Search for 2010-019527-58. Accessed 26/10/2011* [Online]. [Accessed 2011].

2004. *Coronary heart disease statistics: factsheet* [Online]. Available: www.heartstats.org [Accessed].

ABBATE, A., BONANNO, E., MAURIELLO, A., BUSSANI, R., BIONDI-ZOCCAI, G. G., LIUZZO, G., LEONE, A. M., SILVESTRI, F., DOBRINA, A., BALDI, F., PANDOLFI, F., BIASUCCI, L. M., BALDI, A., SPAGNOLI, L. G. & CREA, F. 2004. Widespread myocardial inflammation and infarct-related artery patency. *Circulation,* 110**,** 46-50.

ALAM, S. R., LEWIS, S. C., ZAMVAR, V., PESSOTTO, R., DWECK, M. R., KRISHAN, A., GOODMAN, K., OATEY, K., HARKESS, R., MILNE, L., THOMAS, S., MILLS, N. M., MOORE, C., SEMPLE, S., WIEDOW, O., STIRRAT, C., MIRSADRAEE, S., NEWBY, D. E. & HENRIKSEN, P. A. 2015. Perioperative elafin for ischaemia-reperfusion injury during coronary artery bypass graft surgery: a randomised-controlled trial. *Heart,* 101**,** 1639-45.

ALAM, S. R., NEWBY, D. E. & HENRIKSEN, P. A. 2012a. Role of the endogenous elastase inhibitor, elafin, in cardiovascular injury: From epithelium to endothelium. *Biochem Pharmacol,* 83**,** 695-704.

ALAM, S. R., SHAH, A. S., RICHARDS, J., LANG, N. N., BARNES, G., JOSHI, N., MACGILLIVRAY, T., MCKILLOP, G., MIRSADRAEE, S., PAYNE, J., FOX, K. A., HENRIKSEN, P., NEWBY, D. E. & SEMPLE, S. I. 2012b. Ultrasmall Superparamagnetic Particles of Iron Oxide in Patients with Acute Myocardial Infarction: Early Clinical Experience. *Circ Cardiovasc Imaging*.

ALAM, S. R., SHAH, A. S., RICHARDS, J., LANG, N. N., BARNES, G., JOSHI, N., MACGILLIVRAY, T., MCKILLOP, G., MIRSADRAEE, S., PAYNE, J., FOX, K. A., HENRIKSEN, P., NEWBY, D. E. & SEMPLE, S. I. 2012c. Ultrasmall superparamagnetic particles of iron oxide in patients with acute myocardial infarction: early clinical experience. *Circ Cardiovasc Imaging,* 5**,** 559-65.

ALAM, S. R., SHAH, A. S., RICHARDS, J., LANG, N. N., BARNES, G., JOSHI, N., MACGILLIVRAY, T., MCKILLOP, G., MIRSADRAEE, S., PAYNE, J., FOX, K. A., HENRIKSEN, P., NEWBY, D. E. & SEMPLE, S. I. 2012d. Ultrasmall superparamagnetic particles of iron oxide in patients with acute myocardial infarction: early clinical experience. *Circulation. Cardiovascular imaging,* 5**,** 559-65.

ANDERSON, L. J., HOLDEN, S., DAVIS, B., PRESCOTT, E., CHARRIER, C. C., BUNCE, N. H., FIRMIN, D. N., WONKE, B., PORTER, J., WALKER, J. M. & PENNELL, D. J. 2001. Cardiovascular T2-star (T2*) magnetic resonance for the early diagnosis of myocardial iron overload. *European Heart Journal,* 22**,** 2171-2179.

ANSELMI, A., ABBATE, A., GIROLA, F., NASSO, G., BIONDI-ZOCCAI, G. G. L., POSSATI, G. & GAUDINO, M. 2004. Myocardial ischemia, stunning, inflammation, and apoptosis during cardiac surgery: a review of evidence. *European Journal of Cardio-thoracic Surgery*, 25**,** 304-311.

ASCIONE, R., LLOYD, C. T., UNDERWOOD, M. J., LOTTO, A. A., PITSIS, A. A. & ANGELINI, G. D. 2000. Inflammatory response after coronary

revascularization with or without cardiopulmonary bypass. *The Annals of Thoracic Surgery,* 69**,** 1198-204.

ASOKANANTHAN, N., GRAHAM, P. T., FINK, J., KNIGHT, D. A., BAKKER, A. J., MCWILLIAM, A. S., THOMPSON, P. J. & STEWART, G. A. 2002. Activation of protease-activated receptor PAR-1, PAR-2, and PAR-4 stimulates IL-6, IL-8, and prostaglandin E2 release from human respiratory epithelial cells. *The Journal of Immunology,* 168**,** 3577.

AZUMA, H., HEEMANN, U., TULLIUS, S. G. & TILNEY, N. L. 1994. Host leukocytes and their products in chronic kidney allograft rejection in rats. *Transpl Int,* 7 Suppl 1**,** S325-7.

BABA, T., ISHIZU, A., IWASAKI, S., SUZUKI, A., TOMARU, U., IKEDA, H., YOSHIKI, T. & KASAHARA, M. 2006. CD4+/CD8+ macrophages infiltrating at inflammatory sites: a population of monocytes/macrophages with a cytotoxic phenotype. *Blood,* 107**,** 2004-12.

BAGSHAW, S. M. & GIBNEY, R. T. 2008. Conventional markers of kidney function. *Crit Care Med,* 36**,** S152-8.

BALDUS, S., EISERICH, J. P., MANI, A., CASTRO, L., FIGUEROA, M., CHUMLEY, P., MA, W., TOUSSON, A., WHITE, C. R., BULLARD, D. C., BRENNAN, M. L., LUSIS, A. J., MOORE, K. P. & FREEMAN, B. A. 2001. Endothelial transcytosis of myeloperoxidase confers specificity to vascular ECM proteins as targets of tyrosine nitration. *J Clin Invest,* 108**,** 1759-70.

BALDUS, S., HEESCHEN, C., MEINERTZ, T., ZEIHER, A. M., EISERICH, J. P., MUNZEL, T., SIMOONS, M. L. & HAMM, C. W. 2003. Myeloperoxidase serum levels predict risk in patients with acute coronary syndromes. *Circulation,* 108**,** 1440.

BANBA, K., KUSANO, K. F., NAKAMURA, K., MORITA, H., OGAWA, A., OHTSUKA, F., OGO, K. O., NISHII, N., WATANABE, A., NAGASE, S., SAKURAGI, S. & OHE, T. 2007. Relationship between arrhythmogenesis and disease activity in cardiac sarcoidosis. *Heart Rhythm,* 4**,** 1292-9.

BAROLET, A. W., NILI, N., CHEEMA, A., ROBINSON, R., NATARAJAN, M. K., O'BLENES, S., LI, J., ESKANDARIAN, M. R., SPARKES, J. & RABINOVITCH, M. 2001. Arterial elastase activity after balloon angioplasty and effects of elafin, an elastase inhibitor. *Arteriosclerosis, Thrombosis, and Vascular Biology,* 21**,** 1269.

BELAAOUAJ, A., KIM, K. S. & SHAPIRO, S. D. 2000a. Degradation of outer membrane protein A in Escherichia coli killing by neutrophil elastase. *Science,* 289**,** 1185-8.

BELAAOUAJ, A., KIM, K. S. & SHAPIRO, S. D. 2000b. Degradation of outer membrane protein A in Escherichia coli killing by neutrophil elastase. *Science,* 289**,** 1185.

BELAAOUAJ, A., MCCARTHY, R., BAUMANN, M., GAO, Z., LEY, T. J., ABRAHAM, S. N. & SHAPIRO, S. D. 1998. Mice lacking neutrophil elastase reveal impaired host defense against gram negative bacterial sepsis. *Nature Medicine,* 4**,** 615-618.

BELLEMARE, A., VERNOUX, N., MORISSET, D. & BOURBONNAIS, Y. 2008. Human pre-elafin inhibits a Pseudomonas aeruginosa-secreted peptidase and

prevents its proliferation in complex media. *Antimicrob Agents Chemother,* 52**,** 483-90.

BIERRY, G., JEHL, F., BOEHM, N., ROBERT, P., PRÈVOST, G., DIETEMANN, J. L., DESAL, H. & KREMER, S. 2008. Macrophage Activity in Infected Areas of an Experimental Vertebral Osteomyelitis Model: USPIO-enhanced MR ImagingóFeasibility Study1. *Radiology,* 248**,** 114.

BJERNER, T., ERICSSON, A., WIKSTROM, G., JOHANSSON, L., NILSSON, S., AHLSTROM, H. & HEMMINGSSON, A. 2000. Evaluation of nonperfused myocardial ischemia with MRI and an intravascular USPIO contrast agent in an ex vivo pig model. *J Magn Reson Imaging,* 12**,** 866-72.

BLAND, J. M. & ALTMAN, D. G. 1986. Statistical methods for assessing agreement between two methods of clinical measurement. *Lancet,* 1**,** 307-10.

BOLDT, J. & WOLF, M. 2008. Identification of renal injury in cardiac surgery: the role of kidney-specific proteins. *J Cardiothorac Vasc Anesth,* 22**,** 122-32.

BOLLI, R., BECKER, L., GROSS, G., MENTZER JR, R., BALSHAW, D. & LATHROP, D. A. 2004. Myocardial protection at a crossroads: the need for translation into clinical therapy. *Circulation Research,* 95**,** 125.

BONVINI, R. F., HENDIRI, T. & CAMENZIND, E. 2005. Inflammatory response post-myocardial infarction and reperfusion: a new therapeutic target? *European Heart Journal Supplements,* 7**,** I27-I36.

BORREGAARD, N. & COWLAND, J. B. 1997. Granules of the human neutrophilic polymorphonuclear leukocyte. *Blood,* 89**,** 3503.

BOTHA, A. J., MOORE, F. A., MOORE, E. E., SAUAIA, A., BANERJEE, A. & PETERSON, V. M. 1995. Early neutrophil sequestration after injury: a pathogenic mechanism for multiple organ failure. *J Trauma,* 39**,** 411-7.

BOUTRY, S., BRUNIN, S., MAHIEU, I., LAURENT, S., VANDER ELST, L. & MULLER, R. N. 2008. Magnetic labeling of non-phagocytic adherent cells with iron oxide nanoparticles: a comprehensive study. *Contrast media & molecular imaging,* 3**,** 223-32.

BOYCE, S. W., BARTELS, C., BOLLI, R., CHAITMAN, B., CHEN, J. C., CHI, E., JESSEL, A., KEREIAKES, D., KNIGHT, J., THULIN, L. & THEROUX, P. 2003. Impact of sodium-hydrogen exchange inhibition by cariporide on death or myocardial infarction in high-risk CABG surgery patients: results of the CABG surgery cohort of the GUARDIAN study. *J Thorac Cardiovasc Surg,* 126**,** 420-7.

BRASIER, A. R., RECINOS, A., 3RD & ELEDRISI, M. S. 2002. Vascular inflammation and the renin-angiotensin system. *Arterioscler Thromb Vasc Biol,* 22**,** 1257-66.

BRAUN, J. S., JANDER, S., SCHROETER, M., WITTE, O. W. & STOLL, G. 1996. Spatiotemporal relationship of apoptotic cell death to lymphomonocytic infiltration in photochemically induced focal ischemia of the rat cerebral cortex. *Acta Neuropathol,* 92**,** 255-63.

BUFFON, A., BIASUCCI, L. M., LIUZZO, G., D'ONOFRIO, G., CREA, F. & MASERI, A. 2002. Widespread coronary inflammation in unstable angina. *The New England journal of medicine,* 347**,** 5-12.

BUTLER, J., PARKER, D., PILLAI, R., WESTABY, S., SHALE, D. J. & ROCKER, G. M. 1993. Effect of cardiopulmonary bypass on systemic

release of neutrophil elastase and tumor necrosis factor. *J Thorac Cardiovasc Surg,* 105**,** 25-30.

BUTLER, M. W., ROBERTSON, I., GREENE, C. M., O'NEILL, S. J., TAGGART, C. C. & MCELVANEY, N. G. 2006. Elafin prevents lipopolysaccharide-induced AP-1 and NF- B activation via an effect on the ubiquitin-proteasome pathway. *Journal of Biological Chemistry,* 281**,** 34730.

CARDEN, D., XIAO, F., MOAK, C., WILLIS, B. H., ROBINSON-JACKSON, S. & ALEXANDER, S. 1998. Neutrophil elastase promotes lung microvascular injury and proteolysis of endothelial cadherins. *American Journal of Physiology-Heart and Circulatory Physiology,* 275**,** H385.

CARROLL, T. P., GREENE, C. M., TAGGART, C. C., BOWIE, A. G., O'NEILL, S. J. & MCELVANEY, N. G. 2005. Viral inhibition of IL-1-and neutrophil elastase-induced inflammatory responses in bronchial epithelial cells. *The Journal of Immunology,* 175**,** 7594.

CERQUEIRA, M. D., WEISSMAN, N. J., DILSIZIAN, V., JACOBS, A. K., KAUL, S., LASKEY, W. K., PENNELL, D. J., RUMBERGER, J. A., RYAN, T. & VERANI, M. S. 2002. Standardized myocardial segmentation and nomenclature for tomographic imaging of the heart. A statement for healthcare professionals from the Cardiac Imaging Committee of the Council on Clinical Cardiology of the American Heart Association. *Circulation,* 105**,** 539-42.

CHAKRABORTI, S., MANDAL, M., DAS, S., MANDAL, A. & CHAKRABORTI, T. 2003. Regulation of matrix metalloproteinases: an overview. *Molecular and Cellular Biochemistry,* 253**,** 269-285.

CHIN, A. C., LEE, W. Y., NUSRAT, A., VERGNOLLE, N. & PARKOS, C. A. 2008. Neutrophil-mediated activation of epithelial protease-activated receptors-1 and-2 regulates barrier function and transepithelial migration. *The Journal of Immunology,* 181**,** 5702.

CHRISTEN, T., NI, W., QIU, D., SCHMIEDESKAMP, H., BAMMER, R., MOSELEY, M. & ZAHARCHUK, G. 2012. High-resolution cerebral blood volume imaging in humans using the blood pool contrast agent ferumoxytol. *Magn Reson Med*.

CHRISTEN, T., NI, W., QIU, D., SCHMIEDESKAMP, H., BAMMER, R., MOSELEY, M. & ZAHARCHUK, G. 2013. High-resolution cerebral blood volume imaging in humans using the blood pool contrast agent ferumoxytol. *Magnetic Resonance in Medicine,* 70**,** 705-10.

CHRISTEN, T., SHIMIZU, K. & LIBBY, P. 2010. Advances in imaging of cardiac allograft rejection. *Current Cardiovascular Imaging Reports,* 3**,** 99-105.

COESHOTT, C., OHNEMUS, C., PILYAVSKAYA, A., ROSS, S., WIECZOREK, M., KROONA, H., LEIMER, A. H. & CHERONIS, J. 1999. Converting enzyme-independent release of tumor necrosis factor and IL-1 from a stimulated human monocytic cell line in the presence of activated neutrophils or purified proteinase 3. *Proceedings of the National Academy of Sciences of the United States of America,* 96**,** 6261.

COOPER, L. T., BAUGHMAN, K. L., FELDMAN, A. M., FRUSTACI, A., JESSUP, M., KUHL, U., LEVINE, G. N., NARULA, J., STARLING, R. C., TOWBIN, J. & VIRMANI, R. 2007. The role of endomyocardial biopsy in

the management of cardiovascular disease: a scientific statement from the American Heart Association, the American College of Cardiology, and the European Society of Cardiology Endorsed by the Heart Failure Society of America and the Heart Failure Association of the European Society of Cardiology. *Eur Heart J,* 28**,** 3076-93.

COUDREY, L. 1998. The troponins. *Archives of internal medicine,* 158**,** 1173-80.

COWAN, B., BARON, O., CRACK, J., COULBER, C., WILSON, G. J. & RABINOVITCH, M. 1996. Elafin, a serine elastase inhibitor, attenuates post-cardiac transplant coronary arteriopathy and reduces myocardial necrosis in rabbits afer heterotopic cardiac transplantation. *J Clin Invest,* 97**,** 2452-68.

CRINNION, J., HOMER-VANNIASINKAM, S., HATTON, R., PARKIN, S. & GOUGH, M. 1994. Role of neutrophil depletion and elastase inhibition in modifying skeletal muscle reperfusion injury. *Cardiovascular Surgery (London, England),* 2**,** 749.

CROAL, B. L., HILLIS, G. S., GIBSON, P. H., FAZAL, M. T., EL-SHAFEI, H., GIBSON, G., JEFFREY, R. R., BUCHAN, K. G., WEST, D. & CUTHBERTSON, B. H. 2006. Relationship between postoperative cardiac troponin I levels and outcome of cardiac surgery. *Circulation,* 114**,** 1468-75.

CRUZ, D. N., RONCO, C. & KATZ, N. 2010. Neutrophil gelatinase-associated lipocalin: a promising biomarker for detecting cardiac surgery-associated acute kidney injury. *J Thorac Cardiovasc Surg,* 139**,** 1101-6.

DAHNKE, H., LIU, W., HERZKA, D., FRANK, J. A. & SCHAEFFTER, T. 2008. Susceptibility gradient mapping (SGM): a new postprocessing method for positive contrast generation applied to superparamagnetic iron oxide particle (SPIO)-labeled cells. *Magn Reson Med,* 60**,** 595-603.

DANG, Z., MACKINNON, A., MARSON, L. P. & SETHI, T. 2012. Tubular atrophy and interstitial fibrosis after renal transplantation is dependent on galectin-3. *Transplantation,* 93**,** 477-84.

DAUGHERTY, A., DUNN, J. L., RATERI, D. L. & HEINECKE, J. W. 1994. Myeloperoxidase, a catalyst for lipoprotein oxidation, is expressed in human atherosclerotic lesions. *Journal of Clinical Investigation,* 94**,** 437.

DAY, J. R. & TAYLOR, K. M. 2005. The systemic inflammatory response syndrome and cardiopulmonary bypass. *Int J Surg,* 3**,** 129-40.

DEL ZOPPO, G., GINIS, I., HALLENBECK, J. M., IADECOLA, C., WANG, X. & FEUERSTEIN, G. Z. 2000. Inflammation and stroke: putative role for cytokines, adhesion molecules and iNOS in brain response to ischemia. *Brain Pathol,* 10**,** 95-112.

DESESTRET, V., BRISSET, J. C., MOUCHARRAFIE, S., DEVILLARD, E., NATAF, S., HONNORAT, J., NIGHOGHOSSIAN, N., BERTHEZENE, Y. & WIART, M. 2009. Early-stage investigations of ultrasmall superparamagnetic iron oxide-induced signal change after permanent middle cerebral artery occlusion in mice. *Stroke,* 40**,** 1834-41.

DEVANEY, J. M., GREENE, C. M., TAGGART, C. C., CARROLL, T. P., O'NEILL, S. J. & MCELVANEY, N. G. 2003. Neutrophil elastase up-regulates interleukin-8 via toll-like receptor 4. *FEBS letters,* 544**,** 129-132.

DEWALD, O., ZYMEK, P., WINKELMANN, K., KOERTING, A., REN, G., ABOU-KHAMIS, T., MICHAEL, L. H., ROLLINS, B. J., ENTMAN, M. L.

& FRANGOGIANNIS, N. G. 2005. CCL2/monocyte chemoattractant protein-1 regulates inflammatory responses critical to healing myocardial infarcts. *Circulation Research,* 96**,** 881.

DI MARCO, M., SADUN, C., PORT, M., GUILBERT, I., COUVREUR, P. & DUBERNET, C. 2007. Physicochemical characterization of ultrasmall superparamagnetic iron oxide particles (USPIO) for biomedical application as MRI contrast agents. *International journal of nanomedicine,* 2**,** 609-22.

DIAMOND, J. R., TILNEY, N. L., FRYE, J., DING, G., MCELROY, J., PESEK-DIAMOND, I. & YANG, H. 1992. Progressive albuminuria and glomerulosclerosis in a rat model of chronic renal allograft rejection. *Transplantation,* 54**,** 710-6.

DINERMAN, J. L. & MEHTA, J. L. 1990. Endothelial, platelet and leukocyte interactions in ischemic heart disease: insights into potential mechanisms and their clinical relevance. *Journal of the American College of Cardiology,* 16**,** 207-222.

DIODATO, M. & CHEDRAWY, E. G. 2014. Coronary artery bypass graft surgery: the past, present, and future of myocardial revascularisation. *Surgery research and practice,* 2014**,** 726158.

DOLLERY, C. M., OWEN, C. A., SUKHOVA, G. K., KRETTEK, A., SHAPIRO, S. D. & LIBBY, P. 2003. Neutrophil elastase in human atherosclerotic plaques: production by macrophages. *Circulation,* 107**,** 2829.

DOTSENKO, O., XIAO, Q., XU, Q. & JAHANGIRI, M. 2010. Bone marrow resident and circulating progenitor cells in patients undergoing cardiac surgery. *Ann Thorac Surg,* 90**,** 1944-51.

DOUSSET, V., DELALANDE, C., BALLARINO, L., QUESSON, B., SEILHAN, D., COUSSEMACQ, M., THIAUDIÈRE, E., BROCHET, B., CANIONI, P. & CAILLÈ, J. M. 1999. In vivo macrophage activity imaging in the central nervous system detected by magnetic resonance. *Magnetic resonance in medicine,* 41**,** 329-333.

DREYER, W., MICHAEL, L., WEST, M., SMITH, C., ROTHLEIN, R., ROSSEN, R., ANDERSON, D. & ENTMAN, M. 1991. Neutrophil accumulation in ischemic canine myocardium. Insights into time course, distribution, and mechanism of localization during early reperfusion. *Circulation,* 84**,** 400.

DUBOSCQ, C., GENOUD, V., PARBORELL, M. F. & KORDICH, L. C. 1997. Impaired clot lysis by rt-PA catalyzed mini-plasminogen activation. *Thrombosis Research,* 86**,** 505-513.

DUBREY, S. W. & FALK, R. H. 2010. Diagnosis and management of cardiac sarcoidosis. *Prog Cardiovasc Dis,* 52**,** 336-46.

DUFFIELD, J. S., FORBES, S. J., CONSTANDINOU, C. M., CLAY, S., PARTOLINA, M., VUTHOORI, S., WU, S., LANG, R. & IREDALE, J. P. 2005. Selective depletion of macrophages reveals distinct, opposing roles during liver injury and repair. *J Clin Invest,* 115**,** 56-65.

DUTTA, P. & NAHRENDORF, M. 2015. Monocytes in myocardial infarction. *Arterioscler Thromb Vasc Biol,* 35**,** 1066-70.

EITEL, I., DESCH, S., FUERNAU, G., HILDEBRAND, L., GUTBERLET, M., SCHULER, G. & THIELE, H. 2010. Prognostic significance and determinants of myocardial salvage assessed by cardiovascular magnetic

resonance in acute reperfused myocardial infarction. *J Am Coll Cardiol,* 55**,** 2470-9.

ENGLER, R., SCHMID-SCHÖNBEIN, G. & PAVELEC, R. 1983. Leukocyte capillary plugging in myocardial ischemia and reperfusion in the dog. *The American Journal of Pathology,* 111**,** 98.

ERSOY, H., JACOBS, P., KENT, C. K. & PRINCE, M. R. 2004. Blood pool MR angiography of aortic stent-graft endoleak. *AJR Am J Roentgenol,* 182**,** 1181-6.

FAHIM, T., BOHMIG, G. A., EXNER, M., HUTTARY, N., KERSCHNER, H., KANDUTSCH, S., KERJASCHKI, D., BRAMBOCK, A., NAGY-BOJARSZKY, K. & REGELE, H. 2007. The cellular lesion of humoral rejection: predominant recruitment of monocytes to peritubular and glomerular capillaries. *Am J Transplant,* 7**,** 385-93.

FANANAPAZIR, G., MARIN, D., SUHOCKI, P. V., KIM, C. Y. & BASHIR, M. R. 2014. Vascular artifact mimicking thrombosis on MR imaging using ferumoxytol as a contrast agent in abdominal vascular assessment. *J Vasc Interv Radiol,* 25**,** 969-76.

FELDMAN, A. M. & MCNAMARA, D. 2000. Myocarditis. *N Engl J Med,* 343**,** 1388-98.

FONTAINE, V., TOUAT, Z., MTAIRAG, E. M., VRANCKX, R., LOUEDEC, L., HOUARD, X., ANDREASSIAN, B., SEBBAG, U., PALOMBI, T. & JACOB, M. P. 2004. Role of leukocyte elastase in preventing cellular re-colonization of the mural thrombus. *American Journal of Pathology,* 164**,** 2077.

FRANCART, C., DAUCHEZ, M., ALIX, A. J. P. & LIPPENS, G. 1997. Solution structure of R-elafin, a specific inhibitor of elastase. *Journal of Molecular Biology,* 268**,** 666-677.

FRANGOGIANNIS, N. G. 2006. Targeting the inflammatory response in healing myocardial infarcts. *Curr Med Chem,* 13**,** 1877-93.

FRANTZ, S., BAUERSACHS, J. & ERTL, G. 2009. Post-infarct remodelling: contribution of wound healing and inflammation. *Cardiovasc Res,* 81**,** 474-81.

FRIEDRICH, M. G. & MARCOTTE, F. 2013. Cardiac magnetic resonance assessment of myocarditis. *Circ Cardiovasc Imaging,* 6**,** 833-9.

FRISCH, S. M. & FRANCIS, H. 1994. Disruption of epithelial cell-matrix interactions induces apoptosis. *The Journal of Cell Biology,* 124**,** 619.

GARCIA-DORADO, D., OLIVERAS, J., GILI, J., SANZ, E., PEREZ-VILLA, F., BARRABES, J., CARRERAS, M. J., SOLARES, J. & SOLER-SOLER, J. 1993. Analysis of myocardial oedema by magnetic resonance imaging early after coronary artery occlusion with or without reperfusion. *Cardiovasc Res,* 27**,** 1462-9.

GARCIA-TOUCHARD, A., HENRY, T. D., SANGIORGI, G., SPAGNOLI, L. G., MAURIELLO, A., CONOVER, C. & SCHWARTZ, R. S. 2005. Extracellular proteases in atherosclerosis and restenosis. *Arteriosclerosis, Thrombosis, and Vascular Biology,* 25**,** 1119.

GELLISSEN, J., AXMANN, C., PRESCHER, A., BOHNDORF, K. & LODEMANN, K. P. 1999a. Extra- and intracellular accumulation of

ultrasmall superparamagnetic iron oxides (USPIO) in experimentally induced abscesses of the peripheral soft tissues and their effects on magnetic resonance imaging. *Magn Reson Imaging,* 17**,** 557-67.

GELLISSEN, J., AXMANN, C., PRESCHER, A., BOHNDORF, K. & LODEMANN, K. P. 1999b. Extra-and intracellular accumulation of ultrasmall superparamagnetic iron oxides (USPIO) in experimentally induced abscesses of the peripheral soft tissues and their effects on magnetic resonance imaging. *Magnetic Resonance Imaging,* 17**,** 557-567.

GHUGRE, N. R., RAMANAN, V., POP, M., YANG, Y., BARRY, J., QIANG, B., CONNELLY, K. A., DICK, A. J. & WRIGHT, G. A. 2011. Quantitative tracking of edema, hemorrhage, and microvascular obstruction in subacute myocardial infarction in a porcine model by MRI. *Magn Reson Med,* 66**,** 1129-41.

GONZALEZ, A., RAVASSA, S., BEAUMONT, J., LOPEZ, B. & DIEZ, J. 2011. New targets to treat the structural remodeling of the myocardium. *J Am Coll Cardiol,* 58**,** 1833-43.

GRAY, G. A., MICKLEY, E. J., WEBB, D. J. & MCEWAN, P. E. 2000. Localization and function of ET-1 and ET receptors in small arteries post-myocardial infarction: upregulation of smooth muscle ET(B) receptors that modulate contraction. *Br J Pharmacol,* 130**,** 1735-44.

HAASE, M., BELLOMO, R., DEVARAJAN, P., MA, Q., BENNETT, M. R., MOCKEL, M., MATALANIS, G., DRAGUN, D. & HAASE-FIELITZ, A. 2009. Novel biomarkers early predict the severity of acute kidney injury after cardiac surgery in adults. *Ann Thorac Surg,* 88**,** 124-30.

HAMMOND, M., LAPOINTE, G. R., FEUCHT, P. H., HILT, S., GALLEGOS, C. A., GORDON, C. A., GIEDLIN, M. A., MULLENBACH, G. & TEKAMP-OLSON, P. 1995. IL-8 induces neutrophil chemotaxis predominantly via type I IL-8 receptors. *The Journal of Immunology,* 155**,** 1428.

HANCOCK, W. H., WHITLEY, W. D., TULLIUS, S. G., HEEMANN, U. W., WASOWSKA, B., BALDWIN, W. M., 3RD & TILNEY, N. L. 1993. Cytokines, adhesion molecules, and the pathogenesis of chronic rejection of rat renal allografts. *Transplantation,* 56**,** 643-50.

HANSEN, P. R. 1995. Role of neutrophils in myocardial ischemia and reperfusion. *Circulation,* 91**,** 1872.

HARISINGHANI, M., ROSS, R. W., GUIMARAES, A. R. & WEISSLEDER, R. 2007. Utility of a new bolus-injectable nanoparticle for clinical cancer staging. *Neoplasia,* 9**,** 1160-5.

HATTORI, R., HAMILTON, K., FUGATE, R., MCEVER, R. & SIMS, P. 1989. Stimulated secretion of endothelial von Willebrand factor is accompanied by rapid redistribution to the cell surface of the intracellular granule membrane protein GMP-140. *Journal of Biological Chemistry,* 264**,** 7768.

HAUGER, O., DELALANDE, C., DEMINIËRE, C., FOUQUERAY, B., OHAYON, C., GARCIA, S., TRILLAUD, H., COMBE, C. & GRENIER, N. 2000. Nephrotoxic Nephritis and Obstructive Nephropathy: Evaluation with MR Imaging Enhanced with Ultrasmall Superparamagnetic Iron OxideóPreliminary Findings in a Rat Model1. *Radiology,* 217**,** 819.

HAUSENLOY, D. J., MWAMURE, P. K., VENUGOPAL, V., HARRIS, J., BARNARD, M., GRUNDY, E., ASHLEY, E., VICHARE, S., DI SALVO, C., KOLVEKAR, S., HAYWARD, M., KEOGH, B., MACALLISTER, R. J. & YELLON, D. M. 2007. Effect of remote ischaemic preconditioning on myocardial injury in patients undergoing coronary artery bypass graft surgery: a randomised controlled trial. *Lancet,* 370**,** 575-9.

HAYASHIDANI, S., TSUTSUI, H., SHIOMI, T., IKEUCHI, M., MATSUSAKA, H., SUEMATSU, N., WEN, J., EGASHIRA, K. & TAKESHITA, A. 2003. Anti-monocyte chemoattractant protein-1 gene therapy attenuates left ventricular remodeling and failure after experimental myocardial infarction. *Circulation,* 108**,** 2134.

HEEMANN, U. W., TULLIUS, S. G., TAMATAMI, T., MIYASAKA, M., MILFORD, E. & TILNEY, N. L. 1994. Infiltration patterns of macrophages and lymphocytes in chronically rejecting rat kidney allografts. *Transpl Int,* 7**,** 349-55.

HENDERSON, N. C., MACKINNON, A. C., FARNWORTH, S. L., KIPARI, T., HASLETT, C., IREDALE, J. P., LIU, F. T., HUGHES, J. & SETHI, T. 2008. Galectin-3 expression and secretion links macrophages to the promotion of renal fibrosis. *Am J Pathol,* 172**,** 288-98.

HENRIKSEN, P. A., DEVITT, A., KOTELEVTSEV, Y. & SALLENAVE, J. M. 2004a. Gene delivery of the elastase inhibitor elafin protects macrophages from neutrophil elastase-mediated impairment of apoptotic cell recognition. *FEBS letters,* 574**,** 80-84.

HENRIKSEN, P. A., HITT, M., XING, Z., WANG, J., HASLETT, C., RIEMERSMA, R. A., WEBB, D. J., KOTELEVTSEV, Y. V. & SALLENAVE, J. M. 2004b. Adenoviral gene delivery of elafin and secretory leukocyte protease inhibitor attenuates NF- B-dependent inflammatory responses of human endothelial cells and macrophages to atherogenic stimuli. *The Journal of Immunology,* 172**,** 4535.

HERBORN, C. U., VOGT, F. M., LAUENSTEIN, T. C., DIRSCH, O., COROT, C., ROBERT, P. & RUEHM, S. G. 2006. Magnetic resonance imaging of experimental atherosclerotic plaque: comparison of two ultrasmall superparamagnetic particles of iron oxide. *J Magn Reson Imaging,* 24**,** 388-93.

HERLAAR, E. & BROWN, Z. 1999. p38 MAPK signalling cascades in inflammatory disease. *Mol Med Today,* 5**,** 439-47.

HERTZ, M. I., AURORA, P., CHRISTIE, J. D., DOBBELS, F., EDWARDS, L. B., KIRK, R., KUCHERYAVAYA, A. Y., RAHMEL, A. O., ROWE, A. W., STEHLIK, J. & TAYLOR, D. O. 2009. Scientific Registry of the International Society for Heart and Lung Transplantation: introduction to the 2009 Annual Reports. *J Heart Lung Transplant,* 28**,** 989-92.

HILL, G. E., ALONSO, A., SPURZEM, J. R., STAMMERS, A. H. & ROBBINS, R. A. 1995. Aprotinin and methylprednisolone equally blunt cardiopulmonary bypass-induced inflammation in humans. *J Thorac Cardiovasc Surg,* 110**,** 1658-62.

HIRCHE, T. O., BENABID, R., DESLEE, G., GANGLOFF, S., ACHILEFU, S., GUENOUNOU, M., LEBARGY, F., HANCOCK, R. E. & BELAAOUAJ, A.

2008. Neutrophil elastase mediates innate host protection against Pseudomonas aeruginosa. *The Journal of Immunology,* 181**,** 4945-4954.

HOSHI, K., KUROSAWA, S., KATO, M., ANDOH, K., SATOH, D. & KAISE, A. 2005. Sivelestat, a neutrophil elastase inhibitor, reduces mortality rate of critically ill patients. *Tohoku J Exp Med,* 207**,** 143-8.

HOUGHTON, A. M. G., QUINTERO, P. A., PERKINS, D. L., KOBAYASHI, D. K., KELLEY, D. G., MARCONCINI, L. A., MECHAM, R. P., SENIOR, R. M. & SHAPIRO, S. D. 2006. Elastin fragments drive disease progression in a murine model of emphysema. *Journal of Clinical Investigation,* 116**,** 753.

HOWARTH, S. P., TANG, T. Y., GRAVES, M. J., JM, U. K.-I., LI, Z. Y., WALSH, S. R., GAUNT, M. E. & GILLARD, J. H. 2007. Non-invasive MR imaging of inflammation in a patient with both asymptomatic carotid atheroma and an abdominal aortic aneurysm: a case report. *Ann Surg Innov Res,* 1**,** 4.

HTTP://WWW.BTS.ORG.UK/TRANSPLANTATION/HEART/. 2015. *BHF CVD Statistics Factsheet - UK* [Online]. Available: http://www.bts.org.uk/transplantation/heart/ [Accessed].

HUNT, M. A., BAGO, A. G. & NEUWELT, E. A. 2005. Single-dose contrast agent for intraoperative MR imaging of intrinsic brain tumors by using ferumoxtran-10. *AJNR Am J Neuroradiol,* 26**,** 1084-8.

HYAFIL, F., LAISSY, J. P., MAZIGHI, M., TCHETCHE, D., LOUEDEC, L., ADLE-BIASSETTE, H., CHILLON, S., HENIN, D., JACOB, M. P., LETOURNEUR, D. & FELDMAN, L. J. 2006. Ferumoxtran-10-enhanced MRI of the hypercholesterolemic rabbit aorta: relationship between signal loss and macrophage infiltration. *Arterioscler Thromb Vasc Biol,* 26**,** 176-81.

IRWIN, M. W., MAK, S., MANN, D. L., QU, R., PENNINGER, J. M., YAN, A., DAWOOD, F., WEN, W. H., SHOU, Z. & LIU, P. 1999. Tissue expression and immunolocalization of tumor necrosis factor-alpha in postinfarction dysfunctional myocardium. *Circulation,* 99**,** 1492-8.

ISBIR, C. S., DOGAN, R., DEMIRCIN, M., YAYLIM, I. & PASAOGLU, I. 2001. Aprotinin reduces the IL-8 after coronary artery bypass grafting. *Cardiovasc Surg,* 9**,** 403-6.

JABS, W. J., SEDLMEYER, A., RAMASSAR, V., HIDALGO, L. G., URMSON, J., AFROUZIAN, M., ZHU, L. F. & HALLORAN, P. F. 2003. Heterogeneity in the evolution and mechanisms of the lesions of kidney allograft rejection in mice. *Am J Transplant,* 3**,** 1501-9.

JIN, F., NATHAN, C., RADZIOCH, D. & DING, A. 1997. Secretory leukocyte protease inhibitor: a macrophage product induced by and antagonistic to bacterial lipopolysaccharide. *Cell,* 88**,** 417-426.

JO, S. K., HU, X., KOBAYASHI, H., LIZAK, M., MIYAJI, T., KORETSKY, A. & STAR, R. A. 2003a. Detection of inflammation following renal ischemia by magnetic resonance imaging. *Kidney Int,* 64**,** 43-51.

JO, S. K., HU, X., KOBAYASHI, H., LIZAK, M., MIYAJI, T., KORETSKY, A. & STAR, R. A. 2003b. Detection of inflammation following renal ischemia by magnetic resonance imaging. *Kidney International,* 64**,** 43-51.

JOHANSSON, L., JOHNSSON, C., PENNO, E., BJORNERUD, A. & AHLSTROM, H. 2002. Acute cardiac transplant rejection: detection and

grading with MR imaging with a blood pool contrast agent--experimental study in the rat. *Radiology,* 225**,** 97-103.

JONES, P. L., COWAN, K. N. & RABINOVITCH, M. 1997. Tenascin-C, proliferation and subendothelial fibronectin in progressive pulmonary vascular disease. *The American journal of pathology,* 150**,** 1349.

JORDAN, J. E., ZHAO, Z. Q. & VINTEN-JOHANSEN, J. 1999. The role of neutrophils in myocardial ischemiañreperfusion injury. *Cardiovascular Research,* 43**,** 860.

JU, H., NERURKAR, S., SAUERMELCH, C. F., OLZINSKI, A. R., MIRABILE, R., ZIMMERMAN, D., LEE, J. C., ADAMS, J., SISKO, J., BEROVA, M. & WILLETTE, R. N. 2002. Sustained activation of p38 mitogen-activated protein kinase contributes to the vascular response to injury. *J Pharmacol Exp Ther,* 301**,** 15-20.

KANDOLIN, R., LEHTONEN, J. & KUPARI, M. 2011. Cardiac sarcoidosis and giant cell myocarditis as causes of atrioventricular block in young and middle-aged adults. *Circ Arrhythm Electrophysiol,* 4**,** 303-9.

KANNO, S., WU, Y. J., LEE, P. C., DODD, S. J., WILLIAMS, M., GRIFFITH, B. P. & HO, C. 2001. Macrophage accumulation associated with rat cardiac allograft rejection detected by magnetic resonance imaging with ultrasmall superparamagnetic iron oxide particles. *Circulation,* 104**,** 934-8.

KANSAS, G. S. 1996. Selectins and their ligands: current concepts and controversies. *Blood,* 88**,** 3259-87.

KATUS, H. A., LOOSER, S., HALLERMAYER, K., REMPPIS, A., SCHEFFOLD, T., BORGYA, A., ESSIG, U. & GEUSS, U. 1992. Development and in vitro characterization of a new immunoassay of cardiac troponin T. *Clinical chemistry,* 38**,** 386-93.

KATUS, H. A., REMPPIS, A., SCHEFFOLD, T., DIEDERICH, K. W. & KUEBLER, W. 1991. Intracellular compartmentation of cardiac troponin T and its release kinetics in patients with reperfused and nonreperfused myocardial infarction. *The American journal of cardiology,* 67**,** 1360-7.

KERSTEN, J. R., SCHMELING, T. J., PAGEL, P. S., GROSS, G. J. & WARLTIER, D. C. 1997. Isoflurane mimics ischemic preconditioning via activation of K(ATP) channels: reduction of myocardial infarct size with an acute memory phase. *Anesthesiology,* 87**,** 361-70.

KING, A. E., CRITCHLEY, H. O. D., SALLENAVE, J. M. & KELLY, R. W. 2003. Elafin in human endometrium: an antiprotease and antimicrobial molecule expressed during menstruation. *Journal of Clinical Endocrinology & Metabolism,* 88**,** 4426.

KOOI, M. E., CAPPENDIJK, V. C., CLEUTJENS, K. B., KESSELS, A. G., KITSLAAR, P. J., BORGERS, M., FREDERIK, P. M., DAEMEN, M. J. & VAN ENGELSHOVEN, J. M. 2003a. Accumulation of ultrasmall superparamagnetic particles of iron oxide in human atherosclerotic plaques can be detected by in vivo magnetic resonance imaging. *Circulation,* 107**,** 2453-8.

KOOI, M. E., CAPPENDIJK, V. C., CLEUTJENS, K. B. J. M., KESSELS, A. G. H., KITSLAAR, P. J. E. H. M., BORGERS, M., FREDERIK, P. M., DAEMEN, M. J. A. P. & VAN ENGELSHOVEN, J. M. A. 2003b. Accumulation of

ultrasmall superparamagnetic particles of iron oxide in human atherosclerotic plaques can be detected by in vivo magnetic resonance imaging. *Circulation,* 107**,** 2453-8.

KORBET, S. M. 2002. Percutaneous renal biopsy. *Semin Nephrol,* 22**,** 254-67.

KORKMAZ, B., ATTUCCI, S., JOURDAN, M. L., JULIANO, L. & GAUTHIER, F. 2005. Inhibition of neutrophil elastase by 1-protease inhibitor at the surface of human polymorphonuclear neutrophils. *The Journal of Immunology,* 175**,** 3329.

KROMBACH, G. A., WENDLAND, M. F., HIGGINS, C. B. & SAEED, M. 2002. MR imaging of spatial extent of microvascular injury in reperfused ischemically injured rat myocardium: value of blood pool ultrasmall superparamagnetic particles of iron oxide. *Radiology,* 225**,** 479-86.

KUMAR, A. G., BALLANTYNE, C. M., MICHAEL, L. H., KUKIELKA, G. L., YOUKER, K. A., LINDSEY, M. L., HAWKINS, H. K., BIRDSALL, H. H., MACKAY, C. R. & LAROSA, G. J. 1997. Induction of monocyte chemoattractant protein-1 in the small veins of the ischemic and reperfused canine myocardium. *Circulation,* 95**,** 693.

LAMBERT, J. M., LOPEZ, E. F. & LINDSEY, M. L. 2008. Macrophage roles following myocardial infarction. *International Journal of Cardiology,* 130**,** 147-158.

LANDRY, R., JACOBS, P. M., DAVIS, R., SHENOUDA, M. & BOLTON, W. K. 2005. Pharmacokinetic study of ferumoxytol: a new iron replacement therapy in normal subjects and hemodialysis patients. *Am J Nephrol,* 25**,** 400-10.

LAROSE, E., RODES-CABAU, J., PIBAROT, P., RINFRET, S., PROULX, G., NGUYEN, C. M., DERY, J. P., GLEETON, O., ROY, L., NOEL, B., BARBEAU, G., ROULEAU, J., BOUDREAULT, J. R., AMYOT, M., DE LAROCHELLIERE, R. & BERTRAND, O. F. 2010. Predicting late myocardial recovery and outcomes in the early hours of ST-segment elevation myocardial infarction traditional measures compared with microvascular obstruction, salvaged myocardium, and necrosis characteristics by cardiovascular magnetic resonance. *J Am Coll Cardiol,* 55**,** 2459-69.

LASSNIGG, A., SCHMIDLIN, D., MOUHIEDDINE, M., BACHMANN, L. M., DRUML, W., BAUER, P. & HIESMAYR, M. 2004. Minimal changes of serum creatinine predict prognosis in patients after cardiothoracic surgery: a prospective cohort study. *J Am Soc Nephrol,* 15**,** 1597-605.

LAWACZECK, R., MENZEL, M. & PIETSCH, H. 2004. Superparamagnetic iron oxide particles: contrast media for magnetic resonance imaging. *Applied Organometallic Chemistry,* 18**,** 506-513.

LEE, S., HIROSE, S., PARK, S., CHI, J., CHUNG, S. & MORI, M. 2002. Elafin expression in human fetal and adult submandibular glands. *Histochemistry and Cell Biology,* 117**,** 423-430.

LEE, W. L. & DOWNEY, G. P. 2001. Leukocyte elastase. Physiological functions and role in acute lung injury. *American Journal of Respiratory and Critical Care Medicine,* 164**,** 896.

LEE, W. W., MARINELLI, B., VAN DER LAAN, A. M., SENA, B. F., GORBATOV, R., LEUSCHNER, F., DUTTA, P., IWAMOTO, Y., UENO, T., BEGIENEMAN, M. P., NIESSEN, H. W., PIEK, J. J., VINEGONI, C.,

PITTET, M. J., SWIRSKI, F. K., TAWAKOL, A., DI CARLI, M., WEISSLEDER, R. & NAHRENDORF, M. 2012. PET/MRI of Inflammation in Myocardial Infarction. *J Am Coll Cardiol,* 59**,** 153-63.

LEGER, A. J., COVIC, L. & KULIOPULOS, A. 2006. Protease-activated receptors in cardiovascular diseases. *Circulation,* 114**,** 1070.

LEHRER, R. I. & GANZ, T. 2002. Cathelicidins: a family of endogenous antimicrobial peptides. *Curr Opin Hematol,* 9**,** 18-22.

LENTSCH, A. B., YOSHIDOME, H., WARNER, R. L., WARD, P. A. & EDWARDS, M. J. 1999. Secretory leukocyte protease inhibitor in mice regulates local and remote organ inflammatory injury induced by hepatic ischemia/reperfusion. *Gastroenterology,* 117**,** 953-61.

LEUSCHNER, F., RAUCH, P. J., UENO, T., GORBATOV, R., MARINELLI, B., LEE, W. W., DUTTA, P., WEI, Y., ROBBINS, C., IWAMOTO, Y., SENA, B., CHUDNOVSKIY, A., PANIZZI, P., KELIHER, E., HIGGINS, J. M., LIBBY, P., MOSKOWITZ, M. A., PITTET, M. J., SWIRSKI, F. K., WEISSLEDER, R. & NAHRENDORF, M. 2012. Rapid monocyte kinetics in acute myocardial infarction are sustained by extramedullary monocytopoiesis. *J Exp Med,* 209**,** 123-37.

LI, G., JIA, J., JI, K., GONG, X., WANG, R., ZHANG, X., WANG, H. & ZANG, B. 2016. The neutrophil elastase inhibitor, sivelestat, attenuates sepsis-related kidney injury in rats. *Int J Mol Med,* 38**,** 767-75.

LI, W., SALANITRI, J., TUTTON, S., DUNKLE, E. E., SCHNEIDER, J. R., CAPRINI, J. A., PIERCHALA, L. N., JACOBS, P. M. & EDELMAN, R. R. 2007. Lower extremity deep venous thrombosis: evaluation with ferumoxytol-enhanced MR imaging and dual-contrast mechanism--preliminary experience. *Radiology,* 242**,** 873-81.

LI, W., TUTTON, S., VU, A. T., PIERCHALA, L., LI, B. S. Y., LEWIS, J. M., PRASAD, P. V. & EDELMAN, R. R. 2005. First-pass contrast-enhanced magnetic resonance angiography in humans using ferumoxytol, a novel ultrasmall superparamagnetic iron oxide (USPIO)-based blood pool agent. *J Magn Reson Imaging,* 21**,** 46-52.

LIM, C. C., CUCULI, F., VAN GAAL, W. J., TESTA, L., ARNOLD, J. R., KARAMITSOS, T., FRANCIS, J. M., DIGBY, J. E., ANTONIADES, C., KHARBANDA, R. K., NEUBAUER, S., WESTABY, S. & BANNING, A. P. 2011. Early diagnosis of perioperative myocardial infarction after coronary bypass grafting: a study using biomarkers and cardiac magnetic resonance imaging. *The Annals of Thoracic Surgery,* 92**,** 2046-53.

LIMA, J. A., JUDD, R. M., BAZILLE, A., SCHULMAN, S. P., ATALAR, E. & ZERHOUNI, E. A. 1995. Regional heterogeneity of human myocardial infarcts demonstrated by contrast-enhanced MRI. Potential mechanisms. *Circulation,* 92**,** 1117-25.

LITT, M. R., JEREMY, R. W., WEISMAN, H. F., WINKELSTEIN, J. A. & BECKER, L. C. 1989. Neutrophil depletion limited to reperfusion reduces myocardial infarct size after 90 minutes of ischemia. Evidence for neutrophil-mediated reperfusion injury. *Circulation,* 80**,** 1816.

LIU, W., DAHNKE, H., JORDAN, E. K., SCHAEFFTER, T. & FRANK, J. A. 2008. In vivo MRI using positive-contrast techniques in detection of cells

labeled with superparamagnetic iron oxide nanoparticles. *NMR in biomedicine,* 21**,** 242-50.

LONES, M. A., CZER, L. S., TRENTO, A., HARASTY, D., MILLER, J. M. & FISHBEIN, M. C. 1995. Clinical-pathologic features of humoral rejection in cardiac allografts: a study in 81 consecutive patients. *J Heart Lung Transplant,* 14**,** 151-62.

LUDWIG, A., POLLER, W. C., WESTPHAL, K., MINKWITZ, S., LATTIG-TUNNEMANN, G., METZKOW, S., STANGL, K., BAUMANN, G., TAUPITZ, M., WAGNER, S., SCHNORR, J. & STANGL, V. 2013. Rapid binding of electrostatically stabilized iron oxide nanoparticles to THP-1 monocytic cells via interaction with glycosaminoglycans. *Basic Res Cardiol,* 108**,** 328.

LUISETTI, M., STURANI, C., SELLA, D., MADONINI, E., GALAVOTTI, V., BRUNO, G., PEONA, V., KUCICH, U., DAGNINO, G., ROSENBLOOM, J., STARCHER, B. & GRASSI, C. 1996. MR889, a neutrophil elastase inhibitor, in patients with chronic obstructive pulmonary disease: a double-blind, randomized, placebo-controlled clinical trial. *Eur Respir J,* 9**,** 1482-6.

LUTZ, A. M., GˆPFERT, K., JOCHUM, W., NANZ, D., FRˆHLICH, J. M. & WEISHAUPT, D. 2006. USPIO enhanced MR imaging for visualization of synovial hyperperfusion and detection of synovial macrophages: Preliminary results in an experimental model of antigen induced arthritis. *Journal of Magnetic Resonance Imaging,* 24**,** 657-666.

LUTZ, A. M., WEISHAUPT, D., PERSOHN, E., GOEPFERT, K., FROEHLICH, J., SASSE, B., GOTTSCHALK, J., MARINCEK, B. & KAIM, A. H. 2005. Imaging of macrophages in soft-tissue infection in rats: relationship between ultrasmall superparamagnetic iron oxide dose and MR signal characteristics. *Radiology,* 234**,** 765-75.

MADJID, M., AWAN, I., WILLERSON, J. T. & CASSCELLS, S. W. 2004. Leukocyte count and coronary heart disease:: Implications for risk assessment. *Journal of the American College of Cardiology,* 44**,** 1945-1956.

MAGIL, A. B. 2009. Monocytes/macrophages in renal allograft rejection. *Transplant Rev (Orlando),* 23**,** 199-208.

MAIR, J., DIENSTL, F. & PUSCHENDORF, B. 1992. Cardiac troponin T in the diagnosis of myocardial injury. *Critical reviews in clinical laboratory sciences,* 29**,** 31-57.

MANGANO, D. T., TUDOR, I. C. & DIETZEL, C. 2006. The risk associated with aprotinin in cardiac surgery. *N Engl J Med,* 354**,** 353-65.

MANNISI, J. A., WEISMAN, H. F., BUSH, D. E., DUDECK, P. & HEALY, B. 1987. Steroid administration after myocardial infarction promotes early infarct expansion. A study in the rat. *J Clin Invest,* 79**,** 1431-9.

MARCHANT, D. J., BOYD, J. H., LIN, D. C., GRANVILLE, D. J., GARMAROUDI, F. S. & MCMANUS, B. M. 2012. Inflammation in myocardial diseases. *Circ Res,* 110**,** 126-44.

MARGOLIS, D. J., HOFFMAN, J. M., HERFKENS, R. J., JEFFREY, R. B., QUON, A. & GAMBHIR, S. S. 2007. Molecular imaging techniques in body imaging. *Radiology,* 245**,** 333-56.

MARINESCU, M., CHAUVEAU, F., DURAND, A., RIOU, A., CHO, T. H., DENCAUSSE, A., BALLET, S., NIGHOGHOSSIAN, N., BERTHEZENE, Y. & WIART, M. 2012. Monitoring therapeutic effects in experimental stroke by serial USPIO-enhanced MRI. *Eur Radiol*.

MARINESCU, M., CHAUVEAU, F., DURAND, A., RIOU, A., CHO, T. H., DENCAUSSE, A., BALLET, S., NIGHOGHOSSIAN, N., BERTHEZENE, Y. & WIART, M. 2013. Monitoring therapeutic effects in experimental stroke by serial USPIO-enhanced MRI. *European Radiology,* 23**,** 37-47.

MASSBERG, S., GRAHL, L., VON BRUEHL, M. L., MANUKYAN, D., PFEILER, S., GOOSMANN, C., BRINKMANN, V., LORENZ, M., BIDZHEKOV, K., KHANDAGALE, A. B., KONRAD, I., KENNERKNECHT, E., REGES, K., HOLDENRIEDER, S., BRAUN, S., REINHARDT, C., SPANNAGL, M., PREISSNER, K. T. & ENGELMANN, B. 2010. Reciprocal coupling of coagulation and innate immunity via neutrophil serine proteases. *Nat Med,* 16**,** 887-96.

MATSUZAKI, K., HIRAMATSU, Y., HOMMA, S., SATO, S., SHIGETA, O. & SAKAKIBARA, Y. 2005. Sivelestat reduces inflammatory mediators and preserves neutrophil deformability during simulated extracorporeal circulation. *Ann Thorac Surg,* 80**,** 611-7.

MCATEER, M. A., VON ZUR MUHLEN, C., ANTHONY, D. C., SIBSON, N. R. & CHOUDHURY, R. P. 2011. Magnetic resonance imaging of brain inflammation using microparticles of iron oxide. *Methods Mol Biol,* 680**,** 103-15.

MCELVANEY, N. G., NAKAMURA, H., BIRRER, P., HEBERT, C. A., WONG, W. L., ALPHONSO, M., BAKER, J. B., CATALANO, M. A. & CRYSTAL, R. G. 1992. Modulation of airway inflammation in cystic fibrosis. In vivo suppression of interleukin-8 levels on the respiratory epithelial surface by aerosolization of recombinant secretory leukoprotease inhibitor. *J Clin Invest,* 90**,** 1296-301.

MCMICHAEL, J. W., ROGHANIAN, A., LU, J., RAMAGE, R. & SALLENAVE, J. M. 2005. The antimicrobial antiproteinase elafin binds to lipopolysaccharide and modulates macrophage responses. *American Journal of Respiratory Cell and Molecular Biology,* 32**,** 443-452.

MENTZER, R. M., JR., BARTELS, C., BOLLI, R., BOYCE, S., BUCKBERG, G. D., CHAITMAN, B., HAVERICH, A., KNIGHT, J., MENASCHE, P., MYERS, M. L., NICOLAU, J., SIMOONS, M., THULIN, L. & WEISEL, R. D. 2008. Sodium-hydrogen exchange inhibition by cariporide to reduce the risk of ischemic cardiac events in patients undergoing coronary artery bypass grafting: results of the EXPEDITION study. *Ann Thorac Surg,* 85**,** 1261-70.

MEYBOHM, P., GRUENEWALD, M., ALBRECHT, M., ZACHAROWSKI, K. D., LUCIUS, R., ZITTA, K., KOCH, A., TRAN, N., SCHOLZ, J. & BEIN, B. 2009. Hypothermia and postconditioning after cardiopulmonary resuscitation reduce cardiac dysfunction by modulating inflammation, apoptosis and remodeling. *PLoS One,* 4**,** e7588.

MILLS, N. L., CHURCHHOUSE, A. M., LEE, K. K., ANAND, A., GAMBLE, D., SHAH, A. S., PATERSON, E., MACLEOD, M., GRAHAM, C., WALKER, S., DENVIR, M. A., FOX, K. A. & NEWBY, D. E. 2011. Implementation of

a sensitive troponin I assay and risk of recurrent myocardial infarction and death in patients with suspected acute coronary syndrome. *JAMA,* 305**,** 1210-6.

MILLS, N. L., LEE, K. K., MCALLISTER, D. A., CHURCHHOUSE, A. M., MACLEOD, M., STODDART, M., WALKER, S., DENVIR, M. A., FOX, K. A. & NEWBY, D. E. 2012. Implications of lowering threshold of plasma troponin concentration in diagnosis of myocardial infarction: cohort study. *BMJ,* 344**,** e1533.

MITCHELL, D. N., SCADDING, J. G., HEARD, B. E. & HINSON, K. F. 1977. Sarcoidosis: histopathological definition and clinical diagnosis. *J Clin Pathol,* 30**,** 395-408.

MOCATTA, T. J., PILBROW, A. P., CAMERON, V. A., SENTHILMOHAN, R., FRAMPTON, C. M., RICHARDS, A. M. & WINTERBOURN, C. C. 2007. Plasma concentrations of myeloperoxidase predict mortality after myocardial infarction. *Journal of the American College of Cardiology,* 49**,** 1993-2000.

MOLHUIZEN, H., ALKEMADE, H., ZEEUWEN, P., DE JONGH, G., WIERINGA, B. & SCHALKWIJK, J. 1993. SKALP/elafin: an elastase inhibitor from cultured human keratinocytes. Purification, cDNA sequence, and evidence for transglutaminase cross-linking. *Journal of Biological Chemistry,* 268**,** 12028.

MONTET-ABOU, K., DAIRE, J. L., HYACINTHE, J. N., JORGE-COSTA, M., GROSDEMANGE, K., MACH, F., PETRI-FINK, A., HOFMANN, H., MOREL, D. R., VALLEE, J. P. & MONTET, X. 2010. In vivo labelling of resting monocytes in the reticuloendothelial system with fluorescent iron oxide nanoparticles prior to injury reveals that they are mobilized to infarcted myocardium. *Eur Heart J,* 31**,** 1410-20.

MORRIS, J. B., OLZINSKI, A. R., BERNARD, R. E., ARAVINDHAN, K., MIRABILE, R. C., BOYCE, R., WILLETTE, R. N. & JUCKER, B. M. 2008. p38 MAPK inhibition reduces aortic ultrasmall superparamagnetic iron oxide uptake in a mouse model of atherosclerosis: MRI assessment. *Arterioscler Thromb Vasc Biol,* 28**,** 265-71.

MTAIRAG, E. M., HOUARD, X., RAIS, S., PASQUIER, C., OUDGHIRI, M., JACOB, M. P., MEILHAC, O. & MICHEL, J. B. 2002. Pharmacological potentiation of natriuretic peptide limits polymorphonuclear neutrophil-vascular cell interactions. *Arteriosclerosis, Thrombosis, and Vascular Biology,* 22**,** 1824.

MUROHARA, T., BUERKE, M. & LEFER, A. M. 1994. Polymorphonuclear leukocyte-induced vasocontraction and endothelial dysfunction. Role of selectins. *Arteriosclerosis, Thrombosis, and Vascular Biology,* 14**,** 1509.

NAESENS, M., HEYLEN, L., LERUT, E., CLAES, K., DE WEVER, L., CLAUS, F., OYEN, R., KUYPERS, D., EVENEPOEL, P., BAMMENS, B., SPRANGERS, B., MEIJERS, B., PIRENNE, J., MONBALIU, D., DE JONGE, H., METALIDIS, C., DE VUSSER, K. & VANRENTERGHEM, Y. 2013. Intrarenal resistive index after renal transplantation. *N Engl J Med,* 369**,** 1797-806.

NAGATA, Y., FUJIMOTO, M., NAKAMURA, K., ISOYAMA, N., MATSUMURA, M., FUJIKAWA, K., UCHIYAMA, K., TAKAKI, E.,

TAKII, R., NAKAI, A. & MATSUYAMA, H. 2016. Anti-TNF-alpha Agent Infliximab and Splenectomy Are Protective Against Renal Ischemia-Reperfusion Injury. *Transplantation,* 100**,** 1675-82.

NAHRENDORF, M., PITTET, M. J. & SWIRSKI, F. K. 2010. Monocytes: protagonists of infarct inflammation and repair after myocardial infarction. *Circulation,* 121**,** 2437.

NAHRENDORF, M., SWIRSKI, F. K., AIKAWA, E., STANGENBERG, L., WURDINGER, T., FIGUEIREDO, J. L., LIBBY, P., WEISSLEDER, R. & PITTET, M. J. 2007a. The healing myocardium sequentially mobilizes two monocyte subsets with divergent and complementary functions. *The Journal of Experimental Medicine,* 204**,** 3037.

NAHRENDORF, M., SWIRSKI, F. K., AIKAWA, E., STANGENBERG, L., WURDINGER, T., FIGUEIREDO, J. L., LIBBY, P., WEISSLEDER, R. & PITTET, M. J. 2007b. The healing myocardium sequentially mobilizes two monocyte subsets with divergent and complementary functions. *J Exp Med,* 204**,** 3037-47.

NAJAFI, M. 2014. Serum creatinine role in predicting outcome after cardiac surgery beyond acute kidney injury. *World J Cardiol,* 6**,** 1006-21.

NAKAMURA, H., UMEMOTO, S., NAIK, G., MOE, G., TAKATA, S., LIU, P. & MATSUZAKI, M. 2003. Induction of left ventricular remodeling and dysfunction in the recipient heart after donor heart myocardial infarction: new insights into the pathologic role of tumor necrosis factor-alpha from a novel heterotopic transplant-coronary ligation rat model. *J Am Coll Cardiol,* 42**,** 173-81.

NANKIVELL, B. J. & CHAPMAN, J. R. 2006. The significance of subclinical rejection and the value of protocol biopsies. *Am J Transplant,* 6**,** 2006-12.

NANKIVELL, B. J. & KUYPERS, D. R. 2011. Diagnosis and prevention of chronic kidney allograft loss. *Lancet,* 378**,** 1428-37.

NARA, K., ITO, S., ITO, T., SUZUKI, Y., GHONEIM, M. A., TACHIBANA, S. & HIROSE, S. 1994. Elastase inhibitor elafin is a new type of proteinase inhibitor which has a transglutaminase-mediated anchoring sequence termed ìcementoinî. *Journal of Biochemistry,* 115**,** 441.

NARUKO, T., UEDA, M., HAZE, K., VAN DER WAL, A. C., VAN DER LOOS, C. M., ITOH, A., KOMATSU, R., IKURA, Y., OGAMI, M. & SHIMADA, Y. 2002. Neutrophil infiltration of culprit lesions in acute coronary syndromes. *Circulation,* 106**,** 2894.

NASHEF, S. A., ROQUES, F., MICHEL, P., GAUDUCHEAU, E., LEMESHOW, S. & SALAMON, R. 1999. European system for cardiac operative risk evaluation (EuroSCORE). *Eur J Cardiothorac Surg,* 16**,** 9-13.

NELSON, G. N., ROH, J. D., MIRENSKY, T. L., WANG, Y., YI, T., TELLIDES, G., POBER, J. S., SHKARIN, P., SHAPIRO, E. M., SALTZMAN, W. M., PAPADEMETRIS, X., FAHMY, T. M. & BREUER, C. K. 2008. Initial evaluation of the use of USPIO cell labeling and noninvasive MR monitoring of human tissue-engineered vascular grafts in vivo. *FASEB J,* 22**,** 3888-95.

NEMOTO, E., SUGAWARA, S., TADA, H., TAKADA, H., SHIMAUCHI, H. & HORIUCHI, H. 2000. Cleavage of CD14 on human gingival fibroblasts cocultured with activated neutrophils is mediated by human leukocyte

elastase resulting in down-regulation of lipopolysaccharide-induced IL-8 production. *J Immunol,* 165**,** 5807-13.

NESHER, N., ALGHAMDI, A. A., SINGH, S. K., SEVER, J. Y., CHRISTAKIS, G. T., GOLDMAN, B. S., COHEN, G. N., MOUSSA, F. & FREMES, S. E. 2008. Troponin after cardiac surgery: a predictor or a phenomenon? *Ann Thorac Surg,* 85**,** 1348-54.

NEUWELT, E. A., VÁRALLYAY, C. G., MANNINGER, S., SOLYMOSI, D., HALUSKA, M., HUNT, M. A., NESBIT, G., STEVENS, A., JEROSCH-HEROLD, M., JACOBS, P. M. & HOFFMAN, J. M. 2007. The potential of ferumoxytol nanoparticle magnetic resonance imaging, perfusion, and angiography in central nervous system malignancy: a pilot study. *Neurosurgery,* 60**,** 601-11; discussion 611-2.

NIGHOGHOSSIAN, N., WIART, M., CAKMAK, S., BERTHEZENE, Y., DEREX, L., CHO, T. H., NEMOZ, C., CHAPUIS, F., TISSERAND, G. L., PIALAT, J. B., TROUILLAS, P., FROMENT, J. C. & HERMIER, M. 2007. Inflammatory response after ischemic stroke: a USPIO-enhanced MRI study in patients. *Stroke,* 38**,** 303-7.

NINOMIYA, M., MIYAJI, K. & TAKAMOTO, S. 2003. Influence of PMEA-coated bypass circuits on perioperative inflammatory response. *Ann Thorac Surg,* 75**,** 913-7; discussion 917-8.

NOORA, J., RICCI, C., HASTINGS, D., HILL, S. & CYBULSKY, I. 2005. Determination of troponin I release after CABG surgery. *J Card Surg,* 20**,** 129-35.

NORRIS, D. A., CLARK, R., SWIGART, L. M., HUFF, J., WESTON, W. & HOWELL, S. 1982. Fibronectin fragment (s) are chemotactic for human peripheral blood monocytes. *The Journal of Immunology,* 129**,** 1612.

NUYTINCK, H. K., OFFERMANS, X. J., KUBAT, K. & GORIS, J. A. 1988. Whole-body inflammation in trauma patients. An autopsy study. *Arch Surg,* 123**,** 1519-24.

O'BLENES, S. B., ZAIDI, S. H., CHEAH, A. Y., MCINTYRE, B., KANEDA, Y. & RABINOVITCH, M. 2000. Gene transfer of the serine elastase inhibitor elafin protects against vein graft degeneration. *Circulation,* 102**,** III289-95.

O'NEAL, J. B., SHAW, A. D. & BILLINGS, F. T. T. 2016. Acute kidney injury following cardiac surgery: current understanding and future directions. *Crit Care,* 20**,** 187.

ODA, T., HOTTA, O., TAGUMA, Y., KITAMURA, H., SUDO, K., HORIGOME, I., CHIBA, S., YOSHIZAWA, N. & NAGURA, H. 1997. Involvement of neutrophil elastase in crescentic glomerulonephritis. *Hum Pathol,* 28**,** 720-8.

OHTA, K., NAKAJIMA, T., CHEAH, A. Y., ZAIDI, S. H., KAVIANI, N., DAWOOD, F., YOU, X. M., LIU, P., HUSAIN, M. & RABINOVITCH, M. 2004a. Elafin-overexpressing mice have improved cardiac function after myocardial infarction. *Am J Physiol Heart Circ Physiol,* 287**,** H286-92.

OHTA, K., NAKAJIMA, T., CHEAH, A. Y. L., ZAIDI, S. H. E., KAVIANI, N., DAWOOD, F., YOU, X. M., LIU, P., HUSAIN, M. & RABINOVITCH, M. 2004b. Elafin-overexpressing mice have improved cardiac function after myocardial infarction. *American Journal of Physiology-Heart and Circulatory Physiology,* 287**,** H286.

OKADA, Y. & NAKANISHI, I. 1989. Activation of matrix metalloproteinase 3 (stromelysin) and matrix metalloproteinase 2 ('gelatinase') by human neutrophil elastase and cathepsin G. *FEBS letters,* 249**,** 353-356.

OKADA, Y., WATANABE, S., NAKANISHI, I., KISHI, J., HAYAKAWA, T., WATOREK, W., TRAVIS, J. & NAGASE, H. 1988. Inactivation of tissue inhibitor of metalloproteinases by neutrophil elastase and other serine proteinases. *FEBS letters,* 229**,** 157-160.

OKAMOTO, E., COUSE, T., DE LEON, H., VINTEN-JOHANSEN, J., GOODMAN, R. B., SCOTT, N. A. & WILCOX, J. N. 2001. Perivascular inflammation after balloon angioplasty of porcine coronary arteries. *Circulation,* 104**,** 2228-2235.

OKAYAMA, N., KAKIHANA, Y., SETOGUCHI, D., IMABAYASHI, T., OMAE, T., MATSUNAGA, A. & KANMURA, Y. 2006. Clinical effects of a neutrophil elastase inhibitor, sivelestat, in patients with acute respiratory distress syndrome. *J Anesth,* 20**,** 6-10.

OKAZAKI, T., EBIHARA, S., ASADA, M., YAMANDA, S., SAIJO, Y., SHIRAISHI, Y., EBIHARA, T., NIU, K., MEI, H. & ARAI, H. 2007. Macrophage colony-stimulating factor improves cardiac function after ischemic injury by inducing vascular endothelial growth factor production and survival of cardiomyocytes. *American Journal of Pathology,* 171**,** 1093.

OKUSA, M. D. 2002. The inflammatory cascade in acute ischemic renal failure. *Nephron,* 90**,** 133-8.

ONORATI, F., DE FEO, M., MASTROROBERTO, P., CRISTODORO, L., PEZZO, F., RENZULLI, A. & COTRUFO, M. 2005. Determinants and prognosis of myocardial damage after coronary artery bypass grafting. *Ann Thorac Surg,* 79**,** 837-45.

OWEN, C. A., CAMPBELL, M. A., SANNES, P. L., BOUKEDES, S. S. & CAMPBELL, E. J. 1995. Cell surface-bound elastase and cathepsin G on human neutrophils: a novel, non-oxidative mechanism by which neutrophils focus and preserve catalytic activity of serine proteinases. *The Journal of Cell Biology,* 131**,** 775.

PADRINES, M., WOLF, M., WALZ, A. & BAGGIOLINI, M. 1994. Interleukin-8 processing by neutrophil elastase, cathepsin G and proteinase-3. *FEBS letters,* 352**,** 231-235.

PAPARELLA, D., YAU, T. M. & YOUNG, E. 2002. Cardiopulmonary bypass induced inflammation: pathophysiology and treatment. An update. *Eur J Cardiothorac Surg,* 21**,** 232-44.

PAROLARI, A., PESCE, L. L., PACINI, D., MAZZANTI, V., SALIS, S., SCIACOVELLI, C., ROSSI, F., ALAMANNI, F. & MONZINO RESEARCH GROUP ON CARDIAC SURGERY, O. 2012. Risk factors for perioperative acute kidney injury after adult cardiac surgery: role of perioperative management. *Ann Thorac Surg,* 93**,** 584-91.

PATEL, K. D., CUVELIER, S. L. & WIEHLER, S. 2002. Selectins: critical mediators of leukocyte recruitment. *Semin Immunol,* 14**,** 73-81.

PATTERSON, A. J., TANG, T. Y., GRAVES, M. J., MULLER, K. H. & GILLARD, J. H. 2011. In vivo carotid plaque MRI using quantitative T2* measurements

with ultrasmall superparamagnetic iron oxide particles: a dose-response study to statin therapy. *NMR Biomed,* 24**,** 89-95.

PAUL, L. C. 1999. Chronic allograft nephropathy: An update. *Kidney Int,* 56**,** 783-93.

PEGG, T. J., MAUNSELL, Z., KARAMITSOS, T. D., TAYLOR, R. P., JAMES, T., FRANCIS, J. M., TAGGART, D. P., WHITE, H., NEUBAUER, S. & SELVANAYAGAM, J. B. 2011. Utility of cardiac biomarkers for the diagnosis of type V myocardial infarction after coronary artery bypass grafting: insights from serial cardiac MRI. *Heart,* 97**,** 810-6.

PENNO, E., JOHANSSON, L., AHLSTROM, H. & JOHNSSON, C. 2007. Ultrasmall iron oxide particle contrast agent and MRI can be used to monitor the effect of anti-rejection treatment. *Transplantation,* 84**,** 374-9.

PFUNDT, R., WINGENS, M., BERGERS, M., ZWEERS, M., FRENKEN, M. & SCHALKWIJK, J. 2000. TNF- and serum induce SKALP/elafin gene expression in human keratinocytes by a p38 MAP kinase-dependent pathway. *Archives of Dermatological Research,* 292**,** 180-187.

PILLAY, J., HIETBRINK, F., KOENDERMAN, L. & LEENEN, L. P. 2007. The systemic inflammatory response induced by trauma is reflected by multiple phenotypes of blood neutrophils. *Injury,* 38**,** 1365-72.

POSTLETHWAITE, A. & KANG, A. H. 1976. Collagen-and collagen peptide-induced chemotaxis of human blood monocytes. *The Journal of Experimental Medicine,* 143**,** 1299.

PRINCE, M. R., ZHANG, H. L., CHABRA, S. G., JACOBS, P. & WANG, Y. 2003. A pilot investigation of new superparamagnetic iron oxide as a contrast agent for cardiovascular MRI. *Journal of X-Ray Science and Technology,* 11**,** 231-240.

QI, F., ADAIR, A., FERENBACH, D., VASS, D. G., MYLONAS, K. J., KIPARI, T., CLAY, M., KLUTH, D. C., HUGHES, J. & MARSON, L. P. 2008. Depletion of cells of monocyte lineage prevents loss of renal microvasculature in murine kidney transplantation. *Transplantation,* 86**,** 1267-74.

RADERMACHER, J., MENGEL, M., ELLIS, S., STUHT, S., HISS, M., SCHWARZ, A., EISENBERGER, U., BURG, M., LUFT, F. C., GWINNER, W. & HALLER, H. 2003. The renal arterial resistance index and renal allograft survival. *N Engl J Med,* 349**,** 115-24.

RAMACHANDRAN, P., PELLICORO, A., VERNON, M. A., BOULTER, L., AUCOTT, R. L., ALI, A., HARTLAND, S. N., SNOWDON, V. K., CAPPON, A., GORDON-WALKER, T. T., WILLIAMS, M. J., DUNBAR, D. R., MANNING, J. R., VAN ROOIJEN, N., FALLOWFIELD, J. A., FORBES, S. J. & IREDALE, J. P. 2012. Differential Ly-6C expression identifies the recruited macrophage phenotype, which orchestrates the regression of murine liver fibrosis. *Proc Natl Acad Sci U S A,* 109**,** E3186-95.

RAMACHANDRAN, R., MIHARA, K., CHUNG, H., RENAUX, B., LAU, C. S., MURUVE, D. A., DEFEA, K. A., BOUVIER, M. & HOLLENBERG, M. D. 2011. Neutrophil Elastase Acts as a Biased Agonist for Proteinase-activated Receptor-2 (PAR2). *Journal of Biological Chemistry,* 286**,** 24638.

RAUSCH, M., BAUMANN, D., NEUBACHER, U. & RUDIN, M. 2002. In-vivo visualization of phagocytotic cells in rat brains after transient ischemia by USPIO. *NMR Biomed,* 15**,** 278-83.

RAUSCH, M., SAUTER, A., FROHLICH, J., NEUBACHER, U., RADU, E. W. & RUDIN, M. 2001a. Dynamic patterns of USPIO enhancement can be observed in macrophages after ischemic brain damage. *Magn Reson Med,* 46**,** 1018-22.

RAUSCH, M., SAUTER, A., FRˆHLICH, J., NEUBACHER, U., RAD¸, E. W. & RUDIN, M. 2001b. Dynamic patterns of USPIO enhancement can be observed in macrophages after ischemic brain damage. *Magnetic Resonance in Medicine,* 46**,** 1018-1022.

REEVES, E. P., LU, H., JACOBS, H. L., MESSINA, C. G., BOLSOVER, S., GABELLA, G., POTMA, E. O., WARLEY, A., ROES, J. & SEGAL, A. W. 2002. Killing activity of neutrophils is mediated through activation of proteases by K+ flux. *Nature,* 416**,** 291-7.

REGELE, H., BOHMIG, G. A., HABICHT, A., GOLLOWITZER, D., SCHILLINGER, M., ROCKENSCHAUB, S., WATSCHINGER, B., KERJASCHKI, D. & EXNER, M. 2002. Capillary deposition of complement split product C4d in renal allografts is associated with basement membrane injury in peritubular and glomerular capillaries: a contribution of humoral immunity to chronic allograft rejection. *J Am Soc Nephrol,* 13**,** 2371-80.

REIMER, K. A., MURRY, C. E. & RICHARD, V. J. 1989. The role of neutrophils and free radicals in the ischemic-reperfused heart: why the confusion and controversy? *Journal of Molecular and Cellular Cardiology,* 21**,** 1225.

REYNOLDS, P. R., LARKMAN, D. J., HASKARD, D. O., HAJNAL, J. V., KENNEA, N. L., GEORGE, A. J. & EDWARDS, A. D. 2006. Detection of vascular expression of E-selectin in vivo with MR imaging. *Radiology,* 241**,** 469-76.

RICHARDS, J. M., SEMPLE, S. I., MACGILLIVRAY, T. J., GRAY, C., LANGRISH, J. P., WILLIAMS, M., DWECK, M., WALLACE, W., MCKILLOP, G., CHALMERS, R. T., GARDEN, O. J. & NEWBY, D. E. 2011a. Abdominal aortic aneurysm growth predicted by uptake of ultrasmall superparamagnetic particles of iron oxide: a pilot study. *Circ Cardiovasc Imaging,* 4**,** 274-81.

RICHARDS, J. M., SEMPLE, S. I., MACGILLIVRAY, T. J., GRAY, C., LANGRISH, J. P., WILLIAMS, M., DWECK, M., WALLACE, W., MCKILLOP, G., CHALMERS, R. T. A., GARDEN, O. J. & NEWBY, D. E. 2010. Abdominal aortic aneurysm growth predicted by uptake of ultrasmall superparamagnetic particles of iron oxide

RICHARDS, J. M., SHAW, C. A., LANG, N. N., WILLIAMS, M. C., SEMPLE, S. I., MACGILLIVRAY, T. J., GRAY, C., CRAWFORD, J. H., ALAM, S. R. & ATKINSON, A. P. 2012a. In Vivo Mononuclear Cell Tracking Using Superparamagnetic Particles of Iron OxideClinical Perspective Feasibility and Safety in Humans. *Circulation: Cardiovascular Imaging,* 5**,** 509-517.

RICHARDS, J. M., SHAW, C. A., LANG, N. N., WILLIAMS, M. C., SEMPLE, S. I., MACGILLIVRAY, T. J., GRAY, C., CRAWFORD, J. H., ALAM, S. R., ATKINSON, A. P., FORREST, E. K., BIENEK, C., MILLS, N. L., BURDESS, A., DHALIWAL, K., SIMPSON, A. J., WALLACE, W. A., HILL, A. T., RODDIE, P. H., MCKILLOP, G., CONNOLLY, T. A., FEUERSTEIN, G. Z., BARCLAY, G. R., TURNER, M. L. & NEWBY, D. E. 2012b. In vivo mononuclear cell tracking using superparamagnetic particles of iron oxide: feasibility and safety in humans. *Circ Cardiovasc Imaging,* 5**,** 509-17.

RICHARDS, J. M. J., SEMPLE, S. I., MACGILLIVRAY, T. J., GRAY, C., LANGRISH, J. P., WILLIAMS, M., DWECK, M., WALLACE, W., MCKILLOP, G. & CHALMERS, R. T. A. 2011b. Abdominal Aortic Aneurysm Growth Predicted by Uptake of Ultrasmall Superparamagnetic Particles of Iron Oxide: A Pilot Study. *Circulation: Cardiovascular Imaging*.

RICHARDSON, D., PEPPER, D. & KAY, A. 1976. Chemotaxis for Human Monocytes by Fibrinogen derived Peptides. *British Journal of Haematology,* 32**,** 507-514.

RICHTER, J., NG-SIKORSKI, J., OLSSON, I. & ANDERSSON, T. 1990. Tumor necrosis factor-induced degranulation in adherent human neutrophils is dependent on CD11b/CD18-integrin-triggered oscillations of cytosolic free Ca2+. *Proceedings of the National Academy of Sciences,* 87**,** 9472.

RIDKER, P. M., RIFAI, N., CLEARFIELD, M., DOWNS, J. R., WEIS, S. E., MILES, J. S. & GOTTO, A. M., JR. 2001. Measurement of C-reactive protein for the targeting of statin therapy in the primary prevention of acute coronary events. *N Engl J Med,* 344**,** 1959-65.

RIOU, A., CHAUVEAU, F., CHO, T. H., MARINESCU, M., NATAF, S., NIGHOGHOSSIAN, N., BERTHEZENE, Y. & WIART, M. 2013. MRI assessment of the intra-carotid route for macrophage delivery after transient cerebral ischemia. *NMR in biomedicine,* 26**,** 115-23.

RIOU, L. M., RUIZ, M., SULLIVAN, G. W., LINDEN, J., LEONG-POI, H., LINDNER, J. R., HARRIS, T. D., BELLER, G. A. & GLOVER, D. K. 2002. Assessment of myocardial inflammation produced by experimental coronary occlusion and reperfusion with 99mTc-RP517, a new leukotriene B4 receptor antagonist that preferentially labels neutrophils in vivo. *Circulation,* 106**,** 592-8.

RISTIKANKARE, A., POYHIA, R., KUITUNEN, A., SKRIFVARS, M., HAMMAINEN, P., SALMENPERA, M. & SUOJARANTA-YLINEN, R. 2010. Serum cystatin C in elderly cardiac surgery patients. *Ann Thorac Surg,* 89**,** 689-94.

RIVIERE, C., BOUDGHENE, F. P., GAZEAU, F., ROGER, J., PONS, J. N., LAISSY, J. P., ALLAIRE, E., MICHEL, J. B., LETOURNEUR, D. & DEUX, J. F. 2005. Iron oxide nanoparticle-labeled rat smooth muscle cells: cardiac MR imaging for cell graft monitoring and quantitation. *Radiology,* 235**,** 959-67.

ROBERT, L., ROBERT, A. & JACOTOT, B. 1998. Elastin-elastase-atherosclerosis revisited. *Atherosclerosis,* 140**,** 281-295.

ROBERTS, W. C., MCALLISTER, H. A., JR. & FERRANS, V. J. 1977. Sarcoidosis of the heart. A clinicopathologic study of 35 necropsy patients (group 1) and review of 78 previously described necropsy patients (group 11). *Am J Med,* 63**,** 86-108.

ROGHANIAN, A., WILLIAMS, S. E., SHELDRAKE, T. A., BROWN, T. I., OBERHEIM, K., XING, Z., HOWIE, S. & SALLENAVE, J. M. 2006. The antimicrobial/elastase inhibitor elafin regulates lung dendritic cells and adaptive immunity. *American Journal of Respiratory Cell and Molecular Biology,* 34**,** 634.

ROMSON, J. L., HOOK, B. G., KUNKEL, S. L., ABRAMS, G., SCHORK, M. & LUCCHESI, B. 1983a. Reduction of the extent of ischemic myocardial injury by neutrophil depletion in the dog. *Circulation,* 67**,** 1016.

ROMSON, J. L., HOOK, B. G., KUNKEL, S. L., ABRAMS, G. D., SCHORK, M. A. & LUCCHESI, B. R. 1983b. Reduction of the extent of ischemic myocardial injury by neutrophil depletion in the dog. *Circulation,* 67**,** 1016-23.

RUDOLPH, T. K., SCHAPER, N., KLINKE, A., DEMIR, C., GOLDMANN, B., LAU, D., KOSTER, R., HELLMICH, M., MEINERTZ, T., BALDUS, S. & RUDOLPH, V. 2013. Liberation of vessel-adherent myeloperoxidase reflects plaque burden in patients with stable coronary artery disease. *Atherosclerosis,* 231**,** 354-8.

RUEHM, S. G., COROT, C., VOGT, P., KOLB, S. & DEBATIN, J. F. 2001a. Magnetic resonance imaging of atherosclerotic plaque with ultrasmall superparamagnetic particles of iron oxide in hyperlipidemic rabbits. *Circulation,* 103**,** 415.

RUEHM, S. G., COROT, C., VOGT, P., KOLB, S. & DEBATIN, J. F. 2001b. Magnetic resonance imaging of atherosclerotic plaque with ultrasmall superparamagnetic particles of iron oxide in hyperlipidemic rabbits. *Circulation,* 103**,** 415-22.

RYBICKI, B. A. & IANNUZZI, M. C. 2007. Epidemiology of sarcoidosis: recent advances and future prospects. *Semin Respir Crit Care Med,* 28**,** 22-35.

RYUGO, M., SAWA, Y., TAKANO, H., MATSUMIYA, G., IWAI, S., ONO, M., HATA, H., YAMAUCHI, T., NISHIMURA, M., FUJINO, Y. & MATSUDA, H. 2006. Effect of a polymorphonuclear elastase inhibitor (sivelestat sodium) on acute lung injury after cardiopulmonary bypass: findings of a double-blind randomized study. *Surg Today,* 36**,** 321-6.

SADALLAH, S., HESS, C., MIOT, S., SPERTINI, O., LUTZ, H. & SCHIFFERLI, J. A. 1999. Elastase and metalloproteinase activities regulate soluble complement receptor 1 release. *European Journal of Immunology,* 29**,** 3754-3761.

SADAT, U., HOWARTH, S. P., USMAN, A., TANG, T. Y., GRAVES, M. J. & GILLARD, J. H. 2012. Sequential Imaging of Asymptomatic Carotid Atheroma Using Ultrasmall Superparamagnetic Iron Oxide-enhanced Magnetic Resonance Imaging: A Feasibility Study. *J Stroke Cerebrovasc Dis*.

SADAT, U., TAVIANI, V., PATTERSON, A. J., YOUNG, V. E., GRAVES, M. J., TENG, Z., TANG, T. Y. & GILLARD, J. H. 2011. Ultrasmall superparamagnetic iron oxide-enhanced magnetic resonance imaging of

abdominal aortic aneurysms--a feasibility study. *Eur J Vasc Endovasc Surg,* 41**,** 167-74.

SAGAR, S., LIU, P. P. & COOPER, L. T., JR. 2012. Myocarditis. *Lancet,* 379**,** 738-47.

SAITO, S., TSUGENO, M., KOTO, D., MORI, Y., YOSHIOKA, Y., NOHARA, S. & MURASE, K. 2012. Impact of surface coating and particle size on the uptake of small and ultrasmall superparamagnetic iron oxide nanoparticles by macrophages. *Int J Nanomedicine,* 7**,** 5415-21.

SALEH, A., SCHROETER, M., JONKMANNS, C., HARTUNG, H. P., MODDER, U. & JANDER, S. 2004. In vivo MRI of brain inflammation in human ischaemic stroke. *Brain,* 127**,** 1670-7.

SALLENAVE, J. & SILVA, A. 1993. Characterization and gene sequence of the precursor of elafin, an elastase-specific inhibitor in bronchial secretions. *American Journal of Respiratory Cell and Molecular Biology,* 8**,** 439.

SALLENAVE, J., SILVA, A., MARSDEN, M. & RYLE, A. 1993. Secretion of mucus proteinase inhibitor and elafin by Clara cell and type II pneumocyte cell lines. *American Journal of Respiratory Cell and Molecular Biology,* 8**,** 126.

SALLENAVE, J. M. 2000a. The role of secretory leukocyte proteinase inhibitor and elafin (elastase-specific inhibitor/skin-derived antileukoprotease) as alarm antiproteinases in inflammatory lung disease. *Respir Res,* 1**,** 87-92.

SALLENAVE, J. M. 2000b. The role of secretory leukocyte proteinase inhibitor and elafin (elastase-specific inhibitor/skin-derived antileukoprotease) as alarm antiproteinases in inflammatory lung disease. *Respiratory Research,* 1**,** 87-92.

SALLENAVE, J. M., CUNNINGHAM, G., JAMES, R., MCLACHLAN, G. & HASLETT, C. 2003. Regulation of pulmonary and systemic bacterial lipopolysaccharide responses in transgenic mice expressing human elafin. *Infection and Immunity,* 71**,** 3766.

SALLENAVE, J. M. & RYLE, A. P. 1991a. Purification and characterization of elastase-specific inhibitor. Sequence homology with mucus proteinase inhibitor. *Biol Chem Hoppe Seyler,* 372**,** 13-21.

SALLENAVE, J. M. & RYLE, A. P. 1991b. Purifkation and Characterization of Elastase-Specific Inhibitor. Sequence Homology with Mucus Proteinase Inhibitor. *Biological Chemistry Hoppe-Seyler,* 372**,** 13-22.

SALLENAVE, J. M., SHULMANN, J., CROSSLEY, J., JORDANA, M. & GAULDIE, J. 1994. Regulation of secretory leukocyte proteinase inhibitor (SLPI) and elastase-specific inhibitor (ESI/elafin) in human airway epithelial cells by cytokines and neutrophilic enzymes. *American Journal of Respiratory Cell and Molecular Biology,* 11**,** 733.

SAVILL, J., DRANSFIELD, I., GREGORY, C. & HASLETT, C. 2002. A blast from the past: clearance of apoptotic cells regulates immune responses. *Nature Reviews Immunology,* 2**,** 965-975.

SCHALKWIJK, J., VAN VLIJMEN, I., ALKEMADE, J. & DE JONGH, G. 1993. Immunohistochemical localization of SKALP/elafin in psoriatic epidermis. *Journal of Investigative Dermatology,* 100**,** 390-393.

SCHALKWIJK, J., WIEDOW, O. & HIROSE, S. 1999. The trappin gene family: proteins defined by an N-terminal transglutaminase substrate domain and a C-terminal four-disulphide core. *Biochemical Journal,* 340**,** 569.

SCHELBERT, E. B., HSU, L. Y., ANDERSON, S. A., MOHANTY, B. D., KARIM, S. M., KELLMAN, P., ALETRAS, A. H. & ARAI, A. E. 2010. Late gadolinium-enhancement cardiac magnetic resonance identifies postinfarction myocardial fibrosis and the border zone at the near cellular level in ex vivo rat heart. *Circ Cardiovasc Imaging,* 3**,** 743-52.

SCHILLER, B., BHAT, P. & SHARMA, A. 2014. Safety and effectiveness of ferumoxytol in hemodialysis patients at 3 dialysis chains in the United States over a 12-month period. *Clin Ther,* 36**,** 70-83.

SCHILLER, B., BHAT, P., SHARMA, A., LI, Z., FORTIN, G., MCLAUGHLIN, J. & STRAUSS, W. 2011. Safety of Feraheme¬Æ(Ferumoxytol) in hemodialysis patients at 3 dialysis chains over a 1-year period. *J Am Soc Nephrol,* 22**,** 477A-478A.

SCHMITZ, S. A., COUPLAND, S. E., GUST, R., WINTERHALTER, S., WAGNER, S., KRESSE, M., SEMMLER, W. & WOLF, K. J. 2000. Superparamagnetic iron oxide-enhanced MRI of atherosclerotic plaques in Watanabe hereditable hyperlipidemic rabbits. *Invest Radiol,* 35**,** 460-71.

SCHMITZ, S. A., TAUPITZ, M., WAGNER, S., COUPLAND, S. E., GUST, R., NIKOLOVA, A. & WOLF, K. J. 2002. Iron-oxide-enhanced magnetic resonance imaging of atherosclerotic plaques: postmortem analysis of accuracy, inter-observer agreement, and pitfalls. *Invest Radiol,* 37**,** 405-11.

SCHMITZ, S. A., TAUPITZ, M., WAGNER, S., WOLF, K. J., BEYERSDORFF, D. & HAMM, B. 2001. Magnetic resonance imaging of atherosclerotic plaques using superparamagnetic iron oxide particles. *J Magn Reson Imaging,* 14**,** 355-61.

SCHNORR, J., TAUPITZ, M., SCHELLENBERGER, E. A., WARMUTH, C., FAHLENKAMP, U. L., WAGNER, S., KAUFELS, N. & WAGNER, M. 2012. Cardiac magnetic resonance angiography using blood-pool contrast agents: comparison of citrate-coated very small superparamagnetic iron oxide particles with gadofosveset trisodium in pigs. *Rofo,* 184**,** 105-12.

SCHWENGER, V., HINKEL, U. P., NAHM, A. M., MORATH, C. & ZEIER, M. 2006. Real-time contrast-enhanced sonography in renal transplant recipients. *Clin Transplant,* 20 Suppl 17**,** 51-4.

SEGERS, F. M., DEN ADEL, B., BOT, I., VAN DER GRAAF, L. M., VAN DER VEER, E. P., GONZALEZ, W., RAYNAL, I., DE WINTHER, M., WODZIG, W. K., POELMANN, R. E., VAN BERKEL, T. J., VAN DER WEERD, L. & BIESSEN, E. A. 2013. Scavenger receptor-AI-targeted iron oxide nanoparticles for in vivo MRI detection of atherosclerotic lesions. *Arterioscler Thromb Vasc Biol,* 33**,** 1812-9.

SELVANAYAGAM, J. B., PIGOTT, D., BALACUMARASWAMI, L., PETERSEN, S. E., NEUBAUER, S. & TAGGART, D. P. 2005. Relationship of irreversible myocardial injury to troponin I and creatine kinase-MB elevation after coronary artery bypass surgery: insights from cardiovascular magnetic resonance imaging. *Journal of the American College of Cardiology,* 45**,** 629-31.

SHAH, A. S., ANAND, A., SANDOVAL, Y., LEE, K. K., SMITH, S. W., ADAMSON, P. D., CHAPMAN, A. R., LANGDON, T., SANDEMAN, D., VASWANI, A., STRACHAN, F. E., FERRY, A., STIRZAKER, A. G., REID, A., GRAY, A. J., COLLINSON, P. O., MCALLISTER, D. A., APPLE, F. S., NEWBY, D. E. & MILLS, N. L. 2015a. High-sensitivity cardiac troponin I at presentation in patients with suspected acute coronary syndrome: a cohort study. *Lancet,* 386**,** 2481-8.

SHAH, A. S., ANAND, A., SANDOVAL, Y., LEE, K. K., SMITH, S. W., ADAMSON, P. D., CHAPMAN, A. R., LANGDON, T., SANDEMAN, D., VASWANI, A., STRACHAN, F. E., FERRY, A., STIRZAKER, A. G., REID, A., GRAY, A. J., COLLINSON, P. O., MCALLISTER, D. A., APPLE, F. S., NEWBY, D. E., MILLS, N. L. & HIGH, S. I. 2015b. High-sensitivity cardiac troponin I at presentation in patients with suspected acute coronary syndrome: a cohort study. *Lancet,* 386**,** 2481-8.

SHAH, A. S., GRIFFITHS, M., LEE, K. K., MCALLISTER, D. A., HUNTER, A. L., FERRY, A. V., CRUIKSHANK, A., REID, A., STODDART, M., STRACHAN, F., WALKER, S., COLLINSON, P. O., APPLE, F. S., GRAY, A. J., FOX, K. A., NEWBY, D. E. & MILLS, N. L. 2015c. High sensitivity cardiac troponin and the under-diagnosis of myocardial infarction in women: prospective cohort study. *BMJ,* 350**,** g7873.

SHAPIRO, E. M., SKRTIC, S. & KORETSKY, A. P. 2005a. Sizing it up: cellular MRI using micron-sized iron oxide particles. *Magnetic Resonance in Medicine,* 53**,** 329-38.

SHAPIRO, E. M., SKRTIC, S. & KORETSKY, A. P. 2005b. Sizing it up: cellular MRI using micron-sized iron oxide particles. *Magn Reson Med,* 53**,** 329-38.

SHARMA, A., BHAT, P., SCHILLER, B., FORTIN, G., MCLAUGHLIN, J., LI, Z. & STRAUSS, W. 2011. Efficacy of Feraheme¬Æ(Ferumoxytol) administration on target hemoglobin levels and other iron parameters across 3 dialysis chains. *J Am Soc Nephrol,* 22**,** 485A.

SHERIDAN, F. M., COLE, P. G. & RAMAGE, D. 1996. Leukocyte adhesion to the coronary microvasculature during ischemia and reperfusion in an in vivo canine model. *Circulation,* 93**,** 1784.

SI-TAHAR, M., PIDARD, D., BALLOY, V., MONIATTE, M., KIEFFER, N., DORSSELAER, A. V. & CHIGNARD, M. 1997. Human neutrophil elastase proteolytically activates the platelet integrin aIIbb3 through cleavage of the carboxyl terminus of the aIIb subunit heavy chain. Involvement in the potentiation of platelet. *Journal of Biological Chemistry,* 272**,** 11636-11647.

SIGOVAN, M., BESSAAD, A., ALSAID, H., LANCELOT, E., COROT, C., NEYRAN, B., PROVOST, N., MAJD, Z., BREISSE, M. & CANET-SOULAS, E. 2010. Assessment of age modulated vascular inflammation in ApoE-/- mice by USPIO-enhanced magnetic resonance imaging. *Invest Radiol,* 45**,** 702-7.

SIGOVAN, M., KAYE, E., LANCELOT, E., COROT, C., PROVOST, N., MAJD, Z., BREISSE, M. & CANET-SOULAS, E. 2012. Anti-Inflammatory Drug Evaluation in ApoE-/- Mice by Ultrasmall Superparamagnetic Iron Oxide-Enhanced Magnetic Resonance Imaging. *Invest Radiol,* 47**,** 546-52.

SILVERMAN, E. K. & SANDHAUS, R. A. 2009. Clinical practice. Alpha1-antitrypsin deficiency. *N Engl J Med,* 360**,** 2749-57.

SILVERMAN, K. J., HUTCHINS, G. M. & BULKLEY, B. H. 1978. Cardiac sarcoid: a clinicopathologic study of 84 unselected patients with systemic sarcoidosis. *Circulation,* 58**,** 1204-11.

SIMPSON, A., MAXWELL, A., GOVAN, J., HASLETT, C. & SALLENAVE, J. M. 1999. Elafin (elastase-specific inhibitor) has anti-microbial activity against gram-positive and gram-negative respiratory pathogens. *FEBS letters,* 452**,** 309-313.

SKALI, H., SCHULMAN, A. R. & DORBALA, S. 2013. 18F-FDG PET/CT for the assessment of myocardial sarcoidosis. *Curr Cardiol Rep,* 15**,** 352.

SMALL, W. C., NELSON, R. C. & BERNARDINO, M. E. 1993. Dual contrast enhancement of both T1- and T2-weighted sequences using ultrasmall superparamagnetic iron oxide. *Magn Reson Imaging,* 11**,** 645-54.

SOEHNLEIN, O., LINDBOM, L. & WEBER, C. 2009. Mechanisms underlying neutrophil-mediated monocyte recruitment. *Blood,* 114**,** 4613-23.

SOSNOVIK, D. E., NAHRENDORF, M., DELIOLANIS, N., NOVIKOV, M., AIKAWA, E., JOSEPHSON, L., ROSENZWEIG, A., WEISSLEDER, R. & NTZIACHRISTOS, V. 2007. Fluorescence tomography and magnetic resonance imaging of myocardial macrophage infiltration in infarcted myocardium in vivo. *Circulation,* 115**,** 1384-91.

SPINOWITZ, B. S., KAUSZ, A. T., BAPTISTA, J., NOBLE, S. D., SOTHINATHAN, R., BERNARDO, M. V., BRENNER, L. & PEREIRA, B. J. 2008. Ferumoxytol for treating iron deficiency anemia in CKD. *J Am Soc Nephrol,* 19**,** 1599-605.

SREERAM, G. M., GROCOTT, H. P., WHITE, W. D., NEWMAN, M. F. & STAFFORD-SMITH, M. 2004. Transcranial Doppler emboli count predicts rise in creatinine after coronary artery bypass graft surgery. *J Cardiothorac Vasc Anesth,* 18**,** 548-51.

STANDISH, A. J. & WEISER, J. N. 2009. Human neutrophils kill Streptococcus pneumoniae via serine proteases. *The Journal of Immunology,* 183**,** 2602.

STEFFENS, S., MONTECUCCO, F. & MACH, F. 2009. The inflammatory response as a target to reduce myocardial ischaemia and reperfusion injury. *Thromb Haemost,* 102**,** 240-7.

STEUER, J., BJERNER, T., DUVERNOY, O., JIDEUS, L., JOHANSSON, L., AHLSTROM, H., STAHLE, E. & LINDAHL, B. 2004a. Visualisation and quantification of peri-operative myocardial infarction after coronary artery bypass surgery with contrast-enhanced magnetic resonance imaging. *European Heart Journal,* 25**,** 1293-9.

STEUER, J., BJERNER, T., DUVERNOY, O., JIDEUS, L., JOHANSSON, L., AHLSTROM, H., STAHLE, E. & LINDAHL, B. 2004b. Visualisation and quantification of peri-operative myocardial infarction after coronary artery bypass surgery with contrast-enhanced magnetic resonance imaging. *Eur Heart J,* 25**,** 1293-9.

STEUER, J., BJERNER, T., DUVERNOY, O., JIDÉUS, L., JOHANSSON, L., AHLSTRÖM, H., STÅHLE, E. & LINDAHL, B. 2004c. Visualisation and quantification of peri-operative myocardial infarction after coronary artery

bypass surgery with contrast-enhanced magnetic resonance imaging. *European Heart Journal,* 25**,** 1293.

STEWART, S., WINTERS, G. L., FISHBEIN, M. C., TAZELAAR, H. D., KOBASHIGAWA, J., ABRAMS, J., ANDERSEN, C. B., ANGELINI, A., BERRY, G. J., BURKE, M. M., DEMETRIS, A. J., HAMMOND, E., ITESCU, S., MARBOE, C. C., MCMANUS, B., REED, E. F., REINSMOEN, N. L., RODRIGUEZ, E. R., ROSE, A. G., ROSE, M., SUCIU-FOCIA, N., ZEEVI, A. & BILLINGHAM, M. E. 2005. Revision of the 1990 working formulation for the standardization of nomenclature in the diagnosis of heart rejection. *J Heart Lung Transplant,* 24**,** 1710-20.

SUGAWARA, S., UEHARA, A., NOCHI, T., YAMAGUCHI, T., UEDA, H., SUGIYAMA, A., HANZAWA, K., KUMAGAI, K., OKAMURA, H. & TAKADA, H. 2001. Neutrophil proteinase 3-mediated induction of bioactive IL-18 secretion by human oral epithelial cells. *The Journal of Immunology,* 167**,** 6568.

SUMI, Y., INOUE, N., AZUMI, H., SENO, T., OKUDA, M., HIRATA, K., KAWASHIMA, S., HAYASHI, Y., ITOH, H. & YOKOYAMA, M. 2002. Expression of tissue transglutaminase and elafin in human coronary artery:: Implication for plaque instability. *Atherosclerosis,* 160**,** 31-39.

SUZUKI, J., ISOBE, M., MORISHITA, R. & NAGAI, R. 2010. Characteristics of chronic rejection in heart transplantation: important elements of pathogenesis and future treatments. *Circ J,* 74**,** 233-9.

SWIRSKI, F. K., NAHRENDORF, M., ETZRODT, M., WILDGRUBER, M., CORTEZ-RETAMOZO, V., PANIZZI, P., FIGUEIREDO, J.-L., KOHLER, R. H., CHUDNOVSKIY, A., WATERMAN, P., AIKAWA, E., MEMPEL, T. R., LIBBY, P., WEISSLEDER, R. & PITTET, M. J. 2009a. Identification of Splenic Reservoir Monocytes and Their Deployment to Inflammatory Sites. *Science,* 325**,** 612-616.

SWIRSKI, F. K., NAHRENDORF, M., ETZRODT, M., WILDGRUBER, M., CORTEZ-RETAMOZO, V., PANIZZI, P., FIGUEIREDO, J. L., KOHLER, R. H., CHUDNOVSKIY, A., WATERMAN, P., AIKAWA, E., MEMPEL, T. R., LIBBY, P., WEISSLEDER, R. & PITTET, M. J. 2009b. Identification of splenic reservoir monocytes and their deployment to inflammatory sites. *Science,* 325**,** 612-6.

TAHARA, N., KAI, H., ISHIBASHI, M., NAKAURA, H., KAIDA, H., BABA, K., HAYABUCHI, N. & IMAIZUMI, T. 2006. Simvastatin attenuates plaque inflammation: evaluation by fluorodeoxyglucose positron emission tomography. *J Am Coll Cardiol,* 48**,** 1825-31.

TAMAKUMA, S., OGAWA, M., AIKAWA, N., KUBOTA, T., HIRASAWA, H., ISHIZAKA, A., TAENAKA, N., HAMADA, C., MATSUOKA, S. & ABIRU, T. 2004. Relationship between neutrophil elastase and acute lung injury in humans. *Pulm Pharmacol Ther,* 17**,** 271-9.

TANG, T. Y., HOWARTH, S. P., MILLER, S. R., GRAVES, M. J., JM, U. K.-I., LI, Z. Y., WALSH, S. R., HAYES, P. D., VARTY, K. & GILLARD, J. H. 2008a. Comparison of the inflammatory burden of truly asymptomatic carotid atheroma with atherosclerotic plaques in patients with asymptomatic carotid stenosis undergoing coronary artery bypass grafting: an ultrasmall

superparamagnetic iron oxide enhanced magnetic resonance study. *Eur J Vasc Endovasc Surg,* 35**,** 392-8.

TANG, T. Y., HOWARTH, S. P., MILLER, S. R., GRAVES, M. J., JM, U. K.-I., LI, Z. Y., WALSH, S. R., PATTERSON, A. J., KIRKPATRICK, P. J., WARBURTON, E. A., VARTY, K., GAUNT, M. E. & GILLARD, J. H. 2008b. Correlation of carotid atheromatous plaque inflammation using USPIO-enhanced MR imaging with degree of luminal stenosis. *Stroke,* 39**,** 2144-7.

TANG, T. Y., HOWARTH, S. P., MILLER, S. R., GRAVES, M. J., JM, U. K.-I., TRIVEDI, R. A., LI, Z. Y., WALSH, S. R., BROWN, A. P., KIRKPATRICK, P. J., GAUNT, M. E. & GILLARD, J. H. 2007. Comparison of the inflammatory burden of truly asymptomatic carotid atheroma with atherosclerotic plaques contralateral to symptomatic carotid stenosis: an ultra small superparamagnetic iron oxide enhanced magnetic resonance study. *J Neurol Neurosurg Psychiatry,* 78**,** 1337-43.

TANG, T. Y., HOWARTH, S. P., MILLER, S. R., GRAVES, M. J., PATTERSON, A. J., JM, U. K.-I., LI, Z. Y., WALSH, S. R., BROWN, A. P., KIRKPATRICK, P. J., WARBURTON, E. A., HAYES, P. D., VARTY, K., BOYLE, J. R., GAUNT, M. E., ZALEWSKI, A. & GILLARD, J. H. 2009. The ATHEROMA (Atorvastatin Therapy: Effects on Reduction of Macrophage Activity) Study. Evaluation using ultrasmall superparamagnetic iron oxide-enhanced magnetic resonance imaging in carotid disease. *J Am Coll Cardiol,* 53**,** 2039-50.

TASSANI, P., AUGUSTIN, N., BARANKAY, A., BRAUN, S. L., ZACCARIA, F. & RICHTER, J. A. 2000. High-dose aprotinin modulates the balance between proinflammatory and anti-inflammatory responses during coronary artery bypass graft surgery. *J Cardiothorac Vasc Anesth,* 14**,** 682-6.

TAUPITZ, M., WAGNER, S., SCHNORR, J., KRAVEC, I., PILGRIMM, H., BERGMANN-FRITSCH, H. & HAMM, B. 2004. Phase I clinical evaluation of citrate-coated monocrystalline very small superparamagnetic iron oxide particles as a new contrast medium for magnetic resonance imaging. *Investigative Radiology,* 39**,** 394-405.

TE VELTHUIS, H., JANSEN, P. G., OUDEMANS-VAN STRAATEN, H. M., STURK, A., EIJSMAN, L. & WILDEVUUR, C. R. 1995. Myocardial performance in elderly patients after cardiopulmonary bypass is suppressed by tumor necrosis factor. *J Thorac Cardiovasc Surg,* 110**,** 1663-9.

THYGESEN, K., ALPERT, J. S., JAFFE, A. S., SIMOONS, M. L., CHAITMAN, B. R., WHITE, H. D., KATUS, H. A., APPLE, F. S., LINDAHL, B., MORROW, D. A., CLEMMENSEN, P. M., JOHANSON, P., HOD, H., UNDERWOOD, R., BAX, J. J., BONOW, J. J., PINTO, F., GIBBONS, R. J., FOX, K. A., ATAR, D., NEWBY, L. K., GALVANI, M., HAMM, C. W., URETSKY, B. F., STEG, P. G., WIJNS, W., BASSAND, J. P., MENASCHE, P., RAVKILDE, J., OHMAN, E. M., ANTMAN, E. M., WALLENTIN, L. C., ARMSTRONG, P. W., JANUZZI, J. L., NIEMINEN, M. S., GHEORGHIADE, M., FILIPPATOS, G., LUEPKER, R. V., FORTMANN, S. P., ROSAMOND, W. D., LEVY, D., WOOD, D., SMITH, S. C., HU, D., LOPEZ-SENDON, J. L., ROBERTSON, R. M., WEAVER,

D., TENDERA, M., BOVE, A. A., PARKHOMENKO, A. N., VASILIEVA, E. J., MENDIS, S., BAUMGARTNER, H., CECONI, C., DEAN, V., DEATON, C., FAGARD, R., FUNCK-BRENTANO, C., HASDAI, D., HOES, A., KIRCHHOF, P., KNUUTI, J., KOLH, P., MCDONAGH, T., MOULIN, C., POPESCU, B. A., REINER, Z., SECHTEM, U., SIRNES, P. A., TORBICKI, A., VAHANIAN, A., WINDECKER, S., MORAIS, J., AGUIAR, C., ALMAHMEED, W., ARNAR, D. O., BARILI, F., BLOCH, K. D., BOLGER, A. F., BOTKER, H. E., BOZKURT, B., BUGIARDINI, R., CANNON, C., DE LEMOS, J., EBERLI, F. R., ESCOBAR, E., HLATKY, M., JAMES, S., KERN, K. B., MOLITERNO, D. J., MUELLER, C., NESKOVIC, A. N., PIESKE, B. M., SCHULMAN, S. P., STOREY, R. F., TAUBERT, K. A., VRANCKX, P. & WAGNER, D. R. 2012a. Third universal definition of myocardial infarction. *J Am Coll Cardiol,* 60**,** 1581-98.

THYGESEN, K., ALPERT, J. S., JAFFE, A. S., SIMOONS, M. L., CHAITMAN, B. R., WHITE, H. D., KATUS, H. A., APPLE, F. S., LINDAHL, B., MORROW, D. A., CLEMMENSEN, P. M., JOHANSON, P., HOD, H., UNDERWOOD, R., BAX, J. J., BONOW, J. J., PINTO, F., GIBBONS, R. J., FOX, K. A., ATAR, D., NEWBY, L. K., GALVANI, M., HAMM, C. W., URETSKY, B. F., STEG, P. G., WIJNS, W., BASSAND, J. P., MENASCHE, P., RAVKILDE, J., OHMAN, E. M., ANTMAN, E. M., WALLENTIN, L. C., ARMSTRONG, P. W., JANUZZI, J. L., NIEMINEN, M. S., GHEORGHIADE, M., FILIPPATOS, G., LUEPKER, R. V., FORTMANN, S. P., ROSAMOND, W. D., LEVY, D., WOOD, D., SMITH, S. C., HU, D., LOPEZ-SENDON, J. L., ROBERTSON, R. M., WEAVER, D., TENDERA, M., BOVE, A. A., PARKHOMENKO, A. N., VASILIEVA, E. J., MENDIS, S., BAUMGARTNER, H., CECONI, C., DEAN, V., DEATON, C., FAGARD, R., FUNCK-BRENTANO, C., HASDAI, D., HOES, A., KIRCHHOF, P., KNUUTI, J., KOLH, P., MCDONAGH, T., MOULIN, C., POPESCU, B. A., REINER, Z., SECHTEM, U., SIRNES, P. A., TORBICKI, A., VAHANIAN, A., WINDECKER, S., MORAIS, J., AGUIAR, C., ALMAHMEED, W., ARNAR, D. O., BARILI, F., BLOCH, K. D., BOLGER, A. F., BOTKER, H. E., BOZKURT, B., BUGIARDINI, R., CANNON, C., DE LEMOS, J., EBERLI, F. R., ESCOBAR, E., HLATKY, M., JAMES, S., KERN, K. B., MOLITERNO, D. J., MUELLER, C., NESKOVIC, A. N., PIESKE, B. M., SCHULMAN, S. P., STOREY, R. F., TAUBERT, K. A., VRANCKX, P., WAGNER, D. R., INFARCTION, J. E. A. A. W. T. F. F. U. D. O. M., CHAIRPERSONS, A. T. F. M., et al. 2012b. Third universal definition of myocardial infarction. *J Am Coll Cardiol,* 60**,** 1581-98.

THYGESEN, K., ALPERT, J. S. & WHITE, H. D. 2007a. Universal definition of myocardial infarction. *Eur Heart J,* 28**,** 2525-38.

THYGESEN, K., ALPERT, J. S. & WHITE, H. D. 2007b. Universal definition of myocardial infarction. *Circulation,* 116**,** 2634.

TIEFENBACHER, C., EBERT, M., NIROOMAND, F., BATKAI, S., TILLMANNS, H., ZIMMERMANN, R. & KÜBLER, W. 1997. Inhibition of elastase improves myocardial function after repetitive ischaemia and

myocardial infarction in the rat heart. *Pflugers Archiv European Journal of Physiology,* 433**,** 563-570.

TKALCEVIC, J., NOVELLI, M., PHYLACTIDES, M., IREDALE, J. P., SEGAL, A. W. & ROES, J. 2000. Impaired immunity and enhanced resistance to endotoxin in the absence of neutrophil elastase and cathepsin G. *Immunity,* 12**,** 201-10.

TREMBLAY, G. M., SALLENAVE, J. M., ISRAEL-ASSAYAG, E., CORMIER, Y. & GAULDIE, J. 1996. Elafin/elastase-specific inhibitor in bronchoalveolar lavage of normal subjects and farmer's lung. *American Journal of Respiratory and Critical Care Medicine,* 154**,** 1092.

TRIVEDI, R. A., MALLAWARACHI, C., JM, U. K.-I., GRAVES, M. J., HORSLEY, J., GODDARD, M. J., BROWN, A., WANG, L., KIRKPATRICK, P. J., BROWN, J. & GILLARD, J. H. 2006a. Identifying inflamed carotid plaques using in vivo USPIO-enhanced MR imaging to label plaque macrophages. *Arterioscler Thromb Vasc Biol,* 26**,** 1601-6.

TRIVEDI, R. A., MALLAWARACHI, C., U-KING-IM, J.-M., GRAVES, M. J., HORSLEY, J., GODDARD, M. J., BROWN, A., WANG, L., KIRKPATRICK, P. J., BROWN, J. & GILLARD, J. H. 2006b. Identifying inflamed carotid plaques using in vivo USPIO-enhanced MR imaging to label plaque macrophages. *Arterioscler Thromb Vasc Biol,* 26**,** 1601-6.

TSE, G. H., HUGHES, J. & MARSON, L. P. 2013. Systematic review of mouse kidney transplantation. *Transpl Int,* 26**,** 1149-60.

TSUCHIYA, K., NITTA, N., SONODA, A., OTANI, H., TAKAHASHI, M., MURATA, K., SHIOMI, M., TABATA, Y. & NOHARA, S. 2013. Atherosclerotic imaging using 4 types of superparamagnetic iron oxides: new possibilities for mannan-coated particles. *Eur J Radiol,* 82**,** 1919-25.

TSUJIOKA, H., IMANISHI, T., IKEJIMA, H., KUROI, A., TAKARADA, S., TANIMOTO, T., KITABATA, H., OKOCHI, K., ARITA, Y., ISHIBASHI, K., KOMUKAI, K., KATAIWA, H., NAKAMURA, N., HIRATA, K., TANAKA, A. & AKASAKA, T. 2009. Impact of heterogeneity of human peripheral blood monocyte subsets on myocardial salvage in patients with primary acute myocardial infarction. *J Am Coll Cardiol,* 54**,** 130-8.

TSUNEMI, M., MATSUURA, Y., SAKAKIBARA, S. & KATSUBE, Y. 1996. Crystal structure of an elastase-specific inhibitor elafin complexed with porcine pancreatic elastase determined at 1.9 A resolution. *Biochemistry,* 35**,** 11570-11576.

UEHARA, A., MURAMOTO, K., TAKADA, H. & SUGAWARA, S. 2003. Neutrophil serine proteinases activate human nonepithelial cells to produce inflammatory cytokines through protease-activated receptor 2. *The Journal of Immunology,* 170**,** 5690.

UEHARA, A., SUGAWARA, S., MURAMOTO, K. & TAKADA, H. 2002. Activation of human oral epithelial cells by neutrophil proteinase 3 through protease-activated receptor-2. *The Journal of Immunology,* 169**,** 4594.

URZUA, J., TRONCOSO, S., BUGEDO, G., CANESSA, R., MUNOZ, H., LEMA, G., VALDIVIESO, A., IRARRAZAVAL, M., MORAN, S. & MENESES, G. 1992. Renal function and cardiopulmonary bypass: effect of perfusion pressure. *J Cardiothorac Vasc Anesth,* 6**,** 299-303.

VAN GAAL, W. J., ARNOLD, J. R., TESTA, L., KARAMITSOS, T., LIM, C. C., PONNUTHURAI, F. A., PETERSEN, S., FRANCIS, J. M., SELVANAYAGAM, J., SAYEED, R., WEST, N., WESTABY, S., NEUBAUER, S. & BANNING, A. P. 2011. Myocardial injury following coronary artery surgery versus angioplasty (MICASA): a randomised trial using biochemical markers and cardiac magnetic resonance imaging. *EuroIntervention,* 6**,** 703-10.

VANDIVIER, R. W., FADOK, V. A., HOFFMANN, P. R., BRATTON, D. L., PENVARI, C., BROWN, K. K., BRAIN, J. D., ACCURSO, F. J. & HENSON, P. M. 2002. Elastase-mediated phosphatidylserine receptor cleavage impairs apoptotic cell clearance in cystic fibrosis and bronchiectasis. *Journal of Clinical Investigation,* 109**,** 661-670.

VERRIER, E. D., SHERNAN, S. K., TAYLOR, K. M., VAN DE WERF, F., NEWMAN, M. F., CHEN, J. C., CARRIER, M., HAVERICH, A., MALLOY, K. J., ADAMS, P. X., TODARO, T. G., MOJCIK, C. F., ROLLINS, S. A. & LEVY, J. H. 2004. Terminal complement blockade with pexelizumab during coronary artery bypass graft surgery requiring cardiopulmonary bypass: a randomized trial. *JAMA,* 291**,** 2319-27.

VIALLON, M., MEWTON, N., THUNY, F., GUEHRING, J., O'DONNELL, T., STEMMER, A., BI, X., RAPACCHI, S., ZUEHLSDORFF, S., REVEL, D. & CROISILLE, P. 2012. T2-weighted cardiac MR assessment of the myocardial area-at-risk and salvage area in acute reperfused myocardial infarction: Comparison of state-of-the-art dark blood and bright blood T2-weighted sequences. *J Magn Reson Imaging,* 35**,** 328-39.

VINTEN-JOHANSEN, J. 2004. Involvement of neutrophils in the pathogenesis of lethal myocardial reperfusion injury. *Cardiovasc Res,* 61**,** 481-97.

WAGNER, M., WAGNER, S., SCHNORR, J., SCHELLENBERGER, E., KIVELITZ, D., KRUG, L., DEWEY, M., LAULE, M., HAMM, B. & TAUPITZ, M. 2011. Coronary MR angiography using citrate-coated very small superparamagnetic iron oxide particles as blood-pool contrast agent: initial experience in humans. *J Magn Reson Imaging,* 34**,** 816-23.

WAKAYAMA, F., FUKUDA, I., SUZUKI, Y. & KONDO, N. 2007. Neutrophil elastase inhibitor, sivelestat, attenuates acute lung injury after cardiopulmonary bypass in the rabbit endotoxemia model. *Ann Thorac Surg,* 83**,** 153-60.

WAN, S., YIM, A. P., WONG, C. K., ARIFI, A. A., YIP, J. H., NG, C. S., WAYE, M. M. & LAM, C. W. 2002. Expression of FHL2 and cytokine messenger RNAs in human myocardium after cardiopulmonary bypass. *Int J Cardiol,* 86**,** 265-72.

WEBB, L., CASULA, A., RAVANAN, R. & TOMSON, C. R. 2010. UK Renal Registry 12th Annual Report (December 2009): chapter 5: demographic and biochemistry profile of kidney transplant recipients in the UK in 2008: national and centre-specific analyses. *Nephron Clin Pract,* 115 Suppl 1**,** c69-102.

WELBOURN, C. R., GOLDMAN, G., PATERSON, I. S., VALERI, C. R., SHEPRO, D. & HECHTMAN, H. B. 1991. Pathophysiology of ischaemia reperfusion injury: central role of the neutrophil. *Br J Surg,* 78**,** 651-5.

WESTLIN, W. & GIMBRONE JR, M. 1993. Neutrophil-mediated damage to human vascular endothelium. Role of cytokine activation. *The American Journal of Pathology,* 142**,** 117.

WESTWOOD, M. A., FIRMIN, D. N., GILDO, M., RENZO, G., STATHIS, G., MARKISSIA, K., VASILI, B. & PENNELL, D. J. 2005. Intercentre reproducibility of magnetic resonance T2* measurements of myocardial iron in thalassaemia. *Int J Cardiovasc Imaging,* 21**,** 531-8.

WEYRICH, A. S., BUERKE, M., ALBERTINE, K. H. & LEFER, A. M. 1995. Time course of coronary vascular endothelial adhesion molecule expression during reperfusion of the ischemic feline myocardium. *J Leukoc Biol,* 57**,** 45-55.

WIART, M., DAVOUST, N., PIALAT, J. B., DESESTRET, V., MOUCHARRAFIE, S., CHO, T. H., MUTIN, M., LANGLOIS, J. B., BEUF, O., HONNORAT, J., NIGHOGHOSSIAN, N. & BERTHEZENE, Y. 2007. MRI monitoring of neuroinflammation in mouse focal ischemia. *Stroke,* 38**,** 131-7.

WIEDOW, O., LUADEMANN, J. & UTECHT, B. 1991. Elafin is a potent inhibitor of proteinase 3. *Biochem Biophys Res Commun,* 174**,** 6-10.

WIEDOW, O., SCHRÖDER, J., GREGORY, H., YOUNG, J. & CHRISTOPHERS, E. 1990. Elafin: an elastase-specific inhibitor of human skin. Purification, characterization, and complete amino acid sequence. *Journal of Biological Chemistry,* 265**,** 14791.

WILLINGER, C. C., SCHRAMEK, H., PFALLER, K. & PFALLER, W. 1992. Tissue distribution of neutrophils in postischemic acute renal failure. *Virchows Arch B Cell Pathol Incl Mol Pathol,* 62**,** 237-43.

WITTAMER, V., BONDUE, B., GUILLABERT, A., VASSART, G., PARMENTIER, M. & COMMUNI, D. 2005. Neutrophil-mediated maturation of chemerin: a link between innate and adaptive immunity. *J Immunol,* 175**,** 487-93.

WITTAMER, V., FRANSSEN, J. D., VULCANO, M., MIRJOLET, J. F., LE POUL, E., MIGEOTTE, I., BREZILLON, S., TYLDESLEY, R., BLANPAIN, C., DETHEUX, M., MANTOVANI, A., SOZZANI, S., VASSART, G., PARMENTIER, M. & COMMUNI, D. 2003. Specific recruitment of antigen-presenting cells by chemerin, a novel processed ligand from human inflammatory fluids. *J Exp Med,* 198**,** 977-85.

WU, A. H., FENG, Y. J., MOORE, R., APPLE, F. S., MCPHERSON, P. H., BUECHLER, K. F. & BODOR, G. 1998. Characterization of cardiac troponin subunit release into serum after acute myocardial infarction and comparison of assays for troponin T and I. American Association for Clinical Chemistry Subcommittee on cTnI Standardization. *Clinical chemistry,* 44**,** 1198-208.

WU, K., URANO, T., IHARA, H., TAKADA, Y., FUJIE, M., SHIKIMORI, M., HASHIMOTO, K. & TAKADA, A. 1995. The cleavage and inactivation of plasminogen activator inhibitor type 1 by neutrophil elastase: the evaluation of its physiologic relevance in fibrinolysis. *Blood,* 86**,** 1056.

WU, Y. L., YE, Q., SATO, K., FOLEY, L. M., HITCHENS, T. K. & HO, C. 2009. Noninvasive evaluation of cardiac allograft rejection by cellular and

functional cardiac magnetic resonance. *JACC Cardiovasc Imaging,* 2**,** 731-41.

YANCY, A. D., OLZINSKI, A. R., HU, T. C., LENHARD, S. C., ARAVINDHAN, K., GRUVER, S. M., JACOBS, P. M., WILLETTE, R. N. & JUCKER, B. M. 2005. Differential uptake of ferumoxtran-10 and ferumoxytol, ultrasmall superparamagnetic iron oxide contrast agents in rabbit: critical determinants of atherosclerotic plaque labeling. *J Magn Reson Imaging,* 21**,** 432-42.

YANG, Y., YANASAK, N., SCHUMACHER, A. & HU, T. C. 2010. Temporal and noninvasive monitoring of inflammatory-cell infiltration to myocardial infarction sites using micrometer-sized iron oxide particles. *Magn Reson Med,* 63**,** 33-40.

YANG, Y. M., FENG, X., YIN LE, K., LI, C. C., JIA, J. & DU, Z. G. 2014. Comparison of USPIO-enhanced MRI and Gd-DTPA enhancement during the subacute stage of focal cerebral ischemia in rats. *Acta radiologica,* 55**,** 864-73.

YANG, Y. M., FENG, X. Y., YIN LE, K., LI, C. C., LI, A. N., JIA, J., WANG, X. L., DU, Z. G. & JIN, L. X. 2013. In vivo USPIO-enhanced MR signal characteristics of secondary degeneration in the ipsilateral substantia nigra after middle cerebral artery occlusion at 3T. *J Neuroradiol,* 40**,** 198-203.

YANO, T., MIURA, T., WHITTAKER, P., MIKI, T., SAKAMOTO, J., NAKAMURA, Y., ICHIKAWA, Y., IKEDA, Y., KOBAYASHI, H. & OHORI, K. 2006. Macrophage colony-stimulating factor treatment after myocardial infarction attenuates left ventricular dysfunction by accelerating infarct repair. *Journal of the American College of Cardiology,* 47**,** 626-634.

YAZAKI, Y., ISOBE, M., HIROE, M., MORIMOTO, S., HIRAMITSU, S., NAKANO, T., IZUMI, T. & SEKIGUCHI, M. 2001. Prognostic determinants of long-term survival in Japanese patients with cardiac sarcoidosis treated with prednisone. *Am J Cardiol,* 88**,** 1006-10.

YE, Q., YANG, D., WILLIAMS, M., WILLIAMS, D. S., PLUEMPITIWIRIYAWEJ, C., MOURA, J. M. & HO, C. 2002. In vivo detection of acute rat renal allograft rejection by MRI with USPIO particles. *Kidney Int,* 61**,** 1124-35.

YOSHIMURA, Y., HIRAMATSU, Y., SATO, Y., HOMMA, S., ENOMOTO, Y., JIKUYA, T. & SAKAKIBARA, Y. 2003. ONO-6818, a novel, potent neutrophil elastase inhibitor, reduces inflammatory mediators during simulated extracorporeal circulation. *Ann Thorac Surg,* 76**,** 1234-9.

ZAHLER, S., MASSOUDY, P., HARTL, H., HAHNEL, C., MEISNER, H. & BECKER, B. F. 1999. Acute cardiac inflammatory responses to postischemic reperfusion during cardiopulmonary bypass. *Cardiovasc Res,* 41**,** 722-30.

ZAIDI, S. H., HUI, C. C., CHEAH, A. Y., YOU, X. M., HUSAIN, M. & RABINOVITCH, M. 1999. Targeted overexpression of elafin protects mice against cardiac dysfunction and mortality following viral myocarditis. *J Clin Invest,* 103**,** 1211-9.

ZAIDI, S. H., YOU, X. M., CIURA, S., HUSAIN, M. & RABINOVITCH, M. 2002a. Overexpression of the serine elastase inhibitor elafin protects transgenic mice from hypoxic pulmonary hypertension. *Circulation,* 105**,** 516-21.

ZAIDI, S. H., YOU, X. M., CIURA, S., O'BLENES, S., HUSAIN, M. & RABINOVITCH, M. 2000a. Suppressed smooth muscle proliferation and inflammatory cell invasion after arterial injury in elafin-overexpressing mice. *J Clin Invest,* 105**,** 1687-95.

ZAIDI, S. H. E., YOU, X. M., CIURA, S., HUSAIN, M. & RABINOVITCH, M. 2002b. Overexpression of the serine elastase inhibitor elafin protects transgenic mice from hypoxic pulmonary hypertension. *Circulation,* 105**,** 516-521.

ZAIDI, S. H. E., YOU, X. M., CIURA, S., O'BLENES, S., HUSAIN, M. & RABINOVITCH, M. 2000b. Suppressed smooth muscle proliferation and inflammatory cell invasion after arterial injury in elafin-overexpressing mice. *Journal of Clinical Investigation,* 105**,** 1687-1730.

ZANI, M. L., NOBAR, S. M., LACOUR, S. A., LEMOINE, S., BOUDIER, C., BIETH, J. G. & MOREAU, T. 2004. Kinetics of the inhibition of neutrophil proteinases by recombinant elafin and pre elafin (trappin 2) expressed in Pichia pastoris. *European Journal of Biochemistry,* 271**,** 2370-2378.

ZAWADA, A. M., ROGACEV, K. S., SCHIRMER, S. H., SESTER, M., BOHM, M., FLISER, D. & HEINE, G. H. 2012. Monocyte heterogeneity in human cardiovascular disease. *Immunobiology,* 217**,** 1273-84.

ZEIHER, B. G., ARTIGAS, A., VINCENT, J. L., DMITRIENKO, A., JACKSON, K., THOMPSON, B. T. & BERNARD, G. 2004. Neutrophil elastase inhibition in acute lung injury: results of the STRIVE study. *Crit Care Med,* 32**,** 1695-702.

ZHANG, M., ZOU, Z., MAASS, N. & SAGER, R. 1995. Differential expression of elafin in human normal mammary epithelial cells and carcinomas is regulated at the transcriptional level. *Cancer Research,* 55**,** 2537.

ZHANG, W. R., GARG, A. X., COCA, S. G., DEVEREAUX, P. J., EIKELBOOM, J., KAVSAK, P., MCARTHUR, E., THIESSEN-PHILBROOK, H., SHORTT, C., SHLIPAK, M., WHITLOCK, R., PARIKH, C. R. & CONSORTIUM, T.-A. 2015. Plasma IL-6 and IL-10 Concentrations Predict AKI and Long-Term Mortality in Adults after Cardiac Surgery. *J Am Soc Nephrol,* 26**,** 3123-32.

ZHANG, Y., DODD, S. J., HENDRICH, K. S., WILLIAMS, M. & HO, C. 2000. Magnetic resonance imaging detection of rat renal transplant rejection by monitoring macrophage infiltration. *Kidney Int,* 58**,** 1300-10.

ZHAO, Z. Q., VELEZ, D. A., WANG, N. P., HEWAN-LOWE, K. O., NAKAMURA, M., GUYTON, R. A. & VINTEN-JOHANSEN, J. 2001. Progressively developed myocardial apoptotic cell death during late phase of reperfusion. *Apoptosis,* 6**,** 279-290.

ZHU, J., NATHAN, C. & DING, A. 1999. Suppression of macrophage responses to bacterial lipopolysaccharide by a non-secretory form of secretory leukocyte protease inhibitor. *Biochimica et Biophysica Acta (BBA)-Molecular Cell Research,* 1451**,** 219-223.

ZIAI, F., NAGANO, H., KUSAKA, M., COITO, A. J., TROY, J. L., NADEAU, K. C., RENNKE, H. G., TILNEY, N. L., BRENNER, B. M. & MACKENZIE, H. S. 2000. Renal allograft protection with losartan in Fisher-->Lewis rats: hemodynamics, macrophages, and cytokines. *Kidney Int,* 57**,** 2618-25.

Appendix H: FUTURE STUDIES

IRON NANOPARTICLE ENHANCED MRI IN THE ASSESSMENT OF MYOCARDIAL INFARCTION (IRNMAN) TRIAL

Study Population

All patients will undergo intensive clinical phenotyping including demographics, cardiovascular risk factors, concomitant medication, past medical history, clinical examination and standard clinical haematological and biochemical analyses. All patients will be followed up out to at least 3 months through clinic visits and 12 months by electronic patient record tracking.

We will recruit 80 patients.

Table 1: Inclusion and exclusion criteria

Inclusion Criteria:	**Exclusion Criteria:**
>18 years Plasma troponin concentration >5 ng/mL; upper limit of normal 0.04 ng/mL) Acute myocardial infarction defined according to the Universal Definition of myocardial infarction.(Thygesen et al., 2007b)	Critical (≥95%) left main stem coronary artery stenosis Continued symptoms of angina at rest or minimal exertion Past history of systemic iron overload or haemochromatosis Renal failure (estimated glomerular filtration rate <25 mL/min) Contraindication to magnetic resonance imaging Significant heart failure (Killip class ≥2) Known allergy to dextran- or iron-containing compounds

Study Groups

In the first 40 patients, subjects will receive USPIOs on a specific day after acute myocardial infarction; day 1-3, day 4-9, 10-20 or day 89±14 days (n=10 per group). All subjects will be scanned on days 2-4, 5-10, 11-21 and 74-104 as well as on the day of, and immediately prior to, USPIO administration. This will be subject to patient availability and scanner availability. This will provide an assessment of the time course of the uptake of USPIOs. Half of the recruited patients will receive a second infusion of USPIO at 3 months followed by repeat MRI scanning 24 hours later. This will provide information regarding any residual inflammation at this point, and if absent allow patients to acts as their own controls for scan comparison.

Thus the patient schedule will follow one of the pathways in Figure 1.

Figure 1: Time course of USPIO infusion and MRI scans

Based on this data, we will select the optimum time to administer USPIOs and undertake this in the remaining 40 patients.

Administration

Ferumoxytol (Rienso) will be supplied by Takeda and each vial contains 510 mg of elemental iron in 17 mL (30 mg/mL). It will be administered via a peripheral venous cannula at a dose of 4 mg Fe/kg body weight at a rate of up to 1 mL/sec. We have administered this preparation in our pilot studies without adverse effect.

Magnetic Resonance Imaging

Magnetic resonance imaging will be performed using our British Heart Foundation-funded clinical research 3T magnetic resonance imaging scanner (Siemens 3T Verio) at the Clinical Research Imaging Centre at the Queen's Medical Research Institute, University of Edinburgh.

Standard cardiac imaging breath-held ECG-gated sequences and USPIO imaging will be performed as per the pilot study and EMPIRE trial described in chapters 2 & 3.

Systemic Markers of Inflammation

We will undertake detailed phenotyping of these patients including accurate recording of clinical characteristics, risk factor profile, systemic inflammatory markers (including MCP-1), infarct size and oedema as well as follow them up for clinical outcomes at 3, 6 and 12 months. Prior to each MRI scan, approximately 50 mL peripheral venous blood will be obtained from each volunteer for the measurement of systemic markers of inflammation and inflammatory cell activity such as high sensitivity C-reactive protein (hsCRP), interleukin-6 (IL-6), IL-8, TNFα, MCP-1 and full blood count for differential leucocyte count.

Data Analysis and Statistics

Data will be compared using analysis of variance with repeated measures and unpaired and paired Student's t-test as appropriate. For continuous variables, regression analysis will be performed to explore for associations. Statistical significance will be taken as a two-sided $P<0.05$.

We will be undertaking a time-course assessment of USPIO uptake in 30 patients following acute myocardial infarction. Based on our preliminary pilot data, the mean R2* value for myocardium is 0.041 with a standard deviation of 0.016. Following USPIO administration we expect are a 4-fold increase in the R2* value (0.164±0.051). Given the different time points and gradation of uptake, we wish to be able to detect a 50% increase in R2* value. At 80% power and two-sided $P<0.05$, we will require 10 subjects per group. We will assess key clinical factors such as

infarct size to assess for determinants of USPIO uptake. For a sample size of 60 patients, we will have 80% power at two-sided $P<0.05$ to detect a correlation of ≤ 0.35 between the change in the R2* and clinical correlates. Allowing for drop out due to the multiple scanning regimen, we aim to recruit 80 patients.

Expected Value of Results

We propose to describe, characterise and identify the determinants of USPIO uptake using the clinical model of acute myocardial infarction. This will be the first description of this 'smart contrast agent' in the setting of acute myocardial infarction and, if successful, this technique has many major potential benefits and ramifications. First, it may assist in risk stratifying patients who may have an adverse outcome. For example, intense and persistent USPIO uptake may be associated with adverse remodelling and progression to heart failure. Second, it will provide a method of assessing the inflammatory and reparative processes following infarction. This may be a useful biomarker to assess the impact of therapeutic interventions.

DETECTION OF CELLULAR INFLAMMATION WITH FERUMOXYTOL IN THE HEART: DECIFER-HEART TRIAL

Study Design

This is an open-label comparative investigational cohort study.

Patients from each of the 3 cohorts (see below) and 20 control subjects (with a wide and evenly distributed range of age and sex) will undergo a baseline MRI scan. They will then receive USPIOs immediately after this, with repeat scanning 24 hours later to assess USPIO uptake (Figure 2).

In patient cohorts, MRI scans will be repeated after 3 months to assess response to treatment, or a change in clinical status. Prior to the MRI scans, approximately 100 mL peripheral venous blood will be obtained from each volunteer for the measurement of systemic markers of inflammation and inflammatory cell activity such as high sensitivity C-reactive protein (hsCRP), interleukin-6 (IL-6), IL-8, tumour necrosis factor alpha (TNFα), monocyte chemotactic protein 1 (MCP-1) and full blood count for differential leucocyte count. To characterise the inflammatory cell phenotype, blood will also be taken for flow cytometry to assess the surface expression markers of peripheral blood mononuclear cells (Tsujioka et al., 2009).

Figure 2: Time course of USPIO infusion and CMR scans

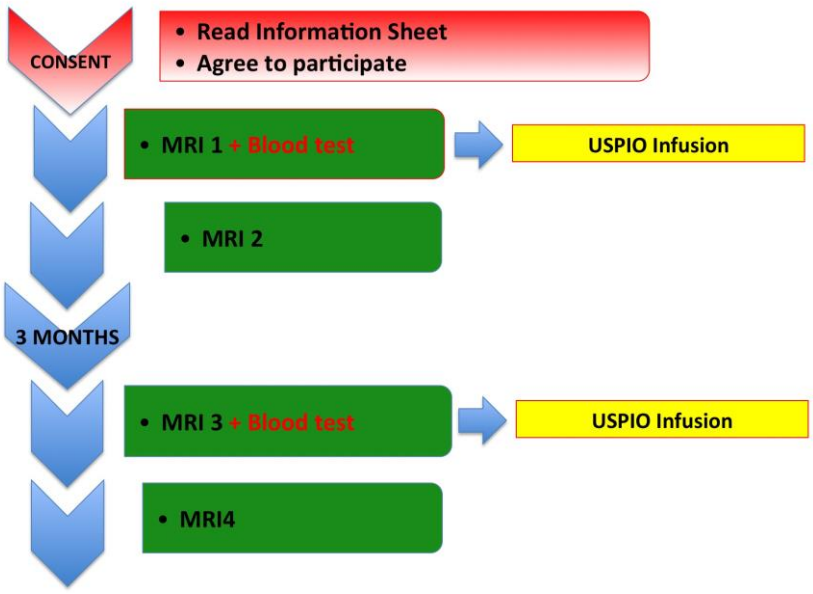

Cohort 1: 20 patients under routine follow up after cardiac transplant.

Patients will be recruited from the national advanced heart failure and cardiac transplantation unit at the Golden Jubilee National Hospital, Glasgow. Currently 121 patients are under regular surveillance and will include a clinical spectrum ranging from no rejection to those with clinical and histological signs of acute rejection. The results of CMR scanning will be compared when possible to biopsy samples in all patients using the International Society for Heart and Lung Transplantation (ISHLT) grading system (which was introduced in 1990 and revised in 2004) (Stewart et al., 2005). We will predominantly recruit patients who exhibit clinical features suggesting differing stages of rejection, although we will also recruit patients who appear well without clinical evidence of rejection.

Cohort 2: 20 patients diagnosed with acute myocarditis. Patients will be recruited from all centres. The clinical diagnosis of acute myocarditis is not well defined and there are no internationally recognised diagnostic criteria. It is therefore a diagnosis of exclusion and maybe caused by infection, chemotherapy, auto-immune conditions or unknown aetiologies. Occasionally patients may undergo myocardial biopsy when a more definitive diagnosis can be made although this is subject to sampling bias (Feldman and McNamara, 2000). Patients with acute myocarditis will be recruited if the diagnosis has been made by a cardiologist based on clinical, biochemical, electrocardiographic, echocardiographic or angiographic data. We will perform a post hoc analysis to define aetiologies. If subsequent to the initial scan, the clinical diagnosis changes from being one of myocarditis, this will exclude the patient from the cohort.

Cohort 3: 20 patients with cardiac sarcoidosis.

Patients will be recruited from the national cardiac sarcoidosis service at the Royal Brompton Hospital with the assistance of Professor Athol Wells and Dr Elizabetta Renzoni. The diagnosis will be made by the internationally recognised guidelines of the "Japanese Society of Sarcoidosis and Other Granulomatous Disorders".(Dubrey and Falk, 2010) Patients with new presentation of active sarcoidosis will be recruited. The Royal Brompton Hospital sees over 150 new cases of sarcoidosis each year with approximately a quarter having cardiac involvement. The total database includes over 1,000 patients with sarcoidosis, of whom approximately 300 have cardiac involvement. We will recruit patients who have been diagnosed clinically with acute cardiac sarcoid by the specialist team. If subsequent to the initial scan, the clinical diagnosis changes from being one of cardiac sarcoidosis, this will exclude the patient from the cohort.

Cohort 4: 20 healthy volunteers.

We will recruit healthy volunteers through advertising, with a wide and evenly distributed range of age and sex. Subjects will have no significant past medical history and be otherwise fit and well in order to act as a normal reference population and to define any non-specific myocardial USPIO uptake.

Patients will be excluded if they have had a diagnosis of myocardial infarction within 1 month, renal failure (estimated glomerular filtration rate <25 mL/min), contraindication to magnetic resonance imaging, past history of systemic iron overload or haemochromatosis, polycythaemia or known allergy to dextran- or iron-

containing compounds. All patients will undergo intensive clinical phenotyping including demographics, cardiovascular risk factors, concomitant medication, past medical history, clinical examination and standard clinical haematological and biochemical analyses.

The research team will track relevant or significant clinical outcomes for up to 5 years after the study is completed, by examining local electronic health records at each centre.

We will recruit 80 participants (over 24 months), 20 in each cohort. Recruitment will take place in three centres; Royal Infirmary of Edinburgh, Golden Jubilee National Hospital in Glasgow and the Royal Brompton Hospital in London.

Sample Size Calculation

There will be tissue resident macrophages as well as possible continued influx of monocytes into the myocardium of the 3 patient cohorts. However the concentration of such inflammatory cells in each condition is unknown. In a pilot study however, we found that the change in myocardial R2* value in patients with myocardial infarction pre and post USPIO was 114+/-60s^{-1} compared to 41±15 s^{-1} in healthy controls. That said, the R2* value in MI patients was however taken from within the infarct area, and an average of infarct and remote myocardial tissue would yield a lower value. Given the less intense anticipated inflammation in our 3 cohorts, we estimate an increase in R2* value of at least 10s^{-1} when compared to controls giving an R2* value least 51s^{-1}. Assuming a two-sided 5% level of significance and 80% power, we would require a sample size of 18 in each group.